UNITED STATES DEPARTMENT OF THE INTERIOR

GEOLOGICAL SURVEY

NATIONAL EARTHQUAKE HAZARDS REDUCTION PROGRAM, SUMMARIES OF TECHNICAL REPORTS VOLUME XXII

Prepared by Participants in

NATIONAL EARTHQUAKE HAZARDS REDUCTION PROGRAM

July 1986

OPEN-FILE REPORT 86-383

Menlo Park, California

1986

INSTRUCTIONS FOR PREPARATION OF SUMMARY REPORTS

1. Use 8 1/2" x 11" paper for both text and figures.
2. Leave at least 1" wide margins at top, sides and bottom.
3. Type headings at top of first page. Headings should include:
    a. Project title
    b. Contract, grant or project number
    c. Name of Principal Investigator(s)
    d. Name and address of institution
    e. Telephone number(s) of Principal Investigator(s)
4. Original copies of text and figures are required. No xerox copies.
5. Type figure captions on the same page as the figure.
6. Only type on one side of the paper.
7. Type all text single spaced.
8. Do not number pages.
9. Do not use staples.
10. All figures must be in black and white. No color figures (color, weak or grey lines will not photo-reproduce).

Gary E. Svenson

UNITED STATES
DEPARTMENT OF THE INTERIOR
GEOLOGICAL SURVEY

NATIONAL EARTHQUAKE HAZARDS REDUCTION PROGRAM, SUMMARIES OF TECHNICAL REPORTS VOLUME XXII

Prepared by Participants in

NATIONAL EARTHQUAKE HAZARDS REDUCTION PROGRAM

Compiled by

Muriel L. Jacobson

Thelma R. Rodriguez

The research results described in the following summaries were submitted by the investigators on May 16, 1985 and cover the 6-months period from October 1, 1985 through May 31, 1986. These reports include both work performed under contracts administered by the Geological Survey and work by members of the Geological Survey. The report summaries are grouped into the three major elements of the National Earthquake Hazards Reduction Program.

Open File Report No. 86-383

The data and interpretations in these progress reports may be reevaluated by the investigators upon completion of the research. Readers who wish to cite findings described herein should confirm their accuracy with the author.

CONTENTS

Earthquake Hazards Reduction Program

Page

Objective (II-1): Prediction Methodology and Evaluation

Develop methods to provide a rational basis for estimates of increased earthquake potential. Evaluate the relevance of various geophysical, geochemical, and hydrological data for earthquake prediction.

1. Develop, operate and evaluate instrumentation for monitoring potential earthquake precursors.

2. Analyze and evaluate seismicity data collected prior to medium and large earthquakes.

3. Obtain and analyze data from seismically active regions of foreign countries through cooperative projects with the host countries.

4. Systematically evaluate data and develop statistics that relate observations of specific phenomena to earthquake occurrence.

5. Develop, study and test prediction methods that can be used to proceed from estimates of long-range earthquake potential to specific short-term predictions..... 202

Objective (II-2): Earthquake Prediction Experiments

Conduct data collection and analysis experiments in areas of California capable of great earthquakes, where large populations are at risk. The experiments will emphasize improved coordination of data collection, data reporting, review and analysis according to set schedules and standards.

1. Collect and analyze data for an earthquake prediction experiment in southern California, concentrating on the southern San Andreas fault from Parkfield, California to the Salton Sea.

2. Collect and analyze data for an earthquake prediction experiment in central California, concentrating on the San Andreas fault north of Parkfield, California..... 260

Objective (II-3): Theoretical, Laboratory and Fault Zone Studies

Improve our understanding of the physics of earthquake processes through theoretical and laboratory studies to guide and test earthquake prediction observations and data analysis. Measure physical properties of those zones selected for earthquake experiments, including stress, temperature, elastic and anelastic characteristics, pore pressure, and material properties.

Most of the technical summaries contained in this volume are for research contracts solicited by RFP-1485. The description in the previous table of contents corresponds to respective Elements and Objectives of that RFP. Additionally some of the summaries are for research objectives that were initiated in earlier years. These objectives are covered in the descriptions found in the following table of contents.

Initiated before FY83

Objective 2. Obtain definitive data that may reflect precursory changes near the source of moderately large earthquakes. Short term variations in the strain field prior to moderate or large earthquakes require careful documentation in association with other phenomena.

Measure strain and tilt near-continuously to search for short term variations preceding large earthquakes. Complete development of system for stable, continuous monitoring of strain.

Monitor radon emanation water properties and level in wells, especially in close association with other monitoring systems. Monitor apparent resistivity, magnetic field to determine whether precursory variations in these field occur. Monitor seismic velocity and attenuation within the (San Andreas) fault zone.----------

Objective 3. Provide a physical basis for short-term earthquake predictions through understanding the mechanics of faulting.

Develop theoretical and experimental models to guide and be tested against observations of strain, seismicity, variations in properties of the seismic source, etc., prior to large earthquakes.----------

Objective 4. Determine the geometry, boundary conditions, and constitutive relations of seismicity active regions to identify the physical conditions accompanying earthquakes.

Measure physical properties including stress, temperature, elastic and anelastic properties, pore pressure, and material properties of the seismogenic zone and the surrounding region.

III. Global Seismicity (G)

Objective 1. Operate, maintain, and improve standard networks of seismographic stations.

Objective 2. Provide seismological data and information services to the public and to the research community.

Southern California Seismic Arrays

Cooperative Agreement No. 14-08-0001-A0257

Clarence R. Allen and Robert W. Clayton
Seismological Laboratory, California Institute of Technology
Pasadena, California 91125 (818-356-6912)

Investigations

This semi-annual Technical Report Summary covers the six-month period from 1 October 1985 to 31 March 1986. The Cooperative Agreement's purpose is the partial support of the joint USGS-Caltech Southern California Seismographic Network, which is also supported by other groups. as well as by direct USGS funding to its own employees at Caltech. According to the Agreement, the primary visible product will be a joint Caltech-USGS catalog of earthquakes in the southern California region; quarterly epicenter maps and preliminary catalogs have been submitted as due during the Agreement period. About 250 preliminary catalogs are routinely distributed to interested parties.

Results

Figure 1 shows the epicenters of all cataloged shocks that were located during the six-month recording period. Some of the seismic highlights of this period were:

Number of earthquakes fully or partially processed: 4458
Number of earthquakes of M = 3.0 and greater: 117
Number of earthquakes of M = 4.0 and greater: 7
Largest event within network area: M = 4.9 (2 October, near San Bernardino)
Number of earthquakes reported felt: 21
Number of earthquakes for which systematic telephone notification to emergency-response agencies was made: 2

This was a relatively dull period from the point of view of southern California seismicity. As is obvious from Figure 1, and has been the case for several years, minor activity remained conspicuous along the San Jacinto fault zone, in the eastern Transverse Ranges and San Gorgonio Pass, in the Lake Isabella area (along the Kern Canyon fault trend), and in the Coso area. Seismicity has remained low to nil along most of the San Andreas fault, including the Bombay Beach segment opposite the Salton Sea, although a M = 3.9 event did occur here 5 days after the close of the reporting period.

Access to network data by "outside" users was markedly improved during the reporting period by the installation of 2 new graphics terminals specifically dedicated to this purpose, although some of the relevant software is still under development. User access has also been facilitated by the fact that the Caltech-USGS staff is now under full production with CUSP on the VAX computer, and the backlog of seismological data is rapidly being whittled away.

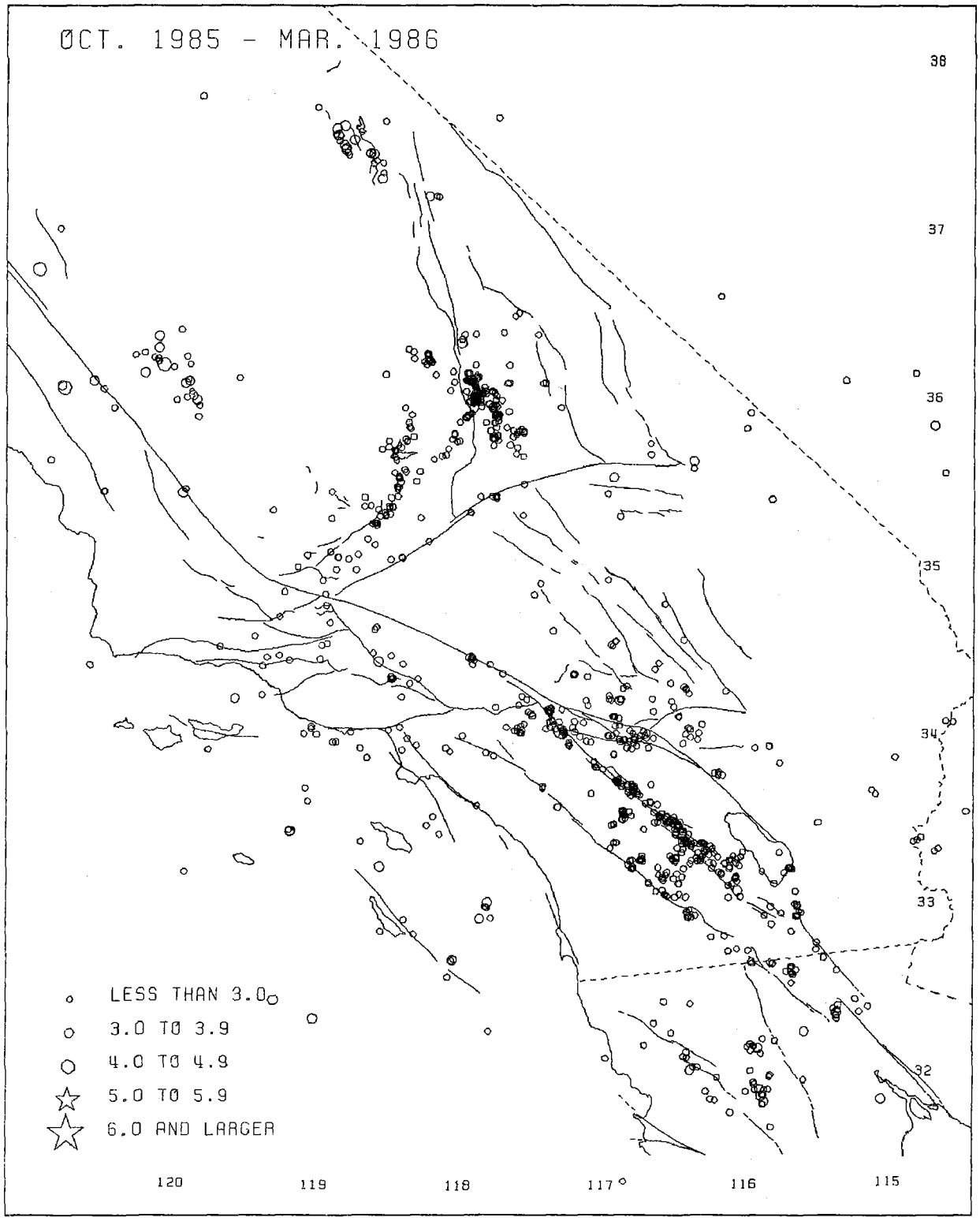

Figure 1.--Epicenters of larger earthquakes in the southern California region, 1 October 1985 to 31 March 1986.

Regional Seismic Monitoring Along The Wasatch Front Urban Corridor And Adjacent Intermountain Seismic Belt

14-08-0001-A0265

W.J. Arabasz, R.B. Smith, J.C. Pechmann, and E.D. Brown
Department of Geology and Geophysics
University of Utah
Salt Lake City, Utah 84112
(801)581-6274

Investigations

This contract supports "network operations" (including a computerized central recording laboratory) associated with the University of Utah 80-station regional seismic telemetry network. USGS support focuses on the seimically hazardous Wasatch Front urban corridor of north-central Utah but also encompasses neighboring areas of the Intermountain seismic belt (ISB). The University of Utah maintains de facto responsibility for earthquake surveillance, including emergency response and direct public interface, for an 800-km-long segment of the ISB between Yellowstone Park and southernmost Utah. The State of Utah, thee U.S. Bureau of Reclamation, the National Park Service and the U.S. Geological Survey (Geothermal Research Program) also contributed support to operation of the University of Utah network during the report period.

Primary products of this USGS contract are quarterly earthquake catalogs and a semi-annual data submission, in magnetic-tape form, to the USGS Data Archive.

Results

1. Network Seismicity

Figure 1 shows the epicenters of 203 earthquakes ($M \leq 4.4$) located in part of the University of Utah study area designated the "Utah region" (lat. 36.75°-42.5°N, long. 108.75°-114.25°W) during the six-month period October 1, 1985 to March 31, 1986. The seismicity includes seven shocks of magnitude 3.0 or greater, several areas of spatial clustering, and three felt events.

The first felt event, M_L 2.4, was felt in Ogden and Clearfield, Utah on October 21 and was located about 20 miles northeast of Ogden. A second event, M_L 3.3, was felt in Logan, Utah on January 13 and was located 10 miles east of Logan. The third felt event occurred on March 24, and was located in central Utah about six miles east of Scipio.

This event, M_L 4.4, was the largest event during the report period and was felt, along with several aftershocks, in the towns of Scipio, Fayette, Gunnison, and Centerfield. A portable array of eight MEQ-800 smoked paper seismographs was deployed to provide high quality aftershock locations and depth constraints. The data obtained from the deployment are currently being analyzed.

The epicenters shown in Figure 1 reflect typical earthquake activity scattered throughout Utah's main seismic region. Several spatial clusters are seen. The clusters of events to the north of the Great Salt lake and the mining-related earthquakes in the vicinity of active underground coal mining near Price in east-central Utah are typical of the Utah region. The cluster in central Utah is associated with the Scipio earthquake.

2. Network Polarity Checks

The maintenance of correct signal polarities is a persistent problem in the operation of any telemetered seismic network. The many varieties of equipment in use, coupled with the fact that a normal station has eight or nine points in the signal path where the signal can be reversed, make it probable that some stations will have incorrect polarities

During the past year, we have developed an electro-mechanical device to test a station's signal polarity. The seismometer is placed on a platform that is separated from the base of the testing device by a molded rubber pad. The tester is actuated by a simple solenoid and bellcrank mechanism. When current is applied to the solenoid this mechanism provides an upward force to the seismometer platform. Since the platform is suspended on the rubber pad there is a small upward displacement of the seismometer. The response of the complete station-telemetry-recorder system to this displacement can then be observed and the polarity of the signal checked. Using this device, we are now methodically checking the polarities of all of our network stations and correcting those that are reversed.

3. Network Calibration Project

Work is continuing on hardware to do a telemetry station calibration by applying a psuedo-random binary sequence current function to the seismometer calibration coil. The field calibration box has been built and most of the important circuits tested. These circuits include the random sequence generator, a DAC circuit to provide different current levels, a precision voltage to current converter-driver, and a circuit to provide the signal that triggers the recording computer. We are now modifying the system to allow simultaneous telemetry of the input calibration signal which will provide accurate control of the system phase response. We anticipate that hardware development for this project will be completed very soon, allowing systematic collection of station calibration data to begin.

Reports and Publications

Brown, E.D., Utah earthquake activity July through September, 1985, Wasatch Front Forum, v. 2, no. 2, 11, 1986.

Brown, E.D., Utah earthquake activity July through September, 1985, Survey Notes, v. 19, no. 3, 12, 1986.

Brown, E.D., Utah earthquake activity October through December, 1985, Survey Notes, v. 19, no. 4, 6, 1985.

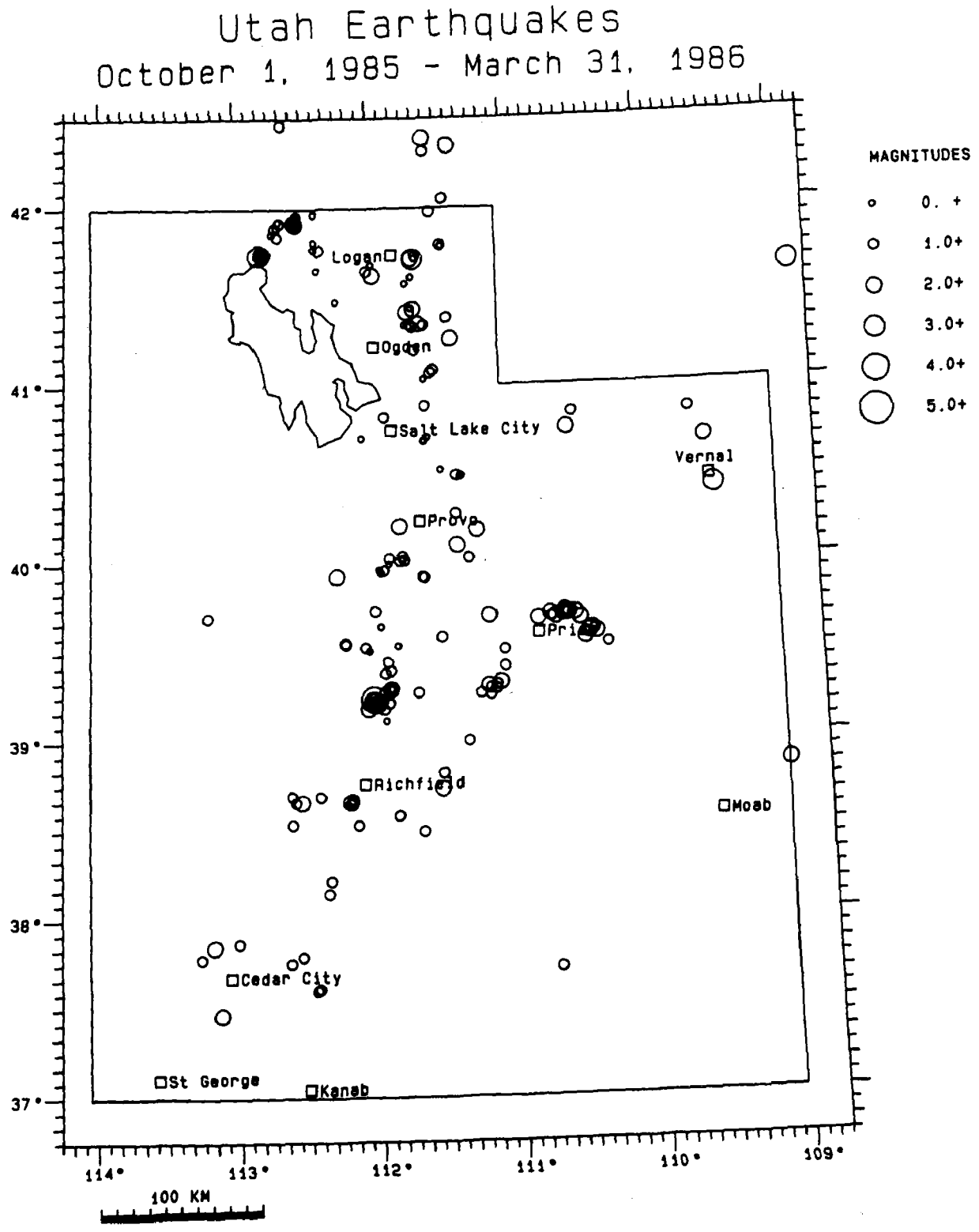
Utah Earthquakes
October 1, 1985 - March 31, 1986
MAGNITUDES
0. +
1.0+
2.0+
3.0+
4.0+
5.0+
Logan
Ogden
Salt Lake City
Vernal
Provo
Richfield
Moab
Cedar City
St George
Kanab
42°
41°
40°
39°
38°
37°
114°
113°
112°
111°
110°
109°
100 KM

Seismological Data Processing

9930-03354

Barbara Bekins and Thomas Jackson

Branch of Seismology
U.S. Geological Survey
345 Middlefield Rd. MS 977
Menlo Park, California, 94025
(415) 323-8111 ext. 2965

Investigations

Computer data processing is now an integral part of seismological research. The purpose of this project is to provide a simple, powerful, computer data processing system to meet the needs of scientists in the earthquake prediction program and monitor earthquakes in northern California. This goal includes maintaining the ability to transfer data and programs over a network and the ability to share data and programs with USGS external contractors.

Results

An Integrated Solutions Optimum System has been purchased to replace the PDP 11/70 UNIX system. The new system provides program virtual addressing, the operating system is fully vendor supported, and it runs about three times faster than the 11/70. Maintenance costs are about one-third the cost of the 11/70 maintenance. This system is a so-called super micro system based on the Motorola 68020 microprocessor. The system was delivered in October of 1985. It was initially delivered with the 68010 processor but has since been upgraded to the 68020 processor. The process of transferring operations from the PDP 11/70 to the new system is proceeding steadily. The new system is now monitoring the RTP seismic data and several users are working on it regularly. The system is connected via the Ethernet to the Seismology branch VAX 750 system. The two systems communicate using the TCP/IP protocol. File transfers and remote logins are supported between them. The 11/70 is expected to be phased out sometime in the next six months.

The Seismology Branch Vax 11/750 running the VMS version 4.2 has become very busy. Various monitoring programs and equipment loans were used to evaluate what the system bottlenecks are. Based on these investigations, new terminal controllers and an additional four megabytes of memory are being purchased for the system. Data from the real time Ppicker and the CUSP processing system are now combined in the CUSP database. Data from the Calnet catalog will be added in the near future.

Work is proceeding on replacing the current system for digitizing of selected earthquakes recorded on FM tapes. This digitizing is presently performed on Data General Eclipse systems. A general purpose digital IO board has been purchased and installed on the Integrated Solutions system for positioning the tape. Work is proceeding on porting the tape control programs which were used on the Eclipses. A Tustin digitizer has been connected to digitize the data. Software which reads in the digitized data from the Tustin to the VAX 750 for storage and analysis has been tested. The replacement digitizing system is expected to be fully operational in the next month.

This project also handles operational support for Seismology users of the office VAX 785. This support consisted of weekly and monthly disk backups to tape, authorizing new users, redistributing Seismology branch disk quotas, assisting users, and occasional miscellaneous activities related to computer operations and system management.

Seismic Source Mechanism Studies In the Anza-Coyote Seismic Gap

14-08-0001-21893

Jonathan Berger and James N. Brune
Institute of Geophysics and Planetary Physics
Scripps Institution of Oceanography
University of California, San Diego
La Jolla, CA 92093

1. Investigations

This report covers the progress of the research investigating the Anza- Coyote Canyon seismic gap for the period of the second half of 1985. The objectives of this research are: 1) To study the mechanisms and seismic characteristics of small and moderate earthquakes, and 2) To determine if there are premonitory changes in seismic observables preceeding small and moderate earthquakes. This work is carried out in cooperation with Tom Hanks, Joe Fletcher and Linda Haar, of the U.S. Geological Survey, Menlo Park.

2. Network Status

During the period of this report, ten stations of the Anza Seismic Network were telemetering three component data. The network was set at a low gain for most of the time of this report to try to record earthquakes up to magnitude 4 occurring inside the array. In December 1985 we ran a high gain experiment for a week sampling every 4 hours to get an estimate of the diurnal variations of ground noise in this frequency band.

There were no significant modifications to the data acquisition equipment.

3. Seismicity

In the six months of summer and fall, the Anza network recorded over 50 events which were large enough to locate and determine source parameters. These events had moments ranging from 1 x 10^{18} to 1.4 x 10^{21} dyne-cm, and stress drops ranging from about 1 to 100 bars (Brune model). The seismicity pattern seems unchanged from what has been observed before (Figure 1). The seismicity does not appear to be associated with the main trace of the San Jacinto fault on the north-west end of the array. These events in this area tend to be between the Hot Springs fault and the San Jacinto fault at depths of 12 to 19 km. The events on the south-east end of the array near the trifurcation of the San Jacinto fault also do not have any obvious associations with the identified fault traces. These earthquakes are occurring at depths between 8 and 12 km. The shallowest events are still occurring in the Cahuilla area.

4. Data Analysis

4.1. Stress Drops

The source parameters which have been determined from events recorded on the Anza array show wide variations, even when they have similar locations. For example, events with stress drops of the order of a hundred bars also have events with very low

stress drops (1/10 bar to 1 bar) nearby. The mechanism by which such low stress-drop events can occur in the same environment as high stress-drop events has not been established.

A preliminary study was conducted to investigate this problem. Initially two sets of data were selected for analysis, one set consisting of five events with stress drops of about 100 bars and a second set with 27 events with stress drops between .1 and 2 bars. The high frequency asymptote on a log-log plot were fit by eye with a straight line for all spectra which appeared to be reasonably approximated in this manner. Each horizontal component was considered an independent measurement (the vertical component was considered separately). The results for the horizontal components where α is equal to the power of high frequency fall-off, i.e. slope on log-log plot.

	$\bar{\alpha}$ average slope	$\Delta\alpha$ standard deviation	N no. of readings	ϵ standard error of mean
High stress drop events	3.67	.57	43	.09
Low stress drop events	2.52	.63	304	.04
Difference	1.15			

The difference in average slope is consistent with the low stress drop events having a lower fall-off than high stress drop events by the the amount theoretically expected between partial stress drop and total stress drop events. The fall-off for both, however, is about a power of about 1.5 greater than predicted, and remains to be explained. This selection of a bimodal sample of stress drops is purely for convenience to emphasize the differences. We checked intermediate stress drop events also, but we do not report the results here. There is a range of stress drops bridging the gap.

An example of the spectra from a high stress drop and a low stress drop event are shown in Figure 2 from station KNW. This figure illustrates features often seen in these comparisons: the high stress drop event is a simple pulse with a well defined corner frequency and relatively steep high frequency fall-off, whereas the low stress drop event is more complex.

A careful analysis of the data revealed that certain stations seemed to reflect site effect distortions in their signals. Stations WMC, LVA, CRY and SND consistently showed lower average corner frequencies and/or higher frequency fall-offs than others, and their signals appeared less pulse-like and more distorted. In order to test the stability of the above result we decided to look at the results with data from these stations removed. Considering only stations RDM, KNW, PFO, BZN and FRD gave the following results

	$\bar{\alpha}$ average slope	$\Delta\alpha$ standard deviation	N no. of readings	ϵ standard error of mean
High stress drop events	3.59	44	29	.08
Low stress drop events	2.32	61	151	.05
Difference	1.27			

Thus, eliminating the questionable stations has slightly changed the average high frequency fall-offs, but the difference between the high stress drop and low stress drop events remains.

The basic observation of importance here is that for a suite of about 30 events the average high-frequency spectral fall-off, α, is approximately 1 unit less than for a suite of five events interpreted as having high stress drops ($\sim$100 bars). Although we need more high stress drop events before we can be sure of the statistical validity of this result, we feel that the data are reliable enough to warrant further study.

4.2. Coherence studies

We ran a small aperture seismic array at PFO during the period of time starting in mid-January and ending in mid-September. We recorded 12 events on multiple stations simultaneously. These events are of high enough quality to allow effective calculation of the body wave coherences. A subset of six of these events were recorded on enough stations to allow frequency wavenumber analysis to be performed.

The computer programs which are being used to analyze the data were also being developed during the period of this report. Programs have been written to calculate two dimensional wavenumber power spectra at discrete frequencies using both simple Fourier transforms and also the "high resolution" technique . We also have adapted a program which stacks two dimensional slowness spectra by frequency. This stacking technique improves the resolution of the slowness and azimuth of the body wave arrivals. Finally a program to calculate coherences has been developed using multitaper techniques. The prelimary results of the coherence analysis show that high coherence can be found up to 50 Hz in P wave arrivals. The shear waves become incoherent by 30 Hz in all of our events. But there is a large scatter in the maximum frequency for the high coherence from event to event for the body waves.

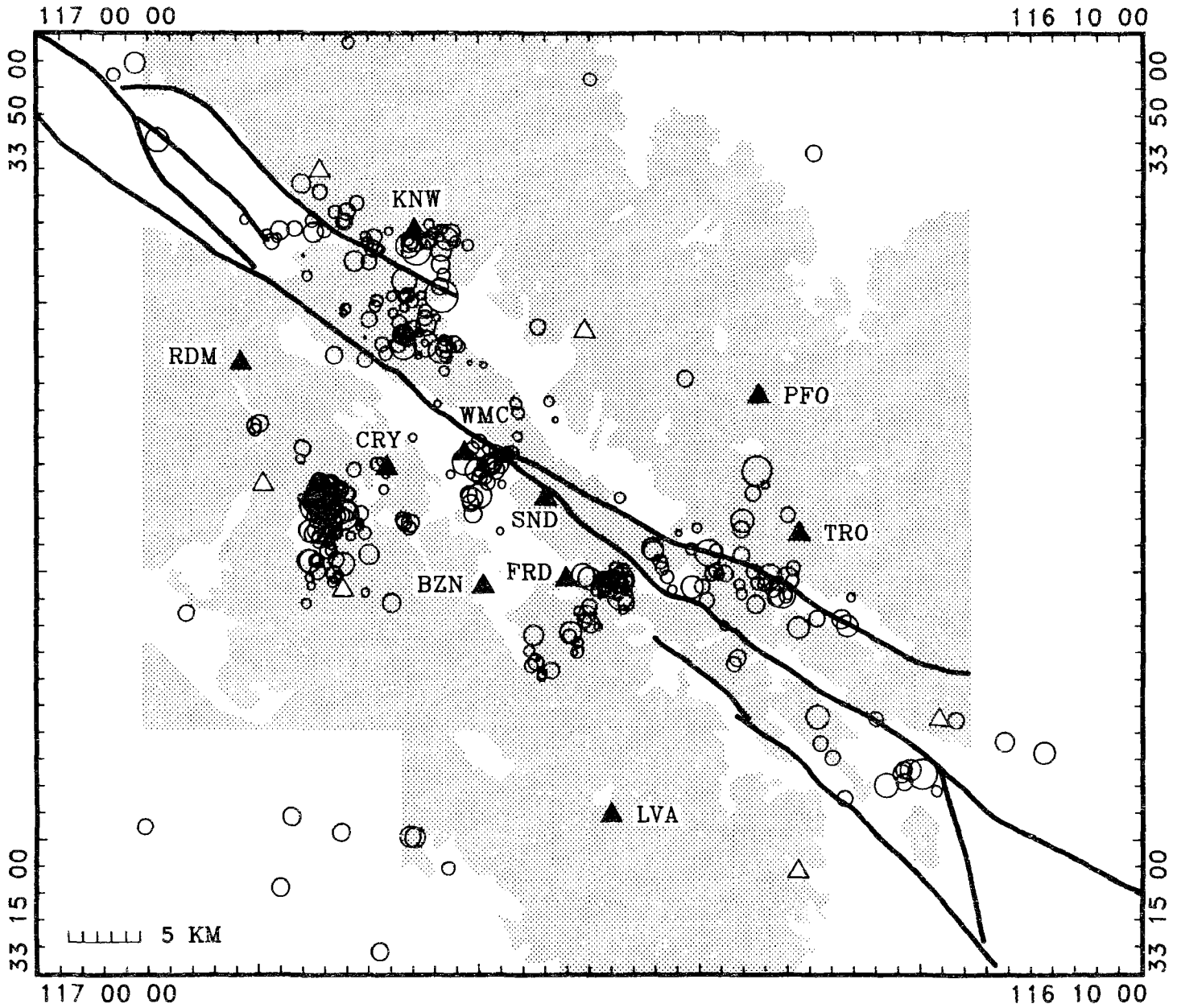
117 00 00
116 10 00
33 50 00
33 15 00
KNW
RDM
PFO
WMC
CRY
SND
TRO
BZN
FRD
LVA
5 KM

Figure 1.

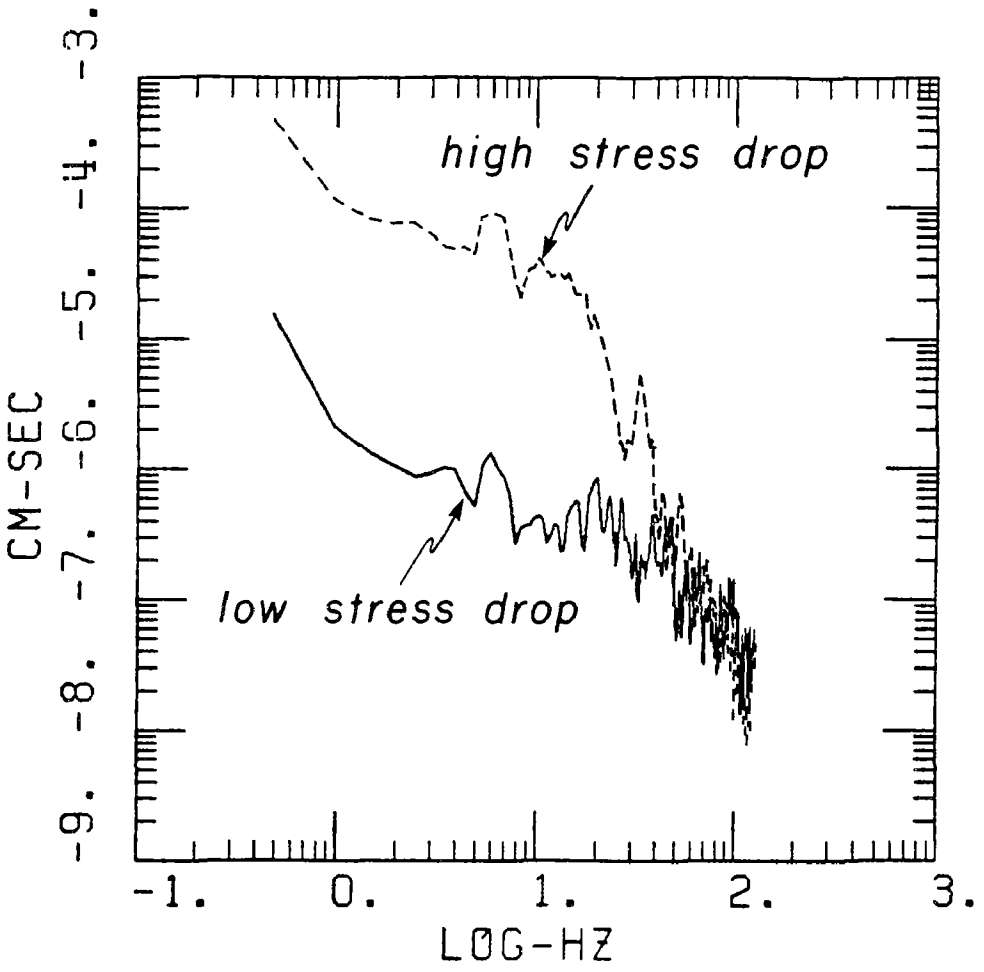

Figure 2.

Central Aleutian Islands Seismic Network

Contract No. 14-08-0001-21896
and Agreement No. 14-08-0001-A0259

Selena Billington and Carl Kisslinger
Cooperative Institute for Research in Environmental Sciences
Campus Box 449, University of Colorado
Boulder, Colorado 80309

(303) 492-6042

Brief Description of Instrumentation and Data Reduction Methods

The Adak seismic network consists of 13 high-gain, high-frequency, two-component seismic systems and one six-component system (ADK) located at the Adak Naval Base. Station ADK has been in operation since the mid-1960s; nine of the additional stations were installed in 1974, three in 1975, and one each in 1976 and 1977.

Data from the stations are FM-telemetered to recording sites near the Naval Base, and are then transferred by cable to the Observatory on the Base. Data were originally recorded by Develocorder on 16 mm film; since 1980 the film recordings are back-up and the primary form of data recording has been on analog magnetic tape. The tapes are mailed to CIRES once a week.

At CIRES the analog tapes are played back at four-times the speed at which they were recorded into a computer which digitizes the data, automatically detects events, and writes an initial digital event tape. This tape is edited to eliminate spurious triggers, and a demultiplexed tape containing only seismic events is created. All subsequent processing is done on this tape. Times of arrival and wave amplitudes are read from an interactive graphics display terminal. The earthquakes are located using a program developed for this project by E. R. Engdahl, which uses corrections to the arrival times which are a function of the station and the source region of the earthquake.

Data Annotations

Earthquake locations are complete through December 1985. Our normal lag time for hypocenter locations is six-to-eight weeks, dependent on the postal service from Adak. The last major field trip to service the network was in July and August, 1984. Because of logistic problems, the westernmost station could not be reached at that time, and we were also unable to make needed return trips to two other far-west stations. Of the 28 short-period vertical and horizontal components, 21 were operating for the period of June through December, 1985.

Current Observations

259 earthquakes were located with data from the network during the six-month time period from July through December, 1985. Epicenters of these events are shown in Figure 1 and a vertical cross-section is given in Figure 2. Only five of the events located within the past six months were large enough to be located teleseismically (USGS PDEs), in keeping with a current low rate of teleseismically observable earthquakes in the region, as we have noted in past reports. (Only four of the five teleseismically recorded events are shown on Figure 1; the fifth is immediately to the east of the mapped area.) The largest of the teleseismically recorded events was one with m_b5.4 which occurred on December 28, near 177.1° W longitude (Figure 1), in the vicinity of Adak Canyon. This is a region in which we are particularly interested, as it may be part of the site of the next large earthquake in the Adak region.

More detailed information about the network status and a catalog of the hypocenters determined for the time period reported here are included in our semi-annual data report to the U.S.G.S. Recent research using these data is reported in the Technical Summary for U.S.G.S. Grants No. 14-08-0001-G881 and 14-08-0001-G1099 in this volume.

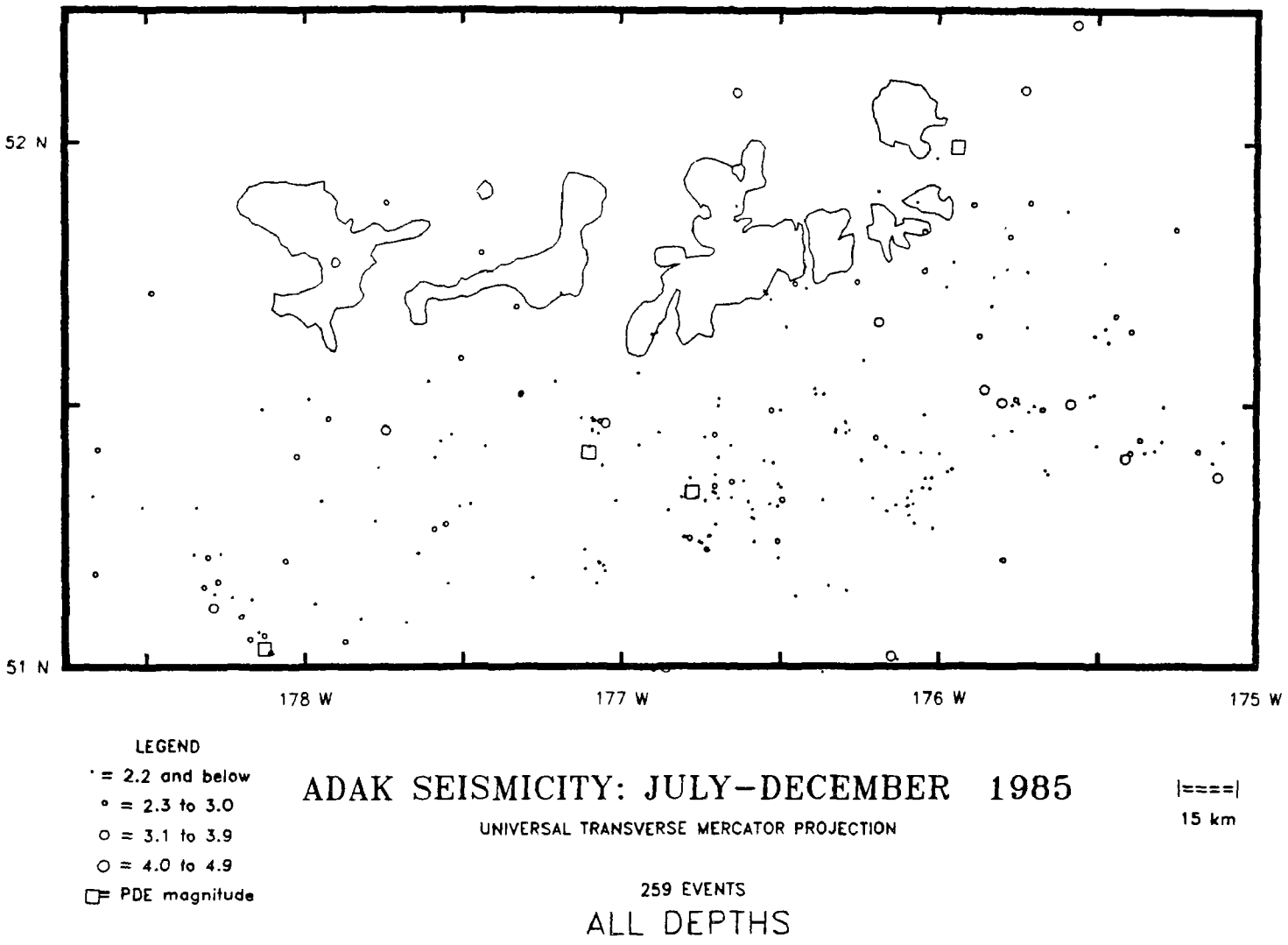

Figure 1: Map of seismicity which occurred from June 1 through December 30, 1985. All epicenters were determined from Adak network data. Events marked with squares are those for which a teleseismic body-wave magnitude has been determined by the USGS; all other events are shown by symbols which indicate the duration magnitude determined from Adak network data. The islands mapped (from Tanaga on the west to Great Sitkin on the east) indicate the geographic extent of the Adak seismic network.

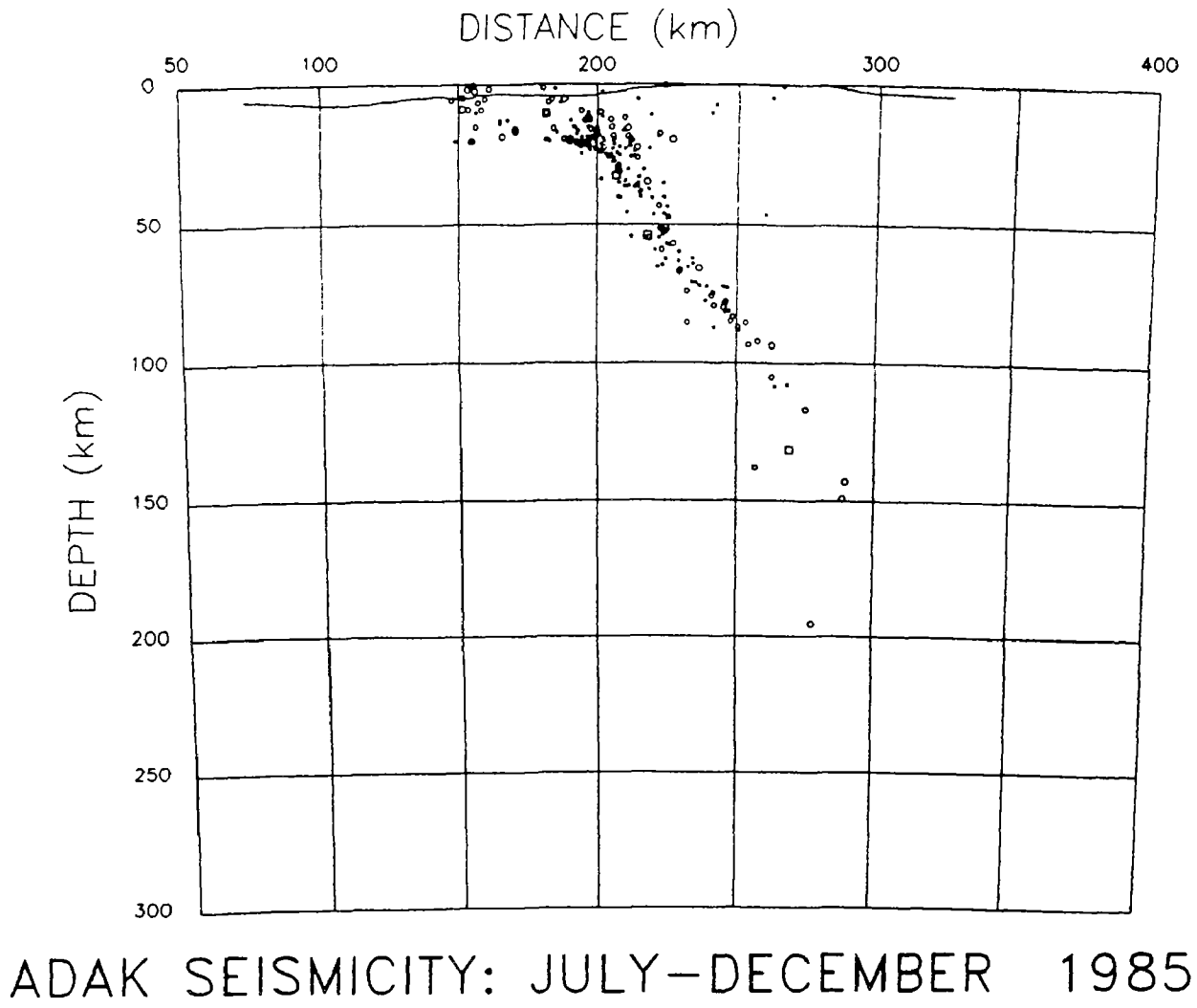

Figure 2: Vertical cross section of seismicity which occurred from June 1 through December 30, 1985. Events are projected according to their depth (corresponding roughly to vertical on the plot) and distance from the pole of the Aleutian volcanic line. The zero-point for the distance scale marked on the roughly-horizontal axis of the plot is arbitrary. Events marked with squares are those for which a teleseismic body-wave magnitude has been determined by the USGS; all other events are shown by symbols which indicate the duration magnitude determined from Adak network data. The irregular curve near the top of the section is bathymetry. Earthquakes deeper than about 100 km depth are mislocated too far south (left) as an effect of the slab on their ray paths to the local stations.

Regional Seismic Monitoring in Western Washington

14-08-0001-A0266

R.S. Crosson and S.D. Malone
Geophysics Program
University of Washington
Seattle, WA 98195
(202) 543-8020

Investigations

Operation of the western Washington regional seismograph network and routine preliminary analysis of earthquakes in western Washington are carried out under this contract. Quarterly catalogs of seismic activity in Washington and Northern Oregon are available for 1984 and 1985, and are funded jointly by this contract and others. The University of Washington operates a total of 79 stations west of 120.5 °W. Twenty seven are funded under this contract. A new station will be installed in the Skagit Valley. A site has been selected and equipment will be installed as soon as weather permits.

This contract provides data for USGS contract 14-08-0001-G1080 and other research programs. Efforts under this contract are closely related to and overlap objectives under contract G1080, also summarized in this volume. Publications are listed in the G1080 summary.

This summary covers a six month period from October 1, 1985 through March 31, 1986. During this period the U.W. seismic network located 415 events west of 120.5 °W. The largest earthquake, M_C 3.9, occurred on February 10, 1986 west of Rockport, Washington. This event was part of a sequence of 11 events larger than magnitude 1.0, including another felt event of magnitude 3.6 on the same day. Four other felt events were located in a similar cluster 20 km to the southeast.

The U.W. runs a statewide sub-network of calibrated stations. Each calibrated station consists of a Geotech S-13 seismometer and a Morrissey-Interface Technology amplifier/VCO package. The calibration curve for this system was given in the previous semi-annual summary. This contract funds two of these S-13 stations. In addition, most of the other stations funded under this contract may also be considered calibrated since the instruments have known response characteristics.

Central California Network Operations

9930-01891

Wes Hall
Branch of Seismology
U.S. Geological Survey
345 Middlefield Road, Mail Stop 977
Menlo Park, California 94025
(415) 323-8111, Ext. 2509

Investigations

Maintenance and recording of 331 seismograph stations (404 components) located in Northern and Central California. Also recording 72 components from other agencies. The area covered is from the Oregon border south to Santa Maria.

Results

1. Modified and installed one hundred-nine (109) VCO/AMPS for greater frequency stability; temperature stability; and dynamic range.
   61 ea J302M to J302ML
   11 ea J402 to J402ML
   29 ea J402 to J402H
   8 ea J502

2. Installed two 8' parabolic antennas on a commercial tower located at Santiago Peak, Cleveland National Forest, Corona, CA. The antennas are part of the Strawberry Peak - Santiago Peak - Pasadena segment of the Southern California Microwave System.

3. Installed all electronics and activated the Southern California Microwave System. Test data is now being telemetered from Edwards AFB to Pasadena via Strawberry Peak and Santiago Peak.

4. All Central California Microwave System facilities were modified to upgrade system from one-way to full duplex capability.

5. Installed equipment and activated the KAR-HOG segment of the Central California Microwave System.

6. Installed a VHF repeater at Mission Peak and Hog Canyon microwave facilities.

7. Completed Procurement Contract for Northern Calif. Instrument Repair Services (14-08-0001-22807).

8. Completed technical evaluation of RFP 1575, Southern California "Seismic Maintenance and Repair".

ALASKA SEISMIC STUDIES

9930-01162

John C. Lahr, Christopher D. Stephens, Robert A. Page
Branch of Seismology
U. S. Geological Survey
345 Middlefield Road, MS 977
Menlo Park, California 94025
(415) 323-8111, Ext. 2510

Investigations

1) Continued collection and analysis of data from the high-gain, short-period seismic network extending across southern Alaska from the volcanic arc west of Cook Inlet to Yakutat Bay and inland across the Chugach mountains.

2) Continued monitoring in the region of the proposed Bradley Lake hydroelectric project on the southern Kenai Peninsula, a cooperative effort with the Alaska Power Authority.

3) Cooperated with the Branch of Engineering Seismology and Geology in operating 19 strong-motion accelerographs in southern Alaska, including 13 between Icy Bay and Cordova in the area of the Yakataga seismic gap.

Results

1) During the past six months preliminary hypocenters were determined for 1726 earthquakes that occurred between August 1985 and January 1986 (Figure 1).
Twenty of these shocks had magnitudes of 4.0 m_b and larger, and the largest had a magnitude of 5.5 m_b. Two of the larger events were located at shallow depth (less than 30 km) within the aftershock zone of the 1979 St. Elias earthquake north of Icy Bay, and two were located north of Glacier Bay. The Glacier Bay shock of September 15 had a magnitude of 5.4 and is the largest event to occur in this area since a magnitude 6.0 shock in 1952. The remainder of these larger events were located in the Aleutian Wadati-Benioff zone of the subducted Pacific plate which extends west and north of Cook Inlet. A magnitude 4.6 m_b shock occurred on September 25 at a depth of 189 km beneath Lake Iliamna. A preliminary focal mechanism for this event determined from regionally recorded P-wave polarities has a steeply dipping tension axis and a nearly horizontal compression axis closely aligned with the local north-northeast strike of the inclined seismic zone. This result is consistent with those of other studies of focal mechanisms from the southern Cook Inlet Wadati-Benioff zone (for example, Pulpan and Frolich, 1985) where it has been suggested that north-south compression is an important component of the stress field within the subducted plate. On December 30, a magnitude 5.5 m_b shock occurred at 50 km depth within the Benioff zone about 30 km northwest of Anchorage and was felt throughout much of the northern Cook Inlet region. Most of the moderate-sized earthquakes that have been located along this segment of the Wadati-Benioff zone by the regional network have had few if any aftershocks, but this recent event was unusual in that it was followed within 16 hours by a sequence that included

12 events with duration magnitudes ranging from 1.1 to 3.1. The largest of these aftershocks was also felt.

Features of the seismicity pattern illustrated in Figure 1 which differ notably from previous time periods include: a tightly clustered swarm of about 40 shocks with magnitudes smaller than 2.5 that occurred in July and August 1985 near the intersection of the Caribou and Castle Mountain faults about 100 km northeast of Anchorage; an apparent decrease in the rate of crustal and shallow Wadati-Benioff zone activity beneath the southern Kenai Peninsula, which is the result of removing six of the nine seismographs that had been operating in this area; and an apparent increase in the rate of shallow seismicity beneath western Prince William Sound, which is the result of both the increased detection capabilty of the network following the installation of three new seismographs on and near Knight Island in the summer of 1985, and a lower magnitude threshold that is applied to this area to select events for processing. Most of the preliminary epicenters of earthquakes occurring beneath western Prince William Sound are located in two clusters, one beneath Knight Island and one about 30 km to the south beneath Latouche Island. The better constrained events are concentrated between 15 and 27 km depth.

In and around the Yakataga seismic gap the pattern of microearthquake activity has remained relatively stable over the past several years, and no obvious changes have been recognized in the recent six months of data that would indicate that a major earthquake is more likely to occur in the next year or two rather than within the next two or three decades.

2) Pronounced secondary phases have been observed on seismograms of several crustal and Wadati-Benioff zone earthquakes that occurred beneath the southern Kenai Peninsula. For the crustal earthquakes, the arrival times of some of these secondary phases are consistent with a simple model in which they are interpreted as reflections from an interface near the top of the underlying Wadati-Benioff zone. Other secondary phases do not fit this simple model and may indicate the presence of shallower velocity interfaces within the crust. These data may provide important constraints on the geometry of the subducted plate beneath this region.

3) During the summer of 1985, five ELOG (Event LOGger) digital seismic data recorders were deployed at four sites in the Talkeetna mountains north of Palmer, Alaska. The triggering parameters for these deployments were derived using telemetered data from the regional seismic network. Preliminary analysis of the field data indicated a very high false trigger rate. Subsequent field testing in California suggested that the high rate of false triggers was due to high frequency noise which is present in the field but which is filtered by the telemetry link. In addition, the triggering threshold was probably set too high. After adjustments were made to the software, including the addition of automatic threshold setting, an ELOG was deployed for three days to detect and record aftershocks of the Mt. Lewis, California earthquake (5.3 m_b) of March 31, 1986. Of 114 aftershocks that occurred during the deployment, 62 events were recorded by the ELOG while 105 were detected by the CALNET real-time processor. The ELOG also recorded 43 non-seismic events, probably cars on the road nearby. Waveforms of the recorded events were stored in solid-state memory and will be used to improve

the seismic-detection and noise-rejection algorithms.

4) Major changes were made in the seismic network during the summer of 1985 to accommodate reduced funding. Fifteen stations had to be terminated and several changes were made in the telemetry circuits, sometimes with poor results. For example, we have experienced problems with station outages in the eastern part of the network where a telephone line was replaced with multiple radio relays; four of the eight stations between Icy Bay and Cordova, the region of the Yakataga seismic gap, have not operated during this past winter. Another change, however, has been satisfactory; one data circuit was switched to the State of Alaska microwave system under a cooperative agreement with the University of Alaska. Improvements were made at some sites, including the addition of solar power at the station on Montague Island and the installation of a circuit to provide absolute timing for the strong-motion recorder at Cordova.

References

Pulpan, Hans, and Frohlich, Cliff, 1985, Geometry of the subducted plate near Kodiak Island and lower Cook Inlet, Alaska, determined from relocated earthquake hypocenters, Bulletin of the Seismological Society of America, v. 75, p. 791-810.

Reports

Pelton, J. R., Astrue, M. C., Lee, W. H. K., and Page, R. A., A Computer-Based System for Interactive Processing of Earthquake Seismograms Recorded on Microfilm, 1209, Bulletin of Seismological Society of America, v. 75, p. 1209-1210.

Lahr, J. C., Stephens, C. D., Page, R. A., and Fogleman, K. A., 1985, Summary of seismic monitoring by the U.S.G.S. southern Alaska netowrk - October 1971 through June 1985, Symposium and workshop, regional seismographic networks, past-present-future, Earthquake Notes, v. 56. p. 93.

Stephens, C. D., Fogleman, K. A., Page, R. A., Lahr, J. C., 1985, Seismicity in southern Alaska, October 1982-September 1983, in, Bartsch-Winkler, Susan and Reed, Kitty, eds., The United States Geological Survey in Alaska: Accomplishments during 1983, U.S. Geological Survey Circular 945, p. 83-86.

Lahr, J. C., Page, R. A., Fogleman, K. A., and Stephens, C. D., 1985, New evidence for activity on the Talkeetna segment, Castle Mountain - Caribou fault system: The 1984 Sutton earthquake, in, Bartsch-Winkler, S., ed., The United States Geological Survey in Alaska: Accomplishments during 1984, U.S. Geological Survey Circular 967, p. 62-63.

Stephens, C. D., Fogleman, K. A., Lahr, J. C., Page, R. A., 1985, Seismicity in Southern Alaska, October 1983-September 1984, in, Bartsch-Winkler, Susan, ed., The United States Geological Survey in Alaska: Accomplishments during 1984, U.S. Geological Survey Circular 967, p. 79-82.

Lahr, J. C., Stephens, C. D., and Page, R. A., 1986, Regional seismic monitoring in Southern Alaska: application to earthquake hazards assessment, in, Hays, W., ed., Workshop on evaluation of regional and urban earthquake hazards and risk in Alaska, U.S. Geological Survey Open-File Report 86- (in preparation).

Stephens, C. D., Lahr, J. C., and Fogleman, K. A., 1985, Southern Alaska Seismicity, 1982 in, Stover, C. W., ed., United States Earthquakes, 1982, U.S. Geological Survey Special Publication (in press).

Lahr, J. C., and Page, R. A., 1986, Evidence for activity of the Castle Mountain fault system: A review for the 1985 NEPEC Workshop, in, Shearer, C. F., ed., Minutes of the National Earthquake prediction Evaluation Council, September 8 & 9, 1985, U.S. Geological Survey Open-File Report 86-92, p. 103-118.

Page, R. A., Lahr, J. C., and Stephens, C. D., 1986, Review of seismicity and microseismicity of the Yakataga seismic gap, Alaska, in, Shearer, C. F., ed., Minutes of the National Earthquake Prediction Evaluation Council, September 8 & 9, 1985, U.S. Geological Survey Open-File Report 86-92, p. 144-158.

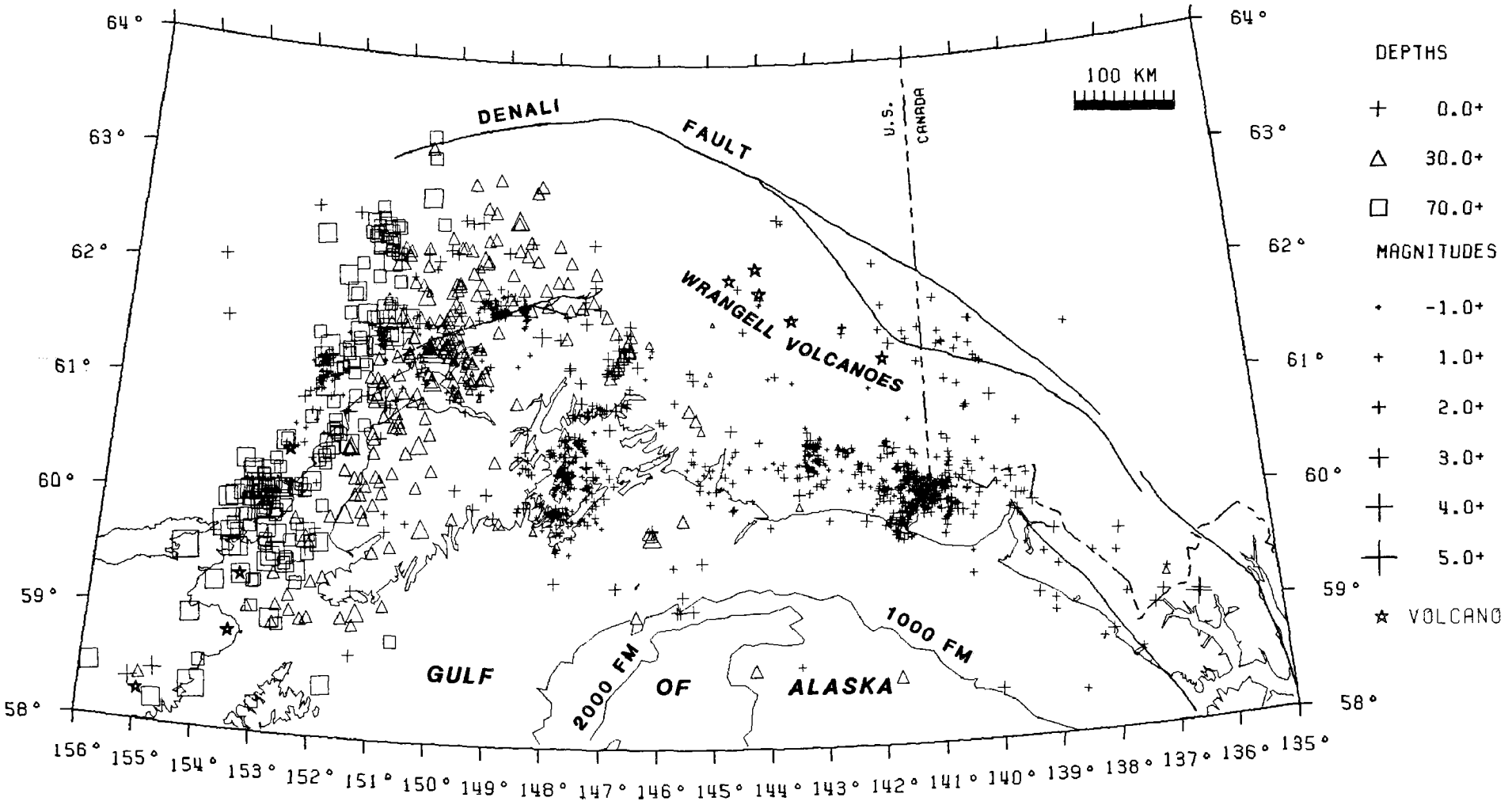

Figure 1. Earthquakes located by the USGS southern Alaska seismograph network during August, 1985 - January, 1986. Epicenters of 1726 events are plotted. Magnitudes are determined from coda-duration or maximum amplitude, and events of magnitude 3 and larger can be as much as one unit smaller than the teleseismic m_b magnitude. The lowest level to which data is processed varies across the mapped area due to uneven station distribution and to criteria used to select earthquakes for processing.

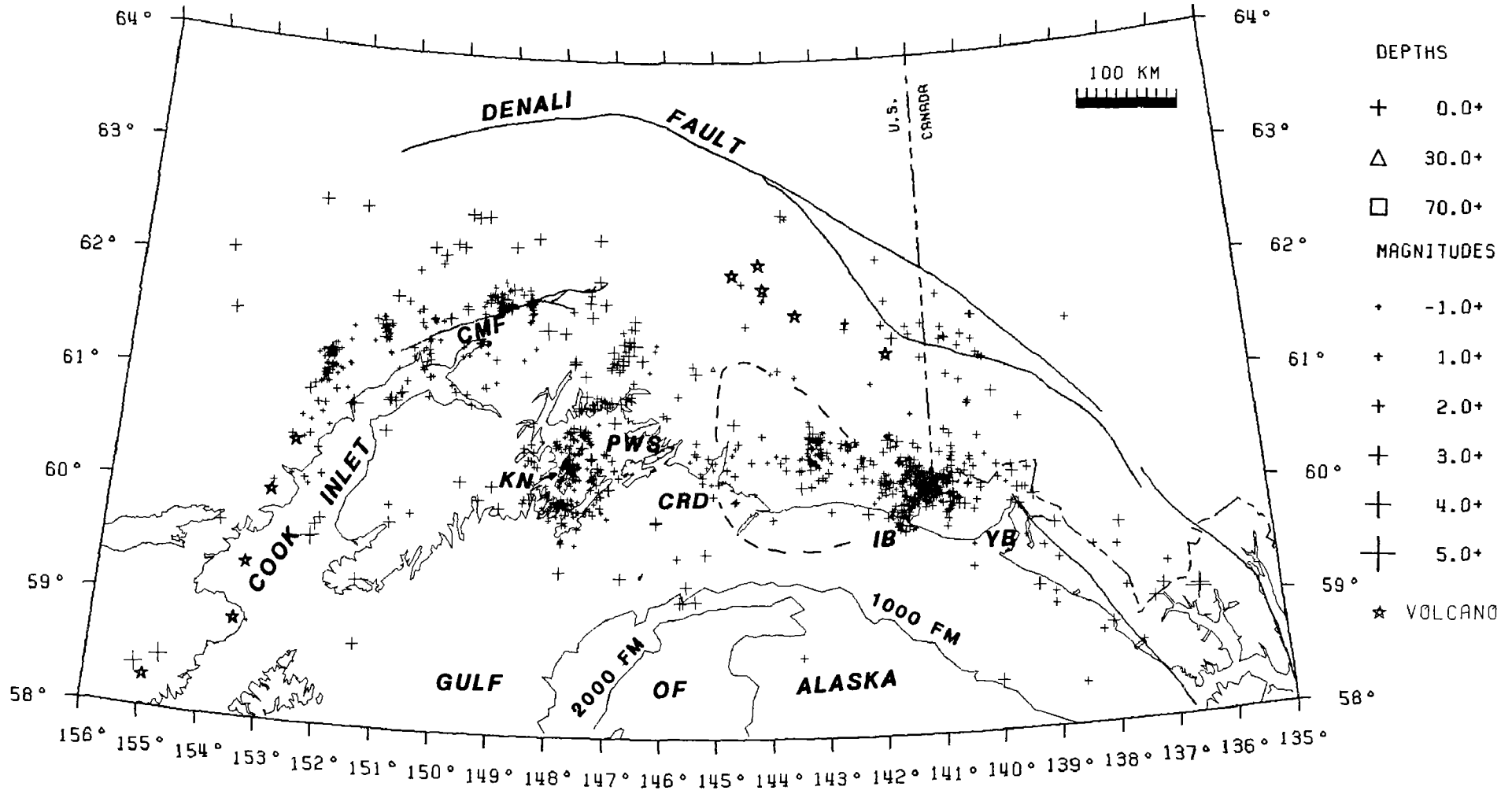

Figure 2. Epicenters of earthquakes from Figure 1 which were located at depths of 30 km or less. Dashed contour indicates inferred approximate extent of Yakataga seismic gap. Abbreviations are: CMF - Castle Mountain fault, CRD - Copper River Delta, IB - Icy Bay, KN - Knight Island, PWS - Prince William Sound, YB - Yakutat Bay.

Seismic Data Library

9930-01501

W. H. K. Lee
U.S. Geological Survey
Branch of Seismology
345 Middlefield Road, Mail Stop 977
Menlo Park, California 94025
(415) 323-8111, Ext. 2630

This is a non-research project and its main objective is to provide access of seismic data to the seismological community. This Seismic Data Library was started by Jack Pfluke at the Earthquake Mechanism Laboratory before it was merged with the Geological Survey. Over the past ten years. we have built up one of the world's largest collections of seismograms (almost all of them on microfilm) and related materials. Our collection includes approximately 4.5 million WWNSS seismograms (1962 - present), 1 million USGS local earthquake seismograms (1966-1979), 0.5 million historical seismograms (1900-1962), and 20,000 earthquake bulletins, reports and reprints.

Recently, we received a few thousand magnetic tapes containing a complete set of digital waveform data of the Global Digital Seismic Network. Although we plan to make these valuable data available to the seismological community, the extent of our service will depend on the available funding. Unfortunately, no funding is available at present to do anything yet.

Twenty data sets that were submitted by projects funded by the USGS External Research Program have been archived, and a description of these data sets may be found in O'Neill, Messier and Lee (1986).

Reports

O'Neill, M. E., Messier, T. M., and Lee, W. H. K., Earthquake Data Archiving and Retrieval System: Archived data sets from the External Research Program, USGS Open-File Report, 86-45, 40 pp., 1986.

Northern and Central California Seismic Network Processing

9930-01160

Fredrick W. Lester
Branch of Seismology
U.S. Geological Survey
345 Middlefield Road M/S 977
Menlo Park, California 94025
(415) 323-8111, ext. 2149

Investigations

1. In 1966 a seismographic network was established by the USGS to monitor earthquakes in central California. In the following years the network was expanded to monitor earthquakes in most of northern and central California, particularly along the San Andreas Fault, from the Oregon border to Santa Maria. In its present configuration there are over 350 single and multiple component stations in the network. There is a similar network in southern California. From about 1969 to 1984 the primary responsibility of this project was to manually monitor, process, analyze, and catalog the data recorded from this network. In 1985 a more efficient and automatic computer-based monitoring and processing system (CUSP) began online operation, replacing most of the manual operations previously performed by this project. For a more complete description of the CUSP system see the project description "Consolidated Digital Recording and Analysis" by S. W. Stewart.

   Since the introduction of the CUSP system the responsibilities of this project have changed considerably. The main focus of the project now is that of finalizing and publishing preliminary network data form the years 1978 through 1984. We also continue to manually scan network seismograms as back-up event detection for the CUSP system, supplement the CUSP data base with data from the back-up magnetic tapes that were detected only visually or by the other automatic detection system (RTP), and assist in the loading of pre-1985 network data into the CUSP data base. Project personnel also act as back-up for the processing staff in the CUSP project. As time permits some research projects are underway on some of the more interesting or unusual events or sequences of earthquakes that have occurred within the network.

   This project continues to maintain the primary data base for the years 1969 - 1984 on both a computer and magnetic tapes for those interested in research on the network seismic data. As soon as the older data are finalized they are exchanged for the preliminary data existing in the data base.

Results

1. Final processing of data for the second half of the calendar year 1982 is complete and those data are ready for publication. Work is currently underway on the final processing of the 1978 and 1983 data. It is expected that data from the second half of 1978 and all of 1983 will be published in 1986. Work is currently underway on the final processing of data for the areas around Lake Shasta, Mt. Shasta, and Lassen Volcanic National Park. Some of these data are very preliminary and need quite a

lot of final processing and analysis, but it is expected that this work will also be complete by the end of 1986.

2. For the time period October 1985 - March 1986 there were an average of 4 to 6 events per day missed by the CUSP automatic detection system. These were added to the existing CUSP data base from the back-up magnetic tape and processed using standard CUSP processing techniques. Most of the earthquakes that were missed occurred in northern California, north of latitude 39 degrees. This is a particular problem in the north because of telemetry noise that exists on those circuits. To avoid producing an abnormally large number of false triggers in the detection system the trigger thresholds are often set higher than normal and therefore some of the real events are missed.

3. Steve Walter is currently investigating some unusual low frequency events that he has detected in Lassen Volcanic National Park over the last four years. Most of these are deep events, focal depths between 15 and 20 kilometers, and most are concentrated west of Lassen Peak. These events are of interest because they resemble events seen in other volcanic regions, particularly Hawaii, that have been associated with magma transport.

4. Quarterly reports were prepared on seismic activity around Lake Shasta, Warm Springs Dam, the Auburn Dam site and Melones Dam for the appropriate funding agencies. Outside funding for the Lake Shasta network ended in February 1986 so those quarterly reports will no longer be submitted. The network will, however, remain in operation with some possible modifications. Quarterly reports on seismic activity in the Mount Shasta area and in Lassen Volcanic National Park were also prepared and distributed to interested agencies and individuals.

5. Work is currently underway on a paper by Mari Kauffmann, Steve Walter, and Rick Lester describing the seismicity in the Klamath Mountains - southern Cascades - northern Sierra Nevada region of California for the years 1977-1984. This paper should be completed in 1986.

Reports

Reynolds, S. L., and Lester, F. W., 1986, Catalog of earthquakes along the San Andreas Fault in central California, January-June 1978, U.S. Geological Survey Open-File Report 86-157, 59 p.

Walter, S. R., 1986, Intermediate - focus earthquakes associated with Gorda Plate subductiuon in northern California, BSSA, v. 76, no. 2, p. 583-588.

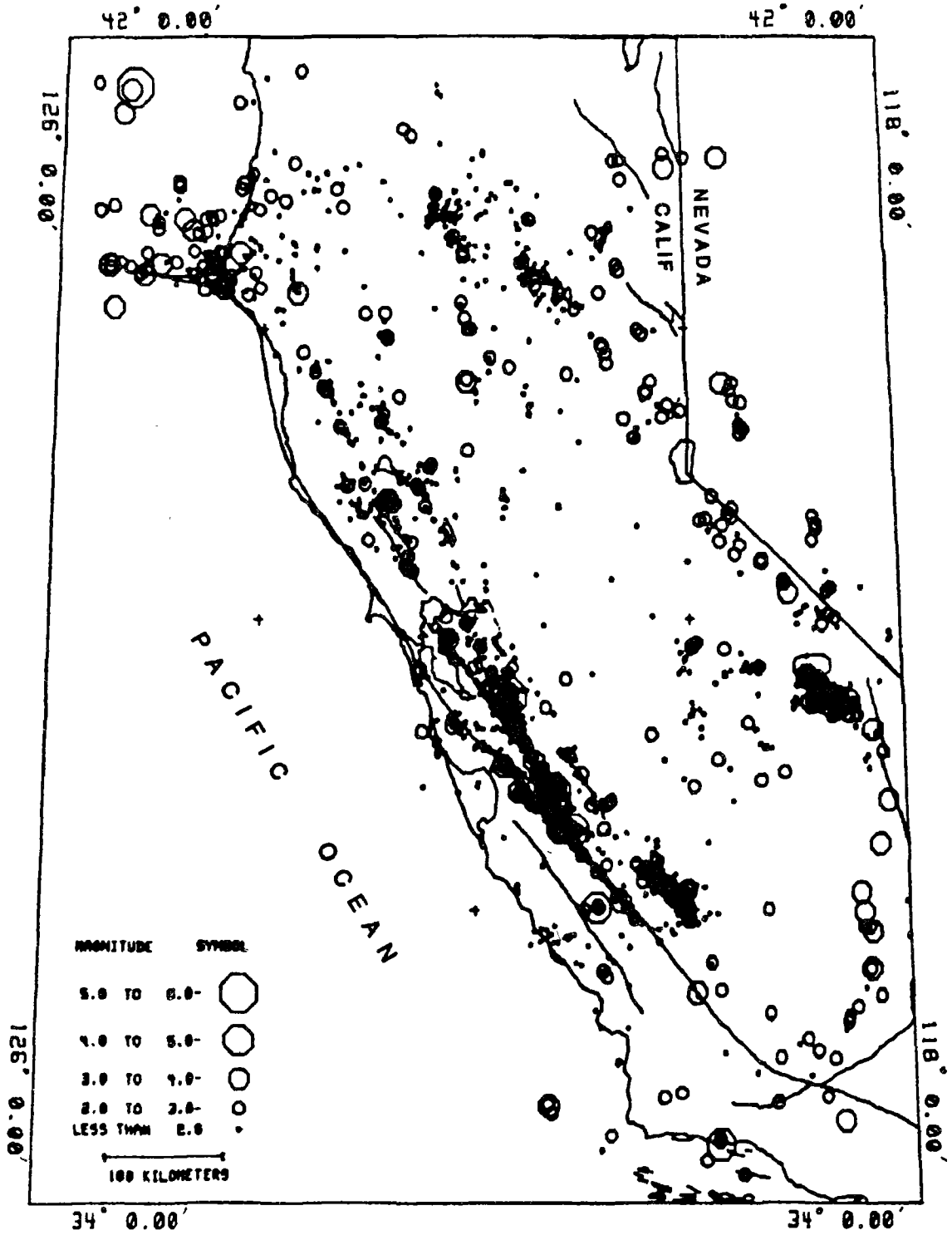

Figure 1. Epicenter map of 7148 earthquakes located by the USGS in northern and central California from October 1985 through March 1986.

Holocene Movement on the Meers Fault, Southwest Oklahoma

R. F. Madole, and Meyer Rubin

Abstract

Stratigraphic relations, differing degrees of soil development, and preliminary radiocarbon ages of three alluvial units indicate that the last major movement on the Meers fault probably occurred in late Holocene time. One alluvial unit is a matrix-supported gravel that was deposited locally on the downthrown side of the fault in response to faulting. This gravel buries a soil formed in the oldest of the three alluvial units and, in turn, is truncated by the youngest alluvial unit. Three preliminary radiocarbon ages (based on a single count) show that deposition of the youngest alluvium probably began in the interval 0.5-1 ka (kilo annum), defining a minimum date for the faulting; the soil probably was buried during the interval 2-4 ka, defining a maximum date for the faulting. The soil in the gravel is weakly developed and similar in degree of development to that in the youngest alluvium, thus supporting a late Holocene age for the gravel and also for the time of faulting. The soil in the oldest of the three units is much more strongly developed. It has a Bt horizon, is leached to a depth of 75 cm, and has stage II carbonate morphology, properties which suggest a late Pleistocene age. A preliminary radiocarbon age of a sample from the lower part of this alluvium suggests that deposition of the unit may have begun 12-14 ka. Two other alluvial units, perhaps deposited within the intervals 90-150 ka and 150-730 ka, provide a basis for determining a history of possible older movement on the Meers fault.

Regional Microearthquake Network in the Central Mississippi Valley

14-08-0001-A0263

Willaim V. Stauder and Robert B. Herrmann
Department of Earth and Atmospheric Sciences
Saint Louis University
P.O. Box 8099 Laclede Station
St. Louis, MO 63156
(314) 658-3131

Investigations

The purpose of the network is to monitor seismic activity in the Central Mississippi Valley Seismic zone, in which the large 1811-1812 New Madrid earthquakes occurred. The following section gives a summary of network observations during the year 1985.

Results

In 1985, 189 earthquakes were located and 57 other nonlocatable earthquakes were detected by the 39 station regional telemetered microearthquake network operated by Saint Louis University for the U. S. Geological Survey and the Nuclear Regulatory Commission. Figure 1 shows 171 earthquakes located within a 4° x 5° region centered on 36.5°N and 89.5°W. Seismograph stations are denoted by triangles and are labeled by the station code. The magnitudes are indicated by the size of the open symbols. Figure 2 shows the locations and magnitudes of 126 earthquakes located within a 1.5° x 1.5° region centered at 36.25°N and 89.75°W. Figures 3 and 4 are similar to Figures 1 and 2, but the epicenter symbols(squares) are scaled to focal depth.

221 teleseisms were recorded by the PDP 11/34 microcomputer in 1985. Epicentral coordinates were determined by assuming a plane wavefront propagating across the network and using the travel-time curves to determine back azimuth and slowness, and by assuming a focal depth of 15 kilometers using spherical geometry. Arrival-time information for teleseismic P and PkP phases has been published in the quarterly earthquake bulletin.

The significant earthquakes occurring in 1985 include the following:

1 7 February 1985, UTC 2344, 36.28°N, 89.45°W: felt at Ridgely, Tennessee. m_{Lg}(10Hz) = 2.8(SLM), m_{Lg}(3Hz) = 2.9<FVMZ>, m_D = 2.4(TEIC).

2 15 February 1985, UTC 1556, 37.23°N, 89.33°W: felt (IV) at Old Appleton, Missouri and at Chester and Tamms, Illinois. Felt (III) at Cairo and Colp, Illinois. Also felt at Belknap, Illinois and

Mayfield, Kentucky. m_{Lg}(10Hz) = 3.3(SLM), m_{Lg}(3Hz) = 2.9<FVMZ>.

3 1 May 1985, UTC 1627, 37.98°N, 87.61°W: felt in the western part of Evansville, Indiana. m_{Lg}(3Hz) = 2.9 <FVM>.

4 4 May 1985, UTC 0707, 36.27°N, 90.77°W: felt (IV) at Biggers, Arkansas. m_{bLg} = 3.1(SLM), m_D = 2.7(TEIC).

5 6 September 1985, UTC 2217, 35.77°N, 93.12°W: felt (V) at Deer, Green Forest, Kingston, Nail, Ozone, and Pyatt. Felt (IV) at Bass, Bruno, Everton, Hasty, Huntsville, Jasper, Mount Judea, Parthenon, Saint Paul, Tilly, Western Grove, and Vendor. Felt throughout much of northwestern Arkansas. m_{bLg} = 3.6(NEIS), m_{bLg} = 3.8(TUL), m_D = 3.3(TEIC).

6 9 September 1985, UTC 2206, 41.85°N, 88.01°W: felt (V) at Clarendon Hills, Edgebrook, Hinsdale, and La Grange. Felt (IV) at Brookfield and Western Springs. Felt (III) at Countryside, Lindenwood, and Villa Park. m_{bLg} = 3.0(NEIS).

7 8 November 1985, UTC 1956, 35.42°N, 91.84°W: m_{Lg}(10Hz) = 3.5(SLM).

8 5 December 1985, UTC 2259, 35.86°N, 89.99°W: felt (V) at Blytheville Air Force Base, Arkansas. Felt (IV) at Blytheville, Osceola, Burdette, Keiser, Joiner, and Tomato, Arkansas. Also felt (IV) at Henning, Tennessee. Felt (III) at Armorel, Dell, Driver, Luxora, and Wilson, Arkansas. m_{Lg}(10Hz) = 3.5(SLM), m_{Lg}(3Hz) = 3.6<FMVZ>, m_{bLg} = 3.9(NEIS).

9 29 December 1985, UTC 0856, 38.49°N, 89.02°W: felt in the Centralia, Iuka, and Salem, Illinois areas. m_{Lg}(10Hz) = 3.2(SLM), m_{Lg}(3Hz) = 3.0<FVMZ>, m_{bLg} = 3.5(NEIS).

ACKNOWLEDGEMENTS

The cooperation of the Tennessee Earthquake Information Center, National Earthquake Information Service, and the University of Kentucky is gratefully acknowledged for providing station readings, magnitude data, and felt information. The results reported were a result of the support from the Department of the Interior, U.S. Geological Survey, under Contract 14-08-0001-A0263 and the U.S. Nuclear Regulatory Commission under Contract NRC-04-81-195-03.

REFERENCES

Central Mississippi Valley Earthquake Bulletin, Department of Earth and Atmospheric Sciences, Saint Louis University. 1985, Nos. 43-45.

PDE Preliminary Determination of Epicenters, Monthly Listings, U. S. Geological Survey, 1985.

TEIC Quarterly Seismological Bulletin, Tennessee Earthquake Information Center, Memphis State University. 1985, Vol. 6, Nos. 1-3.

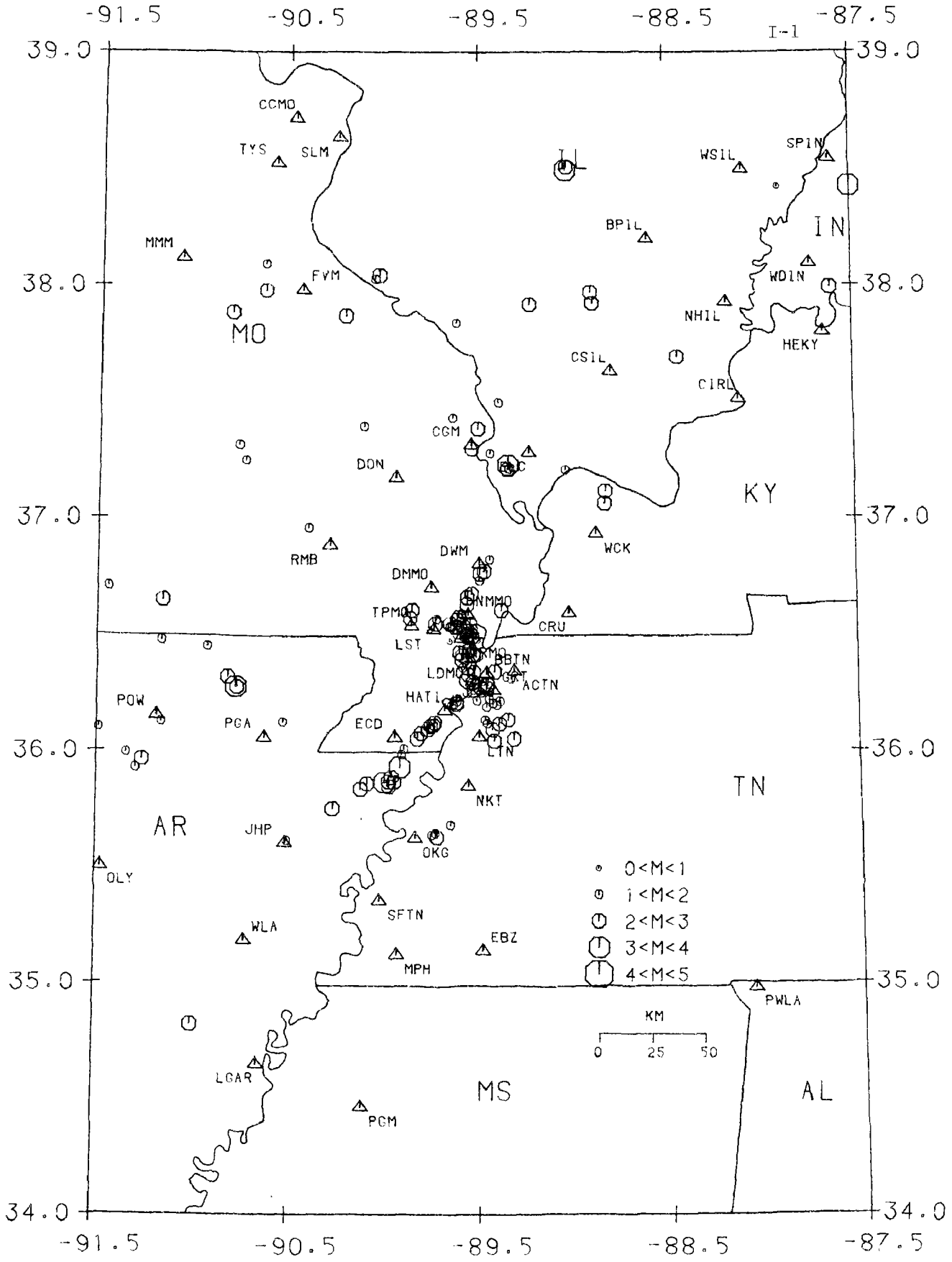

FIGURE 1

REPORTING PERIOD 01 JAN 1985 TO 31 DEC 1985

LEGEND : △ STATION ⊙ EPICENTER

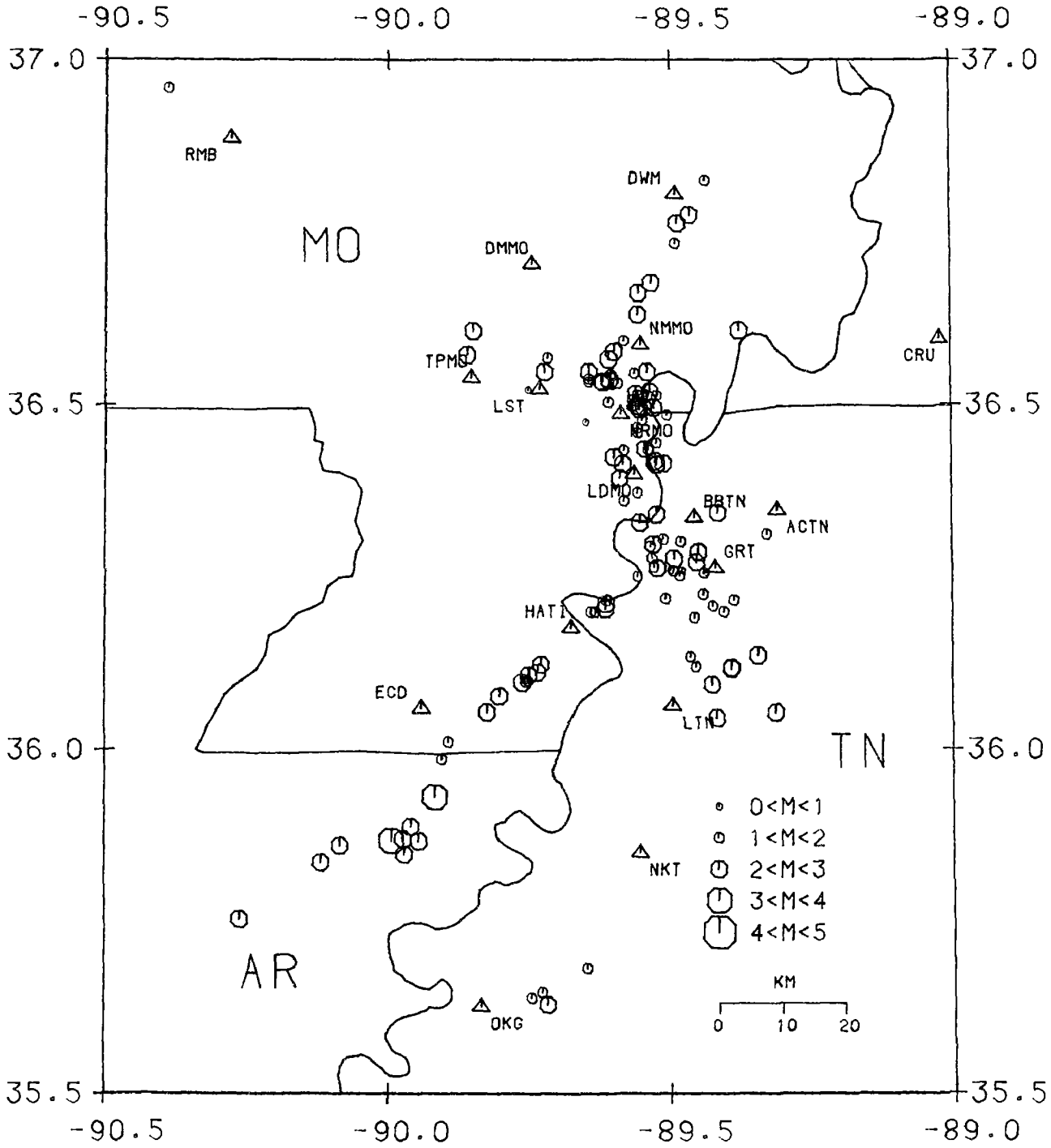

FIGURE 2

REPORTING PERIOD 01 JAN 1985 TO 31 DEC 1985

LEGEND . △ STATION ⊙ EPICENTER

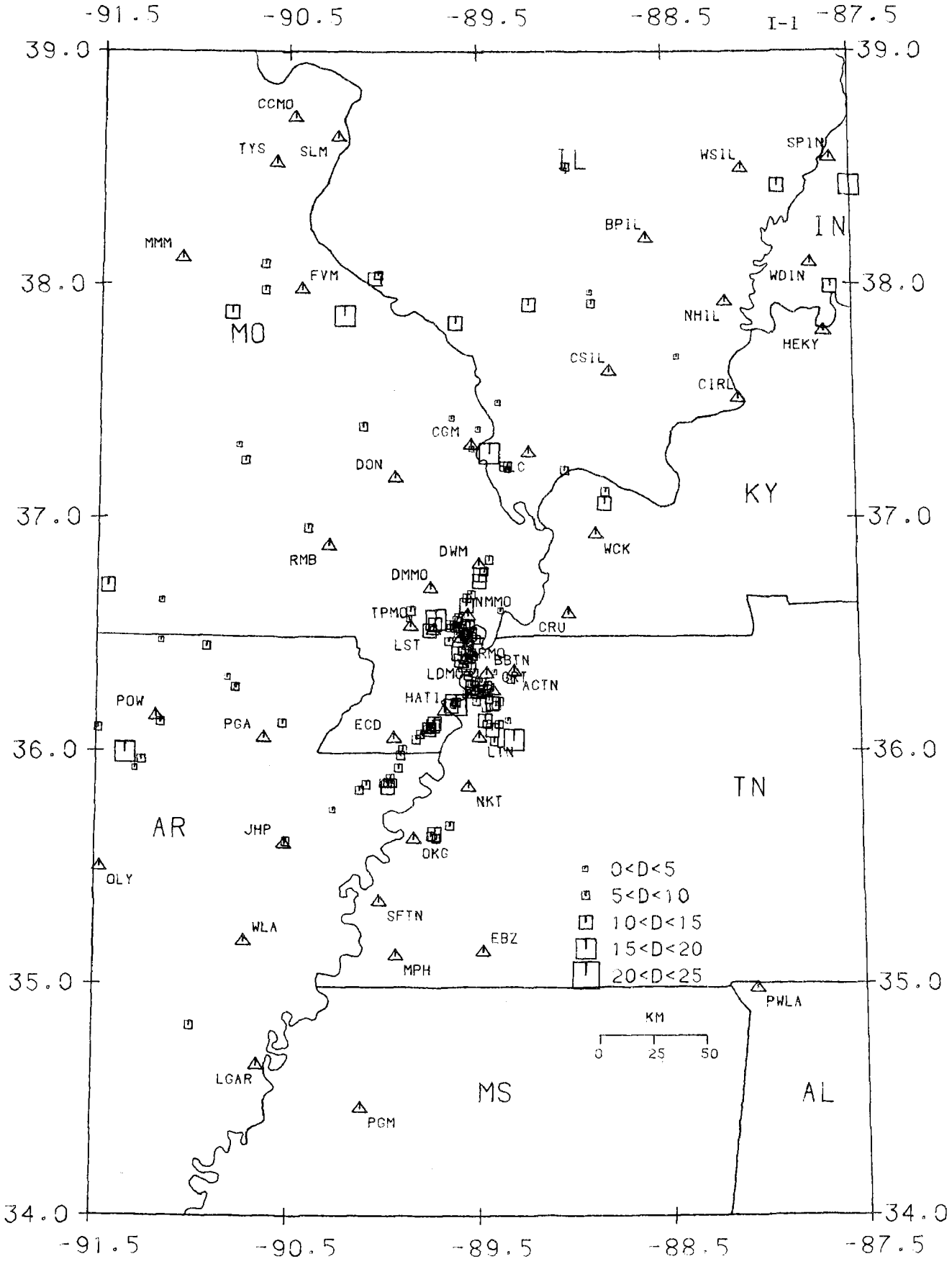

FIGURE 3

REPORTING PERIOD 01 JAN 1985 TO 31 DEC 1985

LEGEND . △ STATION ⊡ EPICENTER

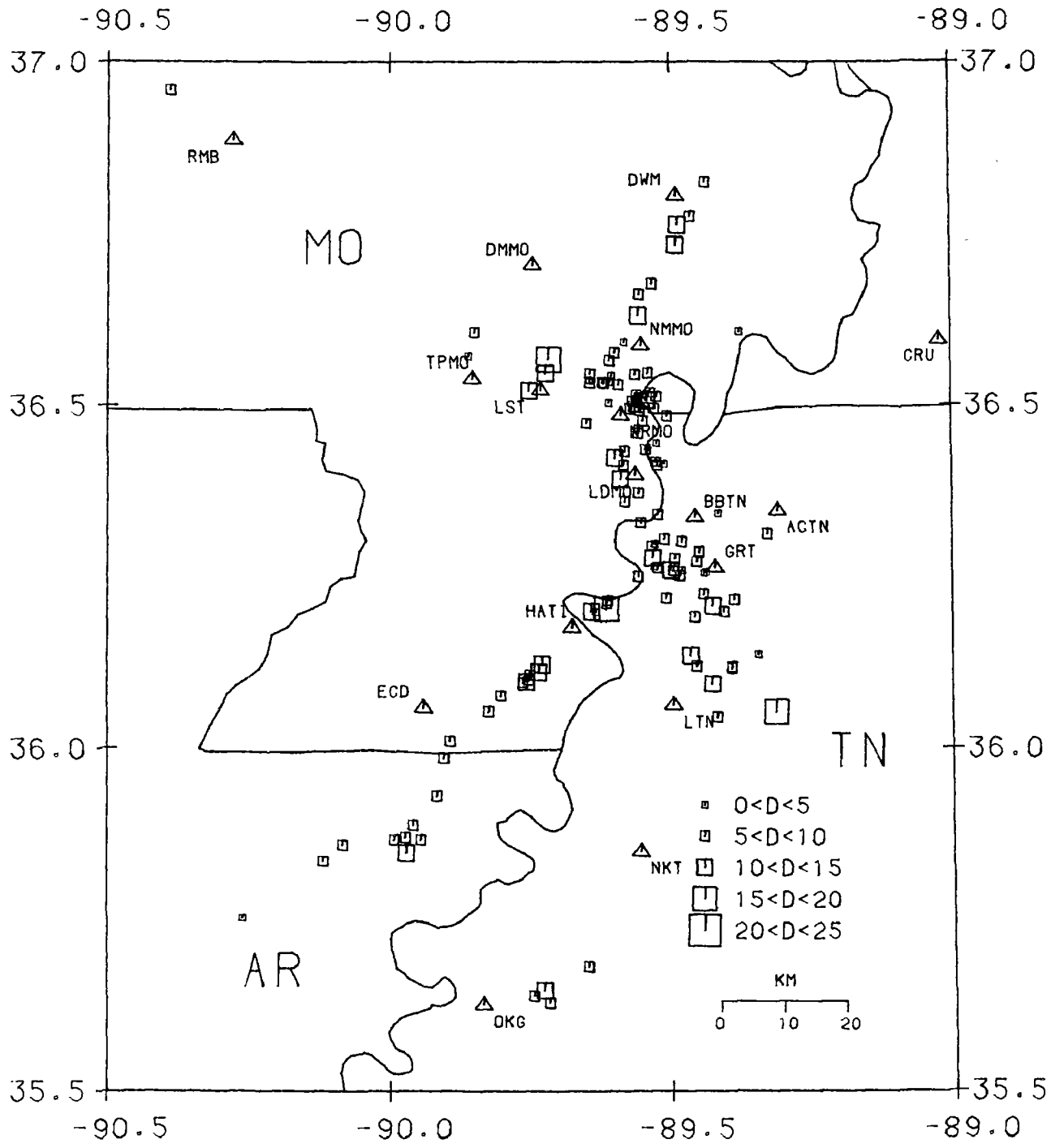

FIGURE 4

REPORTING PERIOD 01 JAN 1985 TO 31 DEC 1985

LEGEND . △ STATION ▫ EPICENTER

Consolidated Digital Recording and Analysis

9930-03412

Sam W. Stewart
Branch of Seismology
U.S. Geological Survey
345 Middlefield Road M/S 977
Menlo Park, California 94025
(415) 323-8111 Ext. 2577

Investigations

The goal is to operate, on a routine and reliable basis, a computer-automated system that will detect and process earthquakes occurring within the USGS Central California Earthquake Network (also known as CALNET). Presently, the output from more than 450 short-period seismic stations is telemetered to a central recording point in Menlo Park, California. Two DEC PDP11/44 computers, and a VAX/750, are used on this project. The 11/44A is dedicated to the task of online, realtime detection of earthquakes and storing the waveforms for later analysis. The 11/44B is used for offline processing and archiving of earthquakes. Both computers have a 512 channel analog-to-digital converter, so the 11/44B can serve as backup to the online system whenever necessary. The two computers can communicate with each other via a simple digital-bit I/O "semaphore" system, and can transfer large amounts of data via a dual-ported disk subsystem or a dual-ported magnetic tape subsystem. The VAX/750 is a general purpose computer used by the Branch of Seismology. We use it as the primary "research" computer for the CUSP system. It holds the primary data base of earthquake summary data and phase card data, which is available for research purposes. We update and maintain the CALNET data on this computer.

Both 11/44 computers use the RSX11M-PLUS (v2.1) operating system. The VAX/750 uses the DEC VMS operating system. Software has been developed largely by Carl Johnson in Pasadena, but with considerable modification by Peter Johnson, Bob Dollar and Sam Stewart, to meet Menlo Park's specific needs. Our applications are all written in Fortran-77, but with heavy use of system functions unique to the RSX or VMS operating systems.

Results

1. During the period October 1985 thru March 1986 approximately 7500 events were processed through the CUSP system. This includes 6300 events that were classified as 'LOCAL' events, i.e., they occurred within or near enough to the network that hypocenters were calculated and the data entered into the catalogs. The remaining 1200 events were either regional or teleseismic events, or unprocessed copies of local events that were too small (Ml 1.0) to be timed, or copies of very large events that had to be 'split' in order to be accomodated by the 11/44 hardware limitations. In addition, a few thousand non-seismic, noise events detected by the online 11/44A computer had to be examined and deleted. Considering only the seismic events, this projects to an annual rate of processing about 15,000 events per year.

2. Calibration pulses generated by the field units are now captured routinely by the online 11/44A earthquake detection system. The onset time of each calibration pulse is timed by the analyst on the 11/44B system. The MEM file for each set of calibrations is then written to an archive tape that contains only calibration pulse files.

On the VAX/VMS 750, the pulses are read in from the ARKIVE tape, and plotted in a format that facilitates detecting network/instrumental hardware problems. The pulses are not yet used to determine complete system response curves. Mary O'Neill Allen has developed programs to analyze the pulses and automatically determine which ones are outside the bounds of acceptable operational parameters. The idea is to determine, objectively, which stations need maintenance done on them.

3. Data from the Rex Allen/Jim Ellis Real Time Processing system (RTP) and the Prototyping system (PRO) are coming into the VAX/VMS 750 system in realtime. The data are entered into the CUSP database system, magnitudes determined from an algorithm developed by Al Lindh, an 'alarm system' (under test) sends a VAX/MAIL message to selected persons if certain hypocenter and magnitude criteria are met, and the data entered into an online catalog. There are 408 stations currently online to the RTP/PRO systems. The hypocentral parameter data are also sent via Ethernet to Fred Klein's Real Time Display (RTD) color terminal and DEC PC where they are plotted automatically.

4. The CUSP earthquake editor (QED) on the VAX/VMS 750 was modified to measure amplitudes and periods as well as the usual phase onset time and first motion direction. The software is quite general in that an amplitude window of any length can be defined, and full- or half-amplitudes and periods can be measured. The automatic analog gain ranging feature of the Alaska Network instrumentation can also be accomodated.

5. CUSP MEM-file tapes from the Pasadena CUSP system for the period October 1983 thru April 1985 were received during this report period. These tapes were copied, and put thru the CUSP system in Menlo Park, resulting in MEM files and tapes consistent with the Menlo Park system.

Reports

Lee, W.H.K., K. Aki, B. Chouet, P. Johnson, S. Marks, J.T. Newberry, A. Ryall, S.W. Stewart and D.M. Tottingham, 1986, A Preliminary Study of Coda Q in California and Nevada. Bulletin of Seis. Soc. Am. (in press).

Peng, J.Y., K. Aki, W.H.K. Lee, B. Chouet, P. Johnson, S. Marks, J.T. Newberry, A.S. Ryall, S.W. Stewart and D.M. Tottingham, 1986, Coda Q Associated Round Valley Earthquake in California. (Submitted to Journal of Geophysical Research)

Seismic Monitoring of the Shumagin Seismic Gap, Alaska

USGS 14-08-0001-21919

John Taber and Klaus H. Jacob
Lamont-Doherty Geological Observatory of Columbia University
Palisades, New York 10964
(914) 359-2900

Investigations

Seismic data from the Shumagin seismic network were processed to obtain origin times, hypocenters, and magnitudes for local and regional events. The processing resulted in files of hypocenter solutions and phase data, and archive tapes of digital data. These files are used for the analysis of possible earthquake precursors, seismic hazard evaluation, and studies of regional tectonics and volcanicity (see Analysis Report, this volume). A yearly bulletin is available for 1984 data and will be available for 1985 data.

Results

The Shumagin network was used to locate 829 earthquakes in 1985. The seismicity of the Shumagin Islands region for this time period is shown in map view and cross section in figure 1. The most notable activity in 1985 was a sequence of events that began with an Ms= 6.5 event in October and included 4 additional events greater than or equal to magnitude 5 The sequence is visible on the map near 54 N,159 W. This is near a similar but smaller sequence that occurred in 1983. Otherwise the overall pattern over this time period is similar to the long term seismicity. Concentrations of events occur at the base of the main thrust zone and in the shallow crust directly above it. The continuation of the thrust zone towards the trench is poorly defined. West of the network (which ends at 163) the seismicity is more diffuse in map view. Below the base of the main thrust zone (~45 km) the dip of the Benioff zone steepens. Part of the double plane of the lower Benioff zone is evident near 100 km depth.

The network is capable of digitally recording and locating events as small as Ml = 0.4 with uniform coverage at the 2.0 level. Onscale recording is possible to ~Ms=6.5 on a telemetered 3 component force-balance accelerometer. Larger events are recorded by one digitally recording accelerometer and on photographic film by 12 strong-motion accelerometers.

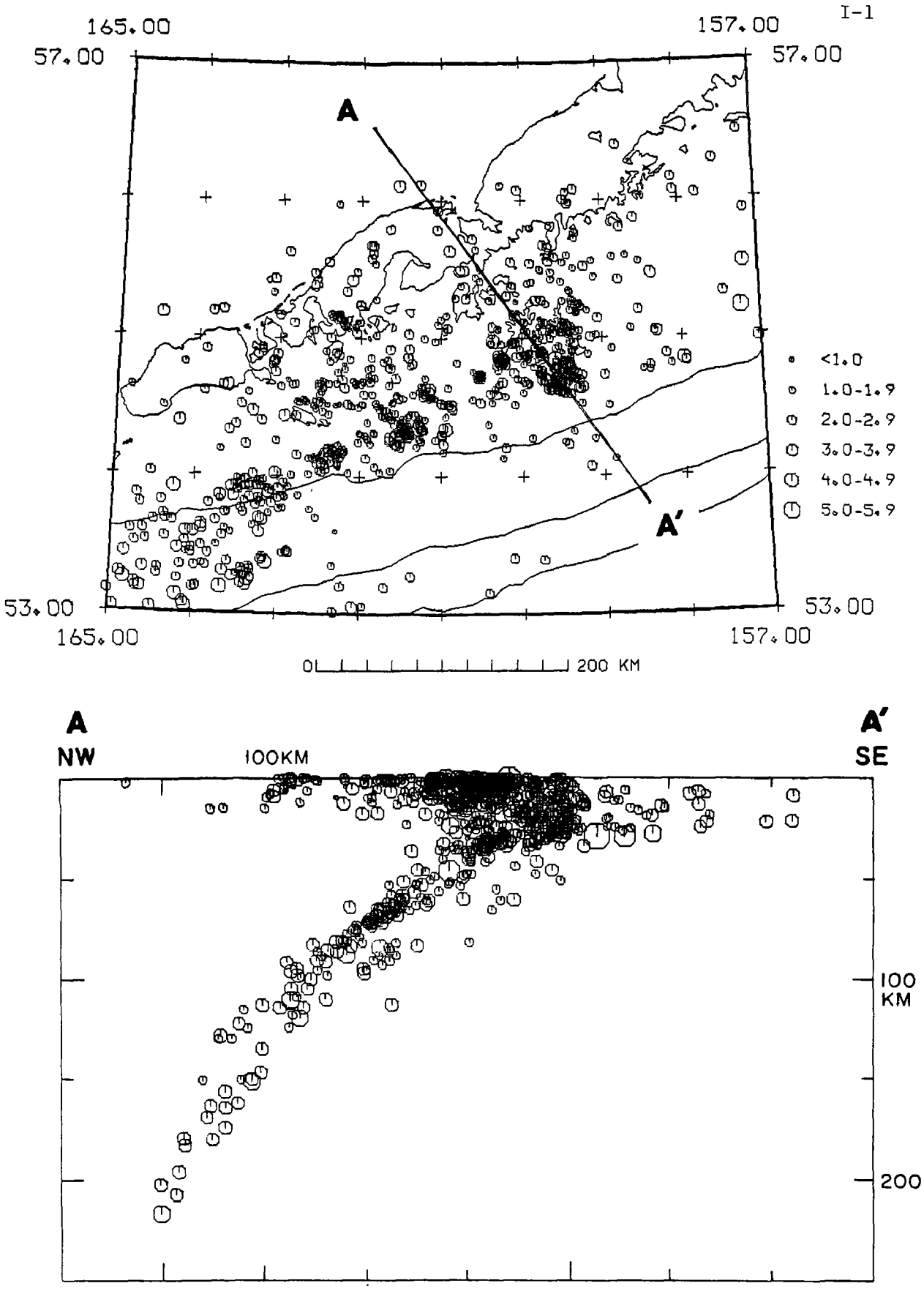

Figure 1. Map view and cross section of seismicity located by the Shumagin network in 1985.

Earthquake Hazard Research in the Greater Los Angeles Basin and Its Offshore Area

#14-08-0001-A0264

Ta-liang Teng
Thomas L. Henyey
Egill Hauksson

Center for Earth Sciences
University of Southern California
Los Angeles, CA 90089-0741
(213) 743-6124

INVESTIGATIONS

(1) Monitor earthquake activity in the Los Angeles Basin and the adjacent offshore area.

(2) Upgrade of telemetry electronics used by remote field stations. The microprocessor-based Optimal Telemetry System has been deployed for field testing at three seismic stations.

RESULTS

(1) The earthquake activity that occurred in the Los Angeles basin and the southern California coastal zone during 1985 is shown in Figure 1. The seismicity rate during 1985 is similar to the rate that was recorded during the previous three years. The earthquake activity in the Los Angeles basin is characterized by single shocks that are scattered throughout the region. Several spatial clusters are observed in the monitoring region. Clusters of seismicity are observed at the northern segments of both the Newport-Inglewood fault as well as the Palos Verdes fault during 1985. The adjacent offshore area in Santa Monica Bay is also characterized by a moderate level of seismic activity. A cluster of earthquakes is observed near the aftershock zone of the 1973 Point Mugu earthquake. The largest earthquake to occur within the Los Angeles basin had a magnitude of 3.6 and was located in San Pedro Bay, just south of the City of Long Beach. In summary, although the 1985 seismicity in the southern California coastal zone and the Los Angeles basin is characterized by several spatial clusters of seismicity, the overall level of activity is moderate to low as compared with the last 10 years of seismicity.

Focal mechanisms have been determined for the M 3.0 earthquakes that occurred in the Los Angeles basin during 1985 (see Figure 2). The event (February 14, 1985) located in San Pedro Bay near the Palos Verdes fault shows oblique reverse faulting with some amount of strike slipe faulting. Three events (March 4, April 5 and April 8, 1985) that occurred along the southern margin of the Transverse Ranges show mostly reverse faulting. These mechanisms are consistent with the fault plane solutions of the 1973 (M=6.0) Point Mugu and the 1979 (M=5.0) Malibu earthquakes.

(2) A second generation of the optimal telemetry system (OTS) is currently being designed and built. The front-end anti-aliasing filters have been upgraded to 7 poles. To minimize electronic noise the microprocessor has been placed on a separate circuit board. The design goals are to achieve a background noise level of 1 mV or less. Field testing of the new OTS is planned to begin in July 1986.

REPORTS

Hauksson, E., T. L. Teng, T. L. Henyey, J. K. McRaney, L. Hsu and G. Saldivar, Earthquake Hazard Research in the Los Angeles Basin and its Offshore Area, U.S.C. Geophysics Laboratory Technical Report #8501, 1985.

Teng, T. L., Application Results of an Optimal Telemetry System, submitted to AGU Fall Meeting, 1985.

Saldivar, G., E. Hauksson and T. L. Teng, The Malibu Earthquake (M=5.0) and Its Aftershock Sequence, southern California, January, 1979, submitted to AGU Fall Meeting, 1985.

Hauksson, E., Constraints on the Velocity Structure of the Crust in the Los Angeles Basin and the Central Transverse Ranges, southern California, submitted to AGU Fall Meeting, 1985.

Teng, T. L. and M. Hsu, A Seismic Telemetry System of Large Dynamic Range, Bull. Seism. Soc. Amer., in press, 1986.

Hauksson, E. and G. Saldivar, The 1930 Santa Monica and the 1979 Malibu, California, Earthquakes, submitted to BSSA, April 1986.

Hauksson, E., T. L. Teng, T. L. Henyey, J. K. McRaney, L. Hsu, M. Robertson and G. Saldivar, Earthquake Hazard Research in the Los Angeles Basin and Its Offshore Area, U.S.C. Technical Report #86-1, February 1986.

st-85-363

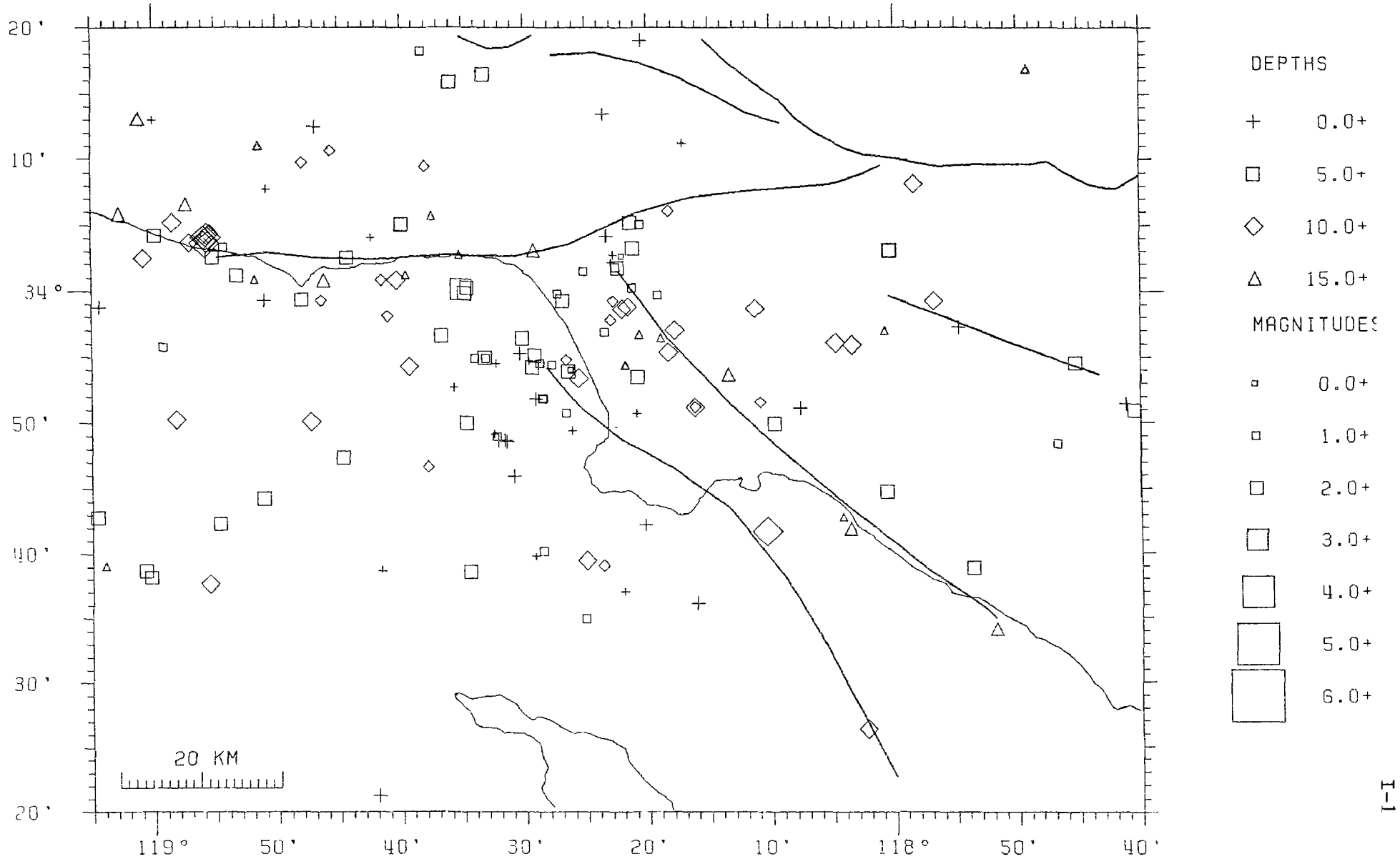

Figure 1. Seismicity in the Los Angeles basin during 1985.

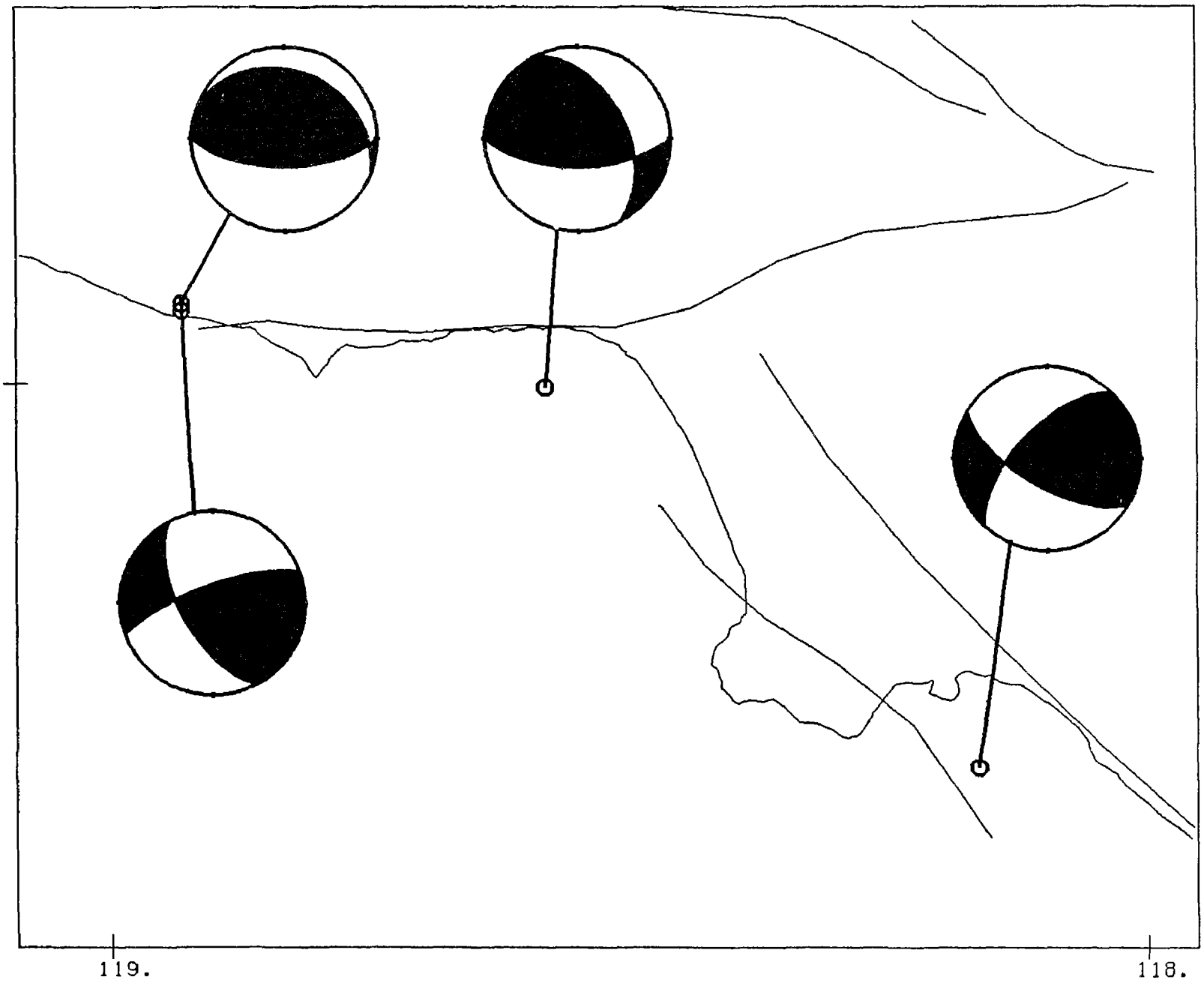

Figure 2. Focal mechanisms of M≥3.0 earthquakes that occurred in the Los Angeles basin during 1985.

Field Experiment Operations

9930-01170

John Van Schaack
Branch of Seismology
U. S. Geological Survey
345 Middlefield Road MS-977
Menlo Park, California 94025
(415) 323-8111, ext. 2584

Investigations

This project performs a broad range of management, maintenance, field operation, and record keeping tasks in support of seismology and tectonophysics networks and field experiments. Seismic field systems that it maintains in a state of readiness and deploys and operates in the field (in cooperation with user projects) include:

a. 5-day recorder portable seismic systems.
b. "Cassette" seismic refraction systems.
c. Portable digital event recorders.
d. Smoked paper recorder portable seismic systems

This project is responsible for obtaining the required permits from private landowners and public agencies for installation and operation of network sensors and for the conduct of a variety of field experiments including seismic refraction profiling, aftershock recording, teleseism P-delay studies, volcano monitoring, etc.

This project also has the responsibility for managing all radio telemetry frequency authorizations for the Office of Earthquakes, Volcanoes, and Engineering and its contractors.

Results

Seismic Refraction

One hundred twenty seismic cassette recorders were used in the PACE experiment along the California Arizona border in late October 1985. The experiment was a success in all respects. Preliminary work is being done in preparation for two refraction experiments to be carried out later in 1986. The first will be in Central Nevada and the second near the Nevada Test Site.

Telemetry Networks

A number of modifications have been made to the Central California Seismic Network telemetry system to reduce telemetry costs and increase reliability. The microwave network is almost completely redundant between Parkfield, CA. and Menlo Park. We have also completed the system as a two way system between Menlo Park and

Parkfield. We are presently testing portions of a cooperative network with the U.S.Army Corps of Engineers. This net will extend between Sacramento and Camp Roberts. Approximately two thirds of our telemetry stations are being carried on the microwave network at a savings of about $130,000 in telephone telemetry costs.

Portable Networks

Six seismic telemetry stations were installed around Ruiz Volcano in Colombia, South America in November 1985. The data were telemetered to a central recording site and recorded on drum recorders. These stations will become part of a permanent network to be operated by the Colombian Government to monitor this active volcano.

Data Processing Center Operations

9930-01499

John Van Schaack
Branch of Seismology
U. S. Geological Survey
345 Middlefield Road- Mail Stop 977
Menlo Park, California 94025
(415) 323-8111, Ext. 2584

Investigations

This project has the general housekeeping, maintenance and management authority over the Earthquake Prediction Data Processing Center. Its specific responsibilities include:

1. Day to day operation and performance quality assurance of 5 network magnetic tape recorders.
2. Day to day management, operation, maintenance, and performance quality assurance of 2 analog tape playback stations.
3. Day to day management, operation, maintenance and performance quality assurance of the U.S.G.S. telemetered seismic network event library tape dubbing facility (for California, Alaska, and Hawaii).
4. Projection of usage of critical supplies, replacement parts, etc., maintenance of accurate inventories of supplies and parts on hand, uninterrupted operation of the Data Processing Center.

Results

Procedures and staff for fulfilling assigned responsibilities have been developed and the Data Processing Center is operating smoothly and serving a large variety of scientific user projects.

Characteristics of Active Faults

9950-03870

Robert C. Bucknam
Branch of Engineering Geology and Tectonics
U.S. Geological Survey, MS 966
Denver Federal Center, Box 25046
Denver, CO 80225
(303) 236-1604

Investigations

1. Scarp degradation studies--Lost River Range, Idaho.

2. Afterslip study--Motagua fault, Guatemala

Results

1. Geomorphic methods of dating fault scarps have proven to be widely useful in studies of paleoseismicity. Such methods typically compare the form of a scarp of unknown age with that of a scarp whose age is well known. However, the influence of lithologic properties of the faulted alluvium (and other site-specific variables) on the rate of degradation is virtually unknown, introducing possibly significant errors in the geomorphically assigned age. In particular, the rate at which the "free face" from the faulting event is destroyed may be particularly sensitive to small variations in the properties of weakly-indurated alluvium and colluvium. Based on extrapolation of the loss of the free face on scarps less than 100 yrs old, Wallace (1977) estimated that the time required for loss of the free face to be in the range of several hundred to several thousand years, a range of possible major importance when dating Holocene age scarps. Recently acquired data from fault scarps produced by an earthquake in 1739 in north-central China (Zhang and others, in press) show that the free face on those scarps is well-preserved on scarps more than 2 m high after nearly 250 years, and locally it is likely to be well preserved for many hundreds of years more. The variability in preservation of the free face along these scarps, however, indicates that subtle lithologic differences locally exert a strong influence on the rate at which the scarp is modified.

   As part of a study to associate variations in the rate of modification of the free face with lithologic and other site specific variables, I have begun photogrammetric documentation of the modification of scarps formed by the Borah Peak earthquake in Idaho. The procedures, developed in collaboration with Sherman Wu of the Branch of Astrogeology, allow monitoring several meter-long intervals of scarp with an X-Y-Z resolution of 1 cm or better. Accurate knowledge of the changes taking place is an essential first step in evaluating the effect of various parameters on the rate and mechanism of degradation. The work is focussing on historic earthquake scarps developed along modified preexisting late-Quaternary scarps. This approach, in contrast to a study of artificial scarps such as roadcuts, offers the opportunity to assess the relative importance of the free face stage on the estimated age of the eroded fault scarp.

The first set of photos was taken in October 1985. The site will be rephotographed in early May 1986 and again in October 1986 to document the changes that occur. The timing of the photographs is intended to aid in identifying possible seasonal effects on the rate of scarp erosion. The photographs, taken with a calibrated mapping camera are being used to compile "topographic" maps referred to a vertical plane. Comparison of one map with another will provide an isobase map of changes on the scarp face.

2. Afterslip following the 1976 Guatemala earthquake was conspicuous at several localities along the Motagua fault (Bucknam and others, 1978). Alinement arrays established across the fault in 1978 (Bucknam, 1978) have been measured periodically through September 1983 by the Instituto Geografico Militar of Guatemala. Figures 1a and 1b show the general nature of the afterslip determined by those measurements at one of the sites. Although the rate of slip is decreasing, it is not decreasing exponentially with time as often noted for afterslip following other earthquakes. Preparation of a report on these data is pending a resurvey of the arrays that has been requested for 1986 to complete the record of afterslip in the decade following the earthquake.

References Cited

Bucknam, R. C., Plafker, George, and Sharp, R. V., 1978, Fault movement (afterslip) following the Guatemala earthquake of February 4, 1976: Geology, v. 6, p. 170-173.

Bucknam, R. C., 1978, Documentation for alinement arrays, Motagua fault, Guatemala: U.S. Geological Survey Open-File Report 78-880, 19 p.

Zhang, Buchun; Yuhua, Liao; Shunmin, Guo; Wallace, R. E.; Bucknam R. C.; and Hanks, T. C. (in press), Fault scarps related to the 1739 earthquake, and seismicity of the Yinchuan graben, Nigxia Huizu Zizhigu, China: Bulletin of the Seismological Society of America.

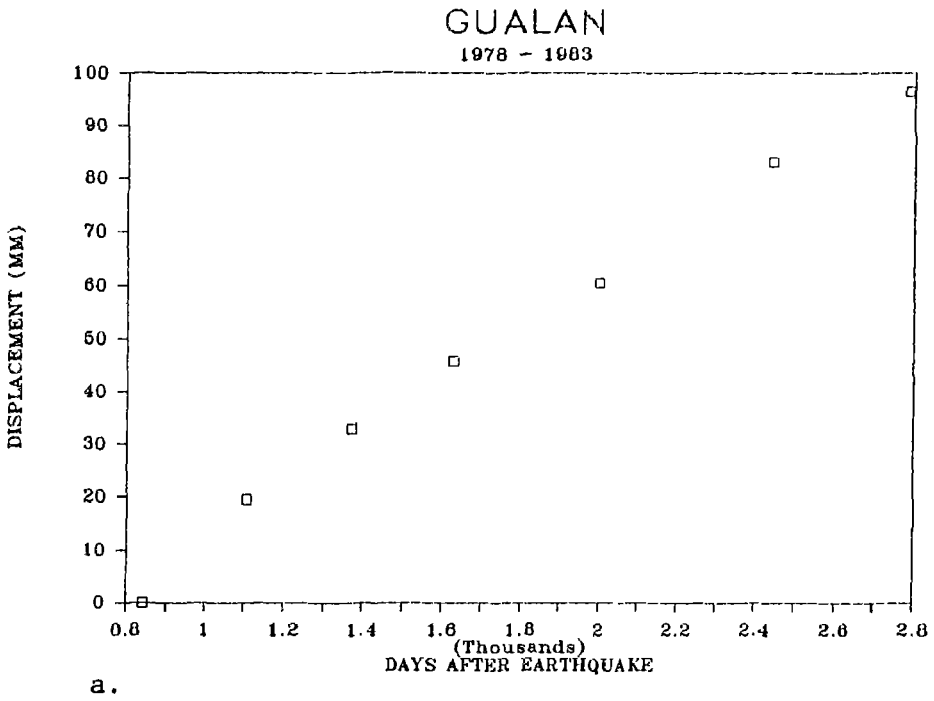

a.

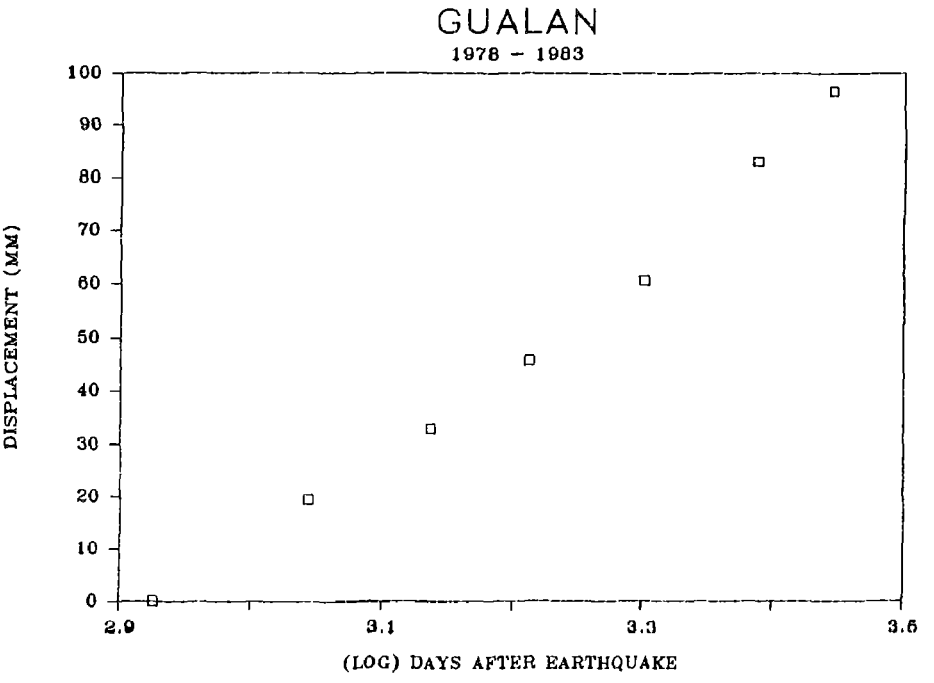

b.

FIGURE 1.--Left-lateral displacement versus time across the Motagua fault, Guatemala at alinement array site "GUALAN."

Comparative Earthquake and Tsunami Potential for Zones in the Circum-Pacific Region

9600-98700

George L. Choy
Stuart P. Nishenko
William Spence
Branch of Global Seismology and Geomagnetism
Denver Federal Center
Box 25046, Mail Stop 967
Denver, Colorado 80225
(303) 236-1506

Investigations

1. Prepare detailed maps and text of comparative earthquake potential for the west coasts of Mexico, Central America, and South America.

2. Conduct investigations of the historic repeat-time data for great earthquakes in the northern Pacific Ocean margin.

3. Conduct investigations into the tectonic mechanisms of major earthquakes in Peru, Chile, and the central Sunda arc in order to assess the likelihood of possible major subduction zone events in those locations.

4. Develop a working model for the interaction between forces that drive plate motions and the occurrence of great subduction zone earthquakes.

5. Develop a rapid method for the estimation of the source properties of significant earthquakes.

Results

1. The probabilistic work has been done for the west coast of Chile and southern Peru (Nishenko, 1985). The highest probability for the recurrence of a great earthquake was assigned to the Valparaiso gap. Confirmation of the theoretical approach was given by the Chile earthquake of March 3, 1985 (M_S 7.8). Considerable stress may remain in the Valparaiso gap. Also having high seismic potential are the areas of Coquimbo-Illapel and Talca-Concepcion. Although their risk is poorly constrained, the areas of Arica-Antofagasta and Mollendo-Arica are considered to have high seismic potential. The probabilistic work for Mexico is completed. Two regions have the highest probabilities for recurrence of large earthquakes within the next two decades: the central Oaxaca gap and the Acapulco-Marcos gap (Nishenko and Singh, in preparation). The Michoacan seismic gap was prominent and in fact a catastrophic earthquake (M_S 8.1) occurred there on September 19, 1985. An analysis of the 1932 Jalisco earthquake was published (Singh et al., 1985).

2. Data on the occurrence of great earthquakes and tsunamis from the Queen Charlotte Islands counterclockwise through the Aleutian Islands have been collected. Evaluation of the probabilistic recurrences in this region will be done by Dr. Nishenko in collaboration with Dr. K. Jacob.

3. Research on the 1974 central Peru earthquake (M_S 7.8) has been completed. One conclusion is that the magnitude of the maximum likely earthquake that can occur here is M_S 8.4. A study on the central Sunda arc earthquake of 1977 (Spence, 1986a) concludes that a great thrust earthquake will not occur at the arc, but that a great normal-faulting earthquake is possible.

4. An evaluation of the ridge-push and slab-pull forces in the context of stresses that lead to great subduction zone earthquakes has been complete (Spence, 1986b).

5. We are developing computer packages that will permit the rapid estimation of source properties of significant earthquakes on a routine basis. We are now routinely using broadband data to obtain depth phases for all earthquakes over m_b 6.0. We are nearly finished with an algorithm that will permit semi-automated on-line computation of radiated energy using as input digitally recorded broadband data for all earthquakes over m_b 6.0.

Reports

Boatwright, J., and G. L. Choy, Teleseismic estimates of the energy radiated by shallow earthquakes: Journal of Geophysical Research, v. 91, p. 2095-2112.

Choy, G. L., 1985, Source characteristics of the Chilean earthquake of March 3, 1985, and its aftershocks from broadband seismograms [abs.]: EOS (American Geophysical Union, Transactions), v. 66, p. 951.

Dewey, J. W., Choy, G. L. and Nishenko, S. P., 1985, Asperities and paired thrust zones in the focal region of the Chilean earthquake of March 3, 1985 [abs.]: EOS (American Geophysical Union, Transactions), v. 66, p. 950.

Nishenko, S. P., 1985, Seismic potential for large and great interplate earthquakes along the Chilean and southern Peruvian margins of South America: A quantitative reappraisal: Journal of Geophysical Research, v. 90, p. 3589-3615.

Nishenko, S., Dewey, J. W., and Choy, G. L., 1985, Spatial variations in aftershock activity during the March 1985, Chilean earthquake sequence and possible tectonic controls [abs.]: EOS (American Geophysical Union, Transactions), v. 66, p. 955.

Singh, S. K., Ponce, L., and Nishenko, S. P., 1985, The great Jalisco, Mexico earthquakes of 1932 and the Rivera subduction zone: Bulletin of the Seismological Society of America, v. 75, p. 1301-1313.

Spence, W., 1986a, The 1977 Sumba earthquake series: Direct evidence for slab pull: Journal of Geophysical Research (submitted).

Spence, W., 1986b, Slab pull and the earthquake cycle: Journal of Geophysical Research (submitted).

Earthquake Hazard Investigations in the Pacific Northwest

14-08-0001-G1080

R.S. Crosson
Geophysics Program
University of Washington
Seattle, WA 98195
(202) 543-8020

Investigations

The objectives of this research are to provide fundamental data and interpretations for earthquake hazard investigations. Currently, we are focusing on seismicity, structure, and tectonic questions related to the occurrence of a hypothetical major subduction earthquake on the Juan de Fuca - North American plate boundary. Specific tasks which we have worked on in this contract period are:

1. Assembling a uniform data-base of all arrival time data available for Washington and northern Oregon from 1970 to the present.

2. Initial studies of tomographic inversion of travel times to determine three-dimensional earth structure.

3. Locations, focal mechanisms and occurrence characteristics of crustal and subcrustal earthquakes beneath western Washington and their relationship to subduction processes.

4. Re-examination of teleseismic travel-times of large events in the Pacific Northwest for evidence of slab location and orientation.

Results

1. We are establishing a uniform base of arrival time data for all network data from 1970 to the present. From 1970 through 1979, data were archived in several different formats, at several sites. 'Pickfiles' of arrival times have been reformatted and events relocated using updated velocity models and location routines. The western Washington data from 1970-1979 and eastern Washington data from mid-1975 through 1979 are complete, and available for research. Eastern Washington data from 1970 through mid-1975 have been retrieved and are being processed.

2. We are beginning to use tomographic inversion of arrival-time data to determine the lateral velocity structure of the Puget Sound area using P and S-wave data recorded by the University of Washington seismic network. We will use local events to determine velocity structure shallower than about 60 km.

At present we are investigating several inversion procedures including simple and multiple interation back projection, direct conjugate-gradient least squares, a Fourier series smoothing method, and convolution techniques. We are investigating three dimensional modeling and the effects of errors and incomplete coverage in the data.

3. A data base of focal mechanisms is being established. The objective of compiling this data base is to use the information to determine the most probable regional tectonic stress in western Washington.

Focal projections of first-arrival polarities have been plotted for more than 400 earthquakes which had ten or more polarities read in routine processing. Focal mechanisms are being determined where possible. Azimuth and plunge of P and T axes must be read from the plots and axes checked to ensure orthogonality. A grading scheme will be implemented to indicate the quality of focal mechanism solutions. Such a grading scheme will consider inconsistent or ambiguous arrivals, and the range of feasible focal mechanisms.

4. Teleseismic residuals from the 1965 Puget Sound earthquake (depth = 60 km) were interpreted by McKenzie and Julian (1971) as evidence of a north-south striking slab dipping 50 degrees east. We recalculated these residuals using both Jeffreys-Bullen and Herrin travel-time tables, and determined that the anomaly is independent of choice of travel-time table. Two other earthquakes of comparable depth, in 1949 (Puget Sound) and 1976 (Pender Island) have similar residual patterns. Several shallow earthquakes in the Pacific Northwest were also analyzed and do not show a consistent distribution.

Articles

Ludwin, R.S., S.D. Malone, R.S. Crosson, 1986 (in press), Washington Earthquakes, 1983, National Earthquake Information Service

Ludwin, R.S., S.D. Malone, R.S. Crosson, 1986 (in press), Washington Earthquakes, 1984, National Earthquake Information Service

Zervas, C.E. , and R.S. Crosson, 1985 (in press), Pn Observations and Interpretations in Washington, BSSA

Reports

Univ. of Wash. Geophysics Program, 1985, Quarterly Network Report 85-C on Seismicity of Washington and Northern Oregon

Univ. of Wash. Geophysics Program, 1985, Quarterly Network Report 85-D on Seismicity of Washington and Northern Oregon

Regional Seismic Monitoring in Western Washington, 1986, Contract 14-08-0001-21861 Final Technical Report 1985.

Univ. of Wash. Geophysics Program,1986 (in preparation), Compilation of Earthquake Hypocenters in Washington, 1980.

Univ. of Wash. Geophysics Program,1986 (in preparation), Compilation of Earthquake Hypocenters in Washington, 1981.

Abstracts

Ludwin, R.S. and Crosson, R.S., 1986, Teleseismic Residuals and Slab Structure in the Pacific Northwest, Earthquake Notes, Vol. 57, no.1, p. 10.

Crosson, R.S., 1986, Where is the Subducted Slab beneath the Pacific Northwest?, Earthquake Notes, Vol. 57, no.1, p. 10.

Investigations of Intraplate Seismic-Source Zones

9950-01504

W. H. Diment
Branch of Engineering Geology and Tectonics
U.S. Geological Survey
Box 25046, MS 966, Denver Federal Center
Denver, CO 80225

Investigations

1. Reprocessing selected parts of 320-km seismic-reflection data in upper Mississippi Embayment to investigate deep structure.

2. Quantitative geomorphic study of stream profiles in the southeastern part of the Ozark Mountains.

3. Interpretation of seismic-reflection data recorded on the Mississippi River.

4. Analysis of level line data in the upper Mississippi Embayment and environs.

5. Interpretation of two trenches excavated across the scarp of the Meers fault in Comanche County, Okla., in conjunction with personnel from the Oklahoma Geological Survey.

6. Interpretation of trench excavated near Blytheville, Ark., in 1982.

7. Analysis of high-resolution reflection data obtained across the Meers fault.

8. Effects of earthquakes on two perennially boiling wells in the Long Valley caldera, Mono County, Calif.

9. Analyses of seismological data from China.

10. Regional studies.

Results

1. Reprocessing of field tape records of seismic-reflection profiles to 11 s two-way traveltime has been completed on four profiles (Dwyer, 1985). An open-file report on them has been technically reviewed. Two abstracts have been published (Dwyer and Harding, 1985; Harding, 1985).

2. A draft report entitled "Analysis of stream-profile data for the eastern Ozark Mountains region and their geologic implications," by F. A. McKeown, M. J. Cecil, B. L. Askew, and M. B. McGrath, has been technically reviewed and has been submitted to BCTR for publication as a USGS Bulletin.

3. The interpretation of part of the seismic-reflection data recorded on the Mississippi River has been completed. (Crone and others, 1986)

4. Compilation and analysis of level line data for the upper Mississippi Embayment and vicinity was completed by Richard Dart and an open-file report is ready for technical review.

5. The two trenches across the Meers fault indicate that the scarp was formed by a reverse fault that dips to the northeast in the shallow subsurface. Nearly all of the deformation in the alluvium is accomplished by warping and flexing with only a small component of brittle deformation. Stratigraphic units in the trenches have a net vertical throw of more than 3 m. Radiocarbon age dates of samples from each of the trenches indicate that the last faulting event is younger than 1,500 yr B.P.

   Recent additional field studies have shown strong evidence that recent displacements on the Meers fault include a large component of lateral slip. Further analysis of the data will hopefully clarify the amount and timing of late Quaternary slip events.

6. The trench, excavated across prominent linear features in the Blytheville, Ark., area of the New Madrid seismic zone, failed to expose any near-surface faults but did reveal numerous liquefaction-induced sandblows that were probably produced by the 1811-1812 earthquakes. A report describing the results of the trenching study has been prepared (Haller and Crone, 1986).

7. A short, high-resolution seismic-reflection line was conducted across the Meers fault in Oklahoma. This data has been processed and shows a fault at approximately 271 m in depth which can be connected to the surface faulting. This fault has a displacement of about 30 m (Harding, 1985).

8. Temperature logs obtained in Chance No. 1 (south moat of the Long Valley caldera, Mono County, Calif.) in 1976, 1982, 1983, and 1985 show a progressive cooling in the uncased part of the hole. Examination of the rate of change suggests that the cooling began to accelerate about the time of the strong earthquakes of May 1980 (Diment and Urban, 1985). Temperature logs from Mammoth No. 1 (near Casa Diablo Hot Springs, 3 km west of Chance No. 1) obtained in 1979, 1982, and 1983 are also being processed and examined for seismically induced phenomena (Urban and Diment, 1984; 1985).

9. Under the Chinese-American Cooperative Earth Sciences Program, K. A. Shedlock and her colleagues from MIT and The Peoples Republic of China have conducted extensive studies of the nature, evolution, and seismicity of several intraplate basins China (Hellinger and others, 1985; Shedlock and others, 1985; Shedlock and Roecker, 1985). These studies are applicable to the better understanding of similar regimes in the United States.

10. L. C. Pakiser and W. D. Mooney perceived the need for the summary/review volume: "Geophysical framework of the Continental United States." A conference was held in Golden between March 17 and 20, 1986 and 24 papers were presented. Manuscripts for review are due in early spring. GSA has agreed to publish the product in their Memoir series.

Pakiser (1985) completed a review of seismic exploration of the crust and upper mantle in the Basin and Range Province.

Reports

Crone, A. J., Harding, S. T., Russ, D. P., and Shedlock, K. M., 1986, Seismic-reflection profiles of the New Madrid seismic zone--Data along the Mississippi River near Caruthersville, Missouri: U.S. Geological Survey Miscellaneous Field Studies Map MF-1863 [in press]

Diment, W. H., and Urban, T. C., 1985, Temperature variations with time in a perennially boiling well in the Long Valley caldera, Mono County, California: Observations in Change No. 1 (1976-83): Geothermal Resources Council Transactions, v. 9, part 1, p. 417-422.

Dwyer, Ruth-Ann, 1985, Seismic-reflection investigation of the New Madrid rift zone near Caruthersville, Missouri: Golden, Colo., Colorado School of Mines, Master's Thesis T-3159, 108 p.

Dwyer, R. A., and Harding, S. T., 1985, Mid-crustal seismic reflections from part of the New Madrid seismic zone: Earthquake Notes, v. 56, p. 26.

_____1985, Midcrustal fault in the New Madrid seismic zone as interpreted from seismic-reflection data: Earthquake Notes, v. 56, p. 72.

Haller, K. M., and Crone, A. J., 1986, Log of an exploratory trench in the New Madrid seismic zone near Blytheville, Arkansas: U.S. Geological Survey Miscellaneous Field Studies Map MF-1858 [in press]

Harding, S. T., 1985, Preliminary results of a high-resolution reflection survey across the Meers Fault, Comanche County, Oklahoma: Earthquake Notes, v. 56, p. 2.

Harding, S. T., 1985, The use of seismic-reflection data to interpret the earthquake history associated with intracratonic earthquakes: Society of Exploration Geophysicists, Expanded Abstracts, 55th Annual International Meeting, p. 188.

Hellinger, S. J., Shedlock, K. M., Sclater, J. G., and Ye, Hong, 1985, The Cenozoic evolution of the North China Basin: Tectonics, v. 4, p. 343-358.

Madole, R. F., and Rubin, Meyer, 1985, Holocene movement on the Meers fault, southwest Oklahoma: Earthquake Notes, v. 56, p. 1.

Pakiser, L. C., 1985, Seismic exploration of the crust and upper mantle of the Basin and Range province: Geological Society of America, Centennial Special Volume 1, p. 453-469.

Shedlock, K. M., Hellinger, S. J., and Ye, Hong, 1985, Evolution of the Xialiao basin: Tectonics, v. 4, p. 171-185.

Shedlock, K. M., Jones, L. M., and Xiufang, Ma, 1985, Determination of elastic wave velocity and relative hypocenter locations using refracted waves. II. Application to the Haicheng, China, aftershock sequence: Seismological Society of America Bulletin, v. 75, p. 427-439.

Shedlock, K. M., and Roecker, S. W., 1985, Determination of elastic wave velocity and relative hypocenter locations using refracted waves. I. Methodology: Seismological Society of America Bulletin, v. 75, p. 415-426.

Shedlock, K. M., Roecker, S. W., and Jin, Anshu, 1985, Crust and upper mantle of the Bohai, China region: Transactions of the American Geophysical Union [EOS], v. 66, p. 987.

Urban, T. C., and Diment, W. H., 1984, Precision temperature measurements in a deep geothermal well in the Long Valley caldera, Mono County, California: EOS [American Geophysical Union Transactions], v. 65, p. 1084-1085.

Urban, T. C., and Diment, W. H., 1985, Convection in boreholes: limits on interpretation of temperature logs and methods for determining anomalous fluid flow, in Proceedings National Water Well Association Conference on surface and borehole geophysical methods in ground-water investigations: National Water Well Association, Worthington, Ohio, p. 399-414.

Investigation of Seismic-Wave Propagation for Determination of Crustal Structure

9950-01896

Samuel T. Harding
Branch of Engineering Geology and Tectonics
U.S. Geological Survey, MS 966
Denver Federal Center, Box 25046
Denver, CO 80225
(303) 236-1572

Investigations

1. Processing and interpreting seismic-reflection lines from Charleston, S.C.

2. Interpreting data gathered from the Crater Flat, Nev.

3. Investigating and processing high-resolution seismic-reflection lines for the following:

   (a) Breccia pipes at the south rim of the Grand Canyon, Ariz.
   (b) Line connecting VH-1 to VH-2 then west across Crater Flat, Nev.
   (c) Line through Tarantula Canyon and east across Crater Flat, Nev.
   (d) Line east of Lathrop Well, Nev., along old railroad grade.
   (e) Line across Sevier Valley south of Aurora, Utah.

Results

1. Three areas near Charleston, S.C., were surveyed using high-resolution seismic-reflection methods to investigate faulting in the uppermost sediments of the Coastal Plain and to investigate tectonic significance of variations in the thickness of shallow sedimentary units. The first survey crossed the Gants(?) fault and coincided with a lower resolution VPISU Vibroseis line. The high-resolution survey showed reverse displacement on a fault with an apparent north dip of 70°, extending from 130- to 680-m depth. Vertical fault displacement was 20 m at 130-m depth and 40 m at 680-m depth, consistent with VPISU results. The reflection data and two 200-m deep wells showed unconformable middle Eocene sediments thickening by 100 m from the fault's downthrown side and its upthrown side. This thickening occurred within a filled channel and had no apparent tectonic significance. In the second survey, two lines were run north-south and eastwest near Hollywood, where there was extensive liquefaction and an exposed small reverse fault. A south-dipping reverse fault was found on the north-south line. The fault could be traced to within 212 m of the surface where it had a vertical displacement of 10 m. The east-west line did not intersect this fault. The exposed fault had no apparent expression at depth. A third survey was run north-west from Fort Dorchester for 2.4 km into the postulated Ashley River fault zone. No significant faulting was seen on this line.

2. As part of the NNWSI program to assess the seismic hazard to the planned Nevada nuclear-waste facilities, two high-resolution seismic-reflection surveys were conducted across two scarps near Beatty, Nev., by employing

the Mini-Sosie high-resolution seismic-reflection technique. The first survey was run across the scarp mapped as the Beatty fault. The site was approximately 6 km south of the town of Beatty. Reflection profiles from this site indicated no evidence of faulting that could be correlated with the scarp. The second survey was located across a prominent down-to-the-west fault scarp on the east side of Crater Flat approximately 26 km southeast of Beatty. The resulting profile had only one distinct reflector that could be carried along the length of the section. This reflector was interpreted to be complexly faulted. A major, nearly vertical fault was projected to the surface fault scarp. This fault (located east of the fault scarp) appeared on a reflector at 160-m depth. This fault, if associated with the scarp, represents a strike-slip fault or a reverse fault, or perhaps a combination of the two . No hint of normal faulting could be seen from the collected data that could be associated with the fault scarp.

3. Still processing breccia-pipe, Crater Flat, Tarantula Canyon, and Sevier Valley data.

Report

Harding, S. T., and Stewart, R. M., 1986, High-resolution seismic-reflection surveys near Charleston, South Carolina: Earthquake Notes, v. 57, no. 1, p. 17.

Harding, S. T., Preliminary results of high-resolution seismic-reflection survey conducted across the Beatty scarp, Beatty, Nevada, and Crater Flat scarp, Nevada: U.S. Geological Survey Bulletin. (Branch approval 8/85)

Swadley, W. C., Yount, J. C., and Harding, S. T., Reinterpretation of the Beatty scarp: U.S. Geological Survey Bulletin. (Branch approval 9/85)

Whitney, S. W., Shroba, R. R., Simond, F. W., and Harding, S. T., Recurrent Quaternary movement on the Windy Wash fault, Nye County Nevada: Geological Society of America Abstracts with Programs. (Branch approval 1/86)

Analysis of Earthquake Data from the Greater Los Angeles Basin and Adjacent Offshore Area, Southern California

#14-08-0001-G-1158

Egill Hauksson
Ta-liang Teng
Geoffrey Saldivar
Center for Earth Sciences
University of Southern California
Los Angeles, CA 90089-0741
(213) 743-7007

INVESTIGATIONS

Analyze earthquake data recorded by the USC and CIT/USGS networks during the last 12 years in the Los Angeles basin to improve earthquake locations including depth and to determine the detailed patterns of faulting in the study region. A study of the 1930 Santa Monica (M=5.2) and the 1979 Malibu (M=5.0) mainshock-aftershock sequences has been completed.

RESULTS

Two moderate-sized earthquakes, the 1930 Santa Monica and the 1979 Malibu earthquake, of magnitude 5.1 and 5.0 have been reported in the Santa Monica Bay, southern California. We have studied these two mainshock-aftershock sequences and the results are presented in a paper by Hauksson and Saldivar (1986). In the paper we show that the 1979 Malibu (M_L=5.0) mainshock-aftershock sequence probably occurred on the eastern end of the Anacapa-Dume fault. The Santa Monica earthquake (M_L=5.1) that occurred August 31, 1930 was relocated using station delays calculated with the 1979 data set. The relocated 1930 epicenter is located near the western end of the Santa Monica fault (Figure 1). The 1979 and 1930 mainshocks thus can be interpreted to define a 6-8 km north-south offset between the Anacapa-Dume and Santa Monica faults. Documenting the segmentation of these two fault systems is important because the lateral offset suggests that they are unlikely to rupture simultaneously in one large earthquake.

We have shown that the Santa Monica Bay 1930 and 1979 mainshock-aftershock sequences are associated with the west-trending reverse faults along the southern margin of the Transverse Ranges. Two very different styles of faulting and crustal deformation occur in Santa Monica Bay. The frontal fault system of the Transverse Ranges, which show predominantly reverse faulting strikes east-west along the northern edge of Santa Monica Bay (Figure 2). In the southern and western part of Santa Monica Bay the tectonic deformation is characterized by right-lateral strike-slip faulting and in some cases reverse faulting along north-northwest-trending faults. Since the Bay is covered by sediments that are being transported out to the Santa Monica basin, the intersection of the west-trending and the north-northwest-trending faults in Santa Monica Bay remains poorly understood. Understanding the relationships between the onshore and offshore faults is necessary to quantify seismic hazards in the Los Angeles basin. The offshore faults constitute special hazards to coastal development through surface rupture,

seismic shaking, ground failure and in rare cases tsunamis.

REPORTS

Saldivar, G., E. Hauksson and T. L. Teng, The Malibu Earthquake (M=5.0) and Its Aftershock Sequence, Southern California, January, 1979, EOS Trans. Amer. Geophys. Union, 66, 953, 1985.

Hauksson, E., Constraints on the Velocity Structure of the Crust in the Los Angeles Basin and the Central Transverse Ranges, Southern California, EOS Trans. Amer. Geophys. Union, 66, 973, 1985.

Hauksson, E. and G. Saldivar, The 1930 Santa Monica and the 1979 Malibu, California, Earthquakes, submitted to BSSA, April 1986.

Hauksson, E., T. L. Teng and G. Saldivar, Analysis of Earthquake Data from the Greater Los Angeles Basin and Adjacent Offshore Area, Southern California, U.S.C. Annual Technical Report #86-5, prepared for the U.S.G.S., 31 pp., 1986.

st-85-363

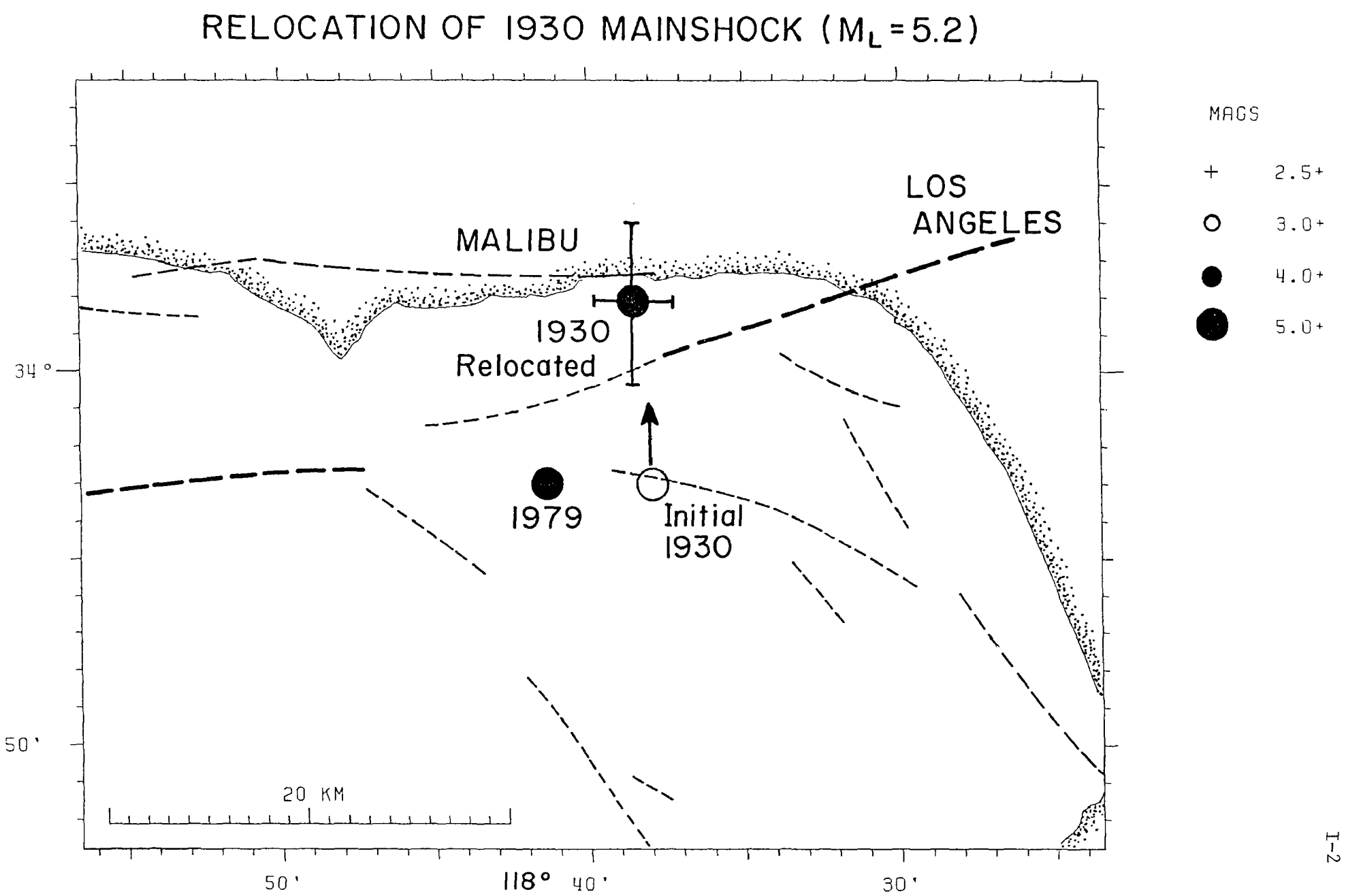

Figure 1. Epicentral map of: 1) 1979 mainshock; 2) the Gutenberg et al. (1932) initial location of the 1930 mainshock; and 3) relocated epicenter of the 1930 mainshock with error bars, based on the 1979 station delays.

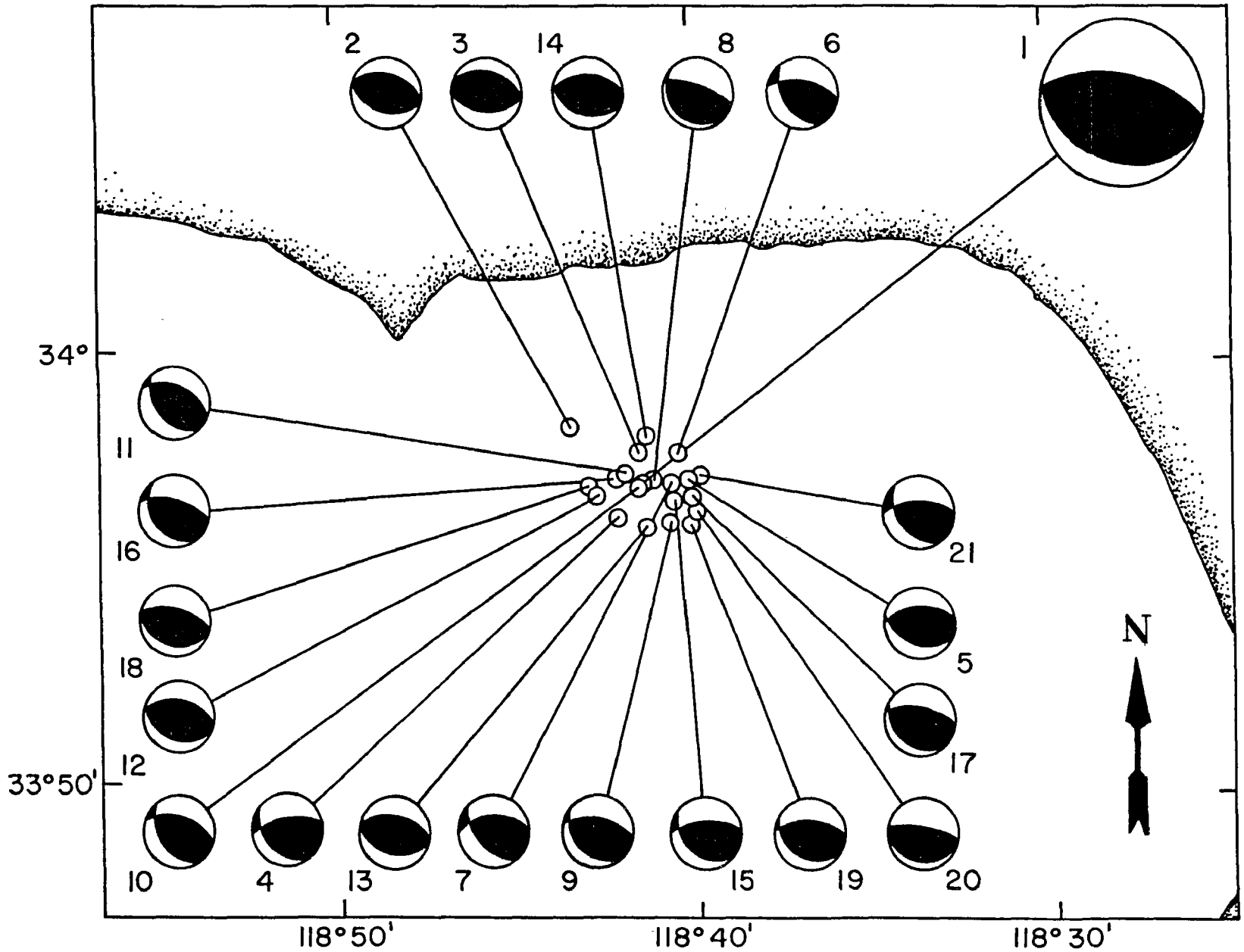

Figure 2. Lower hemisphere focal mechanisms for the 1979 Malibu earthquake (M=5.0) (large symbol to the upper right) and 20 aftershocks of magnitude greater than 3.0. Numbers shown adjacent to each mechanism refer to Table 4.

Seismic Source Characteristics of Western States Earthquakes

Contract No. 14-08-0001-21912

Donald V. Helmberger

Seismological Laboratory,
California Institute of Technology
Pasadena, California 91125
(818)-356-6998

Investigation

A program of continuing study on the characteristics of pre and post - 1962 U. S. earthquakes is progressing. It is based primarily on some recent advances in wave-propagational codes for laterally varying Earth models. Structures with arbitrary variations in two dimensions can now be handled with double-couple type excitations. More precise Green's functions lead directly to a clearer picture of detailed source properties. Four major tasks will be addressed in the next few years, namely;

1.) Extended analysis of low gain (strong motion) recordings of earthquakes to fix the depths of main energy release.

2.) Analysis of body waves at all ranges using direct inversion for fixed earth models and application of the intercorrelation method to measure differences between events and develop master events per region.

3.) Analysis of historic events (pre 1962) using same methods (masters) but on a more regional basis.

4.) Reassessment of events with sparsely recorded strong motions using more accurate Green's functions computed from laterally varying earth models.

Results

A large scale data collection effort of WWSSN and LRSM records is in progress along with waveform inversion for source parameters. The results for representative events was discussed in the last USGS open-file report 86-31. In this report, we briefly discuss the behavior of locally trapped surface waves generated by the San Fernando earthquake.

To treat the complex geology associated with the Los Angeles region, we have developed a fourth-order finite-difference code to generate synthetic strong motions for double-couple sources in elastic media (Vidale et. al., 1985). In the first step we assume a line source running through the source region aligned parallel to the long axis of a basin or geologic structure which is idealized to be infinite in length. A "near field" line excitation is applied such that it produces SH, P and SV vertical radiation patterns compatible with analytic asymptotic dislocation theory. Next, a line-to-point source transformation is applied to the finite-difference results which produces the familiar point source Green's functions. In general, synthetic motion generated by this procedure agree well with those generated by other methods for simple layered models. Results appropriate for the complex but approximately two-dimensional geological structure associated with the San Fernando earthquake are presented in Figure 1. Liu and Heaton (1984) collected strong-motion records from the 11 stations marked by solid triangles in the upper portion of Figure 1. Panel (a) displays the two-dimensional cross-section through the structure from North-to-South derived from the study by Duke et. al. (1978). The transverse components of the data set discussed by Liu and Heaton (1985) are displayed in (b). Note that L166, D068, and D057 are located on hard rock sites in or near the Santa Monica Mountains (see Hanks, 1975) and are amazingly similar in waveshape and amplitude.

Normalizing the motions in waveshapes and amplitude to D068 produces the comparison in Figure 1. The over-all agreement is quite good and a substantial improvement over flat-layered predictions is apparent, especially in amplitude, see Figure 1c. Comparable results for the vertical and radial components are given in Vidale and Helmberger (1986).

A more detailed cross-section displaying the layered structure is given in Figure 2 along with a complete record section in the lower panel. The role of the sloping sides of the basin is to either create or destroy surface waves. When shooting down dip (L.A. basin) the seismic rays are trapped by the sloping structure while the reverse is true for the rays approaching the Santa Monica ridge, see Vidale and Helmberger (1985). Numerical experiments indicate that only deep sources, greater than 8 km, excite surface waves in the L. A. basin with direct S body waves, as is observed in the data. Shallower sources would tend to excite large surface waves in the San Fernando basin which would spill over into the L. A. basin and overwhelm the direct S induced surface waves.

References

Duke, C. M., and A. K. Mal, Site and source affects on earthquake ground motion, *Engineering Report*, UCLA-ENG-7890, 1978.

Hanks, T. C., Strong ground motion of the San Fernando, California, earthquake: Ground displacement, *Bull. Seismol. Soc. Am.*, **65**, 193-225, 1975.

Liu, H.-L., and T. H. Heaton, Array analysis of the ground velocities in the 1971 San Fernando, California, earthquake, *Bull. Seismol. Soc., Am.*, **74**, 1951-1968, 1984.

Vidale, J. E., and D. V. Helmberger, Path effects in strong motion seismology, *Seismic Strong Motion Synthetics*, chapter on, *Methods of Computational Physics*, Ed., Bruce Bolt, submitted, November 12, 1985.

Vidale, J. E., D. V. Helmberger, and R. W. Clayton, Finite-Difference synthetic seismograms for SH-waves, *Bull. Seismo. Soc., Am.*, **75**, no. 6, 1765-1782, 1985.

Vidale, J. E., and D. V. Helmberger, Finite difference modeling of strong motions; 1971 San Fernando Earthquake, in preparation, 1986.

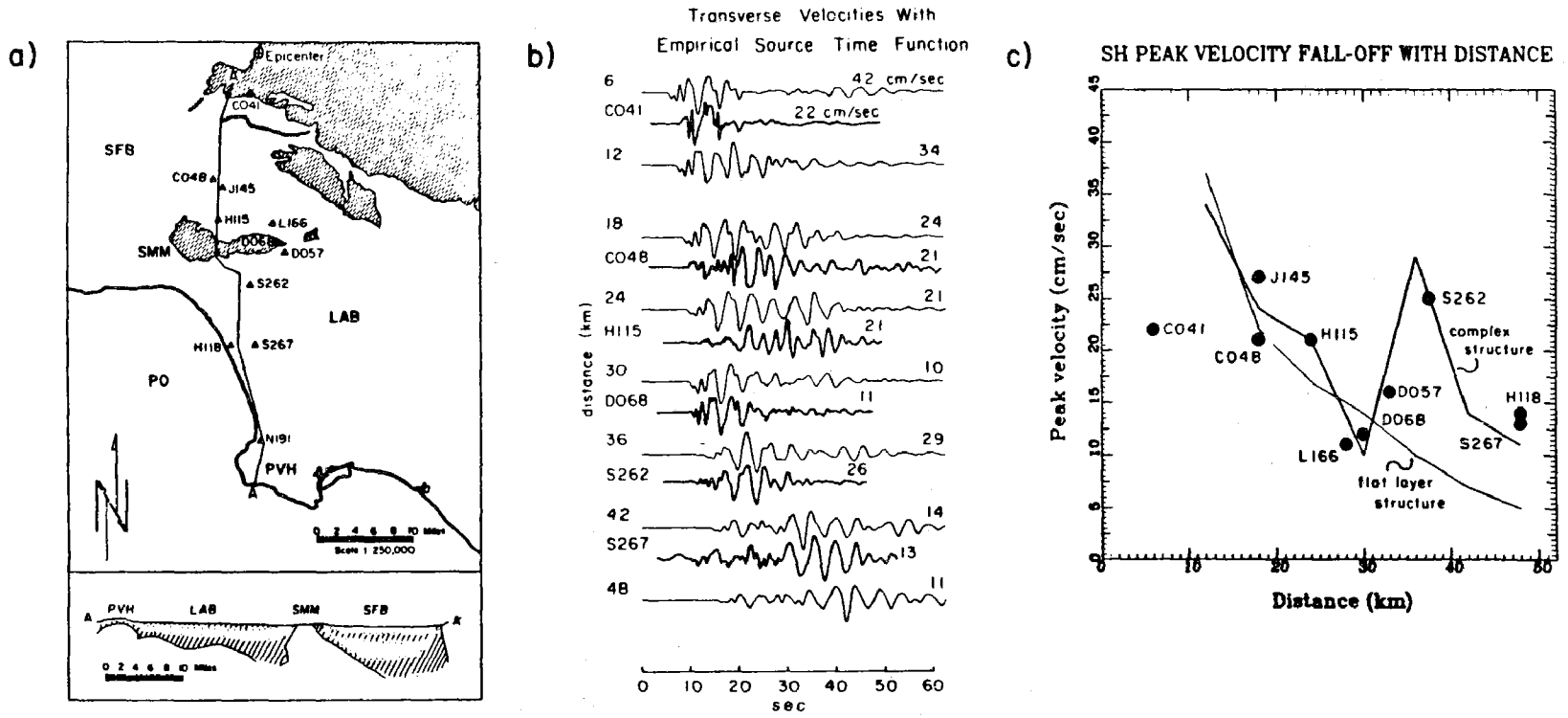

Figure 1: **a)** The locations of a profile of strong motion stations which cross San Fernando Valley (CO48, J145, H115), the hard rock ridge separating the San Fernando Valley (D068, L166, D057) and reaching across the L.A. basin (S262, S267, H118). A cross-section along this profile is displayed on the bottom, after Duke, et. al. **b)** Comparison of the observed transverse component of motion (heavy lines) and synthetics (thin lines). **c)** Comparison of amplitude decay functions with a flat-layered model versus the more realistic model.

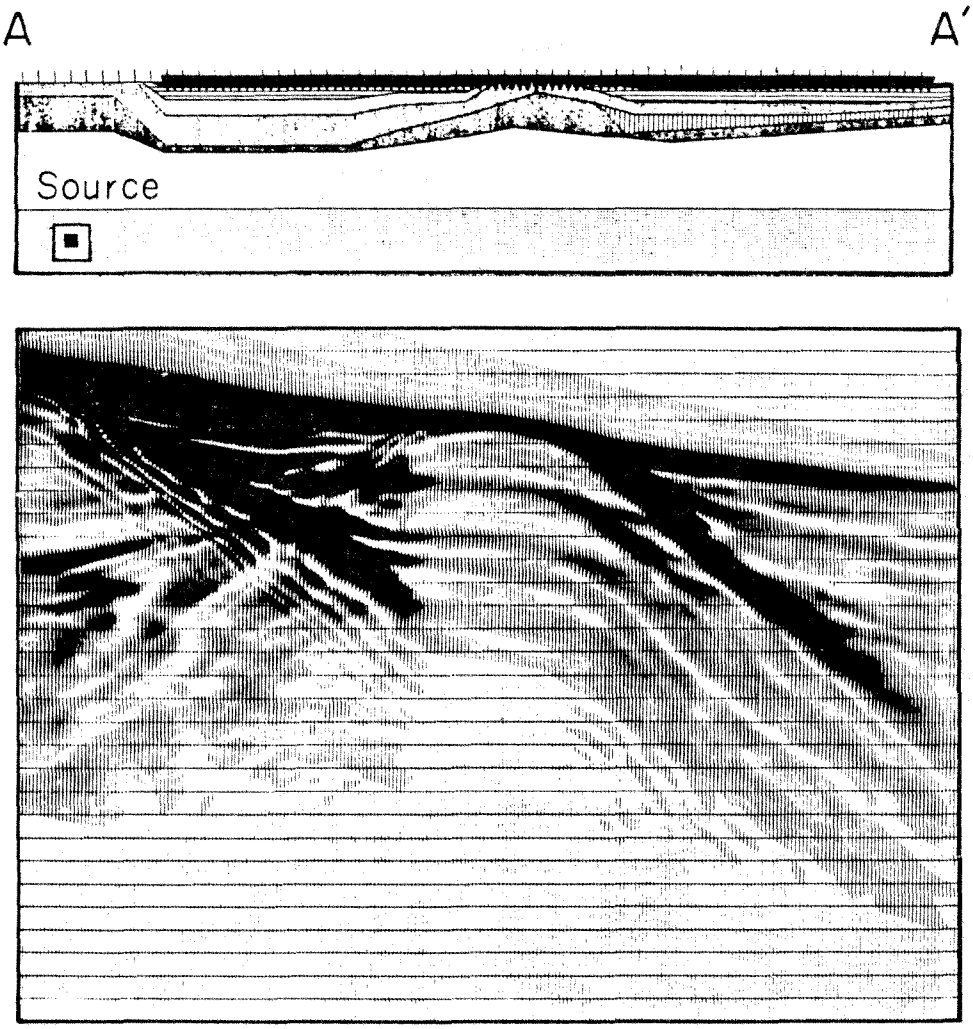

Figure 2: The upper panel contains the cross-section geometry where the velocities range from; .6, 1.4, 1.8, 3.4, 4.0 km/sec from top to bottom. The lower panel contains the record section for the source located at a depth of 10 km.

Earthquake Hazard Research in the Central United States

14-08-0001-G1090

Robert B. Herrmann
Department of Earth and Atmospheric Sciences
Saint Louis University
P.O. Box 8099 Laclede Station
St. Louis, MO 63156
(314) 658-3131

Goals

1. Perform research on the earthquake process in the New Madrid Seismic Zone to delineate the active tectonic processes. 2. Perform more general research relating to the problems of the eastern U. S. earthquake process and of the nature of eastern U. S. earthquakes compared to western U. S. earthquakes.

Investigations

1. A reinvestigation of spectral scaling of earthquakes in the Central Mississippi Valley Seismic zone is underway. Care is being taken to determine a corner frequency versus seismic moment scaling which is obtained from vertical component Lg recordings that have been corrected properly for anelastic attenuation.

2. Surface waves of the January 31, 1986 Cleveland, Ohio earthquake are being studied. Preliminary results points to a strike-slip focal mechanism, with one nodal plane striking approximately north-south, a depth of 8 km, and a seismic moment of about 1.0E+23 dyne-cm. Recent acquisition of Canadian long-period data will refine the strike and depth estimates. An attempt will be made to model the strong motion records of the main shock.

Results

Two papers were given at the 1986 SSA meeting at Charleston, South Carolina, on Lg spectral scaling. This work is being performed by C. Carr and C. Finn. Figure 1 presents preliminary results. The solid curve outlines the corner frequency - seismic moment estimates based on short distance observations made by the USGS in the eastern and western United States (Harr et al, 1986). The symbols in Figure 1 indicate our determinations using earthquakes within the Central Mississippi Valley Regional Seismic Network (local P, local S), events immediately outside the network at distances of 250 - 300 km (Arkansas P and Arkansas Lg), central Mississippi Valley Seismic Network estimates of the 1983 Goodnow, New York earthquake (at a distance of 1000 km), and estimates using the ECTN recordings of the 1982 Miramichi earthquakes. With the exception of the Miramichi values which are station averages, the other estimates are individual station estimates. Variability is seen in the New York data set. All data are corrected for a frequency dependent Q operator. Contrary to the point made by Haar et al, (1986), the Lg estimates match

the short distance estimates well.

We conclude that Lg can be used to estimate source properties and also agree with previous statements by Haar et al (1986) that the earthquake process in the eastern U. S. is similar to that in the western U. S.

REFERENCES

Haar, L. C., C. S. Mueller, J. B. Fletcher, and D. M. Boore (1986). Comments on "Some Recent Lg Phase Displacement Spectral Densities and their Implications with Respect to Prediction of Ground Motions in Eastern North America," Bull. Seism. Soc. Am 76, 291-296.

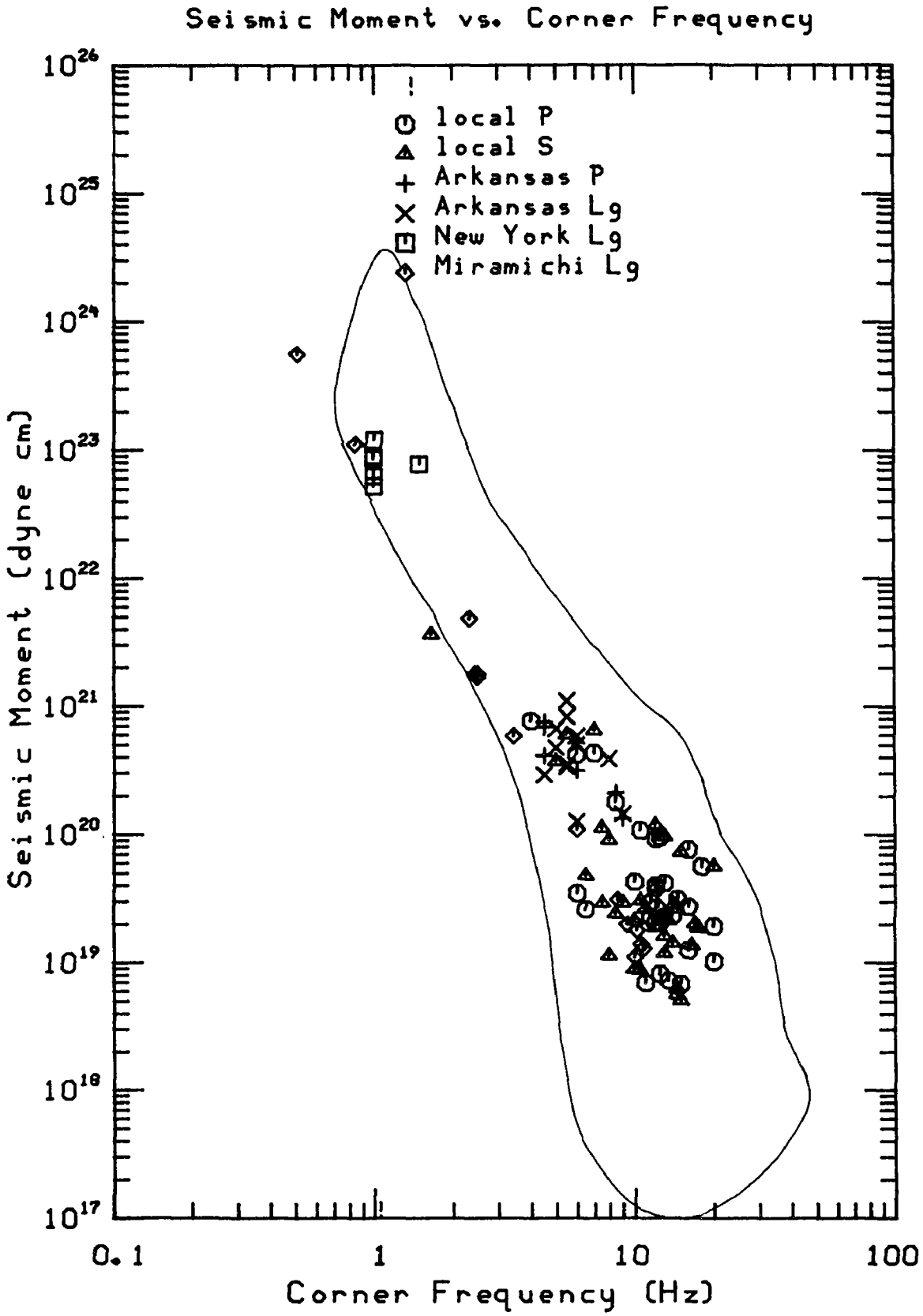
Seismic Moment vs. Corner Frequency
local P
local S
Arkansas P
Arkansas Lg
New York Lg
Miramichi Lg
Seismic Moment (dyne cm)
Corner Frequency (Hz)
10^26
10^25
10^24
10^23
10^22
10^21
10^20
10^19
10^18
10^17
0.1
1
10
100

Tectonics of Central and Northern California

9910-01290

William P. Irwin
Branch of Engineering Seismology and Geology
U. S. Geological Survey
345 Middlefield Road, MS 977
Menlo Park, CA 94025
(415) 323-8111, ext. 2065

Investigations

1. Preparation of a geologic map of the Klamath Mountains and adjacent areas, California and Oregon (scale 1:500,000) for purposes of tectonic analysis of the region.

2. Continued preparation of a geologic map of the Redding 2-degree sheet, California (scale 1:250,000), in collaboration with J.P. Albers and others.

3. Paleomagnetic study to determine the rotational and translational histories of the accreted terranes of northern California, in collaboration with E.A. Mankinen and C.S. Gromme.

4. Extensional tectonics of northern California, in collaboration with R.A. Schweickert.

5. Study of some geologic features related to the San Andreas fault in the Parkfield area.

6. Survey of the literature preparatory to writing a chapter on plate tectonic development for a multi-authored bulletin on the San Andreas fault.

Results

Initial compilation of geologic data from the principal source maps is virtually completed for the Klamath Mountains. The first-order units of the compilation are the accreted terranes. These are subdivided into various Paleozoic and Mesozoic lithogenetic units such as sedimentary rocks, volcanic rocks, ophiolitic rocks, and preamalgamation (syngenetic) plutons. Postamalgamation plutons are indicated separately. Overlap sequences of post-Nevadan strata form the eastern boundary of the Klamath Mountains province: the western boundary is a fault that juxtaposes the rocks of the Klamath Mountains against post-Nevadan strata of the Coast Ranges. Preparation of explanatory material is now underway.

With its abundance of thrust-bounded terranes, the Klamath Mountains are generally thought of as an example of Mesozoic convergence tectonics. However, certain evidence now suggests the possibility that extensional tectonics may have been important in the development of the Klamath Mountains during Tertiary time. Grabens and half grabens of Weaverville Formation (Oligocene) are prominent along a NE-trending zone in the southern part of the province. Some faults that form the grabens are extraordinarily gently dipping. The La Grange fault dips 22 degrees SE and has a remarkably well-developed mylonitic footwall surface. The trace of the La Grange fault is fairly well aligned to the NE with a probable fault boundary between the Trinity ultramafic sheet and the early Paleozoic strata of the Redding section. Various factors including the Oligocene age, the gently dipping normal faults, and the mylonitic surfaces are reminiscent of the metamorphic core complexes of more easterly parts of the Cordillera. This leads us to speculate that the Trinity ultramafic sheet and associated metamorphic rocks may be the equivalent of a metamorphic core complex, and the mylonitic surface of the La Grange fault may be a detachment surface on which the Weaverville Formation and Redding section have slid southeastward. Similarly, northwestward sliding off the Trinity ultramafic sheet may account for the stacked "thrust" plates of early Paleozoic rocks of the Yreka-Callahan area.

Reports

Mankinen, E.A., Gromme, C.S., and Irwin, W.P., 1985, Paleomagnetic constraints on the accretionary history of the Klamath Mountains province, California and Oregon [abs.]: Eos (American Geophysical Union Transactions), v. 66, no. 46, p. 863.

STUDIES OF QUATERNARY FAULTING THROUGH THE ANALYSIS OF SMALL FAULTS AND FRACTURES, NORTH COASTAL CALIFORNIA

Contract no. 14-08-0001-22009

Harvey M. Kelsey
Department of Geology
Western Washington University
Bellingham, WA 98225

Gary A. Carver
Department of Geology
Humboldt State University
Arcata, CA 95521

Investigations

Numerous faults offset late Neogene (mainly Pleistocene) sediments along the California coast in the vicinity of the Mendocino triple junction. These faults are difficult to study because of uniformly poor exposure along the fault trace. Associated with all fault traces is a zone of deformation consisting of fracture sets and small faults. Detailed measurements of such fault-associated deformation in late Neogene sediment, exposed in river banks and road cuts, has substantially improved our understanding of Quaternary faulting. To date, such detailed study has been done at three locations (fig. 1). Fault traces shown on fig. 1 include both faults that demonstrably offset Plio-Pleistocene sediments and the lineaments associated with the Maacama-Garberville fault zone and the Eaton Roughs-Lake Mountain fault zone. Late Quaternary landforms (ridgetop depressions, sag ponds, notched ridges), as well as right lateral offset of distinctive Franciscan melange blocks, suggest these lineaments are traces of faults with Quaternary offset.

Results

Analysis of fracture orientation has helped elucidate both individual fault style and regional strain. Studies to date show a clear association between the style of the major fault (thrust, strike slip) and the orientation of fractures exposed in proximity to the fault zone.

For example, faults of the Mad River fault zone (MRfz) (Carver and others, 1983) in northern California all dip less than 40 degrees within 17 km of the coast (Woodward Clyde Associates, 1980). Stereonets of poles to fractures in close proximity (most cases within 200 m) to these low angle faults reveal a conjugate pair of low angle fractures (fig. 2). The fractures probably developed prior to, and during, initial rupture of the faults through the overlying Pleistocene sediments. The fractures developed before substantial

folding. Evidence for this observation is that unfolded beds near a fault clearly show long angle conjugate fracture pairs and folded beds near a fault show a similar fracture pattern only after fractures are rotated with bedding as bedding is rotated back to horizontal.

A second example of structural analysis of fractures adjacent to a major fault is deformation associated with the Lost Man fault north of Orick, California (Kelsey and Cashman, 1983). Fractures were measured at six localities in Gold Bluffs sediments adjacent to the fault. The fractures were invariably high angle and formed a conjugate set. The Lost Man fault is a high angle lateral fault based on outcrop pattern and on the strain ellipse deduced from the nature of small folds and secondary faulting associated with the fractures (Kelsey and Cashman, 1983).

The above examples suggest that high angle conjugate fractures are closely associated with steeply dipping lateral faults. Low angle fractures appear to be associated with thrust and reverse faults. High angle fractures may be associated with low angle faults, and vice-versa, but they are a distinct secondary population, if present.

Using the above analysis, we suggest that fracture measurement in sediments adjacent to a poorly exposed fault can indicate the dip of the fault and its movement style. Fracture/small fault patterns exhibit either conjugate symmetry (plane strain) or orthorhombic symmetry (non-plane strain). Though quantitative analysis of the fractures in terms of deducing principal strain axes is not yet accomplished, such analysis is probably feasible and will be carried by using the techniques of Reches and Dieterich (1983) and Krantz (1986). At this point, however, we note the consistent fracture-fault association in the field and suggest it is a useful tool to analyse recent faulting characteristics in areas of poor exposure.

Using the above techniques, fracture measurements can be used to document changes in structural style along a fault as it bends. For example, the low angle reverse and thrust faults of the Mad River fault zone (MRfz) (fig. 2) near the coast become less well exposed as the zone trends to the southeast where it merges with the NNW-trending Eaton Roughs fault zone (Kelsey and Allwardt, 1983). The Eaton Roughs fault zone is defined by offset mega-blocks of sandstone and by numerous undrained depressions and instances of unstable ground which together define a straight trace for 66 km to the south-southeast (Kelsey and Allwardt, 1983) (fig. 1). Of interest is the tectonic transition at the bend in the Eaton Roughs-Mad River fault zones near Maple Creek (fig. 2). Systematic fracture measurements in the offset Pleistocene sediments at sites starting near the coast and going inland along the fault toward the fault bend show that fractures change from near horizontal to vertical near the bend (fig. 2). Fracture-fault associations lead to the interpretation that faults of the Mad River zone steepen toward the bend and the faults become part of the high angle Eaton Roughs fault zone to the SSE of the fault bend. Fracture measurement has therefore helped elucidate the nature of the transition between a coastal contractile zone and an inland lateral zone. In this case, the dextral motion of the Eaton Roughs fault is, in part, transferred to low angle thrust motion along the Mad River fault zone.

Fracture-fault association can also be used as a means to decipher contrasting style and relative age of two faults. The faulted Neogene sediments near Garberville, California (location 3 in fig. 1) provided a field example of

this technique. The Garberville sediments are bounded on the northeast by the Dean Creek fault, and on the southwest the sediments are in depositional contact with the Franciscan and this contact is offset along the Garberville fault (fig. 3). Youngest sediments at Garberville are probably early Pleistocene, though most of the unit is Miocene (J. Menack, oral communication, 1985). The Garberville fault appears to trend south-southeast along a well defined lineament toward Laytonville where it connects with the northernmost mapped traces of the Maacama fault zone (Upp, 1982). The dip of the Garberville fault near Garberville and its relation to the Dean Creek fault are uncertain. A possible explanation for these uncertainties is provided by fracture measurements at sites adjacent to each of these faults (fig. 3).

Fractures associated with the Dean Creek fault are low angle and suggestive of a conjugate pair. The conjugate symmetry is only apparent after fractures have been rotated with bedding as bedding is rotated back to horizontal. The Dean Creek fault pattern is less clear than for the thrust faults of the MRfz because the Garberville sediments are older and have subsequently experienced a different stress regime. However, it appears the Dean Creek fault is low angle, perhaps a thrust, and initial faulting pre-dates folding.

Fractures at measurement sites adjacent to the Garberville fault are (with one exception) uniformly high angle (fig. 3). For the Garberville fault, fracture rotation with bedding to the horizontal only creates a confusing mixture of high and low angle fracture. In other words, there is no compelling reason to believe these fractures occurred prior to folding.

Preliminary conclusions for Garberville data are that the low angle fractures near the Dean Creek fault formed early (prior to and during initial folding), and the high angle fractures, associated with the Garberville fault, formed later (after folding). The Dean Creek fault records an episode of SW-NE contraction of the Neogene sediments and the Garberville fault is a later strike slip structure, presumably active today. The Garberville fault postdates folding in the Neogene sediments. The Dean Creek fault may or may not be active--it could rupture under present right lateral shear, but it appears to have formed under a quite different tectonic regime. This tectonic regime may be coincident with a location of the Mendocino Triple Junction (MTJ) due west or southwest offshore, when the San Andreas fault zone terminated well to the south of Garberville. Plate reconstructions suggest this occurred 4-8 my ago (Engebretson and others, 1985). Therefore, fracture analysis has indicated relative ages for these faults and the analysis suggests the Dean Creek fault was formed prior to the passage of the MTJ and thus is less likely to be presently active.

References

Carver, G. A., Stephens, T. A., and Young, J. C., 1983, Quaternary thrust and reverse faulting on the Mad River fault zone, coastal northern California: Geological Society of America Abstracts with Programs, v. 15, no. 5, p. 316.

Engebretson, D. C., Cox, A., and Gordon, R. G., 1985, Relative motions between oceanic and continental plates in the Pacific basin: Geological Society of America Special Paper 206, 59 p.

Jennings, C., 1977, Geologic Map of California, 1:750,000: California Division of Mines and Geology.

Kelsey, H. M., and Allwardt, A. O., 1983, Evidence for a major Quaternary fault zone in the Central Belt Franciscan melange, northern California: Geological Society of America Abstracts with Programs, v. 15, no. 5, p. 316.

Kelsey, H. M., and Cashman, S. M., 1983, Wrench faulting in northern California and its tectonic implications: Tectonics, v. 2, p. 565-576.

Kelsey, H. M., 1986, Late Neogene tectonic deformation along the margins of the central belt malange, northern California: Geological Society of America Abstracts with Programs, v. 14, no. 7, p. 528.

Krantz, R. W., 1986, Orthorhombic fault patterns and three-dimensional strain analysis, northern San Rafael Swell, Utah: Geological Society of America Abstracts with Programs, v. 18, no. 2, p. 125.

Reches, Z., and Dieterich, J. H., 1983, Faulting of rocks in three dimensional strain fields I. Failure of rocks in polyaxial servo-control experiments: Tectonophysics, v. 95, p. 111-132.

Upp, R. R., 1982, Holocene activity on the Maacama fault, Mendocino County, California: (Ph.D. dissertation) Stanford University, 112 p.

Woodward-Clyde Associates, 1980, Evaluation of the potential for resolving the geologic and seismic issues at the Humboldt Bay Power Plane Unit No. 3, Appendices, Woodward-Clyde Consultants, Walnut Creek, California.

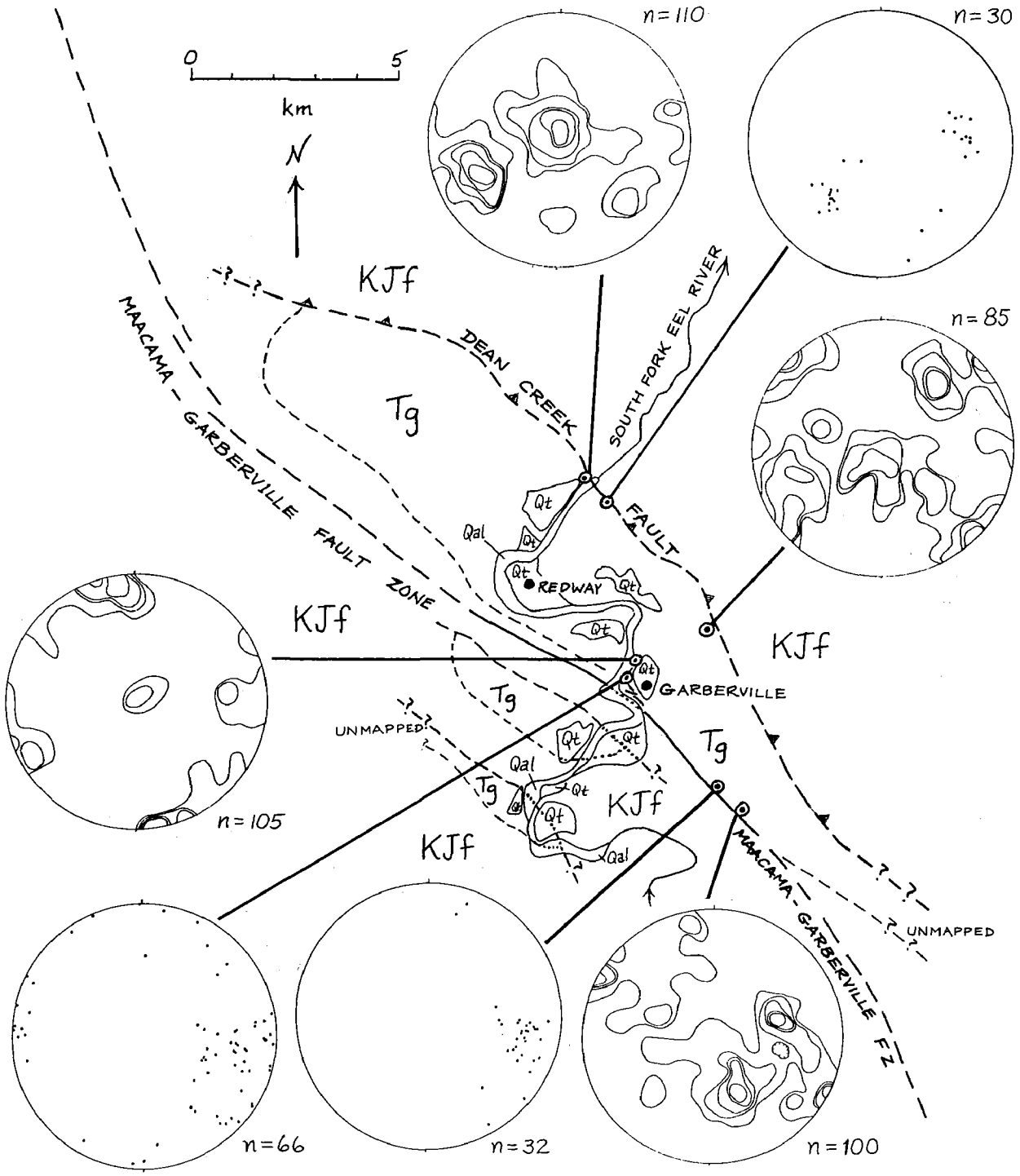

Figure 3. Stereonet plots of poles to small faults and fractures for 7 sites along the faulted margins of the late Neogene sedimentary unit (Tg) near Garberville, California. Pole densities are contoured for sites with more than 80 measurements. Contours are 1, 2.5, 5, 7.5, and 10% per 1% area. The upper 3 stereonets show low angle conjugate fractures associated with the Dean Creek Fault and the lower 4 stereonets show generally high angle, in some instances conjugate, fractures associated with the Maacama-Garberville fault zones.

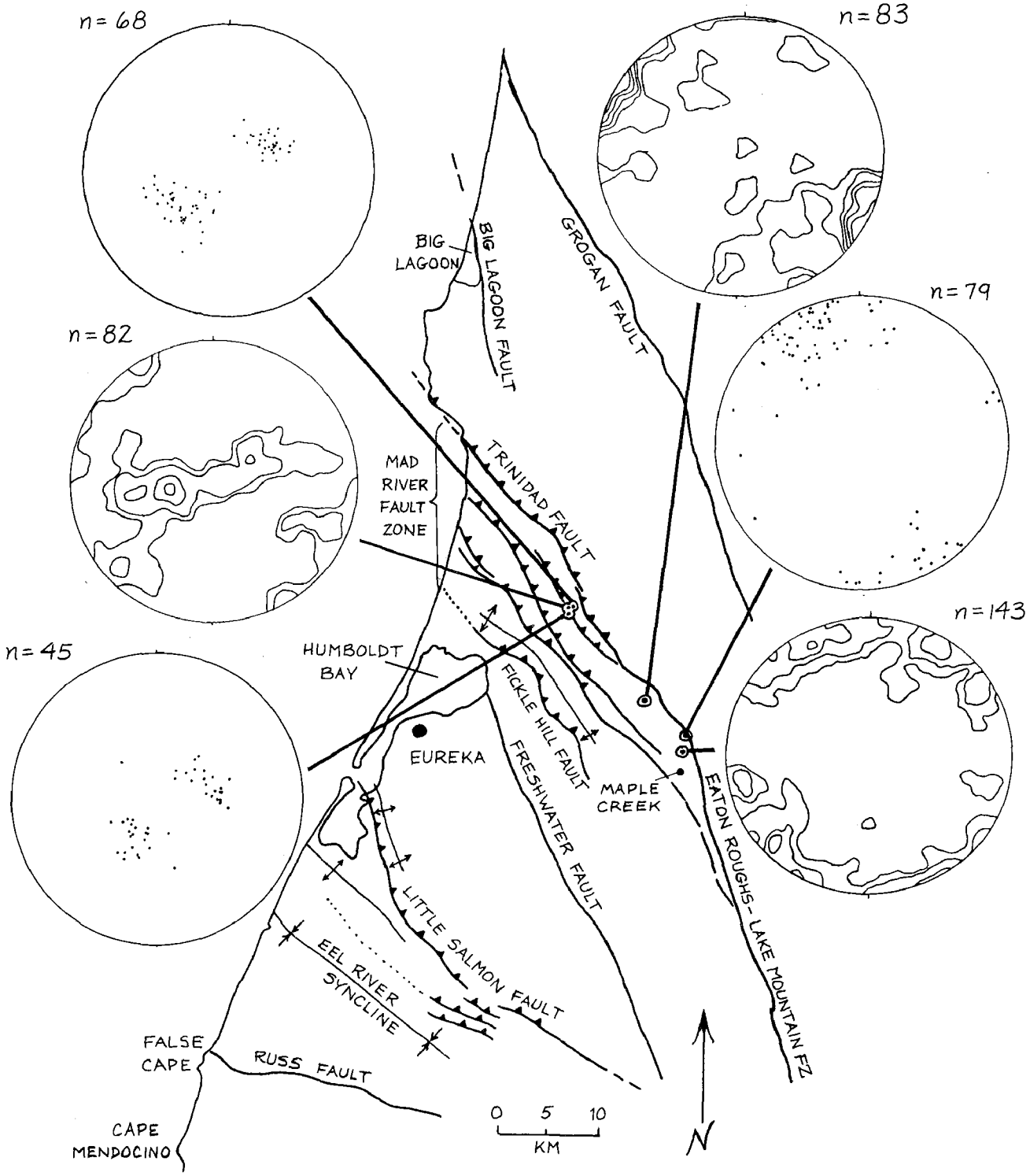

Figure 2. Stereonet plots of poles to small faults and fractures along the NW trend of the Mad River fault zone (MRfz) and along the transition from the MRfz to the NNW-trending Eaton Roughs fault zone. Pole densities are contoured for sites with more than 80 measurements. Contours are 1, 2.5, 5, 7.5, and 10% per 1% area. The western set of plots show the low angle, conjugate fractures typical of deformation near the thrust and low angle reverse faults of the MRfz. The eastern set of plots show the high angle fractures typical along the steeply dipping Eaton Roughs-Lake Mountain fault zone.

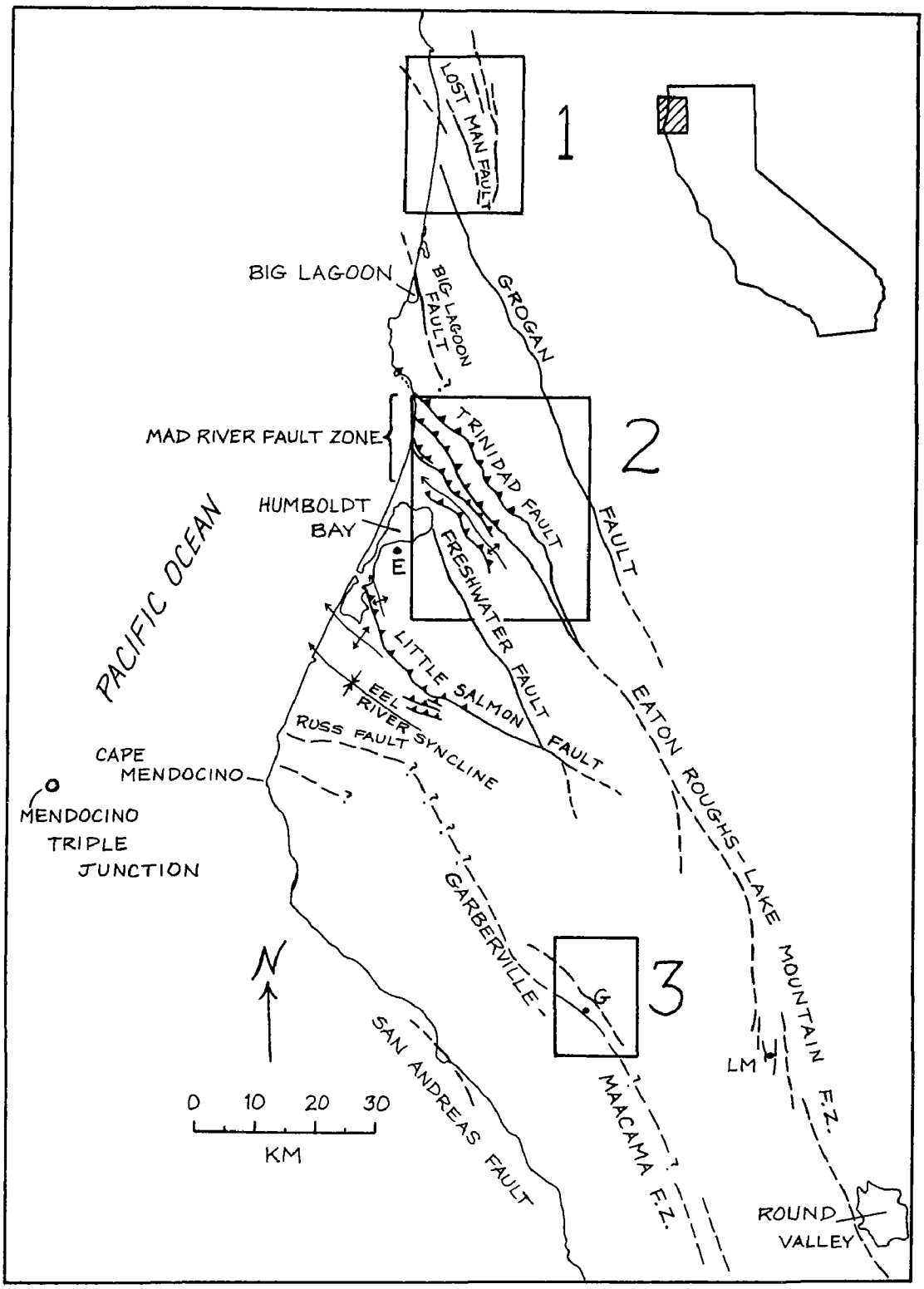

Figure 1. Tectonic map of north coastal California from the latitude of Laytonville north to the mouth of the Klamath River. Mapped faults and Quaternary-age lineaments (see text) from Jennings (1977); Woodward-Clyde (1980); Carver and others (1983); and Kelsey (unpublished mapping). Site 1 is a field area for data in Kelsey and Cashman (1983). Sites 2 and 3 are figs. 2 and 3 respectively of this report. E = Eureka; G = Garberville; LM= Lake Mountain.

Prediction Methodology for Subduction Zone Earthquakes Central Aleutian Islands

Grant Numbers 14-08-0001-G-881/G-1099

Carl Kisslinger and Selena Billington
Cooperative Institute for Research in Environmental Sciences
Campus Box 449, University of Colorado
Boulder, Colorado 80309
(303) 492-6089

Research under these grants is directed toward the discovery of the physical basis for predicting earthquakes in the main thrust portion of a typical island-arc subduction zone and the development of methods for making such predictions. Recent work has been concentrated on: investigation of the fine details of the time-space distribution of seismicity in the Adak seismic zone; mapping of the stress distribution as revealed by the spectral characteristics of the recorded microearthquakes; and application of synthetic seismograms to the improved analysis of the digital data provided by the Central Aleutians Seismic Network. The period covered by this report is October, 1985 - March 1986.

Seismicity in the Adak Zone, 1963-85.

A study of teleseismically-located Adak region earthquakes that was started as a test of the validity of occurrence-rate fluctuations seen in the local network data has proven to be of broader value and interest. By carefully manipulating the data to account, in an approximate way, for mislocations due to lateral heterogeneity under the island arc, it has been possible to isolate the fine details of occurrence rates in narrow N-S strips about 20 km wide, across the seismic zone since 1963. A comparison of the teleseismic catalog (primarily PDE reports) and the catalog based on the local network ($m_b \geq 4.5$ vs $M_D \geq 2.3$) since May, 1976, Figure 1, shows remarkable agreement between the detailed occurrence rates in these strips, in spite of the vast difference in the number of events in the two catalogues, for most of the strips. The deficiency in earthquake numbers under Adak Canyon, interpreted as a deficiency in slip since 1971, and the high rate of activity in the Delaroff block, to the west of Adak Canyon, and in subregion SW2, the activated asperity we have discussed frequently in the past, have been made more quantitative by this analysis. The disagreements between local and teleseismic occurrence rates in a few strips are interpreted as real differences in b-values in these locations. The principal conclusion relevant to the long-range objectives of this research is that our previous findings that Adak Canyon is a likely place for a strong earthquake, $M_s 7$ or larger, in the near future, is still valid, even though the specific prediction for fall, 1985, was a failure. SW2 remains a strongly activated site along the thrust zone, in sharp contrast to the reduced activity in adjacent areas.

It is desirable to convert the numbers of earthquakes into values of seismic slip on the main thrust zone within each of the narrow strips. A major step toward this goal has been achieved by the establishment of empirical relations between magnitude and the seismic moment, average displacement, and source dimension of earthquakes over the magnitude 2 to 6 range. This was done by combining results on seismic moments and fault plane areas to derive average displacements, and using a simple source model (Brune's) to get estimates of the fault dimensions. Moments for the larger events, m_b 5.2 to 5.8, are reported for several Adak events in the PDE monthly reports. Fault areas for these events were estimated from our local

seismicity maps and vertical sections, on which the aftershocks are quite well located. These values for the small events, M_D 1.6-3.5, were taken from a data set compiled for other investigations by F. Scherbaum, who used the spectra of the microearthquakes. Two correlations were made. In one, the equivalent Wood-Anderson magnitude, as calculated by Scherbaum, was used for the small events, and the m_b's given by the USGS for the large ones. In the other set of correlations, M_D was used for the small events (actually $M_D + 0.5$ was used, as this correction has been found in previous work to make the duration magnitudes more nearly in agreement with body-wave magnitudes in the range of overlap). It was gratifying to see that these two totally independent data sets, covering four orders of earthquake magnitude, gave results that lined up very well. The results, which will be very useful in future work, are:

Using M_{WA} for the microearthquakes:

$$\log M_o(\text{Nt·m}) = (7.929 \pm 0.247) + (1.709 \pm 0.067)M$$

$$\log \bar{D}(\text{cm}) = (-3.33 \pm 0.149) + (0.751 \pm 0.0.04)M$$

$$\log L(\text{m}) = 1.333 + 0.48M$$

Using $M_D + 0.5$ for the microearthquakes:

$$\log M_o(\text{Nt·m}) = (9.165 \pm 0.212) + (1.494 \pm 0.062)M$$

$$\log D(\text{cm}) = (-2.789 \pm 0.144) + (0.655 \pm 0.042)M$$

$$\log L(\text{m}) = 1.680 + 0.42M$$

where M_o is the seismic moment, $\bar{D}$ is the average slip in the earthquake, L is twice the radius of a circle with the area of the fault plane (taken as representing the dimensions of the slipped area), M is either M_{WA} or $M_D + 0.5$ for events up to M_D 3.5 or m_b for events greater than 4.5. If the regression of M on M_o is calculated, the results are:

$$M = (-8.488 \pm 0.32) + (0.574 \pm 0.222)\log\ M_o(\text{Nt·m}) \text{ for } M_{WA}$$

and

$$M = (-5.942 \pm 0.387) + (0.656 \pm 0.027)\log\ M_o(\text{Nt·m}) \text{ for } M_D + 0.5$$

These, especially the second, are found to be in close agreement with the magnitude-moment relation suggested by Kanamori and Hanks in 1979,

$$M = -6.03 + \frac{2}{3} \log M$$

The task remains to use these relations to derive seismic slip rates in the 20 km wide strips during the past ten years. The larger events obviously dominate the behavior, as the average slips contributed by the microearthquakes are several orders of magnitude smaller.

One important conclusion of this work so far is that the lumping of seismicity rates with a region even as small as the 250 km segment of the Aleutian arc covered by our network may conceal more information than it reveals, because of offsetting effects of quiescience and activation in small subregions within the zone.

Stress Mapping from Microearthquake Spectral Data.

An on-going task is the systematic mapping of the stress state across the Adak zone on the basis of the spectral characteristic of the numerous earthquakes. This is a labor-intensive project that is progressing steadily. The easternmost sector has been done, with no indications of clear anomalous sites, nor any clear indications of changing distribution of stresses during the eight months prior to a swarm of m_b4.2–4.8 events on August 23, 1985. This eastern zone is covered rather poorly by the network and the current work on the central part of the zone has the benefit of a far larger number of events from which to work.

Synthetic Seismogram Studies.

A new program of improving the interpretation of the Adak network seismograms by comparing them with synthetic seismograms based on the Adak velocity and Q model was started during the period covered by this report. Three research areas will benefit from this effort: seismotectonic studies based on focal mechanisms and stress orientations; studies of wave propagation characteristics of direct, reflected and converted phases; and the studies of stress from the spectra of the observed waves. Experiments on synthetic seismograms with known source parameters have gone far toward explaining the difficulties that have been encountered in using S/P amplitude data for focal mechanism studies. These synthetics have shown how difficult it is to separate the direct S arrival from several strong phases produced by P and S conversions along the path, Figure 2.

These results also show that the S-wave spectra that are used for apparent stress and stress drop determinations are almost certainly contaminated by other arrivals, though the problem is certainly less severe on the horizontal components if the synthetics calculated so far are at all representative of reality.

Now that we are aware of the problem, we are using phase isolaton and polarization filtering techniques to further explore the feasibility of identifying the true S arrival.

The routine use of synthetic seismograms for modelling observed seismograms in different frequency bands allows the isolation of the effects of the source spectrum from the effects of the medium through which the waves travel. Iterative procedures will allow the improvement of the velocity and Q models as Green's function response, which will yield more robust inversion of the seismograms for source properties. This refinement will offer more support to the spectral studies of stress distribution and the transfer of stress along the seismic zone by moderate-energy earthquakes.

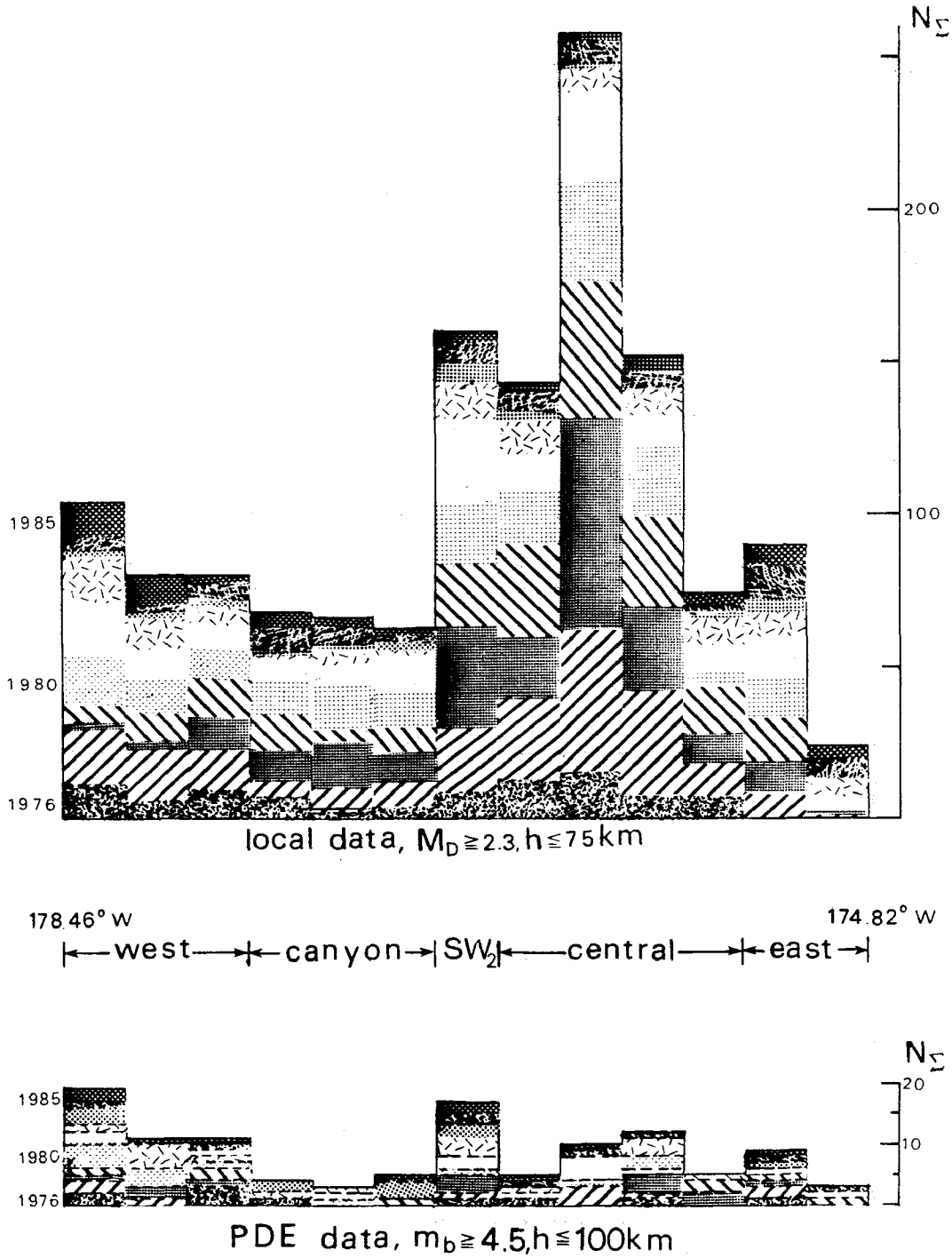

Figure 1. Comparison of seismicity for 1976-1985 in 20 km wide strips along the Adak Seismic Zone. N_Σ is the cumulative number of events, the shading used to indicate each year is indicated on the left. Aftershocks and swarms have been purged and the indicated magnitude cutoff aplied to each catalog to insure completeness of reporting. The depth cutoff for PDE events was chosen to compensate for the systematically too-great depths computed for Aleutian hypocenters. Except for one strip in the Central subregion, in which the small events are very numerous (high b-value), the agreement between the two independent data sets is remarkable. The very low level of activity at all magnitudes in Adak Canyon in recent years is seen, as well as the high rate of moderate earthquakes in SW_2.

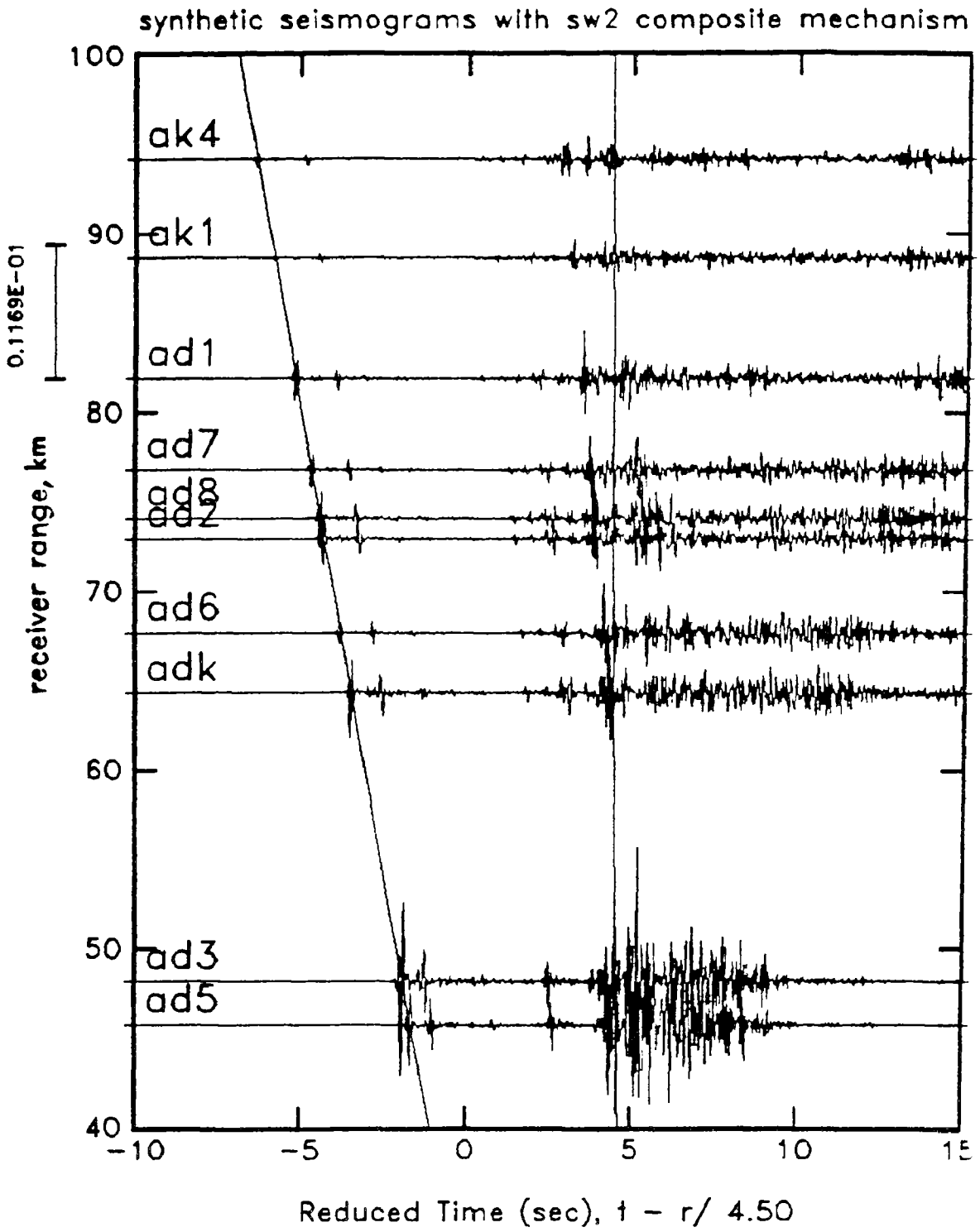

Figure 2. Synthetic vertical component velocity seismograms for an event south of Adak Island, computed for the standard Adak velocity model and an assumed composite focal mechanism. No source spectrum or instrument response function has been included. The reduced P and S arrival times calculated from the velocity model are superimposed across the suite of seismograms. The predicted complexity in the neighborhood of the direct S-wave arrival is obvious even for this preliminary simplified example.

Waveform Analysis of New Brunswick Earthquake Aftershock Data

14-08-0001-22065

C.A. Langston
440 Deike Building
Department of Geosciences
The Pennsylvania State University
University Park, PA 16802
(814) 865-0083

Investigations

1. Obtain and process digital data for aftershocks of the 1982 Miramichi earthquake.

2. Analyze the waveform data for wave propagation effects which may be important in the inversion of source parameters.

3. Develop and implement a master event inversion technique to determine relative and absolute source parameters for the Miramichi aftershocks.

Results

1. Waveform data have been obtained from the U.S.G.S. and have been corrected for instrument response and rotated for use in the waveform analysis for both structure and source parameters.

2. An analysis of site effects is being carried out to determine the effect of near-receiver structure on waveforms. This is being done using the P particle motion from a number of well recorded aftershocks. Results show that although aftershocks vary in source mechanism, the vector particle motion of the P arrival is often coherent for events recorded at the same station. This suggests that near-surface receiver structure has a significant effect on the recorded P waveforms. A resonance feature is seen which commonly dominates the wavetrain with P reverberations existing on the vertical components and P to S conversions prominent on the radial components. Synthetic seismograms computed using the propagator matrix method indicate that a thin low velocity layer corresponding to unconsolidated glacial till is located directly beneath the receivers. Attenuation effects in the thin layer must be included in the computation of the synthetics in order to match amplitude ratios and the relatively longer period of the waveforms on the radial components. The low Q implied by the data is a surprising result and suggests that the "direct" shear waves undergo significant attenuation near the receiver which will then bias kinematic and dynamic source parameters determined from the shear wave data.

3. Theory for the inversion algorithm is being developed. The neccessary computer code is currently being written.

Reports

Williams, David E. and Charles A. Langston (1986). Receiver structure inferred from locally recorded aftershocks of the January 9, 1982 Miramichi, New Brunswick earthquake (Abstract), Trans. A.G.U., 67, 306.

Geologic and engineering studies, Charleston, South Carolina
9950-03868
Stephen Obermeier and Gregory Gohn
926 National Center, Reston, VA
703-648-6791

Investigations undertaken: A field search for prehistoric sand blows has been conducted throughout much of coastal South Carolina, within a belt approximately 30 to 40 km wide that parallels the ocean and extends from North Carolina to Georgia. The search consisted almost exclusively of examining walls of drainage canals, excavated at least 1.7 m deep. About 20 man-weeks were required to locate and examine 12 new sites. About 5 man-weeks were spent collecting wood and humate-rich soil samples that are to be used to age-date the sand blows at many widely scattered sites.

Results obtained: Multiple generations of prehistoric sand blows, interpreted as earthquake induced, have been discovered thoughout coastal South Carolina (see fig. 1). These sand blows extend far beyond 1886 earthquake-induced sand blows, in sediments having approximately the same liquefaction susceptibility based on sediment age and depositional setting. The sesimic source zone for the prehistoric sand blows in unknown. The different distributions of prehistoric and 1886 sand blows have two possible explanations: (1) moderate to strong earthquakes originated in different seismic source locations through time or (2) at least one earthquake much stronger than the 1886 event also originated from the same seismic source as the 1886 earthquake. Seismic source zones may possibly be established only after age-dating sand blows from many widely scattered sies.

Excavations into filled sand blow craters near Hollywood, S. C., have yielded abundant clasts of humate-impregnated sand and sparse pieces of wood. Radiocarbon ages for the humate and wood indicate that at least three prehistoric liquefaction-producing earthquakes have occurred within the last 7,200 years. The youngest prehistoric earthquake occurred around 800 A.D. The average recurrence interval of liquefaction-producing events at the Hollywood site appears to be less than 1800 years.

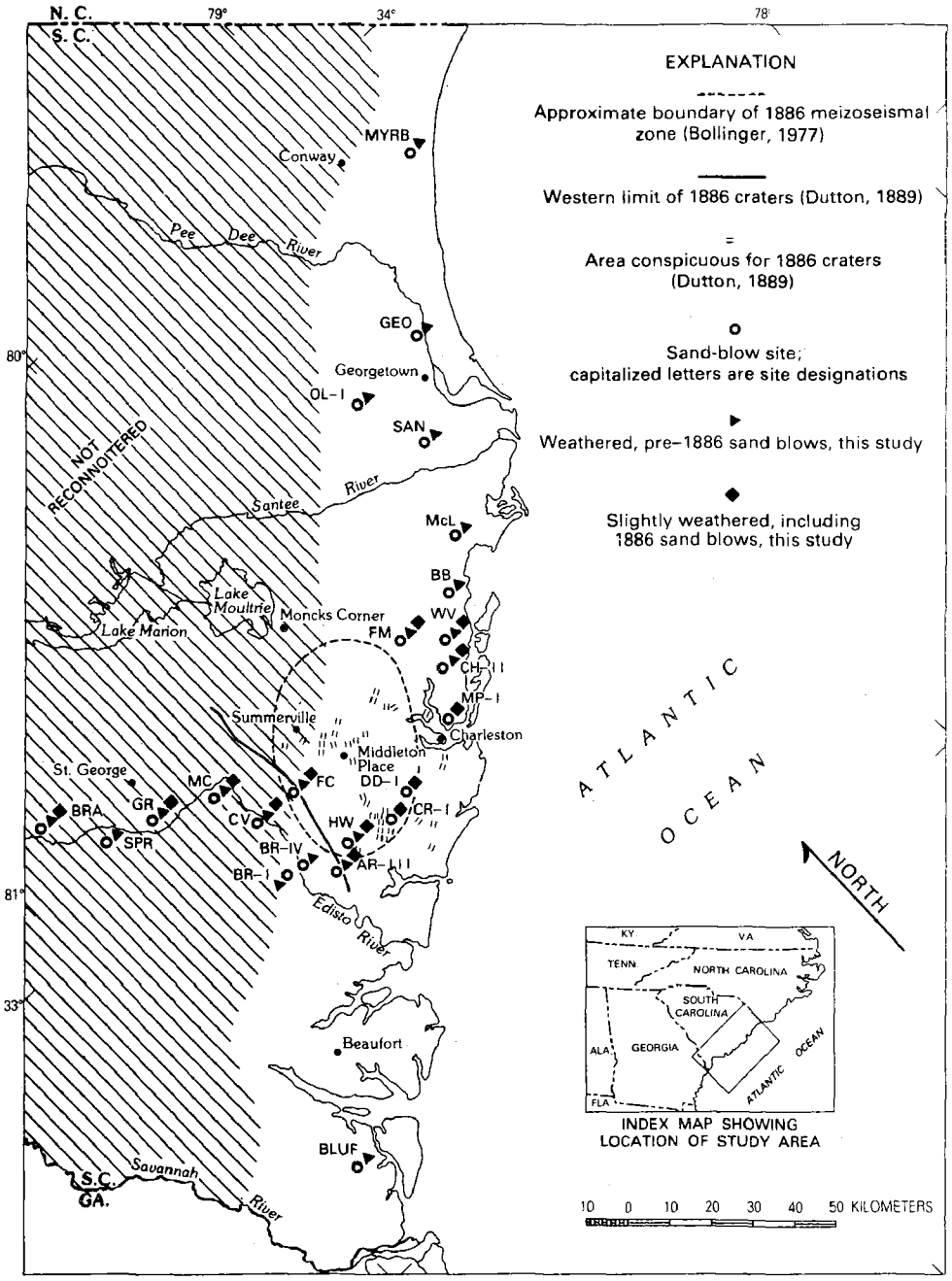

Fig. 1. Map showing 1886 and pre-1886 sand-blow sites. Region without hatching is made up of sediments younger than about 240,000 years (marine-related deposits compose about 80 percent of the region, the rest being fluvial deposits). Hatching delineates region of older marine-related sediments and local younger fluvial sediments. The search for sand blows in fluvial sediments was restricted to Edisto River terraces, inland to site BRA.

Reports:

1. Obermeier, S. F., Jacobson, R. B., Powars, O. S., Weems, R. E., Hallbick, D. C., Gohn, G. S., and Markewich, H. W., in press, Holocene and late Pleistocene (?) earthquake-induced sand blows in coastal South Carolina: Proceedings of the third national conference on eathquake engineering, EERI, Charleston, S.C., August, 1986.

2. Weems, R. E., Obermeier, S. F., Pavich, M. J., Gohn, G. S., Rubin, M., Phipps, R. L., and Jacobson, R. B., in press, Evidence for three moderate to large prehistoric Holocene earthquakes near Charleston, S. C.: Proceedings of the third national conference on earthquake engineering, EERI, Charleston, S. C., August, 1986.

3. Obermeier, S. F., Jacobson, R. B., Weems, R. E., and Gohn, G. S., 1986, Holocene and late Pleistocene (?) earthquake-induced sand blows in coastal South Carolina (abstract): Earthquake Notes, Seismological Society of America, v. 57, no. 1, p. 17.

Array Studies of Seismicity

9930-02106

David H. Oppenheimer
U.S. Geological Survey
Branch of Seismology
345 Middlefield Road, Mail Stop 977
Menlo Park, California 94025
(415) 323-8111, Ext. 2569

Investigations

1. Complete development and documentation of computer algorithms to compute and display earthquake fault-plane solutions.

2. Complete manuscript on state of stress at The Geysers, California and implications for mechanism of induced seismicity.

3. Begin search for earthquake doublets at Parkfield, California to investigate whether "characteristic earthquake" concept can be extended to earthquakes in magnitude range of 1 to 2.5. Examine waveforms of doublets for temporal changes in crustal properties in the seismogenic zone.

4. Analyze main and aftershock sequence of the January 26, 1986 Tres Pinos earthquake.

Results

1. Algorithms for computing and displaying double-couple earthquake fault plane solutions from first motion polarities were completed. The inversion is accomplished through a two-stage grid-search procedure that finds the source model minimizing a normalized, weighted sum of first-motion polarity discrepancies. Two optional weighting factors are incorporated in the minimization: one reflecting the estimated variance of the data, and one based on the absolute value of the theoretical P wave radiation amplitude. The latter weighting gives greater (lesser) weight to observations near radiation lobes (nodal planes). Multiple fault plane solutions are reported for a given earthquake through detection of discrete minimas in the coarse grid search procedure. The fault plane solution uncertainties are computed as a function of the data uncertainty and reported both as the uncertainty in the model parameters (strike, dip, and rake) of the solution as well as those mechanisms for which the solution misfit is less than the 95 percent confidence estimate of the best solution. Both HYP071 and HYPOINVERSE output are permitted as input to the inversion. An Open-File Report which describes the inversion and lists the source code and companion code for displaying the fault plane solutions was completed.

2. A manuscript describing a study of the state of stress at The Geysers, California was completed. The results of this study were discussed in the previous semi-annual technical report and are only briefly summarized

here. Inversion of 210 fault plane solutions at The Geysers shows that the geothermal area is undergoing uniaxial extension in the ESE-WNW direction, consistent with geodetic observations for the surrounding region. Locally observed strains arising from contraction of the steam field do not agree with the stress estimates, indicating that the regional stress field dictates the sense of earthquake slip. The data are equivocal as to demonstrating whether the earthquake activity is induced due to conversion of aseismic to seismic slip, or to increased shear stresses arising from reservoir contraction. The presence of large depositional basins to the north-northeast of The Geysers, together with extension at The Geysers suggests that the extension occurs over the entire region between the Maacama and Bartlett Springs fault strike-slip zones. It appears that the regional extension accounts for the wide-spread presence of Quaternary volcanism in the Clear Lake area.

3. Phase data for earthquakes recorded at Parkfield, California were assembled for the time period 5/70 through 3/86. Substantial efforts were directed towards ensuring that the data set was complete and correct. Algorithms for detection of temporal multiplets through comparison of arrival time patterns at stations common to pairs of earthquakes were applied to the data and dozens of potential earthquake doublets were identified. Existing algorithms for computing spectral ratios, cross spectra, covariance, and time delays of doublets were converted to a VMS operating system, tested, documented, and modified to directly read the CUSP digital seismograms. Current efforts are directed towards verification of doublets identified on the basis of arrival time patterns by waveform comparison and digitizing analog library data as necessary.

4. The M 5.3 Tres Pinos earthquake of 26 January 1986 ruptured a 9 km segment of the Bradley fault SE of Hollister, CA and 7 km east of the Calaveras fault zone. The main shock was preceded by 2.1 s with a M 4.1 foreshock. The mainshock fault plane solution, constructed from P-wave first motions, shows the slip plane oriented at an azimuth of N07W and dipping 83 degrees to the east. Over 300 earthquakes with $M > 1.0$ from the first six days of the sequence were relocated using a one-dimensional velocity model specifically developed for this region. Fault plane solutions for 101 earthquakes of $M > 1.5$ are virtually all dextral strike-slip on nearly vertical planes with a few oblique-slip and dip-slip solutions for events shallower than 5 km. A nearly vertical, curvilinear surface between 3 and 10 km depth is defined by the alignment of the main shock and surrounding aftershock fault plane solutions. This surface is inferred to be the main rupture surface of the Tres Pinos sequence. The dextral-slip planes along this surface vary from a N45W strike at the northern end to a N05W strike (consistent with the main shock) at the southern extent of the aftershock zone. To the northeast of this inferred main shock rupture surface and paralleling it almost its entire length lies a diffuse zone of aftershocks between 7-10 km depth. Fault plane solutions for earthquakes in this zone exhibit dextral-slip, but the average strike of the inferred slip plane is rotated clockwise relative to the aftershocks surrounding the main shock and the trends of mapped faults. Deformation in this region appears to occur by left-stepping echelon dextral shear distributed throughout a volume, rather than by slip on a through-going fault. A comprehensive

paper describing this work together with the results of field investigations (Robert Brown, Malcolm Clark, Katherine Harms, Robert Wallace, Jon Galehouse), isoseismals (Carl Stover), strain (Malcolm Johnston), creep (Sandra Schulz), strong motion (Gary Glassmoyer), and hydrogen data (Moto Sato) is in preparation.

Reports

Oppenheimer, D. H., 1986, Extensional tectonics at The Geysers geothermal area, California, submitted to J. Geophys. Res.

Reasenberg, P., and Oppenheimer, D., 1985, FPFIT, FPPLOT, and FPPAGE: Fortran computer programs for calculating and displaying earthquake fault-plane solutions: U.S.G.S. Open-File Rep. 85-739, 109 p.

Scattering and Q within the Anza Array

14-08-0001-G1182

John A. Orcutt
Institute of Geophysics and Planetary Physics (A-025)
Scripps Institution of Oceanography
La Jolla, California 92093
(619)452-2887

Objective: We are studying waveform data collected with the Anza Array in southern California near the San Jacinto Fault, the location of a recognized seismic gap. The research will investigate the coda of P and S waves, using complete synthetic seismograms in vertically heterogeneous media in conjunction with the observations, with the goal of understanding the waves' generation and the implications of their temporal and frequency characteristics for the anelasticity and heterogeneity of the crust. The use of solely vertically heterogeneous structures permit the incorporation of strong scattering in the model as well as the very important effects of the velocity structure and the presence of a free surface. The use of the high-quality, high dynamic range digital data from Anza may permit the imposition of rough constraints on the source mechanisms of small events in the region using the synthetics described above. This research, involving an investigation of the nature of high frequency earthquake coda, will lead to an evaluation of the proposed use of the inferred *Quality Factor* for earthquake prediction.

Data Selection and Preliminary Analysis: We have undertaken the research for which we were funded this past December. Figure 1 is a plot of earthquake epicenters for a data set we have selected for further analysis, superimposed on a map of the Anza Array. All the events plotted have moments in excess of 10^{19} dyne·cm. The events are generally located within the array where hypocenter locations are quite reliable. The time series for these events have been isolated in a separate database on the IGPP computing ring and we intend to make the data available to other interested parties in a variety of standard tape formats. The application of a wide variety of techniques by a number of investigators would be invaluable. The signal-to-noise ratios for these observations are quite good and, taken as a whole, the azimuthal coverage for any given Anza Array station is quite good. Figure 2 is a representative sample of these data.

The CRAY XMP/48 installed this past October at the San Diego Supercomputer Center (SDSC) represents a new and powerful resource we intend to use in this research. We have ported the wavenumber algorithm, including the facility for frequency dependent Q, to the CRAY and have completed a thorough series of tests. We will be using this computer for the synthetic calculations required by this research. The additional computational power will permit substantially more complex synthetics to be computed than those earlier anticipated when the proposal was initially written.

Mr. Tom Sereno will be completing his Ph.D. thesis on regional wave propagation in the oceans this next month. He will begin working, with Prof. Orcutt, on the project full time in June as a Post-Graduate Research Geophysicist.

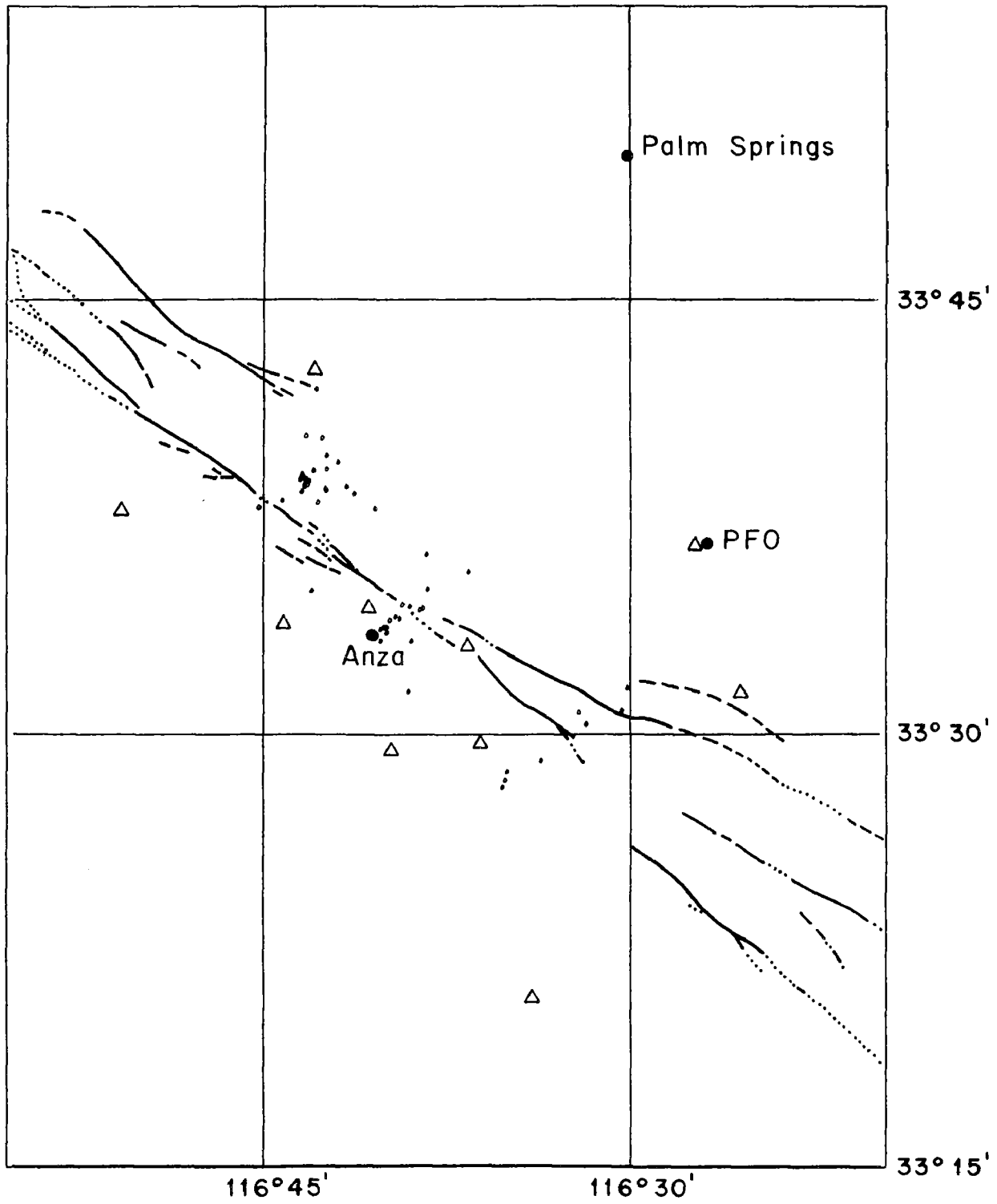

Figure 1. A map of the Anza Array area with epicenters plotted as dots. The triangles represent stations and the San Jacinto and subsidiary faults are sketched for context. All the epicenters have moments in excess of 10^{19} dyne-cm.

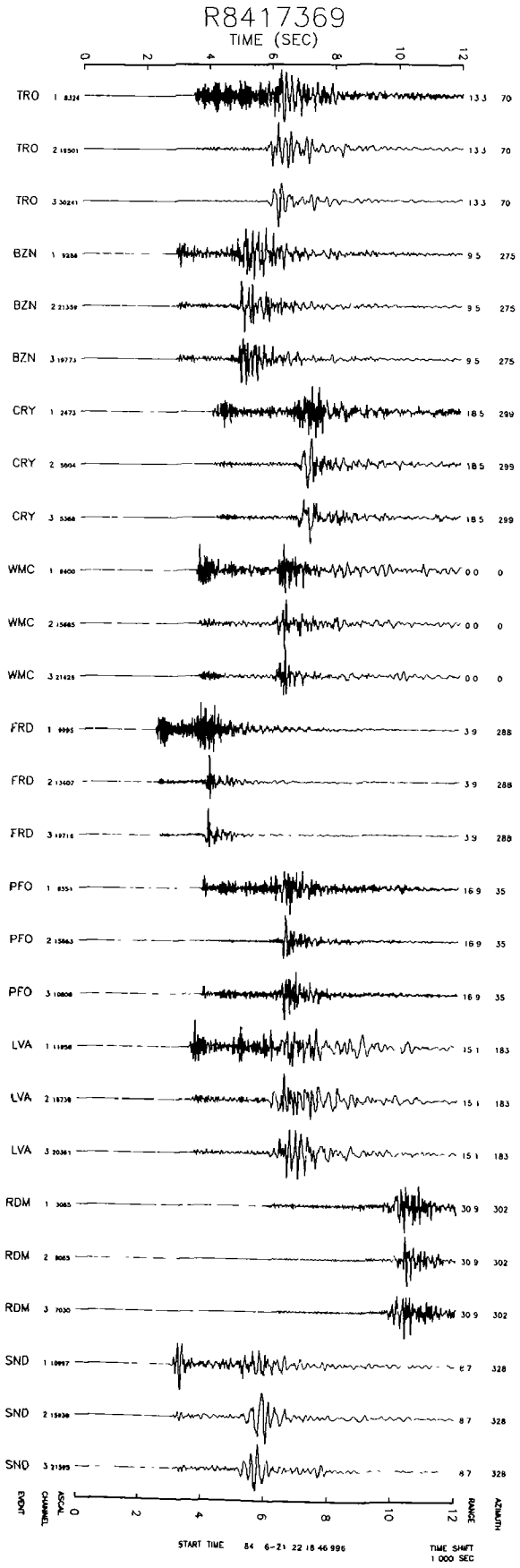

Figure 2. Anza Array seismograms for an event on 21 June 1984. The first trace is the vertical channel while the two horizontals follow as channels 2 and 3. The epicentral range to the event as well as the event azimuth are shown at the top.

EARTHQUAKE RESEARCH IN THE WESTERN GREAT BASIN

Contract 14-08-0001-G1193

W.A. Peppin, E.J. Corbett, and U.R. Vetter
Seismological Laboratory
University of Nevada
Reno, NV 89557
(702) 784-4975

Investigations

This program supports continued studies with research focused on: (1) seismotectonics of the White Mountains Gap; (2) magmatic processes in Long Valley Caldera; (3) the UNR experimental digital network; (4) attenuation changes in earthquake regions connected with volcanism; (5) relocations of Mammoth Lakes earthquakes; (6) analysis of digital waveforms; and (7) digitization of field tapes for a more detailed analysis of the 1978 Wheeler Crest earthquakes. During this contract period progress in each of these areas has been made, and we summarize here only three recent efforts of perhaps greatest interest to the readership of these summaries pertinent to items (1) and (2) above.

Results

Relocations of 1978 Wheeler Crest Aftershocks

Recently Peppin and Honjas (1986) reported master-event relocations of some of the aftershocks of the 1978 Wheeler Crest earthquake (**Figure 1**). These earthquakes are of interest for the new information they might shed on the nature of the 1978 October 4 mainshock (M_L 5.8). We combined data recorded on analog and digital temporary stations deployed independently by UNR and the USGS (left panel of Figure 1), using only the data that could be timed to a precision of 0.02 second or better and not using, for example, the smoke-paper records (in the belief that these can be timed to a precision not exceeding 0.05 second). A pseudo master-event scheme was used (because it was not possible to find a sufficiently large earthquake set having common recording stations), and the results, in agreement with Fuis and others (1979) and Somerville and Peppin (1979), show a north-south trend of epicenters about 10 km long.

The interest in the 1978 earthquake centers around several facts: first, this event initiated activity in the Mammoth Lakes area, and second, there is evidence that magma may be associated with it. This evidence comes from two sources. Julian (1983) found that, like two of the other Mammoth Lakes shocks, the 1978 earthquake produced teleseismic waveforms which could not be explained in terms of a simple double couple source (Julian suggests dyke intrusion along the lines of the source model proposed by Aki, 1984 for these events). Second, Ryall and Ryall (1984), extending their work on S-wave shadowing, found a zone of S-wave shadowing not too far (a few km) from the 1978 epicenter. During the present contract period, we have examined another line of evidence suggestive along these lines, namely the presence of a strong phase preceding S which is possibly a lateral reflection being scattered by a shallow-crustal anomaly. Using the best available records, Peppin and Honjas (1986) have done further work on this phase. In Figure 1 note that those earthquakes for which the pre-S is strong cluster at a few locations. They found that the pre-S times at BIW are strikingly consistent (RMS only 0.02 second) with a lateral reflection

from the south end of Hilton Creek fault at a depth of 1.0 km. This adds another independent line of evidence for a strong crustal anomaly (magma body?) in this vicinity.

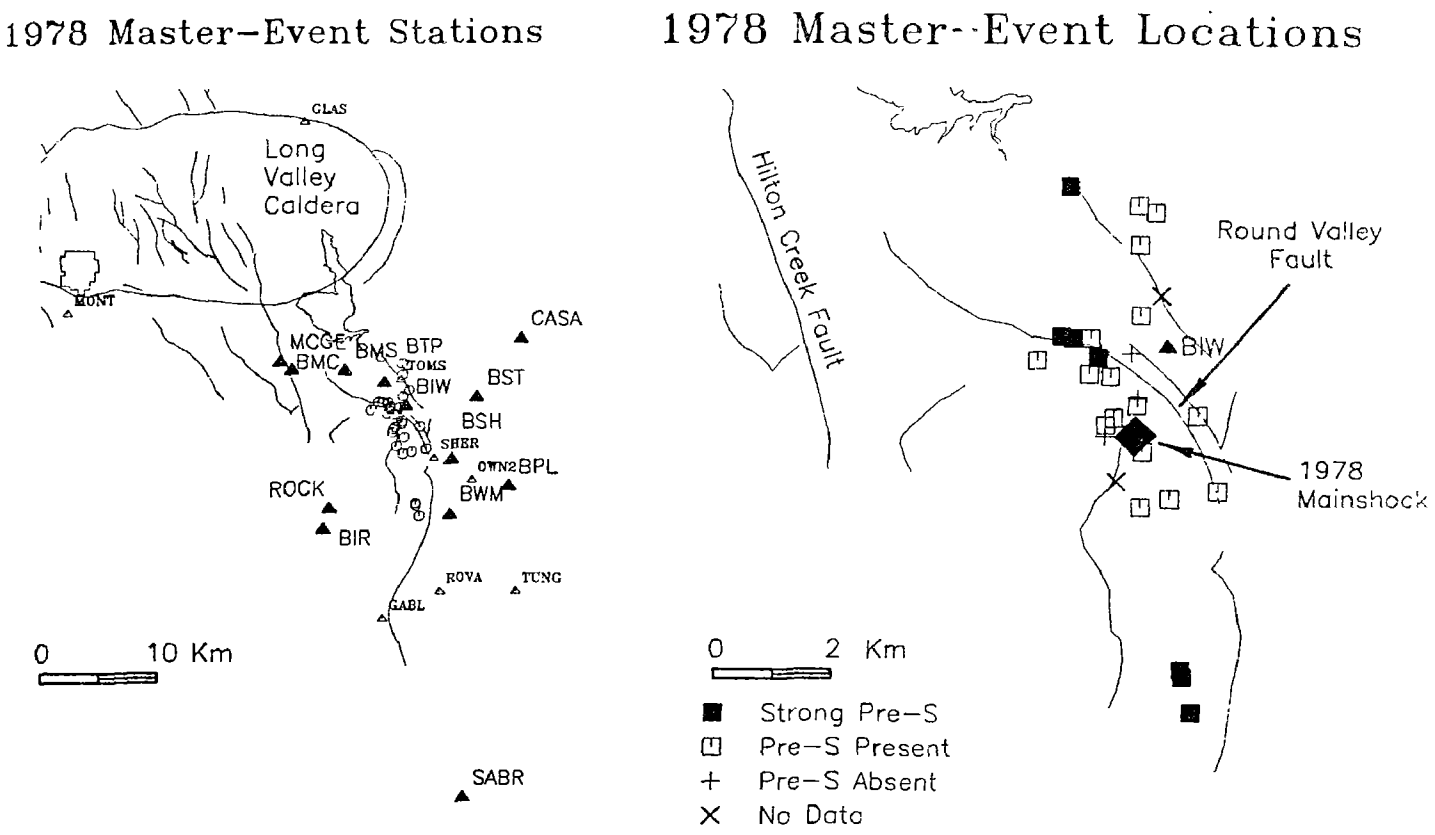

Figure 1. Station distrubution (*left*) and pseudo master-event locations (*right*) of the aftershocks of the 1978 Bishop earthquake (M_L 5.8). Stations available are the triangles; stations used in the locations are solid. Epicenters showing a pre-S phase at station BIW are squares in the right hand panel, with the solid squares those for which the pre-S phase is strong.

Focal Mechanisms.

Work by Vetter (1986) on well-constrained focal mechanisms using the online system data have revealed a pattern in the stress regime that appears to indicate a tectonic boundary. The issue here is that the earthquakes in the vicinity of Mammoth Lakes differ from those nearby in that they share a common axis of extension in the ENE direction. In Vetter's recent work, it was discovered that, while earthquakes to the west of the Round Valley fault (see Figure 1) exhibit ENE extension, earthquakes to the east of the fault show a range of extension axes, ranging from ENE to WNW, the latter being the normal Basin and Range direction. This suggests that we can place quite exactly an eastern boundary on the Mammoth Lakes seismotectonic province: to the east the

mechanisms grade over into the more usual Basin and Range style of events. Much of the data used comprises aftershocks of the November 1984 Round Valley earthquake, whose source mechanism is known to be distinctly different from the other earthquakes (Barker and WAllace, 1986; Corbett and others, 1985).

Travel Times Through the Caldera.

Evidence has been accumulating for another pre-S phase, but this one is seen only at the station SLK, NW of the caldera (**Figure 2**). Also in Figure 2 are plotted observed travel times of P, S, and this pre-S phase, together with simple halfspace travel times for a surface-focus source in a halfspace with a P-wave velocity of 5.85 km/sec and an S-wave velocity of 3.4 km/sec. It is notorious that the pre-S travel times are parallel with the S times. As a result, the time intercept of a straight line drawn through these observations is *negative*. No possible travel path involving flat-lying layers is capable of producing a travel time curve with negative time intercept, and so some other explanation must be sought.

Referring to the map image of Figure 2, it is observed that the earthquakes showing this phase lie in an elliptical zone about 30 km long and 8 km wide whose major axis points toward the reveiver station SLK. It is also noted that this trend passes through Long Valley caldera at about the position of the Sanders (1984) proposed magma bodies, implying a possible connection. In fact, we have concocted a model which can fit these observations. In this model the phase is explained as S leaving the hypocenters which converts to P and then back to S on steeply-dipping faults bounding the caldera. If this interpretation is correct, the data shown herein will give important constraints on the geometry of the magma bodies as proposed by Sanders (1984). The reason is because, under this model, the P conversion is a minimum time path, presumably in the partially melted rocks of the caldera. Consequently, the rays will search for such an anomaly, travelling within it as far as possible. Therefore, the time delay between pre-S and S is a direct measure of P travel time through the anomalous zones. In contrast, the arrivals used by Sanders will tend to steer around such anomalies, giving no such basis for quantitative analysis. We are quite hopeful that the analysis of these waves will lead to marked refinement of Sanders work; this is to be the subject of a Masters thesis project now under way.

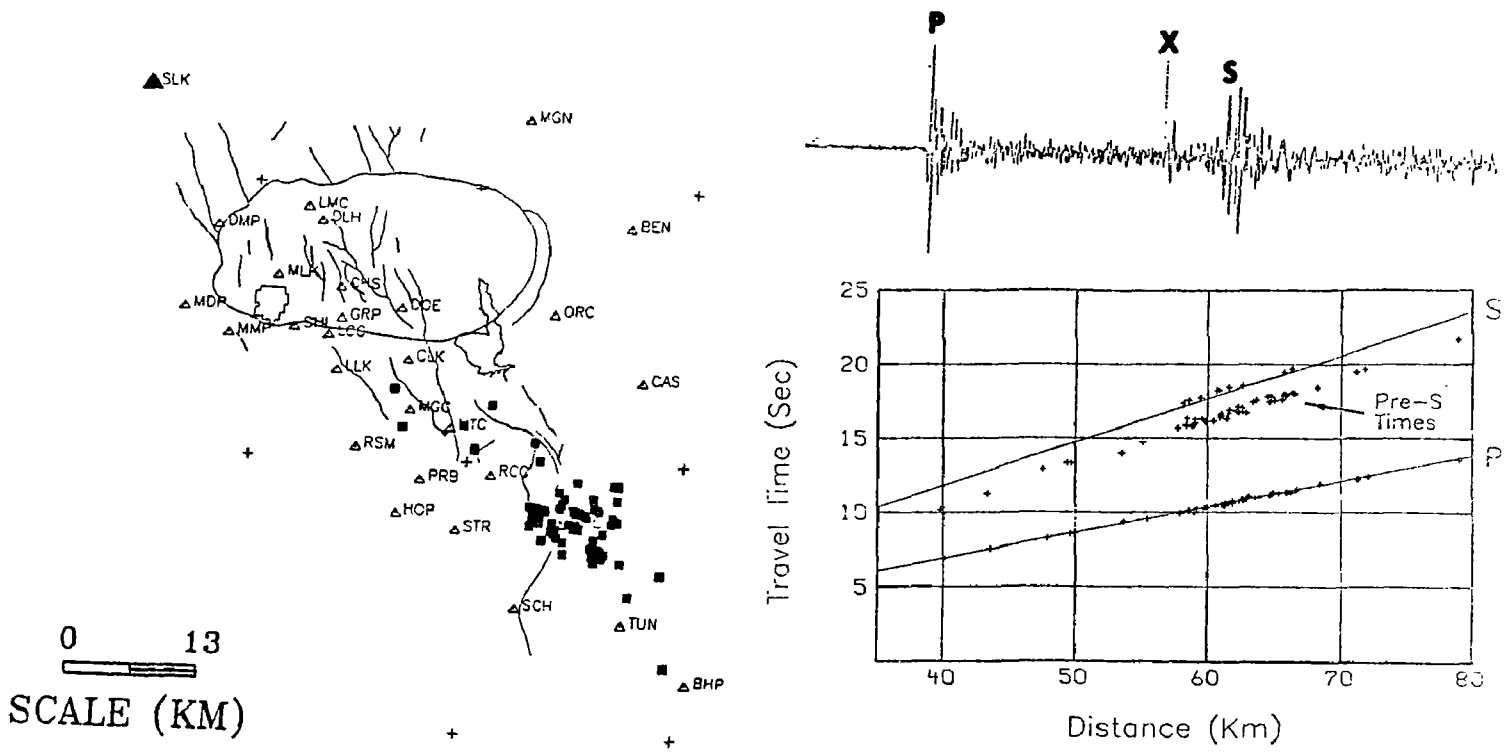

Figure 2. Map view of Long Valley caldera (*left*) showing the earthquakes which produced a pre-S phase at station SLK (upper left, solid triangle). Travel times of P, S, and the pre-S phase are shown in the *right* panel, having the labels "P", "S", and "X", respectively. The lines are simple travel time curves which are for a constant velocity of 5.85 km/sec (lower) and 3.4 km/sec (upper). The pre-S times parallel the S curve and the S observations in the distance range 40 to 80 km.

References

Aki, K., 1984. Evidence for magma intrusion during the Mammoth Lakes earthquakes of May 1980 and implications of the absence of volcanic (harmonic) tremor, *Jour. Geophys. Res.*, **89**, 7689-7696.

Barker, J.S. and T.C. Wallace (in press). A note on the teleseismic body waves from the November 23, 1984, Round Valley, California earthquake, *Bull. Seis. Soc. Amer.*, submitted.

Fuis, G., Cockerham, R.S. and Halbert, W., 1979. Preliminary report on the Bishop earthquake, M_L = 5.8, October 4, 1978: Aftershocks and ground breakage, *Abstracts with Notes, Geol. Soc. Am.*, **11**, 79

Julian, B.R., 1983. Evidence for dyke intrusion earthquake mechanisms near Long Valley caldera, California, *Nature*, **303**, 323-325.

Peppin, W.A. and Honjas, W., 1986. Further evidence on the crustal anomaly (magma body?) near the south end of Hilton Creek fault, Mammoth Lakes, California, *Earthquake Notes*, **57**, 10.

Ryall, A.S. and Ryall, F.D., 1984. Shallow magma bodies related to lithospheric extension in the western Great Basin, western Nevada and eastern California, *Earthquake Notes*, **55**,11.

Sanders, C.O., 1984. Location and configuration of magma bodies beneath Long Valley, California, determined from anomalous earthquake signals, *Jour. Geophys. Res.*, **89**, 8287-8302.

Smith, K.D., D.M. Martinelli, and E.J. Corbett (1985). Focal mechanisms of the November 23, 1984 Round Valley, California earthquakes, *EOS, Trans. Amer. Geophys. Union*, **66**, 952.

Somerville, M.R. and Peppin, W.A., 1979. Recent seismicity patterns near Mammoth Lakes, California, *Earthquake Notes*, **50**, 4.

Vetter, U.R., 1986. Focal mechanisms and the boundary of the Great Basin tectonic province, *Earthquake Notes*, **57**, 21.

Northeastern Seismicity and Tectonics
9510-02388

Nicholas M. Ratcliffe
U.S. Geological Survey, MS 925
Reston, Virginia 22092
and
John K. Costain
Virginia Polytechnic Institute and State University
Blacksburg, Virginia 24061

INVESTIGATIONS

1. Interpretation of VIBROSEIS reflection profiles of the Ramapo Seismic Zone in central New Jersey.

2. Analysis of geology along route.

3. Interpretation of earthquake epicentral data.

RESULTS

1. Analysis of a twelve- and 24-fold VIBROSEIS profile in central New Jersey across the Ramapo fault and zone of high seismicity west of the Newark basin has been completed. The line follows a route (Figure 1) that begins west of the Green Pond syncline, continues east-southeast across Middle Proterozoic gneiss of the Hudson Highlands, and into the Newark basin as far as the second lava flow. Abundant faulting of Mesozoic age is found in the area northwest of the Ramapo fault, where seismicity appears to be concentrated.

2. The migrated version of the line as shown in Figure 2 clearly shows the downdip termination of the second lava flow (labeled b) by the Ramapo fault. A combination of drill-hole data and surface observations indicates that the Ramapo dips 50° to the southeast.

3. Reflections from 0.6 sec to 0.2 sec under the Green Pond syncline show the synclinal and anticlinal form of the Silurian and Devonian strata in the Green Pond syncline. Reflections from the basement rocks under the Hudson Highlands are poorly developed, although a southeast-dipping grain can be detected at 1.0 to 1.6 seconds between CDP stations 160 and 300. These reflections may correspond to thrust faults seen in VIBROSEIS profiles to the south and known to exist from surface observations.

4. Earthquake hypocenters along the profile are portrayed in Figure 3 based on the locations provided in the Regional Seismicity Bulletin of the Lamont-Doherty Network. As in our other profiles, the seismicity west of the Newark basin lies in a southeast-thickening wedge of Proterozoic basement floored by Paleozoic thrust faults, but west of and beneath the major Mesozoic border fault. These data suggest that seismicity west of the Ramapo fault may be caused by movements on brittle Mesozoic faults that bound blocks of material as portrayed in Figure 3.

REPORTS

Ratcliffe, N. M. and Burton, W. C., D'Angelo, R. M. and Costain, J. K., 1986, Seismic reflection geometry of the Newark basin margin in eastern Pennsylvania: Evidence for extensional reactivation of Paleozoic thrust faults: NUREG

Ratcliffe, N. M. and Burton, W. C., in press, Bedrock geologic map of the Poughquag quadrangle, New York: U.S. Geological Survey Geologic Quadrangle Map, GQ___.

Ratcliffe, N. M., Burton, W. C. and Costain, J. K., 1986, Low-angle extensional faulting, reactivated thrust faults, and seismic reflection geometry of the Newark basin in eastern Pennsylvania and New Jersey: Geological Society of America, Abstracts with Programs, vol. 18, no. 1, p. 61.

Ratcliffe, N. M. and Burton, W. C., D'Angelo, R. M. and Costain, J. K., 1986, Low-angle extensional faulting, reactivated mylonites, and seismic reflection geometry of the Newark basin margin in eastern Pennsylvania: Geology, in press.

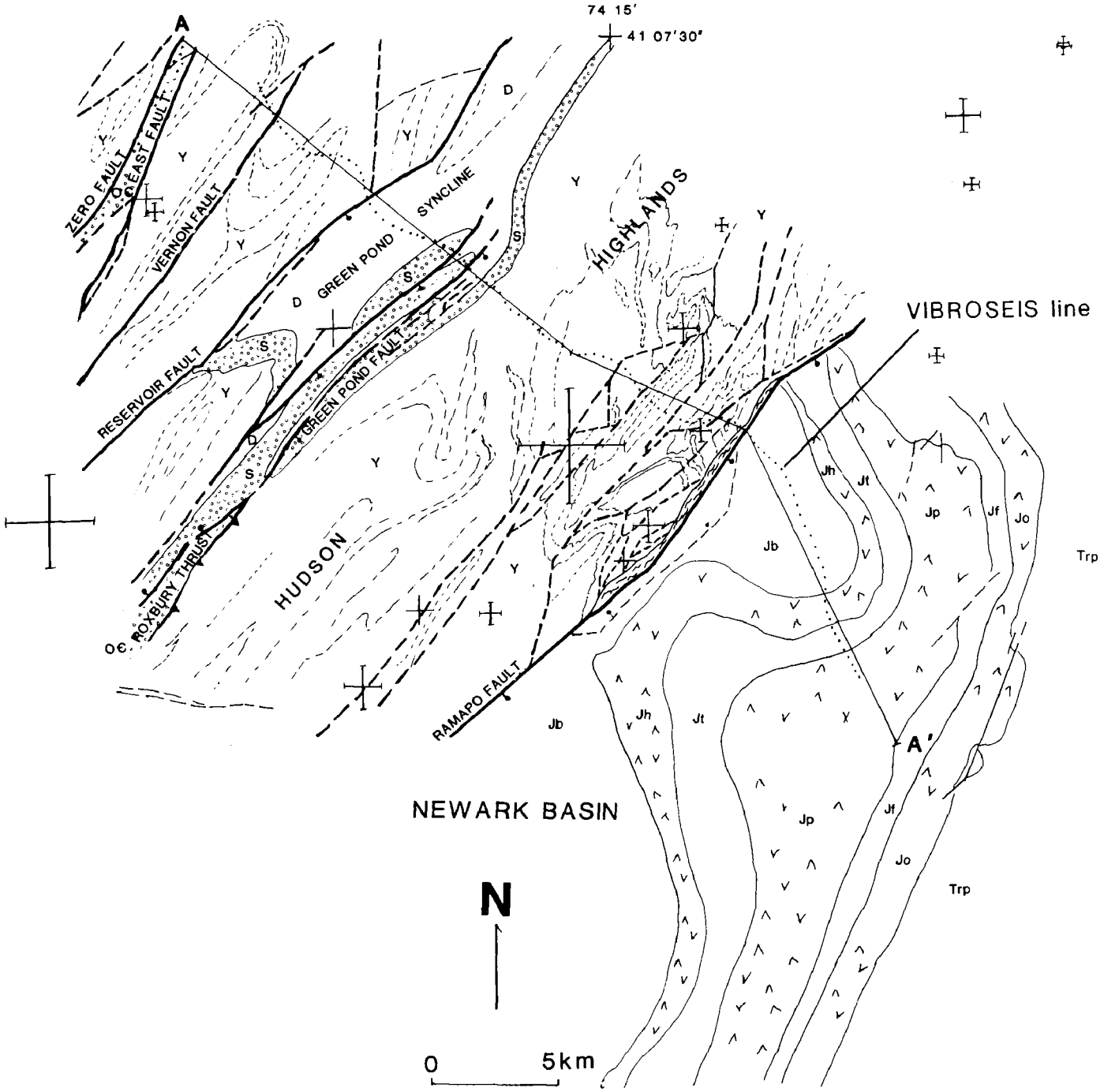

MESOZOIC FAULTS EPICENTERS LINE 6

Figure 1. Route of seismic line 6 in relation to geology and earthquake epicenters.

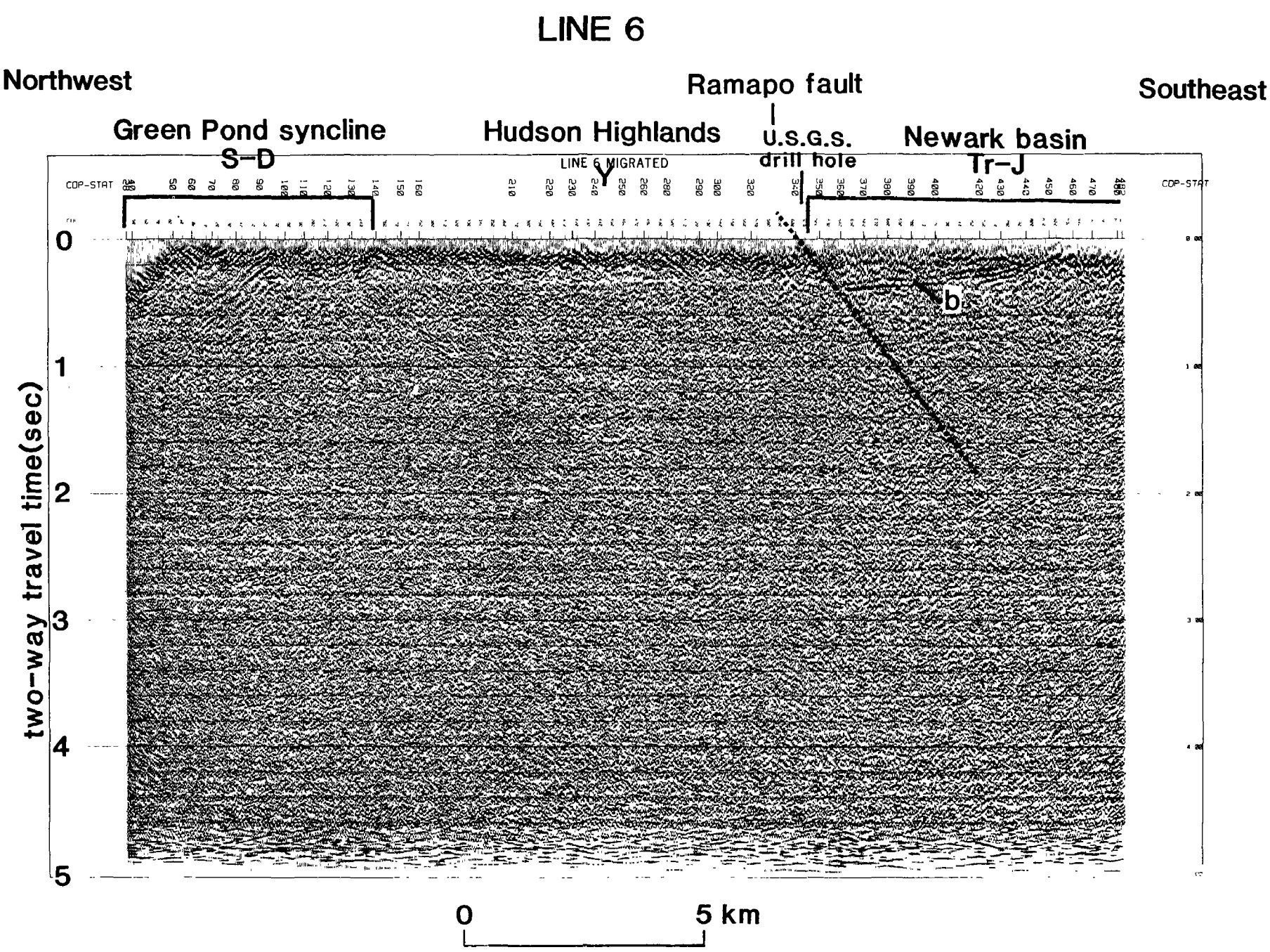

Figure 2. Migrated version of Line 6

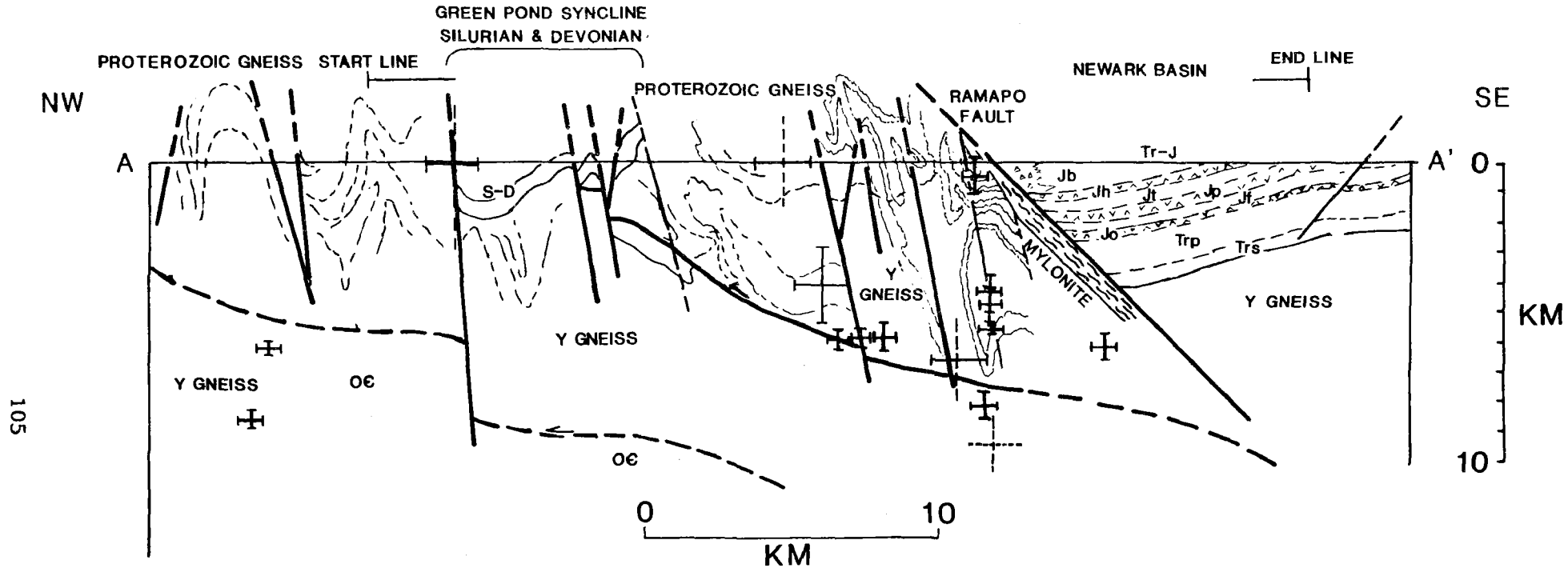

105

CROSS SECTION LINE 6 SHOWING HYPOCENTERS

Figure 3. Geologic cross section and earthquake hypocenters along Line 6.

BASEMENT TECTONIC FRAMEWORK STUDIES SOUTHERN SIERRA NEVADA, CALIFORNIA

9910-02191

Donald C. Ross

Branch of Engineering Seismology and Geology
U.S. Geological Survey
345 Middlefield Road, MS 977
Menlo Park, CA 94025
(415) 323-8111, ext. 2341

Investigations

1. Synthesis of petrographic data for mafic and ultramafic rocks of the southern Sierra Nevada.

2. Compilation of all locations of samples for which Rb/Sr data are known (about 190 localities) north to 36°00' in the southern Sierra Nevada.

3. Petrographic study of thin sections of granitic and metamorphic rocks from the eastern front of the southern Sierra Nevada.

4. Synthesis of chemical data from about 80 sample localities (chemical analyses for main elements and instrumental neutron activation analyses for trace elements from 35°30' to 36°00' N. in southern Sierra Nevada.

Results

1. Study of mafic rocks in the southern Sierra Nevada, particularly the gabbronorite of Quedow Mountain and several related bodies on the west side of the batholith (generally about 25 kilometers or more southeast of Porterville, California) are very similar to mafic bodies that were originally considered to be fragments of the gneissic complex of the San Emigdio-Tehachapi Mountains (for example, the bodies of Live Oak, Breckenridge and Pampa [Ross, 1983]). Studies now suggest that these bodies are scarps of a rather extensive area of gabbronorite to the north. Nevertheless, similar ages of 115 m.y. on the Quedow Mountain rocks (Saleeby and Sharp, 1980) and 110-120 m.y. ages on hornblende-rich mafic complex of the San Emigdio-Tehachapi Mountains (Sams and Saleeby, 1986) suggests that both the gabbronoritic terrane and the largely metaigneous mafic gneiss complex are related.

2. Most instrumental neutron activation analyses for the southern Sierra Nevada show a pronounced "Eu anomaly" (europium value lower than expected in a "normal" rare earth element progression). This is not only true for felsic rocks which show such an anomaly in the central and northern Sierra Nevada, but common for the intermediate and more femic rocks, where such an anomaly is uncommon elsewhere. The presence or absence of a "Eu anomaly" is also of possible correlation value in some granitic bodies. for example, two granodiorites on the east side of the batholith are very similar petrographically though field work suggests they are different. One granodiorite has a strong Eu anomaly and the other has virtually none, suggesting they are not parts of the same unit. Similarly, two mafic Jurassic units were suspected of being closely related, but one (the Sacatar unit) has a pronounced Eu anomaly whereas the "related" quartz diorite of Walker Pass has no anomaly, suggesting the two units are not related. Not only Eu anomalies, but other rare earth element patterns show possibilities of separating or combining some bodies of granitic rock.

3. In Jawbone Canyon (some 30 km NE of Mojave in the eastern Sierra Nevada) a large area of dark rocks has many affinities with the mafic complex of the San Emgidio-Tehachapi Mountains. However, preliminary Rb/Sr studies show that these Jawbone Canyon rocks have a much more "continental signature" than the mafic complex to the west that is primitive and oceanic. Probably these two terranes are unrelated, though they are superficially, at least, similar.

Reports

Ross, D.C., 1986, Basement-rock correlations across the White Wolf-Breckenridge-southern Kern Canyon fault, southern Sierra Nevada, California: U.S. Geological Survey Bulletin 1651.

Detailed Geologic Studies, Central San Andreas Fault Zone

9910-01294

John D. Sims
Branch of Engineering Seismology and Geology
U.S. Geological Survey
345 Middlefield Road, MS 977
Menlo Park, California 94025
(415) 323-8111, ext. 2252

Investigations

1. Field investigations of structural and stratigraphic relationships between late Cenozoic sedimentary units and underlying Franciscan and late Cretaceous units in the Parkfield-Cholame-Coalinga area of the southern Diablo Range.
2. Field investigation of late Holocene and historic slip rates in the Parkfield/Cholame area.
3. Geological consultation and field examination of borehole sites for downhole instrumentation in the Parkfield area.

Results

1. The 40-km-long section of the San Andreas fault (SAF) in the Parkfield-Cholame area is noted for its exotic allochtonous masses of rocks adjacent to the fault zone. Two masses of particular interest are the hornblende gabbro of Gold Hill, which are correlative with rocks at Eagle Rest Peak and in the Logan Quarry; and the volcanic rocks of Lang Canyon that are correlative with the Neenach Volcanics and the Pinnacles Volcanic Formation. Gold Hill, which is bounded by vertical faults, lies to the east of the present main trace of the SAF. The volcanic rocks of Lang Canyon lie 16 km NW of Gold Hill and on the west side of the SAF. The relative positions of the gabbro of Gold Hill and the volcanic rocks of Lang Canyon are reversed with respect to their correlatives to the north and south. This reversal reveals some of the history of movement on the SAF.

   In its initial prefaulted position, the Eagle Rest Peak-Gold Hill-Logan Quarry mass was about 55 km NW of the Neenach-Lang Canyon-Pinnacles mass. First, the Pinnacles and the Logan-Gold Hill body were detached from their parent bodies and transported about 95 km NW; the Pinnacles mass then lay about 30 km NW of Eagle Rest Peak. Second, the SAF locally stepped eastward, and a sliver of the volcanic rocks of Lang Canyon was detached from the Neenach Volcanics and moved 60 km NW. After the 90 km of movement in stage one, the Pinnacles Formation and the volcanic rocks of Lang Canyon thereafter maintained their relative position of about 90 km apart on the west side of the SAF. At the end of the second stage of right-lateral movement, the Logan Quarry mass was opposite the present position of Gold Hill after being transported about 150 km NW of Eagle Rest Peak. The Gold Hill mass was then detached from the Logan gabbro and was emplaced on the east side of the SAF.

2. Provenance studies of the Etchegoin Formation suggest that major paleogeographic changes occurred during the late Miocene and early Pliocene in central California. Provenance of the Etchegoin Formation is inferred on the basis of the lithology and spatial distribution of detritus found within these strata. A suite of detrital grains characterized by quartz associated with green and brown hornblende is interpreted to have been derived from hornblende-quartz-gabbroic rocks adjacent to the Vergeles-Zayante fault. This source is now covered by post-Pliocene rocks, but it is estimated by Ross (1984) to contain about 40 percent hornblendes. Detritus characterized by quartz associated with hornblende, zircon, sphene, epidote, and garnet is similar to that found in sandstone of the Santa Margarita Formation. The similarity in these two heavy minerals suites, and the fact that some of these heavy mineral grains exhibit a variety of crystal shapes and others exhibit multiple degrees of rounding, suggests that this plutonic-rich Etchegoin detritus was recycled from the Santa Margarita Formation. Detritus characterized by quartz associated with green and brown hornblende, epidote, and zircon is found in some sandstone in the Coalinga region, and this detritus is thought to have been derived from plutonic rocks in the Sierra Nevada. A Sierra Nevada source is likely because hornblende, epidote, and zircon are common in the mafic plutonic rocks of the Sierra Nevada. In addition, Sierran plutonic detritus is expected to be found in Etchegoin strata of the Coalinga region because east of the Coalinga region Etchegoin strata grade laterally into the Kern River Formation that is rich in plutonic detritus, which is thought to have been deposited in alluvial fans built westward from the plutonic basement of the Sierra Nevada. The volcanic detritus characterized by volcanic rock fragments associated with brown hornblende and augite or brown hornblende and hypersthene is thought to have been derived from the Mehrten Formation, and subsequently, from coeval volcanic rocks at the crest of the Sierra Nevada in central California. A Sierra Nevada source is likely because: (1) the mineralogy of volcanic detritus in Etchegoin strata is similar to that found in the Mehrten Formation; and (2) the vertical succession of augite-rich to hypersthene-rich volcanic detritus found in Etchegoin strata in the Coalinga region also occurs in the upper Miocene volcanic rocks at the crest of the Sierra Nevada. Severely weathered volcanic detritus that lacks accessory heavy minerals is attributed to recycling of mafic volcanic detritus from the Franciscan sandstone in the Diablo Range. A reworked origin is suspected for this volcanic detritus to account for the alteration and lack of typical volcanic accessory minerals. The metamorphic detritus characterized by metamorphic rock fragments associated with actinolite-tremolite and glaucophane is thought to have been derived from blueschist facies Franciscan rocks in the Diablo Range.

The late Miocene paleogeography of central California, prior to the deposition of Etchegoin strata, was characterized by two marine embayments; one in the San Francisco Bay region, the other in the central and southern parts of the San Joaquin Valley. At this time, the Gabilan Range, Santa Cruz Mountains, and the central part of the Diablo Range were the major emergent region. The paleographic changes that accompanied onset of deposition of the Etchegoin Formation are uplift in the northeastern and southern parts of the Diablo Range, and submergence of the Gabilan Range and most of the Santa Cruz Mountains region. Uplift in the northeastern part of the Diablo Range is thought to be responsible for

changing the locus of deposition of Sierran volcanic detritus from the San Francisco Bay region to the San Joaquin Valley. Emergence of the southern Diablo Range is suspected because arkosic detritus from the Santa Margarita Formation of the southern Diablo Range is found in Etchegoin strata. Submergence of the Gabilan Range and most of the Santa Cruz Mountains region is inferred because detritus characteristic of these regions are lacking in Etchegoin strata; however, the Gabilan Range probably remained a subsea high. The latter stage of deposition of Etchegoin strata are characterized primarily by continued deposition of Sierran and Diablo Range detritus in a restricted San Joaquin basin. The restriction of the San Joaquin basin is attributed to the closure of the southern seaway and a partial blockage by the Gabilan Range subsea high of the seaway outboard of the Coalinga region, and it is reflected in the basin by reduced marine deposition. The restriction caused by Gabilan Range became outboard of the Coalinga region as a result of northwestward movement along the San Andreas fault, which averaged approximately 26 mm/yr during the past 8 Ma. The complex changes in mineralogic composition of Etchegoin strata in the southern Diablo Range thus reflect changes in sediment dispersal caused by emergence and a submergence of nearby and far removed areas of central California.

3. Trenches in Holocene stream deposits near Parkfield reveal offset gravelbars formed by Little Cholame Creek about 3000 ka. The offset, from about 63.5 to 160 m, implies slip rates of from 20 to 50 mm/yr. This range spans the rates determined from nearby Holocene units at the Melendy Ranch and Wallace Creek, and exceeds the long-term rate inferred from the Neenach-Pinnacles volcanic rocks. Rates of Holocene offset are more precise because they span less time and the offset is easily measured. However, the Holocene rate may not be comparable to longer term rates owing to possible variation in the rate of slip for time periods of 100 to 1,000 ka.

4. Several days have been spent by Sims conferring with Malcolm Johnston, Tom Moses, and others associated with the borehole instrumentation projects in determining the best quality sites and site geological conditions that affect drilling and instrumentation. Dave Higgins of my project is in charge of sampling, the boreholes, preparing lithologic logs, and preparing follow-up reports. Results from hole VYCC yielded information on lithology of part of the Santa Margarita Sandstone. The material cored showed that Santa Margarita is composed of detritus derived from the erosion of Salinian block rocks and volcanic rocks of the Neenach-Pinnacles type. This data supports the hypothesis of three phases of movement on the San Andreas in this region developed by Sims (see #1 above).

Reports

Sims, J.D., 1985, Geologic framework for slip-rate studies along the San Andreas fault at Parkfield, California: *American Geophysical Union Transactions*, v. 86, p. 985.

Sims, J.D., 1986, The Parkfield shuffle--displaced rock bodies as a clue to the past-Eocene history of movement on the San Andreas fault in central California: *Geological Society of America, Abstracts with Programs*, v. 18, p. 185.

Perkins, J.A., 1986, Provenance of the Etchegoin Formation: Implications for late Miocene and early Pliocene paleogeography of central California: *U.S. Geological Survey Open-File Report 86-xxx*, 110 p.

O'Day, P.A., and Sims, J.D., 1986, Sandstone composition and paleogeography of the Temblor Formation--Evidence for early- to middle-Miocene right-lateral displacement on the San Andreas fault system: *Geological Society of America Abstracts with Programs*, v. 18, p. 165.

Lienkaemper, J.J., Prescott, W.H., Sims, J.D., and Higgins, C.D., 1985, Parkfield slip history: *American Geophysical Union Transactions*, v. 66, p. 985.

LATE PLEISTOCENE AND HOLOCENE(?) FAULTING BENEATH SAN FRANCISCO BAY, CALIFORNIA

14-08-0001-21917

Doris Sloan and Charlotte Brunner
Department of Paleontology
University of California
Berkeley, CA 94720
(415) 642-7873

INVESTIGATION

The objective of this project was to use stratigraphic and paleontologic methods to investigate the extent, timing and sense of movement of probable faults beneath San Francisco Bay. Previous stratigraphic studies identified offset of late Pleistocene estuarine sediments in boreholes along a transect between San Francisco and Alameda (Sloan, 1981; Laws, 1983; Sloan and Laws, 1983). Distribution of foraminifer and diatom biofacies in the estuarine deposits records transgressive conditions in the bay and a change from brackish marsh to fully marine environments. Offset of these biofacies indicates movement with an apparent vertical displacement of 17 m on several faults.

The approach in the present project was to determine 1) whether late Pleistocene estuarine foraminifer and diatom biofacies are also offset in cores from a San Mateo-Hayward transect; and 2) whether offset can be traced upward through the overlying Wisconsin and Holocene deposits at the San Francisco-Alameda or San Mateo-Hayward transects. Success in tracing late Pleistocene faults northward and southward of the San Francisco-Alameda transect and in recognizing Holocene offset depends on closely-spaced sampling and sufficient preservation of microfossils to permit definition of biofacies. Recognition of Holocene faulting requires, in addition, sufficient change in biofacies to reveal offset.

RESULTS

1. Extent of Late Pleistocene Faulting

The distribution of foraminifers and diatoms was examined in late Pleistocene deposits in five boreholes along the San Mateo-Hayward transect. Preservation of microfossils was sufficient to permit definition of foraminiferal and diatom biofacies, but resolution was not detailed enough to determine whether fault offset occurs. Only 27 percent of the 85 samples examined for foraminifers contained identifiable specimens, and only 54 percent of the samples processed for diatoms contained enough identifiable specimens to permit biofacies determinations. The data show substantial offset of facies suggestive of faulting. However, resolution is not good enough to discriminate between fault offset or rapid facies change. Therefore, it was not possible to determine whether discontinuities in late Pleistocene estuarine sediments at the San Francisco-Alameda transect extend southward as far as the San Mateo-Hayward transect.

Although the objectives relative to late Pleistocene faulting were not realized, valuable stratigraphic and paleontologic data were collected, which extend our knowledge of the depositional setting of the penultimate bay. The biofacies in late Pleistocene deposits along the San Mateo-Hayward transect are similar to those identified at the San Francisco-Alameda transect (Sloan, 1981; Laws, 1982), and are indicative of marsh to subtidal environments. A deepening-upward sequence is preserved. However, shallower conditions prevailed at the San Mateo-Hayward transect than at the more northerly transect. Biofacies changes in uppermost samples in several boreholes suggest a drop in relative sea level. Evidence for small-scale changes in sea level and subaerial exposure of sediments occurs in several boreholes.

2. Timing and Sense of Movement

At the San Francisco-Alameda transect samples from four boreholes were analyzed to determine whether two offsets in late Pleistocene estuarine deposits (Sloan and Laws, 1983) can be traced through the overlying late Pleistocene terrestrial and aeolian and Holocene estuarine deposits. At one locality stratigraphic relationships in the terrestrial and aeolian deposits supports an interpretation of offset. A 3 m sequence of flood basin deposits is present in one borehole but not in the other. In addition, alluvial deposits in the two boreholes appear to be lithologically dissimilar, although no detailed mineral counts were made. Sloan and Laws (1983) argue for vertical offset of the late Pleistocene estuarine deposits at this locality. However, the lack of correspondence of younger sediments in the boreholes suggests lateral rather than vertical offset. It is not possible to determine whether Holocene deposits are offset because no Holocene samples are available from these boreholes.

At the other locality boring logs and soil profiles strongly suggest an offset of Holocene and late Pleistocene terrestrial and aeolian deposits (Bay Toll Crossings, unpublished data). However, examination of the sediments shows that they can be correlated between the boreholes and that lateral facies change can account for the difference between the sediments. The sediments are stream channel deposits and sands of possible aeolian origin. Such sediments can exhibit a high degree of lateral variability. Therefore, apparently only the late Pleistocene estuarine deposits are offset.

Two possible Holocene offsets were investigated, one at the San Mateo-Hayward transect, the other at the San Francisco-Alameda transect. There is much less microfossil variability in the Holocene than in the late Pleistocene estuarine sediments, in which five biofacies can be defined (Sloan and Laws, 1982). Only two biofacies, one intertidal, the other subtidal, occur in the Holocene estuarine samples examined for this study. This does not provide sufficient resolution to determine offset of the deposits, which are relatively uniform in grain size and mineralogy.

At the San Mateo-Hayward transect there is no evidence in the distribution of the biofacies for fault offset of Holocene deposits. It is likely that there is not enough change in the biofacies through time to reveal offset if it were present. It is also possible that the

sampling interval (1.5-3 m) is not small enough to provide the detail necessary to show offset. Alternatively, the faulting that offset the late Pleistocene deposits does not continue into the Holocene.

SUMMARY

Analysis of fault offset in late Pleistocene and Holocene core samples from San Francisco Bay is hampered by the lack of closely-spaced samples, by in-situ and post-collection dissolution of microfossils in estuarine sediments, and by relatively little biofacies change through time in the estuarine sediments. In spite of these problems, data are sufficient to provide some information on timing and sense of movement of late Pleistocene offset at one of three localities investigated and to suggest that movement is restricted to late Pleistocene estuarine deposits at a second locality.

Presently available Holocene core samples are not adequate to analyze possible Holocene sub-bay fault movement. If at some time new boreholes are planned along a transect across San Francisco Bay, every effort should be made to obtain and process samples within a short time (days to a few weeks) so that maximum information is retained. This approach can provide a relatively low-cost method of identifying fault offset if microfossil preservation is good, and closely-spaced samples are available.

REFERENCES

Laws, R.A., 1982. Quaternary Diatom Floras and Pleistocene Paleogeography of San Francisco Bay. Unpublished Ph.D. Dissertation, Department of Paleontology, University of California, Berkeley, CA 94720, 352 pp.

Sloan, D., 1981. Ecostratigraphic Study of Sangamon Sediments Beneath Central San Francisco Bay. Unpublished Ph.D. Dissertation, Department of Paleontology, University of California, Berkeley, CA 94720, 316 pp.

Sloan, D. and R.A. Laws, 1982. Sangamon depositional environments in central San Francisco Bay, California; Geological Society of America Abstr. with Programs, v. 14:4, p. 234.

Sloan, D. and R.A. Laws, 1983. Preliminary evidence for Pleistocene faulting beneath San Francisco Bay; Abstr., Symposium on Late Cenozoic Tectonics and Sedimentation along Faults of the San Andreas System, Pacific Section, Society of Economic Paleontologists and Mineralogists, Sacramento, CA, May 18-21, 1983, p. 133-4.

Seismotectonic Framework and Earthquake Source Characterization--Wasatch Front, Utah, and Adjacent Intermountain Seismic Belt

14-08-0001-G1163

R.B. Smith, W.J. Arabasz, and J.C. Pechmann*
Department of Geology and Geophysics
University of Utah
Salt Lake City, Utah 84112
(801)581-6274

Investigations

1. Comparison of intraplate earthquake behavior in the Intermountain seismic belt and the eastern U.S.
2. P-wave velocity structure of the crust-mantle boundary beneath Utah from network travel time measurements.
3. Earthquake focal mechanisms in the Wasatch Front area during 1981-1986.

Results

1. Despite evident contrasts in stress state and style of contemporary deformation, regions of the (extensional) Intermountain seismic belt and the (compressional) eastern U.S. appear to display some common aspects of intraplate earthquake behavior. These include: diffuse background seismicity, problematic correlation of seismicity with surficial geologic structure, influence locally of pre-Cenozoic detachment structures on rates of seismicity versus depth, low to moderate seismic flux, and long (>1 Ka to >>1 Ka) recurrence intervals of surface faulting. Given the widespread presence of late Pleistocene-Holocene fault scarps in the Intermountain region and their corresponding paucity in the eastern U.S., comparison provides useful insight into using historical and instrumental seismicity as a basis for: source-zone identification, recurrence modeling of moderate to large earthquakes, estimating the minimum threshold of surface faulting, and evaluating implications of low seismicity in the vicinity of late Quaternary faulting (such as along the Meers fault). In the Intermountain region, major active faults are generally not definable by background seismicity, and moderate-size earthquakes smaller than M6 can be argued to have a potential for nearly random spatial occurrence within bounds of broad seismic belts. Superposed epicentral patterns result where seismicity varies above and below low-angle detachment structures, and the recurrence rate of large earthquakes appears to be higher than that extrapolated from background seismicity. Seismic zones in regions of fold and thrustbelt structure in the eastern U.S. display depth-varying seismicity similar to that observed in the Intermountain seismic belt. This notably includes the southern Appalachians of eastern Tennessee and western North Carolina, the Giles County seismic zone of northwestern Virginia, and the Central Virginia seismic zone.

*Graduate students D.T. Loeb and I. Bjarnason also contributed significantly to this project during the report period.

2. Seismic refraction studies have generally concluded that the Utah portion of the Basin and Range province is characterized by an anomalously thin crust (25-28 km) and a very low P_n velocity of 7.4-7.6 km/sec. Although travel time curves of local earthquakes (Δ < 250 km) support this conclusion, travel time curves of near regional earthquakes (250 km < Δ < 700 km) indicate that upper mantle rock with a higher P_n velocity of about 7.9 km/sec is present below the 7.5 km/sec material. The depth structure of these two refractors was investigated by the conversion of travel time residuals to refractor depth using a backwards ray tracing technique and by a modified time term inversion of travel times.

Results indicate that the 7.9 km/sec refractor dips eastward from a depth of about 36 km in western Utah to about 44 km in the western Colorado Plateau and Middle Rocky Mountains of eastern Utah, with most of the increase in depth occurring in a 100-km-wide zone just to the west of the physiographic boundary. The 7.5 km/sec refractor also dips eastward, from a depth of about 25 km in north-central Utah to about 30 km at the eastern margin of the Basin and Range. Refraction results indicate that this refractor deepens in western Utah and disappears in eastern Nevada. Therefore, a wedge-shaped geometry is inferred for the 7.5 km/sec material. The 7.9 km/sec refractor is interpreted to be continuous with refractors of similar velocity that underlie the crust of the central Basin and Range province of eastern Nevada and the Middle Rocky Mountains and Colorado Plateau of eastern Utah, and is therefore interpreted to be the Moho. This contradicts previous interpretations of the 7.5 km/sec material as a mantle or asthenospheric upwarp.

3. A systematic and comprehensive study of focal mechanisms of Wasatch Front earthquakes during 1981-1986 is now well underway. Exhaustive polarity checks of the University of Utah network have been completed. Preliminary focal mechanisms have been done for 20 events of M_L 2.7 or greater. The velocity model that we are using to locate the events and calculate takeoff angles for most of the stations is a horizontally-layered version of the model for the Wasatch Front discussed above and shown in Figure 1. For stations in southeastern Idaho and in the interior of the Colorado Plateau, we use different velocity models to calculate the takeoff angles. These models are similar to the Wasatch Front model in the upper crust, but below 17 km have velocity structures appropriate for these regions. As a check on takeoff angles to be used in the focal mechanisms, we use reduced travel time plots to compare observed travel times to those calculated from the velocity models (Figure 2, top). The sample focal mechanism shown in Figure 2 (bottom) is for a M_L 4.4 earthquake that occurred 10 km southeast of Scipio, Utah on March 24, 1986, at 22:40. The focal depth was fixed to 6.3 km based on aftershock depths determined with the aid of a portable network of 8 stations that was deployed following the event. The mechanism shows a combination of normal and strike-slip movement on a fault plane that strikes either northeast or northwest.

Reports and Publications

Arabasz, W.J. (1986). Common aspects of intraplate earthquake behavior in the intermountain seismic belt and eastern U.S., Earthquake Notes, 57, 12.

Eddington, P.K., R.B. Smith, and C. Renggli (1985). Kinematics of Great Basin intraplate extension, Eos Trans. AGU, 66, 1056.

Jones, C.H., P.H. Molnar, R.B. Smith, and G. Chen (1985). Microearthquake investigation of the Hansel Valley-Pocatello Valley region, northern Utah and southern Idaho, Eos Trans. AGU, 66, 954.

Leu, L.L., and R.B. Smith (1985). Three-dimensional velocity structure of the 1983 Borah Peak, Idaho, earthquake area using geotomographic inversion of aftershock travel times, Eos Trans. AGU, 66, 974.

Loeb, D.T. (1986). The P-wave velocity structure of the crust-mantle boundary beneath Utah, M.S. thesis, University of Utah, Salt Lake City, Utah.

Loeb, D.T., and J.C. Pechmann (1986). The P-wave velocity structure of the crust-mantle boundary beneath Utah from network travel time measurements, Earthquake Notes, 57, 10.

Peinado, J., and W.J. Arabasz (1985). Moment-magnitude relations in the Utah-Idaho region and stress drop-versus-moment behavior, Eos Trans. AGU, 66, 954.

Smith, R.B. (1986). Lithospheric structure, seismicity, and contemporary deformation of the United States Cordillera, submitted to Geol. Soc. Am. DNAG volume on the Cordilleran Orogen: Conterminous U.S.

Smith, R.B., W.C. Nagy, K.A. Julander, J.J. Viveiros, C.A. Barker, W.W. Bashore, and D.G. Gants (1986). Geophysical and tectonic framework: Basin-Range to Colorado Plateau-Rocky Mountain transition, submitted to special volume on Geophysical Framework of the Continental U.S.—Intermontane System.

Thorbjarnardottir, B.S., and J.C. Pechmann (1985). Waveform analysis of preshock-mainshock-aftershock sequences in Utah, Eos Trans. AGU, 66, 954.

Thorbjarnardottir, B.S., and J.C. Pechmann (1986). Constraints on relative earthquake locations from cross correlation of waveforms, submitted to Bull. Seism. Soc. Am.

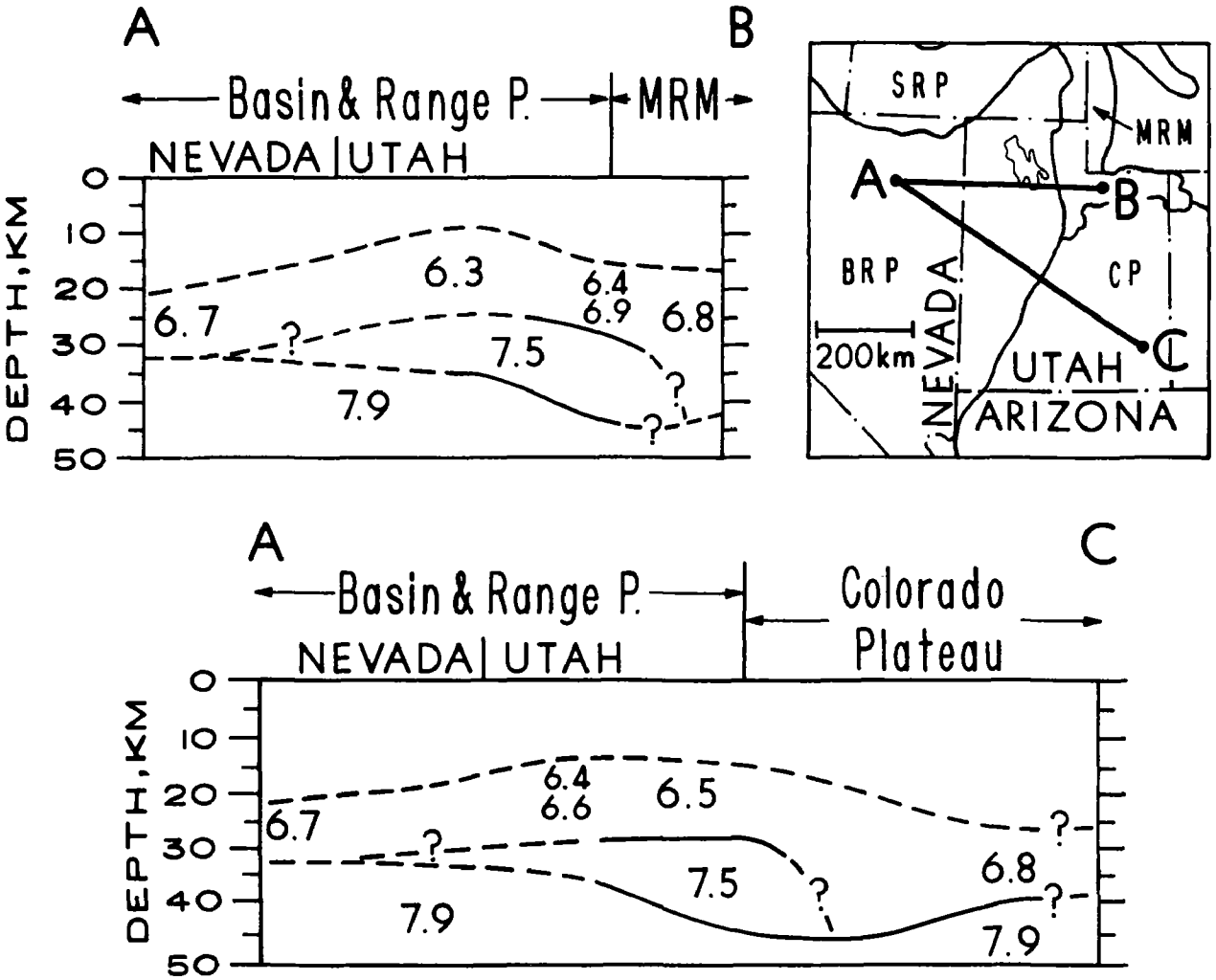

Figure 1. Cross sections showing P-wave velocity structure across the Wasatch Front. The locations of the cross sections ae shown on the index map at the upper right. The structure below the top of the 7.5 km/sec layer is from network travel time measurements. The structure above this layer is generalized from refraction studies. Note the continuous 7.9 km/sec moho beneath Utah which was not detected by refraction studies because data was not recorded out to large enough distances.

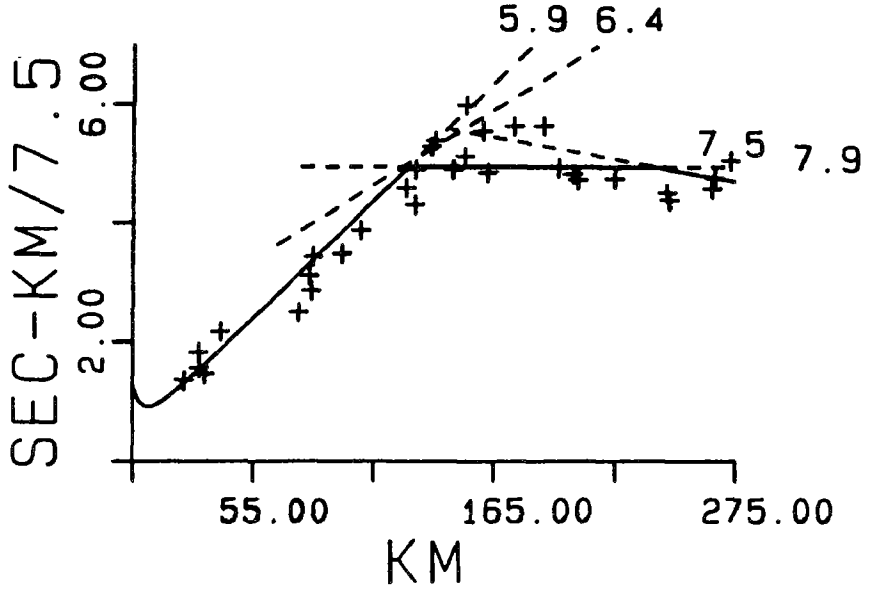

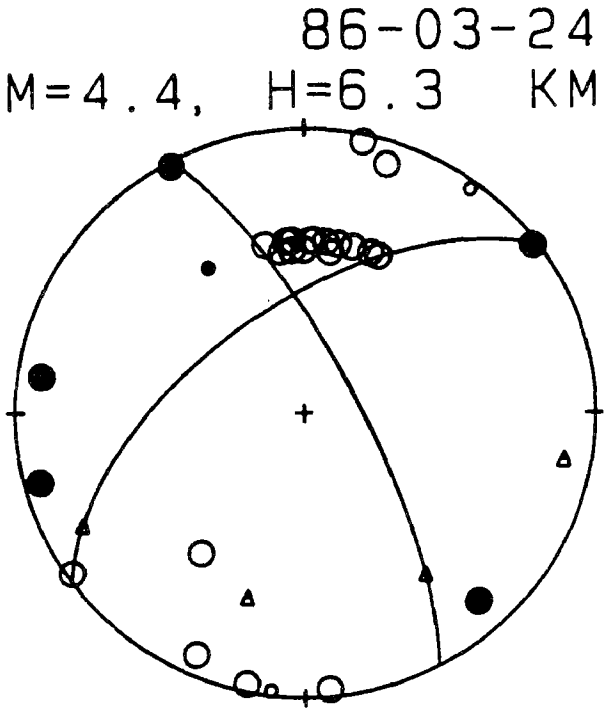

Figure 2. (Top) Reduced travel time plot for a M_L 4.4 earthquake that occurred 10 km SE of Scipio, Utah on March 24, 1986, at 22:40. Solid lines show first arrival travel times calculated from a horizontally-layered velocity model for the Wasatch Front derived from Figure 1. (Bottom) Lower hemisphere P-wave fault plane solution for the same event, constructed using takeoff angles from the revised velocity model shown on the travel time plot. Solid and open circles indicate compressional and dilatational first motions, respectively. Smaller circles indicate less certain readings. The slip vectors, compression axis, and tension axis are shown as triangles.

GREAT EARTHQUAKES AND GREAT ASPERITIES, SOUTHERN CALIFORNIA: A PROGRAM OF DATA ANALYSIS

14-08-0001-G-1096

Lynn R. Sykes and Leonardo Seeber
Lamont-Doherty Geological Observatory of Columbia University
Palisades, New York 10964
(914) 359-2900

Investigations

During 1985 and 1986 we have utilized earthquake data from the CIT-USGS catalog, paleomagnetic determinations, paleoseismicity and historical accounts of seismicity to examine the southern San Andreas fault system.

Results

1. Block rotations in southern California. The discovery that the San Andreas fault system in southern California is characterized by systems of blocks which are currently undergoing rotation is significant for earthquake prediction is several ways. Following are two effects that we are currently investigating:

a) A significant portion of the overall right-lateral plate displacement is taken up by block rotations. This portion may vary in time and space. Accordingly, the corresponding portion that is taken up by right-lateral slip on the major faults will also vary. Thus, slip rate along master faults may be different from place to place, and whether measured geodetically or geologically.

b) Block rotations may effect the earthquake cycle. The stress across a major fault preparing for rupture may be altered by the rotation of an adjacent block. The strength of this fault may increase if normal stress increases as a consequence of block rotation. Thus, block rotation may be related to the length of the interseismic period between great earthquakes and to the timing of rupture.

We are carrying out a detailed structural/paleomagnetic investigation of the southern San Jacinto fault zone addressing the relation between slip in the master fault and rotation of adjacent blocks. Results so far include the discovery of 30° of rotation of the Borrego Badlands during the Quaternary and of many structural features within the Bandlands and in surrounding regions associated with this rotation.

2. Block rotation along the southern San Jacinto fault zone. The 100 km long portion of the San Jacinto zone from the Anza Plateau to the Imperial Valley is characterized by a series of northeast cross faults which span the 3 to 7 km wide zone. Although major earthquakes are associated with right-lateral ruptures on the northwest strands, aftershocks and background seismicity occupy the entire fault zone and are often associated with left-lateral cross faults. A system of faults and blocks across the Coyote Ridge at the northwestern end of this zone could transfer right-lateral shear between two overlapping strands by rapid clockwise rotation. Southeast of Coyote Ridge, the San Jacinto fault zone occupies a broad valley characterized by deformed Plio-Quaternary terrestrial clastics. Several

cross faults are recognized in this young structural domain. Paleomagnetic data from poorly lithified sediments of the Octotillo formation in the Borrego Badlands and straddling the Inspiration Point cross fault, yield normal and reversed characteristic magnetizations that deviate from geomagnetic north and south by 20° to 30° clockwise. This rotation has occurred in the last 0.7 to 1.0 my, since the sediment is younger than 1 my and the sampled reversal older than 0.7 my. The minimum rate of rotation is then 0.3-0.7 μrad/y, corresponding to a minimum overall displacement rate of 0.2-0.5 cm/y for the San Jacinto fault zone. Offset channels and a cluster of 1968 aftershocks associated with the Inspiration Point fault suggest ongoing left slip and clockwise rotation. The triangular Clark Basin between the Borrego Badlands and Coyote Mtn. may reflect pull-apart fanning between rotating and translating portions of the San Jacinto fault zone. A detailed resolution of block kinematics within fault zones such as the San Jacinto fault zone at both the geologic and geodetic time scale may help to understand the pattern of deformation leading to a major rupture.

3. Quiescence of the southern San Andreas fault and adjacent secondary seismicity. The southern San Andreas fault in the area from the Pinto Mountains to Bombay Beach (Salton Sea) is nearly quiescent at the microearthquake level. The closest seismicity is located 3-5 km NE of the fault. The most active region is about 20 km wide and extends from as far north as the Pinto Mountain fault to as far south as the Mecca hills. Relocation of earthquakes using only stations NE of the San Andreas fault and proximal to the activity does not seriously affect epicentral locations, suggesting that the observed offset of epicenters from the San Andreas fault is not an artifact of velocity inhomogeneity. Many of the earthquakes that occur within this region can be ascribed to structures striking NE and conjugate to the San Andreas fault.

Focal mechanisms of earthquakes between 1976 and 1985 were examined. events with essentially common focal mechanisms were found to define linear trends parallel to nodal planes. Structures thus defined are consistent with a NNE axis of maximum compression, in contrast to generally N-S P axes determined in the southern Salton trough and central Transvrese Ranges.

The most consistent feature in the region is that T axes from focal mechanisms of either the normal faulting, strike-slip faulting or a combination of the two have nearly the same azimuth and plunge. This argues that the least compressive stress, which is generally oriented southeasterly, is much smaller than the vertical stress, which is approximately equal to the maximum horizontal compressive stress. Those two stresses interchange to give combinations of normal and strike-slip mechanisms. The pattern changes abruptly as the San Andreas fault changes direction in San Gorgonio Pass. Mechanisms in that area and in a broad area to the west in the Transverse Ranges are characterized by strike-slip and thrust faulting such that the maximum horizontal compression, which is oriented nearly north-south, is much larger than the other two principal stresses. This is in accord with the idea that relatively high stresses are required for the San Andreas fault to slip in the big bend region whereas lower stresses are required for it to slip between Palm Springs and the Salton Sea. This goes along with the developing idea that the Palm Springs to Salton Sea segment of the San Andreas has a repeat time of the order of 150 years in contrast to the major bends or knots which have much longer repeat times.

Three large blocks are bounded by the Pinto Moutain, Blue Cut, Chiriaco and San Andreas faults. The western portions of these blocks are currently

active in response to accumulating elastic strain across a locked San Andreas fault. None of the major E-W striking surface faults are seismically active, however, microearthquakes define E-W en echelon structures in the northern block. A $M_L \approx 4$ event in a previously quiescent locality NE of the 1947 Morongo Valley earthquake occurred in January 1985. This is the largest event to occur in the study area in the period from 1976 to 1985. A second set of 5 events with $3 < M_L < 4$ occurred 14 km to the SE during January. These events fall on a NE striking lineament defined by earlier earthquakes. The asymmetric concentration of activity in the northern portion of the study area suggests that this area has localized higher stress. Alternatively, the closely spaced active structures are uniquely sensitive to the level of stress on the San Andreas fault.

4. Seismicity and fault kinematics along the Brawley seismic zone and adjacent regions. The Brawley seismic zone is the most active section of the San Andreas fault system in southern California. It is defined by a broad band of earthquakes that trends just west of north and connects the southern San Andreas to the Imperial fault. The high rate of microearthquake activity, combined with the shallow nature of the seismicity, the high areal heat flow, the lack of known large (M>6) earthquakes, and the orientation of the fault zone relative to the plate motion vector suggest that the Brawley seismic zone should be dominated by extensional tectonics. Detailed analysis of the microearthquake data from the CIT-USGS catalog reveals, however, that north of the surface rupture involved in the 1979 Imperial Valley earthquake, the Brawley seismic zone is not a single simple fault, but is composed of a complicated series of nearly-orthogonal en echelon northeast striking left-lateral faults that intersect other fault segments striking north or northwest. Very few of the earthquake focal mechanisms examined could be interpreted as pure normal fault solutions. Instead the predominant syle of seismic deformation is strike-slip or oblique strike-slip. Some earthquakes even exhibit focal mechanisms with a large component of reverse faulting. These events are generally located at block corners where faults intersect and could be the result of rotations induced by regional shear. Other earthquake hypocenters define a nearly-vertical northeast-striking planar feature that parallels the southern end of the Salton Sea and conncects the Superstition Hills fault zone with the Brawley seismic zone. Motion along this tranverse structure is also left-lateral and may be accomodating relative slip between the two major fault zones as they converge at the head of Imperial Valley. Such secondary structures may control the distribution of slip between major wrench faults in California, as demonstrated by the occurrence of triggered slip on the Superstition Hills fault after the 1979 event and the occurrence of a large (M_L=5.5) earthquake on the Brawley seismic zone 10 hours after the 1942 Superstition Hills earthquake (M_L=6.5).

References

Bogen, N.L., and L. Seeber, Late Quaternary block rotation within the San Jacinto fault zone, southern California, submitted for publication, 1986.

Nicholson, C., L. Seeber, P. Williams, and L.R. Sykes, Seismicity and fault kinematics through the eastern Transverse ranges, California: Block rotation, strike-slip faulting and shallow-angle thrusts, Journal of Geophysical Research, 91, 4891-4908, 1986.

Nicholson, et al., Seismic deformation along the southern San Andras fault: Implications for conjugate slip and rotational block tectonics, Tectonics, in press, 1986.

Nicholson, et al., Seismicity and fault kinematics along the Brawley seismic zone and adjacent regions (abstract), EOS, Trans. AGU, 1985.

Seeber, L., and C. Nicholson, Block rotation along the San Andras fault system in California: Long-term structural signature and short-term effects in the earthquake cycle, preprint, 1986.

Sykes, L. R., and L. Seeber, Great earthquakes and great asperities, San Andreas fault, southern Calfornia, Geology, 113, 835-838, 1985.

Williams, et al., Quiescence of the southern San Andreas fault and adjacent secondary seismicity (abstract), EOS, Trans. AGU, 1985.

Williams, et al., Seismotectonics of the easternmost Transverse Ranges, California: Patterns of activity on secondary structures, in preparation, 1986.

Tectonic Analysis of Active Faults

9900-01270

Robert E. Wallace
Office of Earthquakes, Volcanoes, and Engineering
345 Middlefield Road, MS 977
Menlo Park, California 94025
(415) 323-8111, ext. 2751

Investigations

1. Evaluation of fault scarps and tectonics of the central Nevada and eastern California seismic belts.

2. Active Tectonics. A project under the auspices of the Geophysics Study Group, National Research Council, National Academy of Sciences. Served as chairman of study group.

3. International Geological Correlation Program (IGCP) - Project 206 - Active Faults of the World.

4. Investigations of active faults in Ningxia and Gansu Province, PRC. Cooperative program in earthquake studies: U.S. Geological Survey/State Seismological Bureau, People's Republic of China.

Results

1. Organized a group of authors to prepare a professional paper on the San Andreas fault. Outlines of 9 chapters are completed and writing has begun.

2. As member of panel on Seismic Hazard Assessment for NRC/NAS, participated in meeting and have begun a chapter on how probabilistic seismic hazard assessment techniques "capture" earth-science information.

3. Unsuccessfully searched for surface faulting related to Tres Pinos, California earthquake of January 26, 1986. Participating as co-author of report on earthquake.

4. National Research Council project on Active Tectonics was completed and a 266-page volume is published.

5. Began a joint paper comparing the San Andreas, Tan Lu, Alpine, and North Anatolia fault and the Median Tectonic Line under IGCP project 206.

6. Completed paper with Chinese colleagues on fault scarps in Ningxia Hui Autonomous Region, China.

Reports

1. Wallace, Robert E., chairman, 1986, Active Tectonics: National Academy Press, Washington, D. C., 266 p.

2. Wallace, Robert E., 1986, Geologic Hazards: The Mexico Earthquake: Scientific and Engineering Implications, Subcommittee on Science, Research and Technology of the Committee on Science and Technology, House of Representatives, Ninety-ninth Congress, Washington, D.C., 1985, No. 54, p. 204-208.

3. Zhang, Buchun, Liao, Yuhua, Guo, Shunmin, Wallace, Robert E., Bucknam, Robert C., and Hanks, Thomas C., 1986, Fault Scarps related to the 1739 earthquake, and seismicity of the Yinchuan Graben, Ningxia, Huizu Zizhiqu, China: Seismological Society of America Bulletin (in press).

4. Bucknam, Robert C., Wallace, Robert E., and Hanks, Thomas C., 1985, Fault scarps related to the 1739 earthquake in Ningxia Hui Autonomous Region, north-central China [abs.]: Transactions, American Geophysical Union, v. 66, no. 46, p. 1067.

5. Wallace, Robert E., 1986, Geologists and Ideas: A History of North American Geology, Centennial Special Volume 1, a review: Science, v. , n.__, p.__ (in press).

Geothermal Seismotectonic Studies

9930-02097

Craig S. Weaver
Branch of Seismology
U. S. Geological Survey
at Geophysics Program AK-50
University of Washington
Seattle, Washington 98195
(206) 442-0627

Investigations

1. Continued analysis of the seismicity and volcanism patterns of the Pacific Northwest in an effort to develop an improved tectonic model that will be useful in updating earthquake hazards in the region. (Weaver, Yelin, Grant, Zollweg).

2. Continued acquisition of seismicity data along the Washington coast and the continued seismic monitoring of the Mount St. Helens area as well as the southern Washington-northern Oregon Cascade Range. The data from this monitoring is being used in the development of models of volcanic processes at Mount St. Helens and seismotectonic models for southwestern Washington. (Weaver, Zollweg, Grant, Shemeta, UW contract)

3. Study of Washington seismicity, 1938-1970. Available helicorder records are being scanned in an effort to determine the completeness of existing earthquake catalogs for the time period that predates the establishment of the existing short-period network. Although records are being reviewed for the entire time period, major emphasis is on the period from 1960 to 1969. The goal of this work is to produce a catalog of located earthquakes that is complete for Washington and northern Oregon above magnitude 4 from 1960 to 1985. (Yelin, Grant, Shemeta)

4. Detailed analysis of the seismicity sequence accompanying the May 18, 1980 eruption of Mount St. Helens. Earthquakes are being located in the ten hours immediately following the onset of the eruption, and the seismic sequence is being compared with the detailed geologic observations made on May 18. (Weaver, Shemeta, UW contract)

5. Study of the larger aftershocks of the Borah Peak, Idaho, earthquake. This work is examining the relation between mapped fault displacements and seismic moment release. (Zollweg)

6. Assistance to the government of Colombia in an effort to establish an effective seismic monitoring program at Nevada del Ruiz. (Zollweg)

Results

1. We have completed the analysis of earthquakes during the ten hours immediately following the 1532 UTC onset of the May 18, 1980 eruption of Mount St. Helens, Washington. (The time-depth pattern was reported in the July 1985 volume in this series, Open-File Report 85-464). The spatial pattern of the earthquake hypocenters has been used to refine the geometry of the magmatic system beneath Mount St. Helens. A shallow magma reservoir (0-3 km) is connected by a narrow conduit (radius on the order of

0.1 km) to a deep magma reservoir located within an earthquake-free volume identified below 7.5 km. This deep reservoir is fault-bounded on the northwest and east. We correlate the low rate of seismicity during the first 4 1/2 hours after 1532 UCT with the eruption of the most evolved magmatic products and suggest that little of the early eruptive volume was transported from depths greater than about 3 km. The maximum period of seismicity corresponds to the tapping of the deeper reservoir (7.5-12 km depth) of less-evolved magmas and the subsequent injection of this magma into the narrow conduit. The deepest earthquakes (>12 km) occurring along the bounding fault to the northwest tend to have nearly all dilational arrivals, and we interpret this as evidence of volume collapse that is related to magma withdrawal from this fault zone to partially re-charge the deep reservoir. We conclude from the earthquake distribution that no significant change in the configuration of the magma system occurred as a result of the May 18 eruption. Our data indicates that no magma transport from depth occurred into the shallow reservoir before May 18; and as a result of this reservoir isolation, the volcanic earthquake sequence that preceded the May 18 eruption was the result of magma already in place within the shallow magma reservoir.

2. Seismicity and the orientation of fault planes from focal mechanisms indicate that Mount St. Helens is located at a dextral offset along the St. Helens seismic zone (SHZ). Because motion on the SHZ is in a right-lateral strike-slip sense, this dextral offset creates extension within a volume of the crust between the offset fault segments. This offset geometry is similar to that for geothermal areas along the San Andreas fault system. We have applied a model derived from these geothermal areas to Mount St. Helens, and find that the data at Mount St. Helens is consistent with the structural and seismological relations defined in San Andreas geothermal areas. The major difference between Mount St. Helens and the geothermal areas is in the ratio of the width of the offset, *(l)* to the seismogenic depth, *(h)*. At Mount St. Helens this ratio is < 1 whereas in the geothermal areas the ratio is about 1. The late-Quaternary volcanic vents near Mount St. Helens strike northeast, similar to the strike of a set of pre-Quaternary faults and intrusive rocks that are mapped north of the volcano; in addition, the deepest earthquakes occurring within the spreading volume are aligned along a northeast-striking fault. All of these northeast-striking features are approximately perpendicular to the regional minimum principal stress. From these observations, we infer that the spatial position of Mount St. Helens is controlled by the junction of the right-stepping offset along the SHZ with the older set of fractures, and that these fractures are favorably aligned with respect to the contemporary regional tectonic stress directions for the transport of magma through the brittle crust. The sense of fault motions predicted by our crustal spreading model is consistent with an apparent component of right-lateral shear measured from geodetic lines around Mount St. Helens during June and July 1980.

3. A seismic monitoring system has been installed on Nevada del Ruiz in Colombia. Routine analysis of the seismic records has begun; this effort includes event identification, event counts, magnitude determination and estimate of seismic energy release, hypocenteral locations, and amplitude and period measurements of the recorded episodes of volcanic tremor.

Reports

Weaver, C. S., Combined regional seismotectonics and the extent of Cenozoic volcanism: An improved first-order geothermal assessment of the Cascade Range? (abs), in, *U. S. Geological Survey Open-File Report, 85-521,* 14-17, 1985.

Baker, G. E., Three component long-period data for the 1949 South Puget Sound,

Washington, earthquake, *U. S. Geological Survey Open-File Report 85-613,* 1985.

Michaelson, C. A., and C. S. Weaver, Upper mantle structure from teleseismic P-wave arrivals in Washington and northern Oregon, *Journal Geophysical Research, vol. 91,* 2077-2094, 1986.

Shemeta, J. E. and Weaver, C.S., 1986, Seismicity accompanying the May 18, 1980 eruption of Mount St. Helens, Washington, *in, Proceedings, Mount St. Helens Five Years Later,* Eastern Washington University Press, Cheney, WA., (in press).

Grant, W. C. and Weaver, C. S., The 1958-1962 earthquake sequence near Swift Reservoir, Washington, *Bulletin of the Seismological Society of America,* (in press).

Physical Constraints on Source of Ground Motion

9910-01915

D. J. Andrews
Branch of Engineering Seismology and Geology
U.S. Geological Survey
345 Middlefield Road, MS 977
Menlo Park, California 94025
(415) 323-8111, ext. 2752

Investigations

Application of the diffusion equation to scarp degradation.

Results

The diffusion model of topographic degradation is a promising means by which vertical offsets on Holocene faults might be dated. In order to calibrate the method, I have examined present-day profiles measured by Robert C. Bucknam of wave-cut shoreline scarps of Late-Pleistocene Lake Bonneville. It may be assumed that these scarps were initially at least as steep as the angle of repose. Offsets range from 1 to 13 m. A parameter called apparent age, defined as the mean-square horizontal extent of the slope function of each profile, is plotted as a function of scarp offset. If linear diffusion held and scarps were initially vertical, apparent diffusion age would be the same for all the shoreline profiles. The points have little scatter, and show a clear trend of apparent age increasing with offset. This increasing trend is too great to be explained only by non-vertical initial scarp slope in a linear diffusion model. It may be explained by the rate of transport of surface material being a nonlinear function of slope. The data are fit by transport proportional to the cube of slope, which implies that the dominant transport mechanism is turbulent overland fluid flow.

Reports

Andrews, D.J., and Bucknam, R.C., 1986, Fitting scarp degradation by a model with nonlinear diffusion [abs.]: *Earthquake Notes*.

Geologic studies for seismic zonation of the Puget Lowland
Project 9540-04004

Brian F. Atwater
Branch of Western Regional Geology
U. S. Geological Survey at Department of Geological Sciences
University of Washington AJ-20
Seattle, Washington 98195
(206) 543-0804 FTS 399-2927

INVESTIGATIONS

This new project concerns both seismic potential (Element I) and ground-shaking hazard (Element III) in the Puget Sound area. The staff is Brian Atwater (full time), Jane Buchanan-Banks (1/3 time), and James P. Minard (contractor).

Seismic potential. Atwater made reconnaissance of late Holocene tidal-marsh deposits as recorders of vertical crustal movement in western Washington. The reconnaissance entailed the study of outcrops and cores on the Pacific Coast near Willipa Bay and Neah Bay, and in the northern Puget Lowland at central Whidbey Island (fig. 1).

Ground-shaking hazard. Buchanan-Banks began compilation of depth-to-bedrock data for the southern Puget Lowland. Minard mapped about one quarter of the Redmond 7.5-minute quadrangle, in the east-central Puget Lowland.

RESULTS

The most notable early results pertain to the potential for great subduction-zone earthquakes in the Pacific Northwest. Whereas monotonous sections of tidal-marsh peat at Whidbey Island suggest gradual submergence throughout the past 5000 years, rhythmically bedded intertidal deposits near Willipa and Neah Bays indicate at least one or two 1-m jerks of submergence during that time. Sudden submergence accompanied great earthquakes along the coasts of southwest Japan (1946), Chile (1960), and Alaska (1964). If similarly coseismic, the jerky submergence near Willipa and Neah Bays confirms previous seismological and geophysical deductions that the Pacific Northwest is subject to great subduction-zone earthquakes.

The evidence for jerky submergence near Willipa and Neah Bays is a stratigraphic sequence in which a tabular body of estuarine mud or sand abruptly overlies peaty tidal-marsh deposits. The mud or sand grades upward into similar tidal-marsh deposits. Scarcity or absence of tidal-marsh rhizomes in this mud or sand indicates deposition below the level at which most tidal-marsh plants live. The tabular shape of the mud or sand indicates that the sequence represents widespread submergence and burial of a marsh, not lateral migration of a tidal creek. The amount of submergence can be roughly equated with the thickness of the mud or sand.

Muddy sequences suggesting sudden submergence near Willipa Bay underlie tidal marsh bordering the Niawiakum River, in SW/4 NW/4 sec. 10 and SW/4 NW/4 sec. 14, T. 13 N, R. 10 W (Bay Center and Nemah 7.5-minute quadrangles). There, three cores penetrated two superposed sequences each suggesting sudden submergence, four additional cores indicate that the upper sequence is tabular along a 300-m transect perpendicular to the river in sec. 10, and streambank outcrops likewise show layer-cake, repetitive strata. The amount of submergence suggested by each of the sequences is in the range 0.7-1.3 m. The general scarcity of sand in the Niawiakum River sections suggests that little or none of this submergence represents local settlement; rather, each jerk probably represents tectonic subsidence. A 50-m-long outcrop in sec. 10, the most seaward of the Niawiakum River sections studied thus far, contains five horizontal layers of very fine sand just above the buried tidal-marsh deposit. There being no other sand in the outcrop, nor hardly any sand in the nearby cores, these laminae suggest that exceptionally strong marine currents--perhaps from tsunami--occurred during or soon after the sudden submergence.

A sandy sequence suggesting jerky submergence near Neah Bay is exposed in two places near extreme high-tide level along the southeast bank of the Waatch (pronounced why'-atch) River, in SW/4 sec. 15, T. 33 N, R. 15 W (Makah Bay 7.5-minute quadrangle). These streambank exposures indicate a single jerk of about 0.8-1.1 m. Much of this submergence conceivably could represent local earthquake-induced settlement, for water-well records reveal that loose, water-saturated sand underlies the area to depths of 30 m or more. The sand above the buried tidal-marsh deposits contains many foraminifers and diatoms of marine or estuarine origin. Accelerator-radiocarbon measurements have been made on a twig and on seeds of a Sitka spruce cone from the sand, and on Triglochin maritima rhizomes from the underlying tidal-marsh deposits. Pending correction for isotopic fractionation, the measurements are consistent with the hypothesis of sudden submergence and further indicate that this submergence took place about 1100 years ago. There is no known evidence along the Waatch River of sudden submergence more recent than this. Sandiness of deposits prevented a search, by means of hand-driven corer, for deposits that might record sudden submergence before 1100 years ago.

The great Alaskan and Chilean earthquakes of the early 1960's are thought to have long repeat times--about 1000 years in the case of areas greatly uplifted during the 1964 Alaskan earthquake--and were each accompanied by tectonic subsidence of a long (~1000 km) coastal belt above a ruptured subduction zone. Similarly, the jerky submergence of Holocene tidal marshes near Willipa and Neah Bays could represent coseismic subsidence accompanying infrequent great earthquakes in the Cascadia subduction zone. Pending further radiocarbon measurements, it is reasonable to suppose that the undated upper sequence near Willipa Bay represents the same earthquake as the dated sequence near Neah Bay, for both are located 140 km from the sea-floor edge of the Cascadia subduction zone (fig. 1). Thus two working hypotheses: (1) a great subduction-zone earthquake struck much of the Pacific Northwest about 1100 years ago; and (2) this was the most recent such earthquake to be accompanied by many decimeters of submergence along the Washington coast.

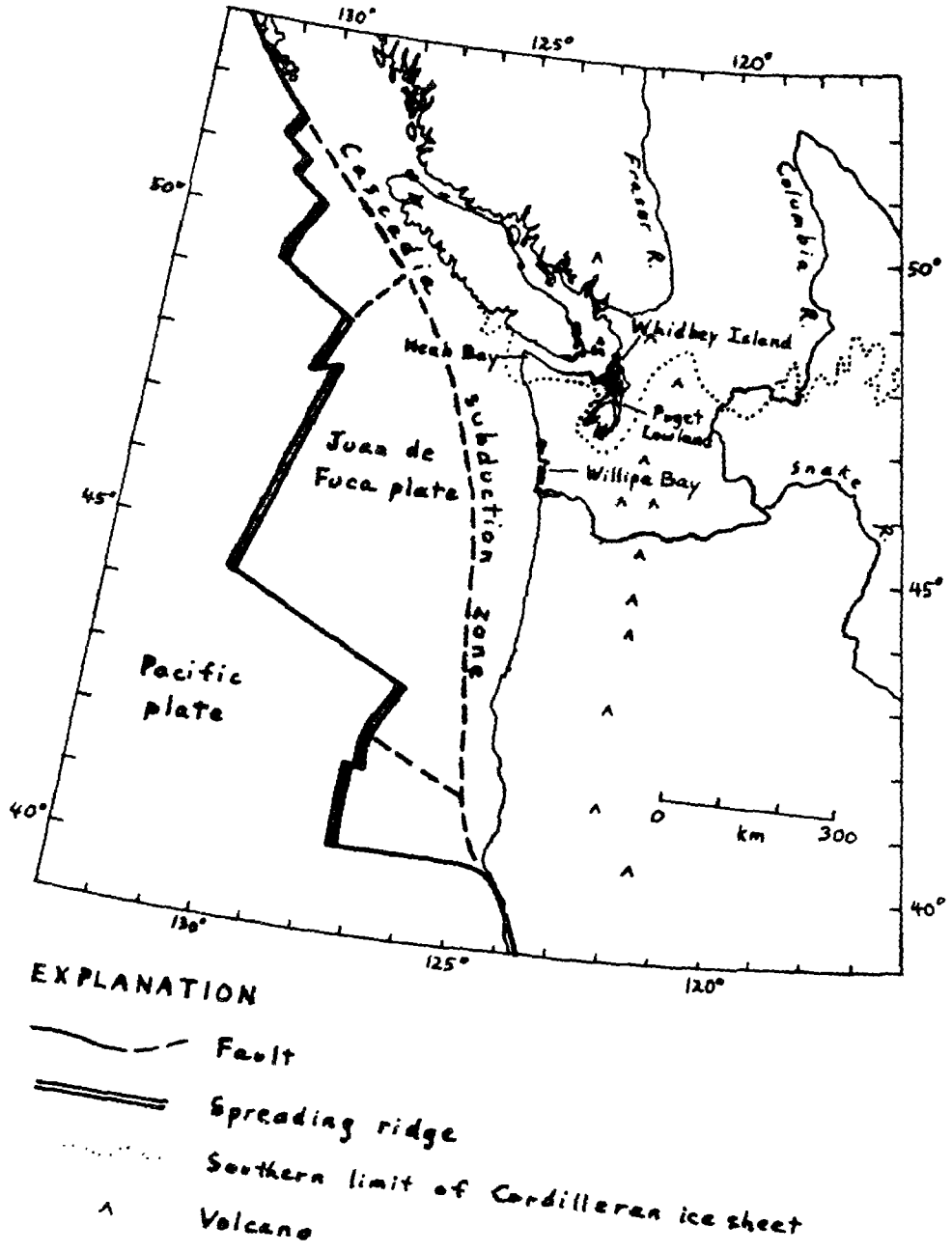

Figure 1. Index map.

Surface Faulting Studies

9910-02677

M. G. Bonilla
Branch of Engineering Seismology and Geology
U. S. Geological Survey
345 Middlefield Road, MS 977
Menlo Park, CA 94025
(415) 323-8111, Ext. 2245

Investigations

1. Threshold earthquake magnitude associated with coseismic surface faulting.
2. Appearance of active faults in exploratory trenches.

Results

Observational data compiled for earthquakes of magnitude less than 6 indicate that the threshold magnitude for earthquakes associated with surface faulting is about M_L 5. The threshold magnitude may actually be smaller because not all earthquakes near M_L 5 have been field checked and faulting at the threshold level is not easily recognized, even immediately after the event. Several factors affect the development and recognition of surface faulting. Surface displacements ranging from a few millimeters to several decimeters have accompanied earthquakes of about magnitude M_L 5. The larger displacements can damage structures, and such a possibility should be considered in regions where shallow earthquakes of about that size can occur. The generally small surface displacements at the threshold magnitude may leave very little evidence in the topography, stratigraphy, or near-surface structure, especially if the displacements are consistently small and recurrence intervals for earthquakes are long. Such conditions may explain the paucity of recognized active faults in some regions of infrequent shallow earthquakes, such as eastern North America.

Review and statistical testing of data related to the expression of faults in exploratory trenches revealed that the previously compiled data base is too small for some types of faults. Additional data that are now available are being compiled.

Reports

Bonilla, M.G., Threshold earthquake magnitude associated with coseismic surface faulting: submitted to *Bulletin of the Association of Engineering Geologists*.

Northern San Andreas Fault System

9910-03831

Robert D. Brown

Branch of Engineering Seismology and Geology
U.S. Geological Survey
345 Middlefield Road, MS 977
Menlo Park, CA 94025
(415) 323-8111, ext. 2461

Investigations

Project activities focused on the Quaternary tectonic history of the San Andreas fault system in California, preparatory to a review chapter on this topic for a planned USGS synthesis of geologic knowledge of the system. I am reviewing published and unpublished data on the San Andreas and related Quaternary faults, and on fold belts and stratigraphic relations that help define both strike-slip and vertical deformation along the fault system during Quaternary time. I am also analyzing relations shown on geologic, topographic and geophysical maps and conferring with other investigators who are, or have been, contributing to knowledge of the Quaternary history of the fault system.

As part of my advisory and liaison duties with the Nuclear Regulatory Commission staff, I continued review of plans for PG & E geologic and geophysical investigations, which are intended to further evaluate earthquake-related issues at Diablo Canyon power plant. This involved meetings and conferences with PG & E, NRC, and USGS staff; geologic interpretations of high altitude aerial photography; limited reconnaissance field work; and reviews of: (1) existing geologic and geophysical data and interpretations, and (2) the utility's work plan for the evaluation program.

Results

1. Prepared an outline for the Chapter on the Quaternary history of the San Andreas, assembled much of the relevant published and unpublished data, and began preparation of manuscript and illustrations.

2. Provided written and oral reviews of the scoping study for the Diablo Canyon long-range seismic program and arranged several meetings between PG & E and USGS personnel to facilitate exchange of information and encourage independent but mutally advantageous geologic and geophysical studies.

3. Provided written and oral information on earthquake hazards to the Bay Area Earthquake Preparedness Project (BAREPP) to support efforts to reduce earthquake hazards in the San Francisco bay region; as a member of BAREPP's advisory board, attended board meetings and conferences.

Reports

None during this period.

LATE QUATERNARY SLIP RATES ON ACTIVE FAULTS OF CALIFORNIA

9910-03554

Malcolm M. Clark

Branch of Engineering Seismology and Geology
U.S. Geological Survey
345 Middlefield Road, MS 977
Menlo Park, CA 94025
(415) 323-8111, ext. 2591

Investigations

1. Late Quaternary history of Owens Valley fault zone, eastern California (Sarah Beanland, M.M. Clark, S.K. Pezzopane, K.K. Harms).

2. Recently active traces of Calaveras fault near Tres Piños, California (J.W. Harden, K.K. Harms, M.M. Clark).

3. Historic slip rates along active faults of California (J.J. Lienkaemper).

4. Investigation of effects of the Quien Sabe earthquake of January 1986 (K.K. Harms, M.M. Clark).

Results

1. Field investigation of the Owens Valley fault zone has identified the 1872 surface rupture from Owens Lake to north of Big Pine over a distance of about 100 km. Dominant slip over most of the rupture was right lateral; the main trace shows no evidence for left slip. A vertical component was subordinate and variable in sense. Most of the 1872 rupture breaks latest Pleistocene beds from Lake Owens in the floor of Owens Valley. Progressively offset channels, meander scars, and scarps indicate at least three 1872-type earthquakes during Holocene time, with a maximum estimated Holocene horizontal slip rate of about 4 mm/yr near Lone Pine.

   Azimuth of the major traces of the 1872 rupture varies from 145° to 175°. The component and characteristics (grabens, sinuosity) of extensional faulting increase with this azimuth. Traces with lower azimuths are straighter and have fewer associated grabens.

2. Soil development rates from the Merced area have been used to date terraces in the Tres Piños area. These terraces are offset along the Calaveras-Paicines fault zone and age determination of the terraces will yield slip rates. Soil development at (radiocarbon) dated localities in the San Francisco Bay Area and near Tres Piños was analyzed and quantified. These dates were from fluvial terrace deposits along Butaño Creek, San Francisquito Creek, Permanente Creek and south of our study area along San Benito Creek. Based on our dated localities, the soil development rates at Tres Piños compare well with those at Merced.

3. The Parkfield slip History project, Lienkaemper et al. (1985), was largely completed except for an attempt to remeasure two alinement arrays at Highway 46; one established in 1966, the other in 1977. All slip data from these future surveys and those of a third alinement array here installed by R.D. Nason in 1968 must be reconciled with fence and highway offset data to determine more accurately the probable interseismic and 1966 event slip at Highway 46. The estimated post-1857 slip deficit at Highway 46 will remain about 3 m regardless of the alinement array data, because the value of slip on the highway fence is well-constrained. All other values given in last semi-annual report stand.

   The 'Map of faulting accompanying the 1966 Parkfield earthquake' by Lienkaemper and Brown (1985) is now available. It is a new 1:12,000 map of the 1966 rupture to help researchers in the Parkfield Prediction Experiment and geologists and others who will map the rupture accompanying the next characteristic earthquake at Parkfield.

4. Investigations were conducted along the Quien Sabe, Bradley and Calaveras faults to determine if ground rupture accompanied the January 26, 1986, earthquake. No evidence of ground rupture was seen on the Quien Sabe or Bradley faults, located in the Santa Ana Valley. A small set of left-stepping en echelon cracks crossed Southside Road at the intersection with the Paicines fault. These cracks, open ~1 mm, appeared fairly fresh when seen on January 26, and may have been associated with the earthquake, but did not extend into the shoulder of the road. The investigators concluded that no ground rupture accompanied the earthquake, with the possible exception of the cracks on Southside Road.

Reports

Clark, M.M., Darrow, A.C., Harms, K.K., Lienkaemper, J.J., Patterson, R.H., 1986, Uncertainties in slip rates, U.S. Geological Survey Bulletin.

Harms, K.K., Clark, M.M., Rymer, M.J., Bonilla, M.G., Harp, E.L., Herd, D.G., Lajoie, K.R., Lienkaemper, J.J., Mathieson, S.A., Perkins, J.A., Wallace, R.E., and Ziony, J.I., 1984, The April 24, 1984 Morgan Hill, California Earthquake: The Search for Surface Faulting in The Morgan Hill, California Earthquake of April 24, 1984 (A Preliminary Report), U.S. Geological Survey Bulletin 1639..

Lienkaemper, J.J., and Brown, R.D., 1985, Map of faulting accompanying the 1966 Parkfield, California, earthquake: U.S. Geological Survey Open-File Report 85-661, scale 1:12,000, 3 sheets, 5 p.

Lienkaemper, J.J., Prescott, W.H., Sims, J.D., and Higgins, C.D., 1985, Parkfield Slip history: EOS, American Geophysical Union, abstract, v. 66, no. 46, p. 985.

Measurements of Northeastern North America Earthquake Magnitudes from 1938 to 1975

14-08-0001-22049

John E. Ebel
Dept. of Geology & Geophysics
Boston College
381 Concord Road
Weston, Massachusetts 02193
(617) 899-0950

Objective: The goal of this research is to measure or re-measure earthquake magnitudes for all local earthquakes from New York, New England and eastern Canada recorded by Weston Observatory of Boston College. The magnitudes are being measured from seismograms from Weston Observatory Benioff instruments and using formulae from Nuttli (1973) as appropriate for the eastern United States. Coda duration magnitudes for the events are also being measured. The magnitude measurements will be used to calculate regressions of magnitude and intensity for the Northeast, as well as to determine recurrence curves for the region using the complete magnitude data set from 1938 to 1984 to be determined by the study.

Project Status: To date, seismograms from the Weston Observatory archives for the time period from 1938 to 1954 have been analyzed for all local or regional earthquakes. For all those earthquakes for which there are recorded signals, Lg-wave amplitude magnitudes using the Nuttli (1973) formulae have been calculated and coda wave durations have been measured. A log of all measurements and results is being maintained and updated.

Preliminary results: The Lg-wave magnitudes of approximately 172 earthquakes have been computed for events from 1938 to 1954. Most of the magnitudes are consistent with the magnitudes or maximum epicentral intensities catalogued by Chiburis (1981), but there are many exceptions to this. Our measurements have found significantly smaller magnitudes for events, principally from Canada, than those reported in Chiburis (1981). There are also several examples of earthquakes where our magnitudes are notably larger than those in Chiburis (1981). Finally, we have computed magnitudes for 48 earthquakes for which there have been no previous magnitude determinations.

Our attempts to use coda durations measured from the seismograms to compute coda magnitudes using the formula of Rosario (1979) have not met with success. The problems have come from the different response of the Benioff instruments than that of the short period local network instrument used in the Rosario (1979) study, from high background noise on some records, and from questionable distance correction factors in the Rosario (1979) formula. Once all the Lg-wave magnitudes have been computed, a new coda duration magnitude formula appropriate for the Weston Benioff instruments will be computed.

REFERENCES CITED

Chiburis, E. F., Seismicity, Recurrence Rates and Regionalization of the Northeastern United States and adjacent Southeastern Canada, prepared for the U. S. Nuclear Regulatory Commission, NUREG/CR-2309, 1981.

Nuttli, O. W., Seismic Wave Attenuation and Magnitude Relations for Eastern North America, J. Geophys. Res., 78, 876-885, 1973.

Rosario, M., A Coda Duration Magnitude Scale for the New England Seismic Network, Master's Thesis, Boston College, 1979, 82 pp.

COASTAL TECTONICS, WESTERN U.S.

9910-01623

Kenneth R. Lajoie

Branch of Engineering Seismology and Geology
U.S. Geological Survey
345 Middlefield Road, MS 977
Menlo Park, CA 94025
(415) 323-8111, ext. 2642

Investigations

1. Uplift and deformation of Pleistocene marine strandlines and deposits in the San Pedro/Long Beach area, Los Angeles County, California.

2. Intra- and inter-shell reproducibility of amino-acid analyses in Saxidomous. This experiment is designed to refine correlations and age estimates of emergent marine strandlines using amino-acid analyses from fossil marine shells.

3. Catalogue of Pleistocene marine fossil localities, west coast U.S.

Results

1. The geology of Deadman Island and Nob Hill in San Pedro was reconstructed from historical records; these classical late Pleistocene stratigraphic fossil localities were destroyed by excavation in the late 1920's. Amino-acid data from fossil marine shells in museum collections indicate that the Palos Verdes Sand and the underlying San Pedro Sand are virtually the same age (between 95 ka and 120 ka); previously, the San Pedro Sand was thought to be much older than the Palos Verdes Sand. Also, amino-acid and paleomagnetic data indicate the underlying Timms Point Silt is between 300 ka and 600 ka in age. Amino-acid data from fossil shells on emergent wave-cut platforms indicate that the three lowest marine terraces are 120 ka or younger in age; the Palos Verdes Sand caps these platforms and the San Pedro Sand is probably the offshore sediment associated with the second and third terraces.

   Amino-acid data from shells in surface outcrops and subsurface borings define seven amino-stratigraphic zones. Their names and tentative ages are:

Mesa	85 (ka)
Pacific	125
Harbor	140-225
Bixby	330
Bent Spring	400-570
Upper Wilmington	660-780
Lower Wilmington	>800

The refined ages of the classical stratigraphic units and the development of a temporal framework provide a more precise means of dating fault activity (Cabrillo and San Pedro faults) and establishing rates of tectonic uplift in this highly urbanized area.

2. Alloisoleucine-Isoleucine ratios of multiple samples from single, well-preserved Saxidomous shells about 60 ka and 100 ka in age range from 0.2 to 0.5, which represents an apparent age range of roughly 30 ka to 200 ka. Samples from hard, inner shell layers near the umbo yield the most consistent results. Much of the scatter in the data in previous studies probably resulted from random sampling. Ratios from at least five shells from each collection should be averaged to obtain a value for a given locality. Also, as many different genera as possible should be used for correlation purposes; intergeneric patterns provide a means of evaluating amino-acid data.

3. Several hundred Pleistocene marine fossil localities have been reported from emergent marine terraces and deposits along the west coast of the U.S. These localities provide the fossils used for dating marine strandlines and determining rates of crustal deformation. Unfortunately, crucial data (elevation, age, species present, and even precise location) are not reported for many localities. Also, many localities have been destroyed or buried, primarily by urban development. To make published and unpublished data more useful, a computer-based catalogue of Pleistocene fossil localites has been established. All known localities have been identified and known pertinent information on each locality is being entered systematically in the data file.

Reports

Lajoie, Kenneth R., 1986, Coastal Tectonics *in* Usselman (ed.), *Studies in Geophysics-Active Tectonics*, National Academy Press, 266 p. (Chapter 6, p. 95-124).

Ponti, Daniel J., Lajoie, Kenneth R., Conlan, Linda M., and McKereghan, Peter F., 1986, Episodic Quaternary marine sedimentation in the southwestern Los Angeles basin [abs.]: *Geological Society of America Abstracts with Programs*, v. 18, no. 2, p. 171.

ADDITIONAL WORK TO DATE PROBABLE EARTHQUAKE DEFORMED BEDS IN KERN COUNTY, CALIFORNIA

Contract 14-08-0001-22018

D. L. Lamar and P. M. Merifield
Lamar-Merifield Geologists, Inc.
1318 Second Street, Suite 25
Santa Monica, CA 90401
Telephone: (213) 395-4528

W. E. Reed
Department of Earth and Space Sciences
University of California
Los Angeles, CA 90024

and
T. K. Rockwell
Geology Department
San Diego State University
San Diego, CA 92182

Investigations

Previous research (Lamar et al, 1979ab) revealed probable earthquake deformed sediments in Kern Lake, Kern County, California. To determine the times of the earthquakes samples of organic material have been collected and submitted for carbon 14 dating under the current contract.

Results

No new results will be available until dating of the carbon 14 samples is obtained.

References

Lamar, D. L., S. G. Muir, P. M. Merifield and W. E. Reed (1979a), Possible earthquake deformed sediments in Kern Lake, Kern County, California: Geol. Soc. Amer., Abstracts with Programs, Vol. II, No. 3., p. 88.

Lamar, D. L., S. G. Muir, P. M. Merifield and W. E. Reed (1979b), Description of earthquake deformed sediments in Kern Lake, Kern County, California: Lamar-Merifield Tech. Report 79-1, Final Tech. Report for U. S. Geol. Survey Contract 14-08-0001-16791.

Earthquake Hazards Studies, Upper Santa Ana Valley and Adjacent Areas, Southern California

9540-01616

Jonathan C. Matti
Branch of Western Regional Geology
U. S. Geological Survey
345 Middlefield Road, MS 975
Menlo Park, California 94025
(415) 323-8111 ext. 2358, 2353

Investigations

1. Studies of the Quaternary history of the upper Santa Ana River Valley. Emphasis currently is on: (a) generation of a liquefaction susceptibility map; and (b) the three-dimensional distribution of the valley fill and its lithologic, lithofacies, and pedogenic character.

2. Neotectonic studies of the San Andreas fault zone and associated fault complexes. The study has focused on: (a) mapping fault strands that deform cyrstalline basement rocks, Tertiary sedimentary rocks, and Quaternary surficial units; (b) identification of Quaternary units to establish Quaternary depositional patterns, relative ages of displacements along various fault strands, and rates of Quaternary fault slip; and (c) interpreting kinematic relations between the Crafton Hills fault complex, the San Gorgonio Pass fault complex, and the modern trace of the San Andreas fault.

Results

1. S.E. Carson and J.C. Matti have concluded the report-writing phase of a liquefaction-susceptibility study in the San Bernardino valley region. A ground-water map that targets 20 shallow-water zones in the upper Santa Ana River valley region has been published (Carson and Matti, 1985), and a map that updates ground-water conditions in the San Bernardino valley has been released in open-file (Carson and Matti, 1986). The latter study shows that ground water in the San Bernardino area has shallowed extensively since 1978 (the most recent period of record for our 1985 report), thus emphasizing the necessity for periodic updates of ground-water conditions.

We also released data from a USGS drilling program in the San Bernardino valley (Carson and others, 1986). Subsurface borings conducted at 27 sites included two drilling operations: solid-stem corkscrew augering to examine the physical stratigraphy, and hollow-stem augering to conduct standard penetration tests in sand and silty sand intervals identified during solid-stem operations. The drilling study resulted in two major findings. (1) The physical stratigraphy of the valley fill varies from place to place, but in general it consists of interlayered sand, silty sand, and clay-rich sediment; pebble and cobble gravel is a minor component where we drilled. Penetration tests show that sand and silty sand layers vary in their degree of compaction, but at all sites loose to moderately firm sand with blow counts from 5 to the high 20's occurs in the interval 0 ft to 30 ft subsurface.

A report interpreting liquefaction conditions in the San Bernardino Valley region has been completed (Carson, and Matti, unpubl.) and is in technical review.

2. J.W. Harden and J.C. Matti are writing up the results of a slip-rate study along the modern trace of the San Andreas fault near Yucaipa; preliminary results have been released (Harden and others, 1986; Terhune and others, 1986). Distinctive red-purple sedimentary rocks of the Miocene Potato Sandstone exposed on Yucaipa Ridge in the San Bernardino Mountains provide a geographically restricted source for gravels transported down Wilson Creek and shed across the modern trace of the San Andreas fault. Soils developed on the terraces containing these unique clasts are progressively older toward the northwest as a result of fault displacements; from young to old, the terraces are at most 225, 850, and 1200 m away from their Wilson Creek source.

Using dated soils from the Central Valley of California and from Cajon Pass northwest of Wilson Creek, a method of "maximum likelihood estimate" was used with Monte Carlo simulations of large data populations to account for soil variability, uncertainty of calibration dates, and the limited number of soils described and sampled. Preliminary age estimates are 7 to 12, 40 to 100, and 70 to 250 ka for the three Wilson Creek terraces.

Maximum-possible slip-rates spanning the Holocene-to-present, Wisconsin-to-present, and Sangamon-to-present are obtained using maximum slip and minimum ages of the displaced terraces. Best-estimates for slip rates for the three time intervals are obtained by restoring the medial axis of each displaced alluvial fan to Wilson Creek and by employing ages of fill at Cajon Creek, assuming that regional pulses of sediment are similar to those at Cajon Pass. The maximum possible rates are 32, 21, and 17 and the best-estimates rates are about 25, 15, and 8 mm/yr for the Holocene, Wisconsin and Sangamon, averaged to the present.

These data indicate that slip rates on the modern trace of the San Andreas fault in the San Bernardino valley have increased progressively during the late Quaternary, culminating in the Holocene rates that are comparable to the 25 mm/yr rate determined in the Cajon Pass region. This conclusion leads to the idea that the modern trace may have evolved gradually during the last 100,000 years or so, and that prior to 100,000 years B.P. some other strand of the San Andreas zone carried most of the slip apportioned to the fault in the Transverse Ranges segment.

3. Continuing studies by J.C. Matti and D.M. Morton are beginning to elaborate the long-term distribution of slip on the San Andreas and San Jacinto faults. Matti and others (1986) proposed that total displacement on the San Andreas fault (sensu stricto) in southern California is about 160 km. Assuming slip commenced with the opening of the Gulf of California 4 or 5 m.y. ago, then the long-term slip rate on the San Andreas is between 32 and 40 mm/year--a rate comparable to the Holocene rate for the fault (about 35-37 mm/year). In the vicinity of the south-central Transverse Ranges, where the San Andreas fault has developed a large left-step in the San Gorgorio Pass region, long-term slip in the San Andreas system has been apportioned between the San Andreas and San Jacinto faults. Morton and others (1986) propose that for the last 700,000 years an average of about 17 mm/year of slip has occurred on both faults, leading to a combined rate of about 34 mm/year. Questions

that remain include the timing of the onset of slip on the San Jacinto fault in relation to the Quaternary evolution of the left step in the San Andreas fault, and variation in slip rate for both faults around the late Quaternary average of about 17 mm for each.

Reports

Carson, S.E., and Matti, J.C., 1985, Contour map showing minimum depth to ground water, upper Sana Ana River Valley, California (1973-1979): U.S. Geological Survey Miscellaneous Field Studies Map MF-1802, 22 p., scale 1:48,000.

Carson, S.E., and Matti, J.C., 1986, contain map showing minimum depth to ground water, San Bernardino Valley and vicinity, California, 1973-1983; U.S. Geological Survey Open-File Report 86-169.

Carson, S.E., Matti, J.C., Throckmorton, C.K., and Kelly, M.M., 1986, Stratigraphic and geotechnical data from a drilling investigation in the San Bernardino valley, California: U.S. Geological Survey Open-File Report 86-225, 78 p., scale 1:48,000.

Harden, Jennifer W., Matti, Jonathan C., and Terhune, Christina, 1986, Late Quaternary slip rates along the San Andreas fault near Yucaipa, California, derived from soil development on fluvial terraces: Geological Society of America Abstracts with Programs, v. 18, no. 2, p. 113.

Terhune, Christina L., Harden, Jennifer W., and Matti, Jonathan C., 1986, Application of a quantified field index of soil development to distinguish relative ages of geomorphic surfaces for regional geologic mapping: Geological Society of America Abstracts with Programs, v. 18, no. 2, p. 192.

Matti, Jonathan C., Frizzell, Virgil A., and Mattinson, James M., 1986, Distinctive Triassic megaporphyritic monzogranite displaced 160 ± 10 km by the San Andreas fault, southern California: a new constraint for palinspastic reconstructions: Geological Society of America Abstracts with Programs, v. 18, no. 2, p. 154

Morton, Douglas, M., Matti, Jonathan C., Miller, Fred K., and Repenning, Charles A., 1986, Pleistocene conglomerate from the San Timoteo Badlands, southern California; constraints on strike-slip displacements on the San Andreas and San Jacinto faults: Geological Society of America Abstracts with Programs, v. 18, no. 2, p. 161.

STUDY OF SEISMIC ACTIVITY BY SELECTIVE TRENCHING ALONG THE SAN JACINTO FAULT ZONE, SOUTHERN CALIFORNIA

Contract 14-08-0001-22033

P.M. Merifield and D.L. Lamar
Lamar-Merifield Geologists, Inc.
1318 Second Street, Suite 25
Santa Monica, CA 90401
(213) 395-4528
and
T.K. Rockwell and C.C. Loughman
Geology Department
San Diego State University
San Diego, CA 92182
(619) 265-4441

Investigations: The objectives of this investigation include determination of the Holocene slip rate and timing of the most recent earthquakes on the Clark fault strand of the San Jacinto fault zone. This strand shows the most convincing geologic evidence of Holocene movement and the largest cumulative displacement of any on the San Jacinto fault zone; however, it has not experienced a ground-breaking earthquake in historic time.

Late Quaternary deposits in the Anza area were mapped by relative age based on soil profile development, and nineteen excavations were made by backhoe along a 1.5-km segment of the Clark fault. Trenches were selected in an area of offset stream channels and ponded alluvium. The ponded alluvium, which is offset about 85-90 m, had produced a radiocarbon age of 9500 years B.P., yielding a minimum slip rate of about 9 mm/yr. (Rockwell et al, 1986). Additional samples of relatively abundant charcoal were collected from several of the excavations for radiocarbon dating.

Results: New slip-rate determinations have been made by radiocarbon dating of charcoal in displaced deposits and by soil profile development of displaced alluvial fans. A sample of charcoal from fine-grained alluvium interpreted to have ponded behind a shutter ridge was dated at 28,650±980 yrs B.P. This date and the offset from the shutter ridge yield a slip rate of 6-18 mm/yr. A piece of charcoal has also been collected from a stream channel offset 200 m from its upstream segment. The absence of stream-laid sediments in the gap between the offset channels coupled with the angularity of the channel wall-fault intersection indicates that the stream did not flow through the gap for any significant period of time following incision.

Therefore the charcoal, which was collected within 1 m of the top of the abandoned channel deposits, will provide a date close to the abandonment of the channel and thus yield a slip rate close to the true slip rate. The charcoal is currently being processed for accelerator measurement.

Dating by soil profile development has also yielded a slip rate. The stream channel which is right-laterally offset 200 m postdates the alluvial fan surface into which it is cut. Soil profiles do not begin to develop until deposition ceases. Because deposition of the fan surface must have ceased by at least the time the stream incised the channel, the degree of soil development in the fan surface provides an estimate of the age of the incision. Both this information and the stream offset provide a maximum slip rate. Comparison of these soils to a dated soil in this area and to other, similar appearing soils in California, provides a preliminary age estimate of 16.5±3 ka and yields a slip-rate estimate of 12.5±3 mm/yr.

The investigation to date has not provided timing of the most recent earthquakes. The fault is buried in places by at least 3.5 m of undisplaced stream deposits and colluvium. Charcoal samples from these deposits have been dated at 870±140 yrs B.P. and 910±120 yrs B.P. These dates are maximums only because the charcoal could be from trees several hundred years old.

Sequential samples of potentially datable material have been collected from colluvium displaced by the fault (Fig. 1). This excavation was studied in detail at the suggestion of David Schwartz, U.S.G.S., Menlo Park, who pointed out that the configuration of the coarser clasts suggests they may have formed at the base of scarps and thus represent discrete events. These samples are being prepared for accelerator measurements.

Reports: Rockwell, T.K., P.M. Merifield, and C.C. Loughman, 1986, Holocene activity of the San Jacinto fault in the Anza seismic gap, southern California, Geol. Soc. Am., Abstracts with Programs, vol. 18, no. 2, p. 177.

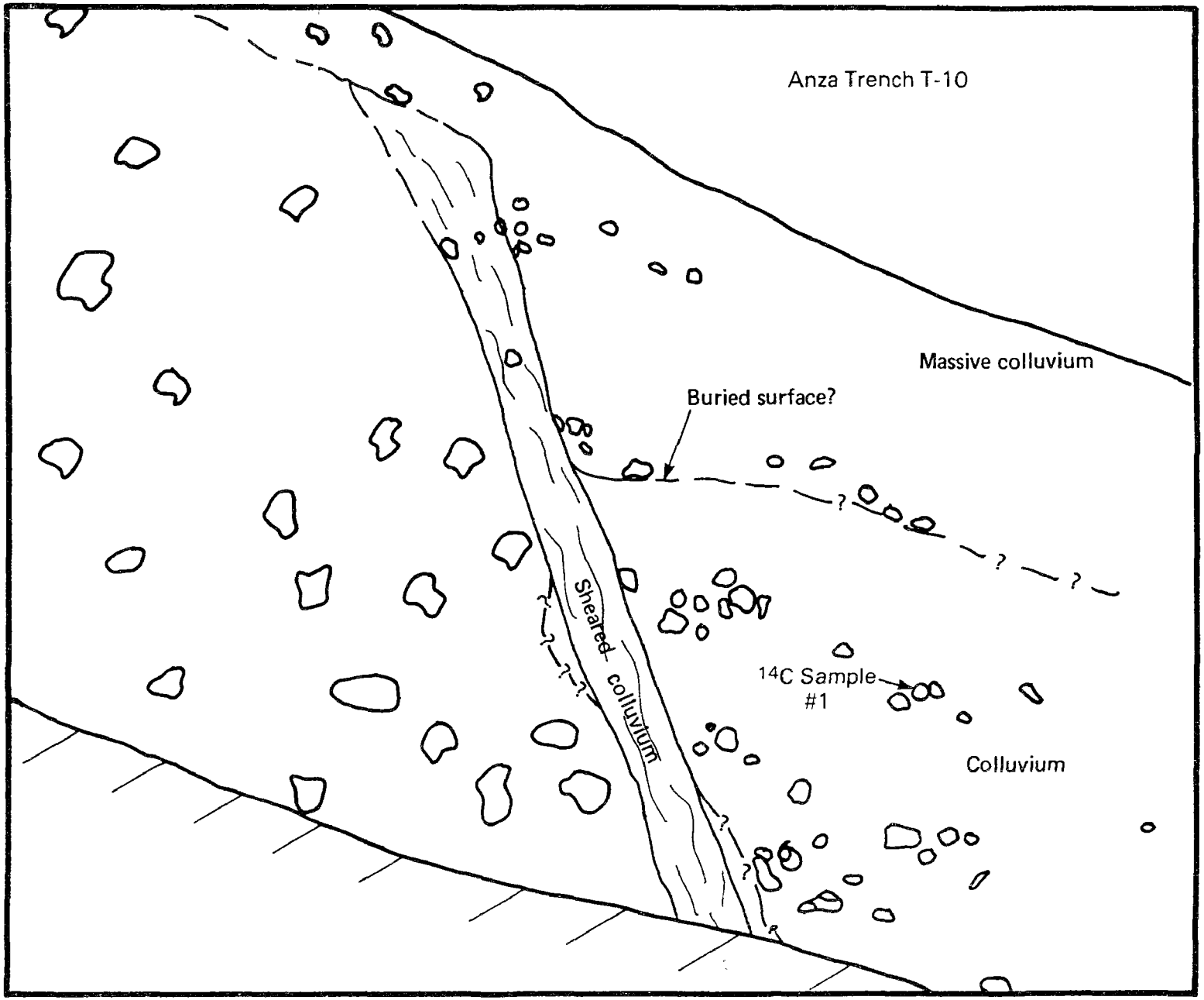

Figure 1 - North wall of trench perpendicular to the Clark fault north of Anza. Concentration of clasts in colluvium may have accumulated at the base of scarps and may represent discrete events.

Structural Framework of the Peninsula Ranges

9540-04040

Douglas M. Morton
Branch of Western Regional Geology
U.S. Geological Survey at Dept. of Earth Sciences
University of California, Riverside
Riverside, California 92521
(714) 787-3429

Investigations

Began study of the tectonic history of the San Jacinto Graben area. Investigation aimed at determining structural details of the graben area and its earthquake history. Began detailed geologic mapping and study of fault related geomorphology of the San Jacinto Valley-Moreno Valley and San Timoteo Badlands.

Results

Analysis of a distinctive conglomerate in the northern part of the San Timoteo Badlands, Riverside County, southern California, suggests strain rates for the San Andreas and San Jacinto faults in this part of southern California have been similar for the last 800,000 to 1,200,000 years. Streams depositing the conglomeratic sediments flowed in a southwestern direction from their source areas, several of which were across all strands of the San Andreas fault in the Bernardino Mountains. Since the deposition of the conglomerate it has been offset right laterally by the San Jacinto fault a minimum of twelve kilometers from its westward continuation.

Reports

Morton, D.M., Matti, J.C., Miller, F.K., and Repenning, C.A., 1986, Pleistocene conglomerate from the San Timoteo Badlands, southern California; constraints of strike-slip displacements of the San Andreas and San Jacinto faults: Geological Society of America Abst. with Programs, vol. 18, no. 2, p. 161.

MORPHOLOGIC DATING OF FAULT SCARPS

14-08-0001-21960

David B. Nash
Department of Geology
University of Cincinnati
Cincinnati, Ohio 45221-013
(513) 475-2834

Investigation

A one dimensional diffusion model successfully predicts the pattern of degradation observed on some transport-limited hillslopes (hillslopes on which more material is loosened and available for transport than the transportational processes are capable of removing), such as the terrace and fault scarps in the West Yellowstone obsidian sand plain investigated in a previous study (USGS contract No. 14-08-0001-19109). According to the diffusion model the, rate of lowering at a point on a hillslope profile is proportional to the curvature of the profile at that point or:

$$\frac{\partial y}{\partial x} = \frac{\partial^2 y}{\partial x^2} \qquad \text{(Eq. 1)}$$

where c is the constant of proportionality and x and y are the horizontal and vertical coordinates respectively of a point on the hillslope profile. The West Yellowstone study demonstrates that the diffusion model may be used to date some scarps on the basis of their morphology (morphologic dating) if their initial morphology is known or may be accurately estimated. Although the initial morphology of a hillslope can usually only be estimated for "cohesionless" materials, limiting morphologic dating to hillslopes underlain by sand and gravels, the primary limitation to the application of morphologic dating, result from c being a function of climate, underlying material, and the orientation of a scarp and thus being site specific.

The current investigation derives c for numerous hillslopes of various ages, underlain by a variety of different materials, in a variety of climatic regions, and having a variety of orientations (aspects) in order to determine the effect climate, material, and aspect have on c.

Results

Terrace scarps of known age at five sites in Wyoming (in the vicinity of Bull Lake, Pinedale, Grand Teton National Park (GTNP), and two locations

within the Wind River Basin) and in the vicinity of Pocatello, Idaho on scarps formed by the Bonneville Flood(s) were studied. A representative sample of profiles were collected from the scarps along with samples of the material into which the scarps were cut. At some locations, detailed maps of the planimetric configuration of the scarp crest lines were made.

A set of terraces in the vicinity of the Jenny Lake Turnout in GTNP was studied particularly intensely (Fig. 1). This terraces set is unique in that the terraces are relatively undisturbed (it had not been appreciated how many terrace surfaces in Wyoming have been cultivated) and are all underlain by a relatively homogeneous alluvium. These terraces are also unique in that they all are about the same age, formed by meltwater discharge during a relatively short period while the glacier stood at the moraine immediately north of the area (Fig. 1). As the glacier withdrew to the north, the meltwater drained east into the Snake River (K. Pierce, personal communique). Analysis of these terraces resulted in some unexpected and disturbing findings.

Assuming that the terrace scarps initially consisted of a nearly horizontal crest and base separated by an inclined scarp face at the angle of repose for the underlying material (approximately 30^{o} for the GTNP scarps - dashed lines in Fig. 2), the diffusion model predicts that the crestal convexity and basal concavity should become progressively more rounded with time (solid line in Fig. 2). If the initial curvature of the scarp basal concavity and crestal convexity are the same, then their curvature at any subsequent time will also be the same (Fig. 2). Many, if not most, of the profiles collected from GTNP have quite different curvatures of the crestal convexity and basal concavity (Fig. 3). The morphologic dating technique used in the West Yellowstone study (Nash, 1984), is based on the gradient of the scarp midsection. That technique is modified in order to determine a scarp's age based on any portion of its profile. The scarp ages based on all of a profile's coordinate points (Fig. 3), and based on the points comprising its basal concavity (Fig. 4), midsection (Fig. 5), and crestal convexity (Fig. 6) alone (referred to as the whole, base, middle, and crest respectively), vary significantly (Fig. 7).

All morphologic dating techniques yield a value for tc, the age of the scarp (t) multiplied by c (henceforth tc will be referred to as the morphologic age). The variation in morphologic age between the parts of scarp profile may result from several causes. Perhaps the initial morphology of the scarps was not of the simple sort shown with the dashed lines in Fig. 2. Study of active and recently abandoned terrace scarps along the nearby Snake River (underlain by the same material) suggest that this is unlikely; their morphology is of the simple sort shown in Fig. 2. Ken Pierce (personal communique) suggests that the basal concavity may be more rounded due to significant deposition of loess. If this were the case, however, the scarp base would consistently yield the oldest age but this is not the case (Fig. 6).

If c for all the scarps is the same (a reasonable assumption because the material and climate are the same for most of the profile scarps) and the age of the scarps (t) is also the same then tc must also be the same. Morphologic dating of the terrace scarp profiles, however, results in widely (by more than one order of magnitude) varying morphologic ages (Fig. 6). There is also a disturbing trend for the morphologic age to increase as a scarp height increases (Fig. 7). Pierce (personal communique) has noted the same trend in

his study of fault scarps in Idaho.

The differences in morphologic age among different portions of the same profile, the trend towards increased morphologic age with increasing scarp offset, and the fact that scarps known to be of about the same age yield vastly different morphologic ages suggest that the diffusion model may have serious limitations for dating hillslopes. Future work on this contract will determine whether the shortcoming in the model that became evident in the GTNP study also occur in the other areas studied. An attempt will also be made to modify the model to fit more closely the observed pattern of degradation.

References

Nash, D.B., 1985, Morphologic dating of fluvial terrace scarps and fault scarps near West Yellowstone, Montana: Geological Society of America Bulletin, Vol. 95, p. 1413-1424.

Figure Captions

Fig. 1. Map of the Jenny Lake Turnout study site in Grand Teton National Park. The scarp face is stippled. The short lines transverse to the terrace scarps represent profile traverse locations (the traverse is numbered at its upslope end).

Fig. 2. Degraded scarp profile generated by the diffusion model (Eq. 1). The straight, dashed lines indicate the initial profile morphology. With time, the scarp face reclines and the basal concavity and crestal convexity become more rounded.

Fig. 3. Profile of terrace scarp TF (Fig. 1). The assumed initial profile is shown with straight dashed lines and the measured profile coordinates are represented with +'s. The solid line represents the closest fit of the diffusion model (Eq. 1) to the whole profile.

Fig. 4. Profile of terrace scarp TF (Fig. 1). The assumed initial profile is shown with straight dashed lines and the measured profile coordinates are represented with +'s. The solid line represents the closest fit of the diffusion model (Eq. 1) to the base of the profile (outside of analyzed are, the line is dashed).

Fig. 5. Profile of terrace scarp TF (Fig. 1). The assumed initial profile is shown with straight dashed lines and the measured profile coordinates are represented with +'s. The solid line represents the closest fit of the diffusion model (Eq. 1) to the middle of the profile (outside of analyzed are, the line is dashed).

Fig. 6. Profile of terrace scarp TF (Fig. 1). The assumed initial profile is shown with straight dashed lines and the measured profile coordinates are represented with +'s. The solid line represents the closest fit of the diffusion model (Eq. 1) to the middle of the profile (outside of analyzed are, the line is dashed).

Fig. 7. Mean values of $\underline{tc}$ for the whole, base, middle, and crest of the terraces shown in Fig. 1. If the diffusion model is correct, all the sets of bars should be about the same height.

Fig. 8. Mean value of $\underline{tc}$ for each terrace scarp in Fig. 1 plotted against the mean offset (height) of the scarp. If the diffusion model is correct, there should be no consistent trend in the data.

Fig. 1

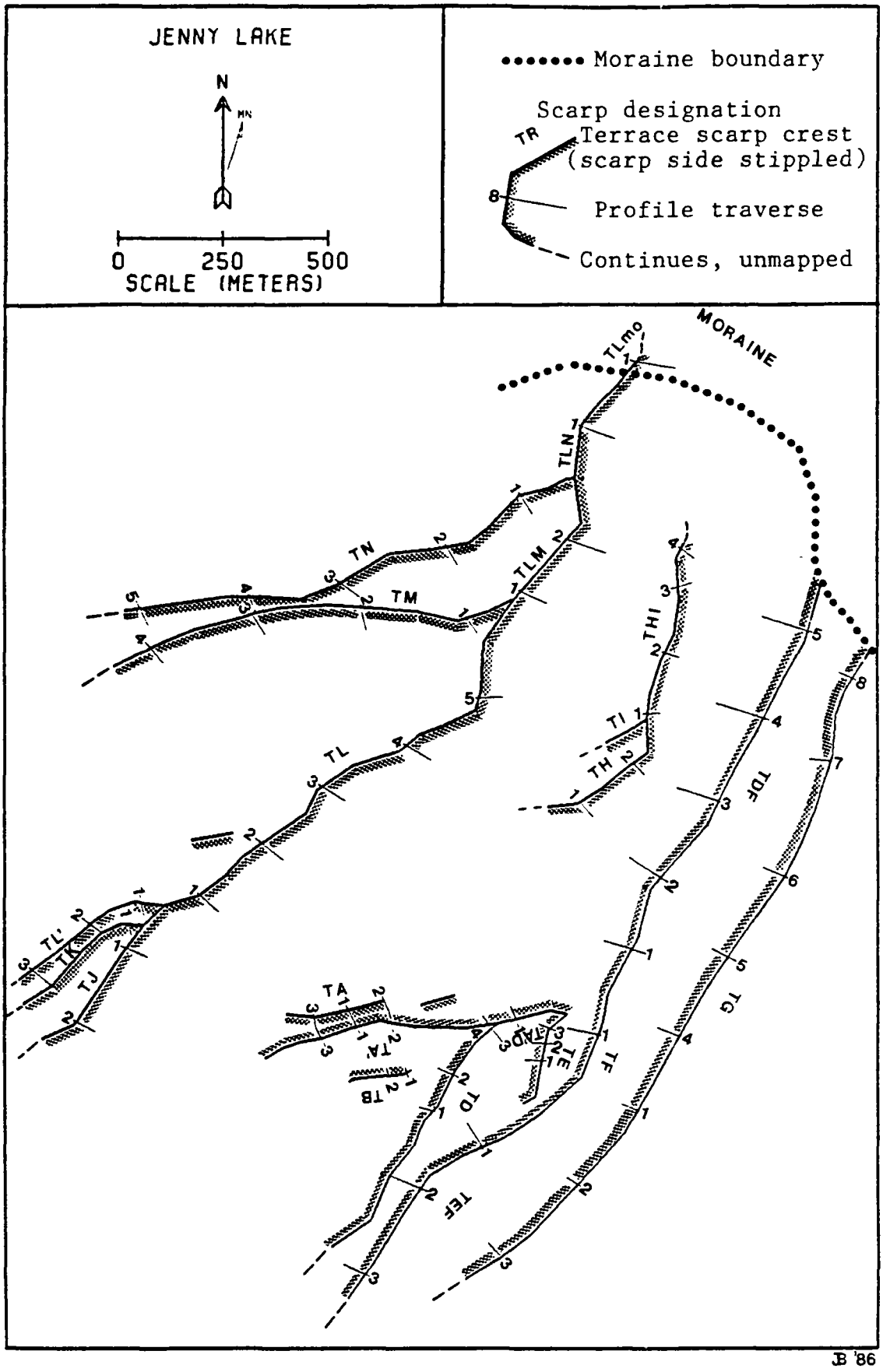
JENNY LAKE
N
MN
0 250 500
SCALE (METERS)
Moraine boundary
Scarp designation
TR
Terrace scarp crest
(scarp side stippled)
8
Profile traverse
Continues, unmapped
MORAINE
TLMo
TLN
TN
TLM
TM
TL
THI
TI
TH
TK
TJ
TA
TB
TD
TE
TF
TG
TDF
TEF
JB '86

#75: Fig. 2: Profile generated by diffusion model

Base slope:	*0.1* °
Midsection slope:	*25.4* °
Crest slope:	*0.0* °
Offset:	*5.0 m*
Initial midsection slope:	*30.0* °
From point 1 to 32 tc:	*5.06 m^2/yr*
Correlation coefficient:	*0.9993*

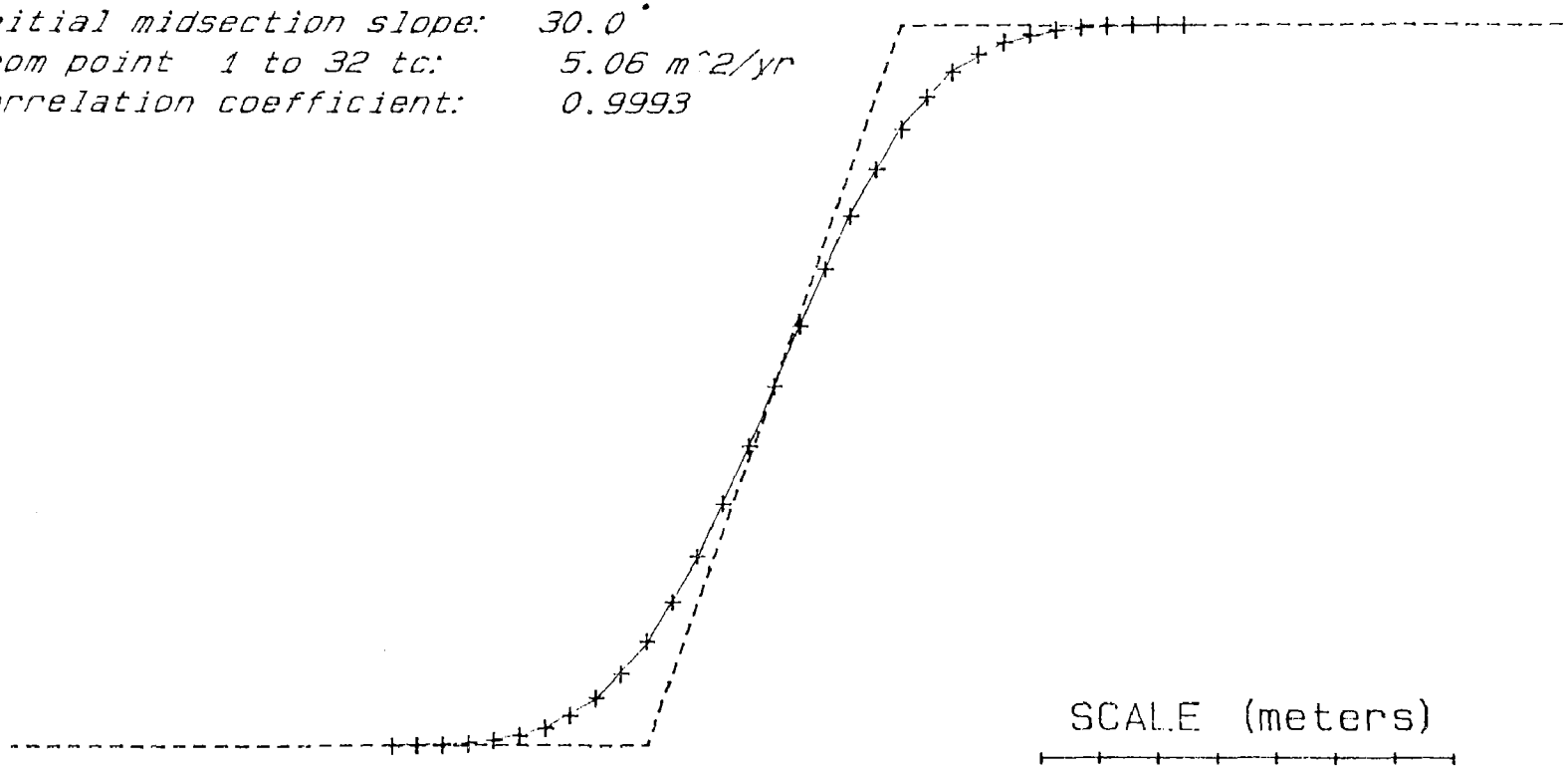

03-03-1986

#19: Fig. 3: Morphologic dating based on whole profile of TF-1

Base slope:	*0.9°*
Midsection slope:	*26.7°*
Crest slope:	*0.0°*
Offset:	*13.0 m*
Initial midsection slope:	*30.4°*
From point 2 to 19 tc:	*23.69 m^2/yr*
Correlation coefficient:	*0.9853*

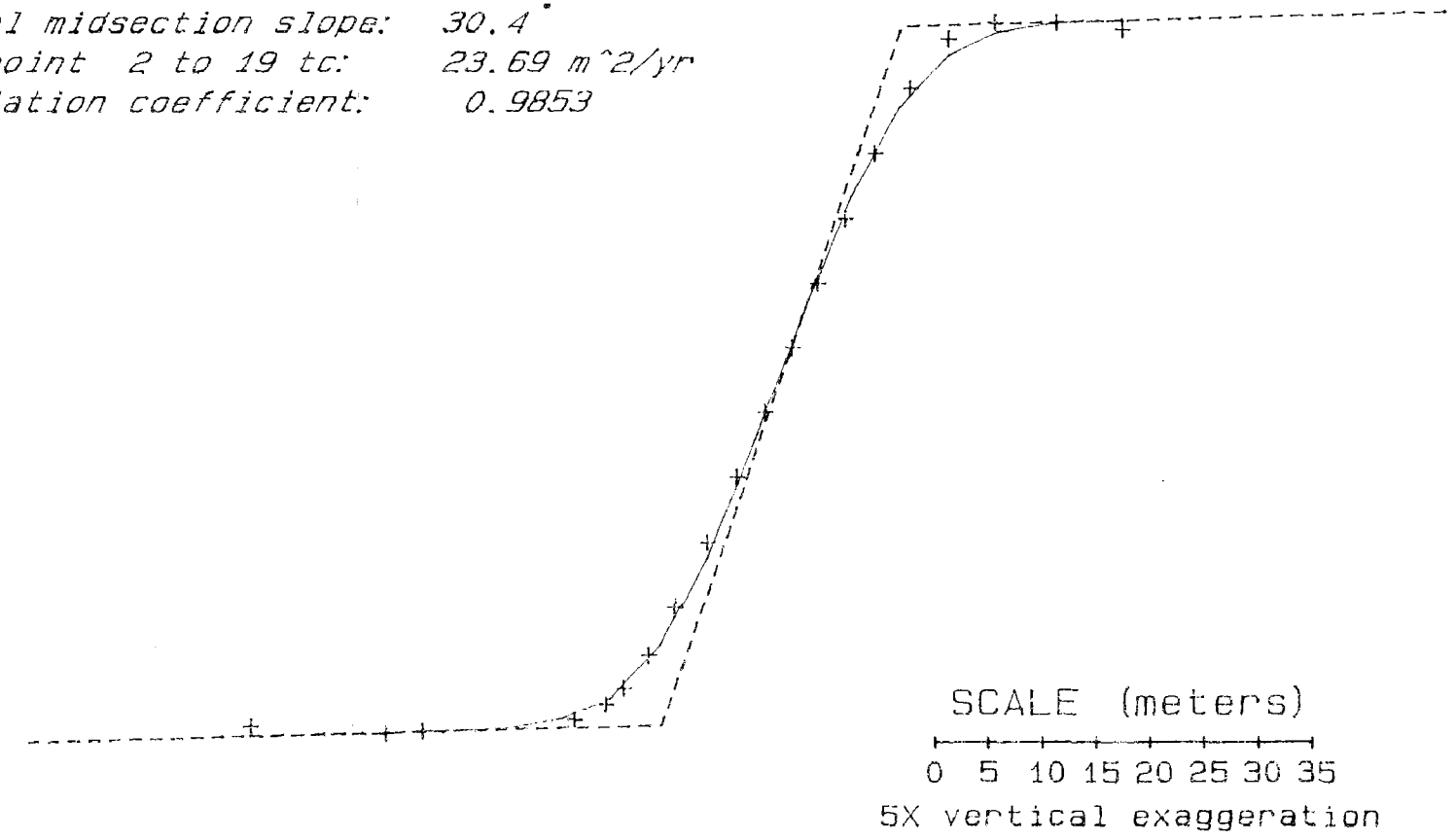

03-03-1986

#19: Fig. 4: Morphologic dating of the base of profile TF-1

Base slope:	*0.9°*
Midsection slope:	*26.7°*
Crest slope:	*0.0°*
Offset:	*13.0 m*
Initial midsection slope:	*30.4°*
From point 2 to 11 tc:	*26.37 m^2/yr*
Correlation coefficient:	*0.9628*

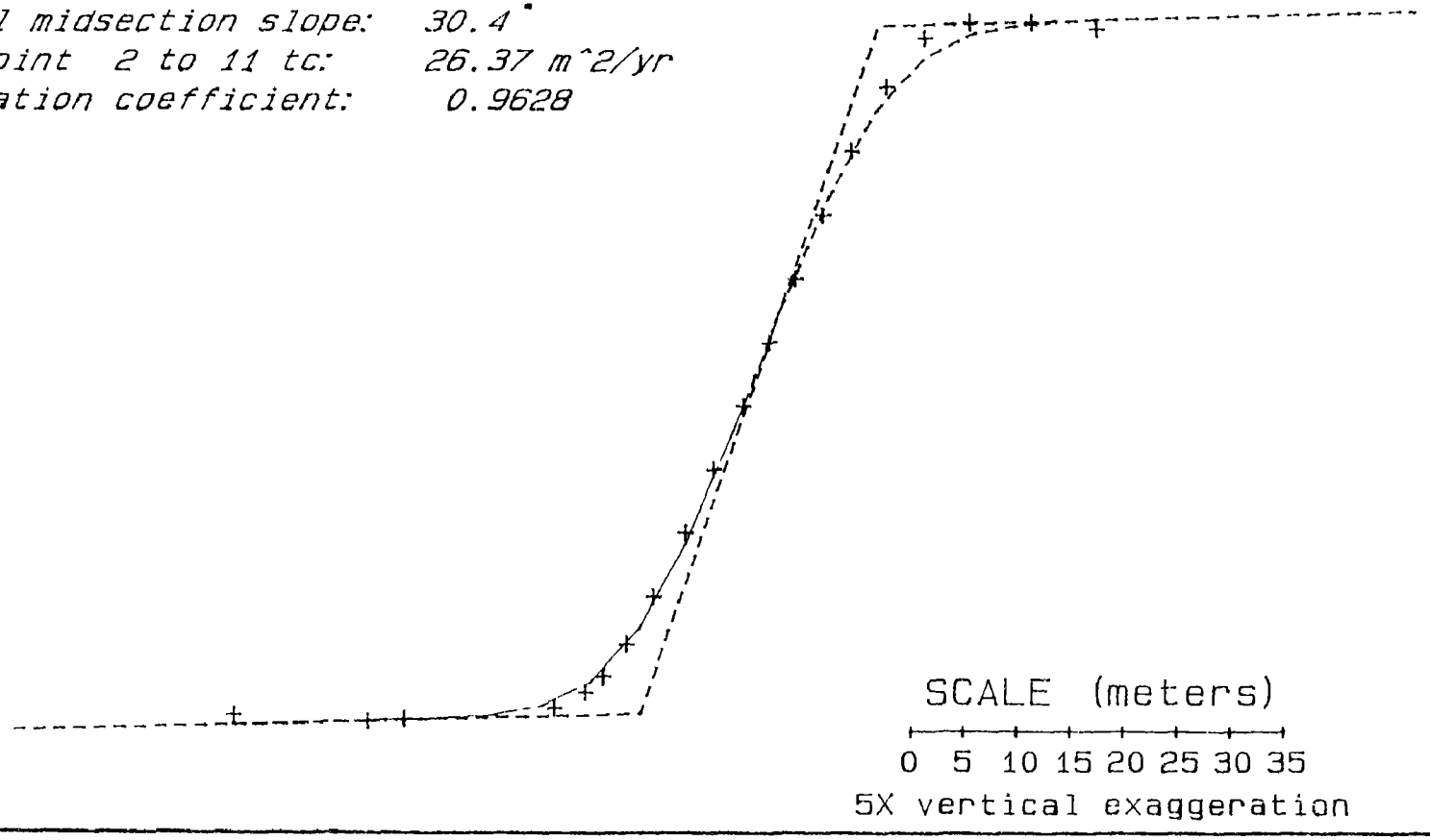

03-03-1986

#19: Fig. 5: Morphologic dating of the middle of profile TF-1

Base slope:	*0.9°*
Midsection slope:	*26.7°*
Crest slope:	*0.0°*
Offset:	*13.0 m*
Initial midsection slope:	*30.4°*
From point 10 to 13 tc:	*33.45 m^2/yr*
Correlation coefficient:	*0.9965*

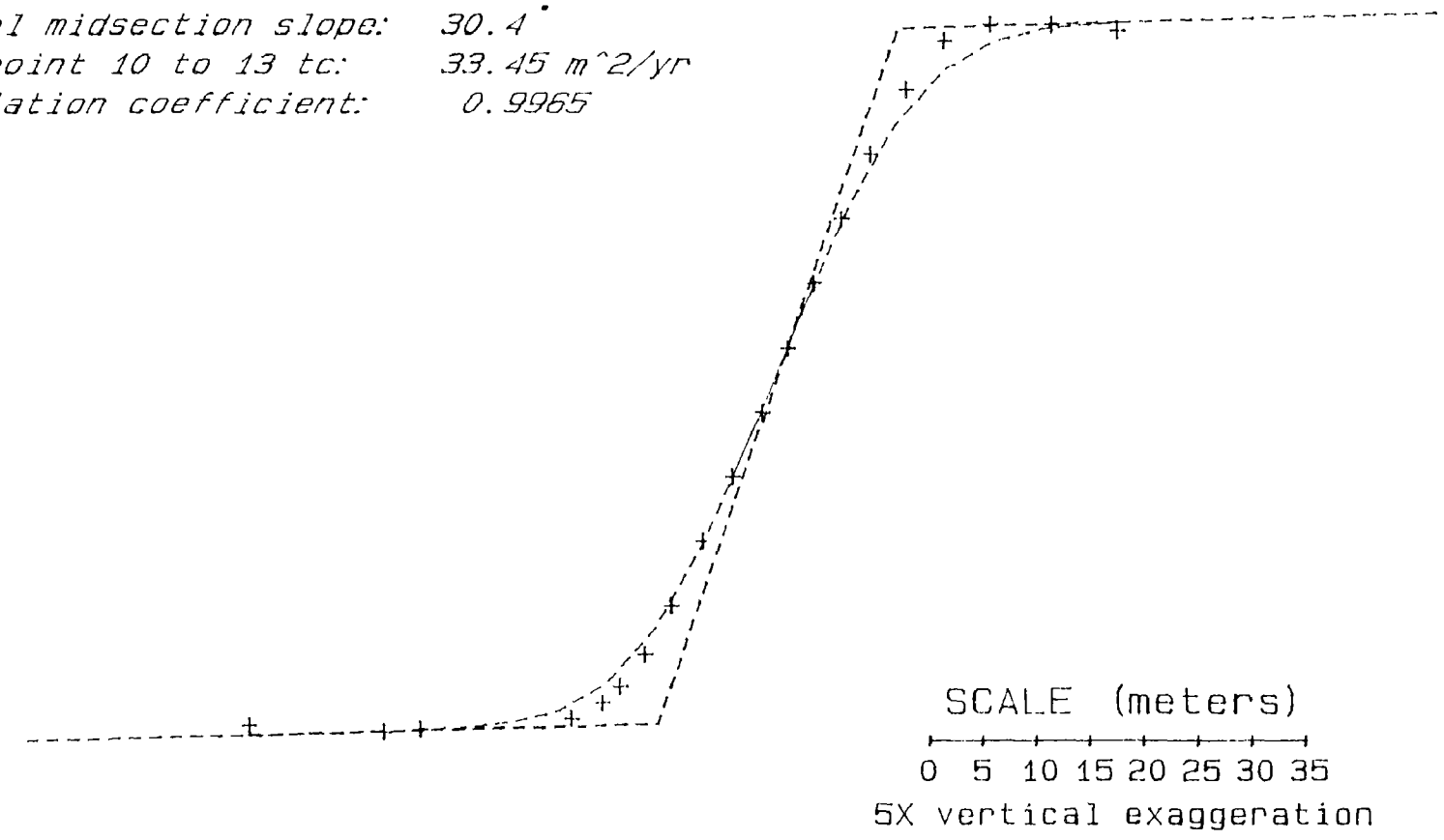

03-03-1986

#19: Fig. 6: Morphologic dating of the crest of profile TF-1

Base slope:	*0.9°*
Midsection slope:	*26.7°*
Crest slope:	*0.0°*
Offset:	*13.0 m*
Initial midsection slope:	*30.4°*
From point 14 to 19 tc:	*20.01 m^2/yr*
Correlation coefficient:	*0.9461*

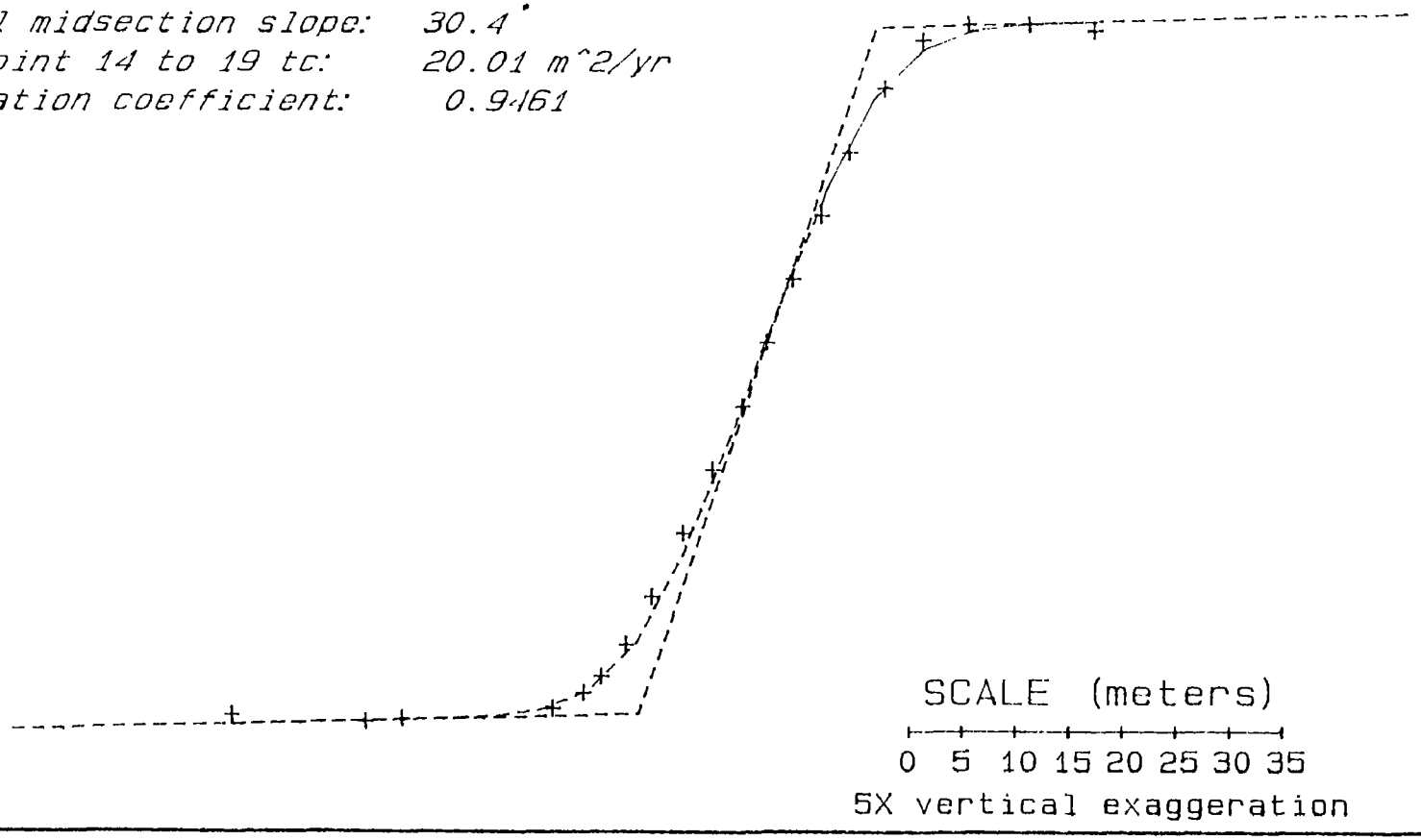

03-03-1986

Fig. 7

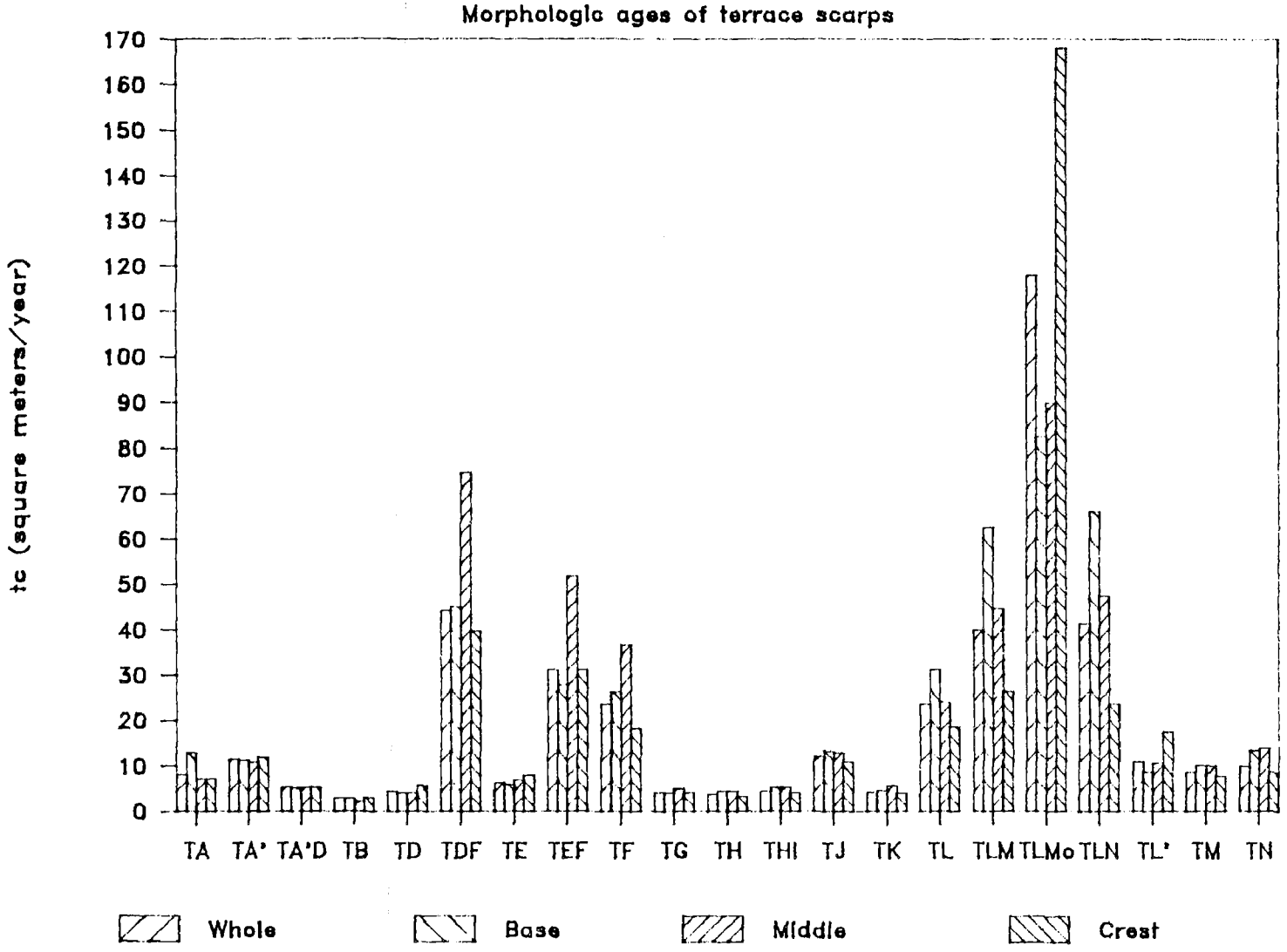
Morphologic ages of terrace scarps
tc (square meters/year)
170
160
150
140
130
120
110
100
90
80
70
60
50
40
30
20
10
0
TA
TA'
TA'D
TB
TD
TDF
TE
TEF
TF
TG
TH
THI
TJ
TK
TL
TLM
TLMo
TLN
TL'
TM
TN
Whole
Base
Middle
Crest

Fig. 8

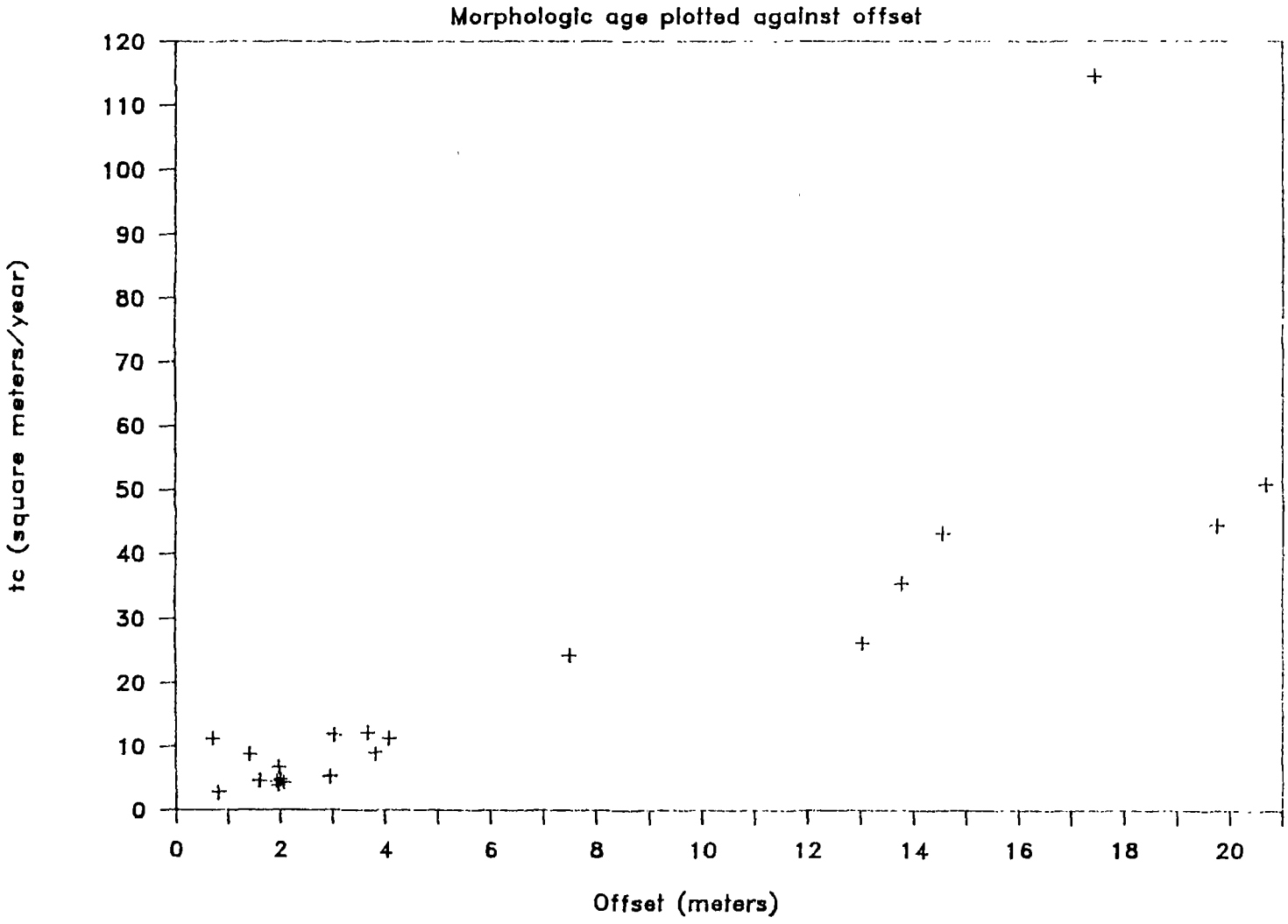
Morphologic age plotted against offset
tc (square meters/year)
120
110
100
90
80
70
60
50
40
30
20
10
0
0
2
4
6
8
10
12
14
16
18
20
Offset (meters)

DETAILED GEOMORPHIC STUDIES TO DEFINE LATE QUATERNARY FAULT BEHAVIOR AND SEISMIC HAZARD, CENTRAL NEVADA SEISMIC BELT

Contract #21970

Philip Pearthree, Julia Fonseca, William B. Bull,
Suzanne Hecker, Oliver Chadwick, and Karen Demsey
Department of Geosciences
University of Arizona
Tucson, AZ 85721
(602)621-6024

Investigations

Geomorphic studies on the timing, distribution, and behavior of late Quaternary faulting in central Nevada are continuing. The findings of this study are being used to determine whether historic rupture patterns have been repeated in the past, to estimate fault recurrence and magnitude of faults with prehistoric ruptures, and to assess the seismic hazards associated with the faults in this area.

Detailed analyses of faulting have been completed in the northern portion of the central Nevada seismic belt (CNSB), from the northern end of the 1954 Dixie Valley surface rupture, through the Stillwater Seismic Gap (SSG) (of Wallace, 1978; Wallace and Whitney, 1984), and the southern and central portions of the 1915 Pleasant Valley surface rupture.

A number of geomorphic tools have been used in our studies. Quantitative evaluation of soil profile development (using the Maximum Horizon Index [MHI] of Harden, 1982) provides a means of correlating surfaces across faults, and of estimating the ages of faulted and unfaulted surfaces, to bracket times of faulting. Fault scarp morphology provides an independent estimate of surface rupture age. Topographic profiles of alluvial scarps have been analyzed using solutions to the diffusion equation, according to the model of Hanks et al (1984); the values of kt (diffusivity scarp age) obtained from the solutions yield age estimates for the scarps.

Latest Pleistocene highstand shoreline terraces and remnants are present in some of the study areas. The shorelines were formed 12 ka, and thus provide an absolute age by which rates of soil development and fault-scarp degradation can be calibrated. Vertical offset and deformation of the originally horizontal shorelines allows comparison with amounts of uplift indicated by fault displacement, while fault/shoreline cross-cutting relationships are an additional means of bracketing timing of faulting.

Relative tectonic activity of mountain fronts has also been assessed by tectonic landform analysis based on criteria such as linearity and steepness of mountain fronts, and degree of alluvial channel entrenchment (technique discussed in Bull and McFadden, 1977).

Work is in progress on the fault-bounded front of the Wassuk Range, adjacent to Walker Lake. The steep, linear mountain front shows pronounced evidence of late Quaternary surface ruptures where alluvial surfaces are present, but scarps are absent or obscured where the surface has ruptured at the bedrock mountain front and/or where the faulting may have occurred below the level of Walker Lake, which immediately bounds the range in several places. The preserved latest Pleistocene Lahontan shorelines along this range, in conjunction with soils and fault scarps, will be integral to interpreting the prehistoric rupture sequence in the area. Analysis of the Toiyabe Range, which is steep and linear but historically unfaulted, is also being undertaken.

Results

Studies incorporating soils and fault morphology in the Dixie Valley-Pleasant Valley portion of the CNSB indicate ages of most-recent prehistoric movement are diachronous along the sites of historic surface rupture, implying that the pattern of historic rupture does not duplicate earlier Holocene patterns. In the central and northern portions of the 1954 Dixie Valley (DV) surface rupture the most recent prehistoric rupture occurred 3 ka, with no definitive evidence of earlier Holocene rupture (Hecker, in review). Faulting of this age extends along at least 20 km, and possibly the entire 40 km, of the SSG. Vertical displacement of latest Pleisotcene shorelines and alluvial surfaces along portions of the SSG suggests the occurrence of an earlier Holocene rupture in the SSG.

The most recent prehistoric surface rupture in two segments of the 1915 rupture in the Pleasant Valley and eastern Sou Hills area apparently occurred during the early Holocene, while the southernmost major segment of the 1915 rupture, along the west side of the Sou Hills, apparently had not previously ruptured since the latest Pleistocene (Fonseca, 1986). Total vertical offset of geologic units, and spatial and temporal patterns of prehistoric and historic surface rupture suggest that the Sou Hills may act as a barrier to fault propagation, analogous to the behavior proposed for other similar transverse structures (Aki, 1979), which may limit the size of individual earthquakes in this region.

Fault scarp and soils data have been collected from several other faulted mountain fronts in the central Nevada region, including the historically unruptured Wassuk Range and the location of the 1954 Fairview Peak surface rupture. Preliminary results indicate that principal segments of FP previously broke in the early Holocene or late Pleistocene, while there were possibly two Holocene surface ruptures along the Wassuk mountain front.

The contrast between prehistoric and historic rupture patterns in the CNSB implies that "belt-filling" behavior along isolated unbroken segments of linear trends of faulting may not necessarily occur. The SSG, however, remains a candidate for a large earthquake in the near future. Mountain-front landform analysis in the CNSB and other ranges in central Nevada indicate that the DV and SSG portions of the CNSB have had the greatest long-term (10^5-10^6 my) uplift rates; several other historically unruptured ranges in central Nevada appear to be at least as tectonically active at this time scale, and may also be likely sites for future large earthquakes. The Wassuk and Toiyabe ranges may be potential candidates for such events.

Continuing work in this project is aimed at increasing our understanding of the spatial and temporal patterns of late Quaternary surface ruptures, and improving our capability of seismic hazard assessment in the Great Basin.

References

Aki, K. (1979). Characterization of barriers on an earthquake fault, J. Geophys. Res. **84**, 6140-6148.

Bull, W.B., McFadden, L.D. (1977). Tectonic geomorphology north and south of the Garlock fault, California, in Geomorphology in arid regions, Doehring, D.O., ed., Proc. 8th Ann. Geomorph. Symp., State Univ. N.Y., Binghamton, 115-138.

Fonseca, Julia (1986). The Sou Hills -- a barrier to faulting in the Central Nevada Seismic Belt, M.S. prepub. manuscr., University of Arizona, 1-47.

Hanks, T.C., Bucknam, R.C., Lajoie, K.R., Wallace, R.E. (1984). Modification of wave-cut and faulting-controlled landforms, Jour. Geophys, Res. **89**, 5771-5790.

Harden, J.W. (1982). A quantitative index of soil development from field descriptions: Examples from a chronosequence in central California, Geoderma **28**, 1-28.

Hecker, Suzanne (in press). Timing of Holocene faulting in part of a seismic belt, west-central Nevada, Bull. Seism. Soc. Am.

Wallace, R.E. (1978). Patterns of faulting and seismic gaps in the Great Basin Province, in Proceedings of Conference VI, Methodology for identifying seismic gaps and soon-to-break gaps, U.S. Geol. Surv., Open-File Rept. 78-943, 857-868.

Wallace, R.E., Whitney, R.A. (1984). Late Quaternary history of the Stillwater seismic gap, Nevada, Bull. Seis. Soc. Am. **74**, 301-314.

Radiocarbon Geochemistry and Geophysics
9570-01568

Stephen W. Robinson
Branch of Isotope Geology

345 Middlefield Road
Menlo Park, California 94025
FTS 467-2858

INVESTIGATIONS

The problem of the application of high-precision radiocarbon calibration curves was investigated with special attention to the statistical significance of the resulting calibrated ages.

Radiocarbon dating was performed in support of the following earthquake related studies:

Quaternary framework for eathquake studies, Los Angeles (John Tinsley)

Tectonic geomorphology of the Mendocino triple junction area (Dorothy Merritts)

Coastal tectonics, Los Angels (Dan Ponti)

Owens Valley fault zone (Sara Beanland)

Coastal tectonics, Washington (Brian Atwater)

RESULTS:

A microcomputer algorithm was developed for calibration of radiocarbon dates against the high-precision (+-15 yrs) dendrochronologic-radiocarbon curves of Stuiver (1982) and Pearson (1983, 1985), which now extend back to 5200 B.C.

REPORTS:

Perkins, James A. and Robinson, Stephen W., Uncertainties Inherent in the use of radiocarbon ages for slip-rate studies: for a U.S.G.S. Bulletin

Engineering

^{14}C Geochronology - 9570-00374

Meyer Rubin

Branch of Isotope Geology
National Center, MS 971
Reston, VA 22092
(703) 648-5350

Results of Investigations Publications:

Evidence for Three Moderate to Large Prehistoric Holocene Earthquakes near Charleston, S.C.

Robert E. Weems, Stephen F. Obermeier, Milan J. Pavich, Gregory S. Gohn, Meyer Rubin, Richard L. Phipps, and Robert B. Jacobson

Abstract

Earthquake-induced liquefaction features (sand blows), found near Hollywood, S.C., have yielded abundant clasts of humate-impregnated sand and sparse pieces of wood. Radiocarbon ages for the humate and wood provide sufficient control on the timing of the earthquakes that produced the sand blows to indicate that at least three prehistoric liquefaction-producing earthquakes (m_b approximately 5.5 or larger) have occurred within the last 7,200 years. The youngest documented prehistoric earthquake occurred around 800 A.D. A few fractures filled with virtually unweathered sand, but no large sand blows, can be assigned confidently to the historic 1886 Charleston earthquake.

Earthquake Geology of the San Andreas and Related Faults in California

14-08-0001-21275

Kerry Sieh
Division of Geological and Planetary Sciences
Caltech, Pasadena, CA 91125
(818) 356-6115

Objective: We have several field studies aimed at the paleoseismicity of active faults in California. Our efforts are focussed on the southern 200 km and northern 300 km of the San Andreas fault, the faults of the Imperial Valley, and the faults associated with volcanic activity in the Mammoth Lakes-Mono Lake region.

Data Acquisision and Analysis: During the past several months our field efforts have been restricted to studies of the southern San Andreas fault and the Salton Trough. We continue to collect data on offset piercing points at the intersection of the shoreline of ancient Lake Cahuilla and the San Andreas fault at Indio. Much of our effort this season has been expended in learning to use our new Total Station and associated peripherals and software to more efficiently map exposures in plan-view and cross-section. Our study of vertical deformation in the Salton Trough is nearly complete. We have only two or three more sites at which we wish to determine the elevation of the most recent shoreline of Lake Cahuilla. Maximum vertical deformation of the 300-year-old shoreline appears to be 1.2 m, at Bat Cave Buttes, on the crest of the Durmid anticline, which straddles the southern tip of the San Andreas fault. Elsewhere, vertical deformation appears to be less than 40 cm. We anticipate that this study, when completed, will provide constraints on long-term rates of deformation inferred from geodetic studies in the Salton Trough.

We have given several papers at recent meetings. These are listed in the references below.

Salyards, S.L., 1986, Thermal and depositional constraints on a block and ash flow deposit from Panum Crater, Mono Co., Calif., from paleomagnetic analysis. Abstracts with Programs, Cordilleran Section, Geol. Soc. America, v. 18, no. 2.

Prentice, C., R. Weldon, and K. Sieh, 1986, Distribution of slip between the San Andreas and San Jacinto faults near San Bernardino, southern California. Abstracts with Programs, Geol. Soc. America Cordilleran Sec.

Sieh, K.E., and M. Bursik, submitted to J. Geophys. Res., Jan. 1986, Most recent eruption of the Mono Craters, eastern central California.

EVALUATION OF ACTIVITY OF THE SAN GABRIEL FAULT ZONE, LOS ANGELES AND VENTURA COUNTIES, CALIFORNIA

14-08-0001-21928

F.H. Weber, Jr.
California Department of Conservation
Division of Mines and Geology
107 South Broadway, Room 1065
Los Angeles, CA 90012
(213) 620-3560

Investigations

Field mapping, compatible with the modified plan described in the previous semiannual report, has continued along the portion of the San Gabriel fault between Castaic and the San Andreas fault near Gorman (Figure 1). Approval of the contract by the State of California in order to do trenching is still being awaited.

Results

In the previous semiannual report (Weber, 1985), geologic relationships involving the northwesternmost and eastern portions of the fault zone were described. Relationships along the northwestern portion of the fault include right lateral displacement of subunits of the Hungry Valley Formation and the Dry Creek syncline developed within rocks of the Hungry Valley Formation, and offset of terrace deposits, all near the northwestern terminus of the fault (Figure 1, Locality 1). About

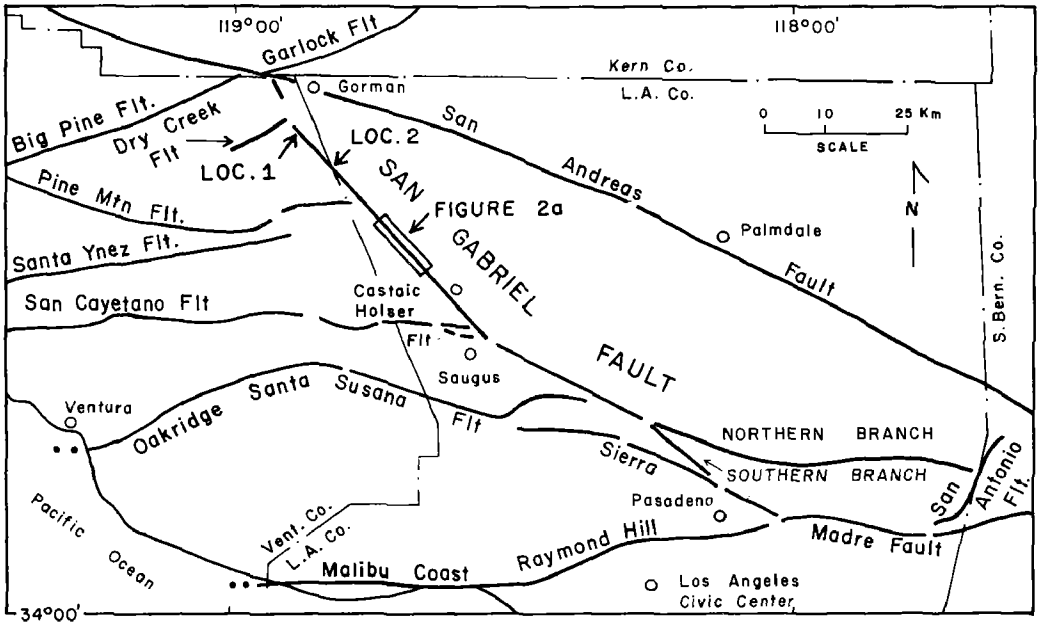

Figure 1. Fault map of a part of southern California showing the San Gabriel fault and the area included within Figure 2, herein. Localities 1 and 2 are referred to in the text.

13 km to the southeast of the terminus, landslide deposits in Beartrap Canyon are offset along the fault (Figure 1, Locality 2). More recent mapping, between 20 and 30 km southeast of the northwestern terminus of the fault (Figure 2a), has disclosed additional important features relative to interpretation of the displacement history of the fault.

Figure 2a covers a segment of the San Gabriel fault in the Whitaker Peak - Palomas Canyon area, about midway between Beartrap Canyon and Castaic. The area was previously mapped by the writer in reconnaissance at 1:24,000 (Weber, 1982), and now is being remapped at a scale of 1:9,600. The mapping thus far has shown that certain rock units can be correlated across the fault, thus implying that lateral displacement is severely limited, as compared to previous estimates. For example, Crowell (1982; and previous reports) has hypothesized that the Devil Canyon conglomerate of the Modelo Formation on the west side of the fault has been displaced right laterally from 35 to 56 km from its source terrane in the San Gabriel Mountains. Commensurate with this aspect of the hypothesis is that the gneissic constituents of the Violin Breccia on the east side of the fault were derived from a source terrane now making up part of the Frazier Mountain - Bear Mountain area far to the northwest of Palomas and Violin canyons. Total right slip on the fault is estimated by Crowell (1982) to be about 60 km.

Relationships depicted in Figures 2a-b present a far different picture. First, the mass of Precambrian Mendenhall Gneiss (gn) and related varieties of gneiss that extends along the west side of the San Gabriel fault from east of Whitaker Peak to nearly the southeast end of Palomas Canyon is not a fault sliver as shown on previous maps. Crowell et al (1982) show the gneiss to lie between the modern San Gabriel fault on the east and the Canton fault, itself offset by faults, on the west. Detailed mapping shows that the gneiss is not separated from granitic rocks (gr) wholly by faults, but has been, instead, intruded by these granitic rocks. Some shearing has occurred along the intrusive contact, as can be seen where it is exposed along the artificial cut for Whitaker Peak Road; but in a natural exposure about 100 m southeast of the road (Figure 2a, Locality 1), the contact is clearly intrusive. In addition, small apophyses of the granitic rocks occur within the gneiss (Figure 2a, Locality 2), and small bodies of the gneiss occur as inclusions within the granitic rocks (Figure 2a, Locality 3). Also, clasts of granitic rocks exposed in cuts in Violin Breccia along Whitaker Peak Road east of the San Gabriel fault (Figure 2a, Locality 8) appear to be identical to the granitic rocks west of the fault.

In addition, Crowell et al (1982) extend the Canton fault to the southeast where it is interpreted as overlain by the Devil Canyon Conglomerate (Tmd). Detailed mapping underway in this very brushy terrain with poor exposures shows a far more complex picture. One point that can be made unequivocably is that the Canton fault is not connected to the fault (Figure 2a, Locality 4) that Crowell et al (1982) show overlapped by the Devil Canyon conglomerate.

Rock units can also be correlated across the San Gabriel fault in the southeasternmost part of the area covered by Figure 2a. Detailed mapping has shown that a small body of gneiss on the east side of the fault (Figure 2a, gn, Locality 5) is equivalent to the lengthy body of gneiss exposed nearby to the northwest on the west side of the fault. In addition, a small outcrop of breccia (Figures 2a, Locality 6), clearly on the west side of the fault, rests on gneissic bedrock from which it apparently is derived. This breccia, identical in lithology to the Violin Breccia exposed widely east of the fault, appears to constitute the base of the Violin Breccia (Figures 2a and 2b, Tvb). Further, Violin Breccia may be correlative with basal breccia (Figures 2a and 2b, Tmb) of the Modelo Formation. Also, a very small body

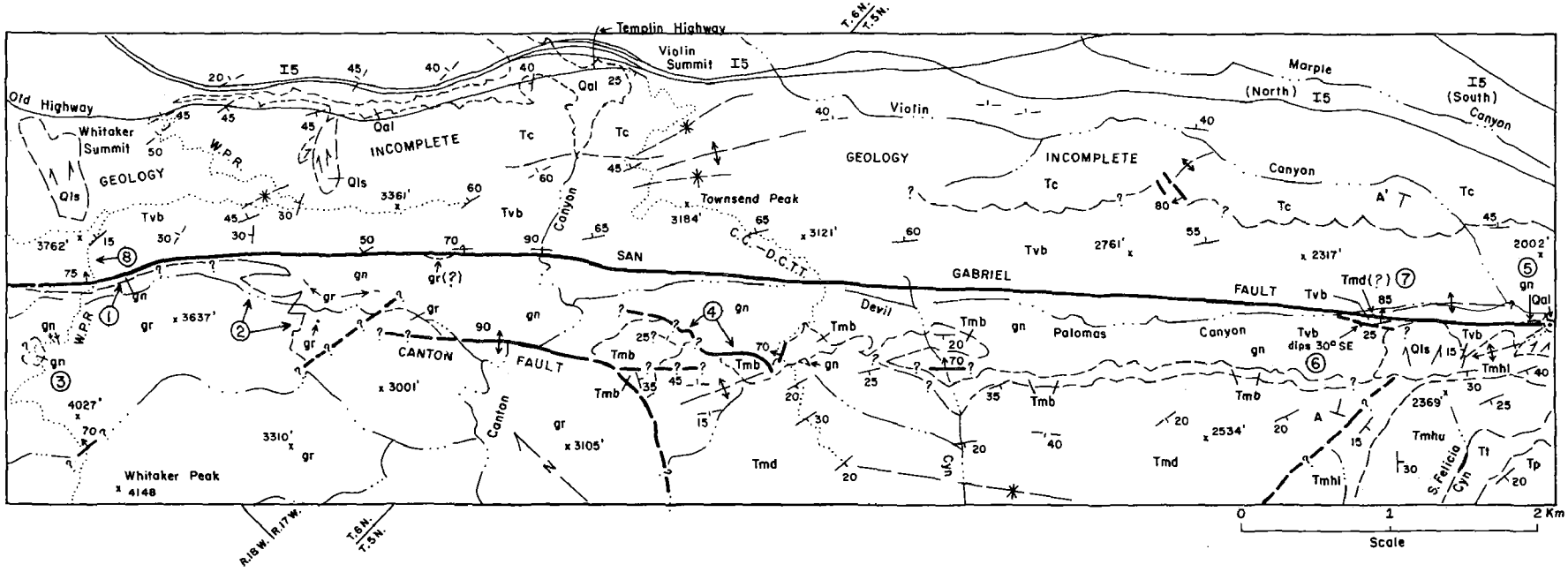

Figure 2a. GEOLOGIC MAP ALONG THE SAN GABRIEL FAULT IN THE WHITAKER PEAK-PALOMAS CANYON AREA, LOS ANGELES COUNTY, CALIFORNIA. Highly simplified from unpublished mapping of part of the Whitaker Peak quadrangle, scale 1:9,600. Explanation of units: Precambrian, Mendenhall Gneiss and related varieties of augen and other gneiss, gn. Cretaceous, granitic rocks, gr. Late Miocene, Violin Breccia, Tvb; Castaic Fm., Tc; Modelo Fm., basal breccia, Tmb; Devil Canyon conglomerate, Tmd; lower and upper Hasley conglomerate, Tmhl and Tmhu. Late Miocene-early Pliocene, Towsley Fm, Tt. Pliocene, Pico Fm, Tp. Quaternary, landslides, Qls. W.P.R., Whitaker Peak Road; C.C.-D.C.T.T. Canton Canyon-Devil Canyon Truck Trail.

of anorthosite clast-bearing conglomerate rests on Violin Breccia on the east side of the fault (Figure 2a, Locality 7). This conglomerate may be correlative with the Devil Canyon conglomerate (Figure 2a, Tmd), heretofore mapped only on the west side of the fault. Interpretive relationships among map units gn, Tvb, Tmb, and Tmd are depicted in Figure 2b. If what is depicted is accurate, then total lateral slip along the San Gabriel fault cannot possibly be as large as previously estimated. An additional consideration is that older alluvium (Figure 2b, Qoa) may be displaced downward relatively along the west side of the principal trace of the fault.

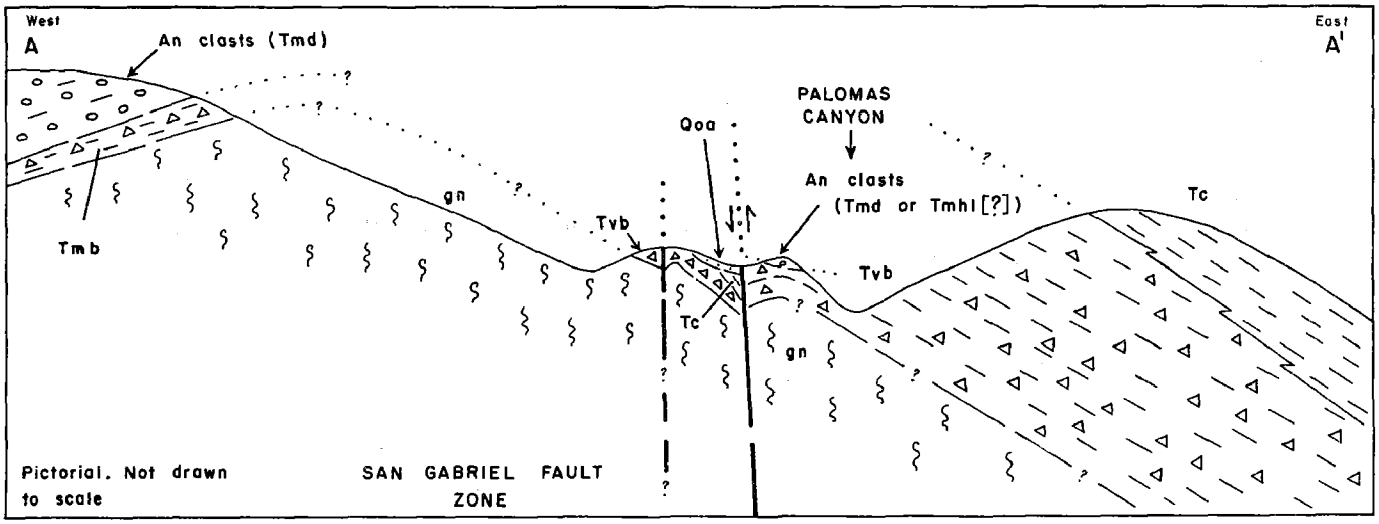

A-A'

Figure 2b. Pictorial cross section across the San Gabriel fault in the southern Palomas Canyon area. Line of profile is on Figure 2a. See caption for Figure 2a for explanation of symbols.

References Cited

Crowell, J.C., 1982, The tectonics of Ridge Basin, southern California, in Crowell, J.C., and Link, M.H., eds., 1982, Geologic history of Ridge Basin, Southern California: Pacific Section, Society of Economic Paleontologists and Mineralogists, Los Angeles, California, p. 25-41.

Crowell, J.C., et al, 1982, Geologic map of Ridge Basin, southern California, in Crowell, J.C., and Link, M.H., eds., 1982, Geologic history of Ridge Basin: Pacific Section, Society of Economic Paleontologists and Mineralogists, Los Angeles, California.

Weber, F.H., Jr., 1982, Geology and geomorphology along the San Gabriel fault zone, Los Angeles and Ventura counties, California (including reinterpretation of slip history and reevaluation of activity): California Division of Mines and Geology Open-File Report 82-2 LA, 157 p.

Weber, F.H., 1985, Evaluation of activity of the San Gabriel fault zone, Los Angeles and Ventura counties, in Jacobsen, M.L., and Rodriguez, T.R., compilers, Summaries of Technical Reports, Volume XXI, National Earthquake Hazards Reduction Program, U.S. Geological Survey, p. 152-156.

Reports

Findings of the study have been utilized in preparation of the following reports completed or published since submittal of the last semi-annual report.

Weber, F.H., Jr., 1985, Geology of the area involving the northwestern terminus of the San Gabriel fault, Los Angeles and Ventura counties, California, in Ridge Basin and the San Andreas fault system, southern California: Guidebook for Los Angeles Basin Geological Society field trip, November 16-17, 1985, p. 68-75. (Leader, J.C. Crowell; Organizers, S.E. Thornton and M. Hall - Burr.)

Weber, F.H., 1986, Geologic relationships between the San Gabriel and San Andreas faults, Kern, Los Angeles, and Ventura counties (California)...A new interpretation: California Geology, v. 39, no. 1, January 1986, p. 5-14.

Weber, F.H., Jr., 1986, Geology along the San Gabriel fault between Saugus and the San Andreas fault, and reinterpretation of structural elements and displacement history, Los Angeles, Kern, and Ventura counties, California; PART I of III, West of Pyramid Lake north to the San Andreas fault: California Division of Mines and Geology Open-File Report (OFR) 85-15 LA.

Weber, F.H., Jr., 1986, Geologic relationships along the San Gabriel fault between Castaic and the San Andreas fault, Kern, Los Angeles, and Ventura counties, California, in Neotectonics in the area between the central and western Transverse ranges, Field Trip No. 10; in Ehlig, P.E., compiler, Guidebook and Volume, Neotectonics and faulting in southern California: Prepared for the 82nd Annual Meeting of the Cordilleran Section of the Geological Society of America, Los Angeles, California, March 25-28, 1986, p. 109-122.

Illustrations were drafted by Robin I. Weber. Word processing was done by Venice Huffman and Virginia Hoskin. The report was reviewed by Cliffton H. Gray, Jr. and Allan G. Barrows, co-principal investigator.

Central California Deep Crustal Study

9540-02191

Carl M. Wentworth
Branch of Western Regional Geology
U.S. Geological Survey
345 Middlefield Road, MS 975
Menlo Park, California 94025
(415) 323-8111 ext. 2474

Investigations

Seismic reflection profiling, in concert with other geophysics and geology, is being used to examine crustal structure between the California Coast Ranges and the Sierran foothills (see map, p. 149, USGS Open-File Report 85-22 for location of profiles; line CC-2 extends a further 30 km into the Sierra Nevada than shown).

1. Processing of reflection lines CC-1 and CC-2 was completed.

2. Recorrelation of the eastern part of reflection line SJ-6 across the eastern San Joaquin Valley at Delano was begun to recover data below the original 6 s of record and thus explore the relation to features in CC-2, 175 km to the northwest.

3. Interpretation of CC-1 and CC-2 continued.

4. Interpretation of lines SJ-3 and SJ-19 at Coalinga was sharpened and a manuscript for a chapter in the Coalinga professional paper was revised.

Results

1. The final stacks for reflection lines CC-1 and CC-2 yielded improved deep record beneath the exposed Franciscan on CC-1, some intrabasement events at the east end of CC-1, and similar, possibly correlative events in the western part of CC-2. Wave-equation migration of the 15-s stacks produced useful record sections down to about 12 s. The most prominent effects of the migration are collapse of the steeper eastern parts of EUR and ELR near the west end of CC-1 and truncation of the layered reflections of WLR by a more steeply west-dipping WMR across their top in the center of CC-2 (see line drawings of stacks, figs. 1 and 2, p. 99-100, in summaries vol. XXI, USGS OFR 86-31).

2. Continuing work on the CC-1/CC-2 transect across the northern San Joaquin Valley, combining present results from reflection, refraction, gravity and magnetics by several cooperating scientists (Wentworth, Colburn, Griscom, Holbrook, Jachens, Mooney, Walter, Whitman, and Zoback) is encouraging. On the west, in the eastern Coast Ranges, oceanic Franciscan rock (5.8 km/s) containing a horizontal lens of magnetic serpentinite extends to a depth of 15 km and yields discontinuous layered reflections that decrease in abundance at 5.0 s. A more poorly layered lower crust (6.9 km/s), probably containing a low velocity zone (5.3 km/s) near 20 km, extends to

M at 29 km, which is marked by the deepest prominent reflections (9.8 s). Steeply east-dipping forearc strata of the Great Valley sequence (GVS) exposed east of the Franciscan are truncated at depths of 1-3 km along the Coast Range thrust (CRT) by a subsurface wedge of Franciscan rock. This wedge peeled up the steeply dipping strata and gently dipping GVS farther east as it was thrust eastward above a west-dipping magnetic basement that is physically continuous with the westward-tilted Sierran block to the east. This anatomy contrasts with the accepted view that the CRT is a Mesozoic subduction zone. A thin, 5.5 km/s layer in the top of that basement beneath the western Great Valley (eroded overthrust remnant of Coast Range ophiolite?) is underlain by a 6.5 km/s upper crust to 15 km and faster lower crust. Beneath the same top layer 12 km farther east, a doubled crust seems indicated by increasing velocity to 7 km/s at 13 km, an inversion to 6.6 km/s and then downward increase to M at 27 km. The upper basement beneath the valley seems composed of several east-dipping (35^{o}) slabs with densities and magnetizations characteristic of mafic to granitic rocks, a structure not clearly evident in the reflection record. A prominent west-dipping midcrustal reflection (WMR), representing a major fault of crustal dimensions, rises eastward beneath the eastern valley and truncates slightly flatter underlying reflections (WLR). WMR crosses through a large inferred granitic mass and merges eastward with discontinuous flat reflections at 2-3 s that extend on beneath the edge of the Sierran batholith. The steeply east-dipping structure of the Foothills metamorphic belt, possibly represented by sparse east-dipping reflections, is probably truncated below by WMR. the middle Sierran crust has a prominent west-dipping reflection fabric, in contrast to expected east-dipping structure. Flat reflections below these events at 14 s may represent M at 36-40 km.

3. The inferred Franciscan identity of the 5.8 km/s wedge of material between west-dipping basement below and Great Valley sequence above at the east front of the Coast Ranges (Wentworth and others, 1984, SEPM special vol. 43) has been complicated by our conclusion that, at Coalinga, the wedge has overridden 4 km of Great Valley sequence (GVS) which also has a velocity of 5.8 km/s. The Franciscan identity of the wedge is based principally on the similarity of its velocity to that observed in Franciscan rock elsewhere and its occurrence beneath GVS, the same position that occupies in exposures in the mountains to the west. We call on a reduction of porosity to nearly zero in the overridden GVS to achieve this increased velocity, relative to the 3.5-5.0 km/s observed in GVS elsewhere. The principal alternative, that the wedge is also GVS, seems unreasonable. This would require abrupt change in the GVS from normal to high seismic velocity without evident cause. Furthermore, particularly at Coalinga, structural relations require thrust emplacement of the wedge, and the resulting gross repetition of section is not observed in the GVS exposed to the west.

4. The timing of wedge emplacement and associated deformation at the east margin of the Coast Ranges is difficult to establish, but may range from late Mesozoic to modern. Thrusting at Coalinga is as recent as 1983, and principal emplacement of the wedge beneath Coalinga anticline began in Pliocene time. Quaternary folding and faulting at the range front is also evident further northwest, and small modern earthquakes with mechanisms like the Coalinga mainshock have occurred near Patterson (Wong and Ely,

1983) and Winters (Eaton, oral commun., 1986). Much of the eastward tilting of the Great Valley sequence (GVS) predates the truncating Quaternary deposits, and may have accumulated through Tertiary time. The Franciscan assemblage was shedding debris to local marine basins in the Eocene, which may mark a major thrusting event that both uplifted the Franciscan and moved it eastward beneath the GVS and lower Tertiary strata. The wedge thrusting should have produced secondary back thrusts in the roof rocks (GVS and Tertiary strata). Such thrusts can account for relations previously interpreted as unconformities, such as that between upper and lower Cretaceous GVS above the Wilburn Springs antiform (Blake and Jones, 1981). These unconformities have been used to constrain timing of Franciscan emplacement, but are now suspect until investigated further. Our inference that the large cross faults in the GVS north of Paskenta are tear faults at the northwest edge of thrust wedges of GVS carried forward of the Franciscan wedge requires many tens of kilometers of thrust transport. This could have begun early in GVS time, but most of the wedge emplacement must post-date the 90-m.y. metamorphic age of rocks near the exposed eastern margin of the Franciscan terrane. Important constraints on timing may come from detailed structural and biostratigraphic work searching for thrusts in GVS-Tertiary section and from analysis of subsidence histories in the Great Valley sedimentary basin.

Reports

Wentworth, C.M., and others, 1985, Structure and tectonic history of the California Coast Ranges--testing an obduction model of Franciscan emplacement inferred from seismic reflection profiles and other geophysical data (abs.): (Program for) DOSECC (Deep observation and sampling of the Earth's Continental Crust) Continental Scientific Drilling Workshop, Houston, Texas, April 29-May 1, 1985, p. 109-112.

Zoback, M.D., and Wentworth, C.M., 1985, Crustal studies in central California using an 800-channel seismic reflection recording system, in Barazangi, M., and Brown, L. (eds.), Reflection seismology: a global perspective: American Geophysical Union, Geodynamics Series, v. 13, p. 183-196.

Recognition of Individual Earthquakes on Thrust Faults (New Zealand)

14-08-0001-21984

Robert S. Yeats
Department of Geology
Oregon State University
Corvallis, Oregon 97331-5506
(503) 754-2484

Kelvin R. Berryman
Earth Deformation Section
New Zealand Geological Survey, D.S.I.R.
P.O. Box 30368
Lower Hutt, New Zealand
(644) 699-059

Investigations

The final report is now being prepared in four parts:

1. Northern South Island, New Zealand and Transverse Ranges, California - a tectonic comparison, by R. S. Yeats and K.R. Berryman.

2. Tectonic map of central Otago based on Landsat, by R. S. Yeats.

3. Geology and neotectonics of the Upper Nevis Basin, South Island, New Zealand, by S. A. Barrow-Hurlbert.

4. Neotectonics of the north half of the Dunstan fault and its intersection with the Blue Lake and Hawkdun faults, South Island, by I. Madin.

Results

We have already pointed out that the Alpine and San Andreas faults are flanked by reverse-fault provinces oriented 45° counter-clockwise to the strike of these faults. However, we have been puzzled by the fact that a reverse-fault province occurs on only the north side of the Alpine fault (Nelson region), and the south side is marked by the Southern Alps, with uplift contours subparallel to the Alpine fault (Figure 1). However, reverse-fault provinces occur farther south in Central Otago and Mackenzie Basin, separated from the Alpine fault by the Southern Alps (Figure 1).

Recent work in California (Hadley and Kanamori, 1978; Yeats, 1981; Webb and Kanamori, 1985) suggests that reverse faults may propagate upward from the brittle-ductile transition through brittle crust to the surface. Granitic crust in the Transverse Ranges may be strong enough to sustain stresses imposed by upward ramping of crystalline rocks over adjacent rocks of similar strength. The Nelson region is also underlain by granitic crust and may behave in the same way. However, the schist and graywacke of the Southern Alps must be weaker than the adjacent granitic crust. Furthermore, the Southern Alps are characterized by very young apparent radiometric ages and by hot springs, suggesting a high geothermal gradient, including temperatures between 140° and 350° C within 2 km of the surface (Allis and others, 1979). In contrast, the California Transverse Ranges and the Nelson region of New Zealand have lower geothermal gradients. In the South Island, uplift rates, based in part on tilt of stranded shorelines of glacial lakes and on heights of marine benches and river terraces, are greater than 10 mm/y in the Southern Alps adjacent to the Alpine fault (Wellman, 1979). The high temperatures close to the surface may be due to the high uplift rates (Allis and others, 1979) and also to frictional shear heating associated with oblique-reverse slip on the Alpine fault (Scholz and others, 1979, Johnston and White, 1983).

The crust in the Southern Alps may be too weak to localize displacement along major reverse faults that extend to the brittle-ductile transition zone. Instead, the displacement may occur anelastically by distributed shear within the schist (Walcott, 1979; Allis and others, 1979). Further southeast, crust with lower geothermal gradient may be brittle enough to support large-scale reverse faulting. The uplift-rate contours of Wellman (1979) are taken as a first approximation of heat-flow gradients, since heat-flow values are not widespread in the South Island. Allis (1986) estimates surface heat flow in the Southern Alps at about 200 mW/m^2. The 4 mm/y uplift-rate contour is shown as a dotted line on Figure 1; rates between the dotted line and the Alpine fault are higher, locally more than 10 mm/y. Figure 1 shows that the faults of Central Otago and Canterbury die out 20-30 km SE of the 4 mm/y uplift-rate contour and 60-80 km SE of the Alpine fault itself. Anelastic rather than brittle failure may also cause the Marlborough strike-slip faults to become diffuse and hard to map close to the Alpine fault. The weaker, hotter crust southeast of the Alpine fault may cause the restraining bend to be smaller in the South Island than the bend in the Transverse Ranges of California.

References

Allis, R. G., 1980, Mode of crustal shortening adjacent to the Alpine fault, New Zealand: Tectonics, v. 5, p. 15-32.

Allis, R. G., Henley, R. W., and Carman, R. W., 1979, The thermal regime beneath the Southern Alps, in Walcott, R. I. and Cresswell, M. M., eds., The Origin of the Southern Alps: Royal Society of New Zealand Bull, 18, p. 79-85.

Hadley, D. M., and Kanamori, H., 1978, Recent seismicity in the San Fernando region and tectonics in the west-central Transverse Ranges, California: Seismological Society of America Bulletin, v. 68, p. 1449-1457.

Johnston, D. C., and White, S. H., 1983, Shear heating associated with movement along the Alpine fault, New Zealand: Tectonophysics, v. 92, p. 241-252.

Officers of the New Zealand Geological Survey, 1983, Late Quaternary tectonic map of New Zealand 1:2,000,000, 2nd ed. New Zealand Geological Survey Miscellaneous Series, Map 12.

Scholz, C. H., Beavan, J., and Hanks, T. C., 1979, Frictional metamorphism, argon depletion, and tectonic stress on the Alpine fault, New Zealand: Journal of Geophysical Research, v. 84, p. 6770-6782.

Walcott, R. I., 1979, Plate motion and shear strain rates in the vicinity of the Southern Alps, in Walcott, R. I. and Cresswell, M. M., eds., The Origin of the Southern Alps: Royal Society of New Zealand Bull. 18, p. 5-12.

Webb, T. H. and Kanamori, H., 1985, Earthquake focal mechanisms in the eastern Transverse Ranges and San Emigdio Mountains, southern California and evidence for a regional decollement: Seismological Society of America Bulletin, v. 75, p. 737-757.

Wellman, H. W., 1979, An uplift map for the South Island of New Zealand, and a model for uplift of the Southern Alps, in Walcott, R. I. and Cresswell, M. M., eds., The Origin of the Southern Alps: Royal Society of New Zealand Bull. 18, p. 13-20.

Yeats, R. S., 1981, Quaternary flake tectonics of the California Transverse Ranges: Geology, v. 9, p. 16-20.

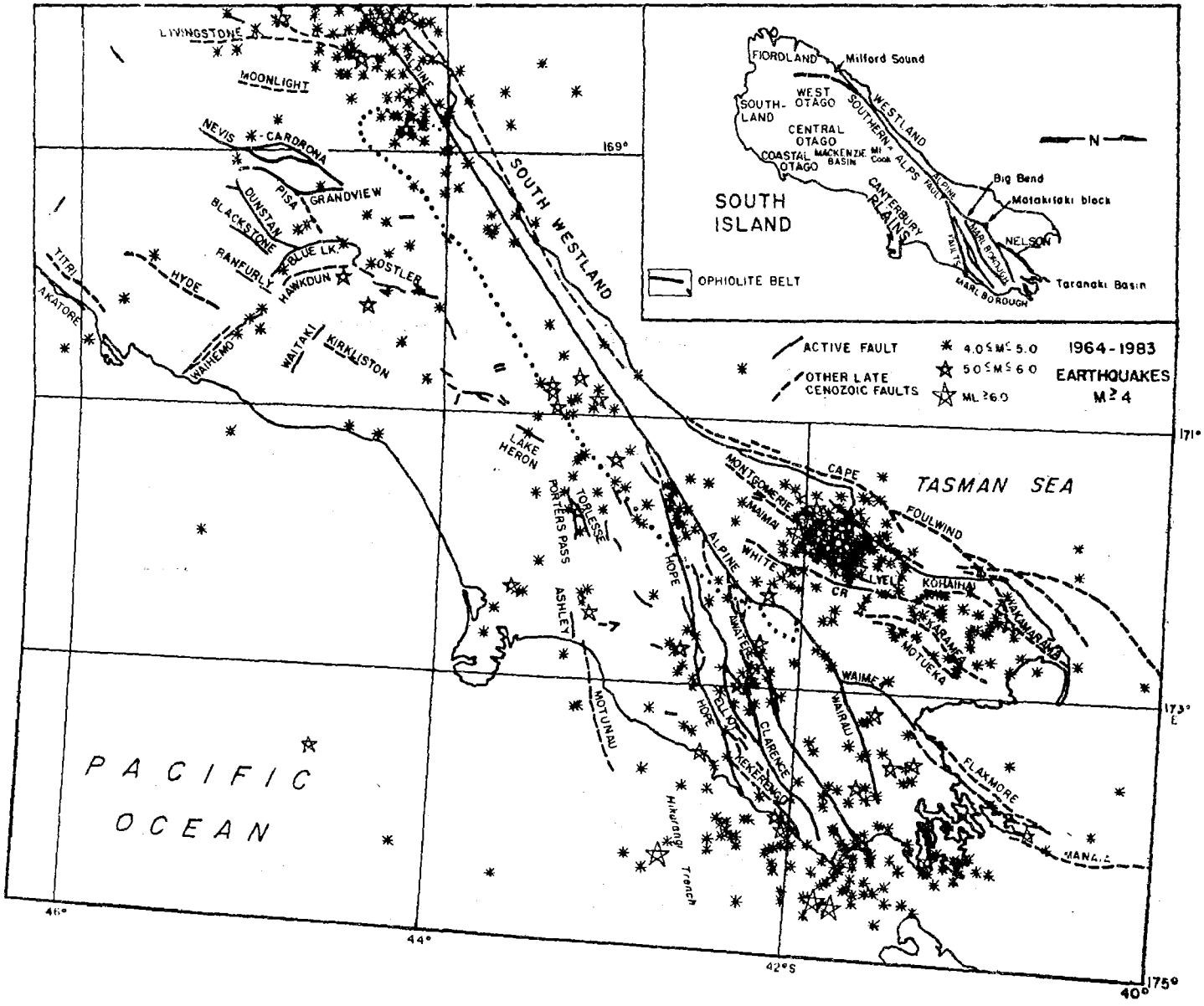

Figure 1. Seismicity and late Quaternary faults of northern South Island, New Zealand. Earthquakes of $M \geq 4$, 1964 through 1983, data from M. Reyners, Geophysics Division, D.S.I.R., plotted by R. Wood, New Zealand Geological Survey. Active faults (solid lines) revised from Officers of the New Zealand Geological Survey (1983) and from Geological Maps of New Zealand, 1:250,000 and 1:1,000,000 published by the New Zealand Geological Survey. Dotted line encloses area of uplift rates higher than 4 mm/y on southeast side of Alpine fault (Wellman, 1979).

Comparative Study of the Neotectonics of the Xianshuihe Fault, China

Grant No. 14-08-0001-G1088

Clarence R. Allen
Seismological Laboratory, California Institute of Technology
Pasadena, California (818-356-6904)

Objectives

The purpose of this study is to investigate, together with Chinese colleagues from the Bureau of Seismology of Sichuan Province, the Xianshuihe fault of western Sichuan. This structure is among the world's most active faults, having producing 3 earthquakes during this century exceeding magnitude 7 along a 200-km length of the zone. At least 6 such events have occurred since 1725. In the more limited 60-km-long segment between Luhuo and Daofu, major earthquakes in 1923, 1973, and 1981 (M = 7-1/4, 7.9, 6.9) were associated with overlapping surficial fault ruptures, and with individual left-lateral displacements as large as 3.6 m. Specific objectives of the study include the questions of (1) whether the current burst of activity is typical of late Quaternary activity, (2) whether the high degree of activity of the fault could be readily ascertained from physiographic features even in the absence of the historic record, and (3) a comparison of neotectonic features of the Xianshuihe fault with those of other active strike-slip faults in China and elsewhere.

Results

This grant commenced on 1 March 1986, and only preparatory work has been carried out to date. The American PI, together with Caltech graduate student Zhou Huawei, is scheduled to leave for China on 6 May for six weeks of field work in Sichuan. The field work will be carried out together with Chinese co-investigators Luo Zhuoli, Qian Hong, and Wen Xueze.

Source and Seismic Potential Associated with Reverse Faulting and Related Folding

14-08-0001-G1165

Edward A. Keller
Dept. of Geological Sciences
University of California
Santa Barbara, California 93106
(805) 961-4207

Objective: Investigate tectonic framework, geometry, and uplift rates associated with folding on upper plates of buried reverse faults. Study sites are Wheeler Ridge, San Emigdio Canyon, and the Los Lobos folds near Bakersfield, California.

Results: The first six months of work on this project have been focussed toward better understanding of rates of uplift at Wheeler Ridge, San Emigdio Canyon, and the Los Lobos folds.

1. The north flank of the San Emigdio Mountains located at the southern end of the San Joaquin Valley is an active fold-thrust belt. In San Emigdio Canyon a mid-to late Pleistocene mountain front is defined by an eroded scarp and the position of the Pleito fault. At this site, a late Pleistocene alluvial fan surface is broadly warped over the principle strand of the Pleito fault, but Holocene deposits are not deformed. Five kilometers to the north at the present topographic range front, gravels of the late Pleistocene fan are steeply dipping but not faulted where they cross the buried Wheeler Ridge fault zone. At the range front, Holocene stream terraces of San Emigdio Creek are deformed and ^{14}C dates coupled to measured deformation suggests an uplift rate of approximately 2 mm/yr. One kilometer north of the present mountain front, alluvial fan segments are being actively folded at the Los Lobos folds. This folding apparently represents late Pleistocene-Holocene northward migration of the topographic expression of the fold-thrust belt. We infer from geophysical data that the folds are on the upper plate of a buried reverse fault. Measured deformation of alluvial fan surfaces over the Los Lobos folds with accompanying ^{14}C dates suggest an uplift rate of about 1.6 mm/yr. Uplift of the present range front at the mouth of San Emigdio Canyon, combined with that at the Los Lobos folds on the alluvial fan immediately to the north suggests a total rate of approximately 3.5 mm/yr.

2. Wheeler Ridge is an east-west trending anticline on the upper plate of the buried Wheeler Ridge fault. Holocene deformation at the eastern end of the anticline is demonstrated where Salt Creek crosses the anticlinal axis. Two alluvial surfaces dated at 7,370 $\pm$ 140 rybp and 11,940 $\pm$ 260 rybp are folded over the structure providing uplift rates 0.6 and 2.1 mm/yr respectively. Assuming an average uplift rate of 1.4 mm/yr (a compromise between minimum and maximum rates) suggests that

the four older Pleistocene surfaces have ages of approximately 15-30 ka, 30-60 ka, 90-150 ka and 220-250 ka (1 ka = 1000 yrs). These age assignments are tentative pending additional age control from ^{14}C dates and uranium-series dates. Uplift, tilting and folding associated with the growth of the anticline are documented by geomorphic surfaces which are higher and older to the west of the eastern terminus of the fold (Figure 1). Soils vary from AC profiles on Holocene surfaces to well-developed argillic and petrocalcic horizons on Pleistocene surfaces. Radio carbon dates, soil chronology, and chronology based upon rate of uplift suggest that the anticline is extending to the east at a rate of about 2 mm/yr. Assuming that the chronology is approximately correct, then the stream that cut the prominent wind gap was defeated approximately 30 to 60 ka ago.

Publications: We have recently published two abstracts:

Laduzinsky, Dennis M., Seaver, Din B., and Keller, Edward A., 1986. "Tectonics of an ative fold-thrust belt." The Geological Society of America, Abstracts with Programs 18 (2): 126.

Zepeda, Ricardo, L., Keller, Edward A. and Rockwell, Thomas K., 1986. "Rates of active tectonics at Wheeler Ridge, Southern San Joaquin Valley, California." The Geological Society of America, Abstracts with Programs 18 (2): 202.

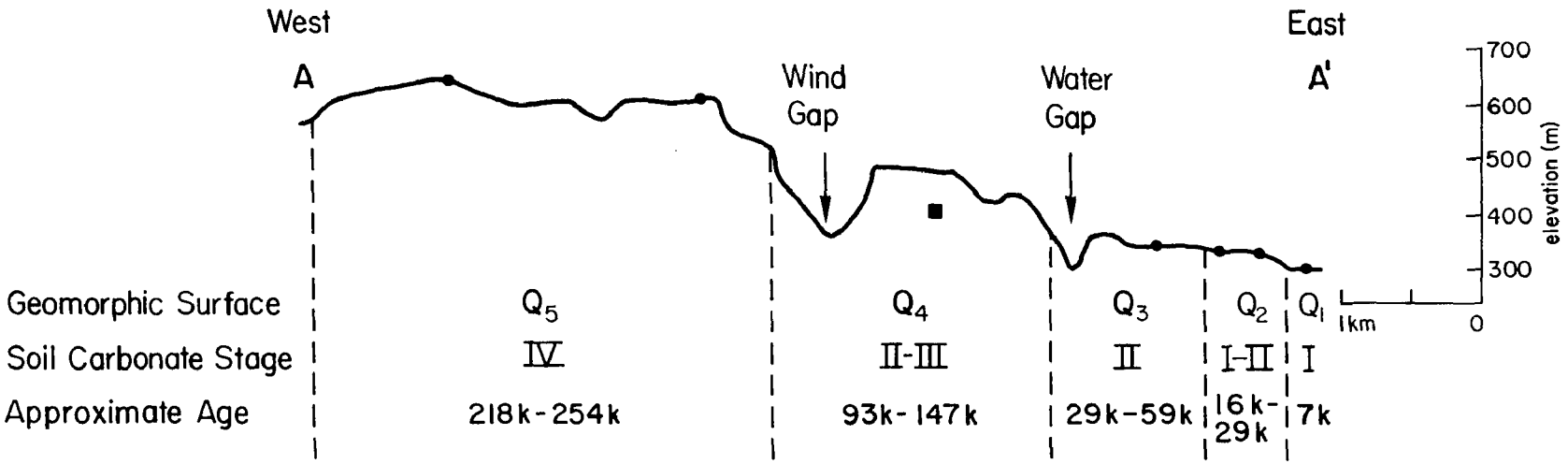

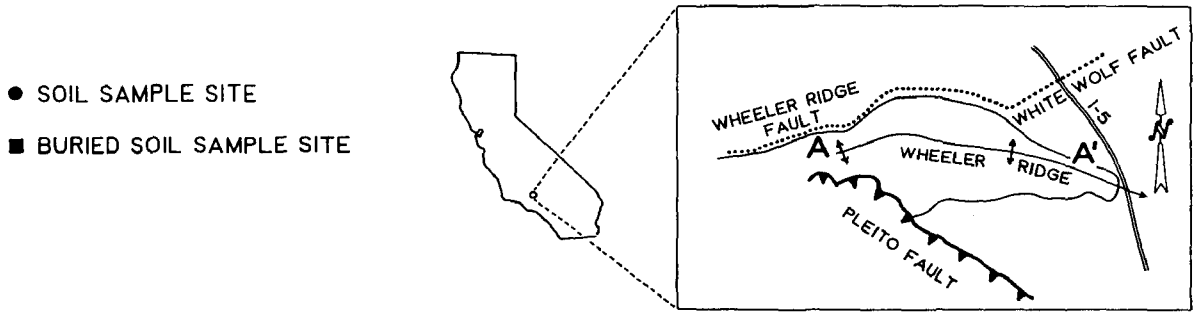

Figure 1

Topographic profile along the crest of Wheeler Ridge. Shown are five geomorphic surfaces with soil carbonate stages and estimated age.

Paleomagnetism of the Neogene Saugus Formation, Transverse Ranges, California: Timing and Deformation Rates of Potentially Active Faults

14-08-0001-G1155

Shaul Levi
Geophysics, College of Oceanography
Oregon State University
Corvallis, Oregon 97331
(503) 754-2912

Objectives: The long term objectives of this study have been to use magnetic stratigraphy to establish the age and sedimentation rates of the Saugus Formation, which is widely exposed in parts of the Transverse Ranges in Los Angeles County, California, in areas undergoing rapid urbanization (Figure 1). These data are necessary for determining the timing and deformation rates of potentially active faults as well as rates of tectonic rotations. The specific objectives of the current phase of our research are:

1) to determine the rates of deformation and uplift of the San Gabriel Mountains along the Tujunga fault, active during the 1971 San Fernando earthquake--paleomagnetism of the Saugus exposed along Kagel Ridge and Little Tujunga Canyon sections;

2) to determine the time of uplift of the Santa Susana Mountains and the initial movement along the Santa Susana fault--paleomagnetism of the Saugus Formation at Horse Flats and the Van Norman Lake section.

Results:

1) The paleomagnetism of the Saugus and underlying Pico/Towsley formations of the composite section including exposures at Kagel Ridge, Little Tujunga Canyon and Marek Canyon (Figure 2) are predominantly of reversed polarity. Four intervals of normal polarity were observed in the Kagel Ridge segment of the composite section, whose total stratigraphic thickness is about 1300 meters. By analogy with the Saugus in the Pico Canyon area near Castaic (Levi et al, 1986), we infer that the Saugus in the Merrick syncline is of Matuyama age, 0.73-2.48 Ma. Since the uppermost zone of normal polarity is overlain by about 500 m of only reversed remanence, we consider it highly unlikely that this normal interval represents the Jaramillo subchron (See Figure 3). We believe that it is most likely that this uppermost normal polarity unit represents the Gilsa subchron (McDougall, 1979). If the normal polarity zones in the Kagel Ridge segment represents the Gilsa, Olduvai, and two Réunion subchrons, then one obtains an average sedimentation rate between 0.7 and 0.9 km/Ma, depending on whether one uses the polarity time scale of McDougall (1979) or Mankinen and Dabrymple (1979).

The mean paleomagnetic direction for 25 sites (inverted to normal polarity) is D=34°, I=47°, α_{95}=5°. The mean inclination is 7° shallower than the expected geocentric axial dipole at this site. The mean declination

is 34°, which would suggest significant clockwise tectonic rotation of this area since about 2.5 Ma ago, comparable to the value observed near Castaic (Figure 4).

2) At the Lower Van Norman Lake ten Saugus sites were sampled for a preliminary paleomagnetic study (See Figure 5). Six of the sites were from the lower Sunshine Ranch member and four from the upper part of the Saugus (Saul, 1975). The sampled section is homoclinal striking almost precisely in the east-west direction and dipping steeply to the north with an average value of about 60°. The sites span a stratigraphic section of about 900 meters. The magnetic polarity was recovered from all ten sites, and the paleomagnetic direction from five of these. The lowest unit records normal polarity, and the overlying nine are reversed (Figure 6). By analogy with results from the Pico Canyon area near Castaic (Levi et al, 1986), we consider that it is most likely that the reversed sequence represents the Matuyama chron. The mean paleomagnetic direction of the five sites (inverted to normal polarity) is D=10°, I=47°, α_{95}=10°.

We have recently sampled about 35 additional sites at the Van Norman Reservoir area and a dozen sites at Horse Flats. Near the syncline axis at Horse Flats we discovered a sedimentary interbed, which might represent an ash fall. It was sent for examination to Dr. Andrei M. Sarna-Wojcicki at the U.S. Geological Survey.

References:

Barrows, A.G., J.E. Kahle, R.B. Saul and F.H. Weber, Jr., 1975, Geologic Map of the San Fernando earthquake area 1:18,000, Calif. Div. Mines Geology Bull., 196.

Jennings, C.W., and Strand, R.G., 1969, Los Angeles sheet: Geologic map of California 1:250,000: California Division of Mines and Geology.

Levi, S., Schultz, D.L., Yeats, R.S., Stitt, L.T., and Sarna-Wojcicki, A.M., 1986, Magnetostratigraphy and paleomagnetism of the Saugus Formation near Castaic, Los Angeles County, California: in Neotectonics and Faulting in Southern California, Cordilleran Section Field Trip Guidebook and Volume, p. 103-108, Geological Society of America, Los Angeles, California.

McDougall, I., 1979, the present status of the geomagnetic polarity time scale: in The Earth: Its Origin Structure and Evolution, M.W. McElhinny, editor, p. 543, Academic Press, London and New York.

Mankinen, E.A. and Dalrymple, G.B., 1979, Revised Geomagnetic Polarity Time Scale for the interval 0-5 m.y.B.P., J. Geophys. Res., v. 84, p. 615-626.

Saul, R.B., 1975, Geology of the southeast slope of the Santa Susana Mountains and geologic effects of the San Fernando earthquake, California Div. Mines and Geology Bull., v. 196, p. 187-194.

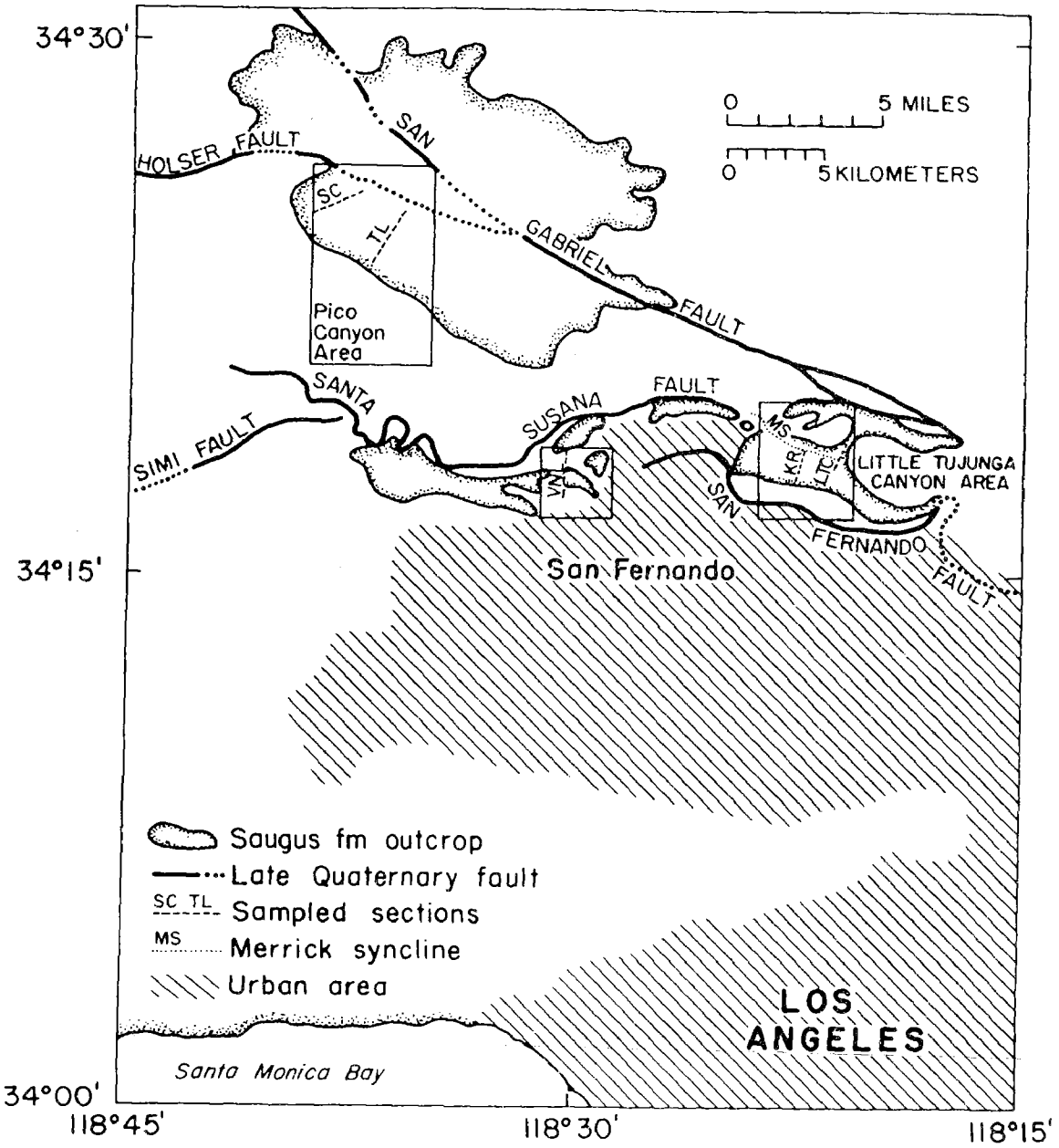

Figure 1. Location of Saugus outcrops in the East Ventura Basin, showing also several Quaternary faults with known potential for ground rupture. Adapted from Jennings and Strand (1969). The rectangles enclose the areas for the present study at the Little Tujunga Canyon area, Horse Flats and the Van Norman Reservoir and also the Pico Canyon area near Castaic (Levi et al, 1986).

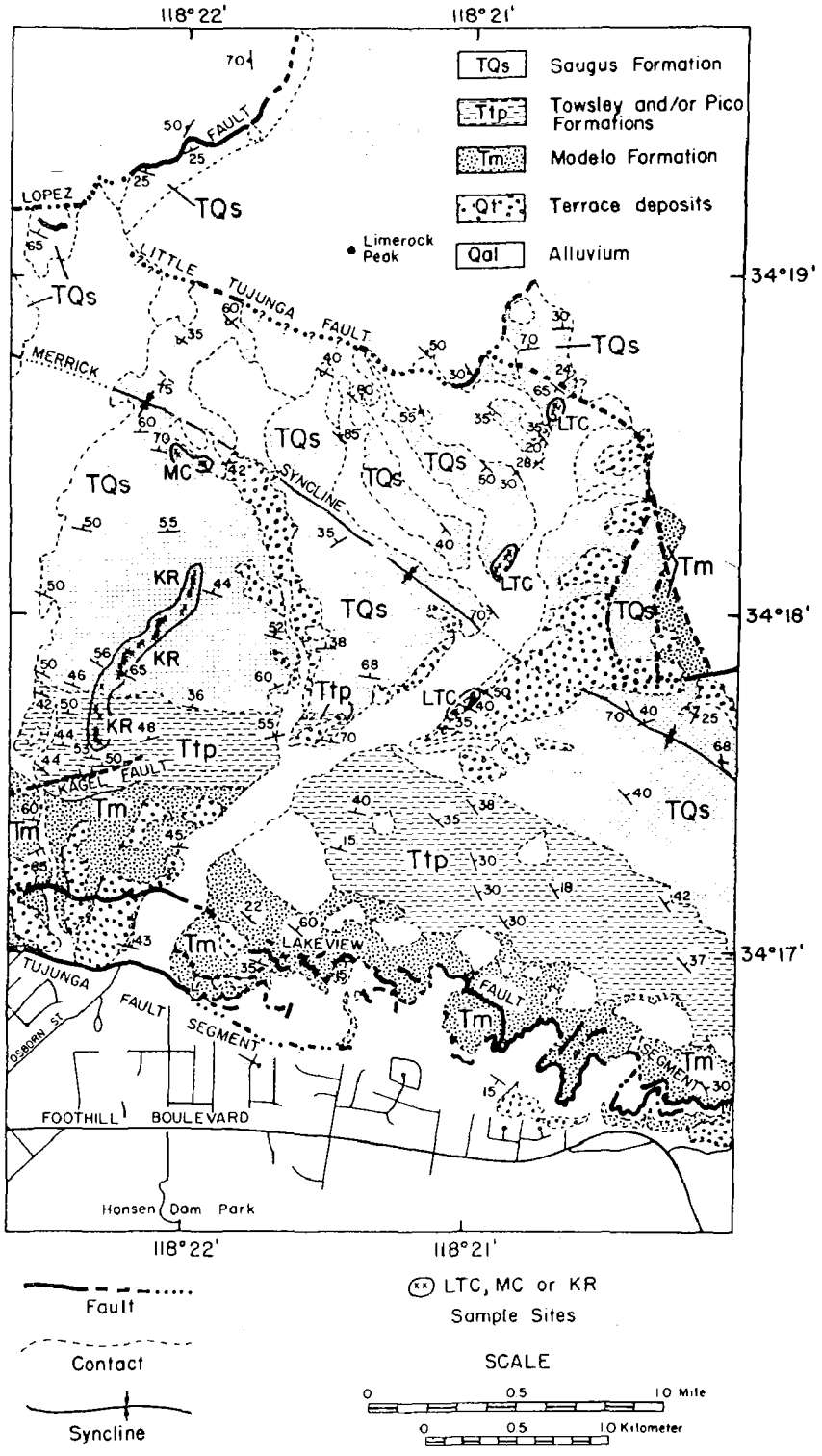

Figure 2. Geologic map of the Little Tujunga Canyon, Marek Canyon, and Kagel Ridge areas. Redrawn and simplified from the "Geologic Map of the San Fernando Earthquake Area," 1:18,000, Barrows et al. (1974). See Figure 1 for location.

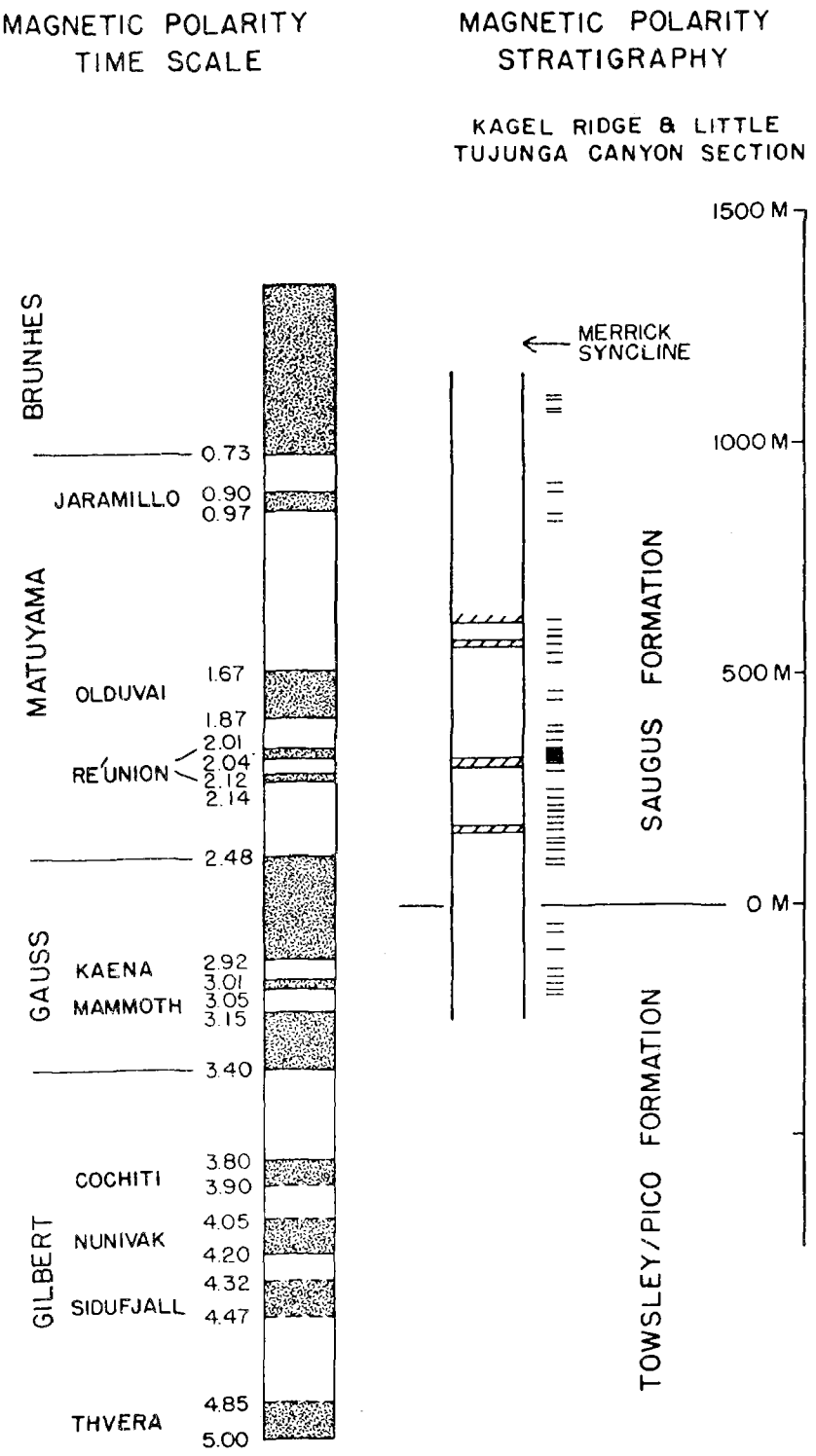

Figure 3. Magnetic stratigraphy of the combined Kagel Ridge, Marek Canyon, and Little Tujunga Canyon sections and the magnetic polarity time scale of Mankinen and Dabrymple (1979). Hatchured (white/unmarked) zones represent normal (reversed) polarity. Dashes along the right side of the stratigraphic column indicate paleomagnetic sampling sites. (The dark zone near 300 m adjacent to the second normal zone from the bottom near 300 m represents unresolved sites due to photo reduction.)

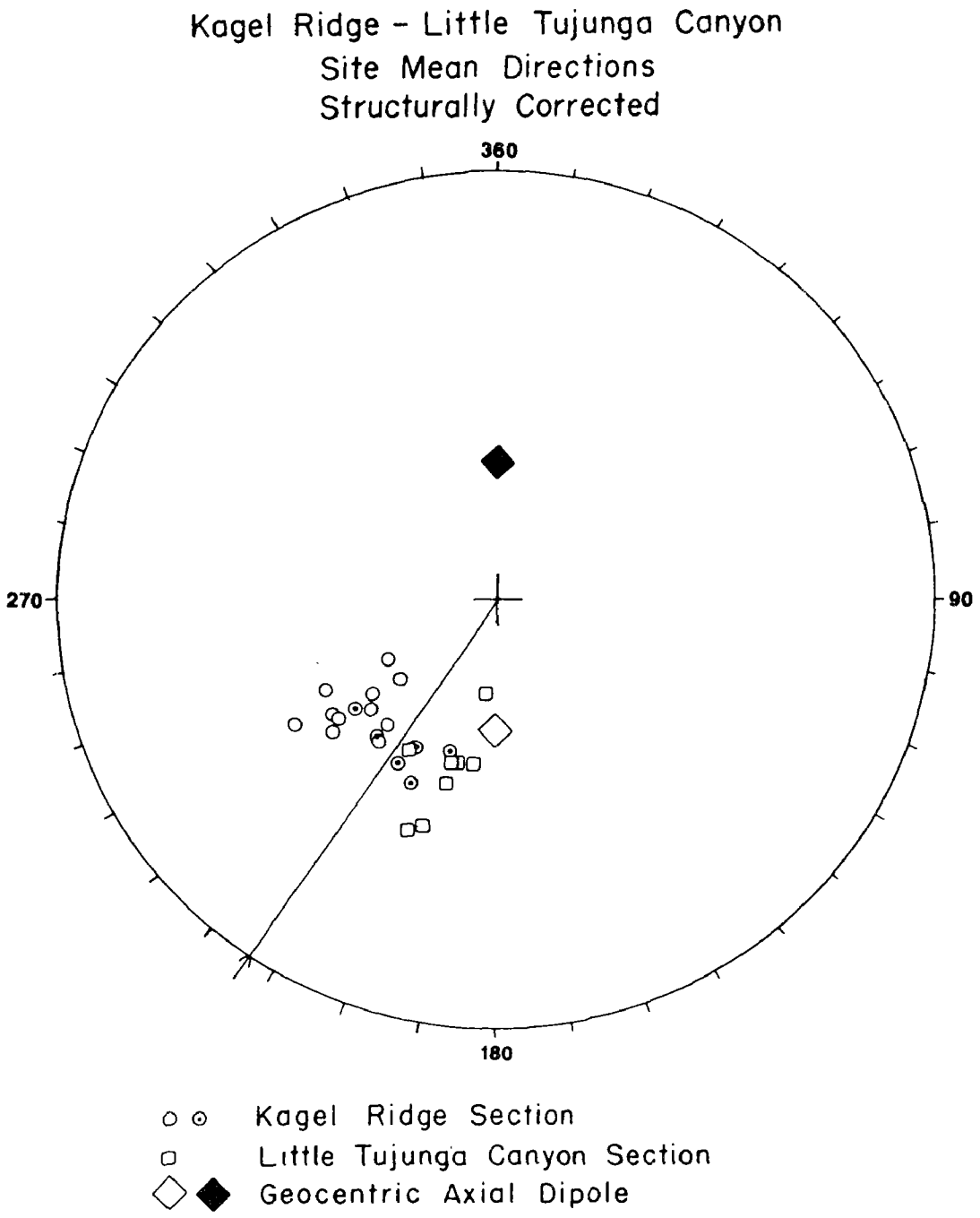

Figure 4. Paleomagnetic directions of Saugus sites in the Little Tujunga Canyon, Marek Canyon, and Kagel Ridge area. Filled (open) symbols represent lower (upper) hemisphere vectors. Open symbols with contral dots indicate normal Matuyama sites inverted through the origin. The arrow along the circumference shows the average declination for the ensemble.

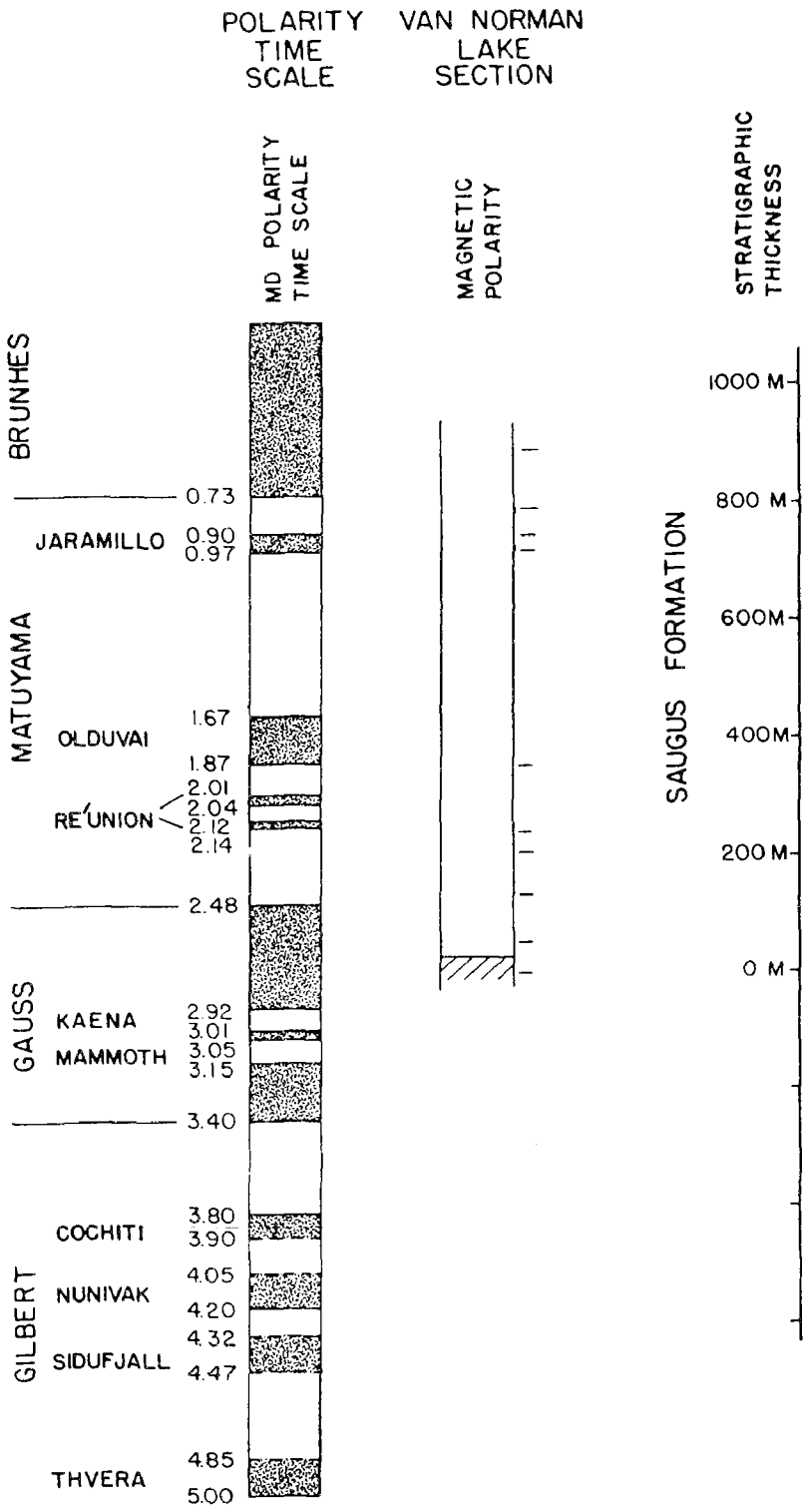

Figure 6. Magnetic stratigraphy along the lower Van Norman Lake and the magnetic polarity time scale of Mankinen and Dalrymple (1979). Hatchured (white/unmarked) zones represent normal (reversed) polarity. Dashes along the right side of the stratigraphic column indicate paleomagnetic sampling sites.

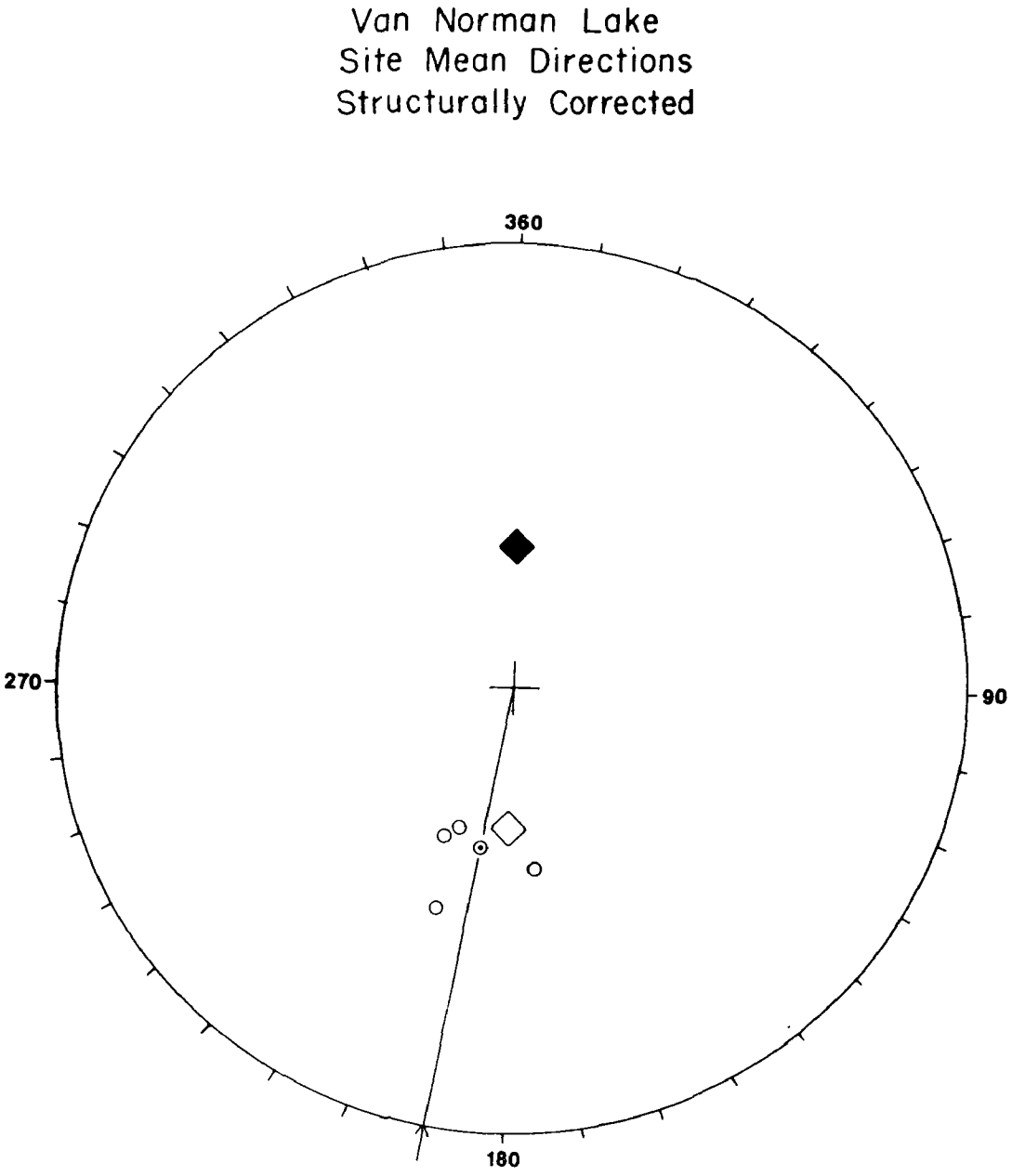

Figure 7. Paleomagnetic directions of Saugus sites along the Lower Van Norman Lake. Filled (open) symbols represent lower (upper) hemisphere vectors. Open circle with central dot represents a normal site which was inverted through the origin. The arrow along the circumference shows the average declination for the sites.

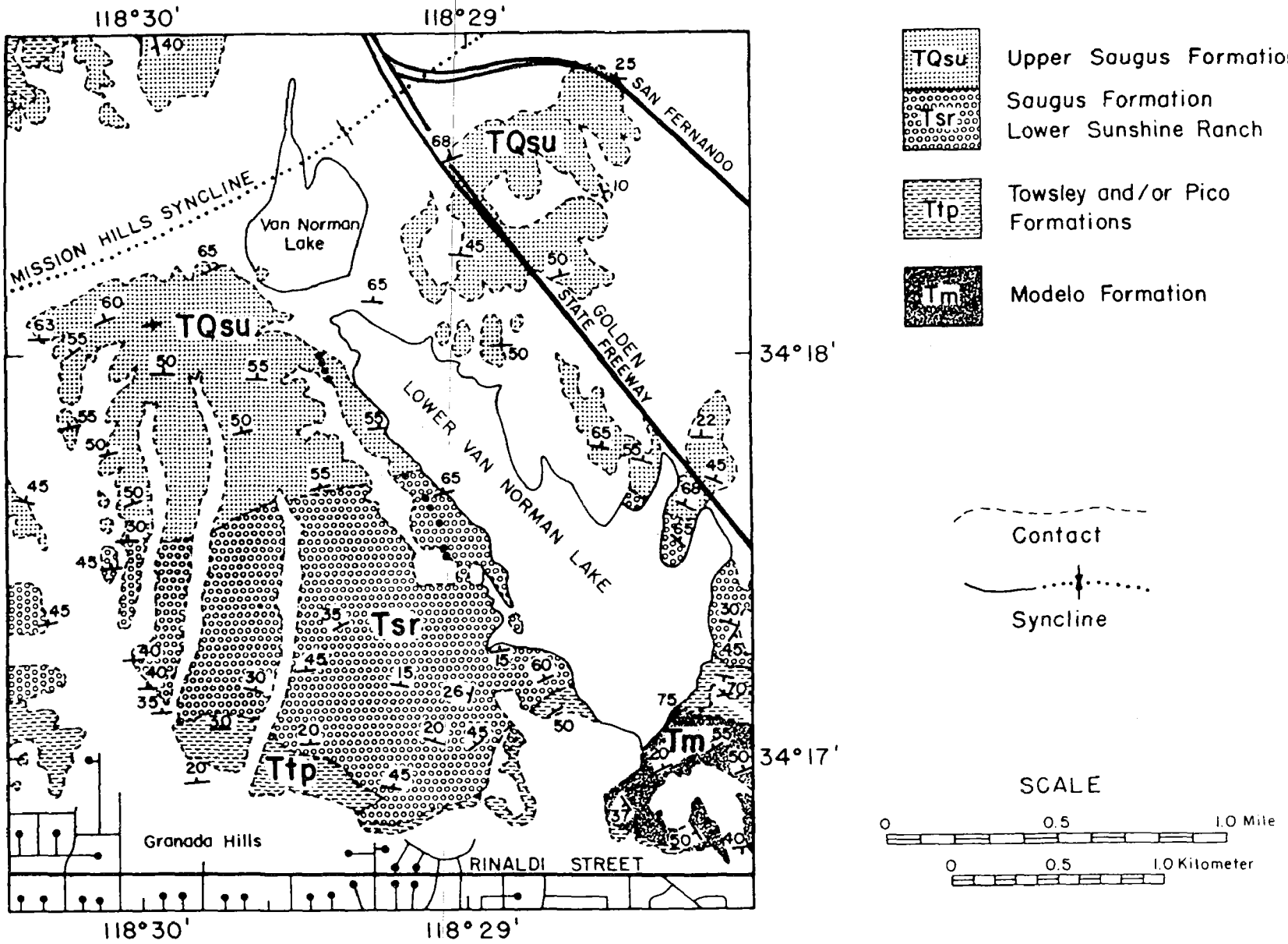

Figure 5. Geologic map of the Van Norman reservoir area, redrawn and simplified from the "Geologic Map of the San Fernand Earthquake Area," 1:18,000, Barrows et al. (1974). See Figure 1 for location.

ANALYSIS OF RECURRENT HOLOCENE FAULTING NORTHERN ELSINORE FAULT

Contract #'s 14-08-0001-G1164 (current)
and 14-08-0001-23176

T.K. Rockwell
R.S. McElwain
Department of Geology
San Diego State University
San Diego, CA 92182
and
D.L. Lamar
Lamar-Merifield Geologists, Inc.
1318 Second Street
Santa Monica, CA 90401

Objectives

The objectives of this investigation are to further constrain the timing of slip events, the displacement per event, and a slip rate on the Glen Ivy North strand of the Elsinore fault zone in Temescal Valley through a detailed study of the faulted late Holocene stratigraphy at Glen Ivy Marsh. The results to date presented here were funded, in part, under contract number 14-08-0001-23176 and continue under contract number 14-08-0001-G1164.

Results

We now have fifteen radiocarbon dates on peat interstratified within silty, sandy, and gravelly units at Glen Ivy Marsh (Table 1). Twelve of the peats are from a three meter thick section which contains over 30 individual peat layers, and it is this section which has been studied the most. Work to date has focused on lateral excavations into the fault zone, revealing a very complex pattern of dominantly transtensive right-stepping faulting. Approximately five meters of the fault have been excavated at 10-30 cm thick intervals to further constrain the timing of prehistoric earthquakes at this site in terms of both ground rupture and seismically produced liquefaction. These data are summarized in Table 2. Further work this year will hopefully constrain the lateral component of faulting by study of the offset margins of several gravel channels.

14C DATES ON PEAT LAYERS AT GLEN IVY MARSH

Peat Layer	Lab #	Radiocarbon Age (Y.B.P.*)	Dendro-corrected A.D. Age
2	A-4029	220 ± 80	1660 A.D. or younger
3?*	A-4400	490 ± 90	1430 +20 -90 A.D.
4	A-4374	590 ± 90	1355 ± 65 A.D.
7	A-4401	380 ± 150	1475 +185 -65 A.D.
8	A-4034	730 ± 100	1275 +100 -65 A.D.
8	A-4375	820 ± 90	1240 +40 -200 A.D.
10	A-4370	630 ± 100	1350 ± 70 A.D.
11	A-4369	780 ± 120	1210 ± 160 A.D.
11-12	A-4033	760 ± 50	1250 ± 40 A.D.
15	A-4376	1020 ± 80	1020 +130 -120 A.D.
20	A-4377	910 ± 60	1125 ± 95 A.D.
22	A-4378	1010 ± 70	1060 ± 80 A.D.
A	A-4372	5130 ± 110	~ 3200 B.C.
B	A-4373	9040 ± 160	~ 7100 B.C.
C	A-4371	10,190 ± 350	~ 8250 B.C.

* There is some confusion as to whether or not this is, in fact, peat 3

Summary of late Holocene Earthquake History at Glen Ivy Marsh

Event	Timing	Size	Comments
Z	Historical; post 1660 A.D.	30-50 cm vertical separation, horizontal separation unknown	Produced extensive liquefaction and ground rupture. Involved glass and pottery in the liquefaction event. This event faults the surface soil which developed after deposition of peat 2, dated at 220 + 80 yrbp (post-1660 A.D.).
X	Between 1360 and 1660 A.D.	2-3 cm vertical separation; horizontal separation unknown	Disrupts peat 3 and not peat 2 in several exposures but appears to cut down-section in the final three cuts, apparently due to stepping of displacement to another stand. Does not significantly offset the sand channel overlying peat 8. Peat 4, which is involved, is dated at 1355±65 A.D. Significant liquefaction in adjacent lateral exposures supports the timing.
V	About 1300 A.D.	Large event: 0 to 20 cm of vertical separation and at least 90 cm of horizontal separation	Produced significant liquefaction. Offsets a gravel channel which overlies peat 8 but does not disrupt a sand channel which immediately overlies the gravel channel. Peat 8 is dated at 1275 +100/-65 A.D. but represents an accumulation of leaves and twigs over a period of years. Thus, the top of the peat and overlying gravel channel slightly postdate the corrected age of the peat, and a tentative event age of about 1300 A.D. is assigned.
T	1260-1275 A.D.	3-5 cm vertical separation, horizontal separation unknown	Faults peat 11 along two strands but does not offset peat 10. Abrupt truncation is not demonstrated at peat 10 because it lies within a 30-50 cm thick fine sand unit and the minor amount of slip may have been absorbed by grain rotation. Liquefaction between peats 11 and 10 indicate an event at this time and is consistent with the non-disturbance of peat 10.
R	About 1060 A.D.	Large event: 10-30 cm vertical separation, horizontal separation unknown	Faults peat 22 but not unit H or peat 20. Peat 22 is dated at 1060 ± 80 A.D. Unit H is draped over the scarp produced by this event. Significant lateral displacement is indicated by a complete mismatch of units below peat 22.

Other events disrupt unit I (buried A horizon) as well as lower parts of the section but have not been resolved at this time.

Very Precise Dating of Earthquakes at Pallett Creek, and Their Interpretation

14-08-0001-G1086

Kerry Sieh
Division of Geological and Planetary Sciences
Caltech, Pasadena, CA 91125
(818) 356-6115

Objective: Recent improvements in radiocarbon dating afford the opportunity to date more precisely the 12 paleoearthquakes recorded along the San Andreas fault at Pallett Creek, California. With Minze Stuiver at the University of Washington and David Brillinger at the University of California at Berkeley, I am attempting to date more precisely the stratigraphic section that contains 12 large earthquakes at Pallett Creek. Two-sigma uncertainties in dates of individual earthquakes are on the order of 100 years at the present time. We hope to reduce the 2σ uncertainties for most of the earthquake dates to 30 years or less. This may enable us to discern patterns of earthquake recurrence and to determine more precisely what variability exists in actual recurrence intervals and the probability of a great earthquake in the next couple decades.

Data Acquisition and Analysis: Minze Stuiver has completed analysis of the first suite of samples. David Brillinger has not yet begun statistical analysis of these data, but my preliminary assessment of the data indicates that we will indeed be able to narrow the dating imprecision of several of the prehistoric earthquakes. For example, event "I" appears to be constrained to 980 ± 10 A.D. The average value for the six intervals between this event and the 1857 earthquake is now constrianed to be 145 ± 2 years. Complete results of this work will be available in late 1987.

Oak Ridge Fault, Ventura Basin, California: Slip Rates and Late Quaternary History

14-08-0001-G1194

Robert S. Yeats
Department of Geology
Oregon State University
Corvallis, Oregon 97331-5506
(503) 754-2484

David A. Gardner
Staal, Gardner & Dunne, Inc.
121 N. Fir Street, Suite F
Ventura, California 93001
(805) 653-5556

Investigations

In February we trenched sites at the Bardsdale Cemetery and the Saticoy Country Club. In addition, we logged a cut in the western Montalvo mound and are now summarizing all information from excavations on this mound in the last decade. Finally, Shell Western E & P Inc. has kindly allowed us to examine 100 km of multichannel seismic data acquired in the 1960's on the nearshore extension of the Oak Ridge fault.

Results (John Powell, Dave Gardner, Bob Yeats, Russ Van Dissen, Tom Rockwell)

1. The Bardsdale Cemetery trench is located on Figure 1. To the south, Oak Ridge is underlain by Tertiary strata with Oligocene Sespe Formation exposed along the axis of the Oak Ridge anticline fairly close to the base of the ridge. The crest of Oak Ridge is underlain by Miocene beds on the south limb of this anticline. Sespe Formation in the covered north limb of the anticline is penetrated by wells drilled in the Santa Clara River floodplain (Figure 2) southwest and northeast of Bardsdale Cemetery (large dots, Figure 1). The surface projection of the Oak Ridge fault (dotted line, Figure 1) is north of the area, probably north of Bardsdale Avenue (Rieser, 1976).

The Santa Clara River is now north of the area, but the scalloped base of Oak Ridge shows evidence that the river formerly flowed along the southern margin of its floodplain. After the river abandoned its channel at the foot of Oak Ridge, alluvial fans were built out from side canyons. Water wells show that the Sespe Formation is overlain by 40-50 m of unconsolidated deposits, including river gravels and alluvial

fan material (Figure 2). The alluvial fan is cut by a fault, north side down, first reported by Yeats and others (1982). Because Sespe Formation of the hanging-wall side of the Oak Ridge fault occurs in the subsurface on both sides of the Bardsdale Cemetery fault, this fault is clearly a subsidiary fault, not the main strand of the Oak Ridge fault.

The trench (Figure 3) revealed alluvial-fan deposits derived from Modelo, Vaqueros, and Sespe strata similar to exposures on the north flank of Oak Ridge. These fan deposits are easy to distinguish from Santa Clara River gravels which are far-derived and include well-rounded clasts of crystalline rocks. The fan deposits include silty sand with gravel, and sand and gravel channel deposits with variable amounts of cobbles and isolated boulders. Soils associated with the fan deposits appear to be Holocene (T.K. Rockwell, oral commun., 1986). Carbon samples from faulted fan deposits will be dated by ^{14}C.

The fan deposits are cut by a normal fault. Distinctive units recognized on both sides of the fault indicate a vertical separation of 1.5 m. Separations are the same for all units, indicating that all offsets recognized in the trench post-date Unit I. However, the total relief on the scarp is 9 m, and no evidence of faulting was observed in the trench north and south of the trench log shown in Figure 2. Possibly much of the relief on the scarp is produced by broad warping.

This appears to be the first evidence of Holocene displacement on a strand of the Oak Ridge fault, but we cannot exclude the possibility of very low-angle slump until we have determined the offset of the base of the river gravels below the level of the trench (Figure 2).

2. The Saticoy Country Club trench was on a lineation mapped by Sarna-Wojcicki and others (1976) as a possible extension of the Ventura fault. We considered the lineations to be possibly related to the Oak Ridge fault. No evidence of faulting was observed in the trench.

References:

Rieser, R. B., 1976, Structural study of the Oak Ridge fault between South Mountain and Wiley Canyon, Ventura County, California: Athens, Ohio Univ. MS Thesis, 93 p.

Sarna-Wojcicki, A. M., Williams, K. M., and Yerkes, R. F., 1976, Geology of the Ventura fault, Ventura County, California: U.S. Geol. Survey Misc. Field Studies Map MF-781.

Yeats, R. S., Keller, E. A., Rockwell, T. K., Lajoie, K. R., Sarna-Wojcicki, A. M., and Yerkes, R. F., 1982, Field trip number 3: Neotectonics of the Ventura basin--road log, in Cooper, J. D., compiler, Neotectonics in southern California: Guidebook prepared for the 78th Ann. Mtg. of the Cordilleran Section of the Geological Society of America, Anaheim, CA, p. 61-76.

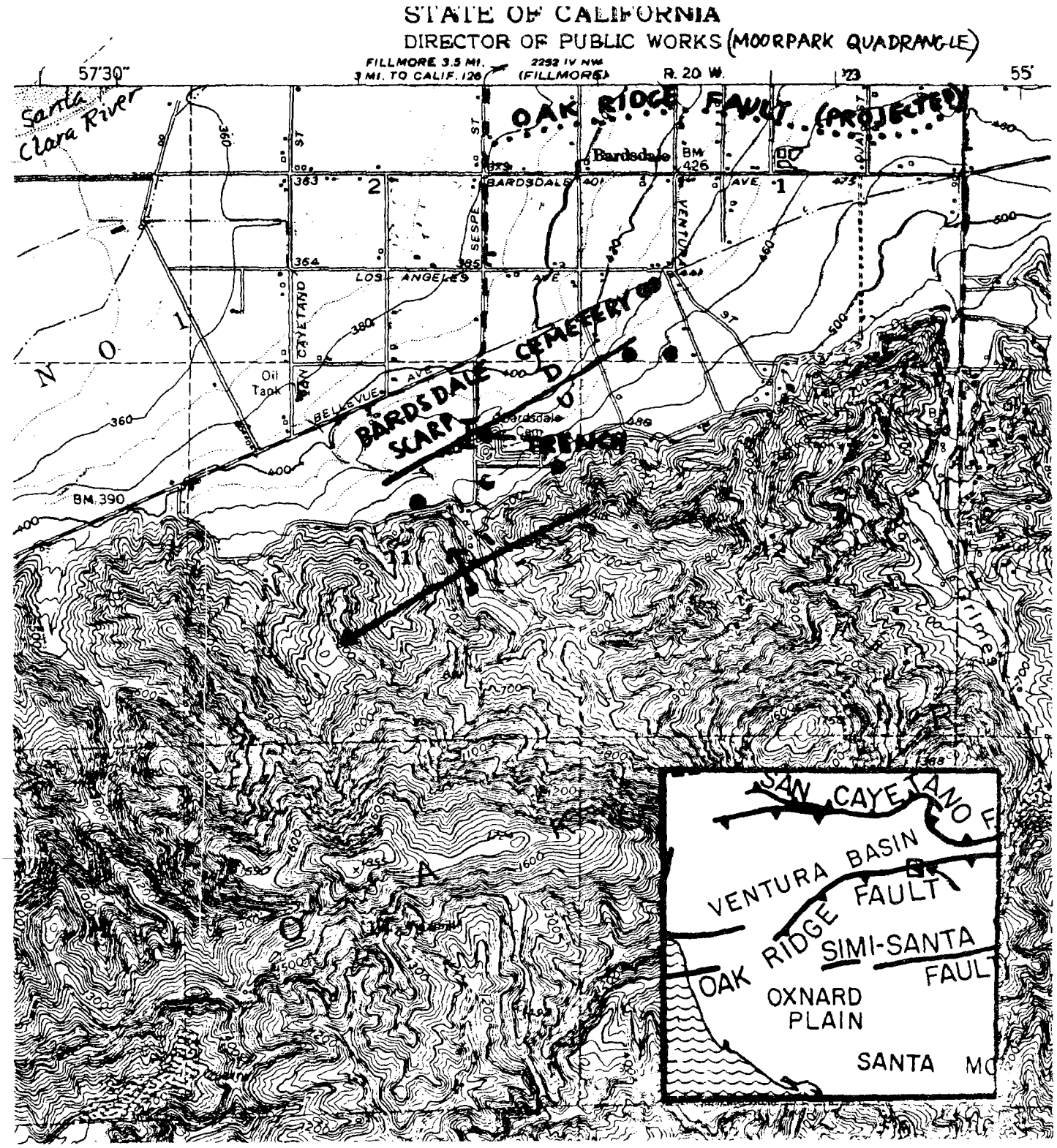

Figure 1. Location of Bardsdale Cemetery trench on Moorpark 7½-minute quadrangle, 1:24,000. Large dots locate oil wells near trench site. Oak Ridge anticline and surface projection of Oak Ridge fault shown.

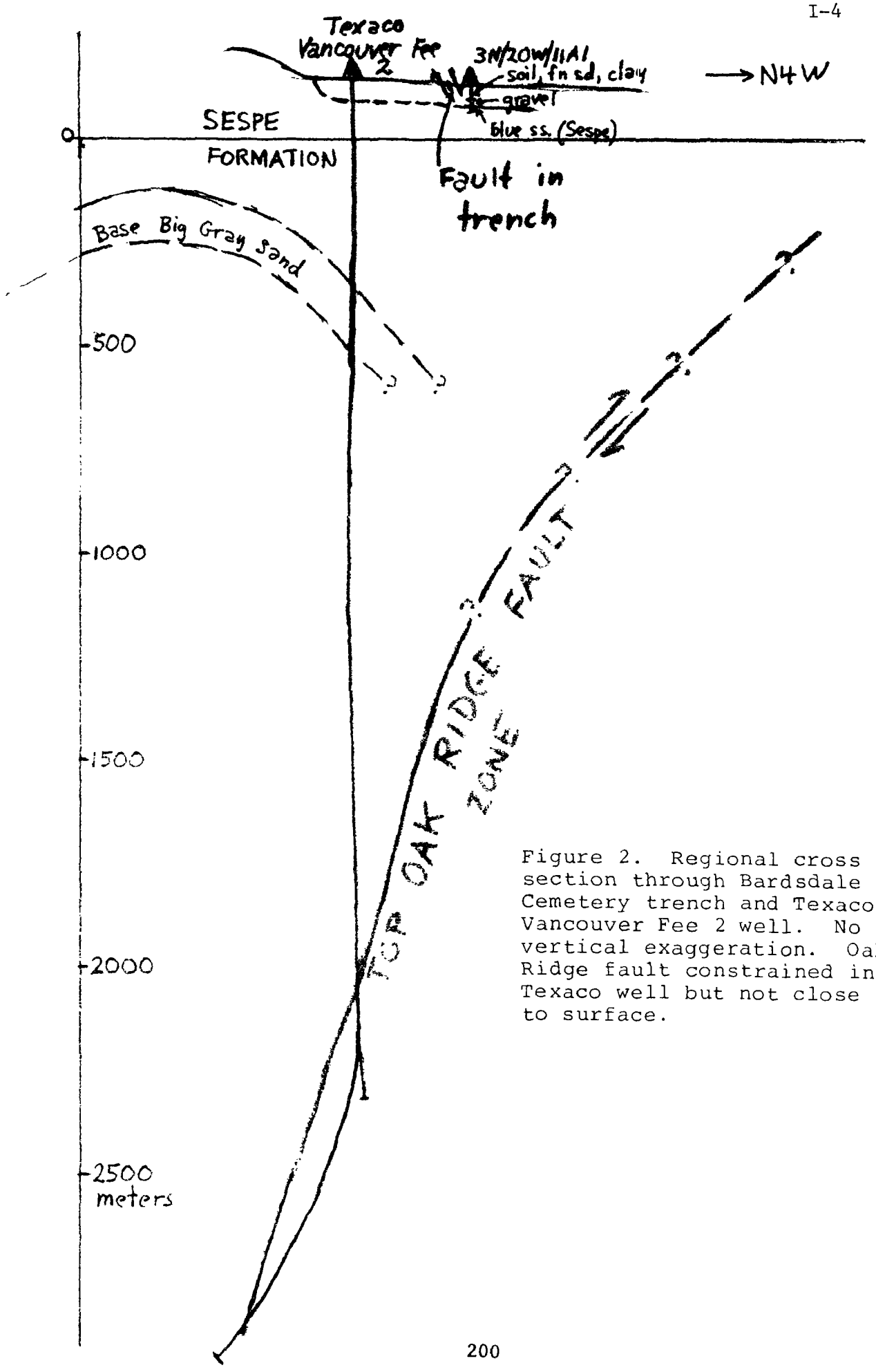

Figure 2. Regional cross section through Bardsdale Cemetery trench and Texaco Vancouver Fee 2 well. No vertical exaggeration. Oak Ridge fault constrained in Texaco well but not close to surface.

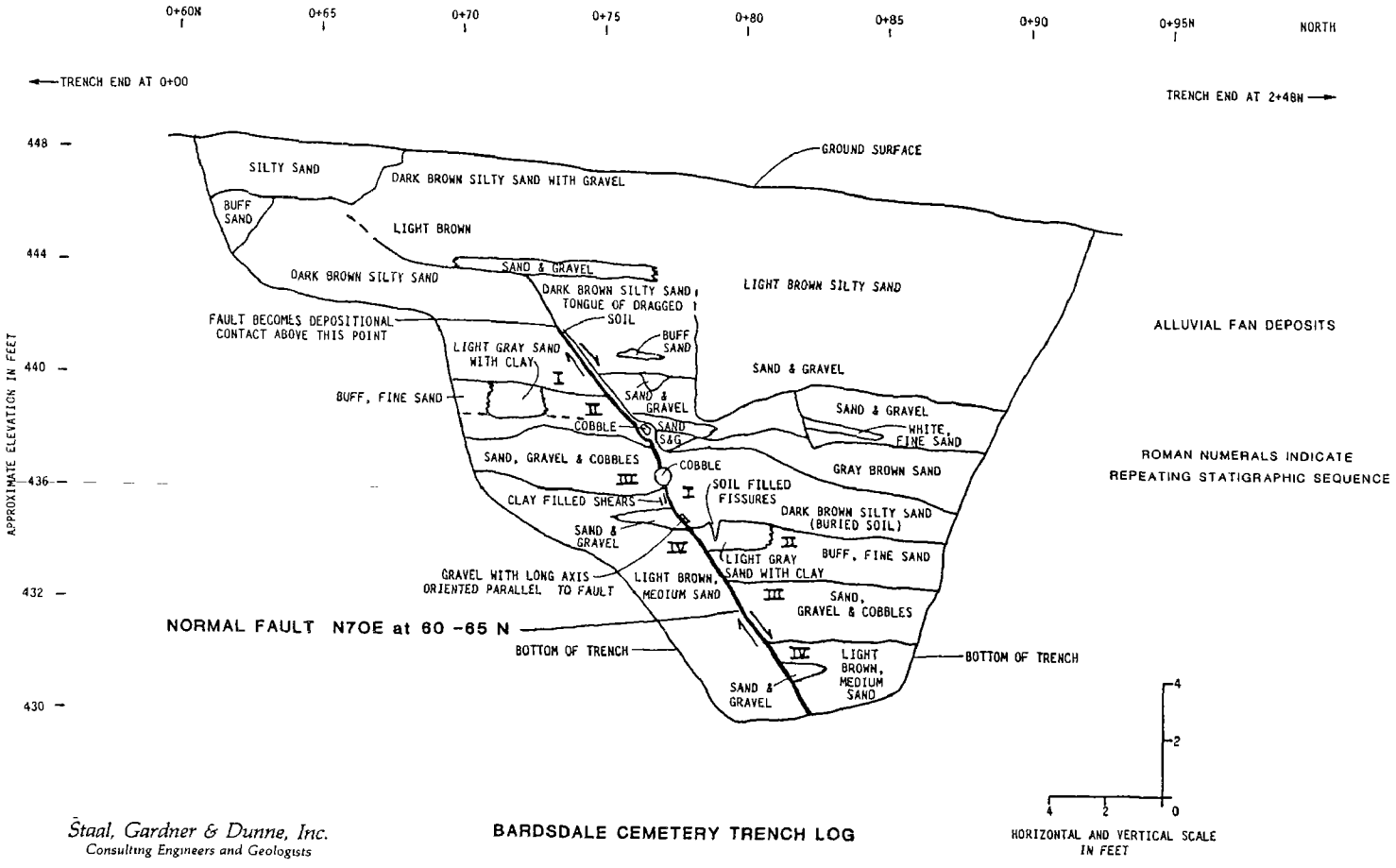

Figure 3. Part of log of Bardsdale Cemetery trench, drawn by John Powell and Dave Gardner.

Analysis of USGS Local Seismic Network Data For Earthquake Prediction

14-08-0001-A-0036
Keiiti Aki
Center for Earth Sciences
Dept. of Geological Sciences
University of Southern California
University Park
Los Angeles, California 90089-0741
(213) 743-3510

Objective: Recently, temporal changes in coda Q^{-1}, have been reported before major earthquakes. They are (1): 1975 Hawaii earthquake (M=7.2), (2): three large earthquakes (M=8.0) in the Kuril-Kamachtka area, USSR, (3): the Petatlan earthquake of 1979 (M=7.6) in Mexico, (4): 1983 eastern Yamanashi earthquake (M=6.0) in Japan, (5): 1976 Tangshan earthquake (M=7.8) and 1975 Haicheng earthquake (M=7.3) in China, and (6): the Misasa earthquake (M=6.2) of October 1983 in Tottori, Japan. The purpose of this study is to use the USGS local seismic network data in central California (CALNET) to systematically investigate the properties of coda Q precursor.

Data Analysis & Results: For the past six months of work on this project, we have mainly focused on the expansion of digital database in central California and coda Q analysis along the San Andreas fault southward form Parkfield to Kern County. These have included the following:

1. The digitized network data for about 300 earthquakes have been processed by our computer program. They are (1) 130 earthquakes in the Parkfield-Coalinga area, (2) 70 earthquakes in the Kern County-Santa Barbara County area and (3) 70 earthquakes in the Long Valley-Bishop area. Furthermore, another set of 300 earthquakes since 1984 to November 1985 along the San Andreas fault is now being processed at USGS, Menlo Park.

2. We found that the parameter m in the frequency-dependence of coda Q ($Q=Q_o f^m$) is independent of time windows for all areas studied. Furthermore, m varies rather strongly from place to place as follows:

m=0.6	for Coyote Lake
0.8 to 0.9	for Parkfield
0.9 to 1.0	for Coalinga
1.2	for Long Valley

These values show a great contrast to the values obtained by Singh and Hermann (1983), who showed that it ranges from 0.1 in the central U.S. to 0.6 in California. According to Wu and Aki (1986), if the attenuation is due to scattering, the 1-D power spectrum of inhomogeneity of the form

$$W(K)=CK^{-m-1}$$

where K is the wave number, can account for the power law frequency dependence of Q. In other words, the area with greater m may be characterized by heterogeneity richer in longer wavelength.

3. We found that the regions near the San Andreas fault show significantly lower Q than the regions away from the fault by 20 to 30% at the level of 95% statistical confidence. A similar significant difference between Coalinga and Parkfield with about 15% lower Q for the latter for frequency above 3Hz can also be observed. The quality factor of the Coalinga crust is higher than

that of Parkfield in spite of the recent earthquake.

4. In general, the regional variation of coda Q become smoother for later time windows. For example, the value of Q_o shows very little variation from region to region for the time window 50 to 100 seconds. This is consistent with the backscattering model in which the latter part of coda samples scatterers in a greater volume.

5. We studied the coda Q^{-1} variation with events which occurred before and after the Round Valley earthquake (M=5.7) of November 1984 in the Mammoth Lakes-Bishop area. The results are remarkable. First, we found that lower Q for shocks after the mainshock than those occurred before the mainshock in regions near the mainshock epicenter as shown in Figure 1. Secondly, we found the opposite, namely higher Q after the mainshock than before for regions farther away from the mainshock epicenter as shown in Figure 2. Thirdly, we found that the lower Q in Long Valley Caldera than outside area observed before the mainshock disappeared after the occurrence of mainshock, and indicating that the temporal variation in coda Q is comparable to its spatial variation. The doughnut model which was invoked for explaining precursory seismicity pattern appears to explain the observed coda Q^{-1} variation associated with the Round Valley earthquake. It also helps to reconcile conflicting results reported in published case studies of the coda Q^{-1} precursor.

6. In addition to the above results from California, we are finding an extremely important result from the coda Q measurement in China through a cooperative work with Dr. Anshu Jin of Institute of Geophysics, State Seismological Bureau. A preliminary results suggests a strong correlation between historical seismicity and coda Q. It appears that the Q_o value of 300-400 may be the critical one. The regions with higher Q than this critical value show no major earthquakes in historical time and those with lower Q show major earthquakes. If this preliminary results is universally valid, we shall have an empirical basis for evaluating the long-term seismicity in the region with no historical records such as the eastern and central U.S.

Reference

Singh, S.K., and R.B. Herrmann, Regionalization of crustal coda Q in the continental United States, J. Geophys. Res., 88, 527-538, 1983.

Wu, R.S., and K. Aki, The fractal nature of the inhomogeneities in the lithosphere evidenced from seismic wave scattering, submitted to PAGEOPH, 1986.

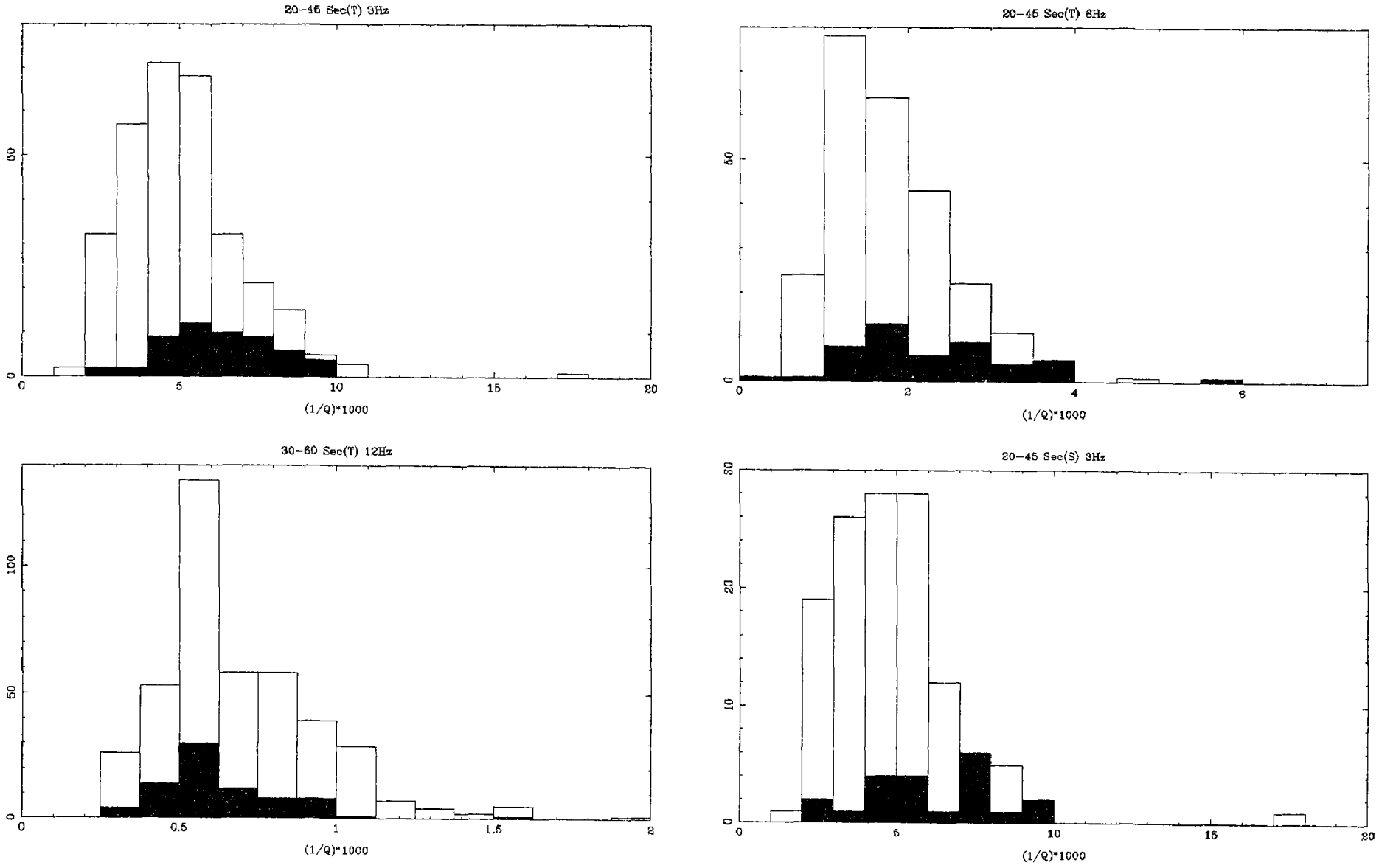

Fig. 1 Histograms of coda Q^{-1} for different frequency bands with statistically significant difference between foreshocks and aftershocks for the regions near the mainshock epicenter of the Round Valley earthquake, 1984. The shaded area is for the aftershocks while the unshaded part is for the foreshocks. The vertical axis shows the number of measurements and the horizontal axis shows the value of Q^{-1}x1000.

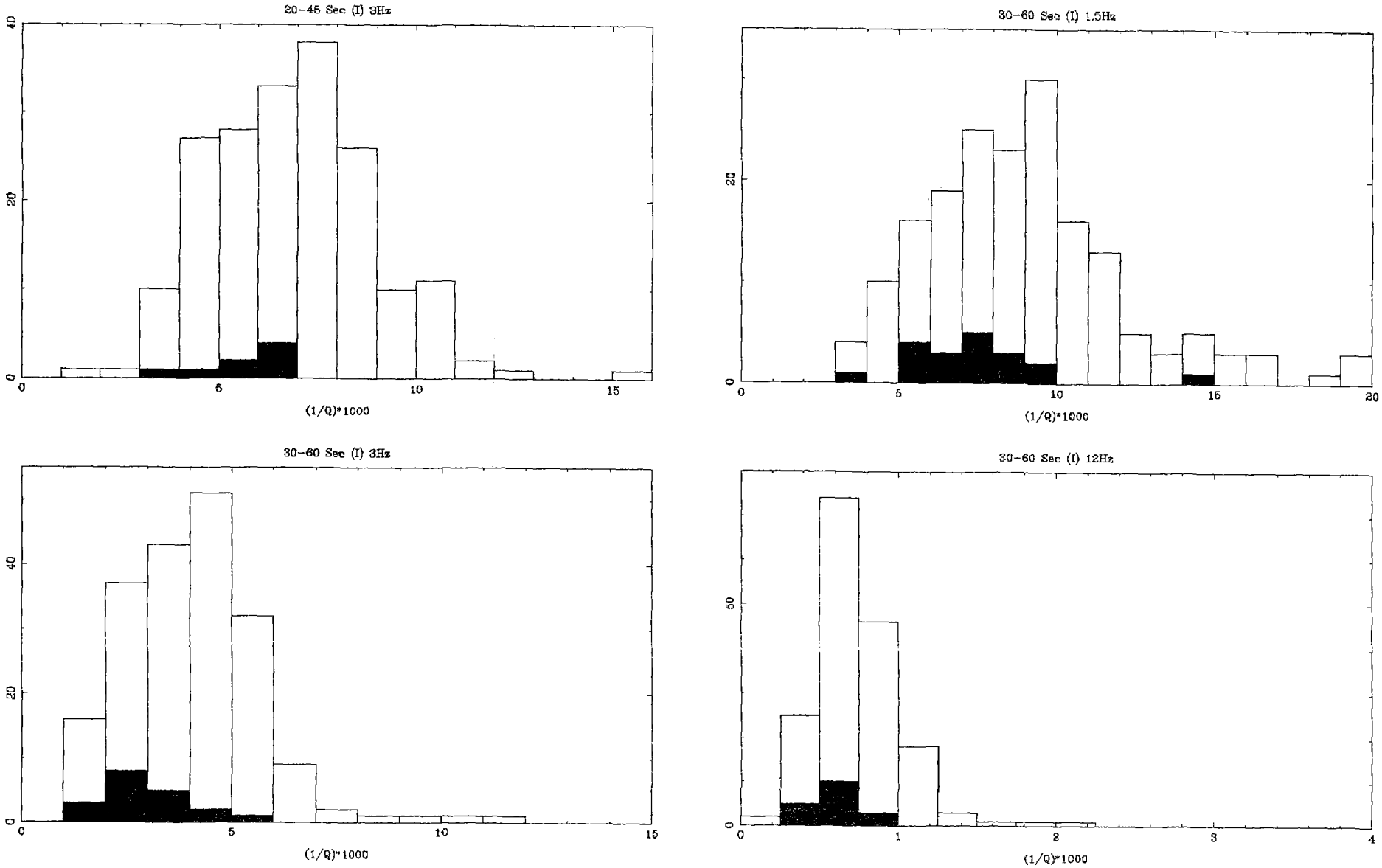

Fig. 2 Histograms of coda Q^{-1} same as Fig. 1 except for the region farther away the mainshock epicenter. Here, region I covers most part of the Long Valley Caldera.

On-Line Seismic Processing

9930-02940

Rex Allen
Branch of Seismology
U.S. Geological Survey
345 Middlefield Road, MS 77
Menlo Park, California 94025
(415) 323-8111 ext 2240

Investigations and Results

This period has been occupied principally in an effort to adapt the Motorola version of the online Real-Time Processor (RTP Mk II) to use as an offline system for the analysis of analog tapes produced by the fiveday recorders used in aftershock studies. These tapes carry 6 seismic channels (3 components at high and low gain), and two timing channels. The requirements of this system are for digitizing and saving the digital samples of all 8 channels at 100 samples per second, but processing only the high-gain vertical for event detection. The tapes are played back at a time compression of 20, requiring the system to deal with 16000 samples per second realtime, and pushing some of the system components well past their design limits. In particular, the Motorola A/D converters were found to be too slow and required extensive modification of their control firmware to get up to the required speed. Critical sections of the FORTRAN picker algorithm were also hand optimized for efficiency and the system now meets speed requirements. Remaining requirements are for writing the resulting traces data out to a magnetic tape suitable for further processing on the offline CUSP system at Menlo Park. The tape deck is now in house and I hope to have the complete system ready for use real soon now.

We are in the process of purchasing new hardware on which to run the online RTP and expect it to be available in about six weeks or so. It will run a 68020 cpu and will allow for expansion to the full capability needed for online surveillance of a large net through through the addition of more 68020's as needed.

Ellis has spent some time adapting the high speed Tektronix graphics interface to work with the I.B.M. PC family of computers. The hardware changes on the Tektronix end have been done, and the computer end has been made to work but thus far at a speed that is too slow to be fully useful.

Ellis is also involved with a multiproject effort to determine the best approach to a new series digital field instruments using , as much as possible, off-the-shelf commercial circuit cards. The C-44 bus was chosen for the project and enough hardware has been purchased to allow a start on development. The first efforts will be development of a digital telemetry instrument and a digital equivalent of the cassette recorders. These two devices are the simplest of those in the "wish book" of new field instruments and probably the most badly needed. Most later instruments will be largely an expansion of the capabilities of these two, so a large portion of the development effort on these first two will be directly applicable to more complicated devices.

Remote Monitoring of Source Parameters for Seismic Precursors

9920-02383

George L. Choy
Branch of Global Seismology and Geomagnetism
U.S. Geological Survey
Denver Federal Center
Box 25046, Mail Stop 967
Denver, Colorado 80225
(303) 236-1506

Investigations

1. Teleseismic estimates of radiated energy. We have developed a method of computing radiated energy from direct measurements of teleseismically recorded broadband body waves.

2. Broadband analysis of large earthquakes. We are using digitally recorded broadband data to detail the rupture process of large, complex earthquakes. We are also deriving source parameters of foreshocks and aftershocks that accompany such large events.

3. Acceleration spectra for subduction zone earthquakes. We are developing an algorithm for obtaining P-wave acceleration spectra for large, shallow-focus, subduction-zone earthquakes.

4. Improvement of NEIC reporting services. Important features of the source-time function are often clearly seen with broadband waveforms. For earthquakes with simple source-time functions, the identification of the direct and surface-reflected phases is straightforward. We are evaluating the feasibility of routinely extracting source parameters from broadband data and incorporating these parameters into the flow of NEIC reporting services.

Results

1. We have applied our algorithm for the computation of radiated energy to two recent earthquakes, the Coalinga earthquake of May 1983, and the Borah Peak earthquake of October 1983. Our results indicate that indirect estimates of energy (for example, those depending on simplistic relations with seismic moment) may overestimate energy if the rupture process involves sizeable component of aseismic slip. We are in the process of implementing a computer package which will enable us to compute radiated energy routinely for all earthquakes with $m_b \geq 6.0$.

2. We are examining the Valparaiso earthquake of March 1985 and the aftershocks that it generated. Using broadband data, we have derived for each of these events a depth, focal mechanism, moment, energy, static stress drop, appparent stress and rupture geometry. The stress drop of the main shock was between 13-60 bars, depending on the assumed rupture geometry.

The aftershocks had stress drops ranging from 2 to 30 bars. The seismic rupture area of the mainshock covered only about one-third of the area defined by the aftershock series.

3. We have compiled the log-averaged P-wave acceleration amplitude spectra of a set of large, shallow-focus, subduction-zone earthquakes ranging in size from M_S 6.2 to M_S 8.1. The spectra of different earthquakes exhibit significant variations in spectral shape. The spectral level of the high frequency acceleration appears more strongly proportional to the asperity areas than the seismic moments of the earthquakes.

4. We have completed a qualitative evaluation of the usefulness of broadband data for quick determination of depth and source characteristics by examining the broadband data set that was compiled for 51 events chosen for special study by the Commission on Practice at the 1985 IASPEI General Assembly in Tokyo. We have already started to introduce the use of broadband data into the flow of NEIC operations. Some estimates of depth are being constrained by depth phases that are now being routinely read from broadband waveforms. In the Monthly PDE Listing, broadband waveforms are now being routinely plotted along with conventional long-period seismograms. We are working on a computer package that will permit the routine computation of radiated energy in a semi-automated on-line mode using as input digitally recorded data from the GDSN.

Reports

Boatwright, J., and Choy, G. L., 1986, Teleseismic estimates of energy radiated by shallow earthquakes: Journal of Geophysical Research, v. 91, p. 2095-2112.

Boatwright, J., and Choy, G. L., 1986, Acceleration spectra for subduction zone earthquakes [abs.]: EOS (American Geophysical Union, Transactions) (in press).

Choy, G. L., 1985, Source characteristics of the Chilean earthquake of March 3, 1985, and its aftershocks from broadband seismograms [abs.]: EOS (American Geophysical Union, Transactions), v. 66, p. 951.

Dewey, J. W., Choy, G. L., and Nishenko, S. P., 1985, Asperities and paired thrust zones in the focal region of the Chilean earthquake of March 3, 1985 [abs.]: EOS (American Geophysical Union, Transactions), v. 66, p. 950.

Engdahl, E. R., and Choy, G. L., 1986, Global analyses of earthquake depth phases and source characteristics using broadband seismogram of body waves [abs.]: EOS (American Geophysical Union, Transactions) (in press).

Nishenko, S., Dewey, J. W., and Choy, G. L., 1985, Spatial variations in aftershock activity during the March 1985, Chilean earthquake sequence and possible tectonic controls [abs.]: EOS (American Geophysical Union, Transactions), v. 66, p. 951.

Seismic Analysis of Large Earthquakes and Special Sequences in Northern California

9930-03972

Robert S. Cockerham, Jerry P. Eaton
and A. M. Pitt
Branch of Seismology
U.S. Geological Survey
345 Middlefield Road, MS-977
Menlo Park, California 94025
(415) 323-8111, Ext. 2963

Investigations

1. Development of regional velocity models and appropriate station corrections to improve hypocenter locations in northern and central California.

2. Acquisition of data necessary to produce California state seismicity maps ($M \geq 1.5$) for 1981-1984.

3. Analysis of 4 August 1985 Kettleman Hills earthquake sequence.

4. Completion of timing and relocation of earthquakes using a much improved velocity model in the Yellowstone National Park-Hebgen Lake Region from 1973 to 1981.

5. Continued monitoring and analysis of the seismicity in the Long Valley area.

Results

1. Regional 1-dimensional velocity models and appropriate station travel-time corrections are being collected or calculated for northern and central California. Areas for which specific models have been obtained are 1) Coalinga-Kettleman Hills, 2) Parkfield, 3) Morgan Hill-Coyote Lake, 4) east san Francisco Bay, 5) San Francisco Peninsula-Santa Cruz Mountain area to northern end of creeping section of the San Andreas Fault, 6) Geysers geothermal area, 7) Mt. Shasta - Mt. Lassen area, and 5) Mono Lake - Long Valley caldera - Bishop area.

2. Hypocentral data from USGS northern and southern California seismic networks, U.C. Berkeley and U. Nevada at Reno seismic networks have been collected and production of California State seismicity maps for 1981 through 1984 of $M \geq 1.5$ earthquakes is in progress. Epicentral maps showing seismicity along the northern and central California coast for the period 1969 through 1985 have been made and are scheduled to be printed by the state of California coastal commission.

3. The M5.5 main shock occurred at a depth of about 12 km along the western edge of the Great Valley about 17 km southeast of the epicenter of the M6.7 May 2, 1983 Coalinga earthquake. The aftershock zone extends nearly

20 km southeast from the main shock epicenter, and its long axis coincides with the northeastern edge of Kettleman Hills. The Kettleman Hills aftersock zone abuts the southeastern end of the Coalinga aftershock zone, but it does not overlap it. The number of Kettleman Hills aftershocks was about tenth the number of Coalinga aftershocks, which is in accord with the difference in the main shock magnitudes. The lengths of the aftershock zones, however, are comparable: about 20 km for Kettleman Hills and 30 km for Coalinga. Focal planes determined from a P-wave plot of first motions are: I) strike N 52° W, dip 78° NE; and II) strike N 52° W, dip 12° SW. We believe that plane II is the fault plane. In this interpretation, the main shock occurred on a thrust fault that strikes N 52° W and dips 12° SW. This solution is similar to that for the Coalinga main shock. The inferred fault surface corresponds in depth and orientation to the 6.5 $\pm$ km/sec "basement" beneath the western edge of the Great Valley.

4. The timing of earthquakes in the Yellowstone National Park-Hebgen Lake region from 1973 to 1981 was completed. The data set of approximately 6000 earthquakes was rerun with a new, improved 1-D velocity model and station travel-time corrections. A catalog of the hypocentral data and epicentral maps are in preparation.

5. The level of seismic activity within Long Valley caldera has continued to decline from 2 to 3 quakes per day ($M \geq 1.0$) in 1984 to an average of less than 1 earthquake per day (Fig. 1a) in 1985. However, the seismicity rate within the Sierran block to the south of the caldera (Fig. 1b) has continued at a level of about 4 events per day ($M \geq 1$). The overall epicentral pattern for this area has remained the same (Fig. 2). From an analysis of approximately 2300 focal mechanisms (700 from the Sierran block south of Long Valley caldera and west of the Round Valley aftershock area, 900 from the Round Valley aftershock area, and 700 from within Long Valley caldera) the conclusions are:

   (a) No systematic change of faulting mechanisms with depth (i.e. strike-slip motion for shallow earthquakes and oblique or normal for deeper earthquakes) either within the caldera or the Sierran block south of the caldera.

   (b) West of the Hilton Creek fault, in general, P-axes are near horizontal and strike NW to NNW and T-axes, also horizontal, strike NE to ENE for both Sierran and caldera earthquakes.

   (c) For earthquakes east of the Hilton Creek fault, i.e. the Round Valley aftershock area, P-axes generally strike N/S and T-axes strike E/W.

   (d) The earthquakes occurring around Mammoth Mt. consistently have, with only a few exceptions, normal faulting focal mechanism solutions with E/W-striking T-axes.

   (e) No radial alignment of P-axes around the resurgent dome for caldera earthquakes is observed.

(f) The spatial variation in P- and T-axes of caldera earthquakes is significantly greater than for Sierran block earthquakes even though the overall trend is similar, i.e. NE-striking and NW-striking T- and P-axes, respectively.

(g) Assuming P and T, then to produce normal faulting on the Hilton Creek fault and the other Sierran frontal faults in the area P must be vertical and T horizontal and striking ENE to E. From the focal mechanism data it is clear that one P-axis has rotated to nearly horizontal while the T-axis has remained in approximately one same orientation as that producing normal faulting along one frontal fault.

Reports

Eaton, J. P., The August 4, 1985 Kettleman Hills, California Earthquake and its aftershocks, Earthquake Notes, v. 57, no. 1, (abst.), 21, 1986.

(A)

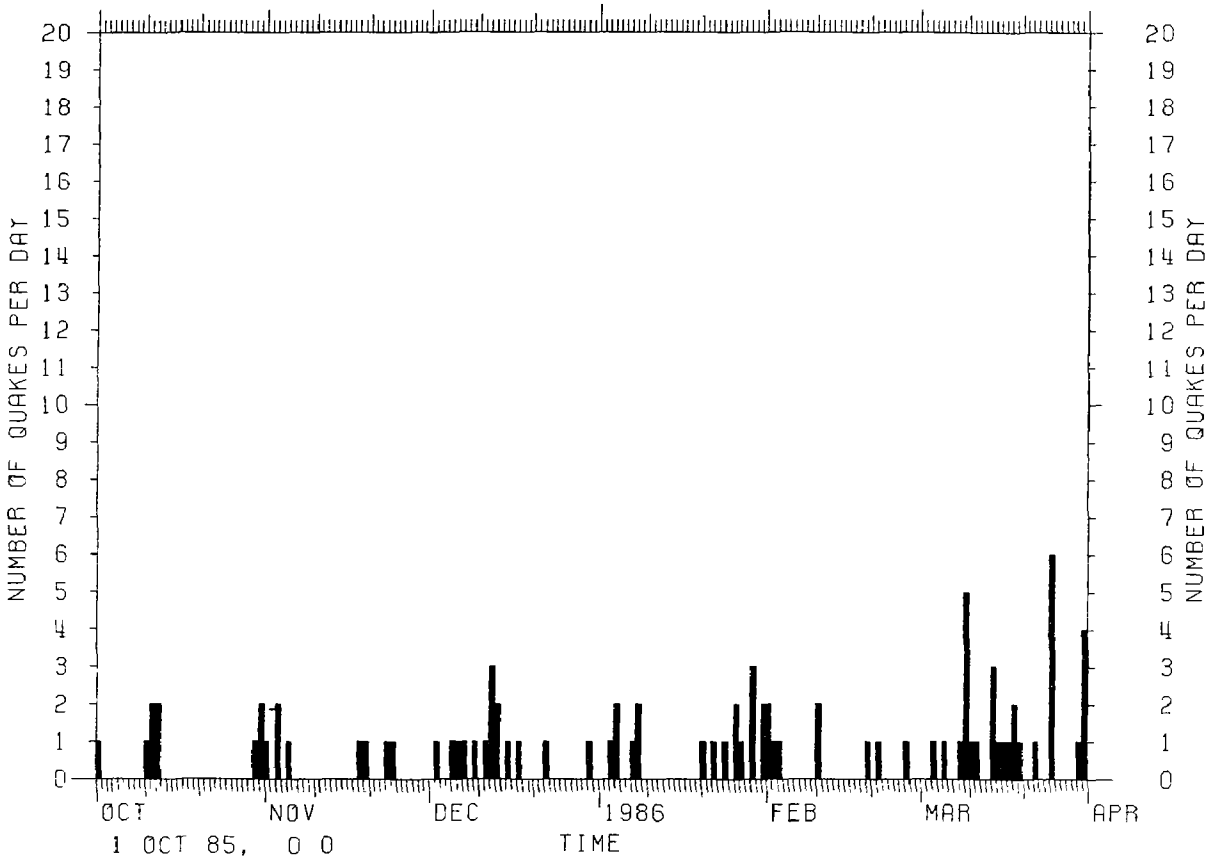
CALDERA QUAKES ONLY
NUMBER OF QUAKES PER DAY
0
1
2
3
4
5
6
7
8
9
10
11
12
13
14
15
16
17
18
19
20
OCT
NOV
DEC
1986
FEB
MAR
APR
1 OCT 85, 0 0
TIME

(B)

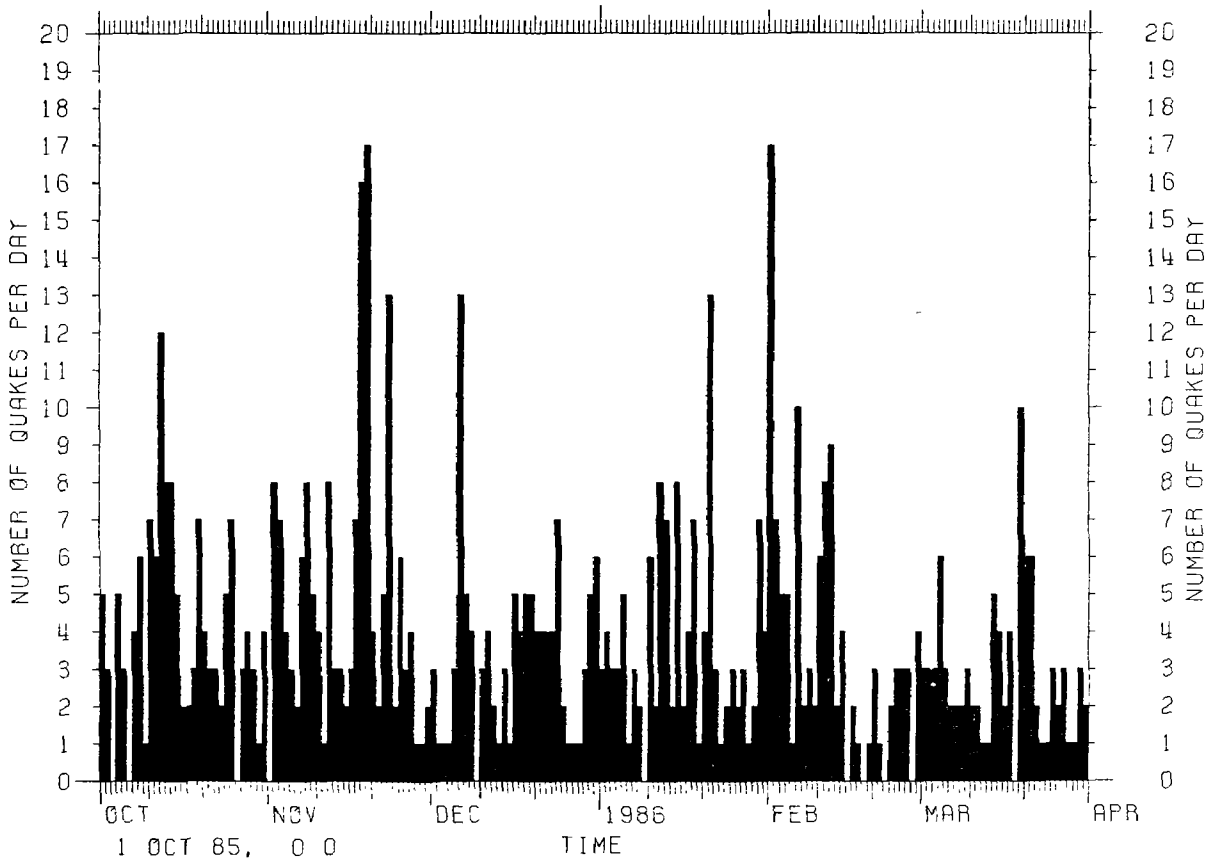
SIERRAN BLOCK QUAKES ONLY
NUMBER OF QUAKES PER DAY
0
1
2
3
4
5
6
7
8
9
10
11
12
13
14
15
16
17
18
19
20
OCT
NOV
DEC
1986
FEB
MAR
APR
1 OCT 85, 0 0
TIME

Figure 1

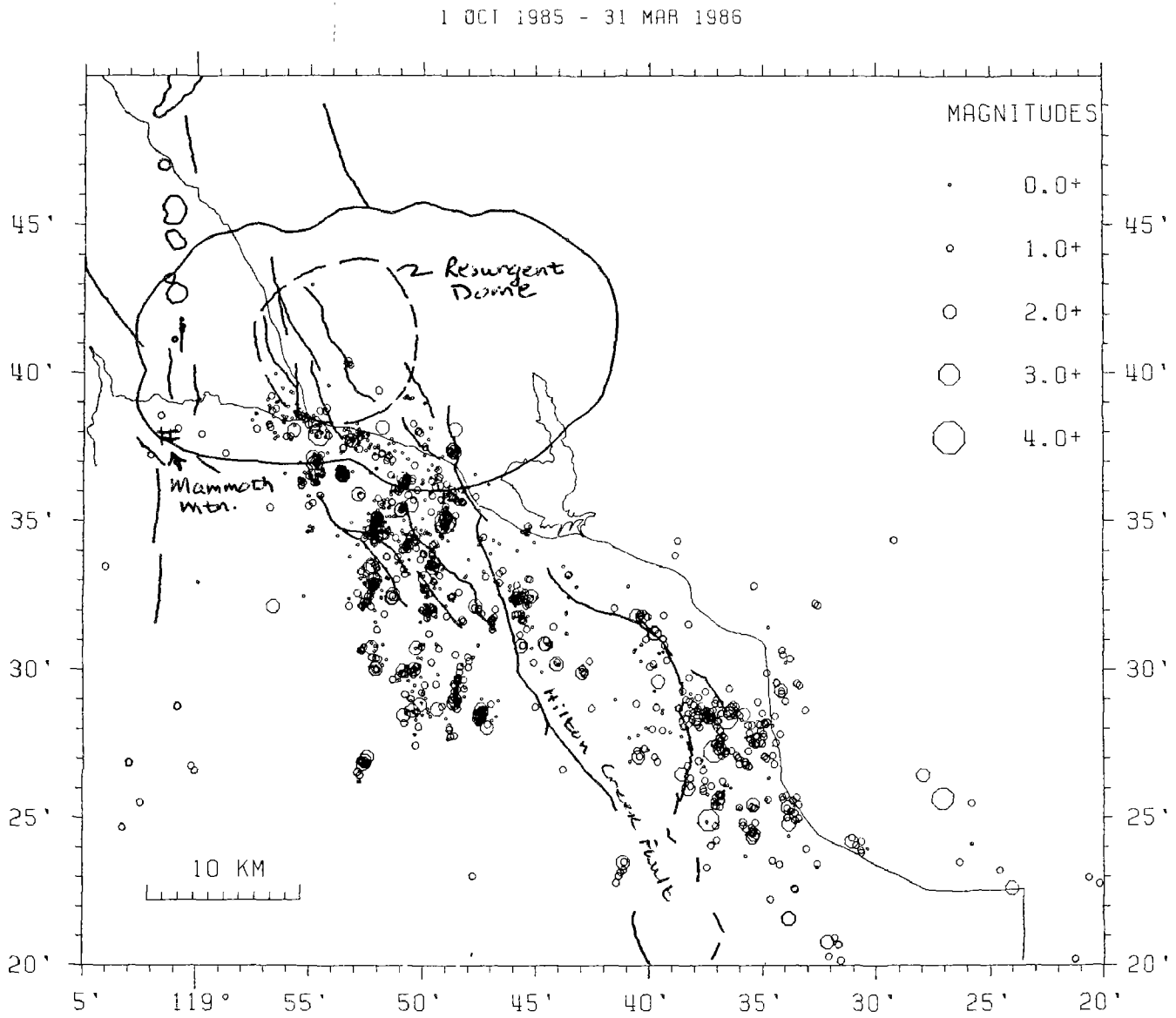
1 OCT 1985 - 31 MAR 1986
MAGNITUDES
0.0+
1.0+
2.0+
3.0+
4.0+
Resurgent Dome
Mammoth Mtn.
Hilton Creek Fault
10 KM
45'
40'
35'
30'
25'
20'
5'
119°
55'
50'
45'
40'
35'
30'
25'
20'

Figure 2

Studies of extensive-dilatancy anisotropy in Western USA

14-08-0001-G1169

Stuart Crampin and Sheila Peacock*
British Geological Survey, Murchison House
West Mains Road, Edinburgh EH9-3LA, Scotland UK
* also at Department of Geophysics, University of Edinburgh
James Clerk Maxwell Building, Edinburgh EH9-3JZ, Scotland UK

Objectives:

1) The primary objective of the contract is to seek to identify shear-wave splitting at closely spaced networks of seismometers in Western USA; particularly at the Anza network.

2) The secondary objective is to present these reports at meetings in North America.

Results:

Shear-wave splitting has now been observed above small earthquakes in Turkey (see Project Reports), Tadzhikistan USSR, Japan, North Wales, and Canada, and in shear-wave vertical-seismic-profiles elsewhere. This shear-wave splitting is caused by propagation through distributions of stress-aligned liquid-filled pores or microcracks, which exist in both sedimentary and igneous rocks in the crust. These cracks are known as extensive-dilatancy anisotropy or EDA. Figure 1 shows equal-area rose-diagrams of the polarizations of the faster split shear-waves at a seismometer network near the North Anatolian Fault in Turkey. These polarizations are aligned parallel to the strike of distributions of parallel vertical EDA cracks, which are themselves aligned perpendicular to the locally dominant tensional stress (N 10°E/N 190°E).

Shear-wave splitting has now been observed at the Anza seismometer network. Figure 2 shows equal-area rose-diagrams of the polarizations of the leading split shear-waves at Anza for two years from September 1983. The Anza network is not ideally suited for the analysis of shear-wave polarizations as the network is too widely spaced for any earthquake to be within the shear-wave window at more than a very few stations. It is also in mountainous terrain and this distorts the edge of the shear-wave window and the shear-wave polarizations. Never-the-less pronouced shear-wave splitting is observed on three-component seismograms which have patterns of shear-wave particle-motion very similar to those observed elsewhere.

Observations elsewhere demonstrate that the surface topography is a major contributor to the scatter in shear-wave polarizations. There is evidence that, if the scatter due to the surface topography could be removed, the orientations of of leading split shear-waves are controlled by the orientations of the EDA microcracks, which are in turn controlled by the stress prevailing in the shear-wave window beneath the stations. The polarizations at Anza are presently being examined in relation to earthquake source parameters and other observations of stress in the Anza

seismic gap.

Shear-wave polarizations are very sensitive to the details of the internal structure along the raypath, and it seems likely that any significant change or build-up of stress before an impending earthquake would result in changes to the orientations or (more likely) the delays between the split shear-waves. We shall continue to seek for such changes in records from the Anza network and at any other suitable networks in California.

Acknowledgements. We thank Joe Fletcher and Linda Haar for their assistance when we visited the USGS, Menlo Park. This research was supported by the Natural Environment Research Council and is published with the approval of the Director of the British Geological Survey (NERC).

Reports

(1) Booth, D.C. & Crampin, S., 1985. Shear-wave polarizations on a curved wavefront at an isotropic free-surface, Geophys.J.R. astr.Soc., 83, 31-45.

(2) Booth, D.C., Crampin, S., Evans, R. & Roberts, G., 1985. Shear-wave polarizations near the North Anatolian Fault: I, evidence for anisotropy-induced shear-wave splitting, Geophys.J.R.astr. Soc., 83, 61-73.

(3) Crampin, S., & Booth, D.C., 1985. Shear-wave polarizations near the North Anatolian Fault: II, interpretation in terms of crack-induced anisotropy, Geophys.J.R.astr.Soc., 83, 75-92.

(4) Crampin, S., Evans, R. & Üçer, S.B., 1985. Analysis of records of local earthquakes: the Turkish Dilatancy Projects (TDP1 and TDP2), Geophys.J.R.astr.Soc., 83, 1-16.

(5) Evans, R., Asudeh, I., Crampin, S. & Üçer, S.B., 1985. Tectonics of the Marmara Sea region of Turkey: new evidence from microearthquake fault plane solutions, Geophys.J.R.astr.Soc., 83, 47-60.

(6) Peacock, S. & Crampin, S., 1985. Anisotropy in the Anza seismic gap, California, EOS, 66, 949 (Abstract).

(7) Crampin, S. & Evans, R., 1986. Neotectonics of the Marmara Sea region of Turkey, J.geol.Soc., 143, 343-348.

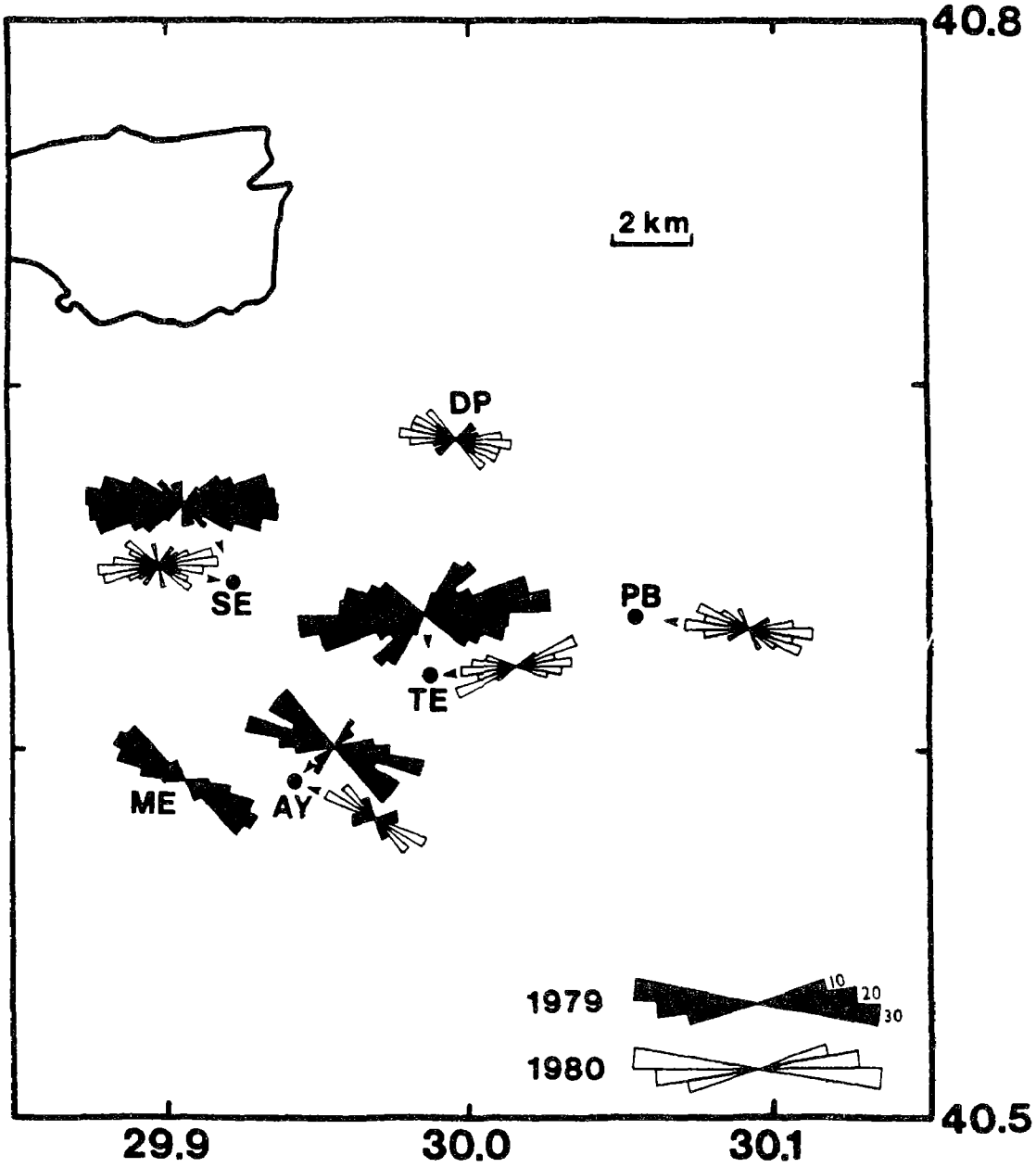

Figure 1: Equal-area rose-diagrams of the polarizations of the faster split shear-waves above a swarm of small earthquakes adjacent to the North Anatolian Fault in Turkey. Polarizations observed for a three months in 1979 and a four months in 1980.

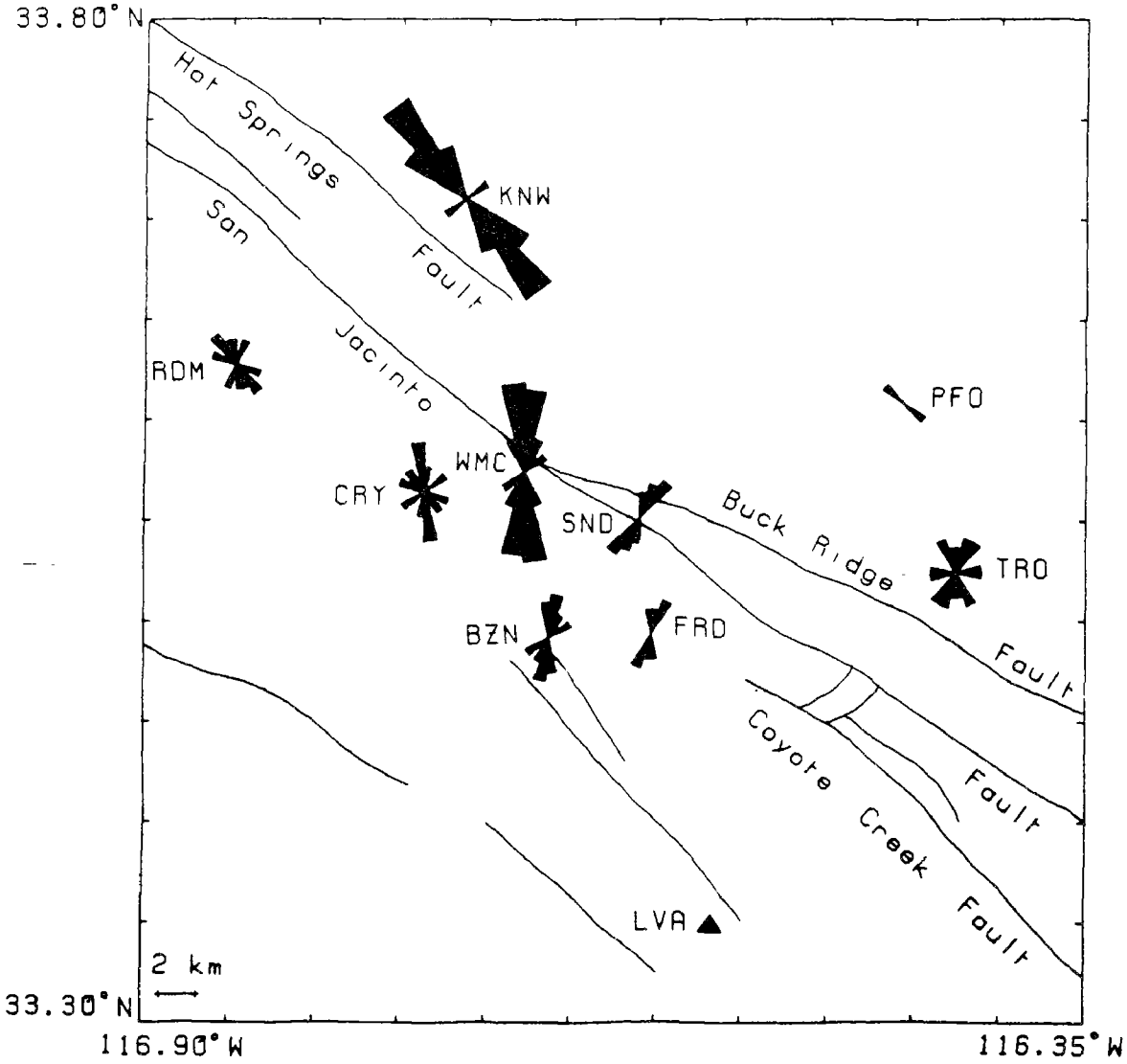

Figure 2: Equal-area rose-diagrams of leading shear-wave polarizations at the Anza seismic network from September 1983 to September 1985.

Analysis of Natural Seismicity at Anza

9910-03982

J. Fletcher
A. Frankel
L. Haar

Branch of Engineering Seismology and Geology
U.S. Geological Survey
345 Middlefield Road, MS 977
Menlo Park, California 94025
(415) 323-8111, Ext. 2384

Investigations

1. Seismicity and source parameters continue to be monitored in and around the Anza seismic gap on the San Jacinto fault. New analog-to-digital converters (ADC) were installed this winter which have better linearity specifications over a broader temperature range and have a better zero-crossover error.

2. An array of nine three-component seismometers was deployed at Pinyon Flat Observatory to investigate the coherence of body and coda waves. These events and ray paths are all occurring within the Southern Californian batholith. A stacking over frequency method developed by Paul Spudich and Tod Bostwick was used to calculate the slowness spectra.

3. Anderson (1986) among others has suggested that the tendency for source radius to be constant for small earthquakes is caused by attenuation filtering out the frequencies higher than a set value which is probably station dependent. Most of the inferred attenuation is presumed to occur near the earth's surface. We are developing a downhole instrument package that will be installed hopefully this summer to measure the attenuation and scattering of seismic waves as they travel the last 300 meters to the earth's surface. Spectral ratios will be calculated over intervals of 150 meters and the spectral modification from scattering will be differentiated from that due to anelastic attenuation.

4. The rupture characteristics of several M 3 earthquakes from the Cahuilla swarm near Anza, California have been determined from waveforms that have had the effect of the ray path deconvolved from the original set of digital seismograms. Small events were used as empirical Green's functions and deconvolved from the larger events yielding source time functions from which the total effect of the path has been removed. A

tomographic inversion of the radon transform of slip velocity also provided estimates of the rupture length and rupture velocity.

Results

1. During the first 3.5 years the Anza array has been in operation, 607 earthquakes have been recorded and located. Figure 1 shows a plot of seismicity during the period 10/1982 to through 1/1985, the station in the Anza array, and the major fault traces. Depths for these events range from less than a kilometer to over 18 km; most of the shallow (less than 5-km-deep) events occur in the Cahuilla area (southwest of the station CRY) and do not appear to be associated with any mapped fault traces. The deepest events (*i.e.*, those with depths greater than 15 km), on the other hand, do appear to be associated with mapped faults. They occur in two areas, one to the north of Anza (beneath station KNW) and to the south, along the Buck Ridge fault.

   Source parameters have been calculated for 516 of the 607 events. These events range in moment from 4.3×10^{16} to 2.6×10^{22} dyne-cm. The corresponding moment-magnitudes range from 0.39 to 4.3. Nineteen events have M_w 3 to M_w 4. Stress drops for these events range from less than 0.1 bar to 244 bars, with the largest moment event having a stress drop of 152 bars.

2. Slowness spectra were calculated for a suite of approximately five events although only four out of a total of twelve events were recorded on 7 or more stations. Of these two are considered to be particularly good because they all triggered well before the P-wave, and have good signal-to-noise ratios. For these data the body waves show strong peaks in the power spectra at the azimuths of the epicenter from the array. Coda comes from the general direction of the epicenter most of the time but significant power is occasionally detected at 90 degrees off azimuth and some backscattering is found. Nevertheless most of the coda appears to be scattered along a vertical profile not horizontally.

   P-wave coherences for some station pairs was high with values of 0.8 up to frequencies as high as 70 to 80 Hz. However for many other pairs values of 0.8 were maintained only up to frequencies of 20 to 30 Hz. Coherences for S-waves generally fell to low values at much lower frequencies than P-waves.

3. The prototype of the velocity transducer package for the downhole system has been designed by Hsi–Ping Lu. A gimbal arrangement that is internal to the downhole case is capable of finding the true vertical if the package is tilted to a maximum of $\pm 10°$ in a 6-inch hole. We plan to deploy a package with this system (Mark Products L–22 2 Hz geophones) in the same package as a Kinemetrics force-balance accelerometer for the deep emplacement at 300 meters depth. We will just use the L–22 system for the shallow hole which will have a depth of roughly half of the deeper hole.

   This downhole package will be installed at either Pinyon Flat Observatory where we ran our coherence experiment and where we also have a permanent station or at station KNW where we believe the rock to be harder and which is located directly over a group of hypocenters. Rays from the hypocenter arrive at this locale at nearly

vertical incidence reducing mode conversions. We may be able to get closer to the rock conditions equivalent to those at hypocentral depths at 300 meters depth near station KNW than at Pinyon Flat Observatory but the latter would provide closer attention because of the technical support at Pinyon Flat.

4. The source time function calculated for the M 3 events suggests a variety of rupture modes similar to the variability found for much larger events. Complex source time functions which indicate multiple ruptures are observed. Stress drops vary substantially from about 10 to 60 bars. A tomographic inversion was used to image slip velocity, using a one-dimensional fault model. A M 2.4 event had a rupture length of 300 meters and a rupture velocity of about the shear velocity. A larger event consisted of two events with an average rupture velocity of 0.8 V_s. These results are similar to those found for much larger events but over much smaller distances and time scales. The differences in stress drops suggest that differences in strength may exist over quite small distances as these events are within just a few hundred meters of each other.

References

Anderson, J. G., 1986, Implication of attenuation for studies of the earthquake source, *Submitted to the AGU Monograph of the Proceedings of the Fifth Ewing Symposium.*

Publications

Fletcher, J., Haar, L., Hanks, T., Vernon, F., Berger, J., and Brune, J., 1986, The digital array at Anza, California: Processing and initial interpretation of source parameters, *submitted to J. Geophys. Res.*.

Fletcher, J. B., Haar, L. C., Vernon, F. L., Brune, J. N., Hanks, T. C., and Berger, J., 1986, The effects of attenuation on the scaling of source parameters for earthquakes at Anza, California, *Accepted for publication in the Proceedings of the Fifth Ewing Symposium, Arden House, N.Y., AGU Monograph.*

Frankel, A., Fletcher, J., Vernon, F., Haar, L., Berger, J., Hanks, T., and Brune, J., 1986, Rupture characteristics and tomographic source imaging of M_L 3 earthquakes near Anza, California, *submitted to J. Geophys. Res.*

Figure Captions

1. Seismicity detected by the Anza array for the period October 1982 to early 1986. The radius of the circles representing the epicenters are proportional to moment. Digital seismic stations and faults are also shown.

117 00 00
116 10 00
33 50 00
33 15 00
RDM
PFO
SND
TRO
BZN
LVA
5 KM

PIEZOMAGNETIC MONITORING OF THE SOUTH PACIFIC REGION
14-08-0001-22021

Michael T Gladwin,

Department of Physics
University of Queensland
St.Lucia, 4067
AUSTRALIA.

ACTIVITIES

1. An array of eight piezomagnetic monitoring stations remains operational in the Papua New Guinea region of the South Pacific. This array is a subset of the original 25 station array deployed in a search for piezomagnetic precursors to very large earthquakes in 1980.

2. The major purpose of this sub array which covers an area of about 40000 square kilometers centered on the city of Rabaul is to assist in the monitoring and ultimate prediction of the expected volcanic eruption in the Rabaul harbour area. The region was placed on a stage 2 alert late in 1983 but has currently been returned to stage 1 status because of the decreased activity over an extended period in 1985.

3. The secondary purpose of the sub array is to continue search for precursory phenomena for large earthquakes. Three large events have been captured to date, and though no coseismic anomalies were observed, several anomalous data sequences have been observed in stations near the epicentral areas. No satisfactory explanations for these events has yet emerged.

4. Preliminary editing of the data from the original larger array has now been completed, and analysis will continue following the termination of this contract.

5. The Rabaul subarray consists of four stations within the caldera symbolised as RAB, TAV, MAT, and BLU. Locations of these stations are shown in figure 1. This inner set are supplemented by four remote (60km) stations from the original array set (NAM, GAS, BUK, and JAC shown in previous reports) which provide remote references for the inner array.

6. The Rabaul sub array is processed in real time, and several significant shifts have been observed in the magnetic field during the past year. No simplistic relationship between volcano induced seismicity and magnetic fields has emerged. Typical offsets are of order 2 to 5 nanoTeslas, which is approximately a factor of 10 above the noise in this environment. Most of these events have occurred at the Rabaul site, though some well documented cases have occurred at the other stations.

7. The period May 1985 to February 1986 has been characterised by low seismicity and very low uplift and tilt rates. In recent months there are indications of increased uplift, and it is planned to continue monitoring from local funding sources beyond termination of this work under U.S.G.S. auspices.

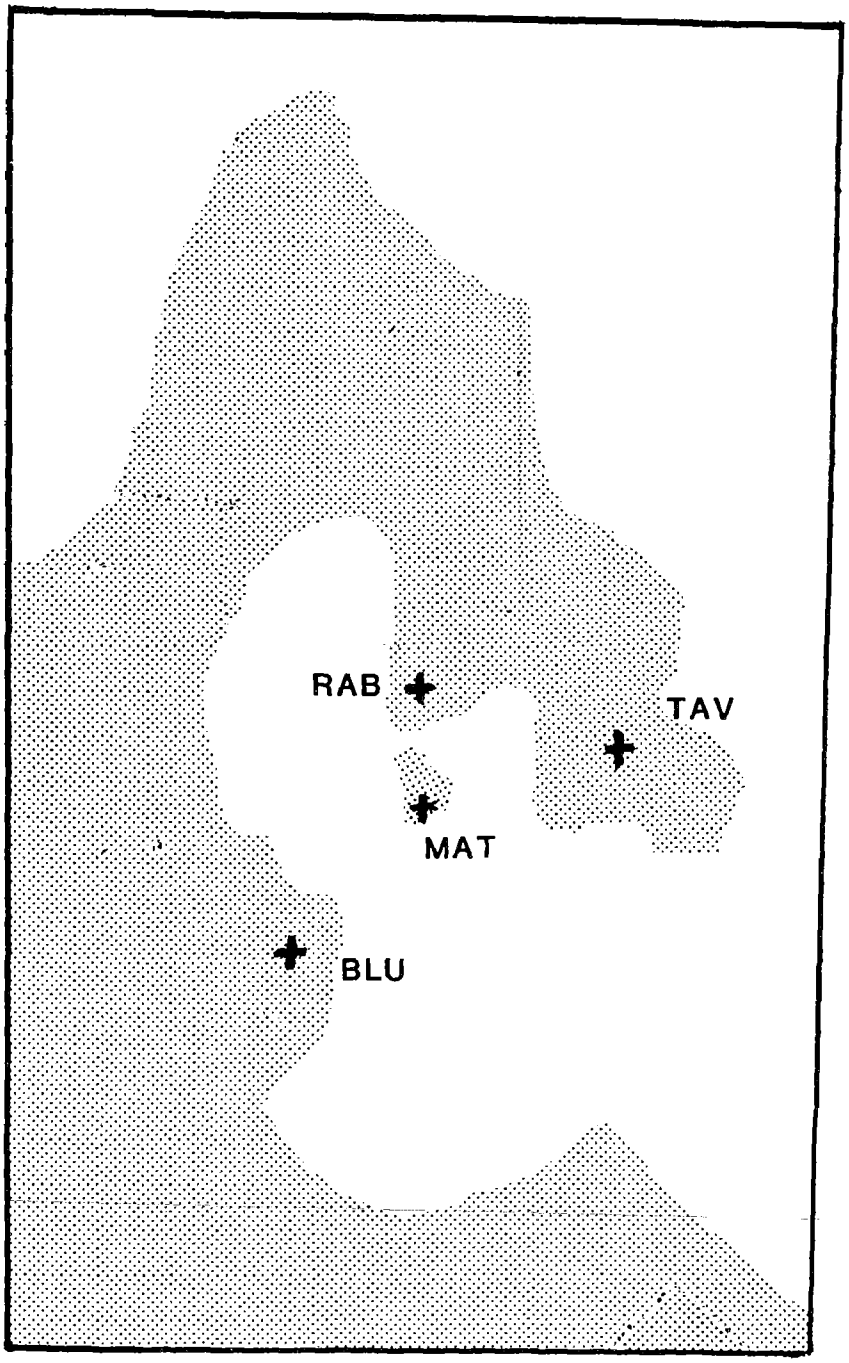

1. Location of the four sites within the Rabaul harbour caldera. The map covers a region of approximately 14 km by 22 km, and the shaded region represents landmass. Uplift in the area has been centered approximately on the site marked MAT.

RESULTS

1. Raw station differences for 1985 for the inner set of stations is shown in figure 2. A scale reference of 10 nanoTeslas is shown in the upper centre of the figure. Station differences involving the site RAB are typified by the gradual decrease beginning about day 115 on this figure. Note that other station differences (excluding RAB) show no significant change over this interval. The stations have been calibrated against a reference magnetometer twice in the interval shown, and the maximum error was two counts ($<$ 0.5 nanoTeslas) in any difference set.

2. The Rabaul site is continuing the tendency to show decrease in the total observed field during 1986. The decrease has in each case occurred in episodes of duration 20 to 40 days.

PUBLICATIONS

Gladwin, M. T., Piezomagnetic monitoring in the South Pacific Region. *I.U.G.G., XVIII General Assembly,* Hamburg, August, 143, 1983.

Gladwin, M.T., Piezomagnetic Monitoring in the South Pacific Region. *Pageoph, 122,* 6,921-923, 1985.

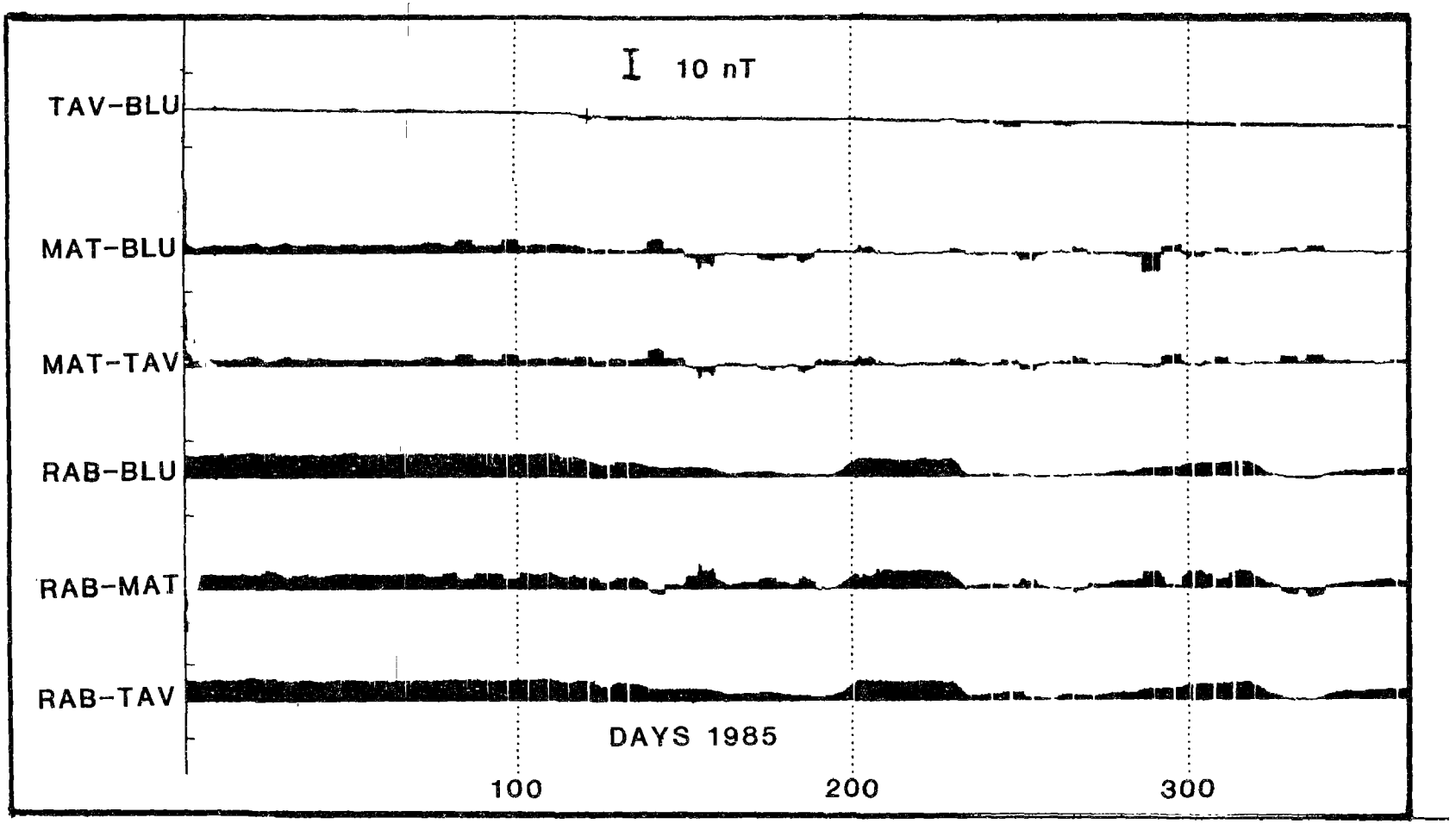

2. Differences of observed magnetic fields between the various sites shown in figure 1. Note that only differences involving the station RAB have shown significant changes in this interval, and that these changes are well above the typical noise fluctuations for the data.

Quantitative Determination of the Detection History of the California Seismicity Catalog

14-08-0001-G-992

R.E. Habermann
School of Geophysical Sciences
Georgia Institute of Technology
Atlanta, Georgia 30332
(404) 894-2860

We have made several major advances during the second half of this project. The first involves regenerating information on stations used for magnitude determinations of specific groups of events in California and the second involves a test of our techniques for identifying and modeling magnitude changes. In addition, we have extended our analysis northward along the San Andreas fault from Parkfield to Bear Valley. Our report on the Bitterwater segment of the San Andreas which describes our results there should be ready soon.

TEST OF TECHNIQUES FOR IDENTIFYING AND MODELING MAGNITUDE SHIFTS

One of the major surprises of our work on the California catalog has been the large number of apparent systematic changes in magnitudes. All three regions we have examined (Calaveras, Parkfield, and Bitterwater) show at least three such changes. We have developed a technique for interpreting these changes which involves modeling the observed magnitude signatures. Our report on the Calaveras fault shows how well this technique works for interpreting very complex magnitude changes even when they are combined with changes in detection (as they many times are).

Some recent work by Poley and Lindh at the USGS provided the first opportunity for an independent test of the results of these modeling techniques. The Parkfield catalog available prior to December, 1985 had magnitudes which were calculated without using station corrections. These are referred to as uncorrected magnitudes. Concern over the effect of the installation of six low-gain stations near Parkfield during November, 1984 prompted the determination of station magnitude corrections for stations in the Parkfield region and recalculation of the magnitudes for all events which occurred since 1983. Comparison of these corrected and uncorrected magnitudes yields an estimate of the systematic change in magnitudes which accompanied the installation of those stations.

Figure 1 shows the differences between the new (corrected) magnitudes and the original magnitudes as a function of time. This Figure demonstrates the difference between random and systematic error in magnitudes quite clearly. Assuming that the corrected magnitudes are accurate, the spread of the data around the mean magnitude difference reflects the random error. The standard deviation of this error varies

in time between 0.07 and 0.14 units. A remarkable change in the mean magnitude difference occurs during November 1984. This difference reflects a difference in systematic error in magnitudes before and after this time. In other words, it shows a clear systematic shift in magnitude estimates. The magnitude of this shift can be determined by comparing the mean magnitude difference before and after the change. Prior to this time the differences have a mean of -0.01. After this time the mean difference is 0.17. The transition between these two groups clearly occurs during November 1984, the time of the station installation. The change in mean difference is 0.18.

We examined the detection history of the Parkfield catalog without knowledge of the installation of the stations during November, 1984 and identified a magnitude decrease in the data at that time. The magnitude signature for this decrease is shown in Figure 2 by squares. It shows the comparison of the seismicity rates during the periods listed for 52 different magnitude bands. The magnitude bands which are bounded by lower magnitude cutoffs (on the right side of the plot) show rate decreases (positive z-values) and those bounded by upper magnitude cutoffs (on the left) show rate increases (negative z-values). This is the pattern expected for a magnitude decrease.

Interpreting this type of change requires modeling of the observed magnitude signature. We use a simple forward modeling approach which relies on one assumption: if the system which generates the seismicity (the earth) is unperturbed, the seismicity rates will remain constant. If this is true, then the first period in the magnitude signature provides a good estimate of what seismicity rates during subsequent periods should be.

In order to construct a synthetic magnitude signature one takes the events during the background period in the observed magnitude signature, applies a known magnitude shift, and recalculates the magnitude signature comparing the original events to the shifted events. This process is repeated for different applied shifts until the best fit between the observed and synthetic magnitude signatures is achieved. The goodness of fit is judged by summing the residuals over all magnitude bands.

This magnitude signature shown in Figure 2 was synthesized using these techniques. The observation of the increase in the larger events suggests that only the smaller events are experiencing the magnitude decrease. For this reason, the magnitude shift was restricted to events smaller than 1.9. The residual sums generated by decreasing the magnitudes of these events by between 0.1 and 0.3 range from 45 down to 28.5 (over 52 magnitude bands) with the minimum at -0.18 or -0.19, indicating that a magnitude decrease of that amount occurred during November, 1984. The synthetic magnitude signature for a decrease of the magnitudes of events smaller than 1.9 by 0.19 is shown by the diamonds in Figure 2. This synthetic fits the observed magnitude signature quite well for most magnitude bands.

The agreement between the magnitude shift determined from the station bias calculations and our analysis is very encouraging. Again, we emphasize that our analysis was done without any knowledge of Poley and Lindh's results or of the station installation during November, 1984. In other words, the catalog alone includes the information necessary for finding systematic changes in magnitudes. This has important implications for studies of catalogs which do not include station magnitude corrections such as the Calnet catalog.

STATION HISTORIES

We have greatly increased the amount of data we are considering in this study by running HYP071 for most of the events in central California between December 1979 and May 1983. We performed this task to regenerate the information about stations used in magnitude calculations in a computer compatible form. This allows us to determine the station distributions used for magnitude calculations for given groups of events. These station distributions can then be used to shed light on the results of the magnitude signature analysis. We are in the process of developing software for searches of this database and will soon be integrating these results with our interpretations. The inclusion of these data will certainly add substantially to our understanding of what controls man-made seismicity changes.

REPORTS (Available on request)

The Detection History of the Calaveras Fault: A preliminary Assessment

The Detection History of the Parkfield Segment of the San Andreas fault: A Preliminary Assessment

The Detection History of the Bitterwater Segment of the San Andreas fault: A Preliminary Assessment

Man-made Seismicity Changes

Constructing Synthetic Magnitude Signatures

ORAL PRESENTATIONS

July 26-27 NEPEC Meeting, Menlo Park (Written summaries included in USGS Open-file Report #85-754):

The Detection History of the Calaveras Fault: A preliminary Assessment

The Detection History of the Parkfield Segment of the San Andreas fault: A Preliminary Assessment

AGU meetings:

Recognition and Evaluation of Seismicity Anomalies in California, EOS,

66, 308.

The Central California Seismicity Catalog: Detection and Reporting History, EOS, 66, 971.

Seismic Quiescence at Parkfield: Real or Man-Made?, EOS, 66, 983.

PAPERS SUBMITTED

Man-Made Changes in Seismicity Rates (to BSSA)

Stability of Magnitudes in the Parkfield, California Region (to BSSA)

Figure 1. Differences between the magnitudes in Lindh and Poley's corrected and uncorrected catalogs as a function of time. The differences are such that positive values indicate lower magnitudes in the uncorrected catalog. The data clearly divides itself into two time periods, before and after November 1984. We identified this as a time of change by analysis of the catalog, with no prior knowledge of the station installation or the magnitude corrections determined by Poley. The difference in means of these two groups of data is an indication of the amount of change in the uncorrected magnitudes. It is 0.18 units, in close agreement with that predicted by our analysis (Figure 2).

Figure 2. Magnitude signature comparing rates between December 28, 1983 and November 27, 1984 to those between November 28, 1984 and June 4, 1985 in the Lindh catalog for the Parkfield region (squares). This plot indicates rate decreases when the data sets with lower cutoffs are examined and increases when those with upper cutoffs are examined. This is the pattern expected for a systematic decrease in magnitudes. The diamonds are the synthetic magnitude signature generated by decreasing the magnitudes of all events during the first period smaller than 1.9 by 0.19 and comparing them to the original unshifted events.

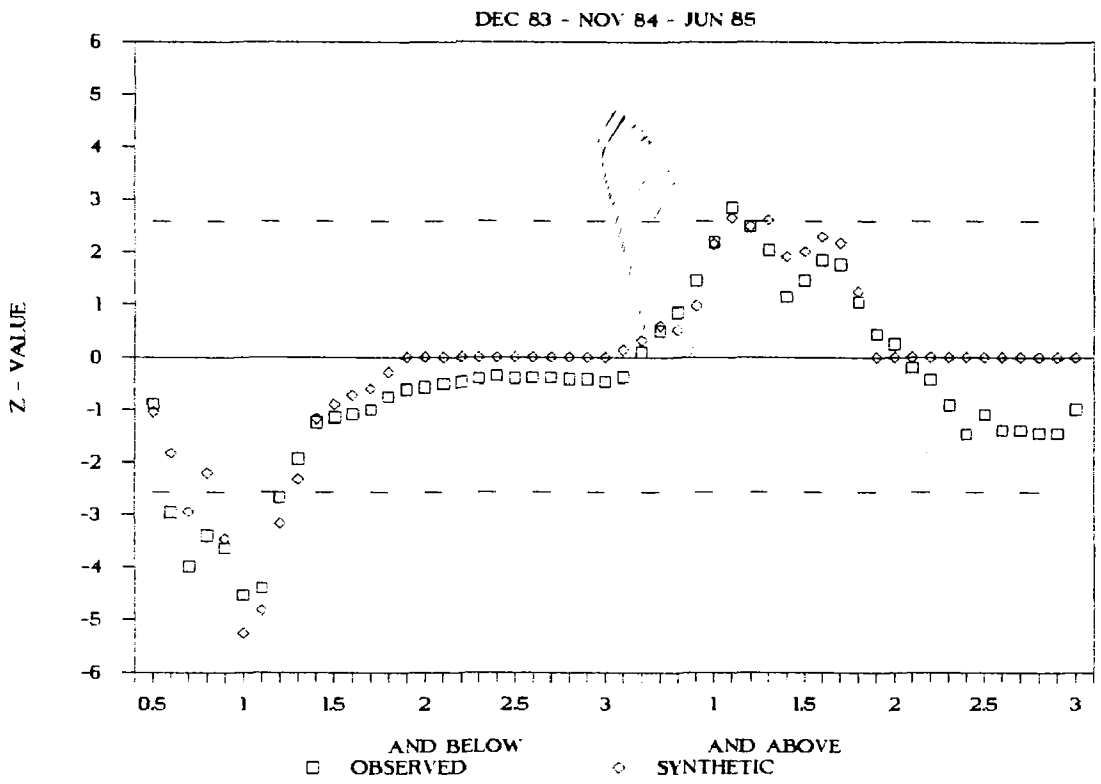

Figure 1.

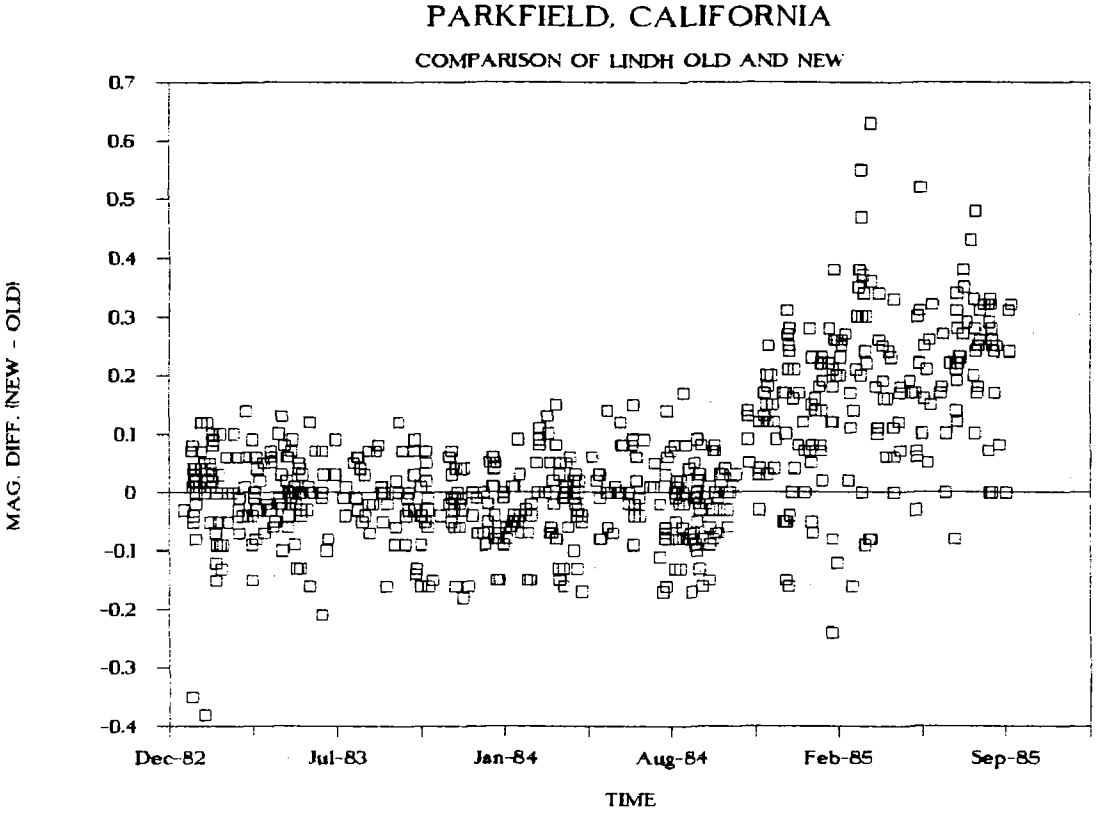

Figure 2.

Instrument Development and Quality Control

9930-01726

E. Gray Jensen
Branch of Seismology
U.S. Geological Survey
345 Middlefield Road - Mail Stop 977
Menlo Park, California 94025
(415) 323-8111, Ext. 2050

Investigations

This project supports other projects in the Office of Earthquake, Volcanoes and Engineering by designing and developing new instrumentation and be evaluating and improving existing equipment in order to maintain high quality in the data acquired by the Office.

Results

A number of new developments were undertaken during this period in addition to on-going and routine projects. One new development is the J120 discriminator. This unit will replace all of the existing OEVE discriminators in California and elsewere in order to standardize the system. The J120 gives improved performance by using sharper bandpass filters, an improved clamping ciruit and a wider output range. The first production units are being assembled now. During the coming weeks 500 will be assembled and tuned.

There have also been improvements in the amplifier/VCO field telemetry electronics. The V02L and V02H are circuits which are piggy-backed to J302 and J402 amp/VCO boards to improve temperature stability. The J502 is an updated version of the J402 incorporating the V02H modifications which is to use an EXAR VCO integrated circuit that is inherently stable but also consumes more power. The J502 and V02H are intended to be used at sites where solar panel power is available and therefore the J502 contains a built-in voltage converter (the amp/VCO's that the V02H will modify already have add-on voltage converters). A modification to improve the low temperature response of these devices was recently made. The V02L uses a temperature compensation circuit with a 4046-type VCO to produce stability at low power. These will be installed at sites without solar power. These circuits which include voltage regulators were also recently modified to permit use of only four batteries to power the package instead of six. So far, 40 J302's have been upgraded with V02L's.

An effort to build small, solid-state digital seismic recorder/telemetry unit has been initiated. Microprocessor boards and accessories have been acquired and development of a prototype is beginning. The demise of the Eclipse A computer which controlled digitizing of Calnet tape has required that this operation be transferred. The system has been rewired to allow an Integrated Solutions computer to control tape operations while a VAX digitizes the data. More computer hardware/sofware debugging is necessary before the system is operational.

Under an agreement between the U. S. Agency for International Development, Naples and the USGS, an electronic engineer from this project travelled to Naples, Italy to assist in the procurement of a network of seismic and deformation monitoring equipment. This network will be installed in an area centered around Pozzoulli where in recent years an uplift of 2 meters and much seismic activity has occurred. Under another agreement with AID, a geophysicist from this project travelled to Manizales, Colombia to assist in the installation of seismic monitoring network following the eruption of the Ruiz Volcano. Six seismic stations with radio telemetry links and drum recorders were installed.

Research has been conducted in preparation for procurement of emergency radio communications equipment for use in the area of large earthquakes where normal communications means are not operating. Research for procurement of an uninterruptible power supply/generator combination to supply critical monitoring equipment in the office was also conducted. Procurement of these items should begin soon.

The microwave telemetry system is continuing to be expanded and upgraded in addition to routine maintenance. Two-way capability between Menlo Park and Parkfield was recently added. A general overall maintenance and upgrade of the Yellowstone network was performed. Fifteen seismic stations were visited and reconditioned, one new station was added and a VHF radio link was added which connects 8 channels of the network to Ricks College in Rexburg, ID. Personnel from this project visited approximately 25 Calnet field stations to perform repairs and maintenance. Maintenance and documentation of the Seismic Cassette Recorder system was also carried out. Numerous seismometers and telemetry radio receivers and transmitters were repaired and calibrated.

Southern California Earthquake Hazard Assessment

9930-04072

Lucile M. Jones
Branch of Seismology
U.S. Geological Survey
Seismological Laboratory 252-21
California Institute of Technology
Pasadena, California 91125

INVESTIGATIONS

1. Routine Processing of Southern California Network Data.

Routine processing of seismic data from stations of the cooperative southern California seismic network was continued for the period October 1985 through March 1986 in cooperation with scientists and staff from Caltech. Routine analysis includes interactive timing of phases, location of hypocenters, calculation of magnitudes and preparation of the final catalog using the CUSP analysis system. About 1500 events are detected each month with a regional magnitude threshold near 1.5. There was little or no active production from late August to early December 1985 while a new computer processing system was being installed. When production resumed in December, the most recent data was processed each day and the backlog analyzed as time permitted. As of the end of March, half of this four month backlog has been processed. Summaries of earthquake activity including locations, time histories and focal mechanisms are produced monthly. This data as well as other information about network operations useful to researchers are published semi-annually in a network bulletin.

2. Foreshocks in Southern California.

Analysis of the characteristics of immediate foreshocks (those that occur within hours or days of their mainshocks) in southern California is continuing. The probability as a function of magnitude and time that any southern California earthquake will be a foreshock has been determined as well as a site-specific result for possible foreshocks to the characteristic Parkfield earthquake. Variations in the probabilities as multiple events occur are now being determined. These results are also applied to real time earthquake hazard assessment.

3. Focal Mechanisms and State of Stress on the Southern San Andreas Fault.

The state of stress on the southern San Andreas fault is being analyzed from focal mechanisms of small and moderate earthquakes with epicenters within 10 km of the active surface trace of the fault from Parkfield to the Salton Sea. Particular attention is being paid to the Cajon Pass region where the San Jacinto fault intersects the San Andreas at the termination of the 1857 rupture zone. Relocations of all $M > 2.6$ earthquakes from 1978 to 1985 have been calculated for more accurate depth and takeoff angle determinations. Focal mechanisms are being determined for all of these events by repicking all first motions from

the digital seismograms. The focal mechanisms are compared to the local seismogenic structures and inverted for information about the state of stress.

RESULTS

1. Foreshocks in Southern California.

Analysis of the earthquakes recorded in the Parkfield region since 1932 has shown that the most likely site of foreshocks to future Parkfield mainshocks is a small area of the San Andreas fault just north of the mainshock hypocenters under Middle Mountain at depths of 6.5 km or greater. This is called the Middle Mountain alarm box. An analytic expression has been derived for the probability that the characteristic Parkfield earthquake will occurs within some time period after a smaller earthquake occur in the Middle Mountain alarm box. This probability is:

$$P(t, T, M) = \left[1 + .307 \times 10^{-.12T} \left(\frac{3135 \times 10^{-.62M}}{1 - \exp(-\lambda t)} \right) - 1 \right]^{-1}$$

where t is the time after the possible foreshock in hours, T is time since 1986/1/1 in years, M is the magnitude of the possible foreshock and $\lambda = 0.022$. From this result, the probability that a M = 4.5 earthquake in the Middle Mountain alarm box in 1988 will be followed within 3 days by the characteristic Parkfield earthquake is 53%.

2. Focal Mechanisms and State of Stress on the Southern San Andreas Fault.

Preliminary analysis of the focal mechanisms of M > 2.6 earthquakes from 1978 to 1985 shows a significant variation in the state of stress with strike along the San Andreas fault. Earthquakes on the Indio section, from the Salton Sea to Banning Pass, and the San Bernardino section, from Banning Pass to Cajon Pass, of the San Andreas have focal mechanisms with right-lateral strike slip, sometimes with an oblique normal component. This slip is occurring along planes striking N40°W to N10°E in the Indio section and along planes striking N70°W to N10°W in the San Bernardion section. In addition, there is a small cluster of earthquakes with right-lateral strike slip and oblique reverse motion along planes striking N60°W to N40°W in the immediate vicinity of the eastern end of the Banning fault. The type of faulting changes abruptly at the end of the 1857 rupture zone at Cajon Pass. From Cajon Pass north to the Carrizo Plains, the majority of focal mechanisms show reverse faulting or oblique reverse faulting on planes striking close to east-west. There are also a few earthquakes with right-lateral strike slip on planes striking east-west to N30°W. There are not enough earthquakes in the Carrizo Plains to characterize its stress state. North of Carrizo Plains in Parkfield, the earthquakes near the fault all show right-lateral strike slip. These results can be interpreted as showing that the state of stress is different along the 1857 rupture zone than elsewhere on the southern San Andreas fault. Inverting these focal mechanisms for stress directions using the techniques on Angelier gives vertical intermediate stresses on all sections of the fault and the horizontal principal stresses shown in figure 1.

REPORTS

1. Jones, L.M., Foreshocks and time-dependent earthquake hazard assessment in southern California, Bull. Seismol. Soc. Amer., 75, 1669-1679, 1985.

2. Jones, L.M., Focal mechanisms and state of stress on the San Andreas fault in southern California (abst.), Trans. Am. Geophys. U., 66, p. 953, 1985.

3. Lindh, A.G., and L.M. Jones, Parkfield foreshock probabilities (abst.), Trans. Am. Geophys. U., 66, no. 46, p. 983, 1985.

4. Norris, R., C.E. Johnson, L.M. Jones, and L.K. Hutton, The southern California network bulletin, January 1 to June 30, 1985, U.S. Geological Survey Open-file Report 86-96, 65 pp., 1986.

5. Jones, L.M., and R.S. Dollar, Evidence of basin-and-range extensional tectonics in the Sierra Nevada: The Durrwood Meadows swarm, Tulare County, California (1983-1984), Bull. Seismol. Soc. Amer., 76, 439-462, 1986.

6. Jones, L.M., and A.G. Lindh, Foreshocks and earthquake prediction at Parkfield, California, in review, to be submitted to Bull. Seismol. Soc. Amer., 1986.

Figure 1

PRINCIPAL HORIZONTAL STRESSES ON THE SAN ANDREAS FAULT

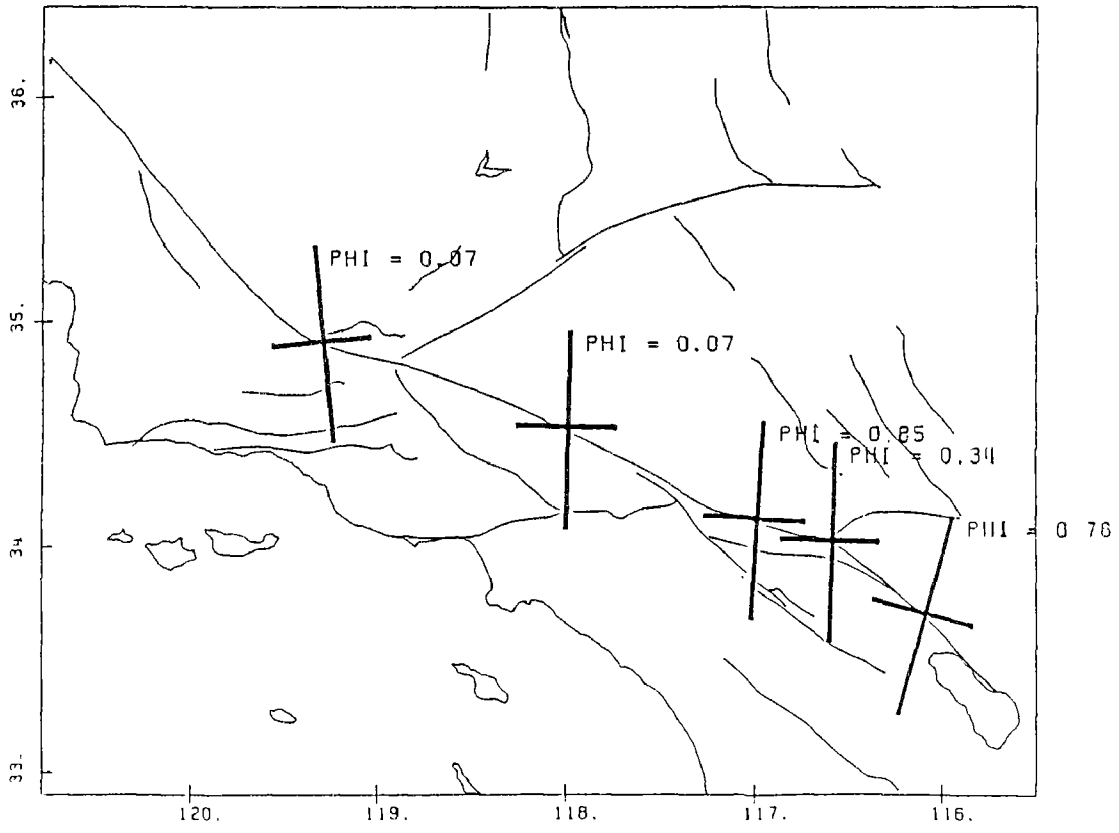

State of Stress Near Seismic Gaps

Contract No. 14-08-0001-G1170

Hiroo Kanamori
Seismological Laboratory, California Institute of Technology
Pasadena, California 91125 (818-356-6914)

Investigations

1) Tectonic Setting and Source Parameters of the September 19, 1985 Michoacan, Mexico, Earthquake
Holly Eissler, Luciana Astiz, and Hiroo Kanamori

2) Source Characteristics of the 1985 Michoacan, Mexico, Earthquake at Short Periods
Heidi Houston and Hiroo Kanamori

Results

1) Tectonic Setting and Source Parameters of the September 19, 1985 Michoacan, Mexico Earthquake

Analysis of body waves and long-period surface waves from the September 19, 1985 earthquake in coastal Michoacan, Mexico shows that the event was an interplate subduction event with a low dip angle fault plane ($\delta = 9^\circ$) striking parallel to the Mid-America trench ($\phi = 288^\circ$) and a small component of left lateral motion ($\lambda = 72^\circ$) with a point source depth of 17 km, and a seismic moment in excess of 1 x 10^{28} dyne cm. The earthquake was a multiple event, with a second source of identical moment, fault geometry, and depth occurring approximately 26 s after the first. Directivity in the body wave time function indicates that the second event occurred roughly 100 km to the southeast of the first. This suggests that the earthquake first broke the northern portion of the Michoacan gap, propagated with low moment release through the rupture zone of the 1981 Playa Azul earthquake, and then broke the remaining asperity in the southern section of the gap. The seismic moment determined from Rayleigh and Love waves is between 1.0 - 1.7 x 10^{28} dyne cm ($M_W = 7.9$ - 8.1), the largest moment determined to date for a Mexico subduction earthquake. Comparison of seismograms at Pasadena from this event with records of other large Mexico events shows that the Michoacan earthquake is basically the same size as the 1932 Jalisco, Mexico earthquake, and clearly larger than other significant events in Mexico since 1932. The seismic moment and the time since the last large earthquake in Michoacan (in 1911) fit an empirical relation between moment and recurrence time found for the Guerrero-Oaxaca region of the Mexico subduction zone. The large aftershock on September 21, 1985 ($M_S = 7.5$) has the same geometry as the mainshock, a somewhat larger source depth (22 km), a simple time function, and a seismic moment between 2.9 - 4.7 x 10^{27} dyne cm ($M_W = 7.6$ - 7.7).

2) Source Characteristics of the 1985 Michoacan, Mexico Earthquake at Short Periods.

Source characteristics of the Sept. 19, 1985 Michoacan, Mexico earthquake and its aftershock on Sept. 21 were inferred from broadband and short-period teleseismic GDSN records. We Fourier-transformed the P wave, corrected for instrument response, attenuation, geometrical spreading, and radiation pattern (including the depth phases), and then averaged to obtain the teleseismic source spectrum from 1 to 30 s. The Michoacan source spectrum is enriched at 30 s and depleted at 1 to 10 s relative to an average source spectrum of large interplate subduction events. Source spectra for the

Sept. 21 aftershock, 1981 Playa Azul, 1979 Petatlan, and 1978 Oaxaca events follow a trend similar to that of the 1985 Michoacan event. This spectral trend may characterize the Mexican subduction zone.

A station-by-station least-squares inversion of the Michoacan earthquake records for the source time function yielded three source pulses. The first two are similar in moment, and the third pulse contains only 20% of the moment of the first pulse. Directivity is evident in the timing. At each station, we measured the time differences between the pulses, and performed a least-squares nonlinear estimation of the strike, distance, and time separation between the pulses to locate them relative to one another. The second pulse occurred 26 s after the first, and 82 km southeast of it, indicating southeastward rupture along the trench. The third pulse occurred 21 s after the second, and about 40 km seaward of it. The two large pulses are also seen in the near-field strong motions.

The mainshock records, spectrum, and time functions contain less high frequency radiation than those of the 1985 Valparaiso, Chile earthquake. Apparently, the Michoacan earthquake ruptured two relatively smooth, strong patches which generated large 30 s waves, but small 1 to 10 s waves. Such behavior contrasts with the Valparaiso event which had a more complex rupture process and generated more 1 to 5 s energy. This difference is consistent with the higher near-field accelerations recorded for the Valparaiso event.

References

Eissler, Holly, Luciana Astiz, and Hiroo Kanamori, Tectonic setting and source parameters of the September 19, 1985 Michoacan, Mexico Earthquake. Submitted to Geophysical Research Letters, February 28, 1986.

Houston, Heidi and Hiroo Kanamori, Source characteristics of the 1985 Michoacan, Mexico earthquake at short periods. Submitted to Geophysical Research Letters, February 28, 1986.

FAULT MECHANICS AND CHEMISTRY

9960-01485

C.-Y. King
Branch of Tectonophysics
U.S. Geological Survey
345 Middlefield Road, MS/977
Menlo Park, California 94025
(415) 323-8111, ext. 2706

Investigations

1. Water temperature and radon content were continuously monitored at three water wells in San Juan Bautista and Parkfield, California.

2. Water level was continuously recorded at six other wells.

3. Water temperature and electric conductivity were periodically measured, and water samples were taken from most of these wells and two springs in San Jose for chemical analysis.

4. Radon content of ground gas was continuously monitored at Cienega Winery, California, and at Nevada Test Site.

Results

This report presents some preliminary data that were periodically measured in ground waters at five wells and two springs distributed along the Hayward and San Andreas faults between Oakland and Cienega Winery since about 1976 (Fig. 1). Temperature and electric conductivity were measured in-situ about once a month with a portable meter (Yellow Spring Instrument Co., Model 33); flow rate was measured at the orifice of sulfur spring #11); and water samples were collected for subsequent chemical (mainly Na^+ content) and isotopic ($^{18}O/^{16}O$) measurements in the laboratory. The results are shown in Figs. 2-8, together with cumulative rainfall data recorded at Berkeley and Gilroy.

David Basler visited the four northern sites on 3/31/86, about 6-12 hours after the mag. 5.3 Mt. Lewis earthquake, and found that the flow rate at sulfur spring #11, located about 20 km SW of the epicenter had increased by a factor of 2 over the background values of approx. 4 gal/min, last measured 5 days before (circles in Fig. 4). The flow rates at several other springs nearby (in the Alum Rock park, east San Jose) also showed visible increases. Similar increases were observed

previously 1 day following the mag. 6.1 Morgan Hill earthquake on 4/24/84 (Fig. 4). However, the waters did not change color this time, as they did in 1984 owing to increased amount of sediments in the water.

The increased water flows following both earthquakes cannot be attributed to rainfall (none between the last two measurements in 1986). The increases are probably not the result of crustal strain changes either, because the springs are situated in a compressional quadrant of one earthquake (Morgan Hill) and a dilatational quadrant of the other (Mt. Lewis). The most likely cause for the increased flow is seismic shaking which may have unclogged the plumbing system of the springs.

The conductivities at the seven sites all began to show a gradual decrease in 1982. Part of the decreases at the four northern sites is probably due to instrumental deterioration (decreased sensitivity of the probe caused by a gradually formed thin layer of deposit on the surface; a duplicate measurement with a new probe on 3/31/86, showed higher readings (solid circles in Figs. 2-5)). However, a significant part of the decrease may still be real as corroborated by the independently measured Na^+ data. The conductivity data for the three other sites, determined with a separate meter, do not appear to have been similarly affected; they showed a recovery to pre-1982 levels during the past several months (Figs. 6-8).

Reports

King, C.-Y., 1986, Mogi's doughnuts (A review of K. Mogi's book on Earthquake Prediction): Nature, v. 319, p. 547.

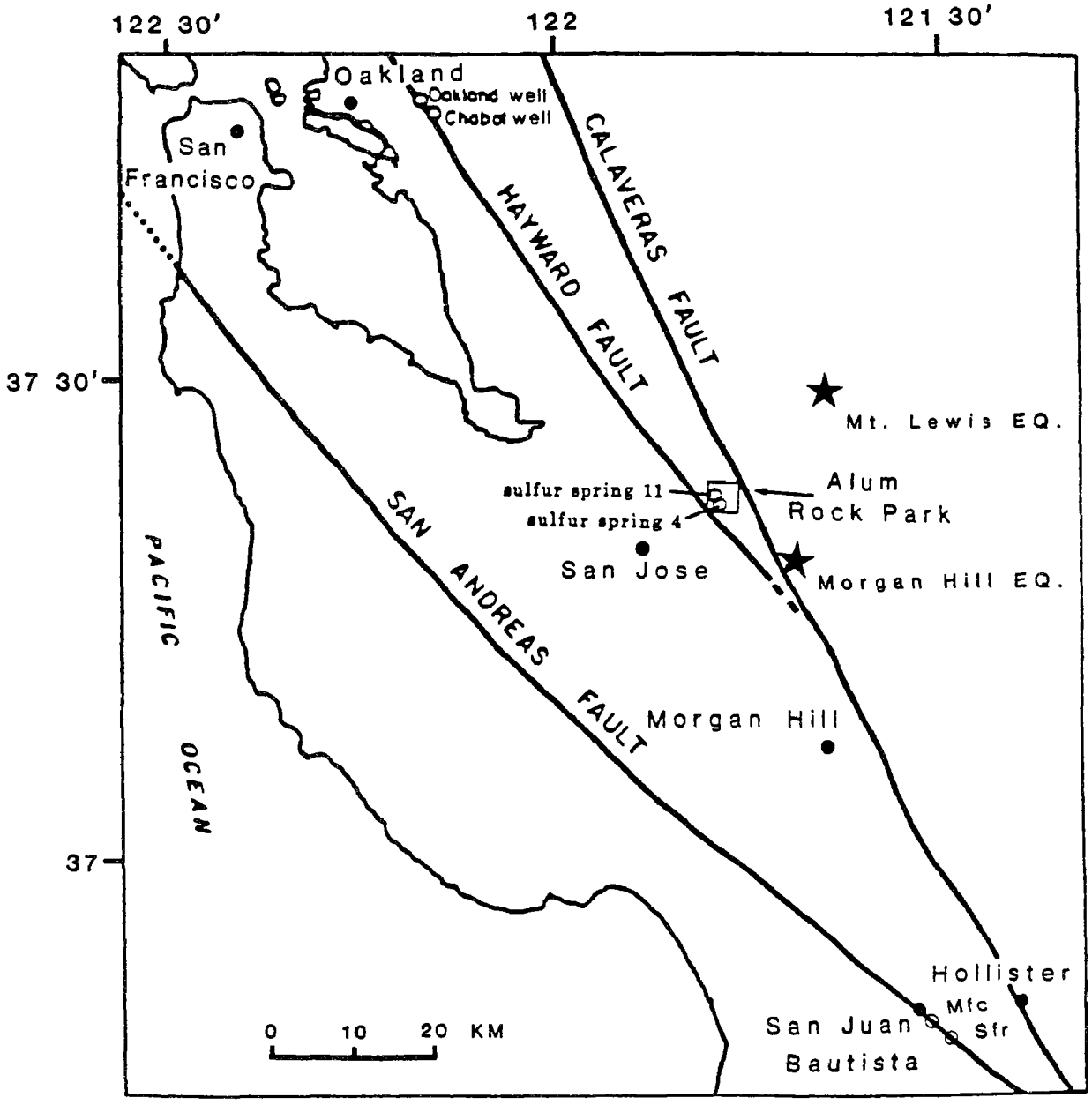

Fig. 1. Location of ground water measurement sites (circles) and epicenters of Morgan Hill and Mt. Lewis earthquakes (stars).

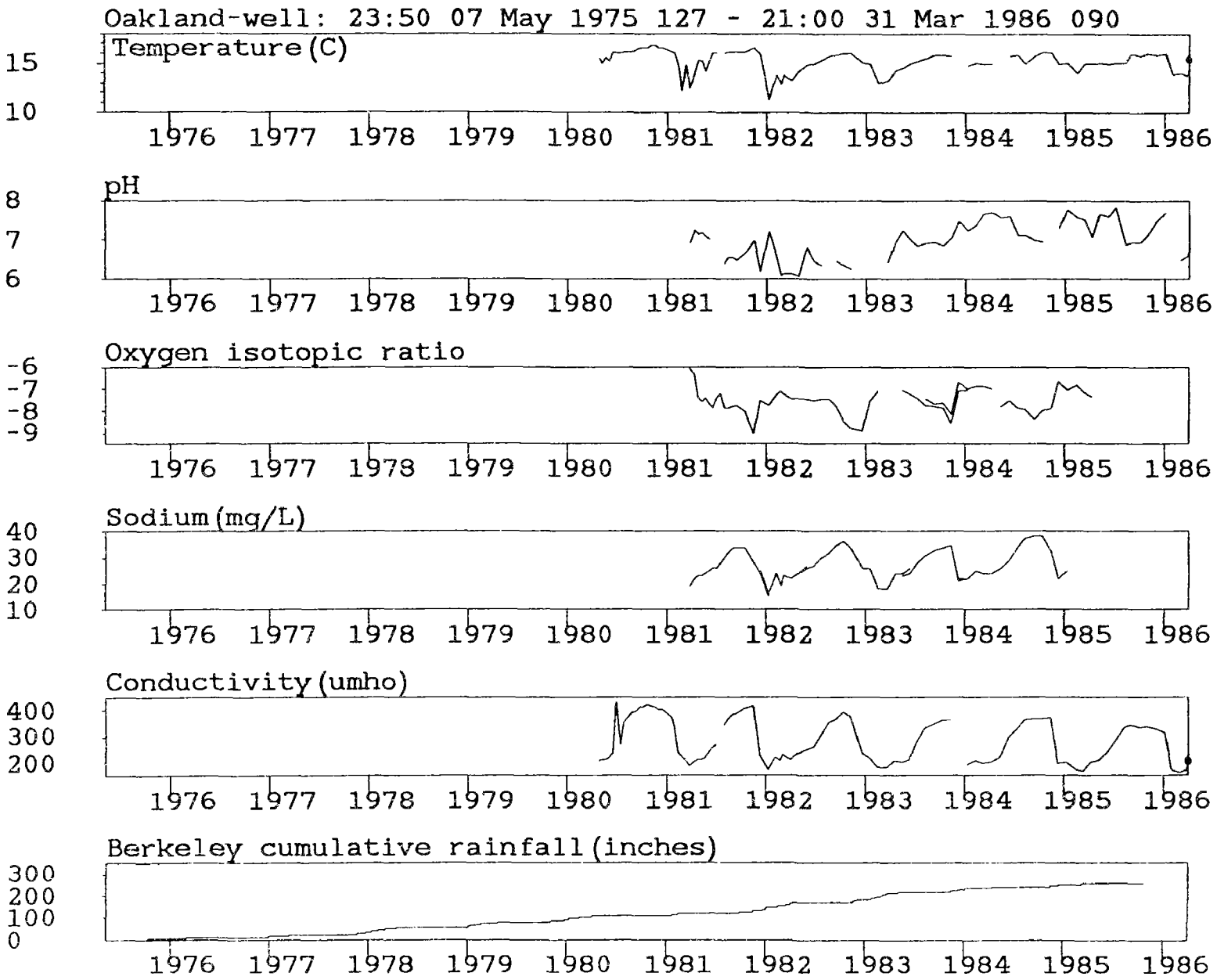

Fig. 2. Ground water data at Oakland well.

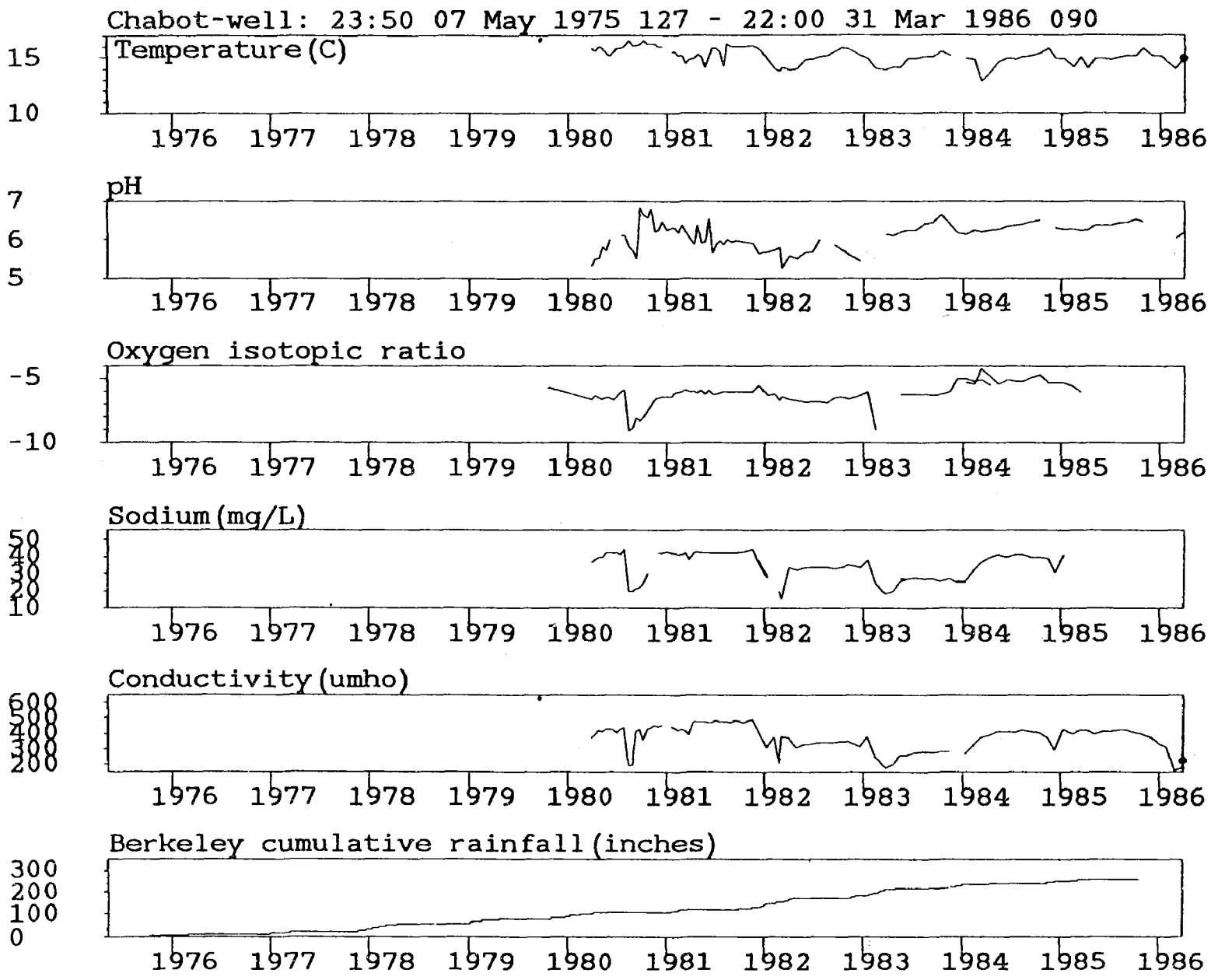

Fig. 3. Ground water data at Chabot well.

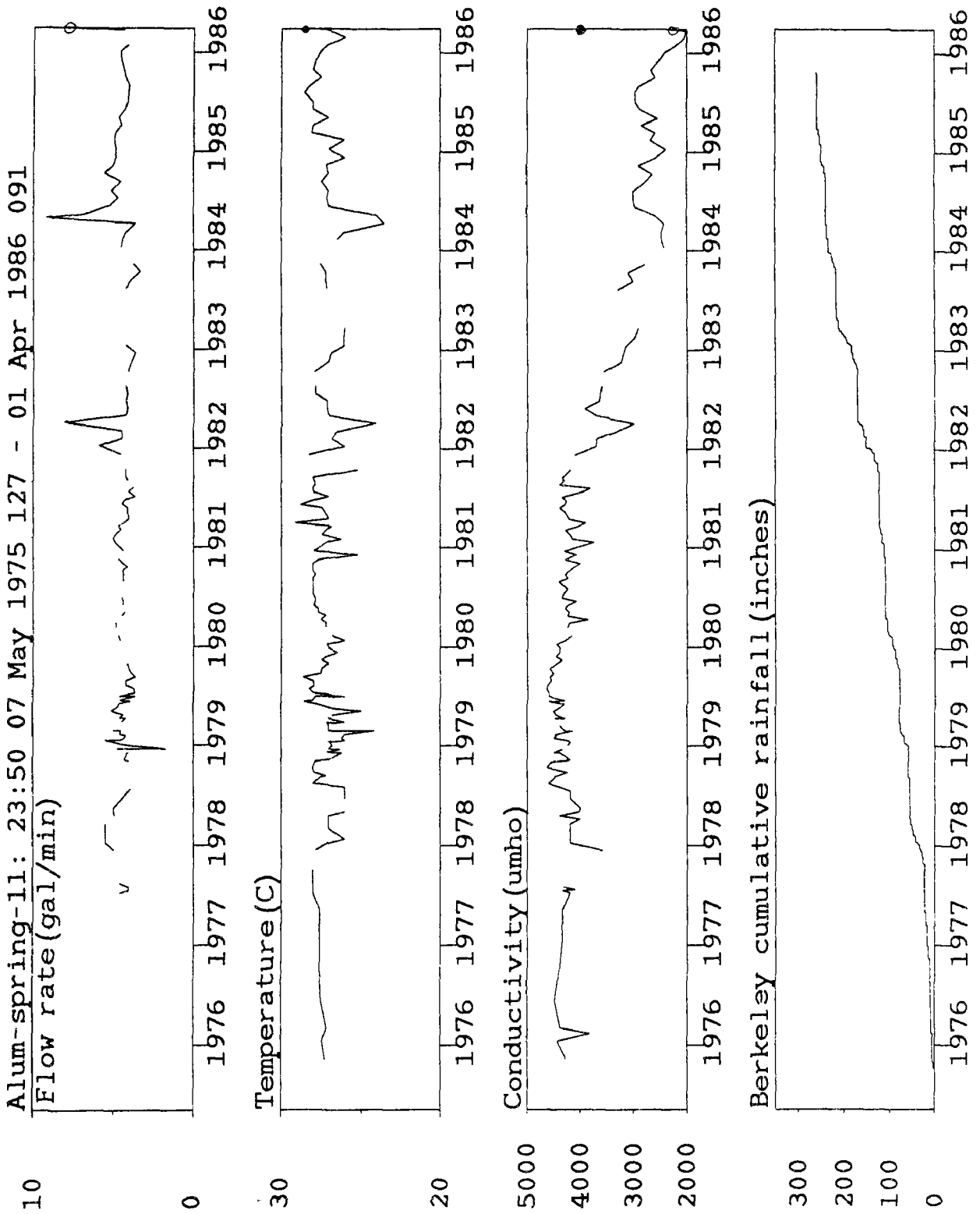

Fig. 4. Ground water data at Spring #11 in Alum Rock park, San Jose.

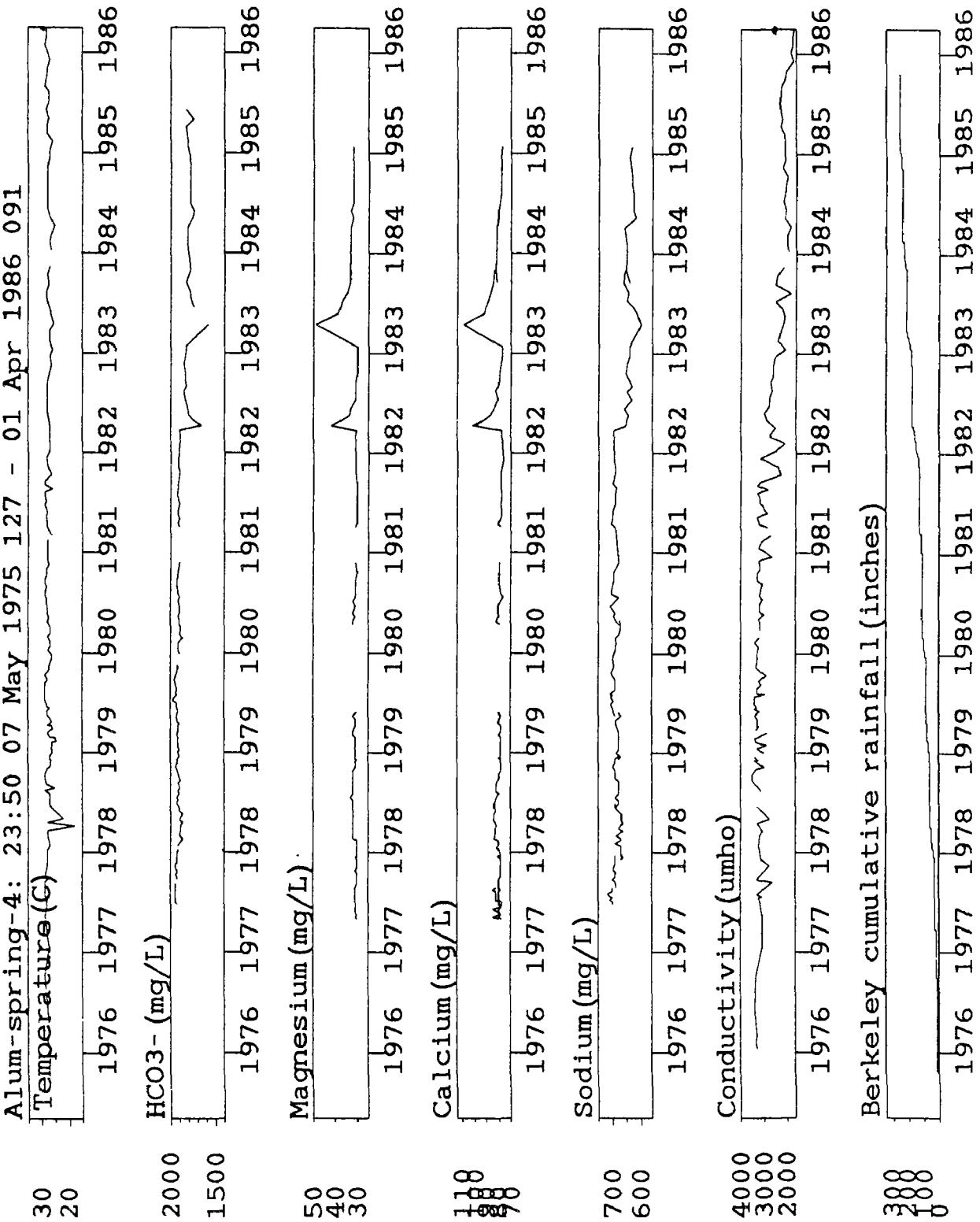

Fig. 5. Ground water data at Spring #4 in Alum Rock park, San Jose.

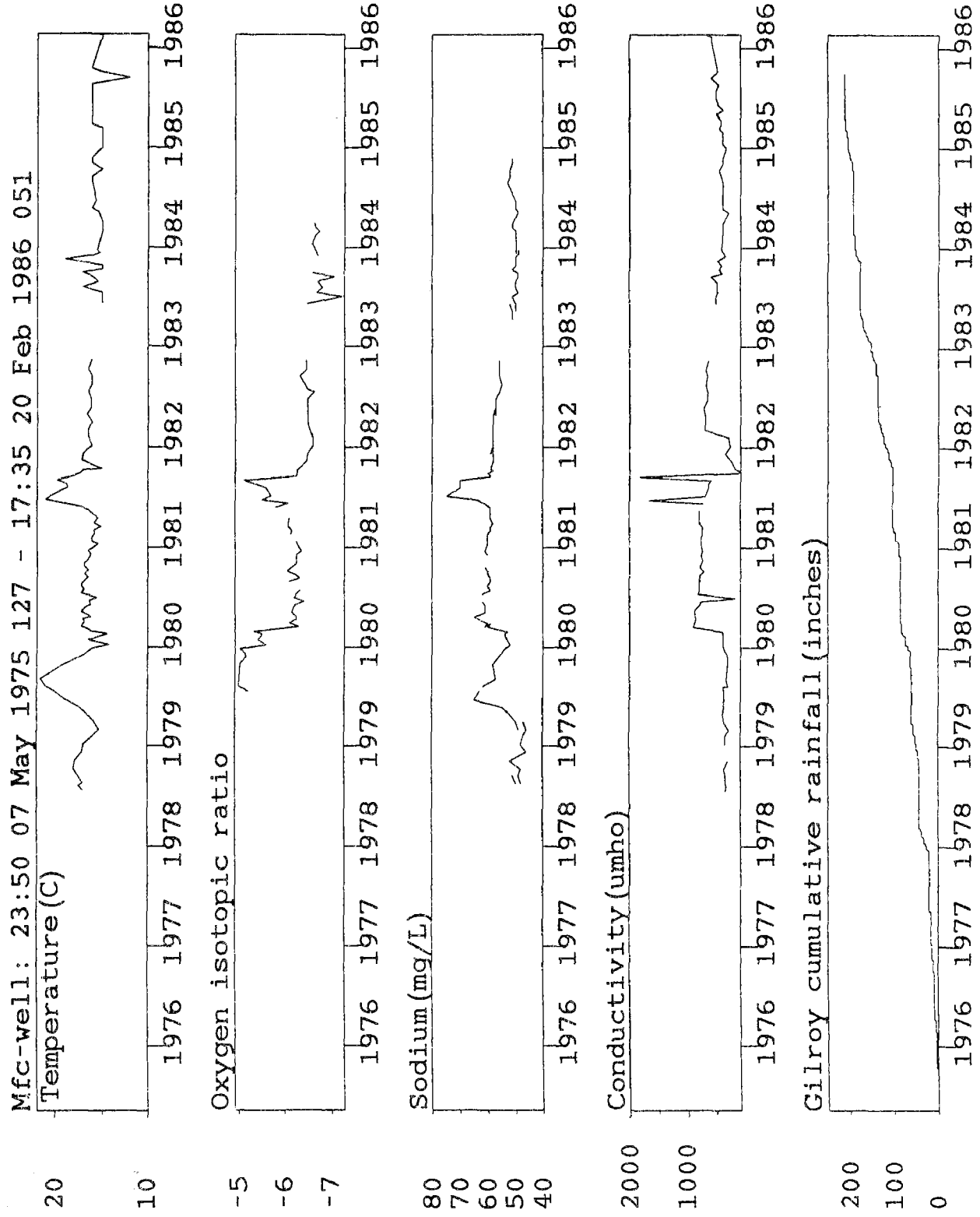

Fig. 6. Ground water data at Mfc well, San Juan Bautista.

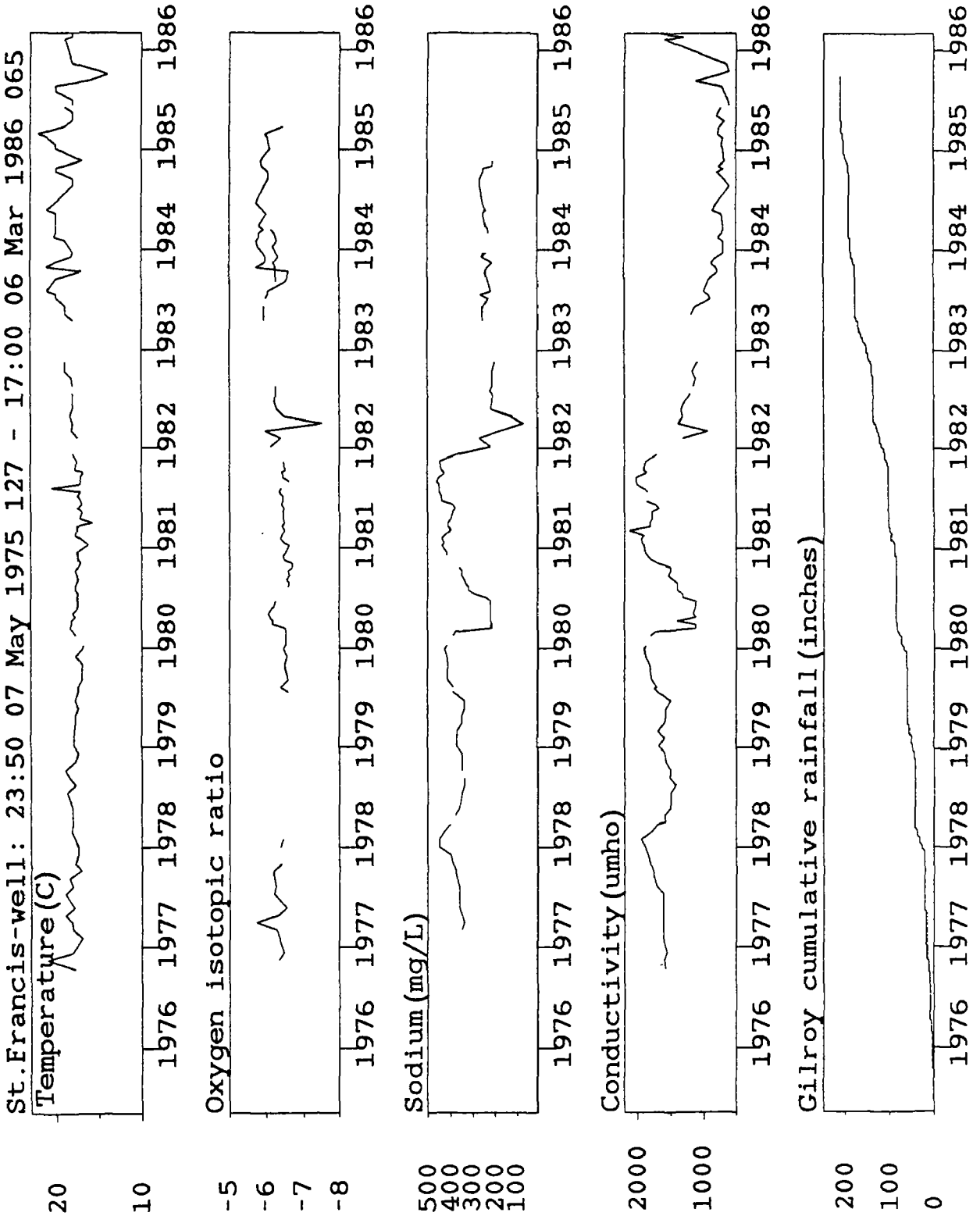

Fig. 7. Ground water data at Sfr well, San Juan Bautista.

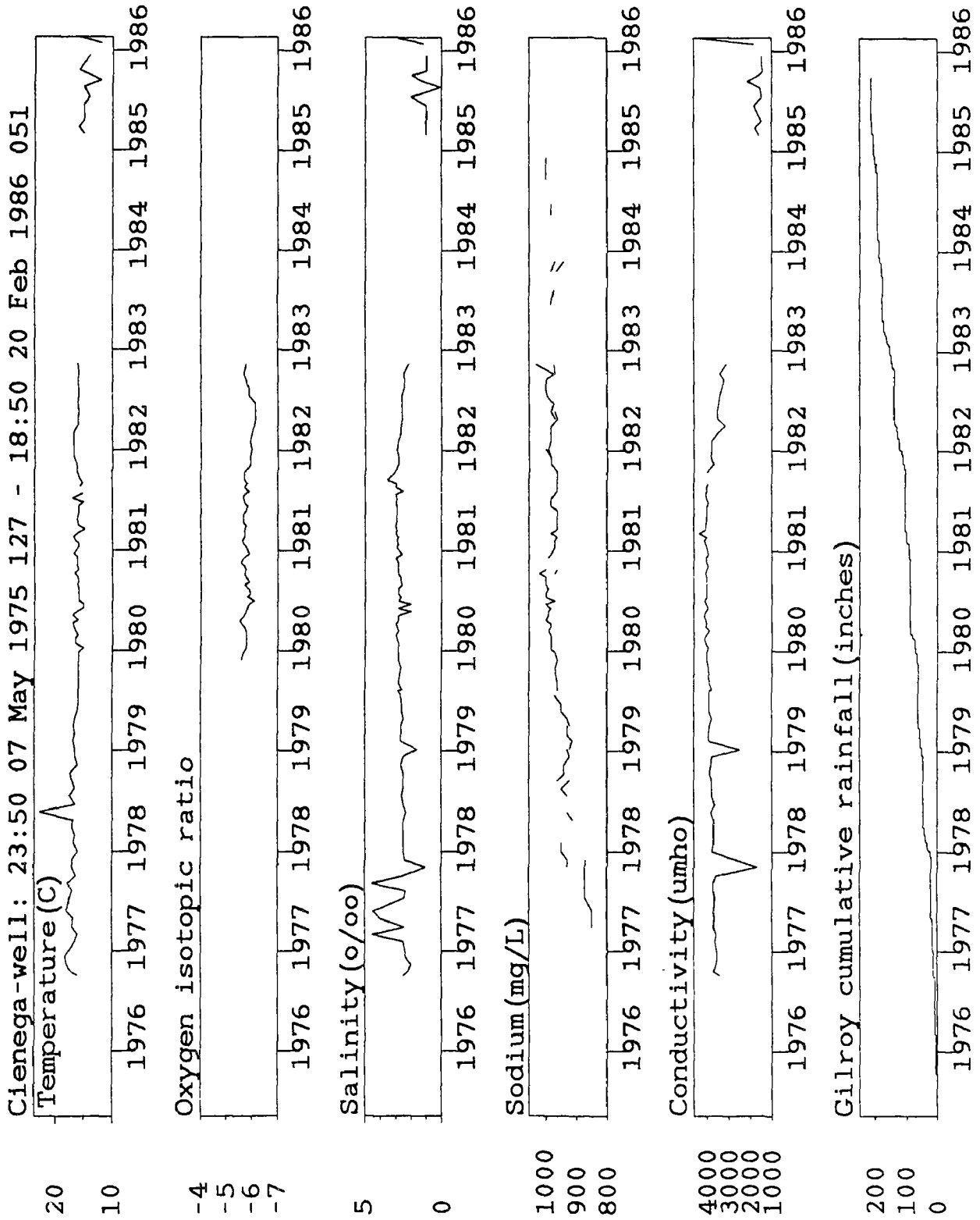

Fig. 8. Ground water data at Cienega Winery well.

SOUTHERN CALIFORNIA CO-OPERATIVE SEISMIC NETWORK

9930-01174

Charles Koesterer
Branch of Seismology
U.S. Geological Survey
525 S. Wilson Avenue
Pasadena, CA 91106
(818) 405-7813

INVESTIGATIONS

1. Operation, maintenance, and recording of the Southern California Seismic Network continued through the reporting period without significant failure. At present 189 U.S.G.S. short period seismograph stations and 66 other agency instruments are telemetered to Caltech for recording onto the CUSP analysis system. Jointly, two analog magnetic tape recorders record 28 of 37 phone lines for back-up of digital recording.

2. Provide logistics, management, and support of office computer systems for three other projects within the Southern California Field Office.

RESULTS

1. Installed the back-bone of the microwave transmission system for seismic telemetry. The link starts at Edwards A.F.B. and goes to Strawberry Peak (San Bernardino Mts.) and then to Santiago Peak (Santa Ana Mts.) and then to Caltech. The system is currently operational with one channel of data and thirteen more channels expected by July 1986.

2. Installed the Ethernet system to the new CIT off-line DEC VAX 750 minicomputer for communication between on-line computers (PDP 11/34's) and the U.S.G.S. VAX 750.

3. Added four stations operated by the University of Southern California to the on-line computer systems.

4. Started construction and testing of 50 new J-502 VCO units for replacement of older VCO units which do not have calibrators.

5. Installed a satellite synchronized clock as the primary timing system for on-line computers and analog magnetic tape recorders.

Microearthquake Data Analysis

9930-01173

W. H. K. Lee
U.S. Geological Survey
Branch of Seismology
345 Middlefield Road, Mail Stop 977
Menlo Park, California 94025
(415) 323-8111, Ext. 2630

Investigations

The primary focus of this project is the development of state-of-the-art computation methods for analysis of data from microearthquake networks. For the past six months Jack Pfluke and I have been involved mainly in starting up a project called "Investigation of signal characteristics of quarry blasts, nuclear explosions, and shallow earthquakes for regional discrimination purposes" for the Defense Advanced Research Project Agency. The objective is to collect high-frequency seismic data generated by quarry blasts, controlled explosions, and shallow earthquakes, to study their signal characteristics, and to develop a method to discriminate between these three different sources.

Results

We identified 48 quaries operating within the U.S. Geological Survey Seismic Network in northern and central California. From November 1, 1984 to October 31, 1985, we identified about 700 quarry blasta and/or earthquakes within 5 km of these quarries. After eliminating quarries that blast infrequently or are located in areas with few shallow earthquakes, we were left with a few potentially useful quarries. We made some initial contacts with quarry operators, and decided to concentrate on the Kaiser Permanente Quarry. This Quarry is located about 3 km from the San Andreas fault and is on top of a small thrust fault that has shallow earthquakes. It is a 30 minute drive from our office and thus field work can be carried out rapidly.

We modified our routine seismic network data processing to pay particular attention to our targeted quarries and save all relevant seismic data so that further analysis can be readily performed. A prototype interactive analysis using a large IBM 3081 computer has been developed, and we just began analyzing the quarry/earthquake data.

We secured cooperation from Kaiser Permanente Quarry to undertake experiments in their quarry. On November 22, 1985, we deployed a total of 40 instruments (6 wide-band 3-component digital GEOS seismographs, 10 3-component analog seismographs, and 24 cassette based vertical-component seismographs) within 5 km of the Kaiser Permanente Quarry to record a quarry blast (about 20,000 lbs of explosives) in more detail than ever had been attempted. We repeated this experiment with 18 instruments on November 26, 1985. The collected data have been played out and are now being analyzed.

We also deployed eight three-component seismograph stations for about one month along a line running a distance of about five kilometers westward of the active rock excavation site. During that month, 15 quarry explosions were

recorded on analog tapes. We have just completed the play out of these events and the best recorded events are now being digitized for further analysis. The books at the Kaiser Permanente Quarry were examined to extract pertinent information on the geometry of the shot holes, amount of explosives used, and the shot delay times. This information will be used to correlate with the recorded signal characteristics.

Willie Lee chaired an AGU ad hoc panel, and organized a special session on "Applications of personal computers in Geophysics" during the Fall AGU meeting in San Francisco. The session was well attended and generated substantial interest in the geophysics community. A proceeding of this specail session will appear in EOS soon.

Reports

Ad Hoc Panel on Personal Computers, Applications of personal computers in geophysics, to appear in EOS (Transact. Am. Geophys. Union).

Lee, W. H. K., and Lahr, J. C., Personal computers in geophysics: a personal overview, to appear in EOS (Transact. Am. Geophys. Union).

Installation and Operation of Two Borehole Tiltmeters at Pinon Flat Observatory

14-08-0001-G-1117

Judah Levine

Joint Institute for Laboratory Astrophysics
University of Colorado
Boulder, Colorado 80309
(303) 492-7785

Investigations

We have drilled two boreholes at Pinon Flat observatory and have installed two tiltmeters in them as outlined in our proposal. The boreholes were drilled in January, 1986, and the tiltmeters were installed a few weeks later.

The boreholes are roughly 80 and 120 feet deep and are cased with a steel pipe that is welded into one continuous casing as it is installed. The orientations of the tiltmeter capsules are determined when the instruments are installed by means of a series of rods extending from the capsule containing the tiltmeter at the bottom of the borehole to the surface.

The outputs of the tiltmeters are digitized 10 times per hour and the digital values are transmitted to our laboratory in Boulder via the existing telephone circuit at the Observatory. The transmission takes places at a fixed time very early every morning and usually takes about 14 minutes to transmit all four channels (two pendulums in two holes).

Results

All of the instruments showed a large initial drift immediately after installation, but the drift on all of the instruments has decreased substantially. The subsequent drift rate is considerably less than one micro-radian per year, although it is far too soon to tell if that rate will be maintained. If it is maintained, that drift rate will be the smallest drift rate we have seen anywhere.

A preliminary estimate of the performance of the pendulums has been completed. The tidal admittance at the

M2 frequency has been computed for each pendulum, using the known azimuth and calibration factor. The results agree very well with the known admittance at Pinon calculated using other instruments at the site.

A problem in the power supply has developed in the last few weeks which has resulted in the tiltmeters becoming very noisy at short periods (although both the secular and tidal tilts are not affected). We have made several trips out to the Observatory to work on the power supply, and we think that we now understand the source of the difficulty, although it is not yet repaired. We expect to complete the repairs by the first week in May.

We plan to continue to operate the tiltmeters and to compare our data with results obtained by other instruments at the site.

CONSTRUCTION OF AN ELECTROMAGNETIC DISTANCE-MEASURING SYSTEM

66701 - 110121

Judah Levine

Time and Frequency Division
National Bureau of Standards
Boulder, Colorado 80303
(303) 497-3903

Investigations

We have completed field tests of our instrument over several baselines up to 25 km long. These tests are preliminary and are designed to evaluate the performance of the dispersion measurement algorithm in a realistic environment.

We have begun the construction of the additional hardware necessary to complete the distance-measuring part of the system. These measurements are in principle much simpler than the dispersion measurements since the signals are so much larger. We anticipate completion of this phase of the work during the summer of 1986.

Results

Our tests of the instrument were conducted in four parts. The first part used very short baselines in the laboratory. These measurements were designed to evaluate the systematic error budget of the electronics and the adequacy of the steering and centering systems that were discussed in previous reports. We found that the steering system must keep the beam centered to within 6 milliradians, and that if this level of control is achieved the system noise is less than the least count of the phase measuring system. Under these conditions, the refractivity is independent of the angle of the beam and is in good agreement with the published refractive constants for the modulator crystals.

The second set of experiments were conducted under field conditions over a baseline about 4 meters long. These experiments were designed to test the stability of the mechanical components in a realistic field environment.

These measurements continued for several days. During the measurement period the temperature varied from 13 degrees C to 23 degrees C, the pressure varied from 812 millibars to 825 millibars and the intensity of the optical beams was manually varied over four orders of magnitude by inserting absorption filters into the path. None of these changes had any effect whatsoever on the data. The sensitivity of the phase meters is 1 part in 4096 of a cycle which is equivalent to a distance of 0.03 mm, and the null result implies that the noise of the instrument in a field environment is less than this value.

The third set of measurements were made over a baseline about 900 m long. This length was chosen to be long enough so that the effects of the atmosphere ought to be observable while at the same time short enough that end-point measurements of atmospheric variables ought to be characteristic of the parameters along the path so that a quantitative comparison between the multiple wavelength determination of the refractivity and calculations using end-point parameters should be possible. During the measurement period the temperature varied from 2 degrees C to 20 degrees C and the pressure varied from 810 millibars to 830 millibars. We found very good correlation between the refractivity determined electromagnetically and the value calculated using end-point measurements on days when the short-term temperature fluctuations were small. On days when the temporal fluctuations were larger, the end-point measurements were not as representative of the average along the path. Although we were unable to explain this effect at the time, we subsequently found that rapid temporal fluctuations implied rather large spatial anisotropy so that the end-point measurements did not represent the average along the path during those periods. Although we were unable to map the spatial anisotropy of the temperature so as to make a quantitative comparison possible, the magnitude of the effect is about right to explain the discrepancy.

The final set of experiments were conducted over a baseline about 25 km long. The temperature varied from -5 degrees C to +5 degrees C during the course of the experiments, while the pressure was quite stable at 818 millibars. The end point temperatures typically differed by about 3 degrees C. These experiments yielded values for the atmospheric attenuation of the beams. We found that the red attenuation coeffecient was 0.00063, while the value for blue was 0.00025. These values imply atmospheric conditions in the range of standard clear to very clear. Consecutive 120 second averages of the refractivity had an rms deviation of 0.27 degrees in phase, which corresponds to a scatter of

less than 1 mm in distance. The values of the refractivity correlated well with the end-point measurements, but the temperature profile along the path was not known. The phase measuring system was able to cope with atmospheric turbulence and dropouts with no error.

Reports

These results were presented at the Fall AGU meeting. A more detailed report is being prepared now.

DETERMINATION OF "WHOLE EARTHQUAKE CYCLE" SYSTEMATICS: CONTINUED STUDIES OF LARGE EARTHQUAKES ($M_S = 7 - 7.5$) ALONG THE MIDDLE AMERICA TRENCH TO REFINE METHODOLOGIES AND MODELS FOR EARTHQUAKE PREDICTION

October 1, 1984 through September 31, 1985

14-08-0001-G977

Principal Investigator: Karen C. McNally
Charles F. Richter Seismological Laboratory
University of California, Santa Cruz
Santa Cruz, California, 95064
(408) 429-4137

Objectives

The objectives of this project are: (1) To continue analysis and evaluation of seismicity data prior to large ($M_W \geq 7.0$) earthquakes in Mexico. (2) To systematically develop and test physical and statistical models of long, intermediate and short term seismicity behavior for earthquake prediction using these data. To monitor ongoing seismcity patterns for prediction experiments, to develop and test methodologies based on (1) and (2). To obtain critical data for interpreting seismic quiescence by operating a field array in a cooperative project with Mexico.

Also, a case history for a large earthquake in Costa Rica is being compiled as follows: (1) Relocate the Samara mainshock in northwestern Costa Rica ($M_S = 7.0$), August 8, 1978; (2) Use Samara mainshock as a calibration event to relocate all WWSSN data, 1964–1983 ($m_b \geq 4.0$), in northwestern Costa Rica; (3) Relocate 1950 ($M_S = 7.7$) mainshock and aftershocks, based on (1) and (2), to refine the definition of the rupture zone area; (4) Relocate all local network data May 1, 1978–November 30, 1978 for the Samara sequence ($\approx$ 370 events, $M_L \geq 2.5$); (5) Finalize waveform modeling of the Samara mainshock for understanding the rupture mechanism and geometries for interpretation relative to the seismicity data; (6) Analyze all data from the new permanent network that pertains to the 1950 rupture zone area (i.e., geometries, fault mechanisms, etc.); and (7) Compare and interpret combined "near field" (i.e., local network) and "far field" (i.e., WWSSN) data from Costa Rica relative to the *whole earthquake cycle model* which is based on relocated global network data for large earthquakes in Mexico.

Results

I. The seismic manifestations ($m_b \geq 4.0$) of the stress accumulation, transfer and release processes associated with 6 large earthquakes ($7.0 \leq M_W \leq 8.1$) along the subduction zone in Mexico are remarkably coherent throughout a complete earthquake cycle of nearly 40 years. At least 3 systematic loading stages are indicated during 15 years prior to the mainshock, in contrast with nondescript background activity observed throughout the remainder of the cycle. This behavior appears to be independent of the mainshock magnitude [in the range $7.0 \leq M_W \leq 8.1$], time elapsed since the previous similar mainshock in the same location [range=31.5 to 74 yrs; median=38 yrs], and the length of the Benioff zone [downdip length from the mainshock ranges from 120 to 250 km]. The characteristic stages of loading are: (1) extensional stress transfer progressing from downdip to updip between 15 and 5 years before the mainshock and culminating in a final slippage of the future rupture zone; (2) quiescence of the future rupture zone between $\approx$ 5 years to 1 year before the mainshock; (3) slab reextension both downdip and updip, concluding in failure of the locked zone with a large mainshock. The complete earthquake cycle was generated by the superposition of 6 case histories with time renormalized to the mainshock occurrence in order to obtain the greatest possible reliability. We relocated all WWSSN and ISC seismic data for Mexico, from 1964 to present, using the JHD method combined with special field study data and also incorporated available and newly constructed earthquake fault-mechanisms into the analysis. The results suggest that seismic failure data follow a rational physical process and also that future work may lead to an accuracy of about one year for anticipating the occurrence of large earthquakes along the subduction zone in Mexico, provided that all WWSSN data ($m_b \geq 4.0$) were available and reprocessed in nearly real time.

II. We describe acceleration signals recorded for nine aftershocks of the September 19, 1985 Michoacan earthquake. To obtain this data set, three A–700 Teledyne–Geotech digital strong–motion instruments were operated temporarily at two sites on the José María Morelos (La Villita) Dam, and at a site located at about 12 km to the west of the town of Zihuatanejo. Peak horizontal accelerations of 0.005 g to 0.031 g were recorded at epicentral distances between 10 and 75 km, for earthquakes with magnitude (m_b) between 4.5 and 5.3. It was observed that the peak accelerations recorded at a site on the embankment of the dam (near the crest) are approximately three times those recorded on the abutment bedrock portion of the dam. Although these sites were spatially separated by no more than 300 m, differences among their records are also significant. Waveforms recorded at the embankment site look more complex than those from the abutment site. This fact, as well as the higher peak accelerations on the embankment, provides evidence of a strong influence of the structure of the dam on the ground motion at the embankment site.

III. The Levenberg–Marquardt non–linear least squares algorithm is used to invert for the crustal velocity structure in the epicentral region of the great ($M_S = 8.1$) Michoacan, Mexico, earthquake of September 19, 1985. The velocity model consists of a layer with linearly increasing velocity overlying a dipping, constant velocity halfspace. Our hypocentral location program uses a velocity model of the same form together with ray tracing. The hypocentral distribution obtained from aftershocks recorded by our local field array delineates a planar structure, roughly 10 km thick, dipping 14° at $N26°E$. This is in good agreement with the source geometry obtained by waveform modelling of the mainshock. The

earthquake hypocentral resolution obtained with this program is significantly better than that from conventional approaches (HYPO) and looks very promising for its applicability in complicated velocity structures like subduction zones.

IV. The size and source complexity of the great (M_S = 8.1) Michoacan, Mexico earthquake can be attributed to both a restriction of the downdip width of the seismic interface between the overriding and downgoing plates, and a uniform distribution of asperities. The seismogenic evidence of strain accumulation during the 20 years prior to the 19 September, 1985 mainshock closely resembles that observed prior to the smaller M_W=7.6 earthquakes in the adjacent Colima (1973) and Petatlán (1979) regions: the subsequent rupture zones are seismically quiescent ($m_b \geq$4.0) for $\sim$ 2.5 – 4 years prior to the mainshocks; the locked thrust interface is loaded by aseismic slip and normal faulting within the downgoing plate below 25–30 km. There is evidence that the 1981 Playa Azul earthquake (M_W = 7.3) is an integral stage of the evolutionary process of strain accumulation and release in the Michoacan area and could thus be considered a foreshock to the great 1985 earthquake. There is also evidence suggesting several episodes of lateral stress redistribution in a southeast direction along the thrust interface, consistent with southeast rupture propagation in the subsequent 1985 mainshock–aftershock sequence.

V. A large earthquake (M_S = 7.0) occurred on August 23, 1978 (00:38:26.96 U.T.) in Sámara, Costa Rica, on the Nicoya Peninsula (9°45.54'N, 85°34.48'W). A complete data set for the 1978 event was analyzed for a period of 115 days before and 33 days after the mainshock, with a total of 273 events well located (104 pre–mainshock events and 169 aftershocks). Historically, this northwestern region of Costa Rica has experienced two other large earthquakes: one in 1916 (M = 7.5), and another in 1950 (M = 7.7). Using the 1978 mainshock as master event, relocated WWSSN ($m_b \geq$ 4.0) seismicity for the period 1964–1984 shows a defined Benioff zone consistent with local findings. Local network data recorded throughout the 148 day observation period provide a more detailed picture of seismic activity than the relocated events that were recorded by the WWSSN for the 1964–1984 period. Seismicity within 50 Km arround the mainshock is relatively low and no activity within a 15 km radius of the mainshock occurs until one minute prior to rupture initiation at a distance of 6.7 km, thus terminating the quiescence which had been maintained in this area throughout the 115 day period. In addition, the local seismic activity before the mainshock is concentrated in thelower, i.e., downdip, portion of the subsequent aftershock zone. The rupture process, therefore, as observed from local network data suggests a weakening process, from downdip to updip, leading to final failure in the mainshock. We also concluded that the 1978 (M_S = 7.0) earthquake is spatially related to the 1950 (M = 7.7) event, implying a variable rupture mode for the same asperity. Another segment of the plate boundary, adjacent to and north of the 1950 and 1978 aftershock zones, ruptured during the 1916 (M = 7.5) event.

NOTE: Lists of earthquake relocations for the Guerrero and Oaxaca, Mexico and Costa Rica regions ($m_b \geq$ 4.0) from 1964–1983 are attached, following.

Publications

Stolte, C., K. C. McNally, G. W. Simila, J. González-Ruiz, A. Reyes, L. Munguía, C. Rebollar, and L. Mendoza, Fine structure of a postfailure Wadati–Benioff zone, *Geophys. Res. Lett.*, accepted, 1986.

Munguía, L., G. W. Simila, K. C. McNally, and H. Thompson, The September 19, 1985 Michoacan earthquake: Aftershock acceleration data recorded by a temporary installation of strong motion instruments, *Geophys. Res. Lett.*, accepted, 1986.

McNally, K. C., J. González-Ruiz, and C. Stolte, Seismogenesis of the 1985 great (M–S=8.1) Michoacan, Mexico earthquake, *Geophys. Res. Lett.*, accepted, 1986.

LeFevre, L. V., and K. C. McNally, 1985, Stress destribution and subduction of aseismic ridges in the Middle America subduction zone, *J. Geophys. Res.*, *90*, 4495–4510.

Abstracts

González, J., McNally, K. C., E. D. Brown and K. Bataille, 1984, The whole earthquake cycle of the Middle America trench, offshore Mexico, *EOS Trans.*, AGU, 65, 998.

Guendel, F., K. C. McNally, J. Lower, E. Malavassi, and R. Saenz, 1984, New evidence regarding subduction mechanisms near the southern terminus of the Middle America trench, Costa Rica, C. A., *EOS Trans.*, AGU, 65, 998.

Barrientos, S., S. N. Ward, K. C. McNally, and R. Stein, 1984, Inversion of moment distribution with depth for the Lost River fault: 1983 Borah Peak Idaho earthquake, *EOS Trans.*, AGU, 65, 998.

González, J., McNally, K. C., E. D. Brown and K. Bataille, 1984, The whole earthquake cycle of the Middle America trench, offshore Mexico, *GEOS Boletin, UGM*, 2.

Grupo de Trabajo en Perfiles Sismicos de Acapulco, 1985, Perfil sismico y microsismicidad en la zona de quietud de Acapulco, *GEOS Boletin, UGM*, 3, 20.

Grupo de Trabajo en Perfiles Sismicos de Oaxaca, 1985, Perfiles sismicos profundos en Oaxaca, *GEOS Boletin, UGM*, 3, 33.

C. J. Rebollar, L. Munguia, A. Reyes, L. Mendoza, J. Gonzalez, C. Duarte, J. Soarez, V. Wong, G. W. Simila, K. C. McNally, C. Stolte, J. González–Ruiz, J. Matter, A. Aburto, G. Nelson, D. Heil, J. Hayes, N. Breen, J. Tagudin, D. Parks, M. O'Mara, E. Gizzi, N. Spriggs, H. Thompson, Y. Koskelo and J. Collins, 1985, Preliminary locations of the aftershock of the September 19/20, 1985 Michoacan, earthquake, *EOS Trans.*, AGU, in press.

McNally, K. C., A. Nava, G. W. Simila, J. González–Ruiz, J. Gonzalez–Garcia and the Interinstitutional Working Group for Seismic Profiling in Guerrero, Mexico, 1985, Deep seismic profiling along the Middle America Trench: A joint Mexico–U.S. interim project of PASSCAL, *EOS Trans.*, AGU, 66, 1071.

Seismicity studies for earthquake prediction in Southern California

January 1, 1985 through December 31, 1985

14-08-0001-22000

Principal Investigator: Karen C. McNally
Charles F. Richter Seismological Laboratory
University of California, Santa Cruz, CA 95064
(408) 429–4137

Objectives.

The objective of the proposed work is to determine the statistical correlation of earthquake clusters (excluding aftershocks) with subsequent moderate and large mainshock events in southern California. Numerous data have already been analyzed uniformly and are available in sufficient quantity to provide results that are statistically meaningful. Using this data base, we will determine the number of earthquake clusters that are followed by large mainshocks compared with those that are not. Similarly, the number of mainshocks that are preceded by clusters, and those that are not, must be ascertained. These correlations will be determined as a function of (1) the magnitude of the mainshock, (2) the minimum magnitude threshold of the seismicity that constitutes a cluster (clustering increases with decreasing magnitude threshold of the seismicity data), (3) the time between the clustering and the mainshock, and (4) the distance (up to $\approx 50km$) between the cluster and the mainshock. The results will be formulated as probabilities for intermediate term (few weeks to few years) predicition applications, with appropriate scaling for compatibility with probabilities that may be used for long term (few years to few decades) predictions. A computer program for automated seismicity monitoring and probability determinations will be written.

Results.

A systematic statistical approach has been used to analyze regional seismicity ($M_L \geq 2.5 - 3.5$) and to identify and extract significant clusters. Data sets from 3 regions are being analyzed for developing automated methods for monitoring and detection: (1) Southern California, (2) Central California, and (3) Mammoth Lakes, California. The Mammoth Lakes study was covered in the report for USGS grant #14-08-0001-20546 for the period 1 January 1984 through 31 December 1984.

A. Earthquake clustering in southern California: review of data base.

In southern California since 1940, there have been ten large earthquakes ($M_L \geq 6$) and two earthquakes of $M_L \geq 5.5$ that we have classified as mainshocks. Statistical analyses of case histories reveal that in all cases these earthquakes were preceded by anomalous clusters of smaller earthquakes within approximately 30-50 km, within 0.2 to 5 years. Forty percent were preceded by an anomalous within 2 years, 90% within 4 years. Fifty–eight percent of the mainshocks were preceded by several anomalies. One anomaly has occurred with no earthquake having yet followed. The possible occurrence of multiple anomalies is a problem for forward prediction monitoring. Consider that an anomaly has occurred; one does not know whether it is the first of several, or the last, before the mainshock. In this situation one must consider the probabilities relative to the times between the *first* anomaly and the mainshock, not the last anomaly. We consider the percentage of earthquakes which occurred as a function of the time from the first anomaly to the mainshock. In 30% of the cases, the mainshock occurred within two years, with no second anomaly. These percentages are similar to actual probabilities, although in detail the probability would also consider the long-term probability, the probability of the cluster being truly "anomalous",and additional probabilities based on other geophysical data. With respect to earthquake monitoring and warning for public prediction applications the following points should be considered. The probability of a mainshock increases with the increasing time uncertainty that a community is willing to tolerate. For example, if the public is only concerned with probabilities of 50% or higher, the time scales of the anomalous data indicate an associated temporal uncertainty of from 0.2 to 5 or 7 years. Also the probability of a mainshock increases if the mainshock magnitude uncertainty is greater, i.e. $M_L \geq 5.4$ rather than $M_L \geq 6.0$. We observe a trend of increasing time of the anomaly with increasing size of the mainshock; however, the number of the largest earthquakes in southern California during the period of instrumental measurement constitutes the smallest sample of observations.

B. Predictability of mainshocks and earthquake clustering in Central California.

The Bear Valley – Stone Canyon (BV-STC) section of the San Andreas fault in central California is a zone of transition from locked to aseismic fault slip behavior. $M_L 4.9 - 5\frac{1}{2}$ earthquakes have occurred every 11.0 ± 1.8 years (95% confidence) since 1936. If less well documented events in 1916 and 1929 are included, the calculated re-occurrence time is 11.0 ± 0.7 years. These data suggest a 95% chance that the next event should occur between Apr 1981 and Aug 1985 (1983.51 ± 2.16) and a 99% chance that the next event occurs between Mar 1980 and Sep 1986 (1983.51 ± 3.24).

Present day aseismic slip rates along the BV-STC to Parkfield (PKFD, 100 km SE of BV-STC) section of the San Andreas fault define a symmetric distribution peaked at midpoint and locked at both ends. This suggests that rates of strain accumulation and release at BV-STC and PKFD may also be similar. A linear fit to the $M_L \geq 4.9$ earthquake sequence in PKFD since 1922 gives an average re-occurrence time of 10.9 ± 1.6 years, which is half the commonly quoted 22 years for $M_L \geq 5.5$ and also has a higher statistical certainty. With 95% confidence this is identical to the BV-STC ($M_L \geq 4.9$) re-occurrence time. The next PKFD earthquake is predicted to occur in 1987.34 (± 4.80 years, 95%), about 4 years after the next predicted BV-STC event. During the last 60 years, BV-STC earthquakes ($M_L \geq 4.9$) have preceded PKFD ($M_L \geq 4.9$) earthquakes by 4.24 ± 1.63 years.

In BV-STC, relocations for all $M_L \geq 4$ earthquakes since 1936 outline a 30 km active fault section and suggest that $M_L 4.9$ to $5\frac{1}{2}$ earthquakes break along equally spaced segments of $\approx$ 6 km. If one segment breaks every 11 years, the repeat time for the entire section is 44 to 55 years, depending upon the interpretation of a 1961 earthquake doublet.

Two distinct patterns suggest that the location of the next $M_L 4.9 - 5\frac{1}{2}$ earthquake in BV-STC should be between 36°36′ and 36°41′, near the location of the 1938 event:

1) The other adjacent segments have produced > 50% more cumulative seismic moment release since 1936 and the 1938 segment has not had a $M_L \geq 4.9$ for 47 years.

2) Large clusters (4 or more events) have preceded other large events locally, as well as elsewhere in California, by $\approx 5 - 10$ years. This segment has had 4 large clusters since 1981 and 8 since 1972.

C. Earthquake potential of the San Gregorio–Hosgri fault zone, California

The seismic and geologic records indicate that the San Gregorio-Hosgri fault system is capable of generating $M = 7.2 - 7.4$ earthquakes. The seismically quiescent San Francisco-Santa Cruz and Monterey-Ragged Point segments of the coastal fault zone may represent seismic gaps and therefore be the most likely segments to next experience $M \geq 7$ earthquakes. The January 23, 1984 Big Sur earthquake ($M = 5.2$) may signal the commencement of the active phase of a seimic cycle preceding a future event on the Monterey-Ragged Point fault segment.

An earthquake catalog was compiled for the central California coastal region and examined visually. Increased seismic activity preceding, and decreased activity following, the 1926 Monterey Bay doublet ($M = 6.2$), and the 1927 Lompoc ($M_w = 7.3$) and 1952 Bryson ($M = 6.0$) earthquakes suggest that the San Gregorio-Hosgri fault system releases strain cyclically via moderate and large ($4 \leq M \leq 6$) earthquakes over 60-100 yr periods. Doughnut-patterned seismicity ($4 \leq M \leq 6$), seismic quiescence bordered by seismic activity, preceded the Monterey Bay, Lompoc, and Bryson earthquakes. These events were also preceded by clustered seismicity ($2.5 \leq M \leq 6$) in the vicinity of the subsequent earthquake epicenter. Presently, the segments of the San Gregorio-Hosgri fault system between San Francisco and Santa Cruz and between Monterey and Ragged Point exhibit similar doughnut-patterned seismicity. A lack of large ($M \geq 6$) events on these segments indicate that they may be seismic slip gaps. The terminations of fault segments that ruptured during the Monterey Bay doublet and the Lompoc and Bryson earthquakes are estimated using an empirical relationship between earthquake magnitude and source area and coincide with the ends of the San Francisco-Santa Cruz and Monterey-Ragged Point segments, supporting the hypothesis that these segments are seismic gaps. A comparison of seismic and geologic slip rates indicates that these segments are characterized by a minimum 0.8 mm/yr or maximum 15 mm/yr slip deficit resolvable by $M = 6.3$ or 7.2 earthquakes, respectively. The maximum expectable earthquakes estimated from fault dimensions are $M = 7.4$ for the San Francisco-Santa Cruz segment and $M = 7.3$ for the Monterey-Ragged Point segment, similar to the larger earthquake magnitudes needed to resolve current slip deficits.

The Monterey-Ragged Point segment is the most poorly understood and therefore most critical link in the fault system. In the Big Sur coastal area, geomorphic and geologic

features related to faulting indicate that the Church Creek, Palo Colorado, and Rocky Creek faults accomodate 30-45 percent of the geologic slip measured on the San Gregorio fault, supporting, but not requiring, a link between the San Gregorio and San Simeon-Hosgri fault zone via the Sur fault zone. The largest historic earthquake recorded on the Monterey-Ragged Point segment since 1800, the January 23, 1984 Big Sur earthquake ($M = 5.2$), and its aftershocks were relocated with HYPO71(revised) and HYPOINVERSE. Focal mechanism solutions for the mainshock and three aftershocks are stylistically similar and indicate predominantly right lateral, strike-slip motion on a $N\,25-31^{\circ}\,W$ striking fault that dips to the northeast. The Rocky Creek and/or closely associated fault appears to have been the source of the earthquakes. The Big Sur earthquake may indicate increasing stress in this area and may signal the beginning of the active phase of a seismic cycle leading up to a large event.

The occurrence of $7 \leq M \leq 7.5$ earthquakes along the San Gregorio or Sur fault zone could have a serious impact in populated areas surrounding Monterey and San Francisco Bays and impair reservoirs and transportation facilities in the Santa Lucia and Santa Cruz Mountains. Whether or not the San Francisco-Santa Cruz and Monterey-Ragged Point fault segments are seismic gaps is critical in the prediction of future events on the coastal fault system. Additional studies are needed to test the hypothesis that these two segments are seismic gaps and to better define the possible time of occurrence of a future $M \geq 7$ event.

Reports

Tuttle, M., 1985, Earthquake potential of the San Gregorio – Hosgri fault zone, California, University of California, Santa Cruz.

Abstracts

Nelson, G. D. and K. C. McNally, 1985, Predictable earthquake sequence near the terminus of a locked zone: Bear Valley – Stone Canyon area; San Andreas fault, central, California, EOS Trans., AGU, *66*,971.

Tuttle, M. P. and K. C. McNally, 1986, Earthquake potential of the San Gregorio – Hosgri fault zone, California, Earthquake Notes, Seismol. Soc. Am., in press.

MAGNETIC FIELD OBSERVATIONS

9960-03814

R. J. Mueller
Branch of Tectonophysics
U.S. Geological Survey
345 Middlefield Road, MS/977
Menlo Park, CA 94025
(415) 323-8111 ext. 2533

INVESTIGATIONS

1) Investigation of total field magnetic intensity measurements and their relation to seismicity and strain observations along active faults in central and southern California.

2) Recording and processing of synchronous 10 minute magnetic field data and maintenance of the 25 station telemetered magnetometer network and its receive telemetry system for central and southern California.

RESULTS

1) Processing and analysis of differential magnetic field and intermediate-baseline geodetic data from nets near the northern end of the Red River fault in Yunnan Province, China.

2) Analysis of magnetic field data for the period before and after the January 26, 1986, M=5.2 - M=5.5, earthquake located ~15 km east of Hollister, California indicated no magnetic field change associated with this event. The closest magnetometer stations (SJNM & HARM) were located ~18 km from the epicenter of the earthquake.

3) Planning of logistics for the installation of 3 component borehole strainmeters in the Parkfield region of California. Installations are scheduled for the summer-fall of 1986.

4) Conversion of three magnetometer stations in the Parkfield region of central California from telephone line telemetry to satellite telemetry systems.

5) Computer programs were implemented on the PDP 11/44 to automatically update the telemetered magnetic field data base on a daily basis. The averaged differenced data from the Parkfield region are compared to predetermined alarm thresholds and the data sets are flagged if the threshold value is exceeded.

No alarm thresholds have been exceeded since mid-February when the system was made operational.

REPORTS

Johnston, M.J.S., Chen Zhong-Yi, and Mueller, R.J., Strain and Magnetic Field Changes on the Red River Fault System Near Dengchaun and Liante, Yunnan, China: 1980-1985, Trans. Am. Geophys. Un., v. 66, p. 1061, 1985.

Mueller, R.J. and Myren, D., Automatic Rezeroing Circuit for Bore-Hole Dilatometer, U.S. Geol. Surv. Open-File Report 86-109, 1986.

Ware, R.H., Johnston, M.J.S., and Mueller, R.J., A Comparison of Proton and Self-Calibrating Rubidium Magnetometers for Tectonomagnetic Studies, J. Geomag. Geolectr., 37, 1051-1061, 1985.

CRUSTAL STRAIN

9960-01187

W.H. Prescott, J.C. Savage, M. Lisowski, N. King
Branch of Tectonophysics
U.S. Geological Survey
345 Middlefield Road, MS/977
Menlo Park, California 94025
(415) 323-8111, ext. 2701

Investigations

The principal subject of investigation was the analysis of deformation in a number of tectonically active areas in the United States.

Results

1. Strain Accumulation in the Yakataga, Alaska, Seismic Gap

Strain accumulation in the Yakataga seismic gap has been estimated from the deformation of a 60 km x 40 km trilateration network surveyed in 1979-1980, 1982, and 1984. The contraction in the approximate direction (N19°W) of plate convergence is 0.19 ± 0.04 μstrain/a. In addition there is a minor (0.07 ± 0.04 μstrain/a) orthogonal extension and a significant right-lateral shear (0.09 ± 0.02 μstrain/a) across a vertical plane striking N71°E. A simple dislocation representation of the plate-interaction model proposed by Lahr and Plafker for the Yakataga seismic gap quantitatively accounts for the observed N19°W contraction and qualitatively accounts for the right-lateral shear, the two strains being associated with the normal and transverse components, respectively, of the oblique convergence between the Yakutat block and the North American plate. The measurements are consistent with strain accumulation building up to a great thrust earthquake in the Yakataga gap. In addition there is a suggestion of right-lateral shear-strain accumulation across the Contact fault, but the interval over which data are available is probably too short to prove such accumulation.

2. Deformation in Long Valley Caldera 1983-1985

A comparison of the deformation measured in the 1983-1984 interval with that measured in the 1984-1985 interval indicates that except for local deformation along the south moat fault deformation in the two intervals does not differ significantly. Specifically, within the resolution Geodolite and leveling surveys there is no evidence for a slowing down of the major

source of deformation (swelling of a magma chamber beneath the resurgent dome).

3. Status of GPS Observations

We have begun a series of experiments designed to investigate the applicability of Global Positioning System (GPS) technology to the measurement of crustal deformation. Experiments involving lines of lengths near 30 km and less than 10 km have already begun. Observations of longer lines should begin next month. Software to process the observations is now operational, if not convenient. Present results have been obtained without the benefit of improved orbits, only the "broadcast orbits" have been employed thus far. Even with these orbits, the first determinations of position difference over a 43 km line indicate repeatability at the level of about 0.3 ppm, over a time period of about 6 months. The nominal precision of the broadcast orbits is 2-5 ppm although the initial results suggest they may be better than expected. Final tests of the precision will require "post-processed" orbits.

4. Continuing Deformation in the Vicinity of the Morgan Hill Earthquake

In previous discussions the large changes following the Morgan Hill earthquake (M_L=6.2, 85/04/24) have been interpreted as evidence of post-seismic slip. This interpretation was supported by an apparent exponential slowing in the rate of change of some of the lines. However, it is becoming apparent that many lines are continuing to change at a rate that has not decayed to the pre-Morgan-Hill-earthquake rate. The post-Morgan Hill changes suggest a continuing major strain episode in the Mt. Hamilton area. Deformation due to the Mt. Lewis (M_L=5.3, 86/03/31) earthquake is undetectable against the background of this strain episode. In fact, the Mt. Lewis earthquake may be a result of this strain episode.

5. Geodolite Instrumentation: Computer-Controlled Data Acquisition

In an effort to improve the accuracy of Geodolite distance measurements and eliminate survey blunders, we have developed computer-controlled data acquisition systems for the Geodolite and for the aircraft-mounted meteorological probes. The meteorological profiles used to correct Geodolite rangings for refractivity have been recorded with a data acquisition computer since 1981. The computer's user interface prompts for all necessary information and accepts average temperature and humidities from each of the two meteorological probes. Probe

malfunctions, identified by a split in the average values, are spotted in the field and corrective actions are taken. Geodolite rangings have been recorded with a data acquisition computer since the summer of 1985. All the necessary Geodolite, reflector, and meteorological data needed to reduce a line length are entered in, or recorded by, the computer. Line lengths are reduced after each pass of the aircraft between the Geodolite and the reflector, and the field reduced values are compared with projected line lengths deduced from previous measurements. If the average distance after two passes is outside of the allowable limit, an additional pass is flown to check the distance. If the measurement is still anomalous, it is repeated later in the day or on the following day after resetting the Geodolite and the reflector. The algorithm used to reduce the line lengths in the field (where only the averages from the meteorological profiles are available) gives the results that are accurate to better than 0.1 ppm. Final reduction of the line lengths in the office is generally completed the day after downloading the data from the field computers to the office computer.

Reports

Estrem, J. E., M. Lisowski, and J. C. Savage, Deformation in Long Valley caldera, California, 1983-1984, J. Geophys. Res. 90, 12683-12690, 1985.

Gross, W. K., and J. C. Savage, Deformation near the epicenter of the Round Valley, California, earthquake, Bull. Seismol. Soc. Am., 75, 1339-1347, 1985.

Savage, J. C., M. Lisowski, and W. H. Prescott, Strain accumulation in the Shumagin and Yakataga seismic gaps, Alaska, Science, 231, 585-587, 1986.

Savage, J. C., and G. Gu, The 1979 Palmdale, California, strain event in retrospect, J. Geophys. Res., 90, 10301-10309, 1985.

Savage, J. C., M. Lisowski, and W. H. Prescott, Strain accumulation in the Rocky Mountain States, J. Geophys. Res., 90, 10310-10320, 1985.

Zoback, M. D., W. H. Prescott, S. W. Krueger, Evidence for lower crustal ductile strain localization in southern New York, Nature, 317(6039), 705-707, 1985.

Seismic Studies of Fault Mechanics

9930-02103

Paul A. Reasenberg
U.S. Geological Survey
345 Middlefield Road, Mail Stop 977
Menlo Park, California 94025
(415) 323-8111, Ext. 2049

Investigations

1. Development of a computer algorithm to obtain double-couple fault-plane solutions from earthquake first-motion polarity data.

2. Investigation of seismicity clustering.

3. Preliminary investigation of the January 26, 1986 Tres Pinos earthquake sequence.

4. Preliminary investigation of the March 31, 1986 Mt. Lewis earthquake.

Results

1. The fault-plane solution program described in the last report was released and is described in Reasenberg and Oppenheimer (1985). Recent application of the program to regional and teleseismic data reveals that the program functions well with these data sets as well as with local data for which it was designed.

2. No new results this reporting period.

3. Hypocenters and fault-plane solutions for the January 26, 1986 (M5.3) Tres Pinos earthquake near the Quien Sabe and Bradley faults east of Hollister, Ca. and its aftershocks, reveal a north-northwest-striking nearly vertical plane that parallels the Bradley fault and is tentatively identified as the mainshock fault plane. Deformation on the plane was apparently dextral strike-slip . Significant off-fault aftershock activity east of the plane in the 6 days following the mainshock is consistent with distributed or left-stepping en echelon dextral shear and inconsistent with movement on a single throughgoing fault surface there.

4. Preliminary determination of the focal mechanism for the March 31, 1986 (M5.7) earthquake near Mt. Lewis, California (approximately 25 km south of Livermore) yields a well-determined strike-slip solution with dextral slip plane striking N5°W and dipping 80°W. This solution and the distribution of aftershock hypocenters are consistent with the presence of a north-striking vertical fault cutting the East Bay Coast Range northeast of the Calaveras fault.

Reference

Reasenberg, P. and D. Oppenheimer, 1985, FPFIT, FPPLOT and FPPAGE: Fortran computer programs for calculating and displaying earthquake fault-plane solutions, U.S. Geological Survey Open-File Report 85-739.

COUPLED DEFORMATION - PORE FLUID DIFFUSION EFFECTS IN FAULT RUPTURE

14-08-0001-G-978

J.W. Rudnicki
Department of Civil Engineering
Northwestern University
Evanston, Illinois 60201
(312)491-3411

Investigations

Dilatant hardening effects due to uplift and near-fault microcracking accompanying fault slip.

Results

We have continued investigating the effects of coupling between pore fluid diffusion and dilatancy accompanying slip on the postpeak deformation of a layer loaded by a combination of shear displacement and normal stess. A fault or frictional surface is assumed to have formed at peak stress and the subsequent deformation is due to a combination of slip on the frictional surface and elastic unloading in the surrounding material. The shear stress on the fault is related to the slip and decreases from a peak value τ_p to a residual value τ_r as the slip increases from zero to δ_0. Dilatancy due to uplift and near-fault microcracking is associated with slip, but saturates when the shear stress reaches τ_r. Calculations are simplified by assuming that the flux of pore fluid into the layer is proportional to the difference between the pore fluid pressure on the fault and that in an exterior reservoir.

As reported previously, we have modelled satisfactorily the observations by Martin [Geophys. Res. Letters, 7, 404-406,1980] of pore pressure stabilization of failure in Westerly granite. The results are, however, sensitive to the detailed shape of the stress versus slip relation and these are not known accurately.

Our recent work has concentrated on determining whether this mechanism of stabilization can be significant for slip under crustal conditons. The main impediment to extending the analysis to this case is the extremely small values of the ratio of the time scale of imposed tectonic straining to that for fluid diffusion. We have, however, recently developed an asymptotic analysis that overcomes this obstacle but we have not yet completed evaluation of the results of this analysis.

We have also been investigating a more elaborate numerical analysis aimed at evaluating the assumption of steady state flow into the dilatant zone. Preliminary results appear not to differ significantly from those of the simpler model.

Hydrogen Monitoring (9980-02773)

Motoaki Sato and Susan Russell-Robinson (FTS 959-6766)
Branch of Igneous and Geotherm Processes
U.S. Geological Survey, MS 959, Reston, VA 22092

Investigations

Hydrogen (H_2) in soil along the San Andreas and Calaveras faults are continuously monitored at eight sites by using fuel-cell sensors and data are telemetered to Menlo Park, CA. Efforts are directed toward the accumulation of valid data, correlations with seismic data, understanding of tectonic and chemical mechanisms for H_2 emissions along active faults, and improvement of the monitoring method.

Results

General: There was one M > 5 earthquake in the vicinity of the monitored area (Tres Pinos earthquake, 27 January 1986, M = 5.5, Fig. 1) during this reporting period. Preseismic H_2 changes were recorded at Wright Road (H2WR in Fig. 1) and Shore Road (H2SH) as shown in Fig. 2.

Anomalous H_2 activities began increasing during December 1985 in the Parkfield segment of the San Andreas fault (Fig. 3). The activities subsided (may be temporarily) near the end of March 1986. A significant point is that two peaks of about 200 ppm magnitude appeared at Gold Hill (H2GH) in mid-December and mid-February for the first time since the installation of this site in July 1982.

Calaveras Fault

Wright Road (H2WR): This site was closest to the epicenter of the Tres Pinos earthquake (12.8 km to NNW), and recorded a large H_2 peak 17 hours prior to the earthquake (Fig. 2). A small increase in H_2 began at about 0800 GMT on January 18, 1986. A rapid increase began at about 0200 GMT on January 25, and culminated in a 1900-ppm at about 0200 GMT on January 26. Telemetry failed between September 12 and December 7, 1985 (corroded battery cable), and again from March 10, 1986 to present (cause undetermined).

Shore Road (H2SH): After exhibiting some anomalous changes earlier (between June 24 and August 8, 1985), there were no anomalous events at this site until November 2, when a 250-ppm (above the baseline) peak appeared (Fig. 1). The anomalous changes continued until the Tres Pinos earthquake. The telemetry line was disconnected during the work to reconstruct the creepmeter, which was damaged by the earthquake. The line was reconnected on March 9, but signal from this site was wild (at least partly due to disturbed telemetry system, although correlation with March 31 earthquake cannot be ruled out).

San Andreas Fault

San Juan Bautista (H2SJ): No events as usual.

Cienega Winery (H2CW): A barely recognizable positive H_2 peak was recorded on 28 January 1986, a day after the Tres Pinos earthquake. This peak, however, may possibly be caused by wine spillage that occurred at the Winery due to the earthquake.

Melendy Ranch (H2MR): No events as usual.

Slack Canyon (H2SC): There was a small peak (30 ppm) on January 31, 1986, after which the H_2 emission level dropped by about 60 ppm (Fig. 3).

Middle Mountain (H2MM): Solar power supply continues to be a problem.

Parkfield (H2PK): There were four broad peaks recorded between December 10, 1985 and March 30, 1986, the largest peak reaching nearly 1000 ppm on January 26 (Fig. 3).

Gold Hill (H2GH): There was a brief 200-ppm peak on December 15, 1985, and a broader 200-ppm peak between February 7 and February 17, in 1986. These peaks were the first substantial peaks recorded at this site since its installation in 1982.

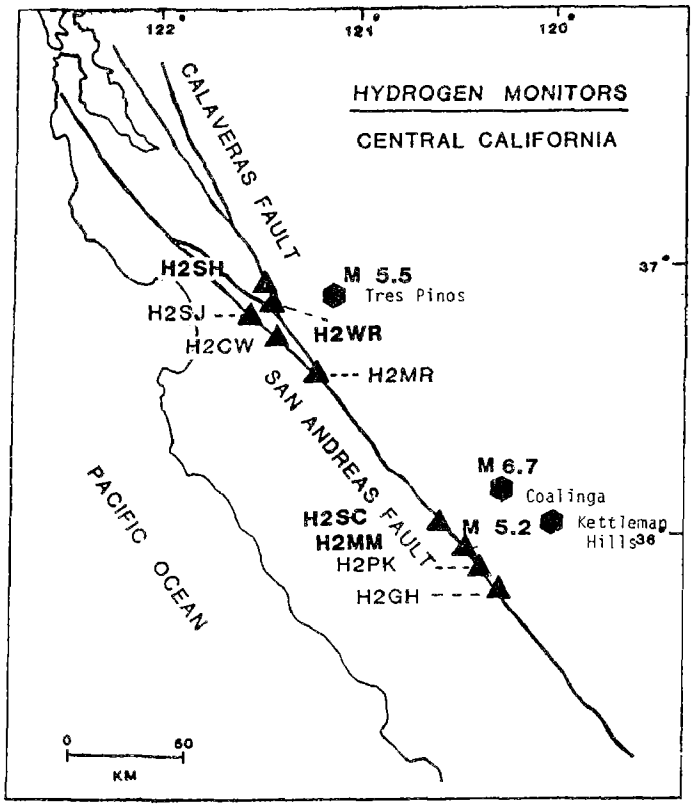

Fig. 1. Locations of hydrogen monitoring sites (triangles) and epicenters of recent M > 5 earthquakes (hexagons) in the monitored area.

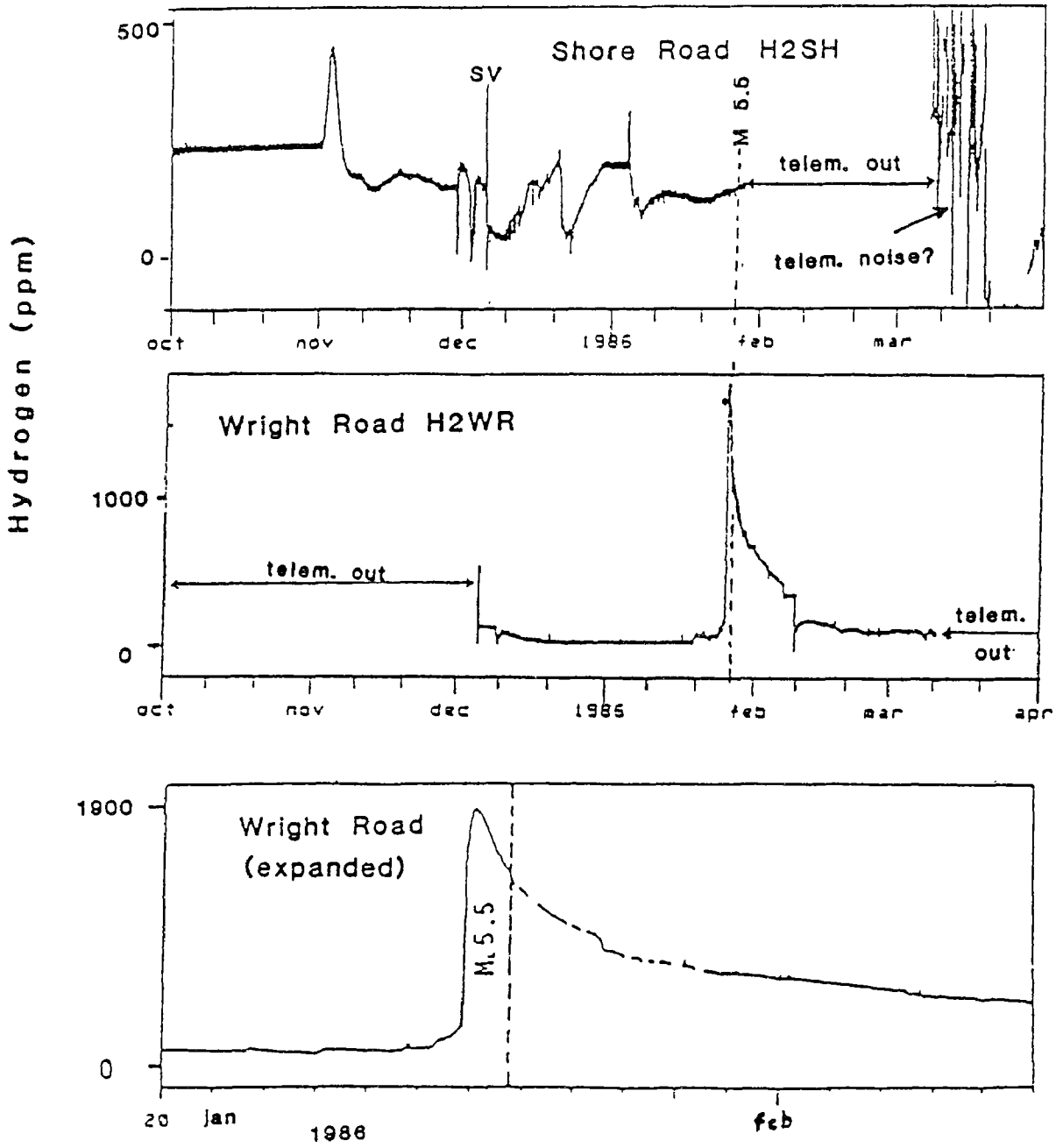

Fig. 2. Hydrogen changes recorded at Shore Road (top) and Wright Road (middle) between Oct. 1, 1985, and April 1, 1986; also time-expanded plot of the Wright Road data between Jan. 20 and Feb.6, 1986 (bottom).

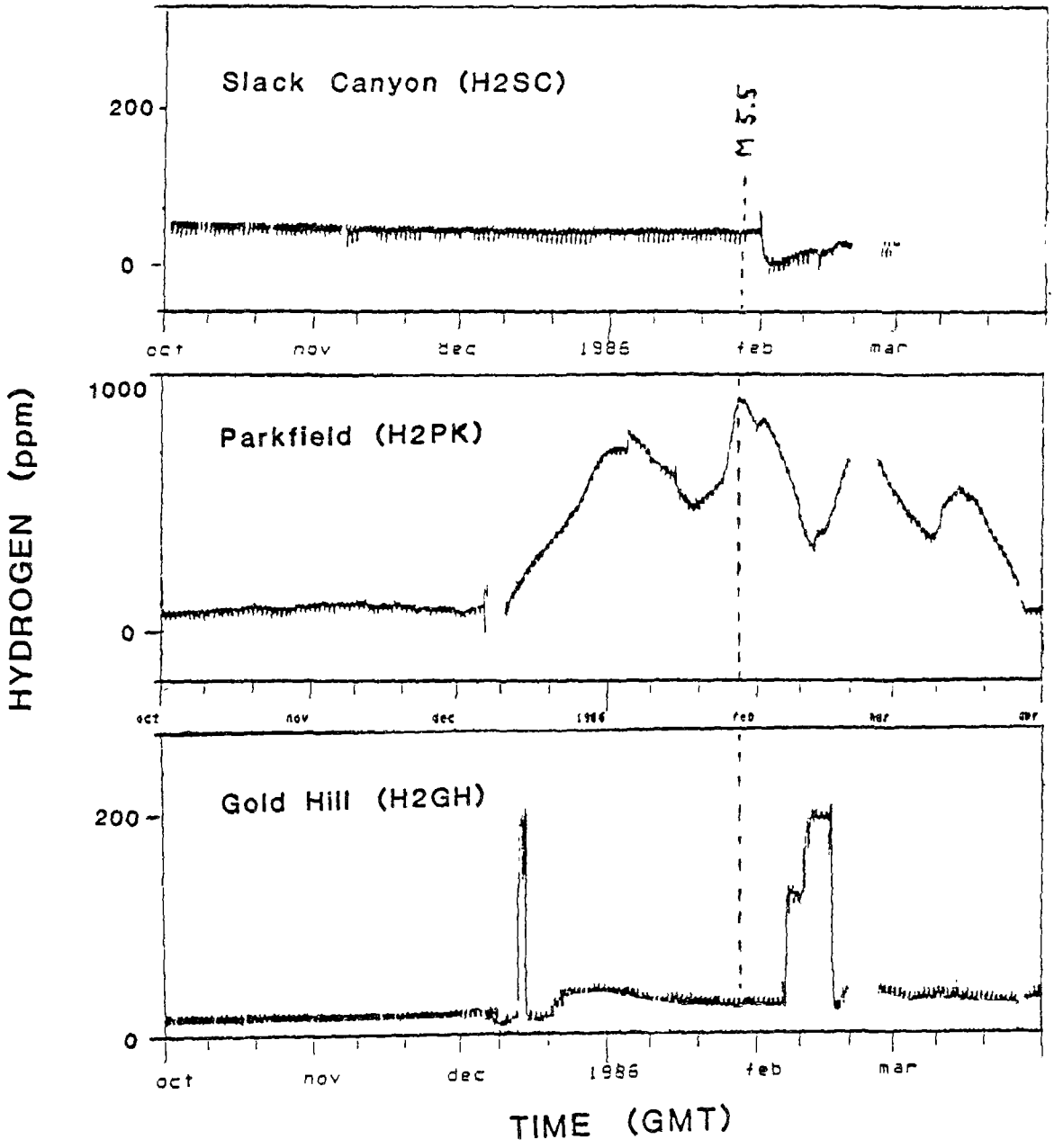

Fig. 3. Hydrogen changes recorded at Slack Canyon (top), Parkfield (middle), and Gold Hill (bottom) on the San Andreas fault between Oct. 1,1985, and April 1, 1986.

FAULT ZONE TECTONICS

9960-01188

Sandra S. Schulz
Branch of Tectonophysics
U.S. Geological Survey
345 Middlefield Road, MS/977
Menlo Park, California 94025
(415) 323-8111 x 2763

Investigations

1. Directed maintenance of creepmeter network in California.

2. Updated archived creep data on PDP 11/44 computer.

3. Installed a new creepmeter to replace creepmeter XDR1 (Durham Ranch) 1.6 km south of Parkfield.

4. Continued to establish and survey alinement array network on California faults.

6. Monitored creepmeter and alinement array data for retardations or other possible earthquake precursors.

Results

1. Currently 29 extension creepmeters operate; 21 of the 29 have on-site strip chart recorders, and 19 of the 21 are telemetered to Menlo Park. A computer program continues to check Parkfield telemetry data once each hour and alert Project personnel via 'beeper' whenever unusual fault movement occurs.

2. Fault creep data from all USGS creepmeter sites along the San Andreas, Hayward and Calaveras faults have been updated through January 1986, and stored in digital form (1 sample/day). Telemetry data covering the period between February 1, 1986, and the present are stored in digital form (1 sample/ten minutes), updated every ten minutes, and merged with the daily-sample data files to produce complete plots when needed.

3. A new 30-meter-long creepmeter (XDR2) was installed across the San Andreas fault 1.6 km southeast of Parkfield to replace the 10-meter-long creepmeter (XDR1) located at the same site since 1969 (Figure 1). Under permit requirements, XDR1 was removed immediately after XDR2 was

completed. The new instrument, three times longer than the old one, may cover more than one trace of the fault, as evidenced by clear changes in soil composition along the trench axis during excavation.

4. Continued to receive and process alinement array survey data every three months for 10 arrays being measured under contract by a private surveying firm. Five of the arrays are in the Imperial Valley and five in Parkfield. Sent out a Request for Proposals for the surveying of five Parkfield arrays every 3 months during the period June 1986 to May 1987. Continued work on a preliminary catalog of alinement array data from 1983 through 1986.

5. Parkfield

In May, 1983, XPK1 creepmeter, 0.5 km west of Parkfield, recorded a 6-mm right-lateral step during the Coalinga earthquake, then right-lateral movement slowed until August 9, 1985. On that day, coincident with a magnitude 3.55 aftershock of the Kettleman Hills earthquake (8/4/85, M 3.5), right-lateral creep at XPK1 resumed at a rate of 15.6 mm/yr for 35 days, followed by an acceleration for 10 days at a rate of 27.4 mm/yr. That period, in turn, was followed by a four-day surge (9/23 to 9/27) of 1.25 mm, after which the creep rate settled to 18.8 mm/yr. It is interesting to note that the average rate for XPK1 from 1979 to May 1983 was 12.5 mm/yr (Figure 2).

During the extremely heavy rains of winter 1985-86, several Parkfield creepmeters recorded unusually rapid movement, reminiscent of speed-ups seen on the same instruments during the heavy rains of 1982-83, just before the Coalinga earthquake.

Hollister-Cienega Valley area

The USGS maintains four creepmeters on the Calaveras fault northwest of the epicenter of the January 26 Tres Pinos earthquake (SHR1, HLS1, HLD1, Figure 1). Three of the instruments no longer record on-site; dial readings are made every three months, and the last routine readings by USGS personnel were on November 1, 1985. However, San Francisco State University personnel surveying in the area on December 7 did make a reading at one creepmeter (HLS1). A comparison between that reading and one the day after the earthquake shows a 4.3 mm difference. It is not certain the movement was related to the earthquake, but Hollister creepmeters traditionally record most of the annual slip in early fall.

The fourth Calaveras instrument is SHR1 (Shore Road), 10 km northwest of Hollister. Although presumably recording on-site and on telephone telemetry at the time of the earthquake, the instrument failed to indicate a response, either then or in the days to come. However, during a routine maintenance visit three days later, the creepmeter was found extended off scale; during an attempted reset, the rod broke. Dial readings at SHR1 indicate a minimum movement of 13+ mm between November 1, 1985, and January 30, 1986. SHR1 normally records approximately 12 mm/yr of creep.

The network also includes six creepmeters on the San Andreas fault west of the epicenter (XSJ2, XHR1, CWN1, CWC3, XFL1, XMR1, Figure 1). Five of the instruments recorded coseismic steps, and three then recorded significant afterslip (Figure 3). Preliminary tests of a fault-interaction model being developed by Robert Simpson of the USGS indicate coseismic step directions recorded on the San Andreas creepmeters are consistent with static changes in shear stress resolved onto the plane of the San Andreas fault resulting from the January 26 earthquake slip.

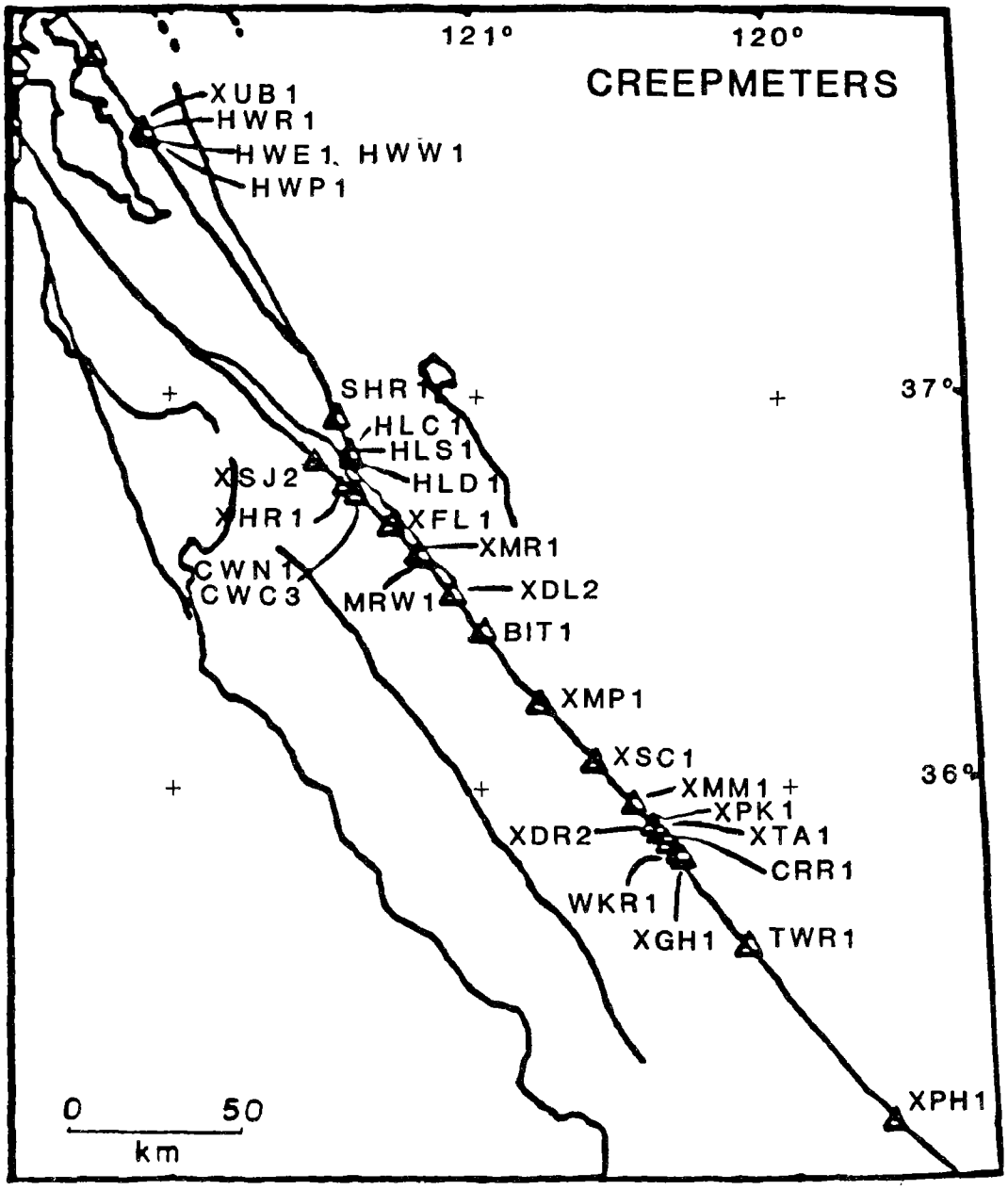
121°
120°
CREEPMETERS
XUB1
HWR1
HWE1, HWW1
HWP1
SHR1
HLC1
HLS1
XSJ2
HLD1
XHR1
XFL1
XMR1
CWN1
CWC3
MRW1
XDL2
BIT1
XMP1
XSC1
XMM1
XPK1
XDR2
XTA1
CRR1
WKR1
XGH1
TWR1
XPH1
37°
36°
0
50
km

FIGURE 1

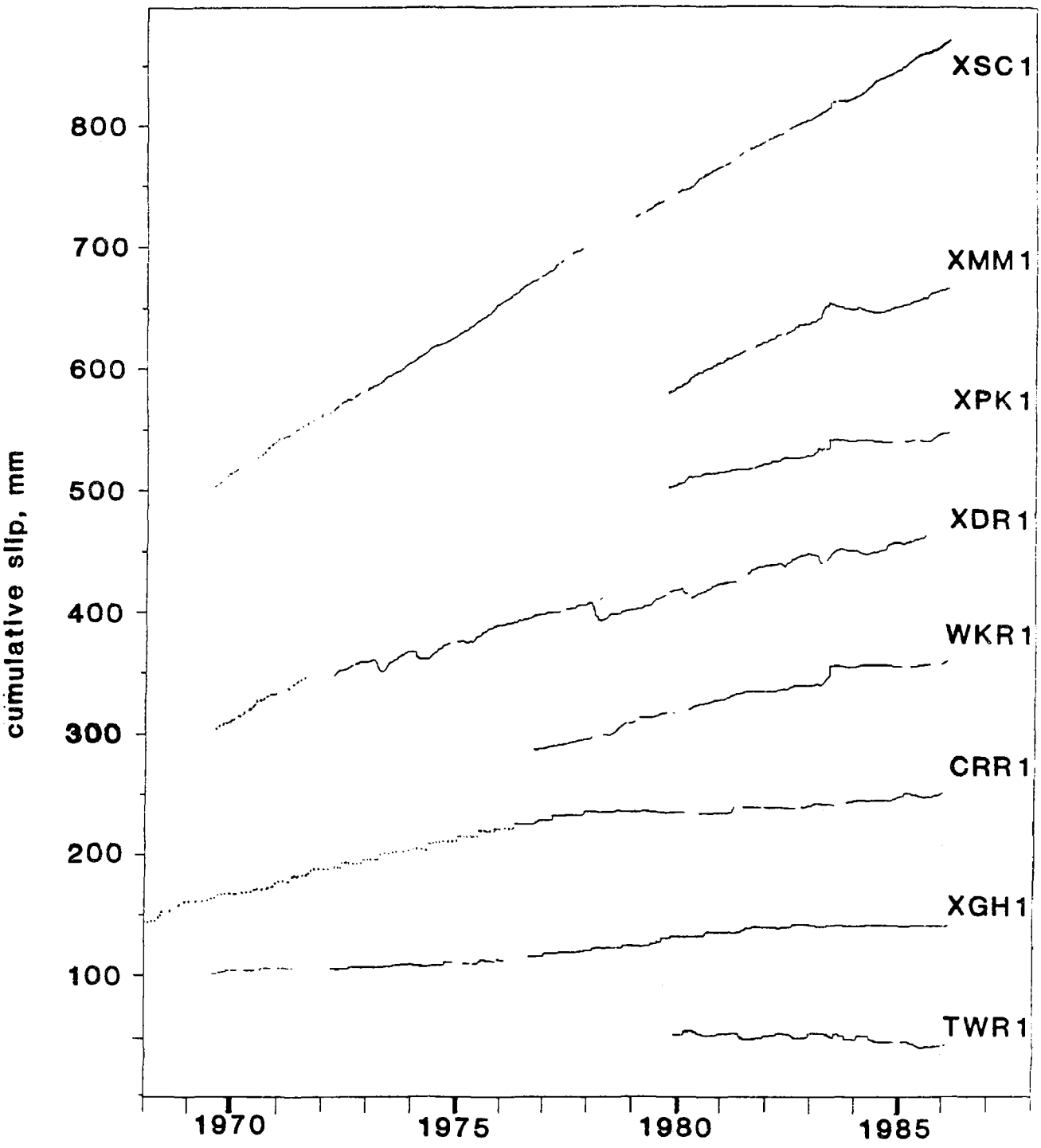

PARKFIELD CREEPMETERS
as of February 1, 1986

FIGURE 2

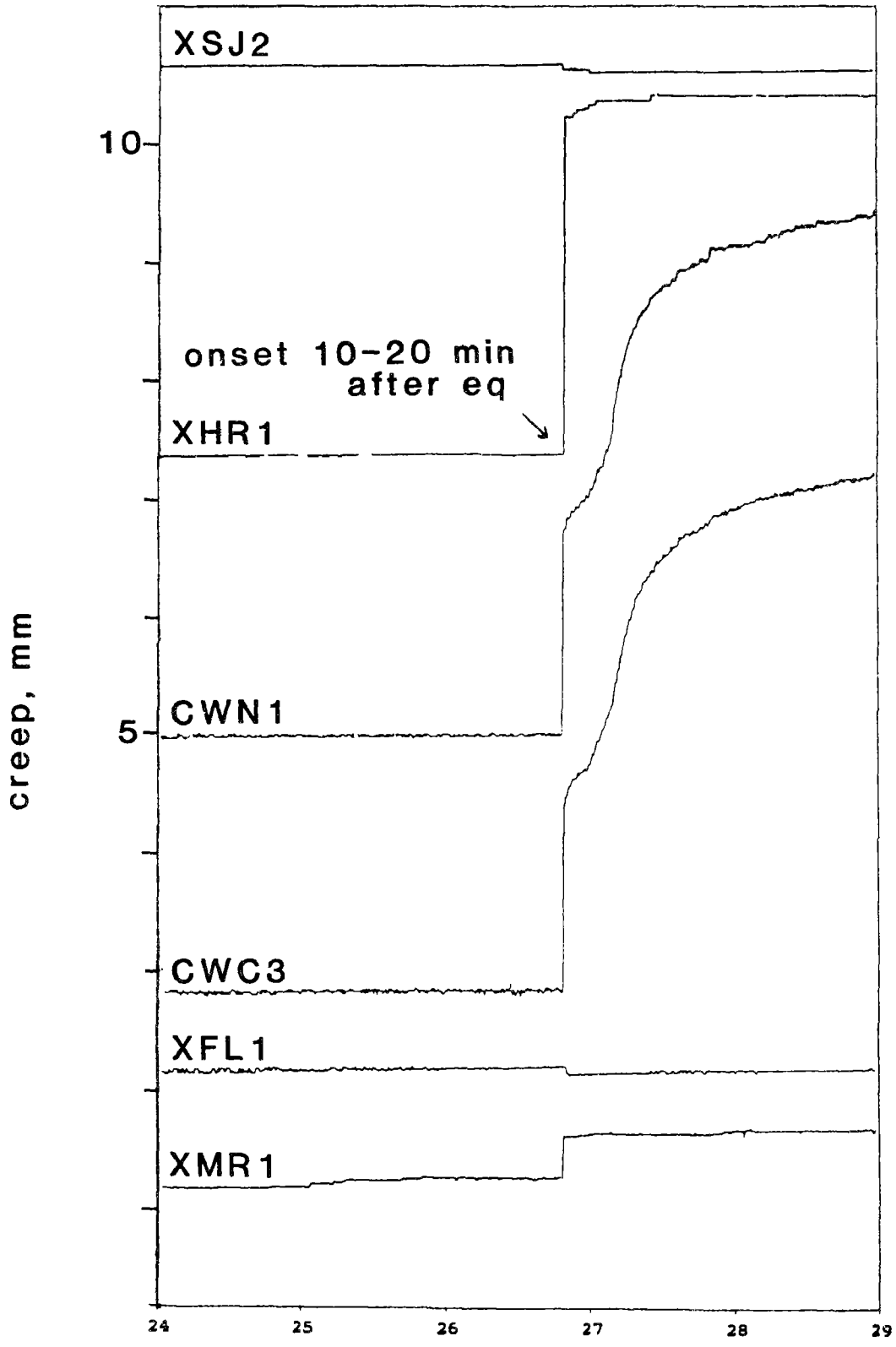

RESPONSE OF SAN ANDREAS CREEPMETERS

TO THE JAN. 26, 1986 EARTHQUAKE

FIGURE 3

Analysis of Seismic Data from the Shumagin Seismic Gap, Alaska

USGS 14-08-0001-G-946

John Taber and Klaus H. Jacob
Lamont-Doherty Geological Observatory of Columbia University
Palisades, New York 10964
(914) 359-2900

Investigations

Digitally recorded seismic data from the Shumagin seismic gap in eastern Aleutian arc, Alaska, are analyzed for detecting space-time variations in the seismicity, focal mechanisms, and dynamic faulting parameters that could be precursory to a major earthquake expected in this seismic gap. The seismic results obtained from the network data are being integrated with crustal deformation data that are independently collected, with volcanicity data of nearby Aleutian volcanoes, and with teleseismic information to identify basic tectonic processes which may be precursory to a great earthquake.

Results

We have begun to analyze an earthquake sequence that occurred in the Shumagin Islands in October and November, 1985. The mainshock (Ms=6.5) was followed by over 60 locatable aftershocks, including four events of magnitude greater than or equal to 5. The sequence occurred after six months of a 38% increase in microseismicity rate within the network and after 5 years of relative quiescence at the Mb$\geq$5.5 level. It was probably the largest sequence within the Shumagins in 20 years and occurred at the same time as increased activity in the Unalaska region to the west. However, no other anamolous behavior has been observed since November, 1985.

The mainshock and aftershocks are plotted in figure 1. The events were located using a master event technique. From the relative location of the mainshock and aftershocks, it appears that the initial direction of rupture was downdip towards the base of the shallowly dipping thrust zone. This is similar to the inferred rupture direction of the main event in a sequence that occurred in 1983 (Taber and Beavan, 1986). The focal mechanism calculated from body wave modeling for the main shock agrees with the dip of the aftershock zone (Figure 1) and is consistant with the first motion data from the local network (Figure 2).

Pavlof volcano had a significant eruption in April, 1985. Seven hours of continuous harmonic tremor, two hours of which was strong enough to be visable at stations 100 km away, was accompanied by a plume that reached 15 km. This eruption breaks the pattern of the last 15 years of yearly eruptions in the fall except during a postulated aseismic slip event in 1978-80 (McNutt and Beavan, 1984). It is not yet clear whether the initial pattern was due to random chance or whether there has now been a change in the stresses in the region.

References

McNutt, S. and J. Beavan, Periodic eruptions at Pavlof volcano, Alaska: The effects of sea level and an aseismic slip event, **EOS, Trans. AGU, 65**, 1149, abstract V42A-08, 1984.

Taber, J.J., and J. Beavan, February 14, 1983 earthquake sequence in the Shumagin seismic gap, Alaska, **Bull. Seism. Soc. Am.**, in press, 1986.

Reports

Jacob, K.H., J.J. Taber, and T. Boyd, Results from earthquake research on the Alaska-Aleutian seismic zone with special focus on the Shumagin Islands seismic gap, USGS Open File Report 86-

92, pp. 37-61.

Taber, J.J., and K.H. Jacob, Recent seismicity data from the eastern Aleutians, USGS Open File Report 86-92, pp. 243-254.

Taber, J.J. and K.W. Hudnut, A transition from a single to a double Benioff zone near the Shumagin Islands, Alaska, **EOS, Trans. AGU, 66**, 958, abstract S12C-13, 1985.

Taber, J.J., T.M. Boyd, and K.H. Jacob, Shumagin Islands earthquake of October 9, 1985, **EOS, Trans. AGU, 67**, 310, abstract S22-11, 1986.

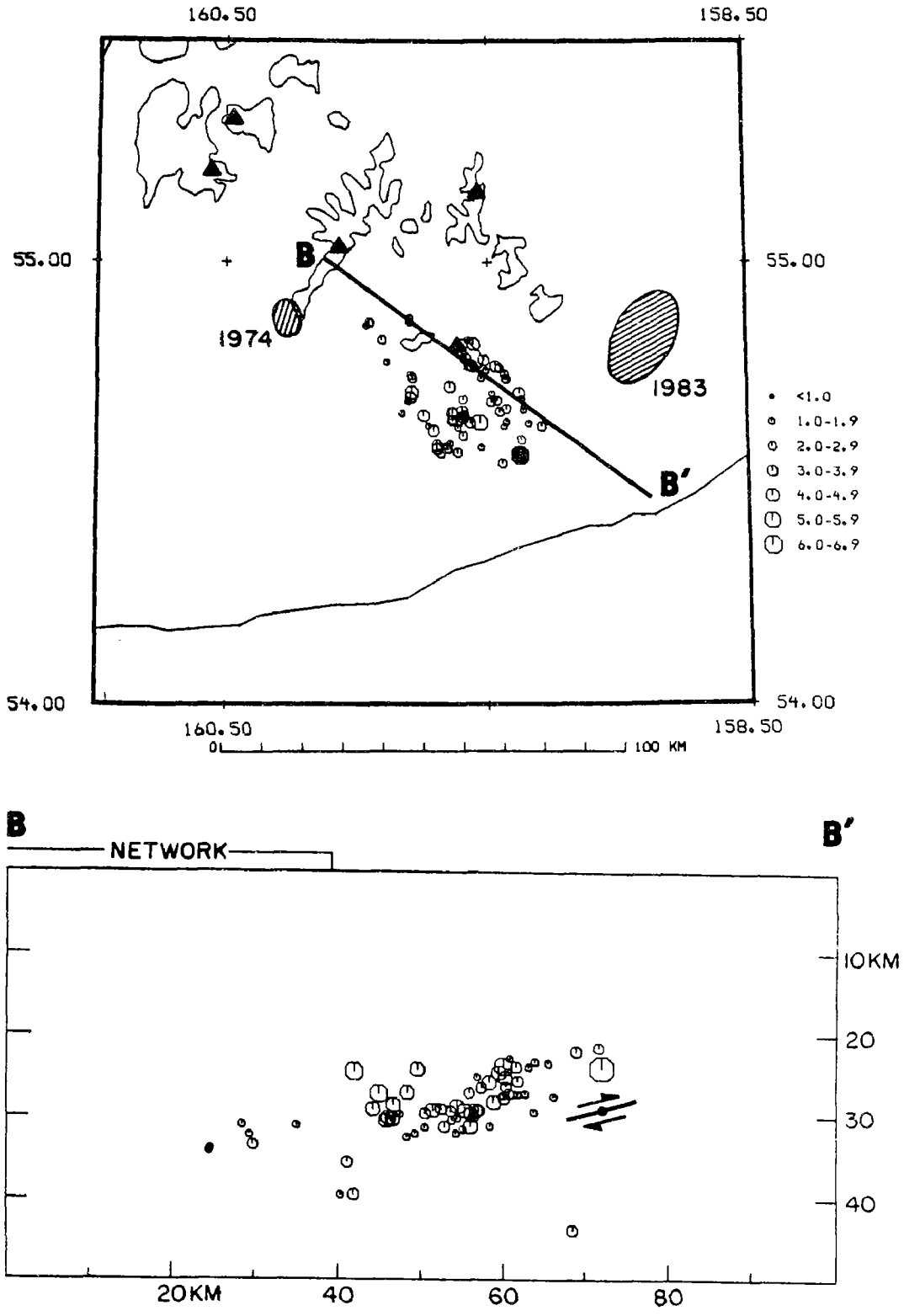

Figure 1. Map view and cross section of the earthquake sequence that occurred in October and November, 1985. Top: The mainshock is the solid circle at the SE edge of the sequence. Stations of the Shumagin seismic network are shown as triangles. The aftershock regions of two recent, nearby sequences are also shown.

Bottom: The fault plane and depth determined by teleseismic body wave modelling is plotted along with the network locations.

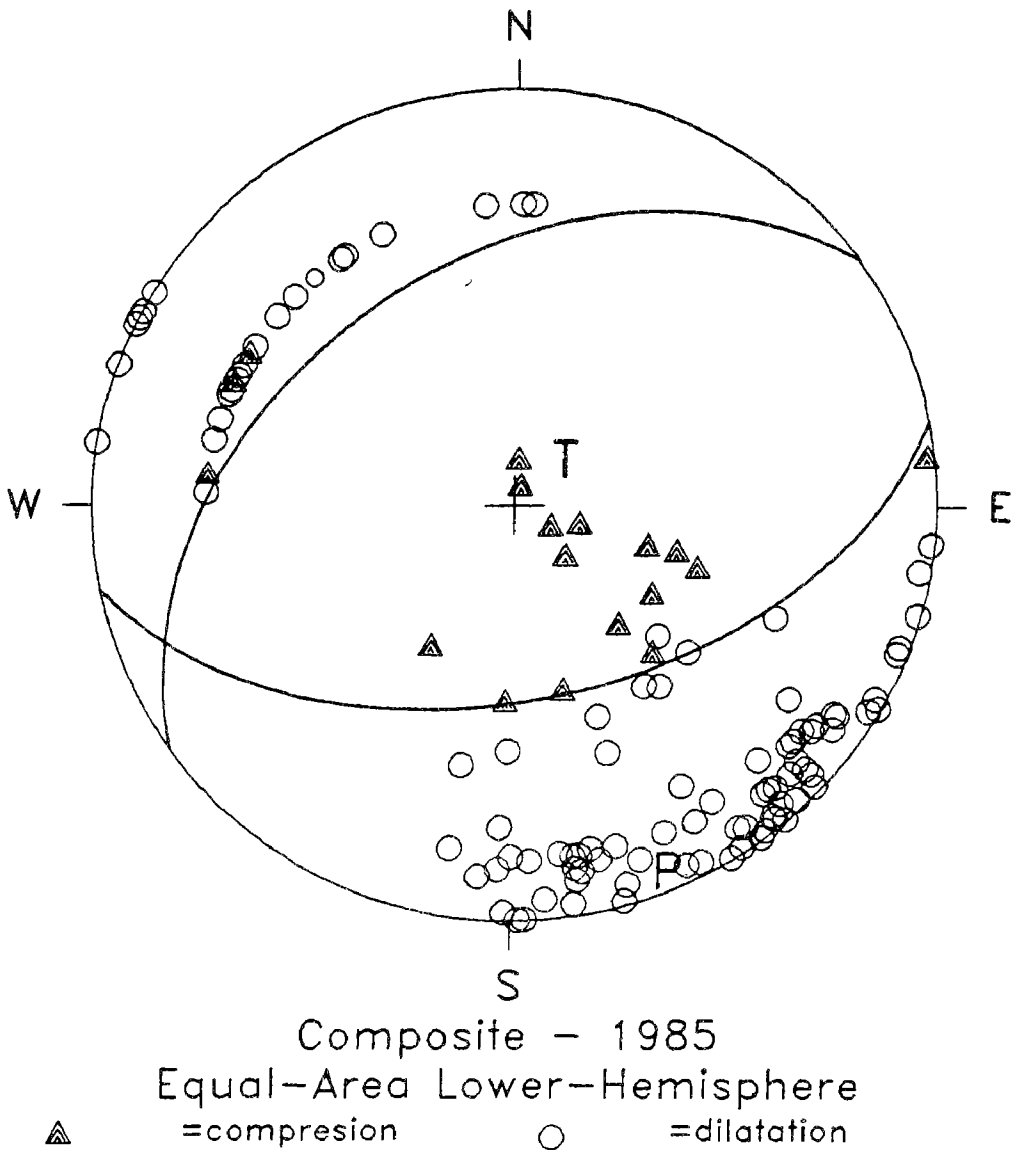

Figure 2. Composite focal mechanism using local data for events in the sequence.

Seismic Evidence for Tectonic Processes

9930-03353

Peter L. Ward
Branch of Seismology
U.S. Geological Survey
345 Middlefield Road
Menlo Park, California 94025
(415) 323-8111, Ext. 2838

Investigations

1. Examine the interrelationship of the segmented nature of volcanic fronts in subduction zones, the segmented nature of the rupture zones of major underthrust earthquakes, and the segmented nature of the ocean floor.

2. Study the temporal relationship between subduction and the formation of major granitic batholiths.

Results

1. The volcanic arc, inland from subduction zones, is segmented. While most young volcanoes within a given segment lie on a remarkably straight line, this line must typically be bent or offset in order to pass through the next group of volcanoes in the adjoining segment. Slip along the underthrust surface of subduction zones is also segmented, as shown by the aftershock zones of major earthquakes that rupture different parts of the plate margin at different times. I have plotted the aftershock zones of large earthquakes on the same time space diagrams as volcanic eruptions reported by Simkin et al. (1981) for Northern Japan to Kamchatka, the Aleutians and Alaska Peninsula, Central America, and parts of South America. These are the most active regions for which the best seismic data are available. The data set includes 167 active volcanoes, 1013 eruptions of moderate and larger size, and 139 earthquakes of magnitude greater than 7.5. When the positions of the most active volcanoes, which tend to occur near segment boundaries, are projected toward the trench along the vector of relative plate convergence, they are found to lie at the ends of the aftershock zones of large underthrust earthquakes. The largest earthquakes rupture multiple segments and in these cases the active volcanoes occur also at several segment boundaries defined by smaller earthquakes or by the alignment of volcanoes. Segmentated slip in subduction zones appears to influence where magma rises to the surface. The eruptions follow the major earthquakes by typically 4 to 23 years, suggesting a strategy for identifying the most important volcanoes to monitor for potential reawakening. The fundamental difficulty in this study is that the potential errors in the data are large enough that it is hard to prove the apparent correlations are statistically significant.

2. The rate of subduction of the Farallon Plate under North America was in excess of 15 cm/year between 56 and 43 my (Jurdy, 1984; Engebretson et al., 1985) and it might have been as high as 38 cm/yr (Alvarez et al., 1980; Tarduno et al., 1986). During the rest of the Cenozoic the convergence rates were much lower and strike-slip motion between the plates seemed to

dominate. This period of rapid subduction was after the youngest granitic plutons in the Sierra Nevada of California and before the period of major rhyolitic volcanism and granite intrusion in the western U.S. The data are less clear elsewhere, but I have been unable to find any example where major granitic batholiths were formed at the same time that major subduction was occurring. Clearly scattered granitic plutons form under arc volcanoes but these are very different from the batholiths that contain almost a continuous line of nearly contemporaneous plutons. Granitic batholiths appear to form in an environment that is distinctly different from, but complementary to, the subduction regime.

References

Alvarez, W., D. V. Kent, I. P. Silva, R. A. Schweickert, and R. A. Larson, 1980, Franciscan complex limestone deposited at 17° south paleolatitude: Geol. Soc. Am. Bull., 91, 476-484.

Engebretson, D. C., A. Cox, and R. G. Gordon, 1985, Relative motions between oceanic and continental plates in the Pacific Basin, Geol. Soc. Am. Special Paper 206, 59 p.

Jurdy, D. M., 1984, The subduction of the Farallon plate beneath North America as derived from relative plate motions: Tectonics, 3, 107-113.

Simkin, T., L. Siebert, L. McClelland, D. Bridge, C. Newhall and J. H. Latter, 1981, Volcanoes of the World, Hutchinson Ross Publ. Co., Stroudsburg, Pa., 233 p.

Tarduno, J. A., M. McWilliams, W. V. Sliter, H. E. Cook, M. C. Blake, Jr., and I. Premoli-Silva, 1986, Southern hemisphere origin of the Cretaceous Laytonville limestone of California, Science, 231, 1425-1428.

Reports

Ward, P. L., 1985, A passive asthenosphere and the origin of hotspots: EOS, Am. Geophys. Un. Trans., 66, 1072.

Ward, P. L., 1986, An apparent correlation between volcanic eruptions and major, shallow, subduction zone earthquakes: Geol. Soc. Am. Abstracts with Programs, 18, 195.

Two Studies of Earthquake Fault Behavior

14-08-0001-G - 1157

Steven N. Ward

C. F. Richter Laboratory
Earth Sciences Board
University of California, Santa Cruz
Santa Cruz, CA 95064
(408) 429–2480

Objective: Analyze the static deformation field of the 1959 Hebgen Lake, Montana earthquake.

The 1959 Hebgen Lake, Montana (M=7.5) earthquake was the largest event to occur in the Basin and Range Province in historic time. It was accompanied by extensive surface deformation, mostly subsidence. Savage and Hastie (1965) modeled the gross coseismic deformation pattern using a rectangular, uniform slip fault. Since then, new techniques have been developed (e.g. Ward and Barrientos, 1986) which are not restricted to uniform slip rectangular faults. We are currently using these techniques to determine the fault slip pattern associated with the Hebgen Lake event.

Data collection: Several classes of data were collected to analyze the coseismic deformation: 1) Leveling lines. Information from 10 lines have been requested from the National Geodetic Survey. These data have been divided into two groups, preseismic and postseismic, according to the date of surveying of each line. In some cases, the period of releveling spans more than 30 years. 2) Highway turning point heights. From the field books of the road leveling by the Bureau of Public Roads and the postseismic releveling by the Coast and Geodetic Survey, an estimation of the subsidence can be assessed in the northern part of the lake. 3) Lake shore height changes, and 4) Fault scarp measurements. The last three types of data were digitized directly from the map by Myers and Hamilton (1964).

Analysis: In the forward analysis, a model is produced and is adjusted by trial and error until a satisfactory fit is observed. In this procedure, all geometrical parameters of the fault plane(s) are allowed to vary and the slip is found by minimizing the sum squares of residuals. Models with both one and two uniform slip fault planes have been considered. Figure 1 shows the data distribution. Triangles represent first and second order leveled benchmarks, squares are lake shore height changes, and crosses are turning point heights. Also, the Hebgen and Red Canyon fault scarps are shown on the northern side of the lake. A–A', B–B', and C–C' are three profiles shown in the subsequent figure. Figure 2 shows six boxes which contain from top left clockwise: 1) Same as Figure 1 with dots representing the two fault planes projected on the surface. We will refer to the eastern plane as plane #1 and the larger western plane as #2. 2) Predicted (dash line) and observed data (solid line) for the releveled benchmarks. Each mark corresponds to 10 km in the horizontal scale and 1 m in the vertical scale. The top box represents data on a roughly east-west (A–A') profile north of the lake. Second and third boxes from top to bottom represent the north-south (B–B') and the east-west (south of the lake, C–C') profiles. 3) The bottom-right box contains the highway turning point heights and the left bottom shows the lake shore height changes. There is an overall general agreement between the observed and predicted values. As expected, data type distribution controls part of the parameters of the model. Benchmarks, turning points and lake shore height changes directly north of Hebgen Lake control the strike of both fault planes. Lake shore data partly constrain the dip of fault #2. Benchmarks on the north-south line control both the depth of burial and the eastern end of fault #1.

In the general inverse procedure, the point sources that simulate the plane are not restricted to have the same moment (or equivalently, slip). Therefore, for a given fault geometry, the variable slip distribution on one or two planes is estimated. This procedure is being implemented at this time.

REFERENCES

Myers, W. B., and W. Hamilton, Deformation accompanying the Hebgen Lake earthquake of August 17, 1959. U. S. Geological Surv. Profess. Paper 435, pp55-98, 1964.

Savage, J. C., and Hastie, L. M., Surface Deformation Associated with Dip-Slip Faulting J. Geophys. Res., 71, 4897-4904, 1966.

Ward, S. N., and S. E. Barrientos, An inversion for slip distribution and fault shape from geodetic observations of the 1983, Borah Peak, Idaho, earthquake, J. Gephys. Res. in press.

Fig. 1. Map view of the leveling routes showing bench marks (triangles), lake height changes (squares), highway turning points and the ruptured segments of the Hebgen and Red Canyon faults (dark lines in the northern part of the lake).

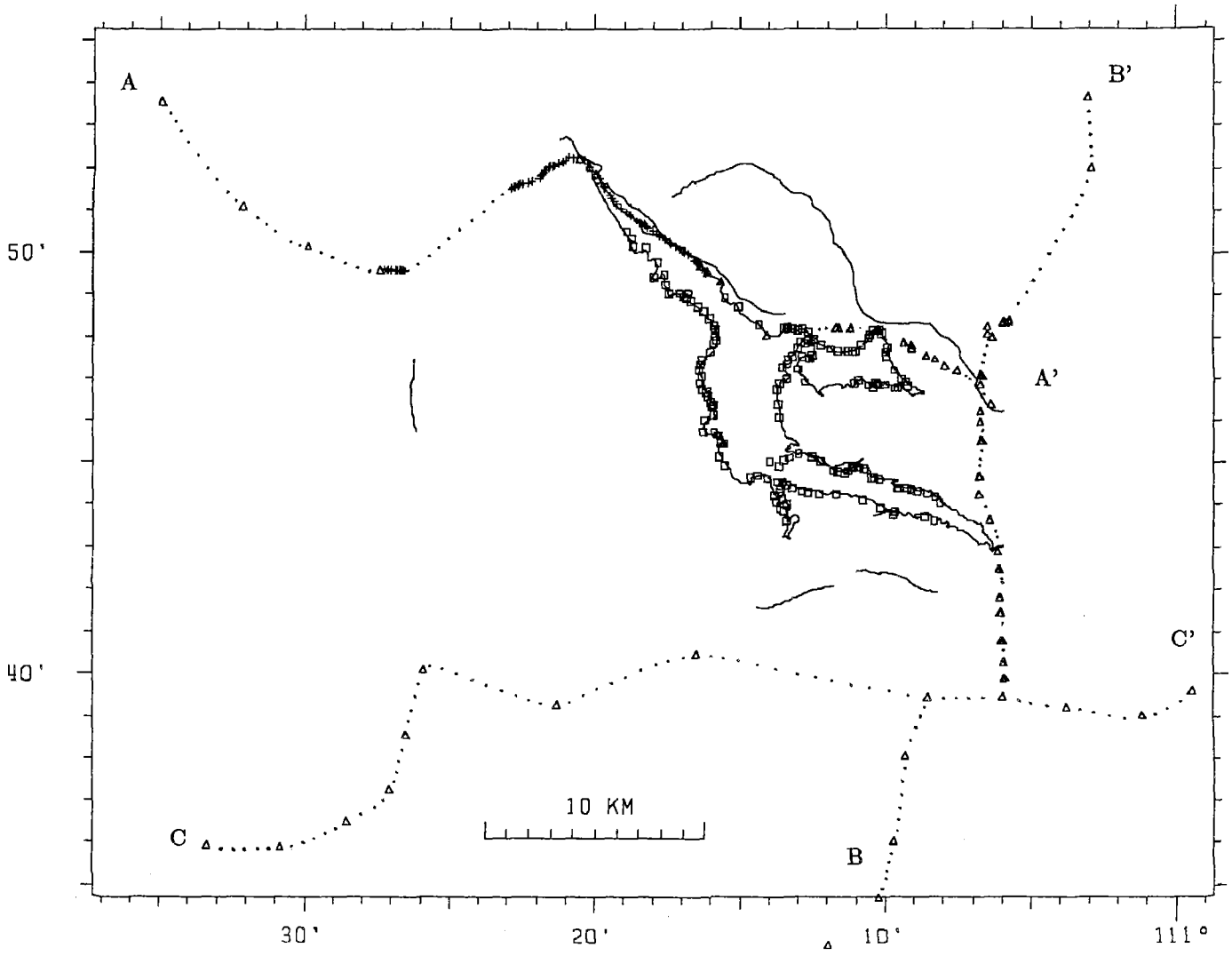

UNIFORM SLIP, TWO PLANES

Fig. 2. From top-left clockwise: 1) Same as Figure 1. Dots represent the surface pojection of the two planes. 2) Predicted (dashed line) and observed (solid line) for the releveled benchmarks along A–A', B–B', and C–C'. 3) Bottom boxes show the highway data and lake shore height changes.

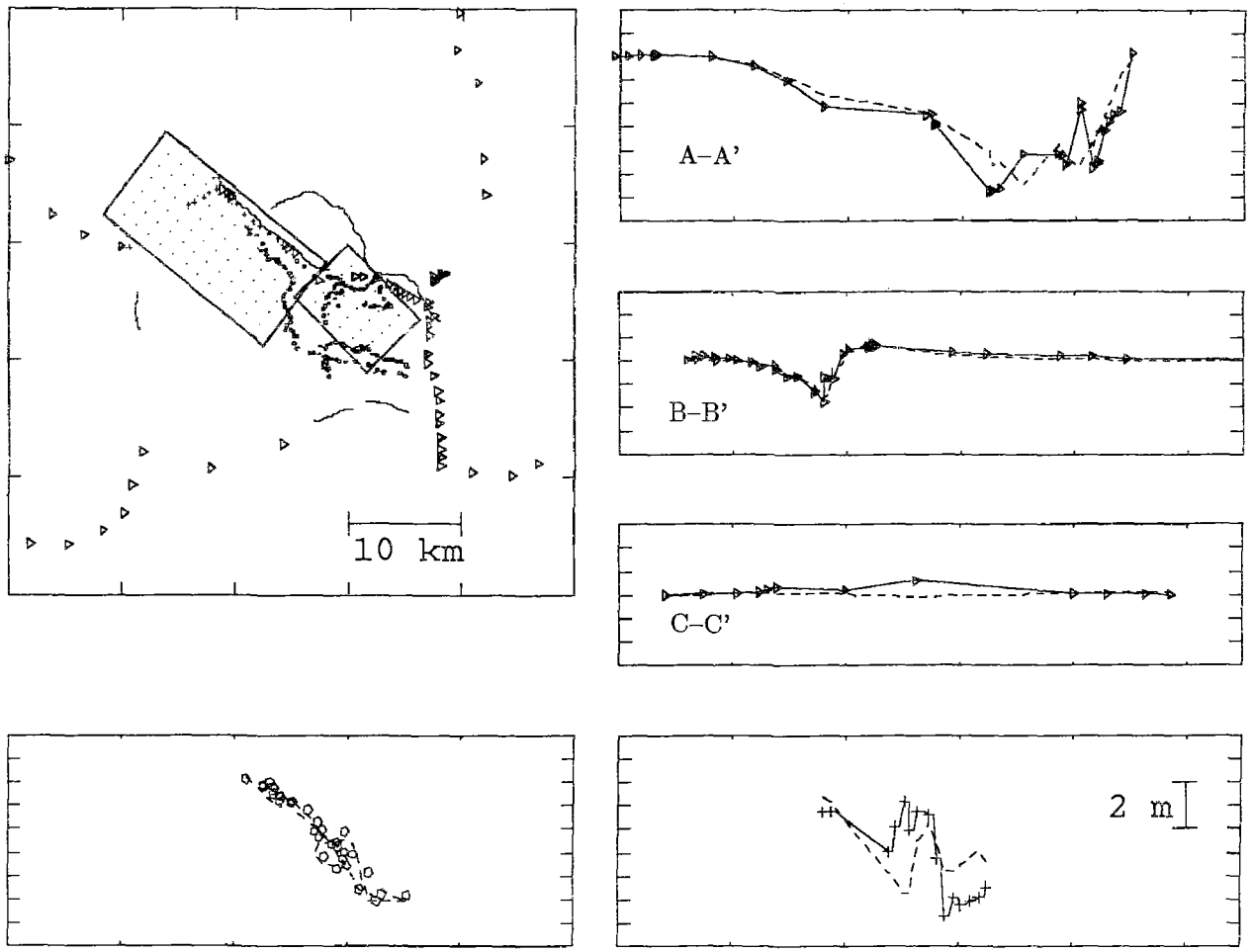

Central American Seismic Studies

9930-01163

Randy White
U.S. Geological Survey
Branch of Seismology
345 Middlefield Road, Mail Stop 977
Menlo Park, California 94025
(415) 323-8111, Ext. 2570

Investigations

Ruiz Volcano, Columbia. On November 13, 1985, Ruiz Volcano erupted, generating catastrophic mudflows that killed about 25,000 people. We left for Colombia immediately and installed 6 telemetered seismic stations to monitor and help predict future eruptions of the volcano. This monitoring effort was carried out initially, principally by David Harlow and is continuing under James Zollwegg. As this monitoring is still underway, results of this work will be detailed later. The most important result of this work is that the largest eruption during the 6 month period following the catastrophic eruption of November 13, 1985, occurred on January 4, 1986 and was successfully predicted and appropriate towns evacuated.

During visits to Colombia, data from four portable seismographs from the 3 1/2 months prior to the catastrophic eruption were examined and are reported below.

Results

Felt earthquakes were first reported at Ruiz volcano in December 1984, and thereafter 15 to 30 events were felt each month through September 1985. Few of these earthquakes, however, were felt beyond the immediate vicinity of the volcano and we estimate that the largest events did not exceed magnitude 4.5. Seismograms from portable instruments indicate that approximately 75 percent of the tectonic earthquakes occurred in small swarms with durations of one to several hours. Sixty events were selected and located in order to determine the locus of the different swarms and seismically active areas. Hypocenters are located at depths of less than 8 km and most occur beneath the volcanic cone. Nevertheless, some earthquakes are located 5 to 10 km from the crater suggesting that nearby faults are either active or were reactivated by the shallow intrusion of magma.

Between July and early September, the rate of seismic energy release was constant. One September 5, however, a clear period of premonitory seismic activity began and continued until September 11 when strong phreatic eruptions began. During this premonitory period the rate of seismic energy release from local tectonic type earthquakes increased by a factor of 5. Also during this period, "periodic tremor", consisting of 5 to 20 minute episodes of harmonic tremor at average intervals of 65 to 85 minutes, was continuously recorded. Phreatic eruptions occurred intermittently until about September 27 and during these eruptions harmonic tremor was recorded continously until October 2, but steadily decreased in amplitude.

In contrast to the premonitory seismic activity in early September, the

seismic energy release rate was very low during the month prior to the November 13 eruption. The only premonitory activity prior to this eruption was a small earthquake swarm November 9, and low level harmonic tremor beginning on November 10 and continuing to November 13. At 15:06 local time on November 13, a blast event of about 15 minutes duration was recorded and minor ash fall was reported about one hour later at towns 35 km NE of the crater. Harmonic tremor mixed with small eruption events followed this small eruption, but diminished rapidly in amplitude and frequency until 21:08 local time. At this time a Plinian eruption started, generating catastrophic mudflows.

Reports

Harlow, David H., Munoz C., Fernando, and Cuellar, Jairo, 1986, Trans. Am. Geophysical Union, v. 67, p. 403.

Crustal Deformation Observatory Part J: Askania Borehole Tiltmeter

14-08-0001-G1153

Frank Wyatt, Duncan Carr Agnew, Hadley Johnson
Institute of Geophysics & Planetary Physics
Scripps Institution of Oceanography
University of California, San Diego
La Jolla, CA 92093
(619) 452-2019

Walter Zürn
Geowissenschaftliches Gemeinschaftsobservatorium Schiltach
Universitäten Karlsruhe
D-762 Wolfach, Heubach 206, FRG

This contract supports the installation and operation of an Askania borehole tiltmeter at Piñon Flat Observatory (PFO) and analysis of data from it. This work is part of the Crustal Deformation Observatory (CDO) program, as a cooperative enterprise with Dr. Walter Zürn of Karlsruhe University (West Germany), who has provided the instrument on loan. The goals of this project are to:

1. Establish techniques (and costs) for emplacing and orienting removable tiltmeters in boreholes of various depths. We have placed special emphasis on developing methods that may be applied at greater depth than has yet been customary; most installations of Askania instruments have been at depths from 10 to 30 m.
2. Compare these borehole tilt measurements with those from adjacent tiltmeters, including both long-base surface instruments and other borehole installations. Such comparisons will enable us to establish sources of instability and noise, and test the accuracy of different techniques.
3. Use a high-quality borehole instrument to accurately monitor tilt in a tectonically active area. The existing long-base tiltmeters sense only east-west tilt.

Askania Installation

The Askania tiltmeter (S/N 11) is on loan from Dr. Walter Zürn (University of Karlsruhe). It arrived in La Jolla in early 1985. We first set it up in the seismic vault at La Jolla, using a clamp attached to the wall of the vault. This is a noisy site (because it is close to the ocean) but convenient, and by operating the instrument there we were able to get valuable experience. (Though we had some English instructions sent by Dr. Zürn, most of the technical material was in German.) When we felt confident of our ability to use the tiltmeter we reinstalled it at PFO, in a vault formerly used by a superconducting gravimeter. This was a more stable site than our La Jolla vault, though subject to large thermoelastic tilts; it gave us a useful opportunity to test the electronics used with the tiltmeter in a field environment, so that they would be ready for the final borehole installation.

Before installing the instrument in the hole we had to design and construct a special watertight housing for it, and cement this housing (and regular casing) into the borehole.

The base of the tiltmeter has a conical socket that is designed to rest on a rounded pedestal; the tiltmeter is held vertical by spikes which bear against the housing wall. For maximum stability at these small bearing surfaces it is important to minimize corrosion, and for this reason the housing was constructed from stainless steel. The ideal design would be to machine the entire housing from a single block of material, but this is not practical, especially since we wish the housing to be as long as possible to get the maximum averaging along the borehole. Instead the housing was constructed from two pieces: a 4.25 m long tube (wall thickness 11.0 mm) and a disc which fit into it and out of which the bearing pedestal was machined. To join these in a stable manner we used a shrink fit: part of the inside of the tube was machined to a diameter slightly less than the disc and then heated, while the disc was cooled in liquid nitrogen. These two could then be fit together; on reaching room temperature they formed an interference fit, giving a tight and, we hope, uniform bond. The lower part of the tube was welded closed to seal the housing and provide a sump beneath the tiltmeter pedestal; an adapter section was welded to the top of the housing for joining to the regular casing in the field (Figure 1).

The Askania tiltmeter requires a hole that is fairly straight and within 3° of vertical. To get the best result we first drilled a pilot hole 27.7 m deep and then reamed it out to 30.5 cm diameter; a second reaming, which extended only to 12 m, allowed installation of a 14-inch casing to prevent near-surface caving. At all stages of drilling and reaming extra stiffeners and guides were used on the drill string, with good results; the completed hole was the straightest yet drilled at PFO. The hole depth was chosen to put the bottom just above the water table.

The final, most important, and most difficult step was to insert the housing and casing and cement them into the borehole. Casing insertion was done with a drill rig. Each section was lowered until its top was flush with the rig platform; a new section was then put atop it, axially aligned, and welded on. Since such welds must be done carefully to prevent leaks, the process is slow though straightforward.

At the same time as the casing was being assembled, sections of grout tubes were also attached in preparation for the least controllable part of the whole process: cementing in. For a shallow hole (such as this one) the time required to weld and insert the casing is short enough that grout may simply be placed into the bare hole and the hole casing pushed into it before it has time to set. For a much deeper hole this ceases to be practical for a number of reasons, and we therefore designed a method which should work in holes of considerable depth.

The basic design is shown in Figure 1: three grout tubes were attached 120° apart around the outside of the casing, running from the top almost to the bottom. At the top they were connected to a distribution manifold; cement pumped into this would flow down the three tubes and back up the hole, cementing in the entire length of casing. (The grout tubes also centered the casing within the hole). Pumping concrete for this distance (60 m) or more is not at all uncommon, as this is a standard distribution procedure at large construction sites.

For the actual grouting the whole system was first flushed with water before pumping began. The grouting process was not entirely successful; the cement clogged before overflowing from the hole. We believe that this was partly because of insufficient pumping pressure (the contractor, as often happens, having assured us in advance of something he could in fact not do) and may also have been because the flushing process was not thorough enough. To partly save the situation we unscrewed one of the top sections of grout tube and filled the hole from the top. Comparison of the volume pumped with the known volume to be filled indicates that most of the hole was filled, though some voids

may remain. We are confident that the lowest section of casing, in which the tiltmeter rests, was properly cemented when the system clogged.

The final step was to install the tiltmeter in its housing, at 24 m depth. This was done on 1985:346, 83 days after drilling and 21 days after cementing. The tiltmeter was simply lowered into the hole; when the instrument reached bottom, the slackening of the lowering cable caused spikes to emerge from the top and anchor the instrument to the cemented-in casing. The clearance between the tiltmeter and the inside of the housing is only 3 mm.

Internal calibration of the tiltmeter is done with a 'ball-calibrator' which causes the pendulum to tilt by a known amount as a small ball is moved to and fro inside the instrument. Calibrations done in the first setup at La Jolla agree with those from PFO (0.5 nrad/least count, $\pm 0.5\%$). A more difficult task is orienting the tiltmeter. This was done by sighting simultaneously on markings on the top of the tiltmeter and on distant reference marks (e.g., Santa Rosa Mountain, 8.1 km south of PFO). This measurement was made using a special optical instrument (the DBAS) developed at the Air Force Geophysics Laboratory and on loan to UCSD. The standard deviation of five separate measurements was 0.5°.

Figure 2 shows data from both components of the Askania beginning a few hours after installation and running through the end of January, 1986. Offsets of order 0.1 μrad caused by nearby drilling (15 m away) and induced cable motion have been removed, but no detrending has been done. Both components show a rapid transient adjustment over the first few days, probably caused by temperature changes as the instrument comes to equilibrium with its surroundings and by stress relaxation of the instrument support points. The NS component (actually at azimuth 170.5°) appears to have settled in very rapidly, while the EW is still equilibrating. We do not yet know the reason for this, or whether it reflects adjustment of the tiltmeter in its housing or creep in the cement that couples that housing to the earth. We are encouraged by the excellent behavior of the NS component to believe that this mode of installation is a good one.

The best tilt records at PFO come from the long-base tiltmeters, and Figure 3 shows a comparison between the Askania data (rotated into the proper azimuth) and the UCSD long fluid tiltmeter (LFT). In this azimuth the Askania tilt is primarily that from the EW component, and therefore shows the same long-term adjustment seen in this component in the previous figure. As a direct comparison, the LFT series was subtracted from the Askania tilt to produce a difference series. The series were each scaled according to their own calibration factors; the good agreement between the tides indicates that these are very nearly correct. The slight residual tide may reflect calibration error or the hydraulic phase lag present in the LFT. Over this time the LFT series has essentially no drift, so the change in the difference series is entirely due to the Askania.

Figure 1.

Borehole Tiltmeter Installation KUA
Piñon Flat Observatory
1985

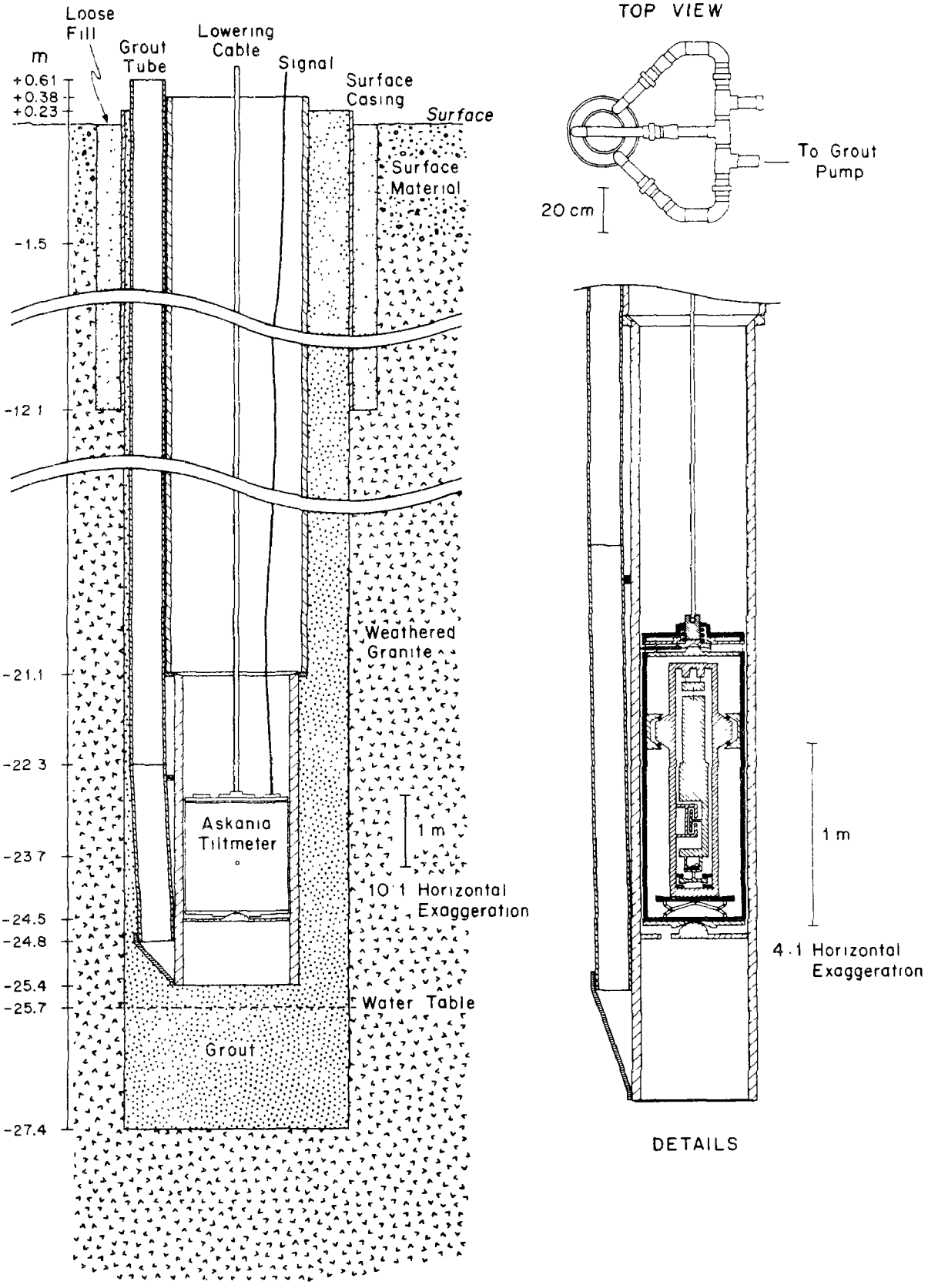

Figure 2.

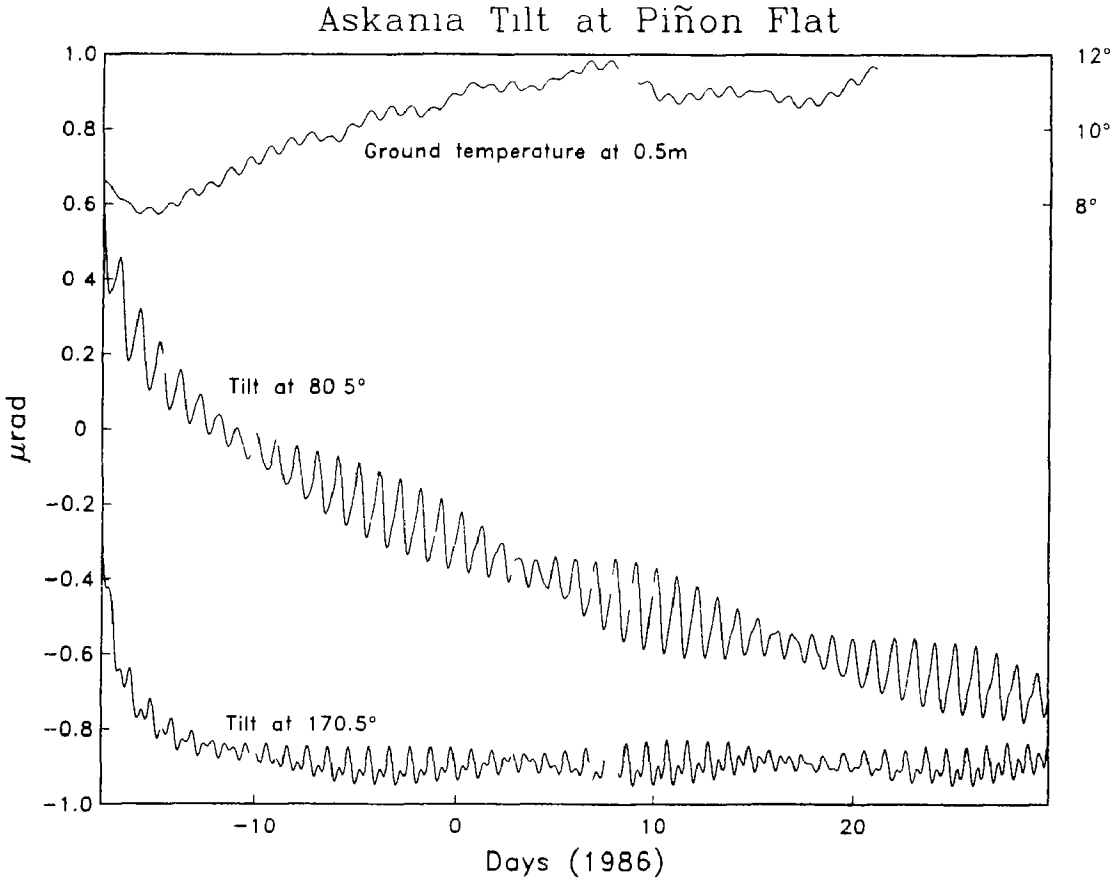

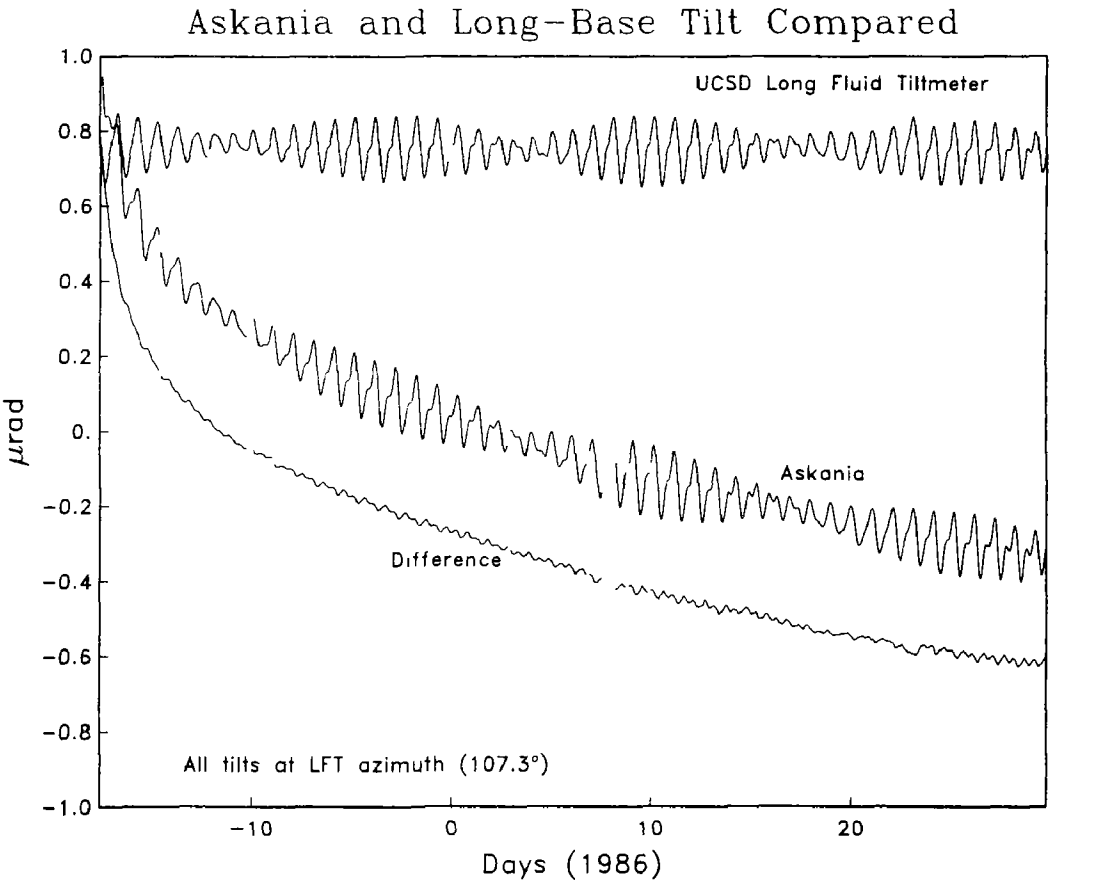

Figure 3.

Piñon Flat Observatory: A Facility for Studies of Crustal Deformation

14-08-0001-G1178

Frank Wyatt, Duncan Carr Agnew,
Mark A. Zumberge, Jonathan Berger
Institute of Geophysics & Planetary Physics
Scripps Institution of Oceanography
University of California, San Diego
La Jolla, CA 92093
(619) 452-2019

This two-year grant helps support the operation of Piñon Flat Observatory (PFO) by providing funds for shared facilities which are used for the development of precision geophysical instrumentation. Matching funds are provided by the National Science Foundation. The work done at PFO includes establishing the accuracy of instruments designed for measuring various geophysical quantities by comparing results from them with data from reference standard instruments. This comparison also allows reliable monitoring of strain and tilt changes in the area near the observatory, between the active San Jacinto fault and dormant southern San Andreas fault systems.

This report reviews recent results from one of the reference standard instruments at the site: a long-base tiltmeter. Liquid-filled tiltmeters have been operated at PFO since 1979; the first of these was only 50 m long. In 1981 this UCSD instrument was extended to 535 m, in parallel with tiltmeters designed earlier by Dr. Roger Bilham, Lamont-Doherty Geological Observatory, and by Dr. John Horsfall, Cambridge University. (A preliminary comparison of these was reported by Wyatt *et al.*, 1984, *Geophysical Research Letters*.) All three of these instruments employ techniques for detecting erroneous motions of the end-monuments; the optical system used in the UCSD instrument was not operational until late 1982. Figure 1 shows the results from that time until the present.

The upper trace in Figure 1 is the difference in fluid levels at the two ends of the sealed, half-filled trough. Below this record is the correction for end-monument motion, formed by taking the difference of vertical strains recorded by the optical anchors at each end; most of the fluid-level signal is just the result of these monument displacements. Subtracting these series yields the corrected tilt at an effective depth of 27 m, the depth of the optical anchors. We may then remove the earth tides to expose the underlying signal (called the Residual in Figure 1). This 3.3-year record ranks among the lowest

variance tilt signals recorded, a testimony to the stability of both this particular sensor and the crust under Pinyon Flat. Whether such well behaved records will prove the rule in other geological settings is subject to conjecture, but we believe it will be so. The residual signal shows the crust to be tilting down to the west (actually at an azimuth of 287.3°) at a rate of 0.097 μrad/a, with variations about this trend no greater than 0.13 μrad. We are just beginning the search for correlations with other low-noise sensors at the site, such as the parallel tiltmeters, borehole strainmeters and tiltmeters, and the long-base strainmeters, in order to judge the tectonic implications of these observations.

The largest signals in Figure 1 occur early in the record, when the end-vaults flooded following two intense thunderstorms. (The downward spikes evident in the residual series at 1983.2 are due to severely perturbing the aquifer under one end of the tiltmeter while drilling nearby.) Figure 2 presents the individual monument displacements for this same period and shows more clearly what happened when the weathered rock under the vault became wet: nearly a millimeter of upward motion for one of the monuments (TAU). In the summer of 1983 sizable A-frames were erected over the vaults to deflect precipitation, and the monuments (particularly TAU) have generally been subsiding since then. There is an indication of a shared annual response with a phase lag of 90° with respect to the ground temperature at 0.5 m depth. For comparison with Figure 1 we note that motions of 50 μm, or one-quarter of a vertical division in Figure 2, correspond to the net annual tilt seen on the 535 m baseline tiltmeter. The 1 mm displacement of monument TAU translates to an erroneous tilt of 1.9 μrad if unaccounted for here, or 5 μrad on a more practical 200-m long instrument. Because these correction signals dominate the tilt estimate , much of our current research efforts are focused on improving these measurements.

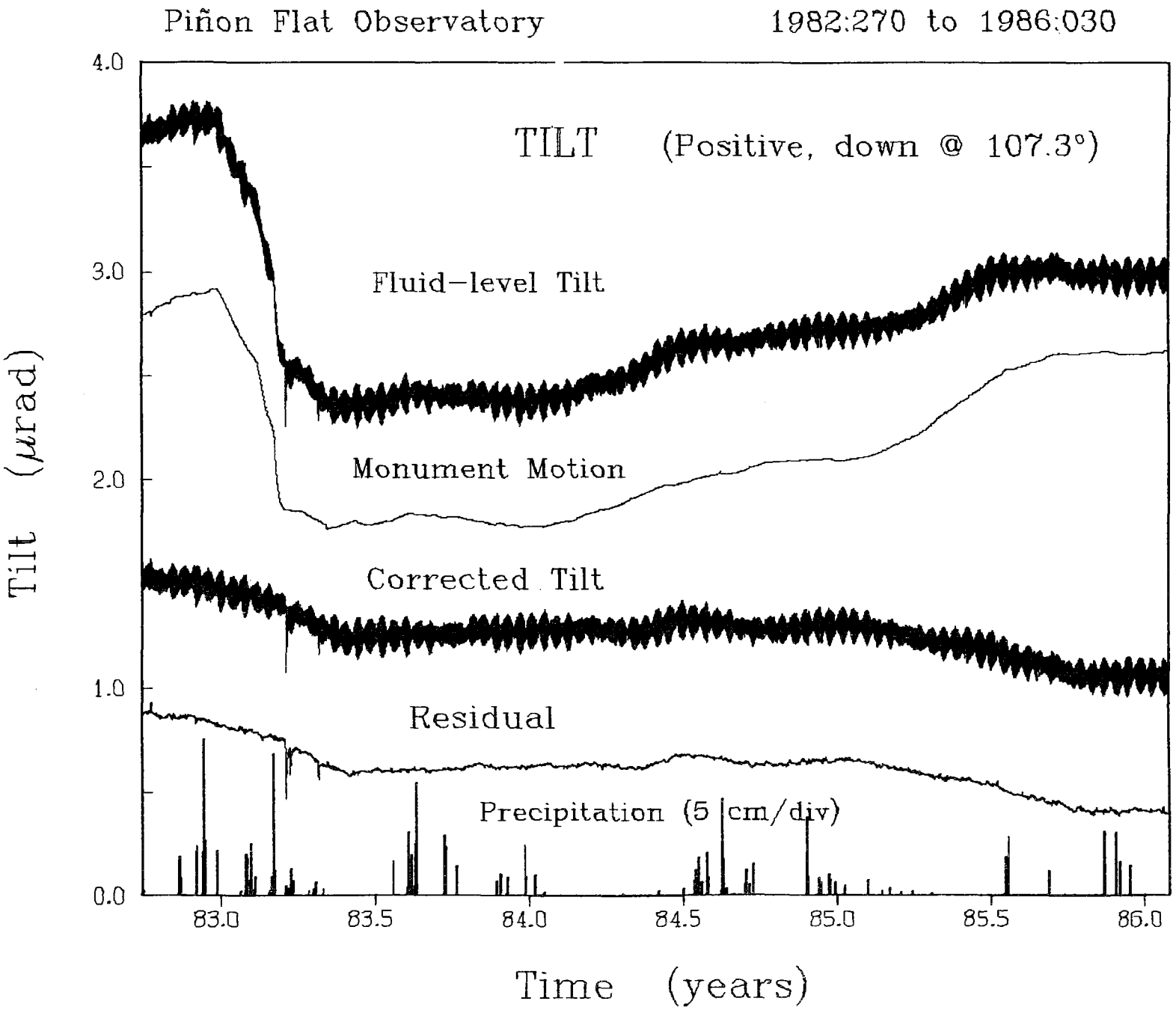
Piñon Flat Observatory
1982:270 to 1986:030
TILT (Positive, down @ 107.3°)
Fluid-level Tilt
Monument Motion
Corrected Tilt
Residual
Precipitation (5 cm/div)
Tilt (μrad)
Time (years)
4.0
3.0
2.0
1.0
0.0
83.0
83.5
84.0
84.5
85.0
85.5
86.0

Figure 1.

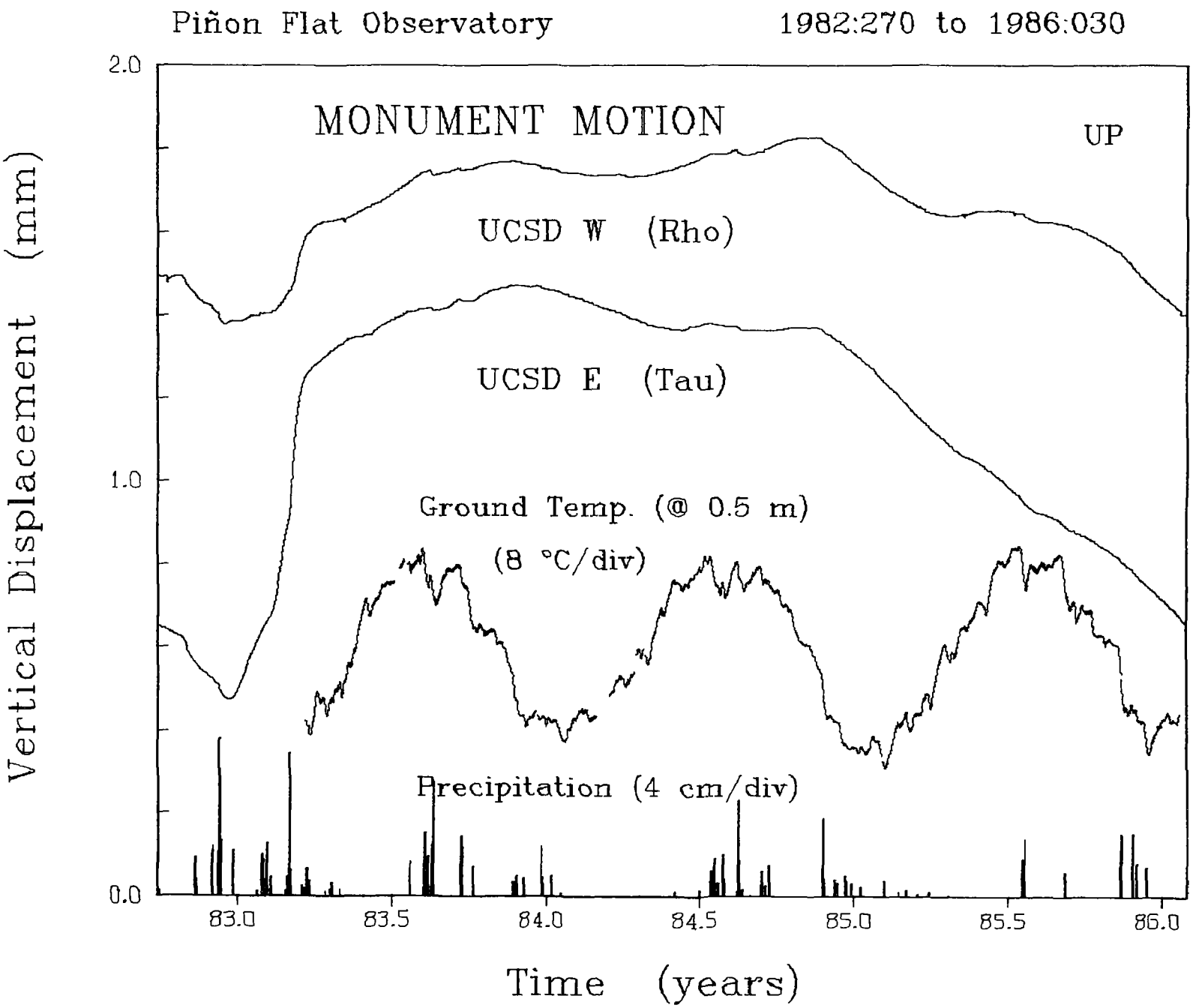
Piñon Flat Observatory
1982:270 to 1986:030
MONUMENT MOTION
UP
UCSD W (Rho)
UCSD E (Tau)
Ground Temp. (@ 0.5 m)
(8 °C/div)
Precipitation (4 cm/div)
Vertical Displacement (mm)
2.0
1.0
0.0
83.0
83.5
84.0
84.5
85.0
85.5
86.0
Time (years)

Figure 2.

Piñon Flat Observatory: Cooperative Studies with Outside Investigators

14-08-0001-G1197

Frank Wyatt and Duncan Carr Agnew
Institute of Geophysics & Planetary Physics
Scripps Institution of Oceanography
University of California, San Diego
La Jolla, CA 92093
(619) 452-2019

This grant provides assistance for those independent investigators working at Piñon Flat Observatory (PFO) under the auspices of the U.S. Geological Survey. This assistance includes: research coordination, instrument operation and testing, data logging, preliminary data reduction, and collaborative data analysis. Much of this effort is part of a cooperative program, called the Crustal Deformation Observatory Project, to evaluate instrumentation for measuring long-period ground deformation in a tectonically active area. The evaluation of these different techniques involves understanding and reducing sources of noise in the instruments as well as developing improved methods to describe measurement error.

Table 1 lists the studies currently underway at Piñon Flat Observatory. Most of these programs are conducted independently, with investigators establishing their own associations to compare results from the common site. Those in the Crustal Deformation Project have a somewhat more formal agreement to share observations. This project focuses on the development of continuously-recording tilt sensors. Several new tiltmeters have recently been added (instrument designation given in parentheses): an Askania tiltmeter at 25 m depth, in cooperation with Walter Zürn of Karlsruhe University (KUA); 24 m- and 36 m-deep tiltmeters designed by Judah Levine and Chuck Meertens of the University of Colorado (BOA and BOB); a revitalized long-base tiltmeter run by Tim Owen of Cambridge University (CAMB); three St. Louis University tiltmeters developed by Sean-Thomas Morrissey replacing commercial units at a depth of 4.5 m (Alpha, Beta, and Delta). Site preparations have also been completed for four more St. Louis tiltmeters: two at a 10 m depth (SLA and SLB) and two at 20 m (SLC, SLD). Figure 1 shows the location of most of these sensors.

In May 1986 the National Geodetic Survey (NGS) will be adding a closely-spaced class A rod mark array (NGS #1-#5). This special cluster will be compared with the optically anchored monuments used by the long-base tiltmeters in an effort to identify sources of noise. Under the direction of Ross Stein, U.S. Geological Survey, the NGS also plans to level annually a calibration loop around the greater Pinyon Flat area. Over the period of a few years this should provide a good constraint on the secular tilt across the observatory.

Table 1.

Studies at Piñon Flat Observatory May 1986

Investigator	Affiliation	Program
Independent Investigations		
D. Agnew	UC San Diego	IDA global seismic network VLP seismometer testing
W. Daily	Lawrence Livermore Labs	Radio wave emissions
W. Farrell J. Berger	UC San Diego	Digital seismometry
D. Garbin L. Brady	Sandia Laboratories	NTS seismic monitoring
M. Gladwin	Univ. of Queensland	Borehole strainmeter
W. Kaula	NGS	Benchmark testing
R. Jachens	US Geological Survey	Relative gravity measurement
M. Johnston	US Geological Survey	Borehole strainmeter studies
J. Langbein	US Geological Survey	Two-color geodimeter
A. Linde S. Sacks	Carnegie Institution of Washington – DTM	Borehole strainmeters
R. Maley	US Geological Survey	Strong motion recording
C. Mitchell D. Trask	NGS JPL	VLBI crustal movement measurements
P. Pammel	DMA – Geodetic Survey	Relative gravity measurement
J. Savage W. Prescott	US Geological Survey	Regional strain monitoring
R. Stein B. Martine	US Geological Survey NGS	Regional leveling – calibration line
F. Vernon J. Fletcher	UC San Diego US Geological Survey	Anza seismic array
F. Wyatt	UC San Diego	Long baseline tiltmeters Long baseline strainmeters Laser optical anchors
M. Zumberge	UC San Diego	Absolute gravity measurement
Crustal Deformation Observatory Project		
R. Bilham J. Beavan	Lamont-Doherty Geological Observatory	Long baseline tiltmeter Benchmark stability
J. Cipar	AF Geophysics Laboratory	Borehole tiltmeter
J. Levine C. Meertens	JILA/CIRES	Borehole tiltmeter
S.-T. Morrissey	St. Louis University	Shallow borehole tiltmeters
T. Owen	Cambridge University	Long baseline tiltmeter
A. Sylvester	UC Santa Barbara	Precision levelling array Benchmark stability
F. Wyatt D. Agnew	UC San Diego	Coordination of research Environmental monitoring Data collection Preliminary data analysis
W. Zürn	Schiltach Observatory	Borehole tiltmeter

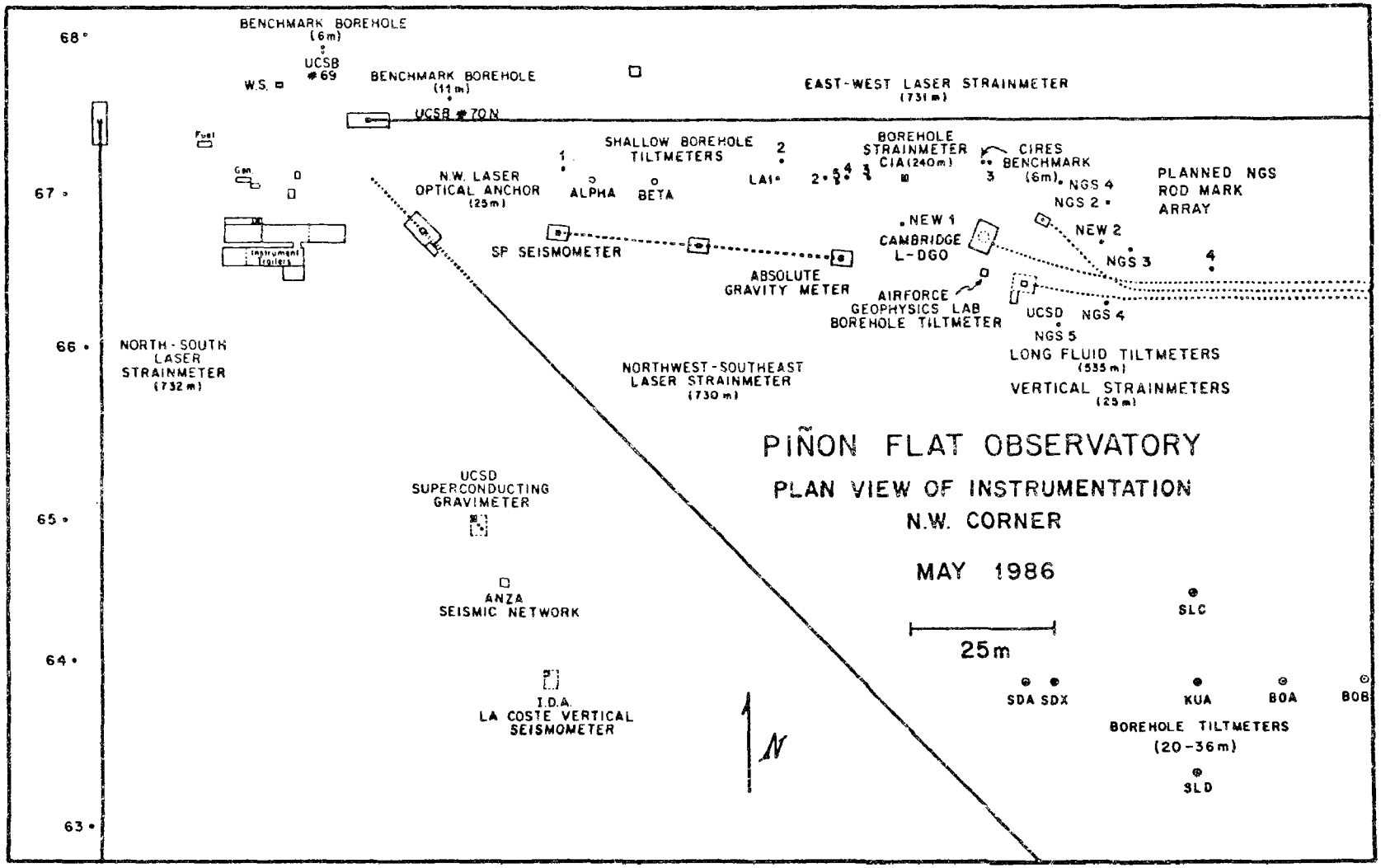
BENCHMARK BOREHOLE
(6m)
UCSB
#69
W.S.
BENCHMARK BOREHOLE
(11m)
UCSB #70N
EAST-WEST LASER STRAINMETER
(731m)
SHALLOW BOREHOLE
TILTMETERS
BOREHOLE
STRAINMETER
CIA(240m)
CIRES
BENCHMARK
(6m)
NGS 4
NGS 2
PLANNED NGS
ROD MARK
ARRAY
N.W. LASER
OPTICAL ANCHOR
(25m)
ALPHA
BETA
LA1
NEW 1
CAMBRIDGE
L-DGO
NEW 2
NGS 3
SP SEISMOMETER
ABSOLUTE
GRAVITY METER
AIRFORCE
GEOPHYSICS LAB
BOREHOLE TILTMETER
UCSD
NGS 5
NGS 4
LONG FLUID TILTMETERS
(535m)
VERTICAL STRAINMETERS
(25m)
NORTH-SOUTH
LASER
STRAINMETER
(732m)
NORTHWEST-SOUTHEAST
LASER STRAINMETER
(730m)
PIÑON FLAT OBSERVATORY
PLAN VIEW OF INSTRUMENTATION
N.W. CORNER
MAY 1986
25m
UCSD
SUPERCONDUCTING
GRAVIMETER
ANZA
SEISMIC NETWORK
I.D.A.
LA COSTE VERTICAL
SEISMOMETER
SLC
SDA SDX
KUA
BOA
BOB
BOREHOLE TILTMETERS
(20-36m)
SLD
N
68°
67°
66°
65°
64°
63°

Figure 1.

ABSOLUTE GRAVITY MEASUREMENTS IN THE LONG VALLEY CALDERA

14-08-0001-22005

M. A. Zumberge, G. Sasagawa, and M. Kappus

Institute of Geophysics and Planetary Physics
Scripps Institution of Oceanography
University of California, San Diego
La Jolla, CA 92093
619/452-2870

Introduction

Data from a variety of geodetic techniques are needed to understand the mechanisms responsible for vertical motions in the earth's crust. Because crustal deformation proceeds slowly, there is an advantage to methods that determine an absolute quantity rather than relative changes between benchmarks. Absolute measurements of gravitational acceleration, based on highly stable length and time standards, are not likely to be contaminated by the instrumental drift and cumulative error that plague many relative geodetic measurements. For vertical motions caused by mechanisms that do not include the addition or subtraction of total mass, g varies with the free air gradient of 3 μGal/cm. The IGPP absolute gravity meter is routinely making measurements with an absolute accuracy of roughly 10 μGal (Zumberge *et al.*, 1986). Thus these measurements are sensitive to changes in height of order 3 cm. Because the measurements are absolute, future results can be compared with those from the present epoch without any ambiguity introduced through the possible instability of reference benchmarks.

Results

Absolute gravity measurements have been conducted in Long Valley, California, since mid 1984, at the Mammoth Lakes Forest Service Visitor's Center (MAM). Four data points acquired over an interval from July 1984 to February 1986 reveal an apparent decrease in gravity at a rate of -18 ± 11 μGal/year at this site in the town of Mammoth Lakes. These results are consistent with deformation rates determined by level lines. Because the uncertainty in the result is of the same order as the result itself, data over a longer period of time will be needed to adequately resolve the time rate of change of g.

Table 1 lists the results of 5 absolute measurements and one relative gravity tie referred to an absolute datum level. Figure 1 plots the observed absolute gravity at each site, transferred to the floor.

Only one absolute measurement has been made thus far at the former Mammoth Lakes Elementary School (MES). Because the site cannot accommodate the absolute instrument during winter months, a LaCoste-Romberg gravity meter (model G-349) was used to make a relative tie between MAM and the doorway to MES during the January 1986 measurement. The uncertainty in height between this relative tie point and the actual absolute site at MES is about 5 cm. The inferred absolute result at MES may thus be biased upwards by as much as 10 μGal. A future survey will determine what this bias really is, and allow its removal.

A weighted least-squares fit to the MAM data satisfies the observations with a linear gravity change of -18 ± 11 μGal/yr. The standard deviation of the data about the line is 6 μGal. If the

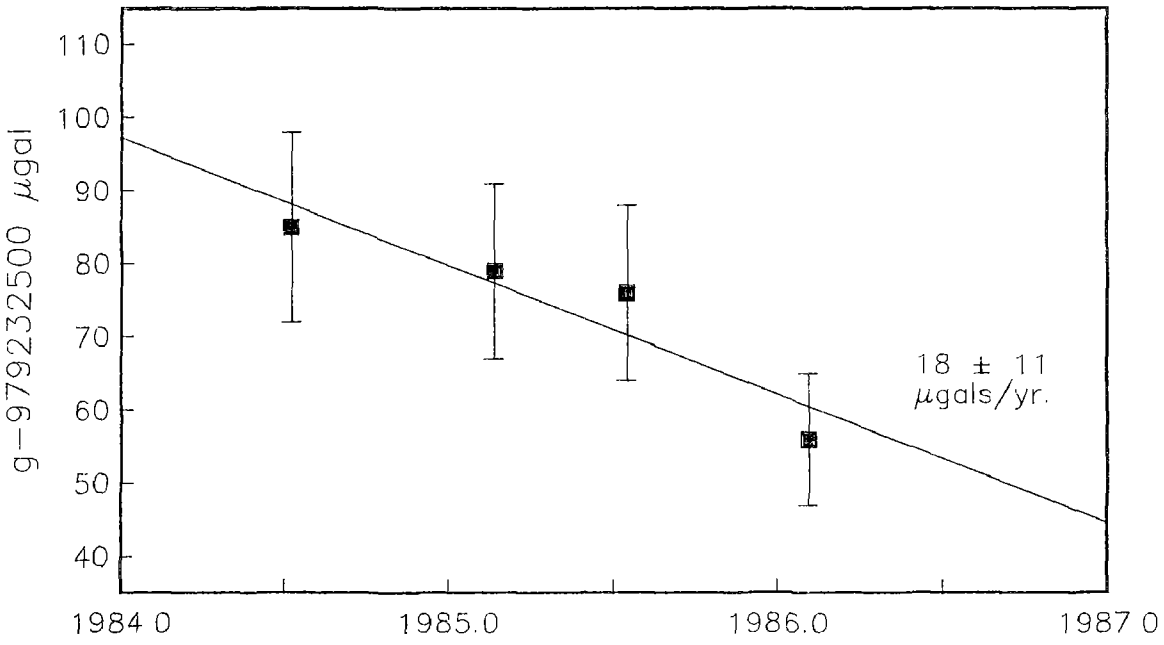

Figure 1. The absolute value of gravity as a function of time at the Mammoth Lakes Forest Service Visitor's Center.

uplift is modeled by the expansion of a point source with conservation of total mass, the observed gravity change elevation change ratio is simply the free air gradient, 308 μGal/m. This implies a 57 ± 36 mm/yr uplift rate at MAM. Jachens and Roberts (1985) suggest a coefficient of -2.5 μGal/cm. Models which involve magma chamber inflation at depth predict a surface change of -2.3 to -2.4 μGal/cm (see, for example, Savage, 1984). Thus our observed gravity change implies uplift between 72 ± 44 mm/yr to 78 ± 48 mm/yr. Leveling studies between 1983 and 1985 show 76 mm of uplift of in this period, corresponding to 38 mm/yr. This is consistent with the absolute gravity data.

The best and simplest explanation for the data at MES is no temporal gravity change. However, the two measurements do not rule out gravity decreases on the order of uplift levels observed with leveling studies.

Firm conclusions on a possible positive uplift rate still require more data. If the uplift continues at its present rate, more absolute gravity data will decrease the uncertainty associated with the $\frac{\Delta g}{\Delta t}$ term.

Table 1. Absolute Gravity Summary

Site	Lat.	Long.	Date	Gradient	g_{floor}	σ_{total}
	°N	°E	yr:day	μgal cm^{-1}	μgal	μgal
MAM	37.65	-118.95	84:191	2.61	979 232 585	13
			85:051		579	12
			85:198		577	11
			86:035		556	9
MES	37.64	-118.85	85:199	2.84	979 269 655	11
			85:035		666†	16

1 gal ≡ 1 cm/sec^2; 1 μgal = 10^{-6} gal = 10^{-8} m/sec^2.

† relative measurement w.r t. MAM result on same day.

References

Jachens, R.C., and C.W. Roberts, Temporal and areal gravity investigations at Long Valley, California, *J. Geophys. Research, 90,* 11,210-11,218, 1985.

Savage, J.C., Local gravity anomalies produced by dislocation sources, *J. Geophys. Res., 89,* 1945-1952, 1984.

Zumberge, M.A., G. Sasagawa and M. Kappus, Absolute gravity measurements in California, *J. Geophys. Res.,* (in press) 1986.

Creep and Strain Studies in Southern California

Grant No. 14-08-0001-G1177

Clarence R. Allen and Kerry E. Sieh
Seismological Laboratory, California Institute of Technology
Pasadena, California 91125 (818-356-6904)

Investigations

This semi-annual Technical Report Summary covers the six-month period from 1 October 1985 to 31 March 1986. The grant's purpose is to monitor creepmeters, displacement meters, and alignment arrays across various active faults in the southern California region. Primary emphasis focuses on faults in the Imperial and Coachella Valleys.

Results

During the reporting period, alignment arrays were resurveyed across the San Jacinto fault at COLTON, across the San Andreas fault at BERTRAM (twice), NORTH SHORE, RED CANYON, and PALLETT CREEK, across the Mission Creek fault at THOUSAND PALMS CANYON, across the Imperial fault at HIGHWAY 80 (twice), TUTTLE RANCH and ALL AMERICAN CANAL, across the unnamed fault at DIXIELAND, across the Superstition Hills fault at SUPERSTITION HILLS, and across the Garlock fault at CHRISTMAS CANYON (twice). Our former alignment array across the Garlock fault at RAND was lost due to construction. Creepmeters were serviced at MECCA BEACH (twice), NORTH SHORE, HEBER ROAD, TUTTLE RANCH, HARRIS ROAD, and SUPERSTITION HILLS. Slipmeters were serviced at MECCA BEACH and LOST LAKE, as well as the two slipmeters in the Parkfield-Cholame area at TAYLOR RANCH and TWISSELMAN RANCH. Nail-file arrays were resurveyed at ROSS ROAD, WORTHINGTON ROAD, and a new array was installed at ANDERHOLT ROAD.

No significant creep events were detected during the reporting period, nor any significant changes in the overall situation as recently described by Louie et al. (1985).

We have recently purchased, partly with grant funds, a Wild Total Station which, with its accessory equipment, incorporates a laser-based EDM (electronic distance measuring) and a theodolite (angle-measuring) device in a single, co-axial, automated, digitally recording system. This instrument will revolutionize our field alignment-array studies, and initial results are very encouraging. Installation of the new creepmeter equipment at SALT CREEK, to utilize SMS-GOES satellite telemetry relay, is underway, although adaptation to the satellite relay system has involved many more problems than we had anticipated.

DIGITAL SIGNAL PROCESSING OF SEISMIC DATA

9930-02101

W. H. Bakun
Branch of Seismology
345 Middlefield Road, MS-977
Menlo Park, California 94025
(415) 323-8111, Ext. 2777

Investigations

Coordination of activities in the Parkfield prediction experiment.

Results

Plans to expand the prediction experiments at Parkfield using the resources available through California AB 938 have been developed. The USGS is preparing to fulfill its intention of issuing a short-term (minutes-to-days) warning of the anticipated Parkfield shock, if sufficient anomalies are recorded.

Reports

Bakun, W. H., A. G. Lindh, and P. Segall, 1985, Overview of Parkfield, California earthquake prediction experiments (abs.) EOS, American Geophysical Union Trans., vol. 66, no. 46, p. 981.

Li, Y. -Z, Y. F. Jin, W. H. Bakun, and F. G. Fischer, 1985, A cooperative seismic network in western Yunnan province, Peoples Republic of China (abs.) EOS, American Geophysical Union Trans, vol. 66, no. 46, p. 1060.

Poley, C. M., A. G. Lindh, and W. H. Bakun, 1986, Parkfield prediction experiment: seismicity updata (abs.), Earthquake Notes, v. 57, no. 1, p. 21-22.

Bakun, W. H., J. Bredehoeft, R. O. Burford, W. L. Ellsowrth, M. J. S. Johnston, L. Jones, A. G. Lindh, C. Mortensen, E. Roeloffs, S. Schulz, P. Segall, and W. Thatcher, 1986, Parkfield earthquake prediction scenarios and response plans (abs.), Trans. Am. Geophys. Un. (EOS), in press.

Bakun, W. H., A. G. Lindh, and T. V. McEvilly, 1986, The Parkfield prediction experiment: an introduction (abs.), Am. Assoc. Adv. Sci., in press.

Bakun, W. H., Li, Y. Z., F. G. Fischer, and Jin, Y. F., 1985, Magnitude and seismic moment scales in western Yunnan, Peoples Republic of China, Seismol. Soc. Amer. Bull., vol. 75, p. 1599-1612.

Li, Y. Z., W. H. Bakun, Jin Yafu and F. G. Fischer, 1985, Magnitude and seismic moment scales in western Yunnan, Peoples Republic of China, J. Seismol. Res., vol. 8, pp. 617-632 (in Chinese).

Synopsis of OCT '85 Parkfield Data

Parkfield seismicity remains at a lower rate than normal, although higher than in September. There were 13 shocks located near Parkfield, only one of which was greater than M=1.5. One M=0.9 shock was located in the Middle Mtn. alarm zone.

The increased creep rate at XPK1 continued throughout October at 18 mm/yr, compared with 12.5 mm/yr for 1979-1983. A new 30-m-long creepmeter was installed at Durham Ranch, replacing the shorter meter that had been operated there. Both the XDR2 and the recently installed XTA1 (Carr Hill) creepmeter are showing left lateral movement. The Work Ranch (WK1) creepmeter is down due to a broken wire.

The two-color laser system down for most of the month is well again and measurements are again being made. Modeling of the measurements in 1985 suggest shallow slip of 25 mm/yr and 18 mm/yr on the Middle Mtn. and Carr Hill sections respectively.

No unusual signals were observed on the water level or borehole dilatometers. The onsite records from the newer water level instruments at Joaquin and Vineyard indicate the presence of good tidal signals, suggesting that these wells probably will serve as sensitive strain monitors.

Synopsis of NOV '85 Parkfield Data

Seismic activity at Parkfield remains low, with only 3 shocks larger than M 1.5 in NOV. The largest shock, at M 1.7, occurred at Turkey Flat on NOV 28 at 0159 GCT. Three shocks with M 1.0-1.5 were located in the Middle Mtn alarm zone. There were no seismic alarm events (beeper-paging alarms) in NOV.

The accelerated creep rate at XPK1 that began with the AUG 9, 1985 Kettleman Hills aftershock continues at about twice the pre-Coalinga earthquake rate. The Work Ranch (now fixed) and Carr Ranch creepmeters resumed right-lateral displacement with the winter rains. There was a 0.5 mm amplitude creep event at XMM1 on NOV 22.

Maintenance completed on NOV 28 by L. Slater on the two-color laser has fixed some of the problems that plagued the system during most of OCT and NOV, and the observation schedule is now getting back to the normal 2-3 times/week. The rapid displacement rates of AUG-OCT for lines to the Middle Mtn section decreased markedly late in OCT. Rapid extension on the line to FLAT in late NOV is consistent with shallow slip at ~26 mm/yr on the fault between Carr Hill and FLAT.

There were no remarkable events on the borehole strainmeters or magnetometers, and the tiltmeters and the Claussen strainmeter show the expected spectacular meteorological effects. There was only one remarkable event recorded by the water wells during OCT and NOV: on OCT 27, the pressure head in the Gold Hill well rose by 4 cm in 2 hours, remained high for 2 days, and began to decline on OCT 29 toward its previous mean. This unexplained event is probably not caused by rainfall, and there were no coincident events on the two Gold Hill dilatometers (except on OCT 30 when both dilatometers reported an apparent extension). The Flinge Flat water well is still down, as is the Eades dilatometer.

There is a need to develop schemes whereby events, alarms, etc. can be rapidly communicated to members of the Parkfield working group. Bill Ellsworth has suggested that a computer mail system be adopted so that any news can be easily sent to all interested parties. Also, we need to have notices of unusual events posted in a prominent place. Stan Silverman and Kate Breckenridge presented samples (attached) of a brief summary of recent (prior 2 days) low frequency data and a map of recent seismicity that will be generated each morning and posted, probably in the hall outside Bakun's office. The format is still in development so that your comments and suggestions are encouraged.

Synopsis of DEC '85 Parkfield Data

Seismicity near Parkfield during December 1985 occurred at twice the average rate with twelve M > 1.5 events. Although there were no Middle Mt. (MM3) seismic alarms, there were two M > 2.5 shocks within the general Parkfield alarm zone resulting in two seismic beeper alerts: a M = 3.11 shock near Slack Canyon on December 14 and a M = 2.97 shock on December 30 near Simmler.

The Work Ranch, Carr Ranch, and Durham Ranch creepmeters all showed significant right-lateral movement, suggesting that these three sites have all now resumed their normal mode of slip; they had written essentially flat creep records since the May 1983 Coalinga shock. The Taylor Ranch instrument continues to show left-lateral motion, probably because of the hillside siting and the winter rains.

Following the maintenance of the two-color source by Larry Slater in early December, data from the two-color electronic distance measuring system improved both in frequency and in less scatter. It is possible that there are unresolved systematic errors in the October-December 1985 data caused by the instrument problems and poor visibility.

The water level, networks recorded no surprising signals during December. The telemetered water level signals from the Gold Hill, Turkey Flat, and Flinge Flat sites are now filtered in real time for barometeric and earth tide effects, preparatory to establishing a real-time alarm system. The water well at Vineyard Canyon has not shown an acceptable earth tide signal and it may be necessary to confine the well to obtain a useable strain monitoring station.

The borehole dilatometer, magnetometer, and tiltmeter networks also recorded no surprising signals in December. The outlook for repairing the damaged electrical cable at the Eades dilatometer site remains bleak. Holes for additional strainmeters at the Vineyard Canyon hilltop site will be drilled soon-tentative starting date of February 1, 1986.

It appears necessary to acquire some means to visit remote sites in winter when normal access by truck, etc over dirt roads is not feasible. It may be necessary to purchase on off-road all purpose vehicles to be stationed near Parkfield.

Synopsis of JAN '86 Parkfield Data

In addition to the Parkfield working group, the three California Division of Mines and Geology Members (Brian Tucker, Chuck Real, and Tony Shakal) of the Parkfield advisory panel were in attendence.

Alerts. A magnitude 2.2 shock occurred at 11 km depth within the MM3 Middle Mt. alarm zone on JAN 28, initiating a level d seismic alert. Water level fluctuation corresponding to 0.04 PPM volumetric change in the Turkey Flat well initiated a level d continuous strain alert. (The fluctuation is thought to be real and related in some way to rainfall.) Two independent level d alerts constitute a c level alert; the Office Chief was notified as specified in the JAN 24, 1986 draft of "Parkfield earthquake prediction scenarios and response plans". No other coincident significant anomalous signals were recognized.

Measurement of the alinement array near the XTA1 creepmeter indicated a slight reversal in the normal right-lateral sense of slip on the main trace of the San Andreas fault. (The last measurement of the alinement array in early November, 1985 was consistent with about 11 mm/year of right-lateral slip.) Recent lack of movement at XTA1 is consistent so that there is no particular reason to suspect the instrumentation at XTA1. Similar lack of right-lateral slip at XDR2 in recent months suggests that the current episode of creep retardation on the Parkfield section extends at least from Carr Hill southeast to the XDR2 creepmeter site.

No surprising signals were recorded on the Parkfield dilatometers or magnetometers. A seismic moment of $3x10^{24}$ dyne-cm was estimated from the dilatometer-GEOS recordings of the S-wave spectra of the Quien Sabe shock of JAN 26. Lower rates and some reversals are apparent on a number of lines in the two-color geodolite network, consistent with the low rates on the nearby

alignment array and creepmeter systems described above. A real-time processing algorithm was installed on JAN 16, 1986 to monitor the water level fluctuations.

Drilling has commenced for new borehole strainmeters at the Vineyard Canyon cluster. One way (Carr Hill to Hog Canyon) transmission on the microwave system was achieved on FEB 5, 1986. Negotiation on extension of the special access to the GOES satellite continue. Negotiations on the Varian lease continue.

Synopsis of FEB '86 Parkfield Data

The heavy rains and their effects on the near-surface geophysical instrumentation near Parkfield were the dominant features of the FEB 1986 period. Total rainfall was 6.18 inches at Gold Hill and 6.63 inches at Turkey Flat; almost all of the rain fell during the FEB 12-20 storm. Separation of tectonic and rain-caused surficial effects remains a difficult problem; if earthquake precursors occur during a rainy period, it will be difficult to separate the tectonic and rain-related components.

There were no seismic alerts in FEB; only one Parkfield shock was larger than M 1.75.

As expected, all of the creepmeters responded to the rainfall; the 5 mm of right-lateral motion on XPK1 in mid-FEB, initially erroneously discounted as the mass floating in a water-filled vault, appears to be real creep associated with rainfall (a creep alert level d(2)).

The borehole dilatometers and the tiltmeters responded to the storms, but there were no strain perturbations of interest; the changes on the dilatometers at the time of the storms are not entirely removed by the barometric corrections so that these apparently are real, not unexpected, pore-pressure effects on the dilatometer outputs.

The Turkey Flat water well instrument pit is flooded. The satellite telemetry was down for much of FEB, at least part of which was caused by problems at the WRD computer facility in Phoenix. All water level fluctuations during FEB are ascribed to barometric pressure variations or to rainfall.

There was a large magnetic disturbance on FEB 7-9, related to a solar flare; the effects can be seen in the differenced magnetic data. These changes are not related to tectonic activity.

A trial run with new electronics and a new computer for the two-color geodolite was conducted during the first week of FEB. The tests were not without problems and the old system, when restored, was compromised by an unexplained offset in the length determinations. These difficulties have been recently overcome, but no reliable two-color data were obtained for most of FEB. The very recent data is consistent with normal trends.

The satellite transmission system had significant dropout problems during the rain storms. No one particular problem has been identified as the cause. Although this is the first significant data dropout due to the satellite telemetry, these problems point out the need for immediate maintenance and also for development of redundant independent data transmission channels.

Synopsis of MAR '86 Parkfield Data

Seventeen earthquakes, only two larger than M 2.0, occurred in the Parkfield region in March 1986. Thus, the relatively low level of recent seismicity near Parkfield continues. There was one level d seismic alert; a M 2.5 shock on March 4 located northwest of MM3 at h=5 km in the Parkfield region alert zone. No other anomalous signals occurred within 72 hours of this alert.

No unusual creep, water well, borehole dilatometer, magnetometer, or two-color geodolite activity that cannot be ascribed to rainfall effects were observed. Rain continued to plague the telemetry data transmission during March. Flooding of the satellite telemetry vault at XMM1 makes reconstruction of the XMM1 creep history problematic until the site can be visited and micrometer readings of the displacement obtained. The surge of creep during this years rainy season (November '85 - April '86) is reminiscent of the surge in creep recorded during the Fall '82 - Spring '83 rainy season that preceeded the 1983 Coalinga earthquake.

No data has been received from the Turkey Flat water well since 13 February due to submersion of the instrument vault. There is a continuing problem in delays of transmission of the water well data from the Phoenix computer center; for as yet unexplained reasons, the water well data has not been adequately received by the satellite system at Menlo Park.

Tests of the new electronics-computer system in the two-color geodolite network continues. When the new system is fully operational, the new computer will provide rapid transmission of the data to the VAX780 in Menlo Park. Pier-tilt readings at most of the reflector sites indicate reasonable levels of pier stability, with exception of the PITT reflector pier. Minimizing the effects of pier instability in the line length calculations will be a major effort in the upcoming summer field season. Trends in line length changes since January 1, 1986 appear to be normal for most lines, but many lines show abrupt changes in slope starting about March 17.

The modelling efforts began a few months ago during Rob Wesson's visit to Menlo Park continue to make progress in addressing outstanding tectonic questions. Bob Simpson provided some provocative results of modelling of the stress changes in the 1983 Coalinga shock on the Middle Mtn. section of the fault. Bob argued that the creep and seismicity changes at the time of the Coalinga shock are somewhat consistent with the calculated stress changes. Paul Segall presented some results of calculations of stress changes inferred from the geodetic observations.

PARKFIELD TWO-COLOR LASER STRAIN MEASUREMENTS

9960-02943

Robert Burford
Branch of Tectonophysics
U.S. Geological Survey
345 Middlefield Road, MS/977
Menlo Park, California 94025
(415) 323-8111, ext. 2574

and

Larry Slater
CIRES
University of Colorado
Boulder, Colorado 80309
(303) 492-8028

Investigations

The CIRES two-color laser ranging system has been operated at the Parkfield CAR HILL site to obtain frequent distance readings to reflector sites shown in Figure 1. Additional measurements were made occasionally to sites without permanent reflectors as well as to reference marks at the permanent sites.

Results

Plots of length changes obtained since late June, 1984 are shown in Figure 2. Details of these changes from October 1, 1985 through March 31, 1986 are shown in Figure 3. The record for station MID (Figure 2) is composed of 2 separate parts owing to loss of the original reflector during late December 1984, with resulting loss of zero. The reflector pier at PITT has shown continuing instability and the line has been dropped. A new station will be established as a replacement (station POMO, Figure 1).

Results of a model, consisting of shallow slip plus uniform strain, indicate that dextral shear (tensor) accumulated at a rate of 1.2 ± 0.2 ppm/yr through March 1986. Dextral shear, presumably caused by deep slip buried beneath a shallow locked zone, was accompanied by 13.6 ± 1.8 mm/yr slip within the upper 1.5 km on the main fault. The model also indicates significant fluctuations in areal dilatation within the network. However, the dilatational component is subject to systematic error due to possible drift in instrument scale. Occasional comparisons between the

observatory instrument and a portable 2-color geodimeter indicate that drift between the two instruments is about +0.4 ± 0.1 ppm/yr (observatory-portable).

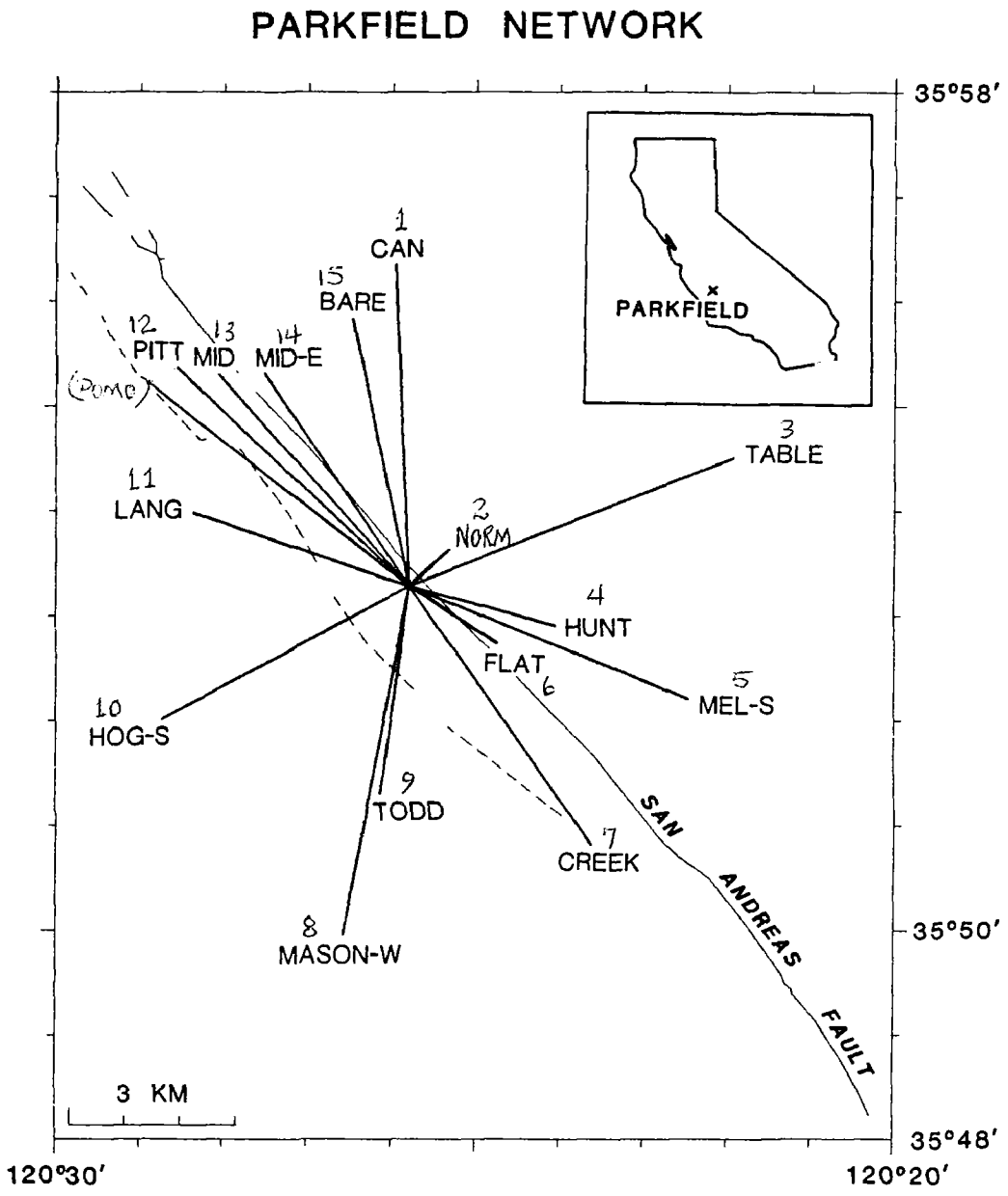
PARKFIELD NETWORK
35°58′
35°50′
35°48′
120°30′
120°20′
PARKFIELD
1
CAN
15
BARE
12
PITT
13
MID
14
MID-E
(POMO)
3
TABLE
11
LANG
2
NORM
4
HUNT
FLAT
6
5
MEL-S
10
HOG-S
9
TODD
7
CREEK
SAN ANDREAS FAULT
8
MASON-W
3 KM

Figure 1

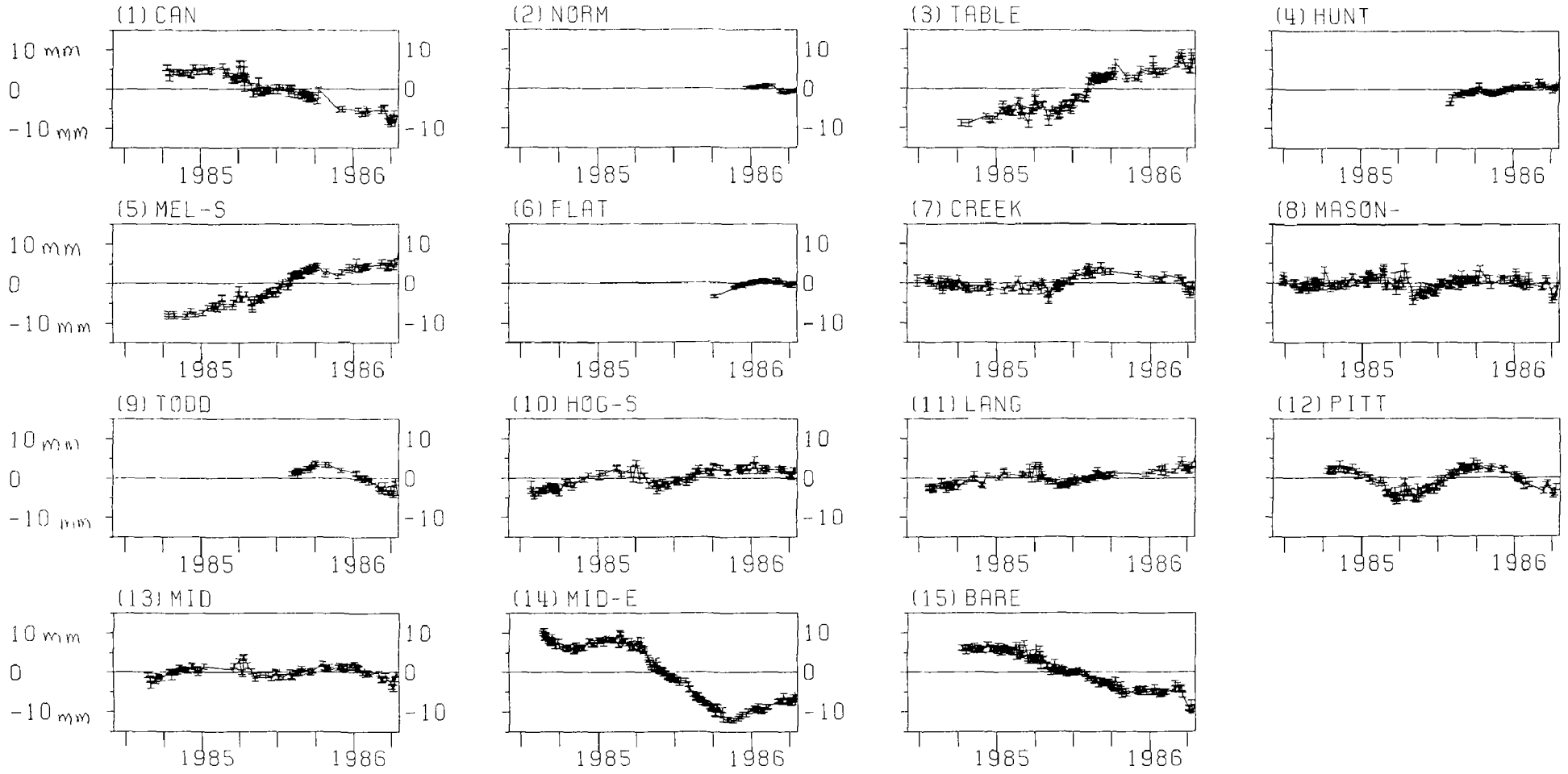
(1) CAN
(2) NORM
(3) TABLE
(4) HUNT
(5) MEL-S
(6) FLAT
(7) CREEK
(8) MASON-
(9) TODD
(10) HOG-S
(11) LANG
(12) PITT
(13) MID
(14) MID-E
(15) BARE
10 mm
0
-10 mm
10
0
-10
1985
1986

Figure 2

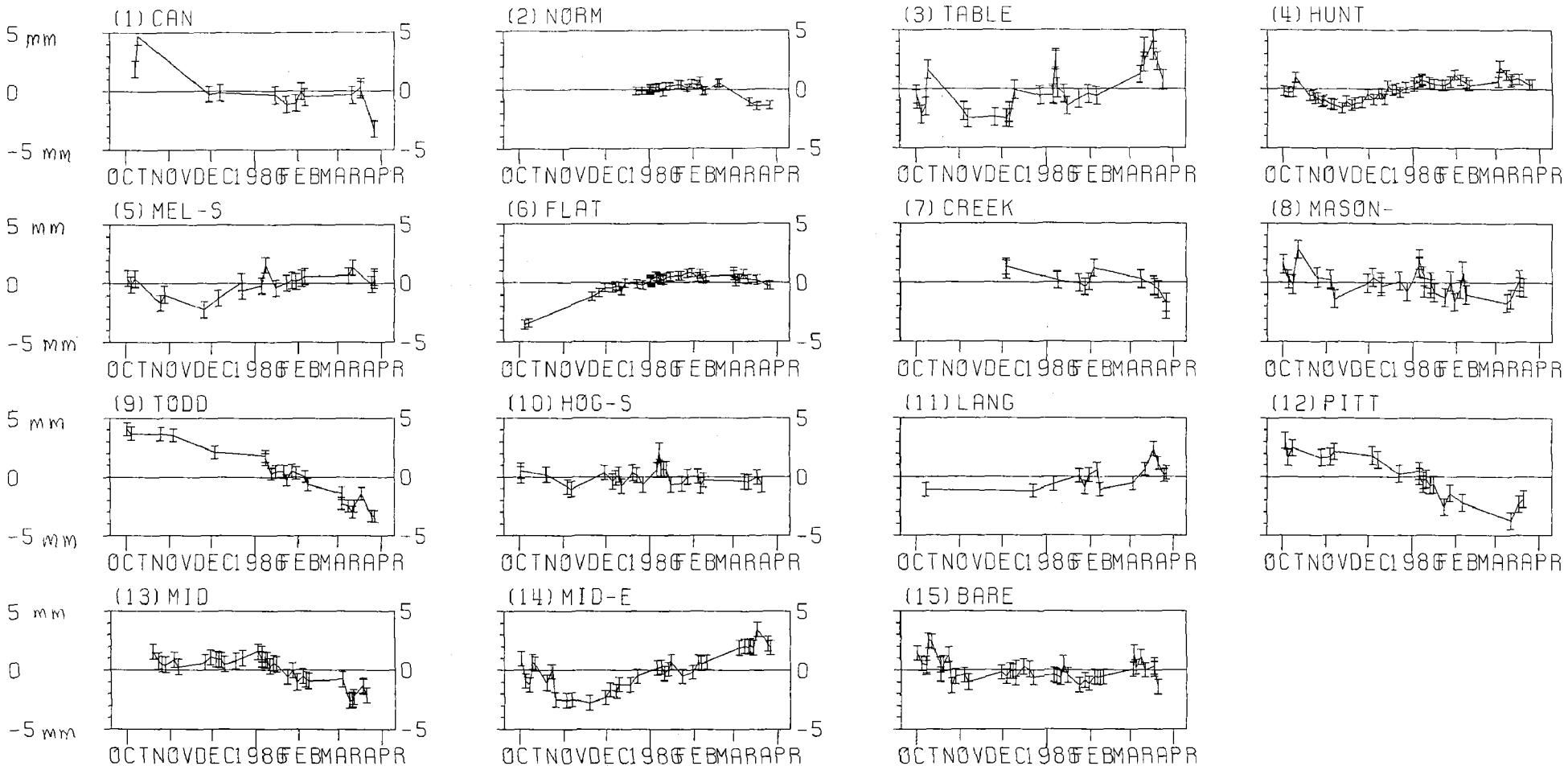
(1) CAN
(2) NORM
(3) TABLE
(4) HUNT
(5) MEL-S
(6) FLAT
(7) CREEK
(8) MASON-
(9) TODD
(10) HOG-S
(11) LANG
(12) PITT
(13) MID
(14) MID-E
(15) BARE
5 mm
0
-5 mm
OCTNOVDEC1986FEBMARAPR

Figure 3

SEARCH FOR ELECTROMAGNETIC PRECURSORS TO EARTHQUAKES
(66730)

William Daily
Lawrence Livermore National Laboratory
P.O. Box 808, L-156
Livermore, California 94550
(415) 422-8623

Joe Tate
Ambient Research
519 Waldo Point
Sausalito, California 94965

Observations of electromagnetic (EM) precursors have been reported for large earthquakes in Japan, Iran, Chile, and the Soviet Union (e.g., by Gokhberg, et al., 1980). In addition, recent observations of very low frequency (VLF) precursors measured by GEOS satellites have been reported by Parrot and Lefeuvre (1984). Mechanisms and semiquantitative models advanced to explain the observations have been discussed by Gokhberg, Gufeld and Dobrovolsky (1979) and Warwick, Stoker, and Mezer (1982). Laboratory demonstration of radio frequency emission from cracking rocks has also been reported (Nitsan, 1977; Vorobev, 1977). Reported herein are the results of a study to search for EM earthquake precursors along the San Andreas Fault system in California, using ground based, broadband electromagnetic monitors.

Several very low frequency radio receivers have been built to monitor broadband EM noise near a fault zone. These receivers have been placed into operation near the San Andreas Fault in 1983 and 1984. It is unlikely that one such monitoring station will be capable of monitoring events along more than a few hundred kilometers of the fault. Therefore, we have emplaced receivers along the San Andreas Fault. The exact location of each site was determined by: 1) the estimated probability of an earthquake of Richter magnitude greater than about 5 (precursors are typically seen only with larger magnitude events); 2) accessibility of site to facilitate deployment and periodic equipment checks; 3) isolation from cultural sources of wide band EM noise; 4) availability of power source and reasonable security. To allow some discrimination of source location, monitoring stations were spaced far enough apart that signals from an event will not be seen equally well by all sensors. If the source region for these signals is deep (a few kilometers), signals at the surface should be confined near the epicenter--attenuation will be high due to propagation long distances through high loss crust from the source. If the source region is near the surface, signals will be measurable at larger distances. From these considerations and published measurements of precursors, we estimate that the locations monitored should be a few hundred kilometers apart, but also chosen for their high potential as an epicenter for a large earthquake. The five locations chosen for placement of monitors are: 1) Coyote Lake, near Morgan Hill; 2) Bear Valley, near Hollister; 3) Turkey Flat, near Parkfield; 4) Adobe Mountain, near Palmdale; and 5) Pinon Flat U.S.G.S. observatory near Palm Springs.

Cultural noise, both narrow band and broadband is the main source of low frequency signal. Narrow band signals are mostly from marine related VLF

transmissions above about 20 kHz. In addition, there are harmonics of 60 Hz from the electric power grid. Broadband signals result from several sources, but especially from automobile ignition systems. Of course, there is a continual lightning-induced low frequency background. Any EM emission associated with a seismically active area will most likely be broadband. Laboratory measurements from cracking rocks are of broadband EM emission. All proposed mechanisms for EM earthquake precursors would result in broadband emissions. Finally, all reported EM precursors were presumed to be broadband emissions. Therefore, for maximum signal to noise ratio, we designed the receivers to be broadband with three bands recorded: 1) 200 Hz to 1 kHz, 2) 1 kHz to 10 kHz, 3) 10 kHz to 100 kHz. Each system uses a three-meter-long vertical monopole antenna referenced to a ground plane. Data is recorded continuously on a strip chart recorder and each station is battery powered.

The broadband capability helps to reduce variation in cultural noise, especially the narrow band (radio station) sources. Reported measurements of events indicate that a high sensitivity system is not required. Each channel has a 60 dB dynamic range (logarithmic amplifiers) recorded on the strip chart recorder. This is used because of its effectiveness, simplicity, reliability, and low cost.

The signal received by each station is very site specific. At some sites, the signal in all frequency bands is continuously highly variable on a time scale of a few hours. At other sites, the measured signal levels are nearly constant for periods of weeks at a time. The reason for this difference is unknown, but some sites may have high levels of cultural noise which would be variable in amplitude.

The largest earthquake on the San Andreas since deployment of our stations had an epicenter near Morgan Hill and occurred on April 24, 1984. Only the station at Coyote Lake was fully operational at the time of and immediately prior to this event. About six days prior to this event a prominent signal minimum which lasts about 28 hours was observed on the station at Coyote Lake. This minimum was recorded in the bands 200 Hz to 1 kHz and 1 kHz to 10 kHz, but the gain was improperly adjusted for the band 10 kHz to 100 kHz so that no data was collected in that frequency interval. The partial data available from the Adobe Mountain (Palmdale) site and the Turkey Flat (Parkfield) site do not show a signal strength reduction comparable to that seen at Coyote Lake (Morgan Hill). However, April 20, 1984, a decrease in ambient EM power similar to that seen at Morgan Hill was reported at Sausalito, California, 120 km to the northwest of Morgan Hill.

Another event on January 26, 1986, of about magnitude 5.0 and centered near Hollister, CA occurred since deployment of our stations. On the Morgan Hill station, two periods of emissions occur, each about one hour long, just prior to the earthquake. These emissions were recorded only in the 10-100 kHz band which includes the frequencies of emissions recorded for the Japanese and Russian earthquakes. No other such emissions are seen in the data for at least the four previous days. At another newly installed station in Sausalito, CA, quasi-periodic (period approx. 15 min.) fluctuations in ambient signal levels were measured for about 6 hours on the 26th.

It is tempting to make a connection between the anomalous EM signals seen at Morgan Hill and Sausalito and the earthquakes that followed at Morgan Hill and Hollister. It is likely premature to make such a connection. On the other hand, the data are encouraging enough to warrant continued monitoring of EM power along the San Andreas until a more complete data set is collected.

Bibliography

Gokhberg, M. B., V. A. Morgounov, T. Yoshino, and I. Tomizawa, "Experimental Measurement of Electromagnetic Emissions Possibly Related to Earthquakes in Japan," J. Geophys. Res., 87, 7824, 1982.

Gokhberg, M. B., I. L. Gufeld, I. P. Dobrovolsky, and G. I. Shevtsov, "Studies of Mechanoelectric Effects under Laboratory Conditions," Preprint N 9, Acad. of Sci. of the U.S.S.R., Moscow, 1980.

Gokhberg, M. B., I. L. Gufeld, and I. P. Dobrovolsky, "On the Sources of Electromagnetic Earthquake Precursors," Preprint N 10, Acad. of Sci. of the U.S.S.R., Moscow, 1980.

Gokhberg, M. B., V. A. Morgounov, and T. Yoshino, "The Experimental Results of Appearance of Electromagnetic Emissions Related with Earthquake at Sugadaira Observatory in Japan," University of Electro-Communications, I - 5 - I.

Nitsan, U., "Electromagnetic Emission Accompanying Fracture of Quartz-Bearing Rocks," Geophys. Res. Letters, 4, 333, 1977.

Parrot, M. and F. Lefeuvre, "Study of VLF Emissions Apparently Associated with Earthquakes from Ground-Based and GEOS Satellite Data, Results of the ARCAD 3 Project and of the Recent Programmers in Magnetospheric and Ionospheric Physics," 2-25 Mai 1984, Toulouse, France, 1984.

Vorob'ev, A. A., "Electromagnetic Radiation in the Process of Crack Formation in Dielectrics," Difektoskopiya, No. 3, 128, 1977.

Theodolite Measurements of Creep Rates on San Francisco Bay Region Faults

14-08-0001-G1186

Jon S. Galehouse
San Francisco State University
San Francisco, CA 94132
(415) 469-1204

We began measuring creep rates on San Francisco Bay region faults in September 1979. Amount of slip is determined by noting changes in angles between sets of measurements taken across a fault at different times. This triangulation method uses a theodolite set up over a fixed point used as an instrument station on one side of a fault, a traverse target set up over another fixed point used as an orientation station on the same side of the fault as the theodolite, and a second traverse target set up over a fixed point on the opposite side of the fault. The theodolite is used to measure the angle formed by the three fixed points to the nearest tenth of a second. Each day that a measurement set is done, the angle is measured 12 times and the average determined. The amount of slip between measurements can be calculated trigonometrically using the change in average angle.

We presently have theodolite measurement sites at 20 localities on faults in the Bay region (see location map). Most of the distances between our fixed points on opposite sides of the various faults range from 75-215 meters; consequently, we can monitor a much wider slip zone than can be done using standard creepmeters. The precision of our measurement method is such that we can detect with confidence any movement more than a millimeter or two between successive measurement days. We remeasure most of our sites about once every two months.

The following is a brief summary of our results thus far:

Seal Cove-San Gregorio fault - We began our measurements on the Seal Cove fault (Site 7) in Princeton, San Mateo County, in November 1979. For the next 6.4 years, the Seal Cove fault showed net movement of only 1.5 millimeters in a right-lateral sense. Any small amount of tectonic slip that may be occurring is difficult to ascertain because of seasonal effects, often involving apparent left-lateral slip that tends to occur toward the end of a calendar year.

Various logistic problems have occurred at our Site 8 across the San Gregorio fault near Pescadero in San Mateo County. The width of fault zone we are monitoring (452 meters) is the widest of all our 20 sites and measuring it is difficult. We have had considerable variations in the amounts and directions of movement from one measurement day to another. The presently-calculated average is 2.4 millimeters per year of right-lateral slip for the past 3.7 years.

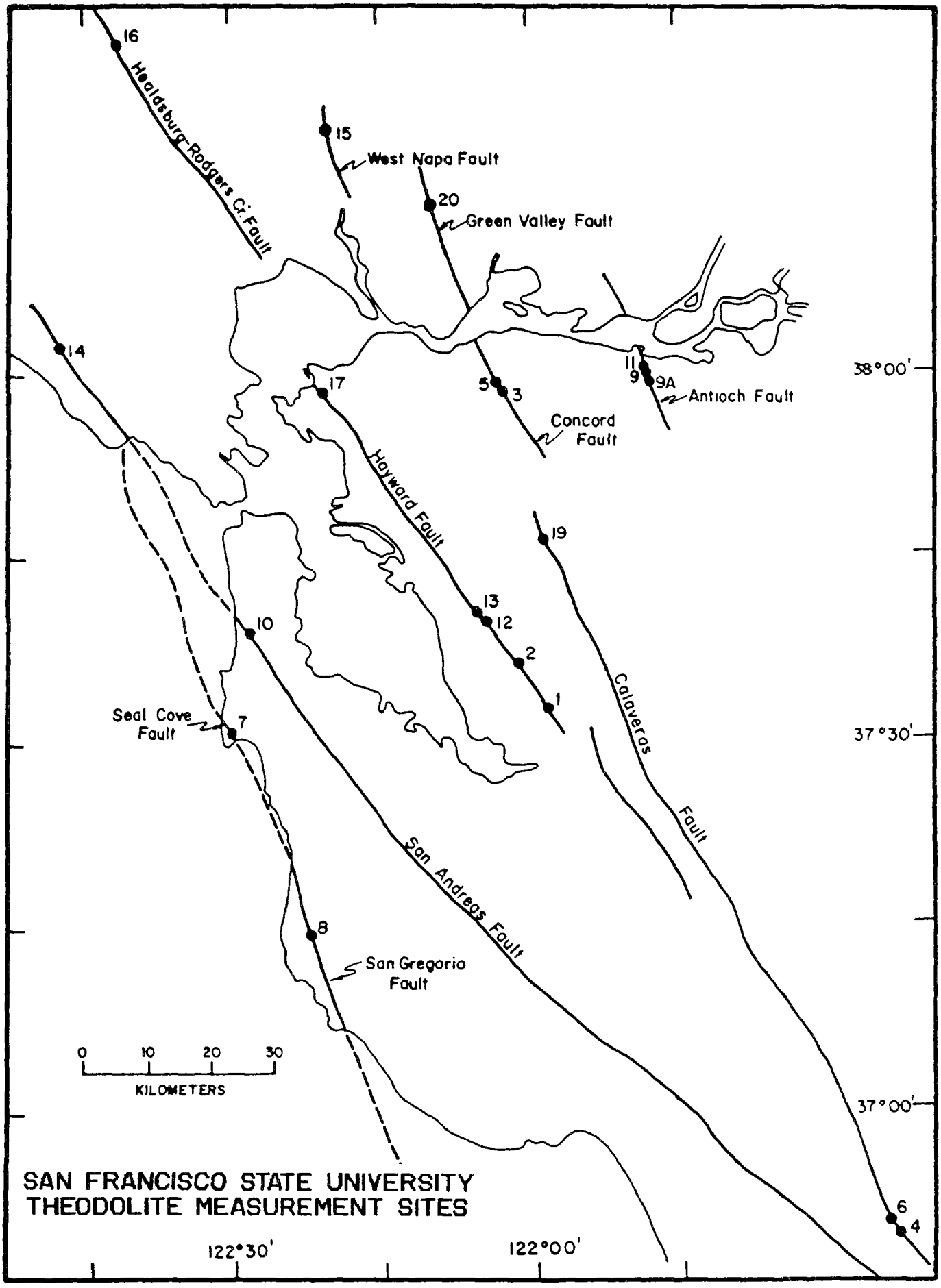
16
Healdsburg-Rodgers Cr. Fault
15
West Napa Fault
20
Green Valley Fault
14
17
5
3
11
9
9A
Antioch Fault
Concord Fault
Hayward Fault
19
13
12
2
1
10
Seal Cove Fault
7
Calaveras Fault
San Andreas Fault
8
San Gregorio Fault
0 10 20 30
KILOMETERS
38°00'
37°30'
37°00'
6
4
122°30'
122°00'
SAN FRANCISCO STATE UNIVERSITY
THEODOLITE MEASUREMENT SITES

San Andreas fault - In the 6 years since March 1980 when we began our measurements across the San Andreas fault in South San Francisco (Site 10), virtually no net slip has occurred. We recently (February 1985) reestablished our Site 14 in Marin County, this time at the Point Reyes National Seashore Headquarters. Preliminary results after one year of measurements indicate right-lateral slip of about one millimeter. Our Site 18 (not shown on the location map.) in the Point Arena area has averaged 1.3 millimeters per year of right-lateral slip in the five years from January 1981 to January 1986. These results indicate that the northern segment of the San Andreas fault is virtually locked, with very little, if any, creep occurring.

Rodgers Creek fault - In the 5.4 years since August 1980, our Site 16 on the Rodgers Creek fault in Santa Rosa has had an average of less than a millimeter per year of left-lateral slip. However, our results show large variations in the amounts and directions of movement from one measurement day to another. These are probably due to seasonal and/or gravity-controlled mass movement effects, not tectonic slip.

West Napa fault - In the 5.7 years since July 1980, our Site 15 on the West Napa fault in the City of Napa has shown virtually no net slip. Similarly to our results for the Rodgers Creek fault, however, large variations up to nearly a centimeter have occurred in both a right-lateral and a left-lateral sense between measurements days. The magnitude of these nontectonic effects is obscuring the small amount of any tectonic slip that may be occurring.

Green Valley fault - We established a new site (Site 20) on the Green Valley fault north of Suisun Bay in June 1984. After 1.6 years, measurements show right-lateral slip at a rate of about three millimeters per year.

Hayward fault - We began our measurements on the Hayward fault in late September 1979 in Fremont (Site 1) and Union City (Site 2). During the next 6.2 years, the average rate of right-lateral slip was 4.7 millimeters per year in Fremont and 4.4 millimeters per year in Union City. However, in the 3.5 month interval from mid-December 1985 to the end of March 1986, the Hayward fault in Fremont moved 10 millimeters in a right-lateral sense. The fault at our site in Union City has continued to move at its average rate.

We began measuring two sites within the City of Hayward in June 1980. During the next 5.5 years, the average annual rate of right-lateral movement was 4.7 millimeters at D Street (Site 12) and 4.4 millimeters at Rose Street (Site 13). However, in the three month interval from mid-December 1985 to mid-March 1986, the fault at Rose Street moved 11 millimeters in a right-lateral sense. The fault at D Street has continued to move at its average rate.

We began measurements in San Pablo (Site 17) near the northwestern end of the Hayward fault in August 1980. For the past 5.6 years, the average rate of movement has been about 3.3 millimeters per year in a

right-lateral sense. However, superposed on this overall slip rate are changes between some measurement days of up to nearly a centimeter in either a right-lateral or a left-lateral sense. Right-lateral slip tends to be measured during the first half of a calendar year and left-lateral during the second half.

In summary, the average rate of right-lateral movement on the Hayward fault is about 4 to 5 millimeters per year. Recently, however, two of our five sites have shown much more rapid movement than the average. This could possibly be a precurser of a forthcoming seismic event of significance on the Hayward fault. We intend to increase the frequency of our measurements in the eastern San Francisco Bay region.

Calaveras fault - We have three measurement sites across the Calaveras fault and the nature and amount of movement are different at all three. We began monitoring our Site 4 within the City of Hollister in September 1979. Slip along this segment of the Calaveras fault is quite episodic, with times of relatively rapid right-lateral movement alternating with times of little net movement. For the past 6.4 years, the fault moved at a rate of 7.5 millimeters per year in a right-lateral sense.

At our Site 6 across the Calaveras fault on Wright Road just 2.3 kilometers northwest of our site within the City of Hollister, the slip is much more steady than episodic. In the 6.3 years since October 1979, the Calaveras fault at this site has been moving at a rate of 13.8 millimeters per year in a right-lateral sense, the fastest rate of movement of any of our sites in the San Francisco Bay region.

U.S.G.S. creepmeter results in the Hollister area are quite similar to our theodolite results. Creepmeters also show a faster rate of movement at sites on the Calaveras fault just north of Hollister than at sites within the City of Hollister itself.

The rate of movement is much lower at our Site 19 in San Ramon, near the northwesterly terminus of the Calaveras fault. Only about one-half millimeter per year of right-lateral slip has occurred during the past 5.4 years.

The epicenter of the 24 April 1984 Morgan Hill earthquake occurred on the Calaveras fault between our Hollister area sites which are southeast of the epicenter and our San Ramon site which is northwest of it. Two papers that we published regarding our theodolite measurements and observations of surface displacement related to the earthquake are listed at the end of this summary. No unusual movement appears to have occurred prior to the Morgan Hill earthquake.

The epicenter of the 26 January 1986 Tres Pinos earthquake occurred on the Quien Sabe fault south of Hollister. It appears that the earthquake may have triggered a few millimeters of right-lateral slip at our site on the Calaveras fault in Hollister. However, no unusual movement occurred either before or after the earthquake at our Wright Road site north of Hollister.

Concord fault - We began our measurements at Site 3 and Site 5 on the Concord fault in the City of Concord in September 1979. Both sites showed about a centimeter of right-lateral slip during October and November 1979, perhaps the greatest amount of movement in a short period of time on this fault in the past two decades. Following this rapid phase of movement by about two months were the late January 1980 Livermore area moderate earthquakes on the nearby Grenville fault.

After the relatively rapid slip on the Concord fault in late 1979, both sites showed relatively slow slip for the next four and one-half years at a rate of about one millimeter per year right-lateral. However, in late Spring-early Summer 1984, both sites again moved relatively rapidly, slipping about seven millimeters in a right-lateral sense in a few months. The rate has again slowed since late August 1984 (through late March 1986).

The overall rate of movement on the Concord fault (combining the two periods of relatively rapid movement with those of slower movement) is about 4.3 millimeters per year (Site 3) and 3.4 millimeters per year (Site 5) of right-lateral slip in the past 6.5 years.

Antioch fault - We began our measurements at the more southeasterly of two original sites on the Antioch fault (Site 9) in the City of Antioch in January 1980. During the next 27 months, we measured a net right-lateral displacement of nearly two centimeters. However, large changes in both a right-lateral and a left-lateral sense occurred between measurement days. Three times left-lateral displacement occurred toward the end of one calendar year and/or beginning of the next. We abandoned this site in April 1982 because of logistic problems and relocated it (Site 9A) just southeast of the City of Antioch in November 1982. The fault at this newer site has shown virtually no net movement for the past 3.4 years.

The more northwesterly of our original sites on the Antioch fault (Site 11) is located where the fault zone appears to be less specifically delineated. In the six years since May 1980, we have measured a slight amount of left-lateral slip. Much subsidence and mass movement creep appear to be occurring both inside and outside the Antioch fault zone and it is probable that these nontectonic movements are obscuring any tectonic slip that may be occurring.

Publications

Galehouse, J.S., 1986, Theodolite Measurements: in Geodetic Observations section of "The Morgan Hill, California Earthquake of April 24, 1984"; U.S. Geol. Survey Bull. 1639, in press.

Galehouse, J.S. and Brown, B.D., 1986, Surface Displacement Near Hollister: in Geological Observations section of "The Morgan Hill, California Earthquake of April 24, 1984"; U.S. Geol. Survey Bull. 1639, in press.

DEEP BOREHOLE PLANE STRAIN MONITORING
14-08-0001-22025

Michael T Gladwin,

Department of Physics
University of Queensland
St Lucia, 4067
AUSTRALIA.

ACTIVITIES

1. Processing of the data from the two borehole tensor strainmeters installed in California in 1983 has been continued. Both instruments have provided data of excellent quality, and reasonable in situ tidal calibration of the various components has now been completed. The instruments used have a useful sensitivity of about 0.3 $n\epsilon$ and stability measured in these installations of approximately 10 $n\epsilon$ per annum. Dynamic range is approximately 140 dB and linearity better than 0.004%. The instrument is most useful in simple shear environments where volume strain is minimal, where diagnostic shear strain data are required soon after installation of an instrument, or where large volumetric noise sources such as migration of water tables dominate the strain field.

2. Two earthquakes of significance have occurred within a few source dimensions since installation. The first was at Morgan Hill on April 24 1984, and the second at Quiensabe, on January 26, 1986. Initial processing of the Morgan Hill event was the subject of a previous report.

3. Further processing of the Morgan Hill, April 24, 1984 earthquake for removal of the effects of grout curing has been performed and has provided new insight into the state of strain at the site during and after the earthquake.

3. Fabrication of three new instruments for installation in the Parkfield region during this summer field season is on schedule. In the new instruments, e ectronic noise has been reduced by more than 30 dB compared with the instruments presently in operation in San Juan Bautista and Pinon Flat.

RESULTS

1. For both earthquakes, the magnitude of the coseismic step observed at the instrument agreed well with that expected from strain step estimates at the San Juan site using the seismically determined moment and source parameters. The strain step and indicated shear strain direction appear to have propagated across the intervening fault zones without significant modification.

2. For both earthquakes, the coseismic step was followed by a period of continued strain release over several hours following the earthquake, indicating that the total moment release associated with the events was significantly larger than that estimated during the (elastic) coseismic event. This effect is illustrated in figure 1, in which the shear data for the coseismic and immediate post seismic period are plotted. The sampling interval in each case is 18 minutes (limited by

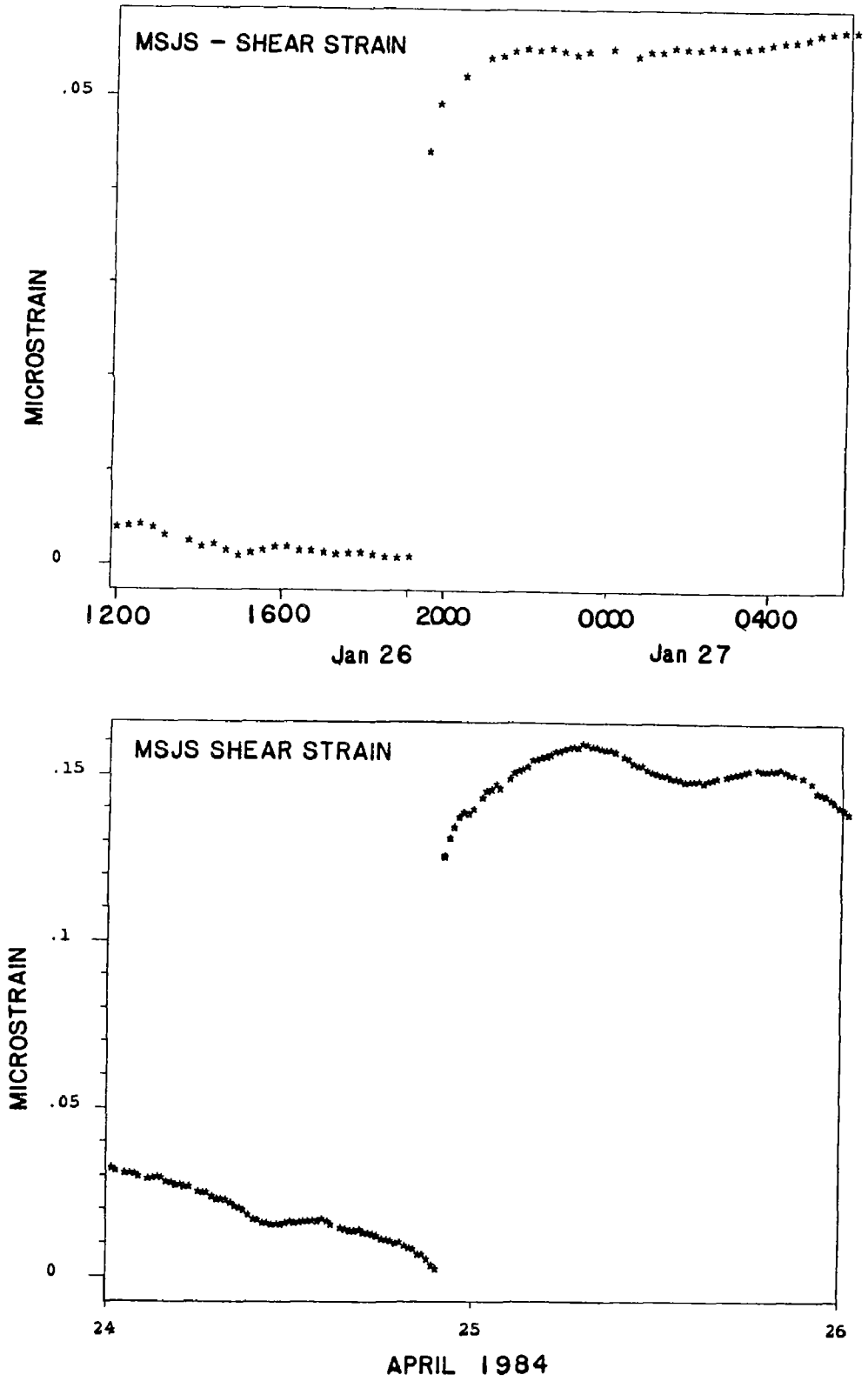

1. Comparison of coseismic and immediate postseismic response for two earthquakes. The coseismic step, whose amplitude is well predicted from the seismically determined source parameters is followed by a clear afterslip sequence. The Morgan Hill event was 51km from the site , and the Quiensabe event (Jan 26, 1986) was 24 km from the site.

the total data throughput in the satellite retrieval system). The time history of the shear strain response for the Morgan Hill event differed significantly from the volumetric strain response during the afterslip phase.

3. For both earthquakes, this afterslip sequence was followed by an extended phase of modified strain response at the site which can be identified as regional strain redistribution following the earthquakes. In both cases, this period is typified by a modified strain rate from before to after the earthquakes.

4. For the Morgan Hill event, the strain redistribution phase was somewhat masked by the final stages of the grout curing following instrument implant on September 29, 1983. Figure 2 shows raw shear strain for the San Juan site beginning four months after installation and showing the step (shear strain relief) of the Morgan Hill event. The smooth curve through the data set is an exponential fit to the data which measures hole relaxation processes following early installation in a region which has a pre-drilling ambient shear strain field. The exponential shown was determined using data before the earthquake only. If we identify the time period plotted as having only a single event of significance, the Morgan Hill strain relief event at MSJS persisted for about four months following the earthquake, and that at that time it recovered in a period of about 3 months to the pre-existing conditions.

5. The residual, that is raw shear data minus the exponential, is plotted in figure 3, which shows that the strain relief event of approximately 150 nanostrain remained reasonably constant following the event until August, then returned to the baseline value (here zero).

6. A comparison of this time history with both geodetic data and with the borehole dilatometer data set at nearby Searle Road is in progress. The dilatometer data also indicates a relatively flat response following the offset at the time of the earthquake and ending in August with significant change in slope, and a general qualitative correspondence with figure 3 indicating that regional strain redistribution is probably involved.

PUBLICATIONS

Gladwin, M. T., High Precision multi component borehole deformation monitoring. *Rev.Sci.Instrum., 55,* 2011-2016, 1984.

Gladwin, M.T., Gwyther, R., Hart, R., Francis, M., and Johnston, M.J.S., Borehole Tensor Strain Monitoring in California. *J. Geophys. Res.* In review.

Gladwin, M. T. and Hart, R. Design Parameters for Borehole Strain Instrumentation. *Pageoph.,123,* 59-88, 1985.

Gladwin, M. T., Hart, R., and Gwyther, R. L. Tidal Calibration of Borehole Vector Strain Instruments.*EOS, (Trans. Am. G. Un.) 66,* 1057, 1985.

Gladwin, M. T. and Johnston, M.J.S. Strain Episodes on the San Andreas Fault following the April 24 Morgan Hill, California Earthquake. *EOS,(Trans. Am.G.Un.), 65,* 852, 1984.

Gladwin, M.T., and Johnston, M.J.S. Coseismic moment and total moment of the April 24, 1984, Morgan Hill and the January 26, 1986, Quiensabe earthquakes. *EOS,(Trans.Am.G.Un.), 67, R 308, 1986.*

Gladwin, M. T. and Wolfe, J. Linearity of Capacitance Displacement Transducers. *J.Sc.Instr. 46,* 1099-1100, 1975.

Johnston, M.J.S., Gladwin, M.T., and Linde, A.T. Preseismic Failure and Moderate Earthquakes. *I.A.S.P.E.I.* , Tokyo, August 19-30, S7-65, 35 ,

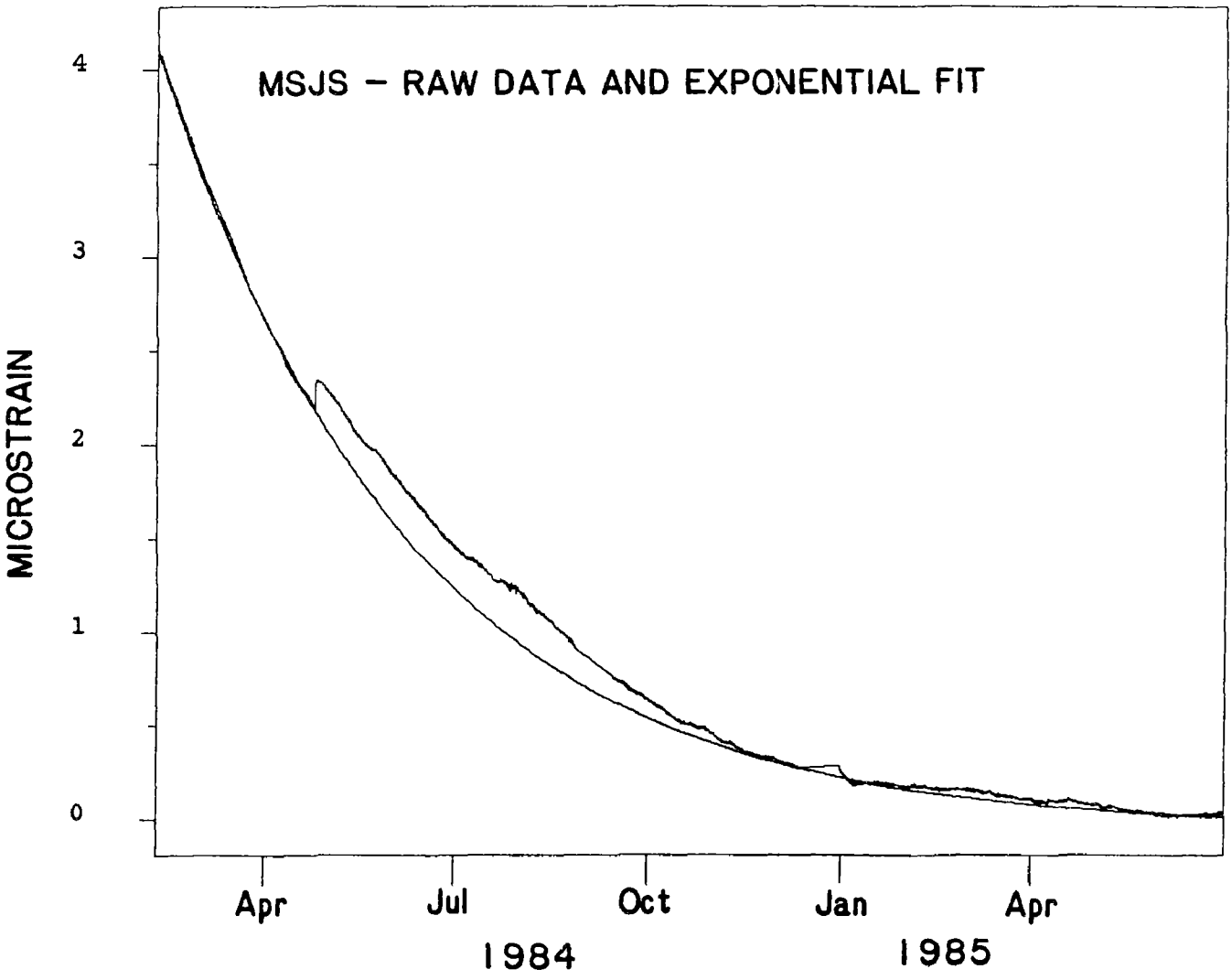

2. Seventeen months of shear strain data from the San Juan instrument showing the exponential decay following implant in a pre-existing shear strain environment. The smooth curve is an exponential fit to the data determined prior to the earthquake. The strain relief of the Morgan Hill event is followed by a return to the pre-existing trend prior to the event.

1985.

Johnston, M. J. S., Linde, A.T., Gladwin, M.T., and Borcherdt, R.D. Fault Failure with Moderate Earthquakes. Tectonophys., In Press.

Johnston, M.J.S., Borcherdt, R.D., Glassmoyer, G., Gladwin, M.T., and Linde, A.T. Static and Dynamic Strain during and following January 26, 1986, Quiensabe, California, Earthquake. *EOS,(Trans., Am. G. Un.), 67,* 16, 308, 1986.

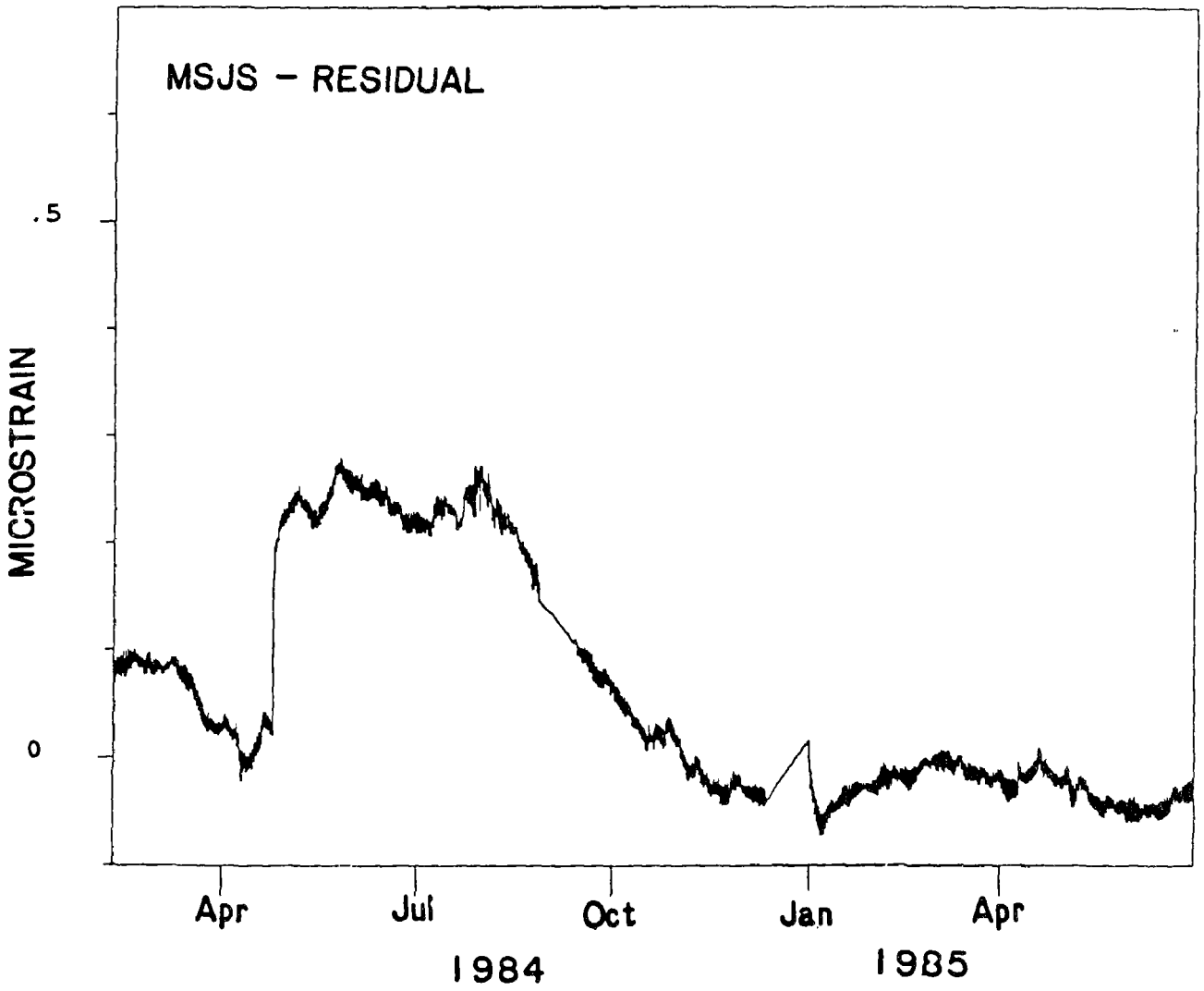

3. Residual indicated in figure 2. The tick marks are each 100 nanostrain and the tidal modulation is evident. The disturbance to the record in December 1984 was caused when the instrument was taken off line for a high sample rate (10Hz) evaluation. The residual shows that the strain relief was relatively constant from April to August, and that it then returned to the zero drift value in a relatively short interval of time.

Deepwell Monitoring along the Southern San Andreas Fault

14-08-0001-G1076

Thomas L. Henyey and Steve P. Lund
Department of Geological Sciences
University of Southern California
Los Angeles, CA 90089-0741
(213) 743-6123

Investigations

We have monitored the variation in water level and temperature within an array of deep wells near the southern San Andreas fault for more than six years. Our data show no variations during 1985 that might be considered related to potential seismic activity along the San Andreas fault.

Results

One goal of our study is to detect large amplitude water-leve variations in the Palmdale region and define their source mechanisms. In general, water-level data sets of several years in duration are needed to assess these long-term strain changes and characterize the water level variability due to known forcing functions such as rainfall and aquifer discharge/recharge. We have previously noted long-term (several year) variations across the Palmdale array that show systematic trends indicative of either long-term strain changes or aquifer storage changes in the Palmdale region. These several-year-long trends are superposed on yearly rainfall cycles, with different wells having different ratios of the several-year to seasonal rainfall response. These long term trends are continuing through 1985.

Several expanded data sets for October-December, 1985 are shown in Figure 1; this was a period encompassing relatively large atmospheric pressure variation, related rainfall, and the only significant earthquake (magnitude 3.7) of 1985 along the San Andreas fault near our array. The quality of data and the correlation across the array for the monthly data sets are outstanding.

We have also previously compared the water level variability in our wells with that of its known forcing functions -- solid earth tidal and atmospheric pressure variations. Our spectral analysis and crosscovariance studies (Henyey and Lund, 1985) have clearly documented that both forcing functions are important contributors to the water-level variation. The coherent water level variation between four different wells, noted in Figure 1, illustrates the systematic response of separate wells to the same solid-earth tidal and atmospheric pressure variations. Almost all of the observed variation (except the longest-term reservoir trends) is due to these known forcing functions. These results are a further indication of the quality and sensitivity of our water-level records. Similar comparisons can be made for all of our sites, although not all have such high sensitivity to solid-earth tidal variations.

One goal of this study is to detect large amplitude water-level variations in the Palmdale region and define their source mechanisms. In general, water-level data sets of several years duration are needed to assess

long-term strain changes and characterize the water level variability due to known forcing functions such as rainfall and aquifer discharge/recharge; these data sets are now becoming available in the Palmdale array.

For example, long-term (several year) variations across the Palmdale array (Figure 2) show systematic trends which may indicate either long-term strain changes within the aquifer rocks or aquifer storage changes in the Palmdale region due to the cumulative effects of seasonal rainfall. These several-year-long trends are superposed on yearly rainfall cycles, with different wells having different ratios of the several-year to seasonal rainfall response. Wells in the north half of the array have smaller relative seasonal responses than do wells in the southern half of the array (with the exception of Phelan which does not show any apparent seasonal trend). Similarly, wells in the north half of the array show relatively less response to solid-earth tides and atmospheric pressure variations than do wells in the southern half of the array.

We have also looked for clear anomalies related to known seismicity in southern California. We have noted no anomaly of either preseismic or coseismic nature during 1985. There were, however, no large earthquakes within or near our array. The largest nearby earthquake occurred on October 31, 1985 near San Bernardino and had a magnitude of 3.7. The timing of this earthquake is noted in Figure 1 relative to the water level variation in four of our wells. We saw no evidence of the earthquake in our data.

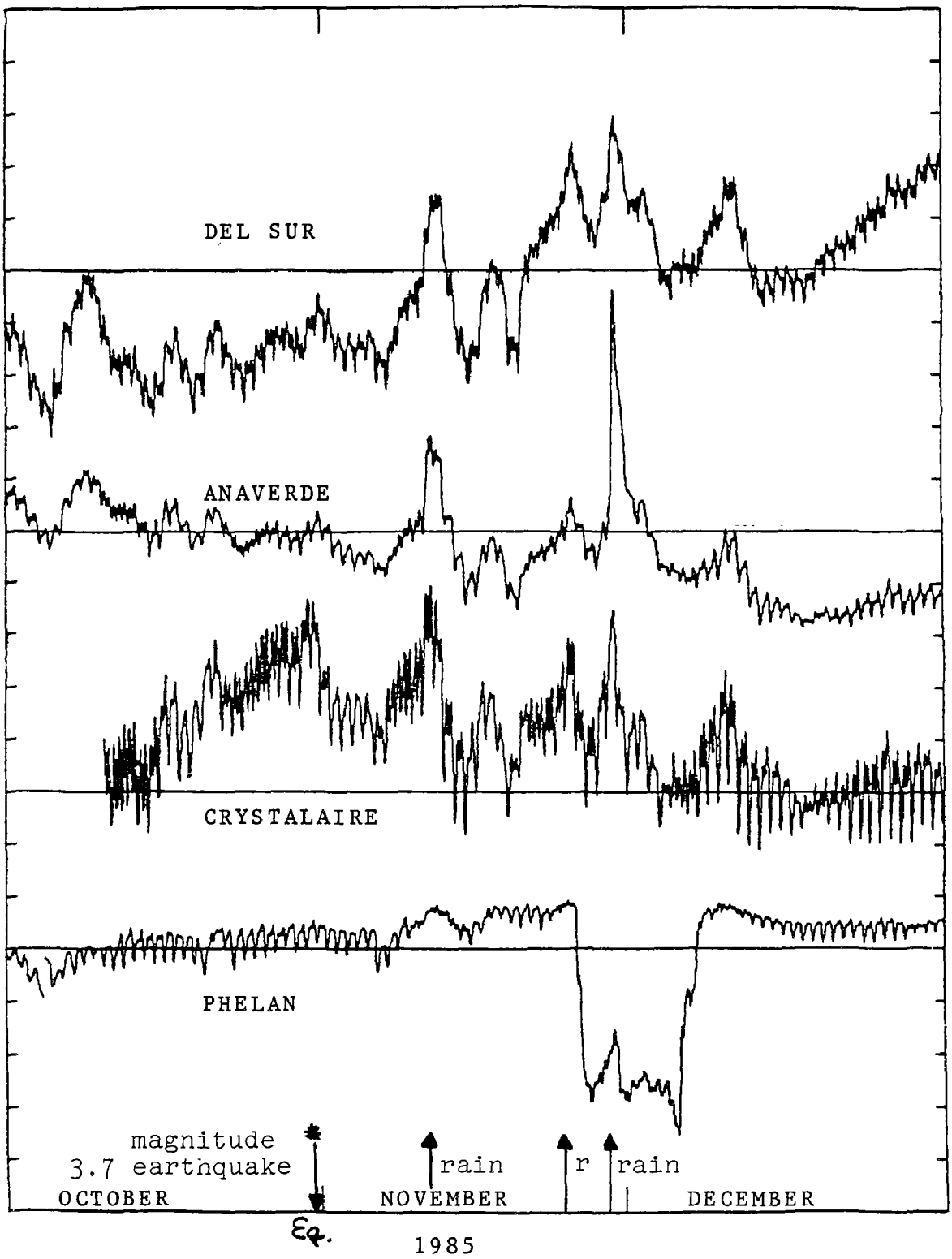

Figure 1: Water level variation from four different wells of the Palmdale array (hourly averaged data). Note strong response of these wells to solid-earth tides and atmospheric pressure changes. Also note the lack of response to magnitude 3.7 earthquake near San Bernardino on October 31, 1985.

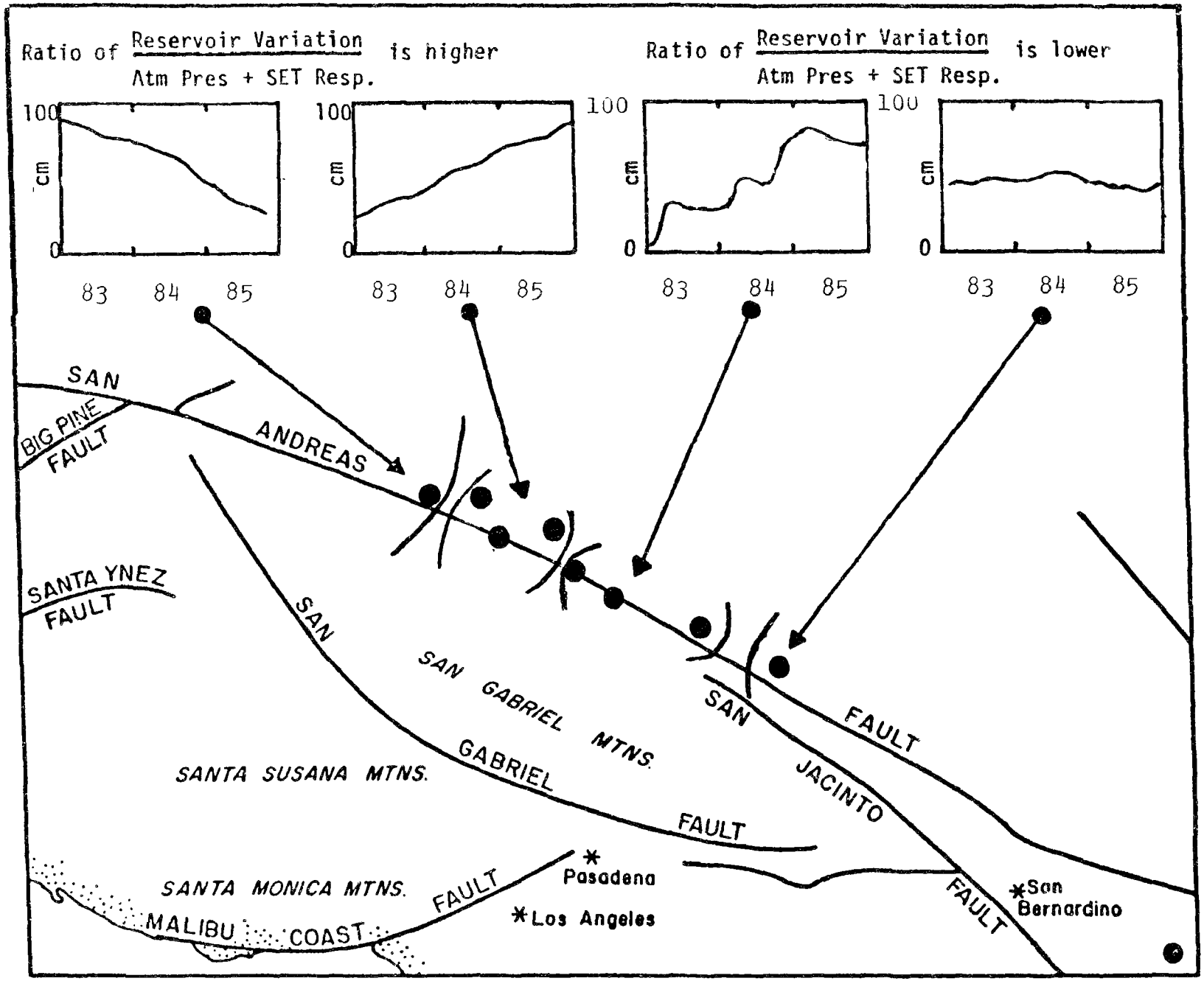

Figure 2: Generalized long term water level variability for the last 3 years along the Palmdale Deepwell array. Distinct but coherent long term behavior can be noted as one progresses from Nothwest to southeast along the array.

Repeat Gravity Studies
9380-03074

Robert C. Jachens and Carter W. Roberts
Branch of Geophysics
U.S. Geological Survey, MS 989
Menlo Park, CA 94025
(415) 323-8111, x 4248

Investigations

1) Remeasured the southern California precision gravity base station network during January, 1986, including a measurement of a station at the Holcomb Ridge 2-color geodimeter site.

2) Remeasured 10 precision gravity stations along a profile oriented perpendicular to the San Andreas fault and passing through Cajon Pass.

3) Received from the contractor and checked preliminary copies of the aeromagnetic survey of the Parkfield area. An OK has been given to the contractor to generate the final copies of the maps and digital data bases.

Results

1) The latest repeat measurement at Holcomb Ridge showed a decrease of 11 microgal from the previous measurement made in May, 1985. This decrease is an accelerated continuation of a trend that measurements at this station have shown since early 1983. A total of nine reoccupations during the past three years have yielded temporal gravity variations that are well correlated with changes in areal strain as measured by John Langbein with the 2-color geodimeter. Decreasing gravity is correlated with areal contraction in the same manner as had been seen earlier at Tejon Pass, Palmdale, and Cajon Pass and the slope of the relationship between areal strain changes and gravity changes is effectively the same value as that seen earlier.

2) The San Andreas cross profile has been measured approximately annually since January, 1983. Although an occasional measurement at an isolated station has deviated from the average at the station by as much as 20 microgal, no systematic pattern of gravity changes relative to the position of the fault is apparent from the data for the past three years.

3) The aeromagnetic map is of excellent quality and displays numerous prominent anomalies due to probable granitic and ultramafic sources. A cursory look at the map in the vicinity of Gold Hill confirms the earlier findings based on a few ground magnetic traverses that the Gold Hill gabbro constitutes a body of limited areal extent, being roughly 4 km long and 1.5 km wide.

Reports

Roberts, C. W., and Jachens, R. C., 1986, High-precision gravity stations for monitoring vertical crustal motion in southern California: U.S. Geological Survey Open-file Report 86-44, 76 p.

TILT, STRAIN, AND MAGNETIC MEASUREMENTS

9960-02114

M.J.S. Johnston, R. Mueller, D. Myren, A. Jones,
C. Mortensen, and V. Keller
Branch of Tectonophysics
U.S. Geological Survey
345 Middlefield Road, MS/977
Menlo Park, California 94025
(415) 323-8111, ext. 2132

Investigations

1. To investigate the mechanics of failure of crustal materials using deep borehole vector and dilational strainmeters data and data from surface strainmeters, tiltmeters, and arrays of absolute magnetometers.

2. To develop physical models of incipient failure of the earths crust by analysis of real-time records of these and other fault zone data.

Results

1. The Kettleman Hills earthquake (M_L 5.5) on August 4, 1985 was recorded on three borehole dilatometers in the Parkfield region of the San Andreas fault at hypocentral distances of 36.3, 37.6, and 38.0 km, respectively. The seismically determined moment was $1.2*10^{25}$ dyne-cm and the preferred focal plane strikes N52°W, with a dip 12°SW (Eaton, 1985). The observed strain data are generally consistent with slip over a plane with this orientation. For the simplest point source model, the volumetric strain calculated at the three dilatometer sites are 0.246, 0.108, and 0.110 μstrain, respectively, whereas the observed strains are 0.305, 0.104, and 0.118 μstrain. It is not clear at this point why the strain observed on the most northern strainmeter near Parkfield is larger than expected. Either the model used is too simple, the properties at this site are not adequately modeled, or (as perhaps indicated by other data) the earthquake triggered some sympathetic slip on the San Andreas with amplitudes of about 0.2 μstrain have been recorded simultaneously on independent instruments and on nearby water wells. These strain transients correspond generally in time with episodes of minor seismicity in the area. The maximum amplitude of a creep wave or strain episode that might occur between a depth of 5 and 10 km on the fault near these instruments and go undetected is about 10 mm.

2. The high sensitivity, wide dynamic range and bandwidth of deep borehole three-component and dilational strainmeters at the shorter periods (0.1 seconds to 10,000 seconds) has not been fully utilized at instrumented sites in California. To remedy this a programmable 16-bit digital seismic event recorder with on-site recording (G.E.O.S.) has been used to record pre-event and event data at more than six sites in California during seismic events, nuclear explosions and in strain noise studies. Power spectral density estimates show general consistency from site to site and, except for about 10 dB of 6 second microseismic noise, decrease with increasing frequency from about -170 dB at about 10 dB per decade of frequency. Peak power in strain seismograms of local earthquakes and nuclear explosions occurs between 0.1 and 1 Hz. Detection of pre-rupture strains at the 10^{-10} strain level appear possible in this period range from these data.

3. Crustal strain data for two nearby earthquakes have been recorded with a 3-component borehole strainmeter installed in a 200 meter borehole near the San Andreas fault at San Juan Bautista, California. These events are the Morgan Hill (M 6.5) earthquake on April 24, 1984, at a distance of 51 km, and the Quiensabe (M 5.5) earthquake on January 26, 1986, at a distance of 24.3 km. The measured coseismic offsets are consistent with moments of $2*10^{25}$ dyne-cm, and $3.7*10^{24}$ dyne-cm, respectively, and axes of maximum shear in directions N33°W and N4°W, respectively. These moments and maximum shear directions are consistent with the seismically determined moments of $2*10^{25}$ and $2*10^{24}$ dyne-cm, respectively, and fault strikes of N33°W and N5°W. In the Morgan Hill record, the coseismic offset data were followed by two distinct phases of continued exponentially decreasing strain (afterslip), with the same maximum shear axis as the main event. The first phase had a time constant of approximately 8 hours and a moment approximately 70% of that released during the elastic event. The second phase had a time constant of several months, in general agreement with the amplitude and time scale of geodetic observations in the area. The Quiensabe earthquake was also followed by two phases of exponentially decreasing postseismic strain. The time scale of the first phase was 2 hours with an additional 20% moment release. The time scale of the second phase was 3 days with a further 20% moment release. We thus identify three contributions to the total moment calculation: 1) coseismic (elastic), 2) continued failure (afterslip) in the immediate source zone, and 3) regional strain redistribution (log-creep). The seismic moments are thus 58% and 71% of the total moments for these earthquakes.

4. Crustal strain preceding, during and following the January 26, 1986, Quiensabe earthquake (M 5.5) was recorded on several Sacks-Evertson dilatometers (SRLS at 27.1 km, GH2S at 151.5 km, and others at greater distances), a 3-component (tensor) strainmeter (MSJS - 24.3 km distant), installed at a depth of about 200 m near the San Andreas fault, and 3-component surface seismic velocity transducers at the dilatometer sites. Dynamic strain and velocity for the foreshock, mainshock, and aftershocks were recorded at a 300 Hz sampling rate and high gain on digital recorders (GEOS). The moment of the earthquake was estimated from displacement spectra generated using the dynamic strain and velocity seismograms and also from the static strain offsets recorded on the strainmeters. The seismic moments determined from the surface velocity transducers at the dilatometer locations are between $1.7\text{-}2*10^{24}$ dyne-cm. As observed for the April 24, 1984, Morgan Hill M 5.5 event, the static moments are larger (between $2\text{-}3*10^{24}$ dyne-cm). Post-seismic strain, consistent with continued failure on the rupture plane, occurred for several days after the earthquake. The post-seismic moment is at least 20% of that of the earthquake. Precursive strains in the days to seconds before the event are again not apparent in the data from the closest instruments, SRLS and MSJS, respectively. The decrease in shear strain and normal strain of 0.01 and 0.05 μstrain, respectively, recorded at the 3-component strainmeter site indicate a decrease in the effective strength ($\sigma_p - 0.6\sigma_n$) for right-lateral failure of the San Andreas fault near this location. The occurrence of the Quiensabe earthquake would make it marginally more likely, therefore, for moderate earthquakes to occur in the locked section of the San Andreas fault in the vicinity of the strainmeters. The axis of maximum shear defined during the seismic phase was N4°W, consistent with the seismically determined strike (N5°W).

5. Strain and seismic records have been obtained for the March 31, 1986, Mt Lewis earthquake to the east of Fremont, California. Copies of these records are shown in Figure 1. These and coseismic offset data have been used to estimate the moment of this earthquake.

6. Four water level monitoring sites have been selected on Lake Crowley in the Long Valley/Mammoth Lakes region. Stills installed at these sites will provide differential water level measurements (tilt) in this seismically active region. The continuous data will be transmitted by the low frequency satellite data collection system to Menlo Park.

7. Arrays of differential magnetometers and intermediate-baseline geodetic nets have been installed and surveyed since 1980 at the northern end of the Red River fault in Yunnan Province. On the basis of seismic recurrence and other evidence a moderate to large earthquake is expected within the next few years. Simple uniform strain models have been fit to the strain data from arrays at Liante and Dengchaun on the northwest extension of the Red River fault. At Liante the primary feature of the data is a uniform well-determined negative dilation of 1.9 μstrain/a. Negative dilation of 1.2 μstrain is evident also in the Dengchaun data with a marginally significant shear in a direction N60°W. Test line data indicate repeatibility in distance measurements during this time to better than 3 mm on a 734 m line. In contrast, the net line length changes are between 10 and 100 mm on lines typically between 4 and 7 km in length. Magnetic measurements in the region of high magnetization on the west side of the fault at Dengchaun show an increase in local magnetic field of up to x nT/a over sites on the east side of the fault. In contrast, no significant magnetic changes have occurred in the Liante array. This result is in accordance with tectonomagnetic theory since the absence of regional magnetic anomalies indicate remanent and induced rock magnetization of less than 0.001 A/m.

8. Sites for 13 potentially borehole strain monitoring sites have been selected in the Parkfield region. Coring and drilling this summe will be done under the direction of Tom Moses. Installation of three 3-component strainmeters and as many as six dilatometers is planned for late summer.

Reports

Bakun, W.H., Bredehoeft, J., Burford, R.O., Ellsworth, W.L., Johnston, M.J.S., Jones. L., Lindh, A.G., Mortensen, C. E., Roeloffs, E., Schulz, S., Segall, P., and Thatcher, W., 1986, Parkfield Earthquake Prediction Scenarios and Response Plans, Trans. A.G.U. (in press).

Gladwin, M.T., and Johnston, M.J.S., 1986, Co-seismic Moment and Total Moment to the April 24, 1984, Morgan Hill, and the January 26, 1986, Quiensabe Earthquakes, Trans. A.G.U. (EOS), (in press).

Johnston, M.J.S., Borcherdt, R.D., and Linde, A.T., 1986, Short period strain ($0.1\text{-}10^5$s): Near Source Strain Field for an Earthquake (M 3.2) near San Juan Bautista, California, J. Geophys. Res. (submitted).

Johnston, M.J.S., Borcherdt, R.D., Glassmoyer, G., Gladwin, M.T., and Linde, A.T., 1986, Static and Dynamic Strains During and Following the January 26, 1986, Quiensabe, California, Earthquake, Trans. A.G.U. (EOS), (in press).

Ware, R.H., Johnston, M.J.S., and Mueller, R.J., 1985, A Comparison of Proton and Self-Calibrating Rubidium Magnetometers for Tectonomagnetic Studies, J. Geomag. Geoelec., 37, 1051-1061.

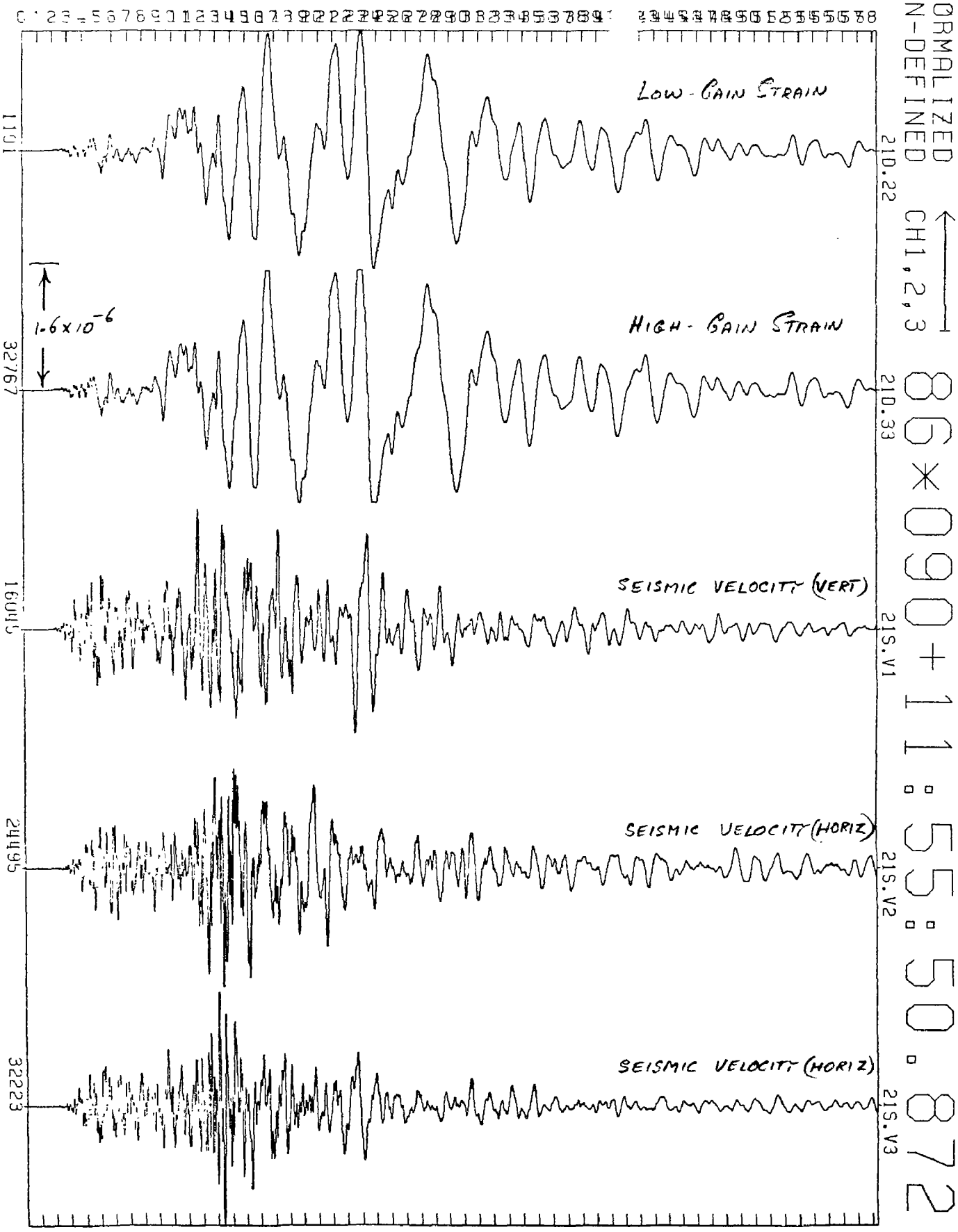

Figure 1. Dilational strain and 3-component seismic velocity recorded at site SRLA during the March, 31, 1986, Mt. Lewis earthquake.

Earthquake and Seismicity Research Using SCARLET and CEDAR

Contract No. 14-08-0001-G1171

Hiroo Kanamori, Clarence R. Allen, Robert W. Clayton
Seismological Laboratory, California Institute of Technology
Pasadena, California 91125 (818-356-6914)

Investigations

1) Earthquake Repeat Time and Average Stress Drop
Kanamori, H. and Allen, C. R.

2) Rupture Patterns and Preshocks of Large Earthquakes in the Southern San Jacinto Fault Zone
Sanders, C., Magistrale, H., and Kanamori, H.

Results

1) Earthquake Repeat Time and Average Stress Drop

We investigated the relation between earthquake repeat time, fault length and magnitude.

Existing data on source parameters of large crustal earthquakes (subduction events are not considered here) over a wide range of repeat times indicate that, for a given magnitude (M_S or M_W), earthquakes with long repeat times have shorter fault lengths than those with short repeat times. A shorter fault length for a given magnitude indicates a larger average stress drop which reflects the average strength of the fault zone. Our result therefore suggests that faults with longer repeat times are stronger than those with shorter repeat times. In terms of an asperity model in which the average strength of a fault zone is determined by the ratio, r_a, of the total area of asperities (strong spots on a fault plane) to the total area of the fault zone, the above result suggests that r_a is proportional to the repeat time. Our result provides a method to estimate seismic source spectra from the fault length and the repeat time of a potential causative fault.

2) Rupture Patterns and Preshocks of Large Earthquakes in the Southern San Jacinto Fault Zone

We relocated the large 1937, 1942, and 1954 earthquakes in the San Jacinto fault zone. The epicenters of the mainshocks, aftershocks, and some preshocks were determined using empirical station corrections obtained from recent small events in the study areas. The 1937 (M_L 5.9) earthquake has an epicenter between the surface traces of the San Jacinto and Buck Ridge faults and aftershocks suggest about 7 km of rupture predominantly to the northwest. A significant increase in small earthquake activity occurred about a year and a half before this event. The 1954 (M_L 6.2) earthquake is located at the southeast end of the mapped trace of the San Jacinto fault, and aftershocks suggest about 15 km of rupture further southeast into an area of folded young sediments with no surface fault trace. This event was preceded by a cluster of small earthquakes which occurred within an eight hour period 10 weeks before the main event and in the eventual rupture zone. The 1942 (M_L 6.3) earthquake is located southwest of the southeast end of the Coyote Creek fault. Large aftershocks of this event are spread over a 15 by 18 km area southwest of the Coyote Creek fault and are not associated with any one fault. The relation of the 1942 event to the San Jacinto fault zone is not simple.

Our study indicates that the area S of the fault plane corresponding to the Anza seismic gap is approximately 18 (length L) x 10 (width W)km^2. The slip rate V along this part of the San Jacinto fault has been estimated to be approximately 10 mm/year. No large earthquake is known to have occurred in this gap since 1899. If these estimates are correct, the seismic moment of an earthquake which might occur in this gap is at least M = μSVT, where μ is the rigidity (assumed to be 3 x 10^{11} dyne/cm^2) and T is the time measured from 1899. Using the values listed above, we obtain M = 4.7 x 10^{25} dyne-cm for the year of 1986.

Figure 1 shows the accumulated moment for the Anza gap in relation to fault length and seismic moment of shallow strike slip events in the world. For the given length of the Anza gap (18 km), the accumulated seismic moment has exceeded the upper bound of the range defined by strike slip earthquakes.

Since the above result depends critically on the estimates of the slip rate, we feel that more work on slip rate and paleoseismicity is needed to evaluate better the seismic potential of this gap.

Figure 1

The relation between the fault length and the seismic moment of shallow strike slip earthquakes in active plate margins. The open and closed circles indicate the data taken from Scholz et al. (1986) and Kanamori and Allen (1986), respectively.

References

Doser, Diane I. and Hiroo Kanamori, Spatial and Temporal Variations in Seismiity in the Imperial Valley (1902 - 1984), *Seismo. Soc. of Amer, Bull., 76,* No. 2, 421-438.

Hearn, Thomas H. and Robert W. Clayton, Lateral velocity variations in Southern California, I. Results for the upper crust from Pg waves, *Seismo. Soc. of Amer, Bull., 76,* No. 2, 495 - 509.

Hearn, Thomas H. and Robert W. Clayton, Lateral Velocity Variations in Southern California, II. Results for the upper crust from Pg waves, *Seismo. Soc. of Amer., Bull., 76,* No. 2, 511 - 520.

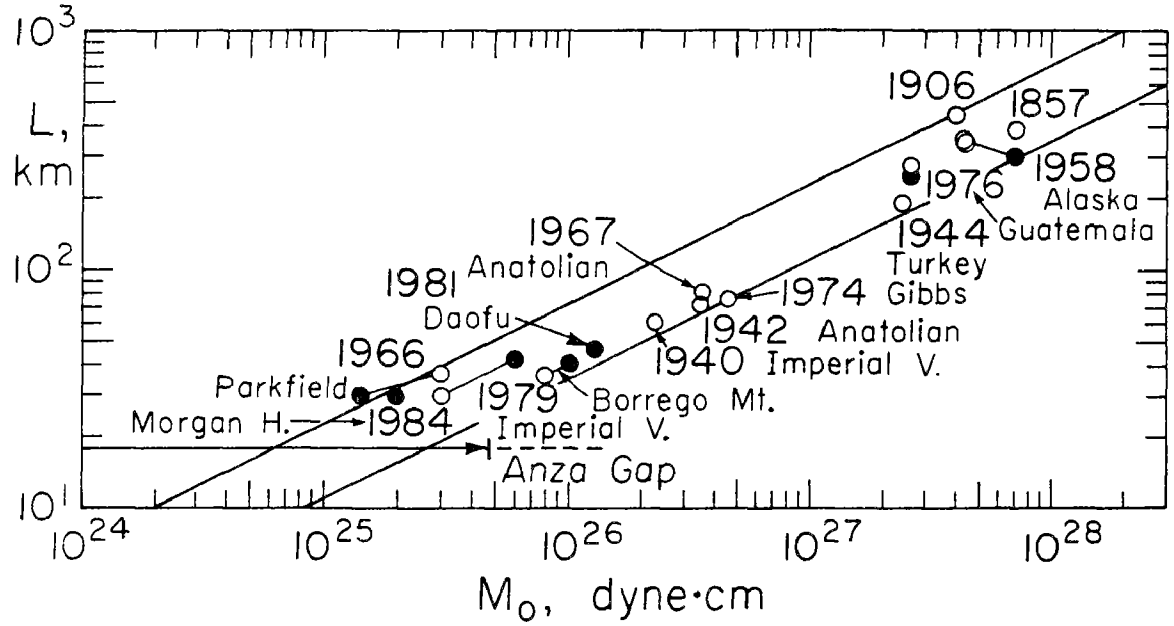
10^3
L, km
10^2
10^1
10^{24}
10^{25}
10^{26}
10^{27}
10^{28}
M_o, dyne·cm
1906
1857
1958
1976
Alaska
1944
Guatemala
Turkey
1967
Anatolian
1981
1974 Gibbs
Daofu
1942 Anatolian
1966
1940 Imperial V.
Parkfield
1979
Borrego Mt.
Morgan H.
1984
Imperial V.
Anza Gap

GEODETIC STRAIN MONITORING

9960-02156

John Langbein
Branch of Tectonophysics
U.S. Geological Survey
345 Middlefield Road, MS/977
Menlo Park, California 94025
(415-323-8111, ext. 2038

Investigations

Two-color geodimeters are used to survey, repeatedly, geodetic networks within selected regions of California that are tectonically active. This distance measuring instrument has a precision of 0.1 to 0.2 ppm of the baseline length. Currently, the crustal deformation is being monitored within the south moat of the Long Valley Caldera in eastern, California, and near Pearblossom, California on a section of the San Andreas fault that is within its Big Bend section. Periodic comparisons with the proto-type, 2-color geodimeter are also conducted near Parkfield, California. These inter-comparison measurements serve as a calibration experiment to monitor the relative stabilities of the portable and proto-type geodimeters.

Results

1) Long Valley

Line-length changes observed on a subset of the baselines shown in Figure 1 still show extension rates on the order of 1 ppm/a for the period between 1 October 1985 and 30 March 1986. These baselines use the station at CASA as a common endpoint. For reference, line-length changes observed from June 1983 through April 1986 are plotted in Figure 2. The rate changes computed for the past year are tabulated below. It is of interest that several baselines, including SHARK, MINER, LOMIKE and TAXI, show an increase in rate for the past six months when compared to the previous 6 month interval.

2. Pearblossom

Due to the high rate of deformation and our limitation of only one operating two-color geodimeter that is currently reliable and portable, the frequency of observations at Pearblossom has been significantly reduced. This network was resurveyed in November 1985, and February 1986. The strain changes from these surveys are plotted in Figure 3 along with the results from the previous measurements since October 30,

1980. The data from the past 6 months is consistent with the previous observations.

3. Instrument Inter-Comparison

The data from 7 sets of measurements, from June 1984 through April, 1986, have been analyzed in terms of the relative change in instrument length scale between the portable and proto-type two-color geodimeters. The data consists of nearly simultaneous measurements of distances using both instruments at a common site and approximately 6 reference monuments located between 1.0 to 7.1 km from the central site at Parkfield, CA. The more recent data uses 14 reference monuments. From these observations, the difference in distances for each baseline using the 2 instruments is tabulated as a function of time. With this method, tectonic strain change is canceled and leaves the relative variation of instrument length scale and the relative displacement of both instrument monuments as the dominant parameters. In examining the differential measurements, 4 scenarios have been considered. The first scenario assumes that neither the monuments or the instrument scale are changing relative to each other. Based upon the aprior errors of the measurements, this model can be rejected at the 99% confidence level. The scenario that allows only the relative length scale of both instruments to change as a function of time can also be rejected at the 99% confidence level. However, the rejection criterium is not satisfied if the two instrument monuments are allowed to be displaced as a function of time. This model being consistent with the data is not surprising considering that these monuments are in clayey soil and within 1/4 km of the San Andreas fault. Expansion and contraction of the soil in response to the rainy and dry seasons can yield displacements of several millimeters.

The addition of variation of instrument length scale to the above, acceptable model, shows a significant reduction in variance. Figure 4 shows the computed results from the last scenario. Before these results can be accepted, it should be emphasized that the covariance is high between the parameters estimating changes in length scale and monument displacements for the data previous to January, 1986. In January, 1986, the network was expanded considerably so that monument displacement could be monitored. The covariance between these parameters for the last two surveys are small (< 0.2).

4. Pinon Flat

An initial survey of a network of 6 baselines was done in March, 1986. Plans call for repeat surveys 3 to 4 times yearly and for comparison of strain data with the shorter baseline instrumentation at Pinon Flat Observatory.

Reports

Langbein, John, and Slater, Larry E., Two-wavelength geodetic measurements of strain accumulation in California, U.S.A., in Proceedings of China-United Symposium on Crustal Deformation and Earthquakes, October 29-31, 1985, Wuhan, China.

Slater, Larry, and Langbein, John, Two-wavelength geodetic measurements: The technique and instrument, in Proceedings of China-United States Symposium on Crustal Deformation and Earthquakes, October 29-31, 1985, Wuhan, China.

Table

Extension Rates Observed by the Two-Color Geodimeter Network in Long Valley

Baseline	Length km	Secular Rates (ppm/a) 1985-25-1985.75	1985.75-1986.29
CASA-SHARK	3.1	0.67 ± 0.13	1.41 ± 0.14
CASA-TILLA	4.2	-0.18 ± 0.11	0.12 ± 0.12
CASA-HOT	6.8	0.49 ± 0.10	0.51 ± 0.11
CASA-MINER	3.9	-0.54 ± 0.13	1.48 ± 0.14
CASA-SHERWIN	4.8	1.36 ± 0.09	1.29 ± 0.10
CASA-KNOLLS	7.1	1.08 ± 0.10	0.83 ± 0.11
CASA-KRAKATAN	7.8	0.80 ± 0.10	0.66 ± 0.10
CASA-SEWER	3.9	1.35 ± 0.15	1.36 ± 0.16
CASA-LOMIKE	2.5	0.92 ± 0.24	1.71 ± 0.26
CASA-RODGER	2.6	0.86 ± 0.31	0.56 ± 0.41
CASA-CONVICT	8.2	-0.03 ± 0.13	0.76 ± 0.14
CASA-TAXI	5.5	0.46 ± 0.18	0.74 ± 0.19
CASA-LOOKOUT	10.4	0.57 ± 0.59	1.31 ± 0.65

Figure Captions

1. Map showing the locations of the baselines that comprise the 2-color geodimeter network within the Long Valley Caldera.

2. Line-length changes for 21 baselines of the two-color geodimeter network. The length changes have been normalized to the nominal length of each baseline. The error bars correspond to one standard deviation.

3. Extensional strain changes inferred from line-length measurements for an 12 baseline network near Pearblossom, California. The strain components are tensor quantities and have been rotated into a coordinate system that is normal and parallel to the local strike of the San Andreas fault.

4. The upper panel is the inferred displacement of the monument used by the portable geodimeter (T-meter) relative to the proto-type (C-meter) monument. Displacements are resolved into the east and north directions. The bottom panel shows the change in relative length scale of both instruments. Scale is computed in ppm rather than in mm for comparison with network areal dilatation.

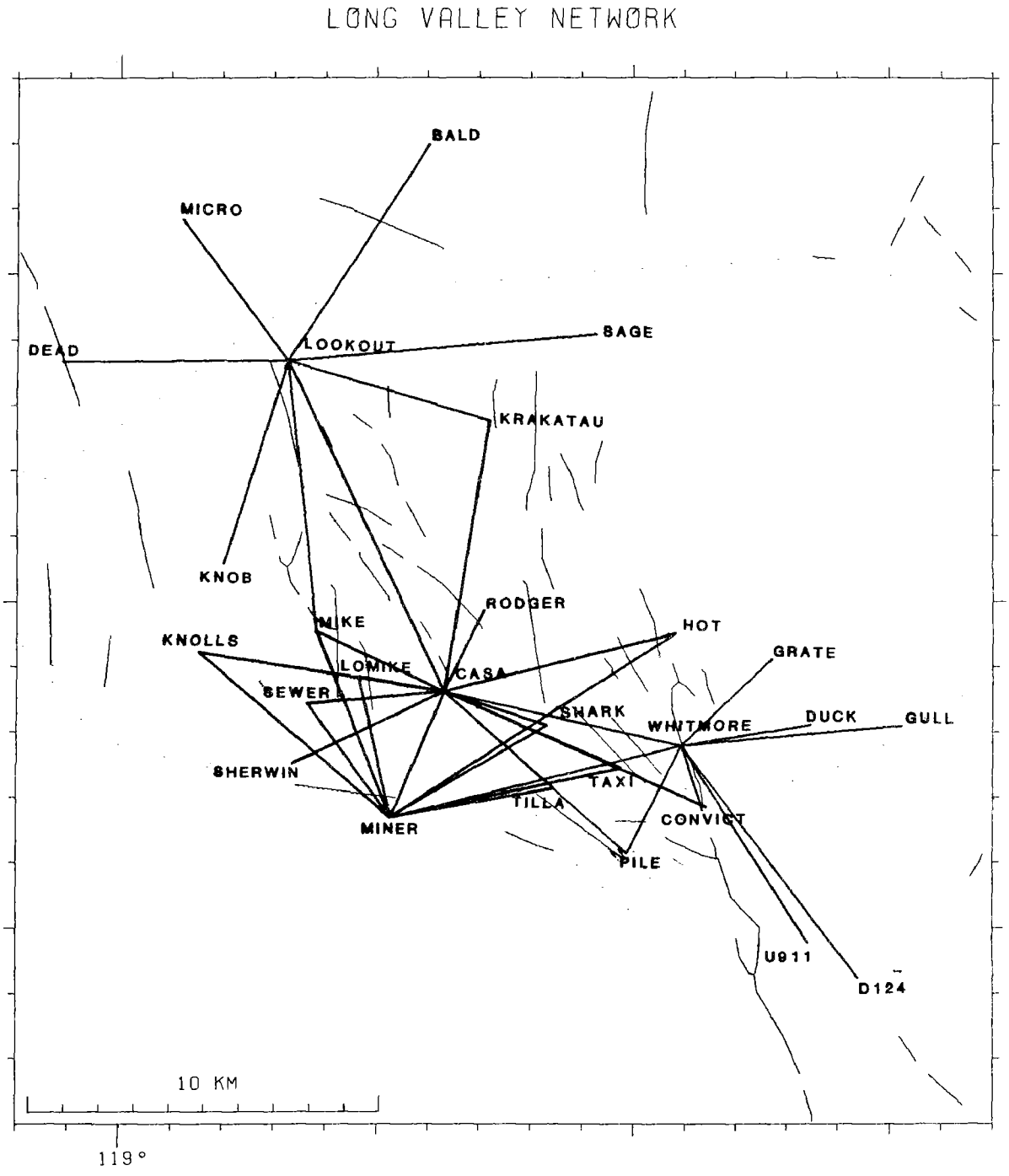
LONG VALLEY NETWORK
BALD
MICRO
DEAD
LOOKOUT
SAGE
KRAKATAU
KNOB
RODGER
MIKE
HOT
KNOLLS
GRATE
LOMIKE
CASA
SEWER
SHARK
DUCK
GULL
WHITMORE
SHERWIN
TAXI
TILLA
CONVICT
MINER
PILE
U911
D124
10 KM
119°

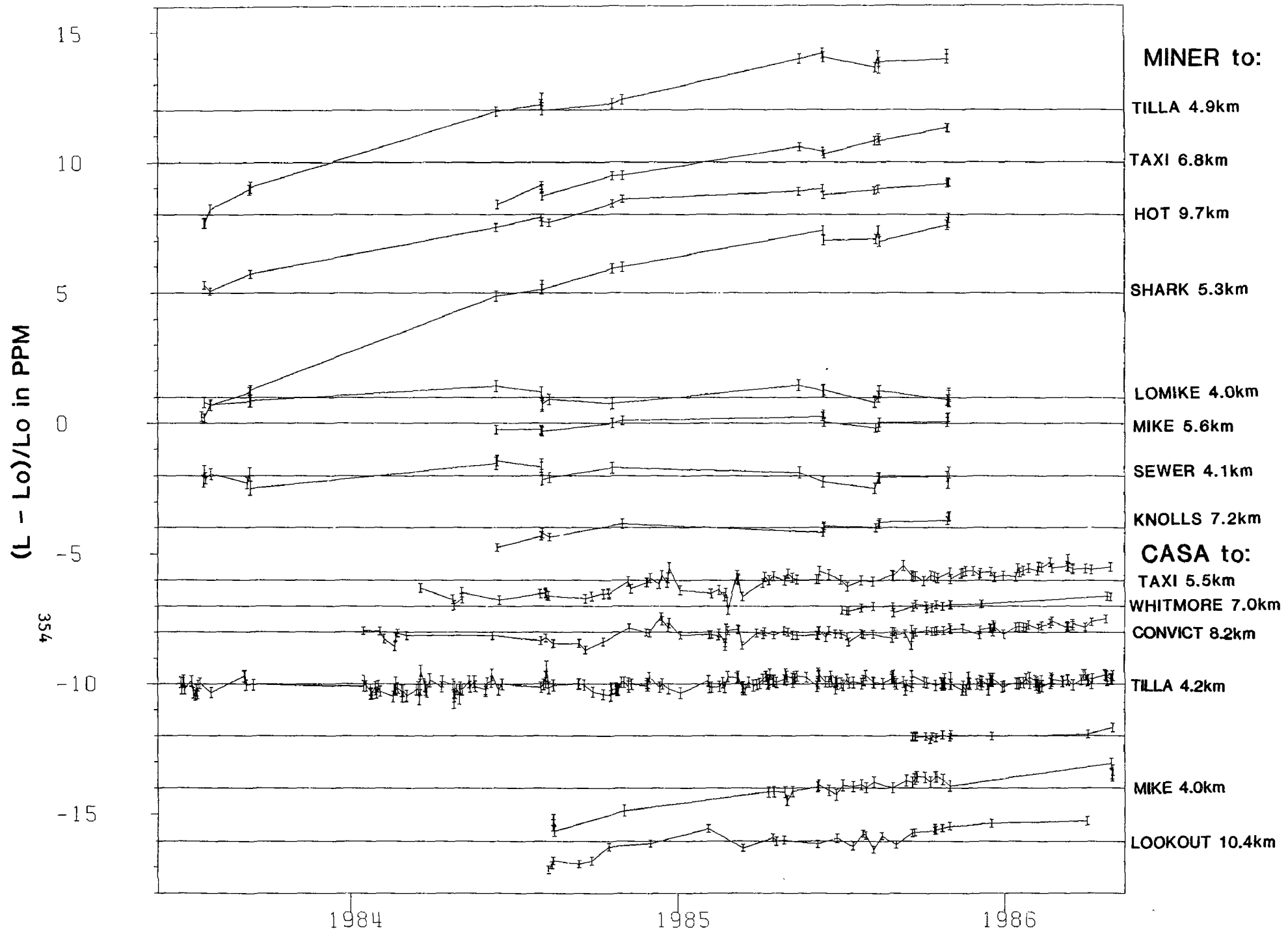
15
10
5
0
-5
-10
-15
(L - Lo)/Lo in PPM
1984
1985
1986
MINER to:
TILLA 4.9km
TAXI 6.8km
HOT 9.7km
SHARK 5.3km
LOMIKE 4.0km
MIKE 5.6km
SEWER 4.1km
KNOLLS 7.2km
CASA to:
TAXI 5.5km
WHITMORE 7.0km
CONVICT 8.2km
TILLA 4.2km
MIKE 4.0km
LOOKOUT 10.4km

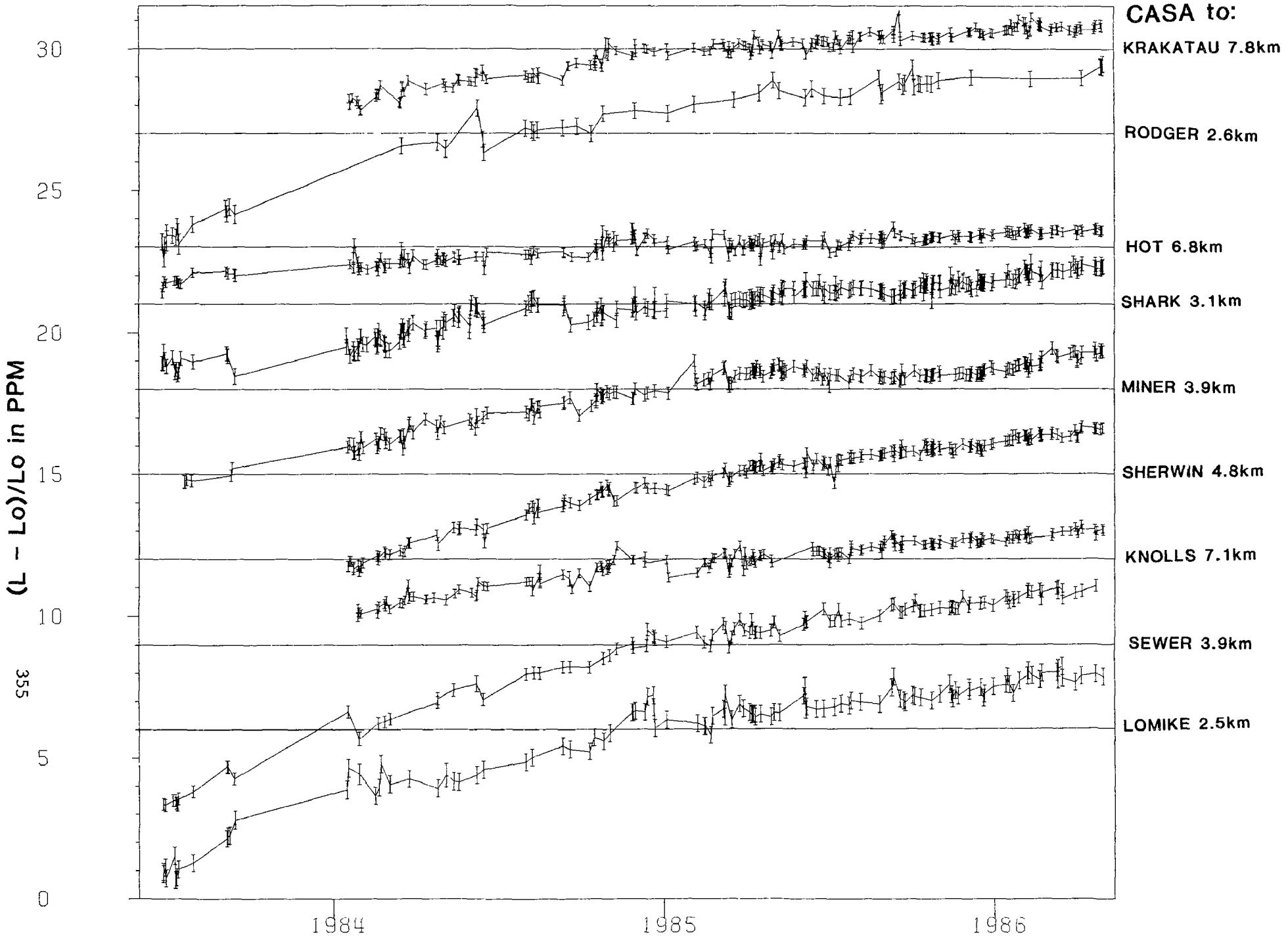
CASA to:
KRAKATAU 7.8km
RODGER 2.6km
HOT 6.8km
SHARK 3.1km
MINER 3.9km
SHERWIN 4.8km
KNOLLS 7.1km
SEWER 3.9km
LOMIKE 2.5km
(L - Lo)/Lo in PPM
0
5
10
15
20
25
30
1984
1985
1986

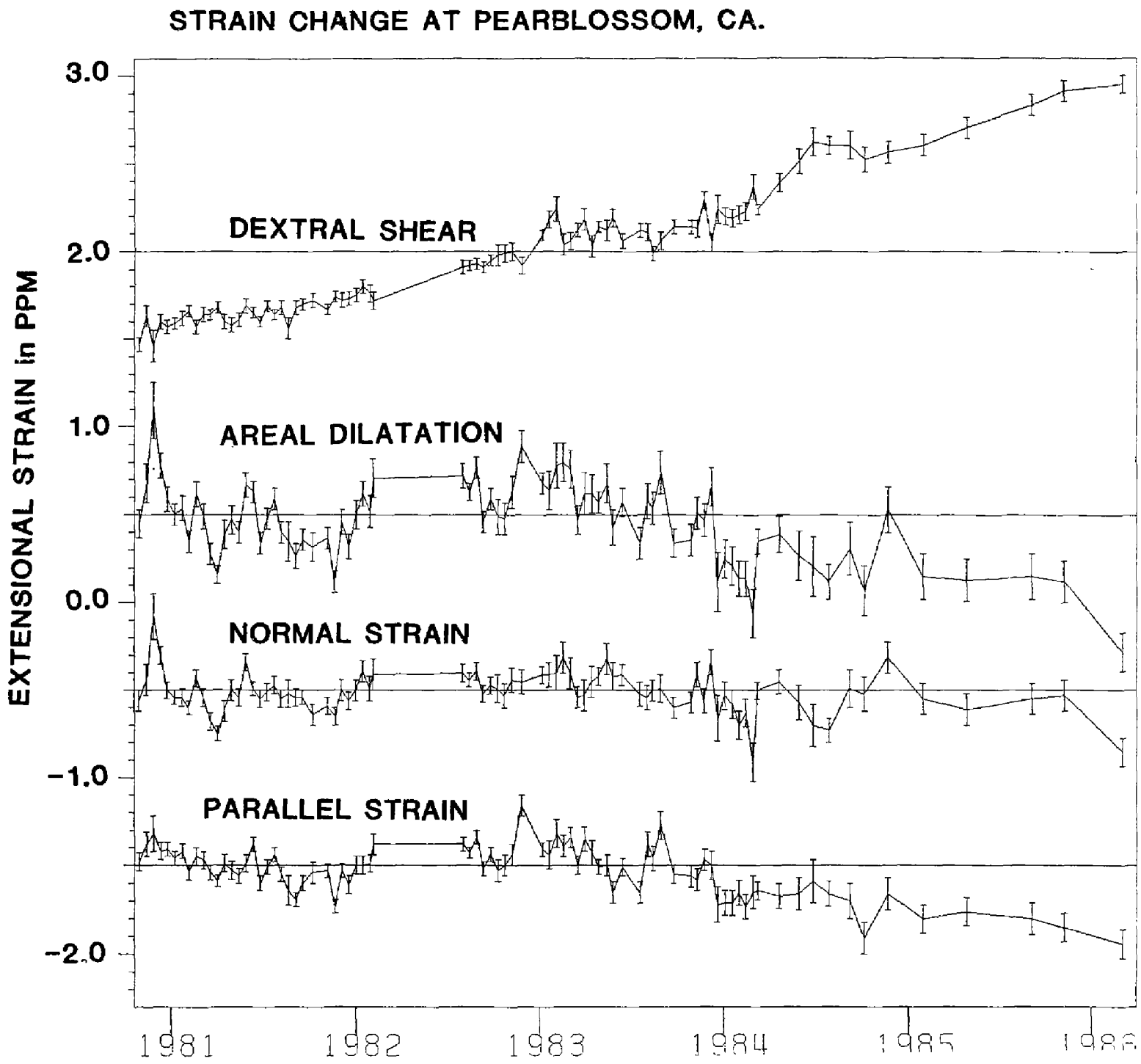
STRAIN CHANGE AT PEARBLOSSOM, CA.
EXTENSIONAL STRAIN in PPM
3.0
2.0
1.0
0.0
-1.0
-2.0
DEXTRAL SHEAR
AREAL DILATATION
NORMAL STRAIN
PARALLEL STRAIN
1981
1982
1983
1984
1985

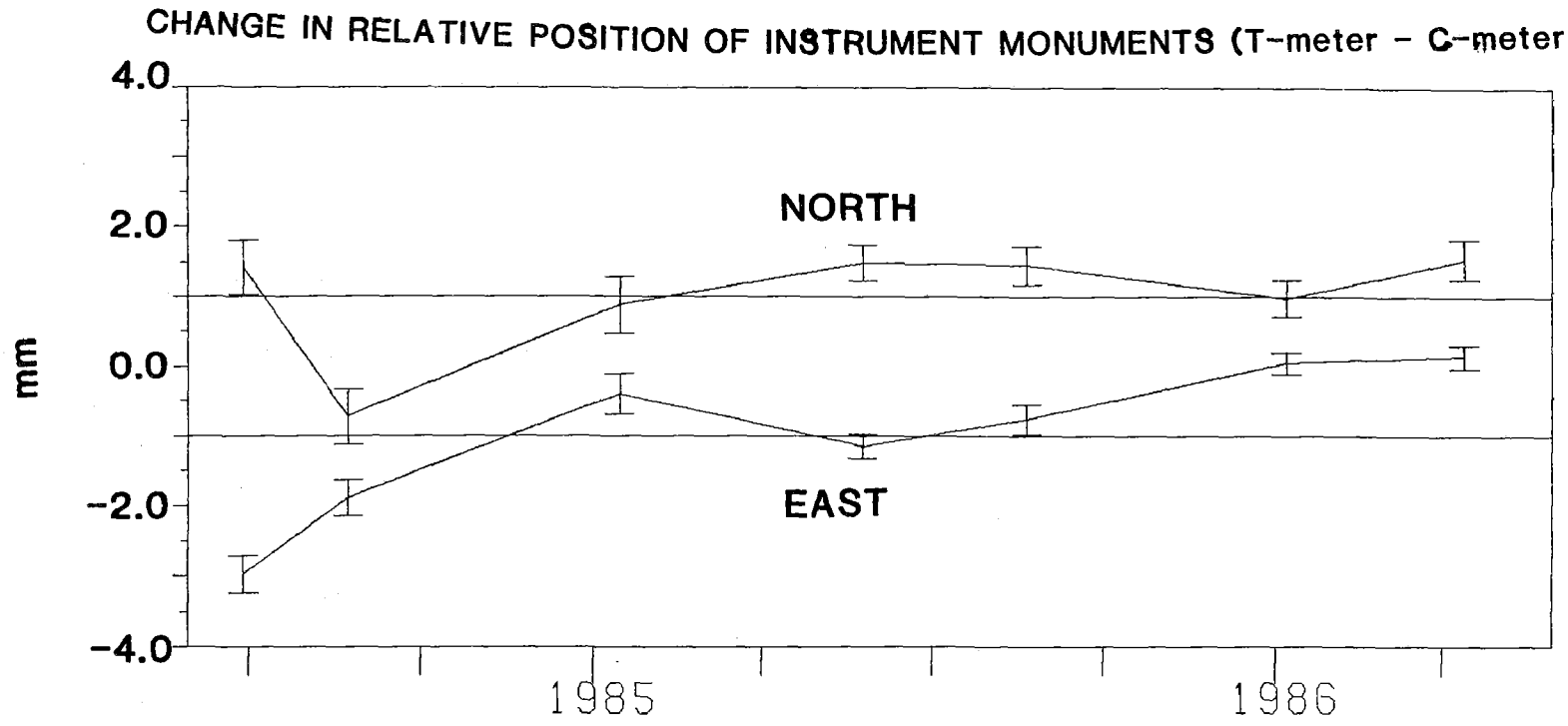
CHANGE IN RELATIVE POSITION OF INSTRUMENT MONUMENTS (T-meter - C-meter)
4.0
2.0
0.0
-2.0
-4.0
mm
NORTH
EAST
1985
1986

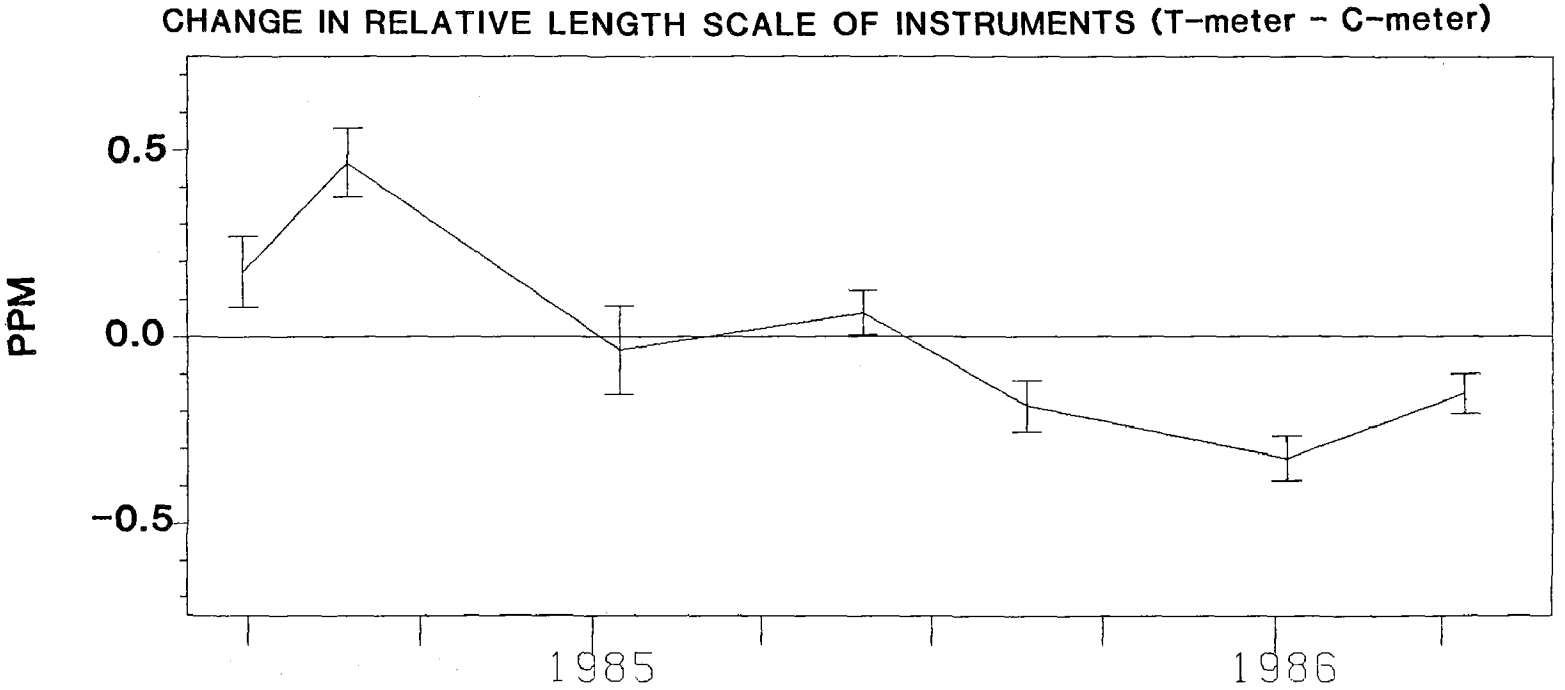
CHANGE IN RELATIVE LENGTH SCALE OF INSTRUMENTS (T-meter - C-meter)
0.5
0.0
-0.5
PPM
1985
1986

Acquisition and Analysis of Data from Sacks-Evertson Strainmeters in California

14-08-0001-G1172

Alan T. Linde
I. Selwyn Sacks
Department of Terrestrial Magnetism
Carnegie Institution of Washington
5241 Broad Branch Rd., NW
Washington DC 20015
(202) 966-0863

A number of Sacks-Evertson borehole strainmeters have been installed in California, primarily in areas adjacent to the San Andreas fault. In this program, in collaboration with the Geological Survey and the University of California, San Diego, we monitor the data and use the information, in conjunction with other relevant seismic and deformation data, in studies of earthquakes and longer term strain changes. Additionally, although routine operation and maintenance of the stations is performed by our colleagues, we aid in non-routine maintenance and upgrades to the instrumentation.

Instrument Operation

The operation of the instruments is monitored primarily by D. Myren of USGS and F. Wyatt of UCSD. During the last year, we have had an unusual number of problems (compared with installations in other areas) with cable leakage. We have made modifications to the electronics for the installed instruments which show signs of water penetration. These modifications allow the instrument to be run with lower downhole voltages to reduce the effects of disassociation of water. Also the instruments are operated in a pulsed mode so that the voltages are applied only for a small fraction of the time. At the time of writing this report, we do not know how successful this modification will be in extending the instrument life. For two instruments yet to be installed, we have designed and constructed modified components to connect the cable to the instrument. This design should result in the instrument being less vulnerable to cable leakage.

Data Analysis

In addition to the low frequency data recording by 12 bit digital telemetry at 10 minute sampling intervals and on analog chart at 0.5 inch/hour, some of the sites have been sampled with 16 bit digital event recorders with sampling rates of up to 100/second. These GEOS recorders have been made available by Roger Borcherdt, USGS. Malcolm Johnston, USGS, provides the data acquisition system for the 10 minute data set and carries responsibility for the primary monitoring and analysis of the data.

These data sets have allowed us to examine some earthquakes in detail. Strain signals from a small event near San Juan Bautista were shown to include a coseismic offset consistent with that calculated from an elastic model using source parameters determined from seismic data (Johnston et al, 1985). However the spectrum of the strain waveform was characteristically different from the equivalent spectrum of the waveform recorded by a surface seismometer at the same site presumably because of the near surface structure in the vicinity of the seismometer.

In another study of several small to moderate sized events (Johnston et al, 1986), we have found good agreement between the calculated and observed coseismic strain steps. Although the instruments were in the near field of the events and strain offsets were detected, the data did not show the presence of significant precursory strain changes in the last few hours before the earthquakes. Any rapid changes in a preparation zone for the earthquake must have been equivalent to at most a few percent of the moment of the earthquake. However some large events in Japan have been preceded by large rapid deformation. More information on this type of behaviour is extremely important in the quest not only to understand the mechanism of earthquake occurence but also to formulate a prediction methodology.

We are presently examining several other types of unusual strain changes which have occurred in the Parkfield region. During last year, there have been strain excursions lasting 20-30 days with amplitudes about a few tenths microstrain. These correlate closely with changes in water level in nearby holes and have been associated with small earthquakes on the San Andreas fault. Preliminary modelling indicates that aseismic slippage on a small patch of the fault could have been the source of these disturbances and produced a stress redistribution which resulted in the earthquake. During the few months before the Kettleman Hills earthquake, increased strain rates were recorded near Parkfield and this change also appears to have been detected by the two color laser geodometer network in that area. It may be that slip on the San Andreas was important in preparing the nearby fault for the earthquake.

References

Johnston,M. J. S., R. D. Borcherdt and A. T. Linde, Measurements of short period strain (0.1 - 10000s): near source strainfield for an earthquake (Ml 3.2) near San Juan Bautista, California. Trans. Am. Geophys. Union, 46, 1093, 1985.

Johnston, M. J. S., A. T. Linde, M. T. Gladwin and R. D. Borcherdt, Fault failure with moderate earthquakes, Tectonophysics, in press, 1986.

Parkfield Prediction Experiment

9930-02098

Allan Lindh
Catherine Poley and Barry Hirshorn
U.S. Geological Survey
Branch of Seismology Mail Stop 977
345 Middlefield Road
Menlo Park, California 94025
415-323-8111, Ext. 2042

Work Continued on:

1. The Parkfield prediction experiment, and
2. Long term earthquake probabilities along the San Andreas system.

Catherine Poley, working with Al Lindh and Bill Bakun, has completed analysis of the last 15 years seismicity near Middle Mtn. This work has been presented to NEPEC and a short paper for Science is ready for internal review. Another project on short term recurrence patterns within the Parkfield preperation zone was presented at the SSA meeting, and is being written up for nature.

Lucy Jones and Al Lindh have completed work on several different approaches to calculating foreshock probability gains at Parkfield. This work has been presented to NEPEC and is being written up for BSSA.

Barry Hirshorn has become the main person processing, cleaning up, and keeping an eye on the RTP data on a daily basis. He also keeps as eye on station and telemetry performance, and runs the weekly station quality meetings.

Working with Peter Johnson, Lindh has completed work on processing the RTP data within the CUSP framework on the Seismology 750, and this is now taking place on a routine basis. Efforts are underway to incorporate this data into the CUSP catalog in a timely and efficient way.

Al Lindh meets with John Van Schaack twice a week to review station performance; thanks to a great deal of cooperation with all involved -- particularly Shirley Marks, who makes available pictures of problem stations in a timely manner -- some progress is being made in holding the net together in the face of reduced funding for station maintenance.

REPORTS

Bakun, W.H., and Lindh, A.G., 1985, The Parkfield, California Earthquake Prediction Experiment, SCIENCE v. 229, no. 4714, pp. 619-624.

Bakun, W.H., Lindh, A.G., and Segall, P., 1985, Overview of Parkfield, California earthquake prediction experiments (abs.) EOS, 66, p. 982.

Lindh, A.G., and Jones, L.M., 1985, Parkfield Foreshock Probabilities (abs.) (abs.) EOS, v. 66, p. 982.

Poley, C.M., and Lindh, A.G., 1985, (abs.) Recent Seismicity at Parkfield, California, EOS, v. 66, p. 982.

Poley, C.M., Lindh, A.G., and Bakun, W.H., 1986, (abs.) Parkfield Prediction Experiment: Seismicity Update, Earthquake Notes, vol. 57, p. 21-22.

Active Seismology in Fault Zones

9930-02102

Walter D. Mooney
Gary S. Fuis
U.S. Geological Survey
Branch of Seismolgoy
345 Middlefield Road, Mail Stop 977
Menlo Park, California 94025
(415) 323-8111, Ext. 2569

Investigations

1. Continuation of analysis of seismic-refraction data in southern Alaska. This is part of the Trans-Alaska Crustal Transect (TACT) (Fuis, Ambos, Mooney, Page).

2. Continued analysis of the crustal structure of the Central Valley of California (Mooney, Walter, Whitman, Colburn).

3. Completion of manuscript on the seismic properties of fault zones (Mooney and Ginzburg).

4. Revision and re-submission of manuscript on deep crustal structure of Yunnan Province, PRC (Mooney).

5. Continued analysis of seismic refraction data from Maine and Quebec (Luetgert, Klemperer, Mann).

6. Analysis of crustal structure of western Arizona - southern California (PACE) from seismic refraction data. (Fuis, McCarthy, Wilson).

Results

1. In 1984, the U.S. Geological Survey initiated the Trans-Alaska Crustal Transect (TACT) program--a coordinated geological and geophysical study of the structure, composition and evolution of the Alaskan crust along the Trans-Alaska oil pipeline corridor from Valdez to Prudhoe Bay and across the adjacent Pacific and Arctic continental margins. TACT is a major element of the multi-institutional Trans-Alaska Lithosphere Investigation (TALI). The TACT project was launched in southern Alaska; in succeeding years the investigations will shift northward with the goal of completing the transect by the end of the decade.

   As part of the continuing Trans-Alaska Crustal Transect (TACT) program, the USGS in 1985 recorded two seismic-refraction lines in southern Alaska with 120 seismographs. The Cordova Peak (CP) line, 120 km long with 9 shots, extended southward to the Copper River delta a 1984 refraction profile along the Richardson Highway that terminated in the central Chugach Mts. The Montague (MG) line, 135 km long with 7 shots, ran southwestward from Cordova along Hawkins, Hinchinbroo, and Montague Islands.

In both the Chugach terrane (CGT) and Prince William terrane (PWT), exposed rocks are marine clastic and volcanic rocks, but CGT rocks are older (Mesozoic vs. Cenozoic) and metamorphosed to greenschist facies. Preliminary 1985 results indicate different velocity structures in the two terranes. In the CGT, the exposed rocks (V_p=5.5-5.9 km/s) overline mafic(?) rocks (V_p=6.8-7.1 km/s) that shoal southward from 7-km depth under the central Chugach Mts. to 2-3 km depth near the boundary with the PWT. In the PWT, the exposed rocks (V_p=5.1-5.6), extending to 2-6-km depth, overlie a layer of relatively uniform velocity (V_p=6.1-6.2), extending to at least 10-km depth. Unlike the CGT, the PWT velocity structure does not closely resemble that of oceanic crust.

Results from 1984 suggest the CGT and Peninsular-Wrangellia (composite) terrane north of it are rootless, truncated at 10-km depth. At great depth are a series of north-dipping low- and high-velocity zones that may be relict subduction assemblages.

2. The Great Valley of California is a 700-km-long by 100-km-wide sedimentary basin situated between the granitic and metamorphic terrane of the Sierra Nevada and the Franciscan subduction complex of the Coast Ranges. The Great Valley is of geologic interest not only as a prolific oil-bearing province, but also as a key to the tectonic evolution of central California.

   In 1982 the U.S. Geological Survey collected six seismic refraction profiles in the Great Valley of California: three axial profiles with a maximum shot-to-receiver offset of 160 km, and three shorter profiles perpendicular to the valley axis. The crust of the central Great Valley is laterally heterogeneous along its axis, but generally consists of a sedimentary section overlying distinct upper, middle, and lower crustal units. The sedimentary rocks are 3-5 km thick along the profile, with velocities increasing with depth from 1.6 to 4.0 km/s. The basement consists of four units: (1) a 1.0-1.5 km thick layer of velocity 5.4-5.8 km/s, (2) a 3-4 km thick layer of velocity 6.0-6.3 km/s, (3) a 1.5-3.0 km thick layer of velocity 6.5-6.6 km/s, and (4) a laterally discontinuous, 1.5 km thick layer of velocity 6.8-7.0 km/s. The mid-crust lies at 11-14 km depth, is 5-8 km thick, and has a velocity of 6.6-6.7 km/s. On the NW side of our profile the mid-crust is a low-velocity zone beneath the 6.8-7.0 km/s lid. The lower crust lies at 16-19 km depth, is 7-13 km thick, and has a velocity of 6.9-7.2 km/s. Crustal thickness increases from 26 to 29 km from NW to SE in the model.

   Although an unequivocal determination of crustal composition is not possible from P-wave velocities alone, our model has several geological and tectonic implications. We interpret the upper 7 km of basement on the NW side of the profile as an ophiolitic fragment, since its thickness and velocity structure are consistent with that of oceanic crust. This fragment, which is not present 10-15 km to the west of the refraction profile, is probably at least partially responsible for the Great Valley gravity and magnetic anomalies, whose peaks lie about 10 km east of our profile. The middle and upper crust are probably gabbroic and the product of magmatic or tectonic underplating, or both. The crustal structure of the Great Valley is dissimilar to that of the adjacent Diablo Range, suggesting the existence of a fault or suture zone

throughout the crust between these provinces.

Livermore Valley:
We have interpreted two USGS seismic refraction profiles to determine the upper crustal structure east of Livermore, CA. The profiles are reversed over 33 km, with station spacing of 250-600 m. One profile was shot over Tertiary sediments in a WNW direction. The profile crosses an inferred contact between Great Valley rocks and the Franciscan terrane, the Greenville-Tesla Fault. The other profile was shot over Tertiary and Cretaceous Great Valley rocks east of the fault, in a NW direction parallel to the regional strike.

The NW strike line shows a wide variation in structure at depths less than a kilometer, including a low velocity wedge (2.1 km/sec) within the Cretaceous rocks. Cretaceous rocks surrounding the wedge have velocities of 3.5 km/sec at the surface, increasing to 4.1 km/sec at depth. A 5.5 km/sec layer underlies these rocks at 4.5 km depth and dips 5 degrees to the NW.

The WNW line displays different apparent velocity structures on either side of the fault. East of the fault the velocity structure is in accord with the interpretationof the NW profile. West of the fault is a 2.6 km thick layer of Tertiary sediments (2.1-3.2 km/sec) overlying a 5.0 km/sec basement. We interpret the high velocity basement as Franciscan assemblage rocks.

3. The internal properties within and adjacent to fault zones are reviewed based principally on laboratory, borehole, and seismic refraction and reflection data. The deformation of rocks by faulting produces effects ranging from intra-grain microcracking to severe alteration of the rocks. Whereas saturated microcracked and mildly fractured rocks do not exhibit a significant reduction in velocity, borehole measurements in densely fractured rocks do show significantly reduced velocities, with the amount of velocity reduction generally proportional to the fracture density. Highly fractured rock and thick fault gouge along the creeping portion of the San Andreas fault is evidenced by a pronounced seismic low velocity zone (LVZ), whereas an LVZ is either very thin or absent along locked portions of the fault. Thus there is a correlation between fault slip behavior and the seismic velocity structure within the fault zone; high pore pressure within the pronounced LVZ may be conducive to fault creep. Deep seismic reflection data indicate that crustal faults sometimes extend through the entire crust. Modelling of this reflection data and geologic evidence are consistent with a composition of deep faults consisting of highly foliated, seismically anisotropic mylonites.

4. We report results of a cooperative Sino-American geophysical investigation of crustal structure and tectonics in southwest China. Yunnan province, that are of study, is located at the eastern end of the Himalaya-Burma arc, just southeast of the Tibetan plateau. Tectonically active, with major through-going faults, the region is highly seismic. The prominent Red River fault, for example, shows suybstantial recent movement and is considered a boundary between major crustal blocks. Historical records yield evidence for some 40 major earthquakes (probably of magnitude 6 or greater) in the last 400 years. In this century such

earthquakes have occurred at a rate of aobut three every 10 years. The largest recent shock in western Yunnan, of magnitude 7, severely damaged the old town of Dali in 1925. Chinese scientists have estimated a 120-year recurrence interval for the 1925-type earthquake.

Seismic refraction profiles in Yunnan province, southwestern China, define the crustal structure in an area of active tectonics on the southern end of the Himalaya-Burma arc. The crustal thickness rnges from 38 to 46 kilometers, and the relatively low mean crustal velocity indicates a crustal composition compatible with normal continental crust and consisting mainly of meta-sedimentary and silicic intrusive rocks, with little mafic or ultra-mafic rocks. This suggests a crustal evolution involving sedimentary processes on the flank of the Yangtze platform, rather that the accretion of oceanic island arc, as previously proposed. An anomalously low upper mantle velocity observed on one profile but not on another at right angles to it may be indicative of active tectonic processes in the mantle, or of seismic anisotropy.

5. In recent years, the northern Appalachians have been recognized as being composed of several distinct terranes, having distinguishably separate orogenic histories prior to coalescence in their present form. Recently, active seismic experiments (both reflection and refraction) have been undertaken crossing the Appalachians in Maine and Quebec to characterize the crustal velocity structure. Preliminary results show upper crustal velocities that range from 5.7-6.3 km/sec with localized regions of low velocity within the upper crust. Secondary arrivals provide evidence for a higher velocity lower crust (6.8-7.2 km/sec) below 22 km. Crustal thickness varies from 38-40 km in NW Maine to 32-35 km in the coastal volcanic belt.

   A particular fruitful approach to the analysis of the refraction data has been the examination of wide-angle reflections from the Moho and from horizons in the lower crust through the use of normal moveout corrected record sections. This examination has provided (1) regional measures of crustal thickness; (2) a measure of variation from region to region of the reflective character of the crust; and (3) evidence for local abrupt changes in depth to the Moho. The latter may be, in some instances, related to the boundaries between recognized terranes.

   The Avalon terrane, which extends along the eastern seaboard of New England, has recently been considered to be a suspect terrane, believed to have been accreted after the Taconic orogeny (Ordovician) and probably during the Devonian. The geology of the area consists principally of late Precambrian and Cambrian sedimentary and volcanic rocks intruded by Devonian plutons, similar to composition and age to rocks found in western Europe.

   Six shots were recorded along a 145-km profile parallel to the northeastern coastline of Maine within the Avalon terrane. An upper crustal model for the first 10 km has been determined using 2-d modelling programs which accounts for all first arrivals on the travel-time curves for each of the shots. To determine the lower crustal structure, deeper reflections were analyzed by applying normal moveout (NMO) corrections routinely used in reflection processing. The NMO record sections contain

easily distinguishable major reflective boundaries at approximately 4, 7, and 10 to 10.5 sec. The latter, deeper reflection corresponds to the crust-mantle boundary. Preliminary results show a correspondence between the crustal thickness in the Avalon terrane and its counterparts in Europe.

Six shots were recorded along a 145-km profile parallel to the northeastern coastline of Maine within the Avalon terrane. An upper crustal model for the first 10 km has been determined using 2-D modelling programs which accounts for all first arrivals on the travel-time curves for each of the shots. To determine the lower crustal structure, deeper reflections were analyzed by applying normal moveout (NMO) corrections routinely used in reflection processing. The NMO record sections contain easily distinguishable major reflective boundaries at approximately 4, 7, and 10 to 10.5 sec. The latter, deeper reflection corresponds to the crust-mantle boundary. Preliminary results show a correspondence between the crustal thickness in the Avalon terrane and its counterparts in Europe.

6. During 1985 the U.S. Geological Survey initiated the Pacific-Arizona Crustal Experiment (PACE), a multidisciplinary transect across western Arizona, southern California, and the offshore Pacific continental margin. 260 km of reversed seismic-refraction data were recorded as a part of PACE along two perpendicular profiles centered over the Whipple Mountain metamorphic core complex in southeastern California. This experiment, consisting of a total of 30 shots, 20 shotpoints, and an average station spacing of 500-1000 meters, represents the most-detailed geophysical study-to-date of the crustal structure beneath a metamorphic core complex.

   Although analysis of the PACE seismic-refraction experiment has just begun, several significant results are already evident. First, a sharp velocity discontinuity is present thoughout the survey at a depth of 13-16 km separating a 6.0 km//sec upper crust from a 6.5-7.2 km/sec middle crust. Second, laterally-discontinuous, 6-8-km-thick low-velocity zones (LVZs) are evident both above and below this mid-crustal discontinuity. The upper crustal LVZs are analogous to those previously identified in the northern Basin and Range Province, but the lower-crustal LVZs have no counterpart in the western U.S. Finally, the crust is 24-26 km thick beneath the Whipple Mountains and is underlain by a 7.8 km/sec mantle.

   These seismic-refraction results, when combined with CALCRUST seismic-reflection studies, suggest that the crust in eastern California and western Arizona is composed of both high- and low-velocity layers that range in thickness from tens to thousands of meter and that are laterally continuous over horizontal distances of tens of kilometers. These layers appear to outline large-scale boudins elongated in a northeast direction -- the direction of extension of the metamorphic core complexes.

RESULTS

Colburn, R., and Mooney, W.D., 1985, Crustal structure of the Great Valley,

California: Axial profile, EOS, Transactions Am. Geophys. Union 66, p. 973; (manuscript submitted to Bull. Seis. Soc. Am. 4/86).

Daley, M.A., Ambos, E.L., and Fuis, G., 1985, Seismic refraction data collected in the Chugach Mountains and along the Glenn Highway in southern Alaska in 1984: U.S. Geological Survey Open-File Report 85-531, 32 pp., 12 plates.

Fuis, G.S., Ambos, E.L., Mooney, W.D., an Page, R.A., 1985, Velocity structure of accreted terranes of southern Alaska, EOS, Transactions Am. Geophys. Union 66, p. 1074.

Hwang, L., and Mooney, W.D., 1985, Qp and velocity modeling of seismic refraction data: Central Valley, Ca., EOS, Transactions Am. Geophys. Union 66, p. 973; (manuscript submitted to Bull. Seis. Soc. Am. 2/86).

Luetgert, J.H., 1985, Depth to Moho and characterization of the crust in the northern Appalachians from 1984 Maine-Quebec seismic refraction data, EOS, Transactions Am. Geophys. Union 66, p. 1074.

Meltzer, A.S., Levander, A.R., and Mooney, W.D., 1985, Interpretation of seismic refraction profiles east of Livermore, Ca., EOS, Transactions Am. Geophys. Union (abst.), 66, p. 973.

Mann, C.E., and Luetgert, J.H., 1985, Seismic refraction data within the Avalon terrane, eastern Maine: analysis of 2-D structure from normal moveout record sections, EOS, Transactions Am. Geophys. Union (abst.), 66, p. 1074.

Whitman, D., Walter, A.W., and Mooney, W.D., 1985, Crustal structure of the Great Valley, California: Cross Profile, EOS, Transactions Am. Geophys. Union 66, p. 973.

Fuis, G.S., and Ambos, E.L., 1986, Deep structure of the Contact fault and Prince William terrane: preliminary results of 1985 TACT seismic-refraction survey, in U.S. Geological Survey in Alaska, Accomplishments during 1985: U.S. Geological Survey Circular (in press).

Ackermann, H.D., Mooney, W.D., Snyder, D.B., and Sutton, V.D., Preliminary interpretation of seismic refraction and gravity studies west of Yucca Mountain, Nevada and California U.S.G.S. Circular "Studies of the Southern Great Basin", M. Carr (edit) (in press; 21 pp., 10 fig.).

Fuis, G.S., McCarthy, J., and Howard, K., 1986, A seismic-refraction survey of the Whipple Mountains metamorphic core complex, southeastern Calif.: A progress report from PACE: Geological Society of America Abstract with Program, Rock Mountain Section Meeting, Spring 1986 (in press).

Fuis, G.S., Walter, A.W., Mooney, W.D., and McCarthy, J., Crustal velocity structure of the Salton Trough, western Mojave Desert, and Colorado Desert, from seismic refraction (abs.): Geological Society of America Abstracts with Programs, Cordilleran Section Meeting, Spring 1986 (in press).

Gettings, M.E., Blank, H.R., Mooney, W.D., and Healy, J.H., 1986, Crustal Structure of Saudi Arabia, Jour. Geophy. Res. (in press; 45 pp., 8 figs.)

Kan, R.J., Hu, H.X., Zeng, R.S., Mooney, W.D., and McEvilly, T.V., 1986, Crustal structure and tectonics of Yunnan Province, Southwest China, from seismic refraction profiles, SCIENCE (in press; 11 pp. 4 fig.).

McCarthy, J., Fuis, G.S., and Howard, K., seismic-refraction studies across the Whipple Mountains, Calif.: A progress report from the Pacific-Arizona Crustal Experiment (PACE) (abs.): Geological Society of America Abstracts with Programs, Cordilleran Section Meeting, Spring 1986 (in press).

Mooney, W.D., and Ginzburg, A., 1986, Seismic measurements of the internal properties of fault zones, in, The Internal Properties of Fault Zones, C.Y. Wang (edit.) PAGEOPH (in press); 24 pp. 6 fig.

Page, R.A., Plafker, George, Fuis, G.S., Nokleberg, W.J., Ambos, E.L., Mooney W.D., and Campbell, D.L., 1986, Accretion and subduction tectonics in the Chugach Mountains and Copper River Basin, Alaska: Initial results of the Trans-Alaska Crustal Transect: Geology, v. 14 (in press).

Plafker, Geroge, Ambos, E.L., Fuis, G.S., Mooney, W.D., Nokleberg, W.J., Page, R.A., and Campbell, D.L., Late Mesozoic and early Tertiary accretion and subduction along the southern Alaska continental margin (abs.): Geological Society of America Abstracts with programs, Cordilleran Section Meeting, Spring 1986 (in press).

Valdez, C. M., Mooney, W.D., Singh, S.K., Meyer, R.P., Lomnitz, C., Luetgert J.H., Helsley, C. and Lewis, B.T.R., 1986, Crustal structure of Oxaca, Mexico, from seismic refraction measurements, Bull. Seis. Soc. America, 76, p. 547-563.

Tiltmeter and Earthquake Prediction Program in S. California and at Adak, AK

14-08-0001-21244

Sean-Thomas Morrissey
Saint Louis University
Department of Earth and Atmospheric Sciences
P.O. Box 8099 - Laclede Station
St. Louis, MO 63156
(314) 658-3129

I: Task 1: The Tiltmeter System

Objective: To continue to improve the performance of bubble sensor tiltmeter systems and to investigate other sensor systems for use in moderate depth boreholes, seeking relatively low-cost, readily deployed instrumentation.

Accomplishments: Most of the effort during this period related directly to the second task, but included some changes in the upper borehole pipe adapter to better fit the installation system engagement tool and allow 20 indexed orientation positions rather than 2. A set of switch-selectable very low gain bridge AC amplifier/demodulators was prepared for use in the early phases of each deep-hole installation. These increase the available dynamic range of the sensor to 140 db, from 10^{-2} radians (about 0.57 degree) to 10^{-9} radian, without using the electronic zeroing system.

II: Task 2: The Installation Method

Objective: To improve the installation methods for borehole instruments with a goal of installing them as deep as 100 meters.

Accomplishments: We are nearing the completion of the design and testing of the remotely controlled installation system that will allow precise installation (within 1 ppm of vertical) with the sensor housing bonded directly to the host rock. At depths up to 20 meters, the system uses two hand tamping rods for control and packing of the sand; beyond this depth. the electrically controlled pneumatic tampers will have to be used. An unforeseen situation has urged us toward completing the pre-leveling system, in that the holes drilled in November 1985 at Pinon Flat were not vertical. but inclined toward the southwest by about 1^{o}, an offset of 15 cm in a 10 m hole. (See the CDO report). Since this was half the diameter of the hole, the previously evaluated hand-held alignment tool would not work, since it would be against the borehole collar. So the pre-leveler system has been completed, and the hole brace. which remotely locks the pre-leveler assembly about 4 meters from the bottom, was redesigned to provide a preset offset that would cause precise vertical alignment of the system at that point. With these completions, we were in a position to do 20 m depth installations, so all the cables and flexible conduits have been rebuilt in 75' lengths.

These two assemblages of systems that are temporarily lowered into the hole to accomplish the remote installations become rather heavy to be lowered and precisely positioned with delicacy by hand, so a variable speed motor-winch was built, and a portable frame assembled as a guyed "A" frame from a pair of heavy duty extension ladders. The 7 m height of this frame (the assembled length of the pre-leveler, with a tiltmeter attached at the bottom and the brace at the top, is 6 m high) required a large 4 m x 4 m base frame, much too large to be used on top of the test tower that simulates a 12 m hole for hand-aligned test installations at the CCMO test site. Consequently, a 2 m deep, 1 m diameter pit at CCMO was deepened to 10 meters by digging by hand. Four small 12 cm instrument boreholes were drilled in the bottom, protected by a base platform and ABS collars. The 10 m long, 30 cm diameter "casing" can be installed in turn over each of these, and inclined so as to simulate the field conditions. We plan to test inclinations as much as 2^{o}, or an offset of 15 cm at the hole brace. If we install four tiltmeters at the 10 m depth of this test pit, we will record the data for evaluation and comparison.

For deeper installations (beyond 20 m), we have done some further work on the pneumatic tamper. A very compact tamper was designed, such that eight can be used in a single 15 cm circle. We are searching for compact double-acting electric air valves. Figure 1 is a functional diagram of the complete remote installation system. The concept still requires a dry hole for the installation process, which should be experimented with at about the 100 m depth.

III: Task 3: The Digital Data System

Objective: To continue to develop and operate a digital data acquisition system to acquire geodetic data and to thoroughly monitor the environment of the instrument installations.

Accomplishments: The Adak digital system continues to operate well. One of the floppy disk drives failed for yet unknown reasons, but a spare on hand at Adak was quickly installed and only about 6 hours of data were lost. The data base is now continuous for 68 months. Two prototypes of the 16 bit data acquisition system continue to run well; the clocks were trimmed to within 1 second per month, and the ADC provided with a 20 ppm/year voltage reference.

IV: Task 4: The Data Interpretation

Objectives: To process the digital data and make efforts to remove the environmental noise from the data, so as to establish the intrinsic long-term stability of the tiltmeters. Various analysis techniques are then utilized to present the data in meaningful formats such that any precursory tilt events would become evident.

Accomplishments: Because of other priorities, little new data analysis programming was done. In preparing figures for the current round of proposals, previous concepts were generally applied. Of interest was to further examine the Adak data after the pits were back filled with bagged dirt to provide the greatly increased thermal mass and stability

reported last time. Figures 2 and 3 show the raw data for the last 8 months, along with the temperature data. Figures 4 and 5 show the data after being corrected for the temperature by the least-squares fitting process; note that the scales are 5x those of the raw data. Short-term coherence is interesting except for the rainfall events, and the overall long-term behavior is also encouraging.

V: Problems and Plans

A) Problems Encountered: As mentioned in the last report, this program was discontinued after an unfavorable evaluation of the proposal in response to RFP1586. Consequently, the considerable funding reserved for the final installation phase (travel, housings, masts, etc.) of the scientifically orphaned Palmdale tiltmeters (after the infamous bulge went away) was re-budgeted for continuation of the instrumentation development and research aspects of the effort. A no-cost extension was provided through October 1986.

B) Future Plans: In response to Announcement 7121, a proposal was submitted to continue this instrumentation research effort as part of the Crustal Deformation Observatory, part (i), at Pinon Flat. See that report for the status of that effort.

C) There is a possibility that we will lose the services of our valued project technician, and with Grahm-Rudman and a renewed suspicion of borehole tiltmeters staring at us, it is probably unwise and also unlikely that we will be able to replace this person in the near future. The consequences are no less than potentially terminal for this research program.

Figure 1

Functional Diagram of Remote Control Borehole Tiltmeter Installation System

II-2

Surface		Borehole
A) Utility Carrier: 110 VAC	→	TV camera, etc., in borehole
1) TV: 12" TV monitor	←	RCA miniature TV camera
focus control	→	remote focus motor
lighting control	→	upper, lower lights
2) Supplies dispensing: portable air compressor 40 psi	→	air reservoir
right, left sand push buttons	→	air valves → air cylinders → sand gates, right, left
right, left water push buttons	→	solenoid valves on water reservoirs (available sand mix 6.7 liters) (available water 2.2 liters)
B) Pre-Leveling Machine		
1) Hole brace on cable slackening	→	brace in hole
2) x, y axis pre-leveling control (variable speed, polarity)	→	x, y DC gear motors: → (drive warping screws)
limit indicators	←	limit switches
DC supply	→	x, y coarse level indicators (optical pendulum, beam splitter, Si cells)
3) Coarse level indication	←	coarse level out, $\pm 5^{o}$
4) Tiltmeter electronics system (with low gain option PC cards)	→	electrolytic bubble on tapered cast stainless housing
5) x, y output monitor	←	fine level out, $\pm 10^{-3}$ to $\pm 10^{-6}$
6) Tiltmeter release cable	→	retracts locking pins, frees tiltmeter
C) Pneumatic Tamping System		
1) Air supply: 40 psi, 0.8 cfm: oil-less compressor → tank → regulator → filter → regulator → mist oiler	→	downhole air reservoir
2) Tamping control: eight push buttons (compass points) (electronically switched option of tamp - drop or drop - tamp - lift sequence varies firmness)	→	Double acting air valves → Eight double acting floating tamper cylinders: (3/4" bore x 2" stroke)
3) Tamper hoist control	→	Gear motor → lift cables → position indicator
Position monitor in mm, digital meter	←	(rack driven multi-turnpot)
Limit indicators	←	Limit switches

Figure 2,3 : Adak west site raw data after filling the access pits.

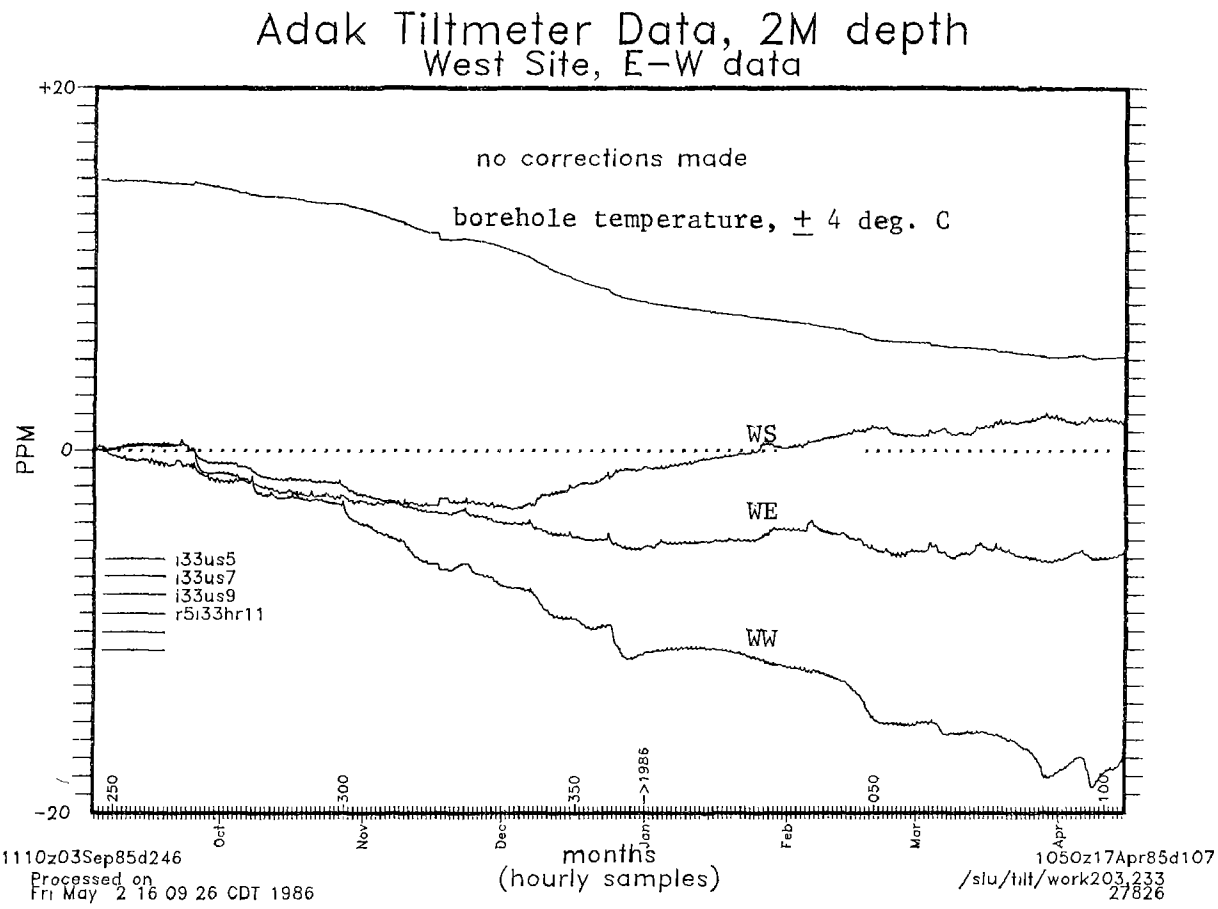

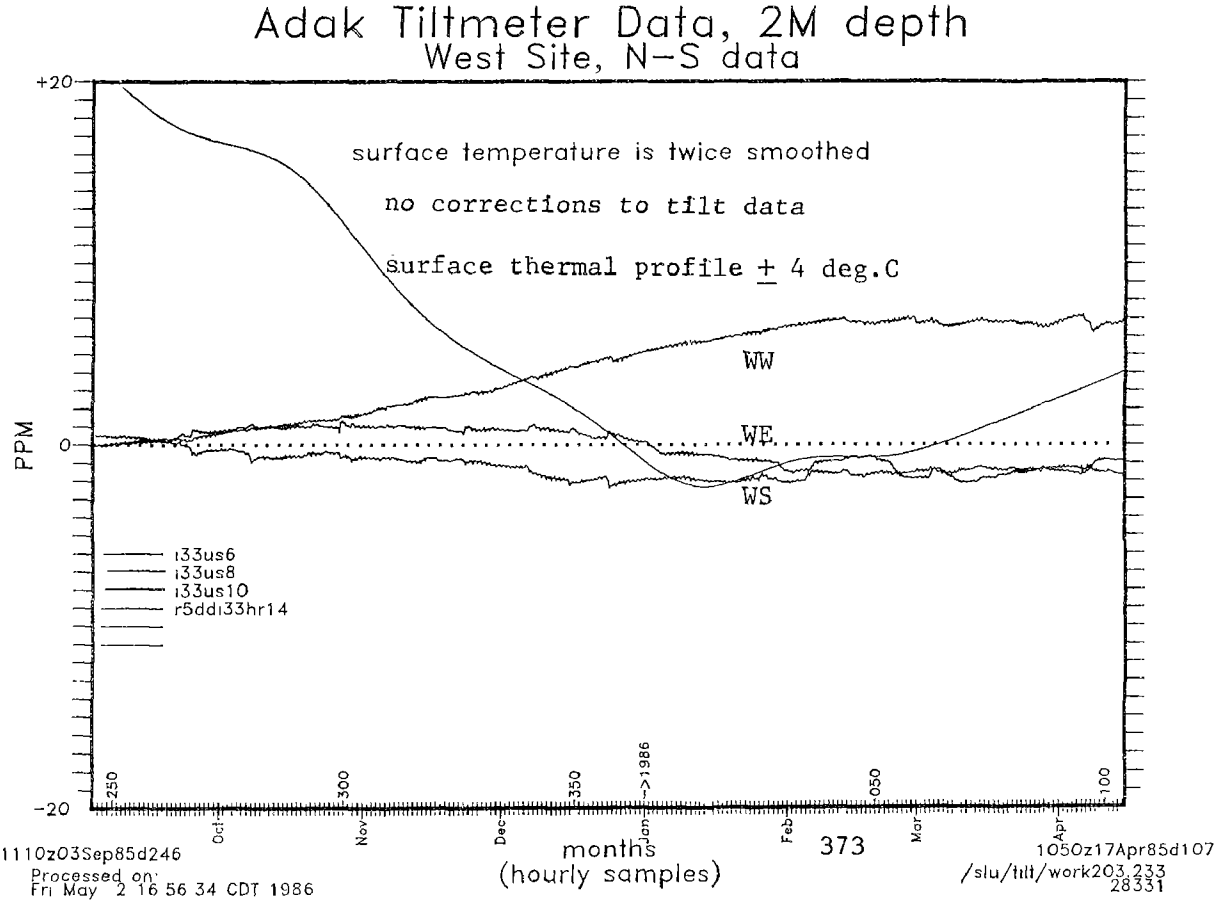

Figure 4,5: Residual tilt after fitting and removing direct thermal data.

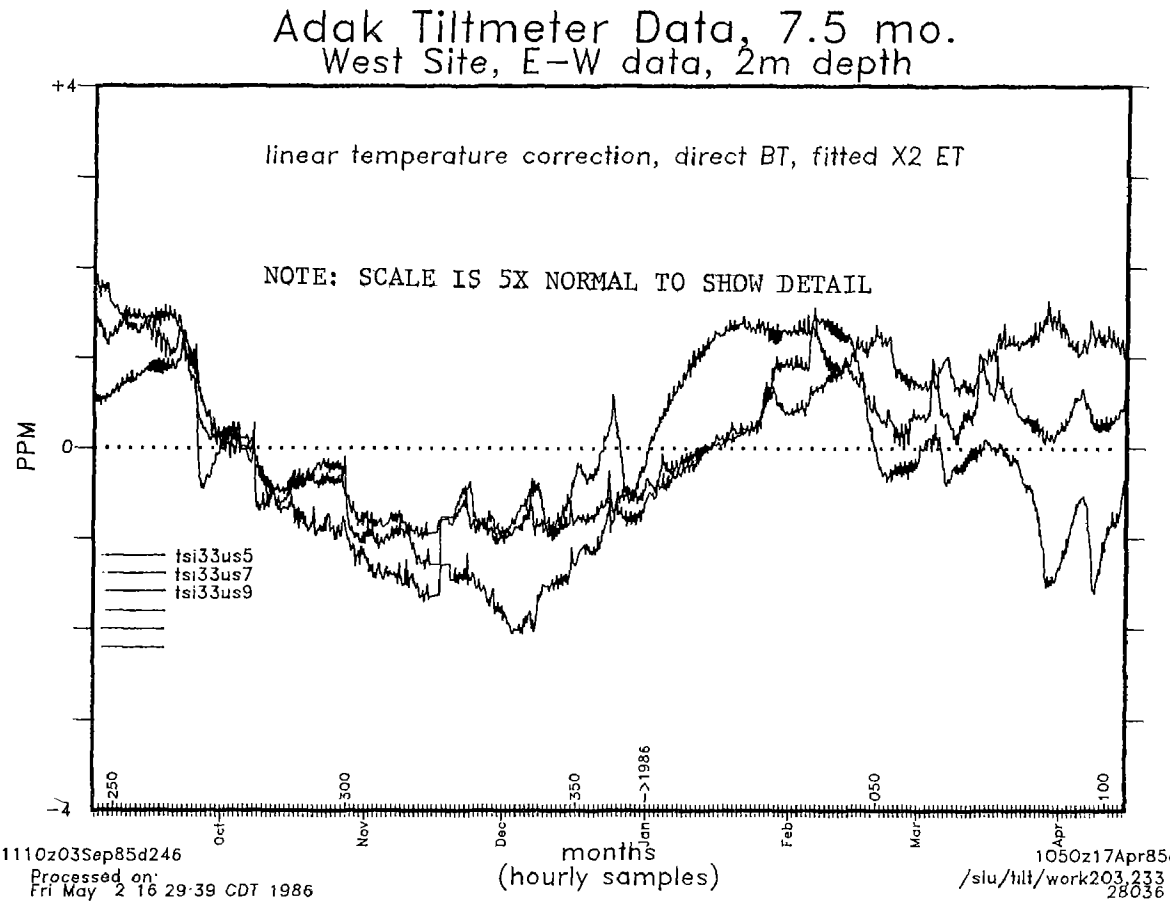

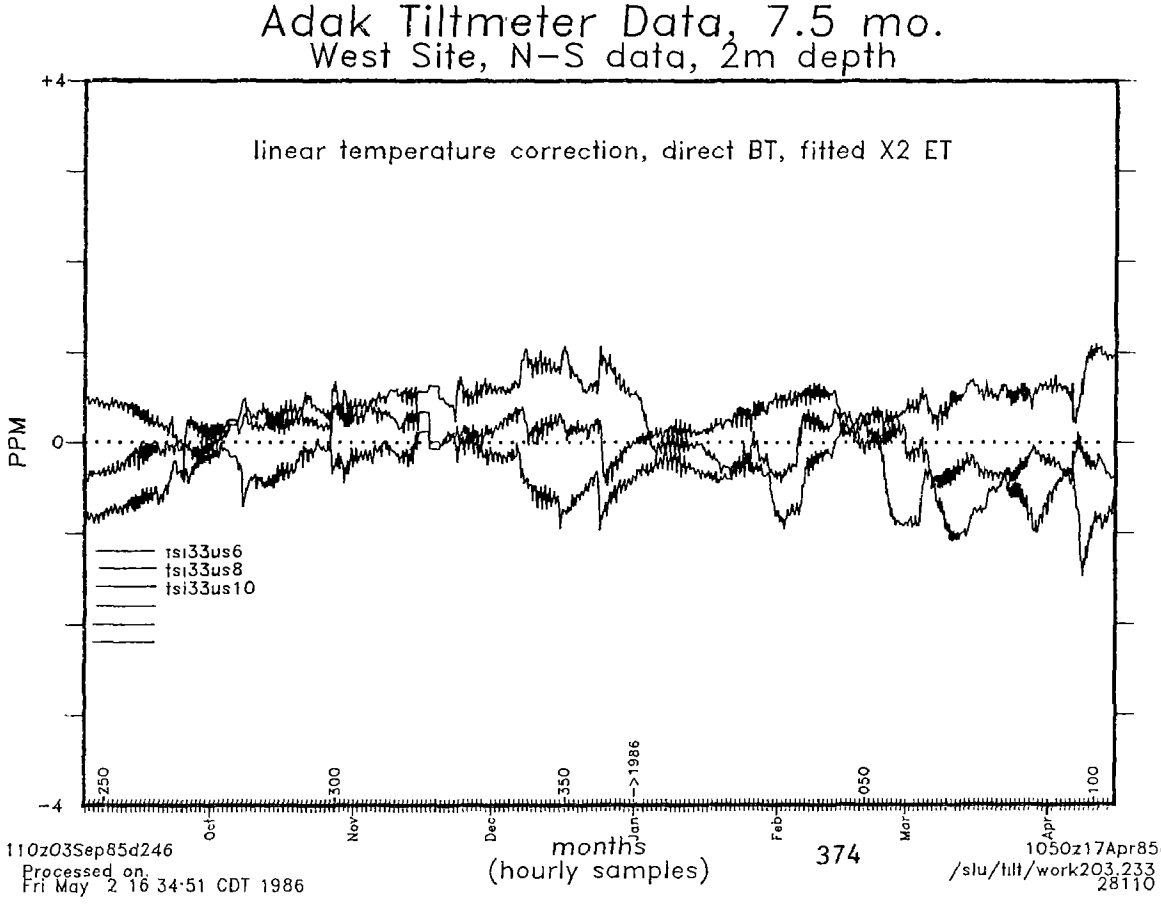

Crustal Deformation Observatory, Part (i)
Shallow Borehole Tiltmeters

14-08-0001-21939

Sean-Thomas Morrissey
Saint Louis University
Department of Earth and Atmospheric Sciences
P.O. Box 8099 - Laclede Station
St. Louis, MO 63156
(314) 658-3129

Objective: To apply the latest innovations and technology of instrumentation and installation methods to the shallow borehole tiltmeters at Pinon Flat such that their performance, particularly with regard to longterm stability, will compare more favorably with the data from the long baseline tiltmeters.

Accomplishments:

1) 5 m deep installations: These units were fitted with new electronics and borehole housings and reinstalled in May 1985, and the data available at the time of the last report seemed to indicate that there may have been significant changes in the annual trend of one or two components in the first two months of data after reinstallation. However, longer data sets indicate that the previous annual trends from each location were resumed within a week or two after the installation. This is a somewhat surprising result for two reasons:

First, there was not a dramatic decrease in diurnal thermal noise as had occurred at Adak when the tiltmeter electronics were replaced. On further examination, we find that since the previous CDO electronics units were installed near the bottom of the 5 meter pits, they were exposed to diurnal variations of about 0.2°C, and annual variations of about 8°C, whereas the Adak electronics, in exposed surface enclosures, measured diurnal variations in excess of 20°C, and annual variations of 50°C. The new electronics at Pinon Flat are at the top of the pits, and sealed baffles in the pits attempt to minimize the diurnal variations at the bottom. Moving the Alpha electronics down into the pit in November 1985 made no measurable difference in the diurnal signal, as expected.

The second surprising result of the reinstallations was that after the transient of a few hours to two weeks, each of the six components resumed the annual trend that it had been following for months before. This was true even though the sensors had been rotated 90° upon reinstallation, effectively interchanging the NS and EW components of the instrument, indicating that there are no problems with the tiltmeters, but that the incoherent noise is in the ground, and that deeper depths are necessary. This data is shown in Figures 1, 2, and 3. The larger transient on the Gamma unit is because the bubble mounting threads seized during reassembly and could not be freed. This so stressed the mount and the pipe that the data at first appeared useless, but it now

seems to have resumed the annual cycle. The thermal data was not connected to the digital system until later, and there are some problems with it in these figures, as noted.

2) 10 and 20 m deep installations. The task here is to install two instruments in 10 meter boreholes, and attempt deeper holes, possibly 20 meters. We have proven the 10 meter technique at the CCMO (Creve Couer, MO) test site, and in designing and testing installation tools for the deeper holes, found that we could adequately control manual tamping rods over the 20 meter depth. This meant that with the pre-leveler device, 20 meter installations should be feasible. A further problem at Pinon Flat is that the water table is at about 26 meters. In November 1985, two 10 meter and two 20 meter holes were drilled. Although the driller had constructed special long stabilizers for the 8" bore, and long stabilizers as well as 8" diameter drill stems for the 12" reaming, the holes all inclined to the southwest by about 1 degree, or half the diameter of the hole in the 10 m hole. This meant that the hand-held alignment tool would not work, so the remote pre-leveler has been completed and tested in a hand dug 10 m pit at the CCMO test site. (See the other report for more details.) We plan to install both the 10 m and 20 m instruments in May 1986, along with our digital telemetry system to provide the volume of data we need.

Plans and Problems

In response to RFP 7121, a proposal was submitted to the USGS to continue this work, and also to merge the basic tiltmeter and instrumentation research aspects of the former Palmdale program. Continuation of operation of the Adak tiltmeters was also included, as long as this PI is operating the CIRES seismic network there.

A problem has arisen in that the technician for these programs has resigned, and with the uncertainties of funding, he will not be able to be replaced in the near future, seriously jeopardizing our ability to meet our objectives.

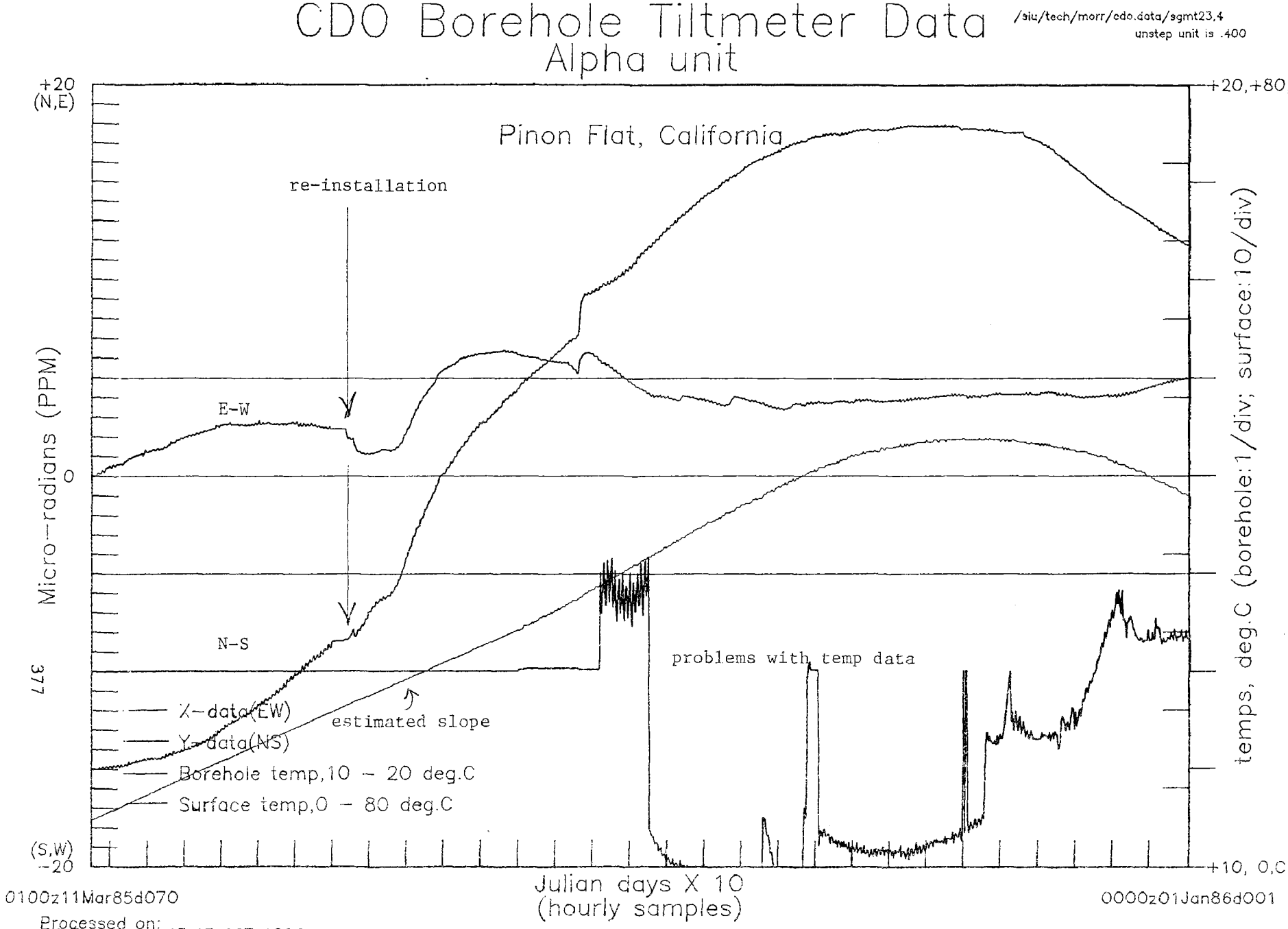

Figure 1. CDO Alpha unit before and after re-installation

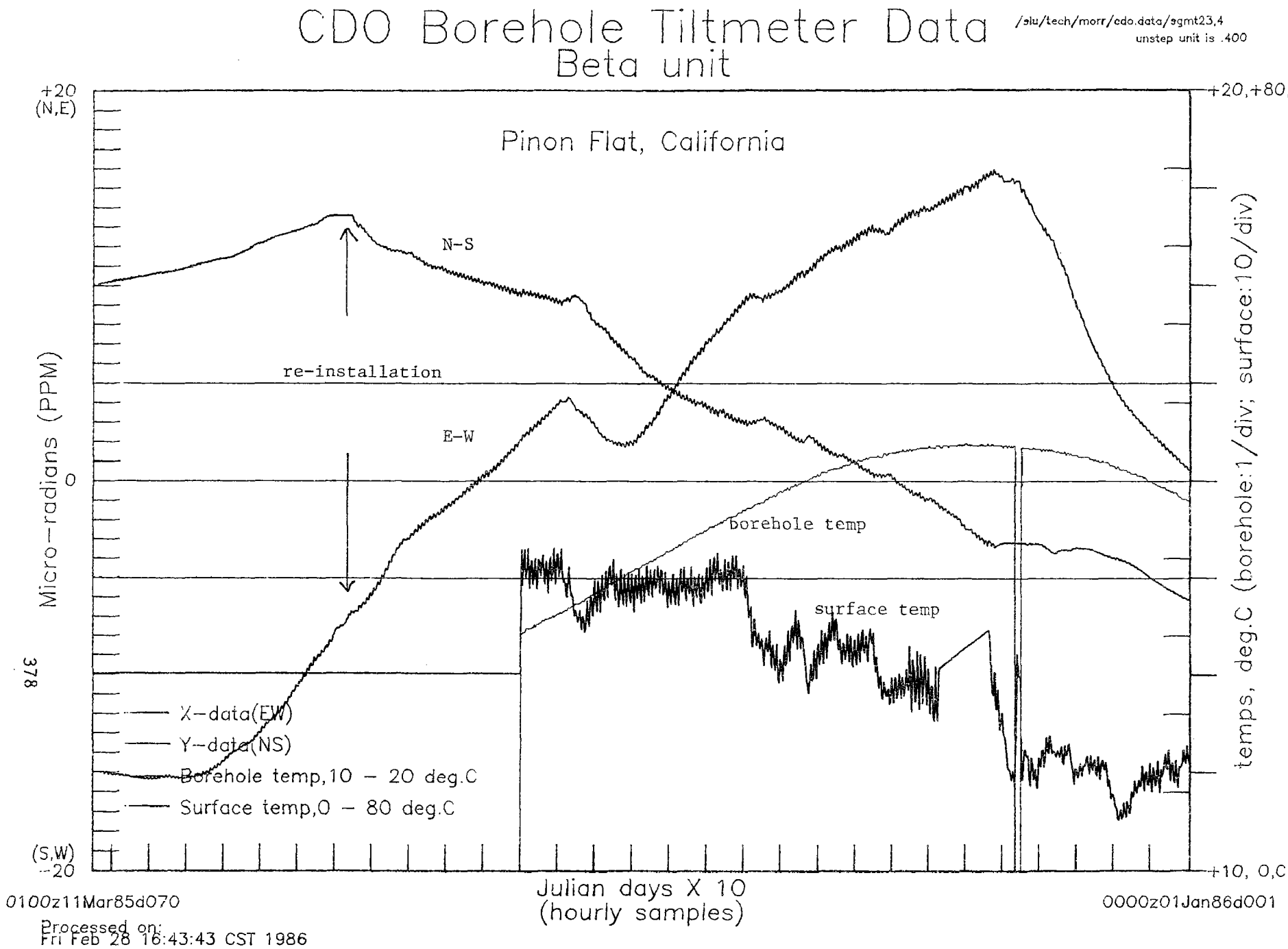

Figure 2. CDO Beta unit before and after re-installation

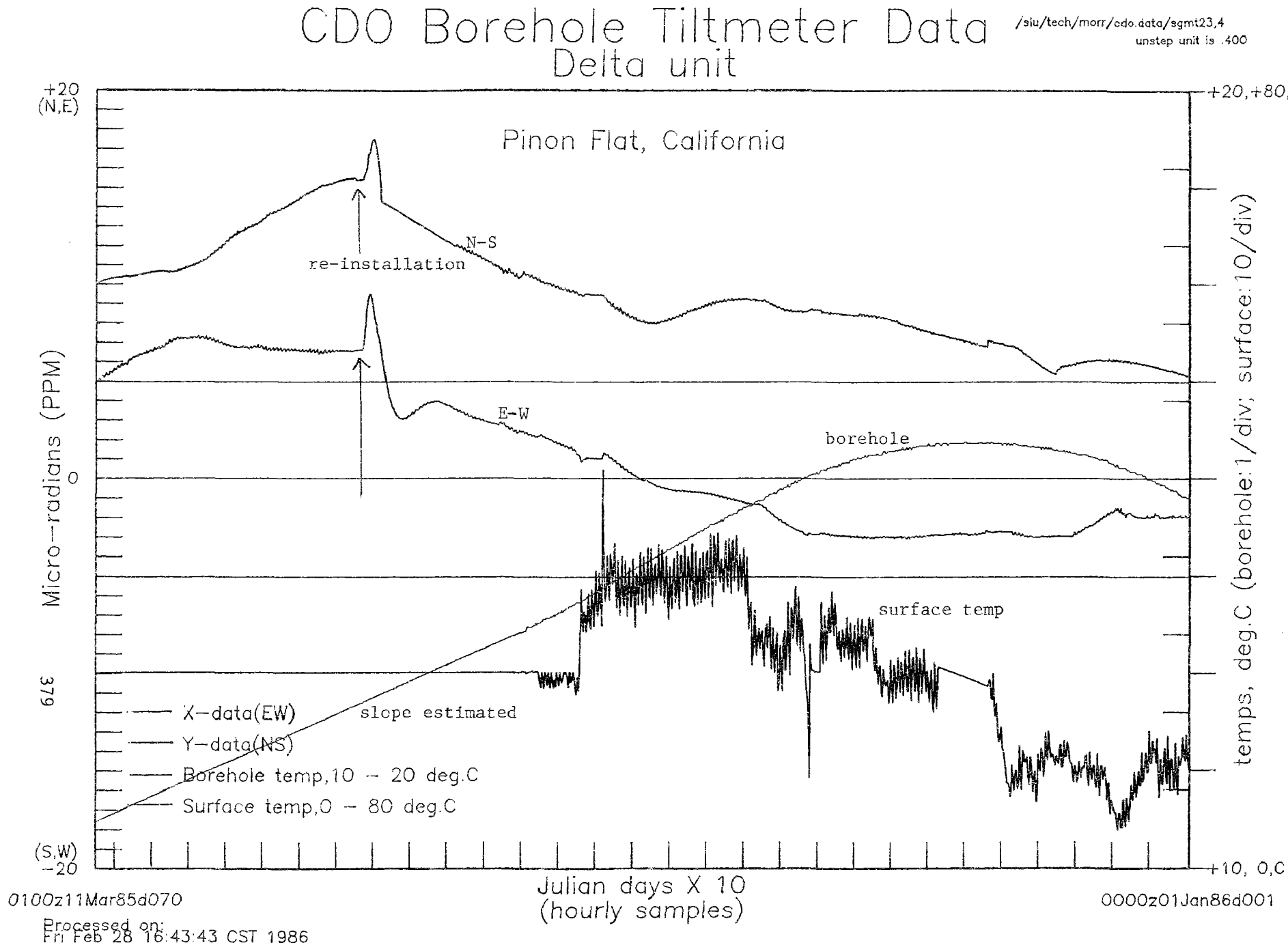

Figure 3. CDO Delta unit before and after re-installation.

Cooperative Tiltmeter Program at Parkfield, California

14-08-0001-G1204

Sean-Thomas Morrissey
Saint Louis University
P.O. Box 8099 - Laclede Station
St. Louis, MO 63156
(314) 658-3129

Objective: To apply the latest state-of-the-art technology to shallow borehole tiltmeter installations and data acquisition in the Parkfield area, which is forecast to be the locale of a moderate earthquake in the near (3-8 years) future. Considerations of the current failure model, based on known creep data and fault-constituitive models, allows locating the tiltmeters such that probability of acquiring large coherent signals during the precursory stages is enhanced. The cooperative aspect involves the assistance of the U.S. Geological Survey in site selection, preparation, maintenance, and data acquisition.

Accomplishments: We contracted for drilling two 10 m and one 20 m holes at both Gold Hill and Turkey Flat early in November 1985, but on November 6, with the drillers already on the road, we were informed that the Gold Hill site was temporarily not available because of permitting problems. So we planned three 20 m holes at Turkey Flat. Refraction in May 1985 showed the top of the Franciscan sandstone at about 6 meters, where it was encountered. The first hole (North) was finished to 20 m with the 30 cm bore, but when the small 12 cm bore for the tiltmeter was made, a clay pocket was encountered, so the hole was re-cemented to 18 m.

Similar problems with clay lenses occurred in the other holes, all in a line separated by 20 meters. The driller had fabricated special stabilizers for the 12" reamer, and had only 60' of drill stem, so he was not able to drill the small bore past the clay pockets, which were small and dispersed. An 8" test hole was drilled without hitting a clay pocket to 69' (the bit and hammer are 9' long), but another hole 2 m away encountered a pocket of gravel at 58'. Several other holes were abandoned, so the net result of our efforts were two 10 m holes and one 19 m hole. In the future, we should plan on going considerably deeper if possible, and probe the ground with a fast 6" bit first. There is seep water in the 19 m hole, up to about 15 m, but the seep is slow enough that the hole can be pumped (with a water jet pump) during installation. The tiltmeter has no problem running submerged, as most of the Adak units are.

Future Plans

The review panel has recommended that the instruments not be installed until after the CDO instruments are installed in 10 m and 20 m holes, which is planned for May 1986. Because of reductions in the program, we will need the assistance of the USGS in providing shelters and data telemetry when the instruments are installed, which will probably be in

the fall, since the major Adak seismic network service trip will occupy the PI's time in July and August.

The current program is funded through December 1986, and a response to RFP1721 was submitted to continue to operate it for another year. No further installations are planned, unless the USGS decides to provide 20 m holes at Gold Hill.

EXPERIMENTAL TILT AND STRAIN INSTRUMENTATION

9960-01801

C.E. Mortensen
Branch of Tectonophysics
U.S. Geological Survey
345 Middlefield Road, MS/977
Menlo Park, California 94025
(415) 323-8111, ext. 2583

Investigations

1. The satellite telemetry system has been operational in the Parkfield and Mammoth regions for some time. Most of the strainmeters, creepmeters, tiltmeters, magnetometers and hydrogen monitor stations in these areas are being telemetered via the GOES satellite to the Direct Readout Ground Station (DRGS) in Menlo Park. As of April 1986, 79 Data Collection Platforms (DCPs) are returning more than 280 channels of data to the DRGS. Most of these transmit data in 1 minute time windows every 3 hr. However, 35 DCPs transmit data from 116 sensors at ten minute intervals. Of these, 16 DCPs are reporting data from 30 separate instruments in the Parkfield region; 7 DCPs are returning data from 15 instruments in the Mammoth region; 3 DCPs return data from as many instruments in southern California and 4 DCPs operate at sites in central California. At most of these sites the old digital telemetry system based on phonelines and radio links is still being operated in parallel with the satellite system. This is likely to continue in until we are collectively brave enough to turn off the old system. The old system has been eliminated at 11 sites.

   Stan Silverman has the DRGS operating under the control of dual AT&T PCs. Following a period of several days of downtime in February, we decided to order duplicate parts to insure backup of most of the DRGS.

   The satellite system is proving to be more reliable than the telephone-based system, principally due to the elimination of problems associated with the quality of phonelines. However, the current west spacecraft, GOES 3, has a badly inclined orbit. This causes some lost transmissions at certain times of the day. Shortly before this writing GOES 7 was destroyed during launch. This will cause some rethinking on the configuration of our uplinks and downlink. The DRGS is more reliable now than the old telemetry

receiver system. Difficulties associated with full implementation and finalization of the satellite telemetry system now appear to be mostly administrative rather than technical in nature.

In January Malcolm Johnston and Carl Mortensen travelled to Washington and met with representatives of the National Environmental Satellite Data and Information Service (NESDIS), the agency that operates the GOES system. An extension of the 2-year special operating agreement between NESDIS and the Geologic Division was requested and should be forthcoming soon. It was agreed that we would setup a test to determine whether the random reporting mode of operation could be used to monitor data from Parkfield. In this mode of operation frequent transmissions are available only when they are required, with the intervals of frequent transmissions being activated by some trigger. Several triggering techniques will be tested and evaluated. A re-evaluation of our special operating agreement will occur in one year, at which time we will hopefully have some results from this test.

2. In November 1985, Dr. Richard Adler of the Naval Postgraduate School, Monterey, established a site for monitoring radio frequency emissions near the Cienega Winery, south of Hollister, California. Analysis of the data is coordinated by Carl Mortensen. The experiment monitors emissions at 150.75 MHz and 38.45 MHz using sensitive receivers and antennas polarized and oriented in different directions.

3. In October, Carl Mortensen travelled to China and presented a paper at the U.S.-China Symposium on Crustal Deformation and Earthquakes. Visiting the Seismological Laboratories at Wuhan and at Shanghai, it was possible to examine the instrumentation and techniques used by the Chinese to monitor crustal deformation, and to examine much of their extensive data sets of crustal deformation measurements spanning times of significant nearby earthquakes.

4. Networks of tiltmeters, creepmeters and shallow strainmeters have been maintained in various regions of interest in California. A network of 14 tiltmeters located at seven sites monitor crustal deformation within the Long Valley caldera. Other tiltmeters are located in the San Juan Bautista and Parkfield regions. Creepmeters are located along the Hayward, Calaveras and San Andreas faults from Berkeley to Parkfield, and shallow strainmeters are located in the Parkfield region. A tiltmeter station, consisting of a pair of biaxial instruments, is operated at Cape Yakataga, Alaska. Observatory type tiltmeters and strainmeters are located at the Presidio Vault in San Francisco

and a tiltmeter is sited in the Byerley Seismographic Vault at Berkeley. Data from all these instruments are telemetered to Menlo Park via the GOES satellite, by phonelines and radio links, or both.

Results

1. A system to monitor radio-frequency emissions was installed in November, 1985, on the Hollister Hills State Vehicular Recreation Area, near the Cienega Winery, Hollister, California. The most sensitive channels seem to be 150.75 MHz, with vertical polarization, pointed NW and 38.45 MHz, with horizontal polarization, pointed SE. Data from these channels, digitized at a 1 hr sample interval, are shown in Figure 1. These data span the time of the M=5.2 earthquake near Tres Pinos on January 26, 1986. No signal significantly above the noise level is evident preceeding the event, however, there are some interesting small fluctuations following the quake. Dr. Richard Adler of the Naval Postgraduate School, Monterey, manages this experiment. The measurement system is discussed in detail by Whyms, 1985.

Reports

Mortensen, C. E. and M. J. S. Johnston, 1985, Monitoring Crustal Deformation: A Review of Instrumentation, in Proceedings of the U.S.-China Symposium on Crustal Deformation and Earthquakes, Wuhan, PRC, in press.

Reference

Whyms, Michael L., 1985, Design of a Space-Based Sensor to Predict the Intensity and Location of Earthquakes from Electromagnetic Radiation, Naval Postgraduate School, Monterey, California, MSEE Thesis.

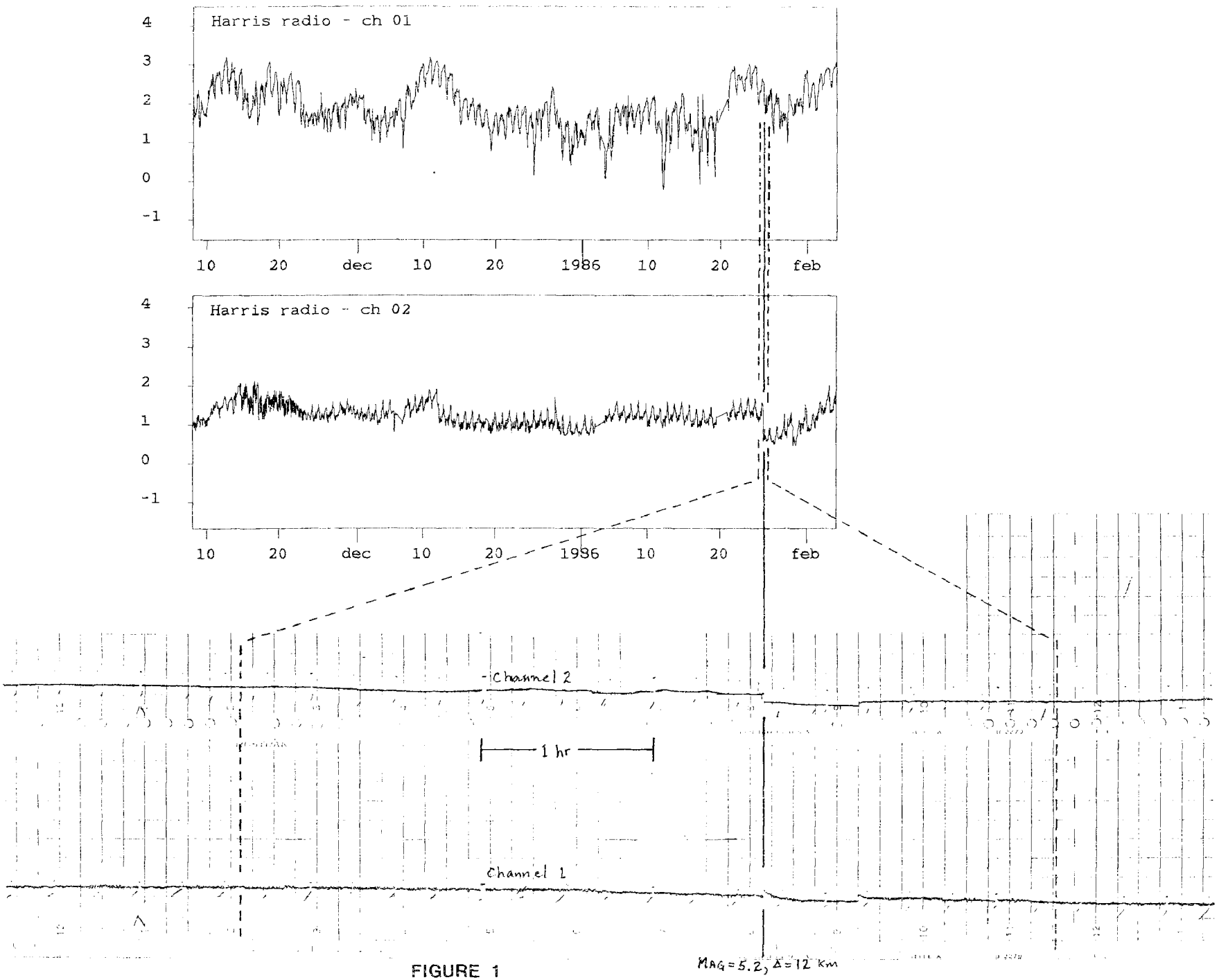
Harris radio - ch 01
4
3
2
1
0
-1
10
20
dec
10
20
1986
10
20
feb
Harris radio - ch 02
4
3
2
1
0
-1
10
20
dec
10
20
1986
10
20
feb
Channel 2
1 hr
Channel 1
MAG = 5.2, Δ = 12 km

FIGURE 1

Dilatometer Operations

9960-03815

G. Douglas Myren
Branch of Tectonophysics
U.S. Geological Survey
345 Middlefield Road, MS/977
Menlo Park, California 94025
415-323-8111, ext. 2705

Investigations and Results

Since October of 1985 most of the time has been spent on instrument maintenance. However, we were able to remove the bugs from the automatic valve opener and now have it installed at all instruments except Devils Postpile and Adobe Mtn. It is now working well enough to be incorporated in the electronics of the next six dilatometers on order from Carnegie.

Our regular maintenance includes the GEOS data recorders installed at Searle Road, Gold Hill, Punchbowl, and Devils Postpile. Under direction from Malcolm Johnston and Roger Borcherdt, we have increased the range of the dilatometer recordings by not only recording signals at the 36db level, but also at the 0db (*64 vs. unity gain) level. This current recording method is incorporated only at Searle Road, but will be implemented at all GEOS sites.

There were no holes drilled in the fall of 1985. In late January of 1986 two holes were drilled at the top of Vineyard Canyon Road, near Parkfield, California. Of these two holes one proved productive for instrument installation. It has been decided that a 3-component strainmeter will be installed at this site later this summer.

Tom Moses has let a contract for core drilling at 13 potential sites for strainmeter installation. This drilling will begin this spring. The cores will be taken to approx. 660'; information from the cores will tell us whether the rock at depth meets the criteria for instrument installation at any of the 13 sites. Drilling of instrument size holes will begin after site locations have been selected.

Three additional holes will be drilled in the Parkfield area; at Taylor Ranch (near Eades), at Gold Hill (near existing dilatometers), and at Frolich (a straightening of the existing hole). Three component strainmeters will be installed at Eades and Gold Hill, and a dilatometer at Frolich.

Six dilatometer strainmeters arrived in late March with cable arriving in the middle of April. These six instruments have commercially developed cable head-connectors (marine environment). These six along with two from the 1983 Carnegie trip gives us 8 instruments ready for installation. Plans at this time call for 4-6 (dilatometer, 3-component) strainmeters to be installed in the Parkfield area this year.

Reports

Mueller, R. J. and Myren, D., 1986, Automatic Rezeroing for USGS Operated Bore-hole Strainmeters, Open-File Report No. 86-___ (for review).

Helium Monitoring for Earthquake Prediction

9570-01376
G. M. Reimer
U.S. Geological Survey, MS 963
Denver Federal Center
Denver, CO 80225
(303) 236-7886

Investigations

The variations of helium in soil-gas from sample collecting stations along the San Andreas Fault near San Benito, California continue to be observed and related to nearby seismic activity. A system to monitor soil-moisture and temperature had been installed to determine if soil-moisture measurements might provide information that could normalize the seasonal helium variations. Data is being accumulated to evaluate this theory.

Results

For the early part of the past year and a half, there has been relatively little seismic activity and few helium decreases. This relationship is valuable in that it provides information on the frequency of helium decreases that might randomly occur. In contrast to this quiescence, helium data for the last 6 months (Figure 1) indicate that the concentrations have been more variable than anytime in the previous 5 years. Also of signficance is the fact that several seismic events have occurred in the vicinity during this same time preriod; of particular note is the M=5.5 of January 26, 1986 near Hollister. That event and subsequent aftershocks could be the reason for the observed helium variations. The helium variations are continuing which indicate effects of the additional aftershocks or other discrete seismic events such as the late March event.

Reports

Reimer, G. M., 1985, Prediction of central California earthquakes from soil-gas helium fluctuations: Pageoph, v. 122, p. 369-375.

FIG. 1. HELIUM SOIL-GAS CONCENTRATIONS NEAR SAN BENITO, CA.,

3.0 MOVING AVERAGE THROUGH 86091.

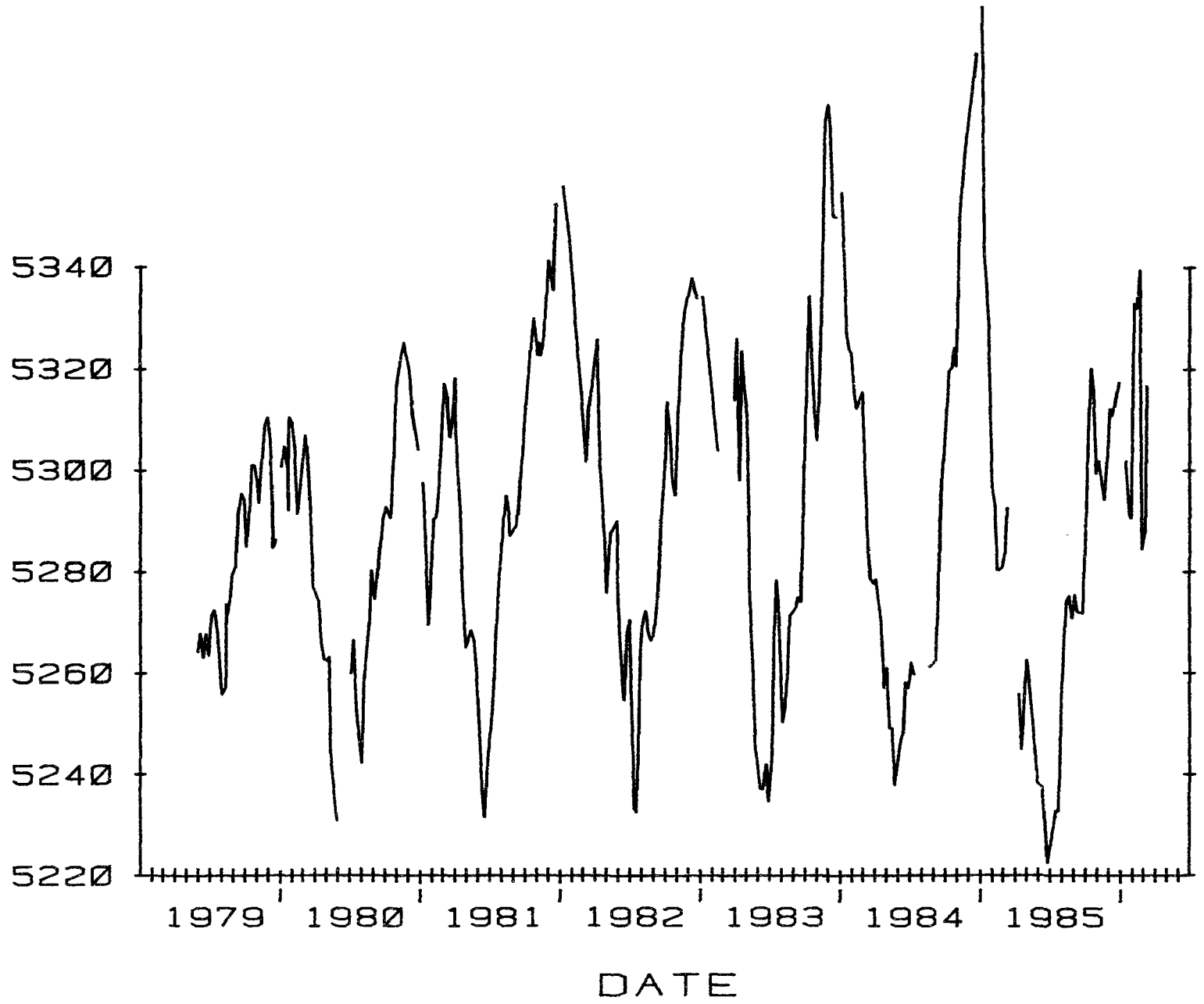

Mechanics of Faulting and Fracturing

9960-02112

Paul Segall and Ruth Harris
Branch of Tectonophysics
U.S. Geological Survey
345 Middlefield Road, MS/977
Menlo Park, California 94025

Investigations

1. Analysis of trilateration data near Parkfield, California in the transition between the central creeping zone and southern locked zone of the San Andreas fault.

Results

Trilateration measurements have been made by various agencies since 1959 near Parkfield, California, in the transition zone between the central creeping section and the southern locked section of the San Andreas fault. Within the transition zone there are several creepmeters and alinement arrays, four small-aperture trilateration networks, and a broad trilateration network extending 70 km southwest from the San Andreas fault to the Pacific coast (Figure 1). Shallow slip rates determined by creepmeters and alinement arrays decrease from 25-30 mm/yr in Slack Canyon northwest of the Parkfield rupture zone, to zero at Highway 46 at the southeastern end of the rupture zone (Figure 2).

We have inverted the average rates of survey line-length change to estimate the distribution of slip rate on the fault. The shallow fault slip rate is specified to fit the observed decrease in creep rate from the creeping to the locked zone. Whereas the total fault-parallel motion across the network is 25.5±4.6 mm/yr, the geodetic data cannot uniquely resolve the deep fault slip rate. Solutions ranging from 25.5 mm/yr slip below 14 km to 33 mm/yr below 22 km fit the data equally well. In either case, solutions providing acceptable fits to the data have little or no slip in the 1966 rupture zone (Figure 3). Analysis of model resolution indicates that the data are capable of detecting the presence of a locked or slowly slipping zone, but cannot resolve the details of the locked zone geometry, particularly the depth of its lower boundary. Features of the slip-rate distribution with characteristic dimensions less than 10 km are essentially unresolvable at seismogenic depths. Considering the resolution of the data, the locked

zone predicted by the inversions coincides quite closely with the rupture surface of the 1966 earthquake as delineated by its aftershocks. The hypocenter of the main shock is located at the northwest end of the locked zone, and the aftershocks extend some 30 km southeastward into the zone of negligible interseismic slip (Figure 3). From the difference between the slip rate in the seismogenic zone and the deep slip rate we estimate a rate of moment deficit accumulation. This rate is compared to the geodetically determined seismic moment of the 1966 earthquake. The comparison indicates that the strain released by the last Parkfield earthquake recovers in 18 to 23 years, although the data would permit this number to be as slow as 5 years or as great as 29 years.

We calculate station velocities from the data, removing the ambiquities in rigid-body motions by minimizing the difference between the observed velocities and those predicted by the inversions. In general, there is a good fit between the observed station velocities and those predicted by the inverse models (Figure 4). There is, however, a systematic difference between the observed and predicted motions. The residual motions show a spatially uniform contraction of 0.08 ± 0.01 μstrain/yr normal to the SAF, equivalent to 6.4 ± 1.1 mm/yr of NE-SW shortening. An alternate adjustment that minimizes the velocity components normal to the fault yields NE-SW shortening rate of 3.6 ± 1.5 mm/yr. The orientation of the shortening is consistent with geologic and seismic evidence of recent folding and reverse faulting in the region. The inferred contraction rate falls within Minster and Jordon's (S.E.P.M. Pac. Sect., v. 38, 1984) bounds of 3.7 to 13 mm/yr normal to the SAF.

Reports

Harris, R. and P. Segall, 1985, Determination of the Slip Deficit Along the Parkfield, CA Section of the San Andreas Fault From the Inversion of Trilateration Data, Trans. Amer. Geophys. Union (EOS), v. 66, p. 985.

King, N. E., P. Segall, and W. Prescott, 1986, Geodetic Measurements Near Parkfield, 1959-1984, submitted to J.G.R.

Segall, P. and R. Harris, 1986, Deformation in the Transition Between the Central Creeping and Southern Locked Zones of the San Andreas Fault, Trans. Amer. Geophys. Union (EOS), v. 67, p. 359.

Segall, P. and R. Harris, 1986, Slip Deficit at Parkfield Revealed by Inversion of Geodetic Data, Amer. Assoc. Adv. Science Annual Meeting.

Segall, P. and R. Harris, 1986, Slip deficit on the Parkfield, California, section of the San Andreas fault as revealed by the inversion of geodetic data, in review.

Segall, P. and C. Simpson, 1986, Nucleation of ductile shear zones on dilatant fractures, Geology, v. 14, p. 56-59.

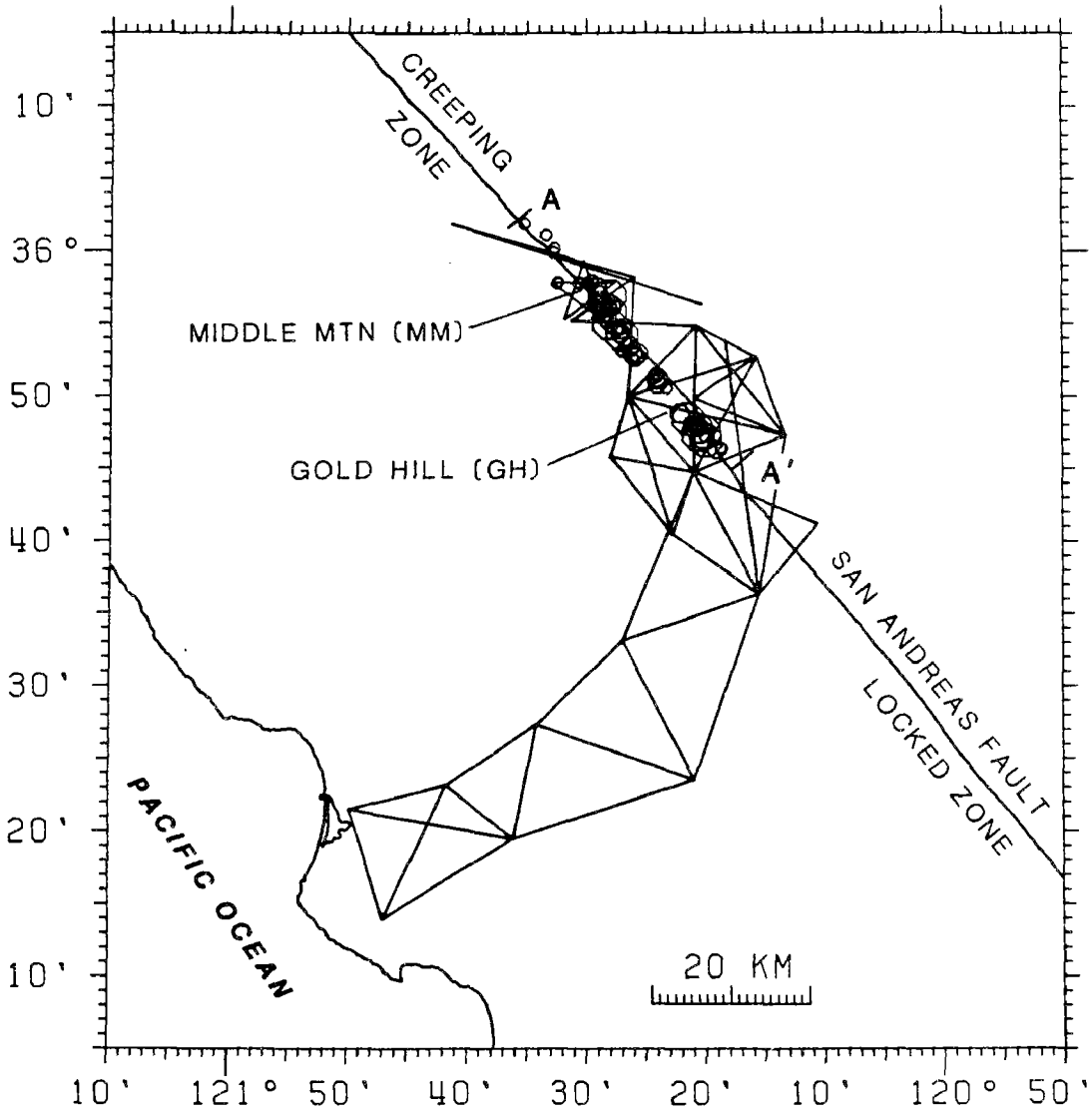

Figure 1. Parkfield trilateration network. Straight lines represent geodetic survey-lines used in interseismic-slip-rate inversion. 1966 Parkfield mainshock (star) and M > 2 aftershocks (circles).

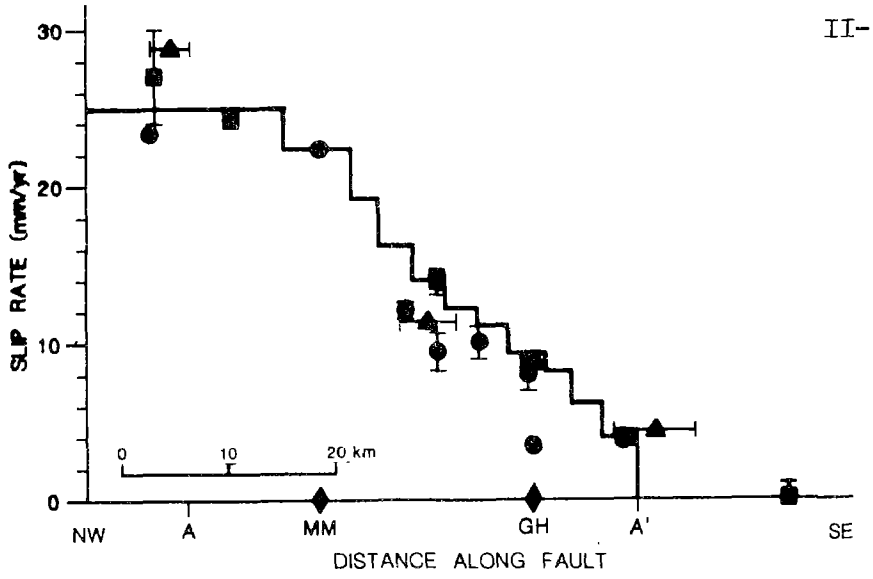

Figure 2. Shallow-fault-slip rate versus distance along fault, showing average slip-rate as measured by creepmeters (circles), alignment arrays (squares), and short-baseline trilateration networks (triangles). Heavy line shows shallow-fault-slip-rate profile used in interseismic inversions. MM = Middle Mountain, GH = Gold Hill.

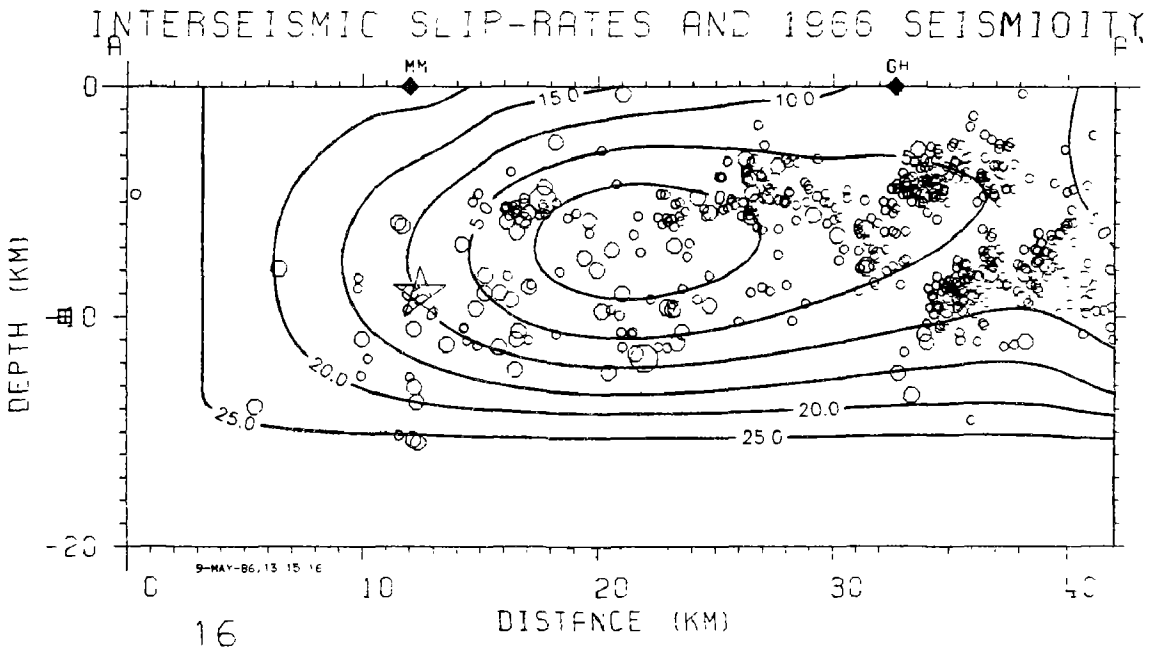

Figure 3. Interseismic-slip-rate pattern determined by inversion of long baseline trilateration data. Contours indicate slip-rate in mm/yr. Longitudinal cross section of 1966 aftershocks (circles) and mainshock (star) projected onto model fault plane outlines rupture surface of 1966 Parkfield earthquake. MM = Middle Mountain, GH = Gold Hill.

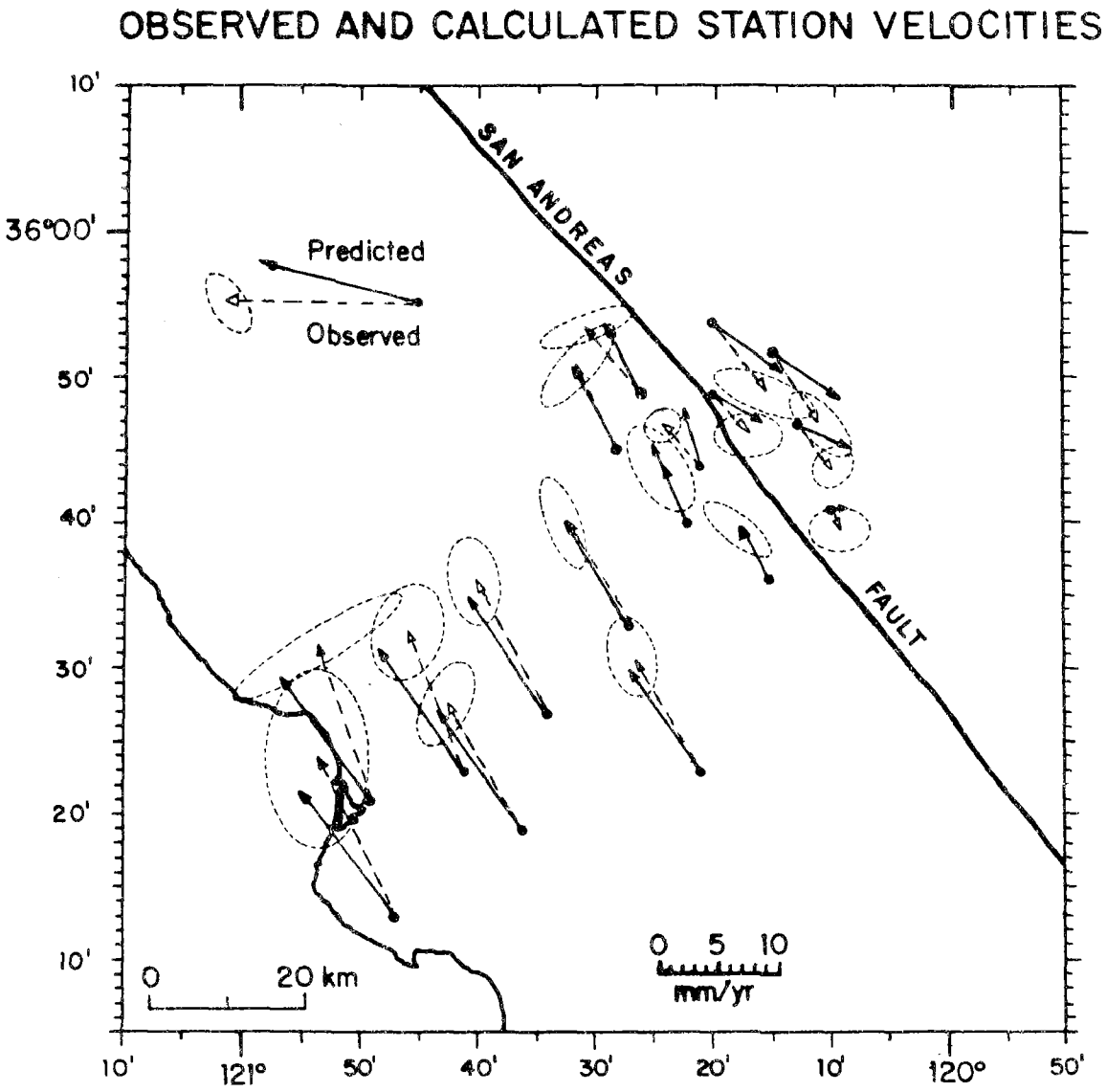

Figure 4. Velocities of geodetic survey marks. Observed velocities (dashed vectors) with 95% confidence ellipses, as well as velocities predicted by inverse model (solid vectors) are illustrated.

LOW FREQUENCY DATA NETWORK

9960-01189

S. Silverman, K. Breckenridge, J. Herriot,
U.S. Geological Survey
Branch of Tectonophysics
345 Middlefield Road, MS/977
Menlo Park, California 94025
415-323-8111, ext. 2932

Investigations

1. Real-time monitoring, analysis, and interpretation of tilt, strain, creep, magnetic, and other data within the San Andreas fault system and other areas for the purpose of understanding and anticipating crustal deformation and failure.

2. Compilation and maintenance of long-term data sets free of telemetry-induced errors for each of the low frequency instruments in the network.

3. Enhancements to satellite-based telemetry system for reliable real-time reporting and archiving of crustal deformation data.

4. Development and implementation of backup capabilities for low frequency data collection systems.

5. Specialized monitoring and display of data relevant to the Parkfield region.

Results

1. Data from low frequency instruments in southern and central California have been collected and archived using the Low Frequency Data System. In the six months over four million measurements from 160 channels have been received via telephone telemetry and subsequently transmitted to the Low Frequency 11/44 UNIX computer for archival and analysis. In the same period, more than 50 satellite platforms have been monitored, accounting for an additional four million measurements on the 11/44 system.

2. The project continues to operate a configuration of one PDP 11/44 computer running the UNIX operating system and two PDP 11/03 computers running real-time data collection software. Two AT&T PC 7300 computers have been installed as backup machines for collection of satellite and telephone

telemetered data. The 11/44 has been operational as our analysis machine with less than 1% down-time. The two 11/03 machines operate redundantly for robustness. Data from the Network are been made available to investigators in real-time. Events such as creep events can be monitored while they are still in progress. The prediction working group has made extensive use of the timely plots produced routinely by Kate Breckenridge.

3. The project continues to use a five meter satellite receiver dish installed in Menlo Park for retrieval of real-time surface deformation data from California, and South Pacific islands. The GOES geostationary satellite together with transmit and receive stations makes possible a greatly improved telemetry system. Additional reporting platforms containing waterwell and climate data are being added to the collection end of the system. Further expansion of the number of platforms monitored is anticipated.

4. Software has been developed to operate two AT&T PC 7300 computers as backup systems for collection and storage of data from satellite and telephone data collection systems. The 7300 computers have been linked to the 11/44 system so that data may be transferred between systems and users may access the AT&T machines via the 11/44 computer.

5. The project continues to take an active part in the Parkfield prediction activities. Programs have been implemented to automatically plot strain and creep records, as well as to record the status of the satellite telemetry system for the Parkfield region. These plots are routinely available on a daily basis. Stan Silverman has automated hourly monitoring of strain data with an alert system for dilatometers in the Parkfield area. No alerts have been recorded since the system has been operational. Kate Breckenridge continues as the alternate monitor for Parkfield creep events, which includes contact via paging system during periods of increased activity. Processing which monitors creep events has been expanded to include satellite telemetry. The system has signalled alerts for creep events on several occasions and has also notified researchers of malfunctioning field equipment. Research and planning of computing resources required for the Parkfield data-center has been ongoing.

6. Processing of telemetered magnetometer data has been automated on the 11/44 system and an alert system has been implemented for instruments in the Parkfield region. No alerts has been raised since the system has been in operation.

7. The project has continued to provide real-time monitoring of designated suites of instruments in particular geographical areas. Terminals are dedicated to real-time color graphics displays of seismic data plotted in map view or low frequency data plotted as a time series. During periods of high seismicity these displays are particularly helpful in watching seismic trends. The system is used in an ongoing basis to monitor seismicity and crustal deformation in central California and in special areas of interest such as Mammoth Lakes.

A 2-Color EDM Observatory Near Parkfield, California

14-08-0001-22056

Larry E. Slater
CIRES
University of Colorado
Boulder, Colorado 80309
(303) 492-8028

Investigations Undertaken: A segment of the San Andreas fault near Parkfield in central California has been subjected to periodic moderate earthquakes. The earthquakes (approximately magnitude 6) have occurred approximately every 22 years since the great 1857 earthquake. The last Parkfield earthquake of that magnitude struck in 1966.

Because of several similarities between the earlier earthquakes other investigators have issued a formal prediction for the next expected Parkfield earthquake. U.S. Geological Survey co-workers Al Lindh and Bill Bakun estimate there is a 95% chance that the next magnitude 6 Parkfield earthquake will occur in 1988, plus or minus 5 years. Since the region of fault slip is thought to be centered near Parkfield it was decided that a dense geodetic network of intermediate length lines would assist in monitoring crustal deformation changes and possible precursors to the expected earthquake.

Effort and Results: Early in 1984 we began selecting and installing retro-reflector sites to be used with the CIRES 2-color EDM instrument. It was decided to construct a radial array similar to those used earlier in Hollister and Pearblossom, California. The 2-color instrument is housed in a protective shelter on a hilltop approximately 1 km south of Parkfield. A combination of permanent and portable retro-reflectors are used to monitor over 20 lines that range in length from 1 to 8 kms. These reflectors provide good azimutal coverage on both sides of the San Andreas fault near the center of the expected earthquake displacement.

A field assistant measures the Parkfield array several times each week and transmits the data to both the U.S. Geological Survey and the University of Colorado. The measurements generally show a precision of 1 mm or less. We are now in the process of upgrading the 2-color instrument to allow easier operation and instant transmission of new data.

Measurements of the Parkfield array were begun late summer 1984 and have continued to the present with only minor interuptions due to electronic or laser problems and a few cases of vandalism to the reflector sites.

Figures 1 and 2 present approximately 20 months of data from 2 adjacent lines. Mid is a 5 km line that does not cross the San Andreas fault but is nearly parallel to it. Mideast is also nearly 5 km in length, however

it does cross the fault. Both lines extend from the instrument site to the northwest. The reflectors are approximately 1 km apart with the San Andreas fault between them and nearly equidistant from each of them.

The large offset in the data from Mid that occurred in early 1985 was the result of unfortunate vandalism. If that offset is removed the line length has been quite stable as might be expected since the line does not cross the fault. The creep rate on the fault is, however, substantially higher to the northwest than at the instrument site so some extension of the line to Mid might be expected.

The data from Mideast shows a very interesting episode of line-length change in 1985. The onset and termination of the episode is fairly abrupt and reminiscent of similar behavior observed near Hollister in the late 70's. The overall rate of compression on Mideast is close to that expected from other long-term data but the rate during this episode is approximately 3 times higher (3 cm/a). The extension observed on Mideast during early 1986 is very difficult to explain by any right-lateral slip on the San Andreas fault. A stress relaxation in the direction of the fault might produce such a change in line length but such a relaxation should also be apparent on Mid.

Since these 2 lines are so close to each other it is possible to remove any instrument movement by simply subtracting one of the data sets from the other. Also, because the lines are nearly equal in length, errors caused by atmospheric monitoring errors are largely removed. The difference data set is slightly different than Mideast but the episode remains very clear. The shear strain between these 2 reflectors is very high during 1985.

Long term changes are in good agreement with nearby creepmeter measurements conducted by the U.S. Geological Survey. The stability of these reflector monuments is checked periodically and appears to be good.

mid
5060.0 meters
20
0
20
change of length (mm)
6-23-84
day
4-30-86

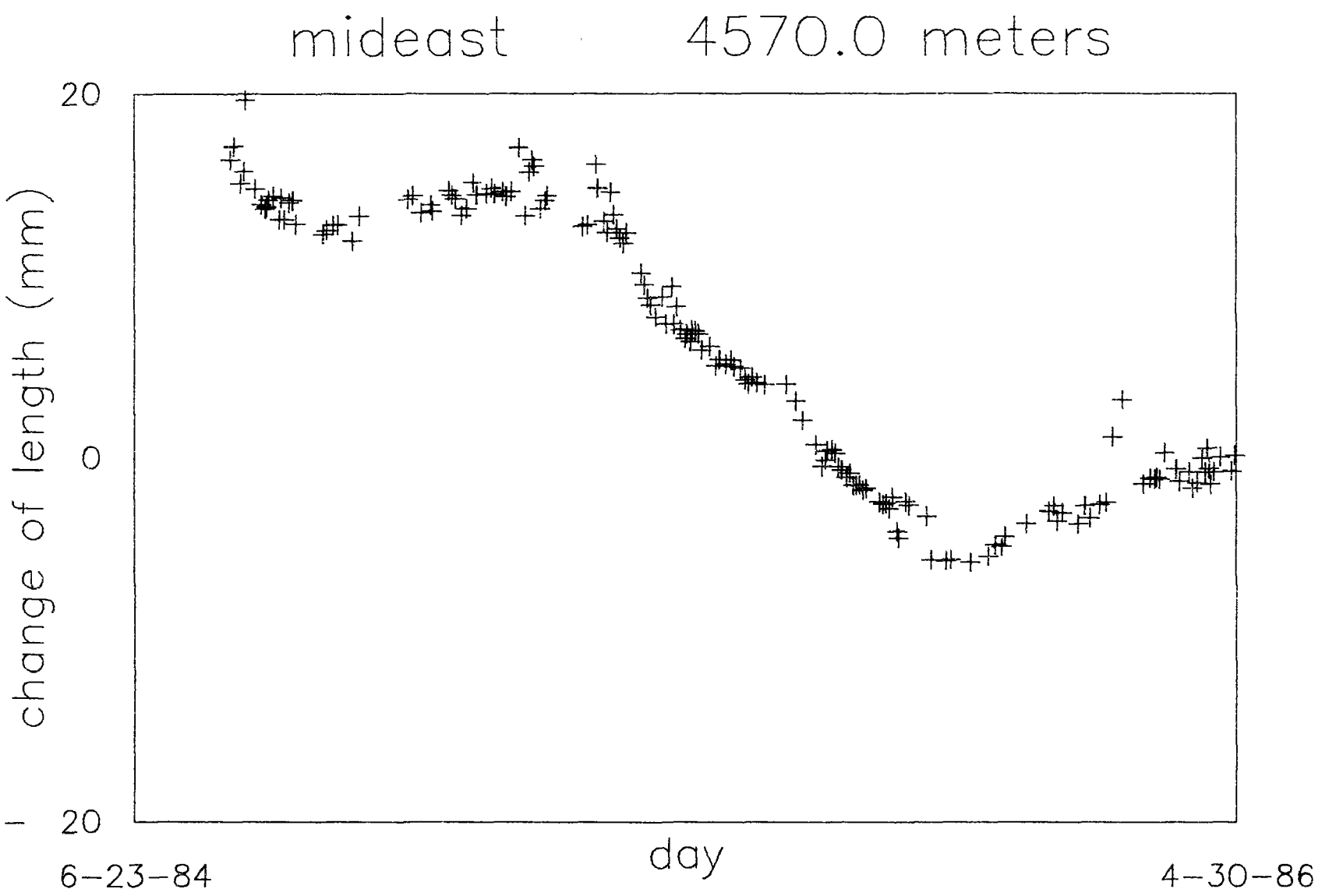
mideast 4570.0 meters
20
0
20
change of length (mm)
6-23-84
day
4-30-86

Dense Seismograph Array at Parkfield, California

9910-03974

Paul Spudich
Branch of Engineering Seismology and Geology
U.S. Geological Survey
345 Middlefield Road, MS 977
Menlo Park, California 94025
(415) 323-8111, ext. 2395

Investigations

1. Design and installation of a dense seismograph array at Parkfield.

Results

This array is a cooperative venture involving the USGS and the Electric Power Research Institute (EPRI). The array will consist of 28 surface elements and 8 downhole elements. Twenty-one of the array elements will contain both a three-component force-balance accelerometer and a three-component geophone, probably a 2 Hz L-22. The remainder will be accelerations only. The downhole elements will be buried at depths ranging from 7-1/2 to 120 m. The maximum separation between surface elements will be 3-4 km, and the minimum separation between them will be about 10 m. All elements will be connected to a local central computer facility by underground wires, and all data will be digitized using a 16-bit digitizer at 200 samples/s. The combined use of accelerometers, geophones, and 16-bit digitization will guarantee both unclipped recording of all seismic events exceeding ground noise, and good resolution of small events. We expect to make nearly complete recordings of the foreshock and aftershock sequence.

The site of the array will be on the Scobie Ranch (35° 15.5'N, 120° 16.6'W), where hard Temblor sandstone outcrops. This region is about 7 km off the San Andreas fault near the *en echelon* offset of the San Andreas in the Cholame Valley. The landowners have already given us verbal permission to install the array described herein.

The instrumental system we have chosen is rather like the ANZA seismic network (Berger and others, 1984) with wires replacing radio links between the seismographs and central recorder. Most array elements will contain a three-component accelerometer and a three-component velocity geophone. For recording the sensor outputs we have chosen a distributed-intelligence system that maximizes data capacity and reliability. Six channels of analog sensor output go into a commercially available electronics package made by Refraction Technology (Ref-tek) containing a 16-bit analog-to-digital converter (A/D), 512 Kbytes of memory for data, and an 80C86 microprocessor. These Ref-tek packages will be located at the array elements when space permits and when digital signal transmission is required to achieve acceptable signal-to-noise ratios. Otherwise, they will be located in the central computer structure. Each package does independent trigger calculations, sends trigger information to the front-end MicroVax via a local-area-network (LAN), and performs other status

checking. Data recovery by the MicroVax will be initiated when it detects a pre-defined number of triggers within a specified time window. Digital ground velocity and acceleration data packets are then transmitted to the Micro Vax via the LAN.

The primary source of reliability in this arrangement is that each Reftek package operates continuously like an independent RAM-based strong motion accelerograph. If a signal exceeding a pre-defined threshold is detected, then the field unit will store that data in RAM and not allow it to be erased until a specific command is given. This operation mode requires no telemetry.

The front-end MicroVax receives digital data blocks and trigger information from the field units via the Computrol interface. It stores data locally in the 500 Mbyte Megatape tape drive and forms disk files of the data (trigger times, time series) on the backend MicroVax II. The MicroVax boots from a hard disk, floppies, or ROM but then runs using memory only. Consequently, a disk failure will not cause a loss of data. Critical spare parts, including a Megatape drive, will be kept on site. Data/status information can be communicated to Menlo Park by satellite, microwave telemetry, or phone lines.

It is envisioned that the system described above will be operational early in 1987. The exact date is difficult to predict because it depends on several unknowns such as the time various funds become available and the equipment delivery schedules. However, to provide some form of instrumental coverage until it is operational, we will install a temporary array based on 10 portable DR-100 and 10 GEOS recorders. These recorders will all be housed in the central computer building and will be connected together to provide common time and triggering. They will be connected to surface sensors via buried analog cables.

References

Baker, J., Baker, L., Brune, J., Fletcher, J., Hanks, T., and Vernon, F., 1984, The Anza array: A high dynamic range, broadband, digitally radiotelemetered seismic array: *Bulletin, Seismological Society of America*, **74**, 1469-1481.

Reports

None.

MODELING AND MONITORING CRUSTAL DEFORMATION

9960-01488

Ross S. Stein, Wayne Thatcher
Branch of Tectonophysics
U.S. Geological Survey
345 Middlefield Road, MS/977
Menlo Park, California 94025
(415) 323-8111, ext. 2120

Investigations

1. Study of deformation accompanying and following dip-slip faulting in regions of compressional tectonics (1983 M = 6.5 Coalinga, CA, earthquake), and in regions of extensional tectonics (1983 M = 7.0 Borah Peak, ID, and 1959 M = 7.3 Hebgen Lake, MT, earthquakes).

2. Analysis of a field test to study the accumulation of refraction error in historical leveling surveys, and correction of southern California data for refraction and rod error.

Results

1a. Postseismic Deformation Associated with Large Intraplate Earthquakes

Leveling surveys carried out following the 1983 Coalinga (M_s = 6.5) and 1983 Borah Peak (M_s = 7.2) earthquakes, supplemented by less complete results from other intraplate dip-slip shocks, are used to determine the pattern and mechanism of short-term (~1 year) postseismic intraplate deformation. Movements differ notably from those observed following large plate boundary thrust events. Although the postseismic deformation is discernible, it is small, averaging only ~5% of the coseismic movements and having nearly the same spatial pattern. Clearly, such motions are best explained by continued minor slip on the same fault that ruptured during the earthquake itself. In contrast, short-term movements following intraplate thrust events are large (~20% coseismic), differ markedly from coseismic deformation, and are conveniently explained by transient slip downdip of the coseismic rupture plane. However, limited evidence from intraplate shocks indicates a temporal broadening of the movement profile, suggesting a deepening of slip or ductile deformation. Resurveys at

Coalinga and Borah Peak covering the first 2 years after the mainshock reveal modest deformation caused primarily by continued slip on the coseismic fault. The results in hand indicate significant differences between intraplate and plate boundary environments, both in the rheological properties beneath the seismogenic zone and consequently in the mechanics of strain accumulation and release in these regions. (Thatcher and Stein)

1b. Geodetic and Geologic Investigations of the Coalinga Anticline

Buried alluvial plains in the banks of Los Gatos Creek, positioned chiefly by radiocarbon dating of measured stratigraphic sections, provide structural datums as old as 2500 yr B.P. that can be traced discontinuously from synclinal Pleasant Valley to the axial part of the Coalinga anticline about 10 km downplunge from the epicenter of the M_L-6.7 earthquake of May 2, 1983. The buried plains of 2000 and 2500 yr B.P. nearly parallel the present surficial alluvial plain. If the initial profiles of the 2000- and 2500-yr-B.P. plains were parallel to the profile of the present alluvial plain, then the Coalinga anticline has probably grown no faster than 1 meter per 1000 yr during the past 2000-2500 yr. This average growth rate implies an average repeat time of at least 250 yr for major earthquakes of the late Holocene, provided that all the growth has occurred in coseismic increments of about 0.25 m, the 1983 increment suggested by geodetic leveling near Los Gatos Creek. The average growth rate could be higher and the repeat time consequently shorter if natural levees or broader depositional humps are fortuitously superposed atop structural bulges in the alluvial plains of 2000 and 2500 yr B.P. An average late-Holocene repeat time of at least 250 yr is compatible with the average Quaternary repeat time of 500-1500 yr that has been previously inferred from the maximum dip of tilted bedding in the Tulare Formation near the 1983 epicenter. Long repeat time in the Holocene is also compatible with several other lines of negative evidence that collectively argue against a high average rate of anticlinal growth during the latest Pleistocene and Holocene. For example, no conspicuous terrace higher than the presently surficial alluvial plain lines the gap through which Los Gatos Creek crosses the Coalinga anticline. If terraces were elevated at this gap during the latest Pleistocene and Holocene, perhaps they were uplifted too slowly to escape erosion by lateral stream migration. (Stein, Atwater, King, and others)

2. Saugus-Palmdale, CA, Field Test for Refraction Error in Historical Leveling Surveys

A field test was conducted in southern California during May-June 1981 to study the accumulation of unequal refraction error along a 50-km-long route rising 612 m between Saugus and Palmdale, California. The route has been leveled repeatedly since 1955, with observed elevation changes of 200 mm. The experiment was designed to compare leveling characteristic of the period before 1964 with contemporary leveling, to measure the parameters that control atmospheric refraction, and to remove the refraction error from the surveys. The observed temperature structure was well represented by a power law relation, $T = a + bz^c$, and depended on atmospheric conditions and the ground surface beneath the line of sight. The refraction-corrected leveling satisfies specifications and standards for First Order control surveys. Correction for refraction using Kukkamaki's balanced-sight equation effectively removed the observed 51 mm divergence between short- and long-sight leveling. Some simplified forms of the correction, where dT is approximated from T or the ground surface properties, perform equally well. The historical leveling surveys over the Saugus-Palmdale grade were corrected for refraction errors based on the results of the experiment, and also for rod scale errors considered in previous investigations. The corrected cumulative uplift near Palmdale reached 65 $\pm$ 16 mm with respect to Saugus during the period 1955-65. This is about one-third the value obtained before correction for refraction error. The corrected displacement profiles reveal previously unrecognized deformation in the epicentral region of the M_L = 6.4 1971 San Fernando earthquake during the decade preceeding the mainshock. (Stein, Whalen, Holdahl, Strange, and Thatcher)

Reports

Atwater, B. F., J. C. Tinsley, R. S. Stein, D. A. Trumm, A. B. Tucker, D. J. Donahue, A. J. T. Jull, L. A. Payden, 1985, Alluvial plains and earthquake recurrence at the Coalinga anticline: submitted to the U.S. Geol. Surv. Prof. Pap. on the 1983 Coalinga Earthquake, 45 pp.

Stein, R. S., 1985, Evidence for surface folding and subsurface fault slip from geodetic elevation changes associated with the 1983 Coalinga, California, Earthquake, submitted to the U.S.G.S. Professional Paper on the Coalinga Earthquake, 45 pp.

Stein, R. S., and S. E. Barrientos, 1985, Planar high-angle faulting in the Basin and Range: Geodetic analysis of the 1983 Borah Peak, Idaho, earthquake, J. Geophys. Res., v. 90, 11,355-11,366.

Stein, R. S., C. T. Whalen, S. R. Holdahl, W. E. Strange, and W. Thatcher, 1985, Saugus-Palmdale, California, field test for refraction error in historical leveling surveys, Journ. of Geophys. Res., special issue on Vertical Crustal Motions, v. 91, in press.

Stein, R. S., and R. C. Bucknam, 1986, Quake replay in the Great Basin, Natural History, v. 95 (June).

Thatcher, W., 1986, Geodetic measurement of active tectonic processes, in Active Tectonics - Impact on Society, R.E. Wallace, ed., National Research Council, Washington, D.C., 155-163.

Thatcher, W., 1986, Cyclic deformation related to great earthquakes at plate boundaries: Models and observations, Proc. Int'l Symp. on Recent Crustal Movements, Wellington, New Zealand, in press.

Abstracts

Atwater, B. F., J. C. Tinsley, R. S. Stein, D. A. Trumm, and A. B. Tucker, D. J. Donahue and A. J. T. Jull, 1985, Progress toward estimation of earthquake recurrence at Coalinga anticline, California, EOS, 66, 1093.

Stein, R. S., C. T. Whalen, S. R. Holdahl, and W. E. Strange, 1985, Saugus-Palmdale, CA field test for refraction error in historical leveling surveys, EOS, 66, 856.

Thatcher, W., and R. S. Stein, 1985, Postseismic deformation from intraplate earthquakes: Comparison with plate boundary events, EOS, 66, 1093.

NEARFIELD GEODETIC INVESTIGATIONS OF CRUSTAL MOVEMENTS, SOUTHERN CALIFORNIA

Contract No. USDI-USGS 14-08-0001-21997

Arthur G. Sylvester
Department of Geological Sciences, and
Marine Science Institute
University of California
Santa Barbara, California 93106
(805) 961-3156

INVESTIGATIONS

Repeated surveys of 24 of 45 existing precise leveling arrays across active faults were done during the contract period. Ten new arrays were established and surveyed at least twice, chiefly across the central and southern San Andreas fault, and across the San Jacinto fault. The leveling array at Pinyon Flat Geophysical Observatory was resurveyed twice, and the array at Dalton Canyon Geophysical Observatory was abandoned.

The purpose of these surveys is to search for and monitor the spatial and temporal nature of vertical displacement across active and potentially active faults. Thus, we document pre-, co- and post-seismic displacement and creep, if any, especially where seismographic, paleoseismic and geomorphic data indicate current or recent fault activity. The investigations are intermediate in scale between the infrequent, regional geodetic surveys traditionally done by the National Geodetic Survey, and point measurements by continually recording instruments such as creepmeters, tiltmeters, and strainmeters. All surveying is done according to First Order, Class II standards.

RESULTS

The principal accomplishment in 1985 was the establishment of the 10 new leveling arrays across the central and southern San Andreas fault, the northern end of the San Jacinto fault, and the western half of the Garlock fault. Each new array was resurveyed at least twice during the contract period.

Two relevelings in 1985 across the San Andreas fault in Parkfield show that the northeast fault block has continued to rise at about 3 mm/yr relative to the southwest block. The cumulative vertical separation across the fault is nearly 15 mm since 1980.

Two relevelings across the Sierra Madre fault in Arroyo Seco, Pasadena, showed that the mountain side of the fault rose 4 mm relative to the valley side during 1985 without accompanying detectable earthquake activity. The cumulative relative displacement is 15 mm since 1978.

Following the Round Valley earthquake (M 5.7) of 23 November 1984, the southwest fault block rose 2 mm relative to the northeast block across the Hilton Creek fault, 15 km west of the earthquake epicenter. A releveling in 1985 showed that the southwest block subsided 1 mm, leading to the interpretation that a strain transient passed through the array following the earthquake, similar to oscillations we have observed elsewhere following nearby earthquakes.

Newly established leveling arrays across the San Jacinto fault in San Bernardino and San Jacinto showed anomalous tilts and offsets before and after a M 5.1 earthquake on the fault on November 1, 1985. Only one survey had been done of each array prior to the earthquake, and only one survey was done in the contract period after the earthquake, so interpretation of the tilt and offset anomalies is tenuous.

The floor of a quarry near Lompoc continued to tilt at a rate of nearly 20 microradians per year in response to lithostatic rebound due to the removal of rock in the quarrying operations; however, only negligible displacement was observed across the fault in the quarry floor, and that was probably co-seismic movement related to a small earthquake in the quarry in April 1985. The total tilt of the quarry floor is well over 60 microradians since 1981.

Arrays across young fault scarps in Death Valley show continued stability to 1 ppm ever since they were established in 1970 with the exception of a single bench mark at the northeast end of the Artist's Drive array which has been rising at a rate of 0.5 mm/yr. The array was lengthened by two more bench marks to provide more control on the rising benchmark.

Resurveys of all other arrays during the 1985 contract period failed to reveal noteworthy height or tilt changes.

Earthquake Process

9930-03483

Robert L. Wesson
Branch of Seismology
U.S. Geological Survey
922 National Center
Reston, Virginia 22092
(703) 648-6785

INVESTIGATIONS

1. Analysis of theoretical and numerical models of the processes active in fault zones leading to large earthquakes.

2. Analysis of seismological and other geophysical data pertinent to understanding of the processes leading to large earthquakes.

3. Analysis of the potential for earthquakes induced by deep well injection.

RESULTS

1. The San Juan Bautista earthquake of October 3, 1972 (M_L 4.8), located along the San Andreas fault in central California, initiated an aftershock sequence characterized by a subtle, but perceptible, tendency for aftershocks to spread to the northwest and southeast along the fault zone. The apparent dimension of the aftershock zone along strike increased from about 7-10 km within a few days of the earthquake, to about 20 km 8 months later. In addition, the mainshock initiated a period of accelerated fault creep, as observed at two creepmeters situated astride the trace of the San Andreas fault within about 15 km of the hypocenter of the main shock. The creep rate gradually returned to the preearthquake rate after about 3 years. Both the spreading of the aftershocks and the rapid surface creep are interpreted as reflecting a period of rapid creep in the fault zone representing a readjustment following the failure of a "stuck" patch or asperity during the San Juan Bautista earthquake. Numerical calculations suggest that the behavior of the fault zone is consistent with that of a material characterized by a viscosity of about 3.6×10^{14} poise, although the real rheology is likely to be more complicated. In this model, the main shock represents the failure of an asperity that slips only during earthquakes. Aftershocks represent the failure of second order asperties which are dragged along by the creeping fault zone.

2. On January 31, 1986, at 11:46 EST an earthquake of magnitude 4.9-5.0 occurred about 40 km east of Cleveland, Ohio, and about 17-18 km south of the Perry Nuclear Power Plant. The earthquake was felt over a broad area including 11 states, the District of Columbia, and parts of Ontario, Canada, caused intensity VI-VII at distances of 15 km, and generated relatively high accelerations (0.18 g) of short duration at the plant. Twelve aftershocks were detected as of April 15, 1986, with most

occurring within the first 14 days. The latest was on March 24, 1986. Two of the aftershocks were felt. Coda magnitudes for the aftershocks ranged from -0.5 to 2.5. Focal depths for all the earthquakes range from 3 to 7 km.

One aspect of this sequence was the possibility that the recent earthquakes were induced by deep injection well activities. Three wells are currently operating within 15 km of the earthquakes and there was concern expressed that the wells may have played a substantial role in triggering the earthquake activity.

At present, the analysis of available stress measurements seems to indicate that the state of stress in northeastern Ohio is close to the theoretical threshold for small earthquakes as predicted by the Mohr-Coulomb failure criterion. This should not be surprising given the history of small earthquakes in the region.

Although given the present state of stress, triggering of small earthquakes by fluid injection would not be surprising, the distance of the January 31, 1986 earthquake and its aftershocks from the wells (with the possible exception of the very small earthquake on March 12, 1986), the lack of any small earthquakes near the bottom of the wells, the history of small earthquakes in the region prior to the initiation of injection, and the attenuation of the pressure field with distance from the injection wells, all argue for a "natural" origin for the earthquake. Therefore, although triggering remains a possibility, the probability that the injection played a significant role in triggering the earthquake, based on the information currently available, must be regarded as low. The analysis of the possible relation between the injection wells and the January 31, 1986, earthquake has indicated nothing to suggest than an earthquake larger than that expected for the broad region should be expected near the injection wells.

REPORTS

Wesson, R. L., Modelling aftershock migration and afterslip of the San Juan Bautista earthquake of October 3, 1972, Tectonophysics, in press.

Wesson, R. L., Modelling surface fault creep events (abstract), Earthquake Notes, v. 57, p. 11, 1986.

Wesson, R. L. (editor), Studies of the January 31, 1986, northeastern Ohio earthquake, U.S. Geological Survey Open-File Report (in press).

ROCK MECHANICS

9960-01179

James Byerlee
U.S. Geological Survey
Branch of Tectonophysics
345 Middlefield Road, MS/977
Menlo Park, California 94025
(415) 323-8111, ext. 2453

Investigations

Laboratory experiments are being carried out to study the physical properties of rocks at elevated confining pressure, pore pressure and temperature. The goal is to obtain data that will help us to determine what causes earthquakes and whether we can predict or control them.

Results

As part of the cooperative program of earthquake research between the U.S. Geological Survey and the People's Republic of China, we have been carrying out laboratory experiments to determine the friction and fluid flow properties of a variety of fault gouges to get a better understanding of the rheological properties of fault zones in the deep crust. Our present results show that (1) at a given temperature, the phyllosilicate-rich gouges show a greater tendency to stick-slip and also larger stress drops in experiments run at the lower of 2 confining pressures. (2) At a given confining pressure the phyllosilicate-rich gouges show a greater tendency to stick-slip with increasing temperature. (3) Granite gouges show only stable sliding at all the temperatures and confining pressure investigated. (4) Phyllosilicate-rich gouges support higher stress levels with increasing temperature and decreased strain rate. (5) The granite gouge showed no variations in frictional strength with temperature or strain-rate. Thus, our results indicate that fault zones containing a larger percentage of phyllosilicates will behave quite differently than if the gouge is composed of crushed framework silicates in or below the crust where the temperature is greater than 200°C.

Reports

Byerlee, J., C. Morrow, D. Moore, Ma Jin, Liang Shi, Zhang, Bo-Chong, 1985, Laboratory studies of the rheological properties of fault zones, E.O.S. Trans. Am. Geophys. Union, v. 66, No. 46, p. 1060.

Lockner, D., J. Byerlee, 1985, A case for displacement dependent instabilities in rock, E.O.S. Trans. Am. Geophys. Union, v. 66, No. 46, p. 1100.

Moore, D., J. Byerlee, 1985, Deformation textures developed in heated fault gouge, E.O.S. Trans. Am. Geophys. Union, v. 66, No. 46, p. 1100.

Morrow, C., J. Byerlee, 1985, A physical explanation for transient stress behavior during shearing of fault gouge at variable strain rates, E.O.S. Trans. Am. Geophys. Union, v. 66, No. 46, p. 1100.

Summers, R., D. Lockner, J. Byerlee, 1985, Temperature and velocity dependence of friction in granite, E.O.S. Trans. Am. Geophys. Union, v. 66, No. 46, p.1100.

PERMEABILITY OF FAULT ZONES

9960-02733

James Byerlee
Branch of Tectonophysics
U.S. Geological Survey
345 Middlefield Road, MS/977
Menlo Park, California 94025
(415) 323-8111, ext. 2453

Investigations

Laboratory studies of the permeability of rocks and gouge are carried out to provide information that will assist us in evaluating whether in a given region fluid can migrate to a sufficient depth during the lifetime of a reservoir to trigger a destructive earthquake. The results of the studies also have application in the solution of problems that arise in nuclear waste disposal.

Results

The permeability of Westerly Granite decreased by a factor of 25 during a 2-week experiment in which a heated, aqueous fluid was passed down a temperature gradient through the rock. Conditions of the experiment were: confining pressure = 60 MPa, pore water pressure = 20 MPa, pore pressure difference = 1 MPa, temperature range = 300-92°C. The altered, experimental sample was examined using scanning electron microscopy and compared with the starting material: (1) about half of the grain boundaries in the starting material that involve quartz are cracked, as are most such grain boundaries in the altered sample; (2) grain boundaries between feldspars are closed in both the starting material and the altered sample; (3) intragrain cracks occur in feldspar and quartz in both samples; (4) both intragrain and grain boundary cracks contain a platy Si-rich filling near the low-temperature edge of the sample and massive fillings that are both Ca-rich and Si-rich in the high-temperature region. Utilizing a rate equation for precipitation and dissolution of quartz, we have calculated the reduction or porosity that would be expected from dissolution and homogeneous reprecipitation of quartz as the fluid moved through the sample. Based on these calculations, the maximum porosity reduction is 8% which corresponds to a 22% reduction in permeability. The observed reduction was 96% of the initial value, indicating that other processes contributed to the permeability reduction. Two such processes are non-homogeneous precipitation and crack healing.

Reports

Moore, D., Morrow, C., Byerlee, J., 1986, High temperature permeability and ground water chemistry of some Nevada Test Site tuffs, J. Geophys. Res., v. 91, No. B2,pp. 2163-2171.

Morrow, C., Bo-Chong, Zhang, Byerlee, J., 1986, The effective pressure law for the permeability of Westerly granite under cyclic loading, J. Geophys. Res., v. 91, No. B3, pp. 3870-3876.

Mechanics of Earthquake Faulting

9960-01182

James H. Dieterich
U.S. Geological Survey
Branch of Tectonophysics
345 Middlefield Road, MS/977
Menlo Park, California 94025
415-323-8111, ext. 2573

Investigations

Constitutive Properties of Faults with Variable Normal Stress

Work continued on the experimental measurement of fault constitutive properties under conditions in which normal stress is independently varied during slip. The goal of this study is to develop a more general formulation for rate- and state-variable fault constitutive laws which currently assume constant normal stress.

Nucleation and Triggering of Earthquake Slip

Analysis and modeling of the processes associated with the nucleation and triggering of earthquake slip was continued. Emphasis was given to further development of analytic solutions that permit simple calculations for earthquake potential under time varying stress conditions.

Deformation Mechanics of Active Volcanoes

Models for the growth and persistence of Hawaiian volcanic rifts were developed. The problem is important to the understanding of large earthquakes on Kilauea and Mauna Loa volcanoes.

Modeling of Dynamically Propagating Ruptures with Rate- and State-Dependent Friction

Paul Okubo implemented a rate- and state-dependent fault constitutive relation into a dynamically propagating fault rupture calculation. The constitutive formulation used for the calculations is based on earlier experimental results and direct observation of dynamically propagating ruptures from large scale laboratory faulting experiments.

Results

Constitutive Properties of Faults with Variable Normal Stress

Mark Linker completed necessary equipment modifications to conduct fault slip tests with continuous high speed servo-control of normal stress and slip rates. Tests show that normal stress history has an important effect on the state variable employed to represent sliding history effects. Following a change in normal stress, the return of fault friction to steady state conditions is governed by a characteristic sliding distance comparable to that observed in slip speed stepping experiments. An effect previously reported by Bruce Hobbs of CSIRO, Australia indicating an instantaneous but transient decrease in strength at the time of an increase in normal stress could not be verified by our experiments.

Nucleation and Triggering of Earthquake Slip

No new results to report.

Deformation Mechanics of Active Volcanoes

Models for the processes governing the growth and persistence of Hawaiian rifts have been examined and the results are currently being prepared for publication. Hawaiian volcanic rifts are characterized by long-term persistence and cumulative dike injection widths on the order of a kilometer or more. To account for these characteristics, processes permitting the expansion of the rifts and for continued existence of dike trapping stresses must operate. Analyses of a variety of models indicate that faulting of the type that occurred during the 1975 Kalapana earthquake can operate to permit rift expansion and to preserve the trapping stresses that guide the dikes into the rift zones. Analysis of previously proposed models based on gravity loading alone or shallow gravity sliding of the flanks appear incapable of permitting the apparent persistence of the rift zones.

Modeling of Dynamically Propagating Ruptures with Rate- and State-Dependent Friction

Numerical modeling of dynamic crack growth governed by the state-variable fault friction model was done with a boundary integral solution method. Tests were performed to compare the results using state-variable fault strength with results from simple slip weakening models and to evaluate the effects of initial conditions in governing

rupture propagation. For both classes of models characteristics of the rupture propagation are governed by the fault strength parameter $S = (\tau_p - \tau_o)/(\tau_o - \tau_r)$, where τ_o, τ_p and τ_r are the initial, peak and final shear stresses, respectively. Over a range of values for S the state-variable calculations are consistent with the slip-weakening calculations in that both predict an unstable jump from propagation at the Rayleigh wave speed to the shear wave speed and then smooth propagation to the P-wave speed. However, the unstable transition in rupture speed occurs at shorter fault propagation distances in the state-variable model. This occurs because the state-variable model permits fault slip to occur at stresses below the peak yield stress level. The effect of varying prestress over the entire rupture surface are also qualitatively similar in these calculations. For smaller values of S the transition occurs at shorter distances from the rupture nucleation. In the state-variable model both the initial fault creep rate and the state-variable must be specified to set a value for S. Tests were carried out that demonstrate that rupture growth calculated for one initial rate and state condition can be matched by a different initial rate and state condition if the value of the parameter of S is preserved.

Reports

Dieterich, J. H., 1986, A Model for the Nucleation of Earthquake Slip, accepted and in press: Proceedings Volume Ewing Symposium on Earthquake Mechanics, 26 p.

Dieterich, J. H., 1986, Nucleation and Triggering of Earthquake Slip: Effect on Periodic Stresses, submitted to Tectonophysics, 21 p.

Okubo, P. G., 1986, Experimental and Numerical Model Studies of Frictional Instability Seismic Sources, Ph.D. Thesis, Massachusetts Institute of Technology, 162 p.

Okubo, P. G., and Dieterich, J. H., 1986, Constitutive Relations for Dynamic Fault Slip, accepted and in press: Proceedings Volume Ewing Symposium on Earthquake Mechanics, 16 p.

In Situ Stress Measurements

9960-01184

John Healy
Branch of Tectonophysics
U.S. Geological Survey
345 Middlefield Road, MS/977
Menlo Park, California 94025
415-323-8111, ext. 2535

Investigations and Results

An important part of our work during this reporting period has been the effort devoted toward the improvement of our packer systems that we use for stress measurements. We have concentrated on two major areas of improvement: the development of a reliable resettable packer system and the development of a packer system that will contain high pressures in the isolated interval. We have been working on this problem with TAM International, a packer manufacturer from Houston, Texas. We have achieved interval pressures in excess of 7,500 psi using a 5-1/2" packer in a 7" test hole and we have developed an adequately reliable resettable mechanism which was tested in our measurements at Black Butte and Cajon Pass.

An earlier measurement program in the Black Butte hole was terminated due to lack of funds, so we returned to complete the stress measurements at that site. The Black Butte site was chosen to fill in data on a profile of stress measurements perpendicular to the San Andreas fault. It was anticipated that this data point would confirm early interpretations about the variation of stress with distance from the fault. The Black Butte measurements, which are of high quality, are completely different in both magnitude and direction of stress. The measurements indicate that Black Butte is close to a state of incipient thrust faulting in a direction that is not consistent with the regional stress field. We believe that these data have important implications about the nature of observed stresses and we are working on the interpretation of these data.

During the reporting period we made a series of measurements in the Cajon Pass drill hole. The primary purpose of these measurements was to obtain data that would help us estimate the stress and temperature that will be encountered to 5 km. The temperature gradient that was observed in this hole was high and indicates that packer systems and other electronic

equipment used in the deep hole will have to withstand temperatures in the neighborhood of 200°C. The stress regime observed in the existing drill hole that extends to a depth of 5,800' suggests that the rocks are in a state of incipient normal faulting. Some observers might take these observations in conjunction with our measurements at Black Butte, suggesting that stress is a capricious quantity and, at least as measured in shallow holes, not indicative of major tectonic processes. We believe that this view is incorrect. The stress field we observe is not explainable in terms of simplistic elastic models. We believe there are a number of straightforward and relatively simple explanations that can account for these observations. We think that an important step in understanding the distribution of stress is the development of a better model to describe the rheology of granitic rocks. We think that our data provide conclusive evidence that a purely elastic model cannot be used to explain the observations. We also believe that the data suggest that the details of local geology are important in understanding the observations. We think it is premature to propose an explanation for the limited data available, but the observations illustrate the critical importance of obtaining data from deep holes.

We have completed the digital recording system to measure water level with high accuracy and have installed this system and are now recording data in the Hi Vista well. The system is relatively inexpensive and consists of Hewlett-Packard packers and electronics, and we believe it will be very useful in making observations in the future. We propose to use this system in China as part of the earthquake prediction program there.

We worked with Tom McEvilly at U.C. Berkeley and Peter Leary at the University of Southern California to conduct a VSP survey in the Hi Vista hole. Tom McEvilly provided both a large stress wave vibrator, a P-wave vibrator, and his new VSP recording system. Peter Leary provided USC's downhole seismometer and clamping system. The main purpose of this survey was to test Stewart Crampin's proposal that shear waves will be polarized along the direction of principal stress. Hi Vista is a hole drilled at a site where we have data on both stress magnitude and direction, as well as data on P-wave anisotropy from a special seismic refraction experiment. The VSP survey was very successful and the data are being interpreted by the Berkeley group.

Jack Healy has been working with a number of colleagues on a paper describing the seismic structure of the lower crust and the implications of high fluid pressure in the crust. A review of the seismic refraction or reflection data that is now available in large quantities strongly suggests that properties of

the lower crust are distinctly different in most areas from those of the upper or granitic crust. One possible explanation for this difference might be the state of fluid pressure in the lower crust as opposed to the fluid pressure in the upper crust. We have worked with John Bredehoeft and Claus Prodehl to try to provide some synthesis on the available data to provide a theory that would help us evaluate the physical properties and composition of the lower rocks. If it turns out that the lower crustal rocks are in fact different from the upper crustal rocks, then it seems appropriate to reevaluate and resurrect the term "Conrad discontinuity" because of its historical significance as the boundary between the upper "granitic" crust and the lower "basaltic" crust. This is an extremely broad topic in geological and geophysical literature and we are currently trying to prepare a paper on the Conrad discontinuity as a way of subdividing this task and describing the available evidence in an orderly fashion.

We are working with the borehole geophysical group at Stanford to develop new techniques to analyze new data. Jim Springer has completed digitization of our televiewer records in the Cajon Pass drill hole and is preparing a paper on these data for presentation at the next AGU meeting. Steve Hickman digitized some of the televiewer records from the Crystallaire hole and with the aid of the new techniques found new breakouts in this hole which give us important new information on the stress direction at this site.

We are continuing work at the nuclear waste disposal site and hope to make additional measurements there during this fiscal year. We have selected two sites in Crater Flat and are currently trying to obtain access to previously drilled holes VH1 and VH2. A major part of our effort in this program is the development of the packer systems described above and the work on improving our quality assurance procedures which is required for all projects in this program. We are making good progress in these areas and anticipate completion of all required quality assurance in the near future.

We are working closely with Ken Fox in Denver in preparation of long-term plans for determining the regional stress field in the vicinity of Yucca Mountain. We are proposing that measurements be made at 20 sites in holes drilled specifically for the measurement of stress. We envision a three-year program with most of the measurements being completed in the first two years. In an effort to search for suitable off-site drill holes we have logged a number of holes drilled by a mining company in their exploration program. The results of this search have not been successful but we will continue to try to find or use any hole that becomes available to use.

Reports

Healy, J. H. and Urban, T. C., 1985, In situ fluid pressure measurements for earthquake prediction: an example from a deep well at Hi Vista, California, Pure and Applied Geophysics, v. 122, p. 255-279.

Healy, J. H. and Zoback, M. D., 1986, In-situ stress measurements at Cajon Pass (abs.): EOS, Transactions of the American Geophysical Union, v. 67, no. 16, p. 380.

Mooney, W. D., Gettings, M. E., Blank, H. R., and Healy, J. H., 1985, Saudi Arabian seismic-refraction profile: A travel-time interpretation of crustal and up mantle structure: Tectonophysics, v. 111, p. 173-246.

Springer, J. E., Barton, C., and Zoback, M. D., 1986, Natural fracture distribution and drilling-induced borehole elongation in the Cajon Pass well, California (abs.): EOS, Transactions of the American Geophysical Union, v. 67, no. 16, p. 380.

Stierman, D. J. and Healy, J. H., 1985, A study of the depth of weathering and its relationship to the mechanical properties of near-surface rocks in the Mohave Desert: Pure and Applied Geophysics, v. 122.

Stierman, D. J., 1986, Effective stress and the water table in fractured granitic rocks (abs.), EOS, Transactions of the American Geophysical Union, v. 67, no. 16, p. 373.

Stock, J. M. and Healy, J. H., 1984, Magnitudes and orientations of stress in an extensional regime, Yucca Mountain, Nevada, GSA Abstracts with Programs, v. 16, no. 6.

Stock, J. M., Healy, J. H., Hickman, S. H. and Zoback, M. D., 1985, Hydraulic fracturing stress measurements at Yucca Mountain, Nevada, and relationship to the regional stress field, Journal of Geophysical Research, v. 90, no. B10, p. 8691-8706.

Stock, J. H., Healy, J. H. and Svitek, J., 1986, Hydraulic fracturing stress measurements at Black Butte, Mojave Desert, CA (abs.), EOS, Transactions of the American Geophysical Union, v. 67, no. 16, p. 382.

Stock, J. M., Healy, J. H., Svitek, J., and Mastin, L., 1984, Report on televiewer log and stress measurements in holes USW G-3 and UE-25P#1, Yucca Mountain, Nevada Test Site, U.S. Geological Survey Open File Report.

Svitek, J. F., Healy, J. H., and Stokely, C. O., 1986, Testing packers for stress measurements in deep boreholes (abs.), EOS, Transactions of the American Geophysical Union, v. 67, no. 16, p. 382.

Zoback, M. D. and Healy, J. H., 1984, Friction, faulting, and in-situ stress, Annales Geophysicae, v. 2, no. 6, p. 689-698.

Constitutive Relations for Frictional Rock Sliding and Computer Modelling of the Elastic-Sliding Interactive System

14-08-001-G1191

Bruce E. Hobbs
CSIRO Division of Geomechanics
Box 54, Mt. Waverley, 3149
Australia
(03) 235-1355

Objective: This project is aimed at (i) generalizing the constitutive relations for frictional sliding already developed by Dieterich (1979, 1981) and Ruina (1980, 1983) by including a dependence upon normal stress and at (ii) modelling the interaction between constitutive behavior of the fault and the elastic response of the surrounding rocks using hybrid distinct element-boundary element codes.

Experimental Studies: The past six months have been spent in tuning up the large capacity shear frame shown in Figure 1. This frame is designed to apply shear loads across rock samples with a maximum surface area of 250 mm by 500 mm. The normal and shear forces of up to 880 KN are supplied by two bi-directional load actuators under hydraulic pressure and control is provided by two MTS servo-control units. We have installed two new load cells immediately adjacent to the specimen to measure normal and shear loads close to the specimen. Experiments can be conducted with servo-control on any of the four parameters: sliding velocity, normal displacement, normal force or shear force (all measured at the specimen). Data acquisition is by a newly installed HP320 computer with a HP 3852A data acquisition system; this gives us data acquisition rates of 150 KHz on 20 switched channels. The HP 320 computer will also be used for control purposes. The apparatus is being used to examine the response of shear stress to changes in normal stress at constant sliding velocity.

Modelling Studies: The single degree of freedom spring-slider system with one and two state variable constitutive laws has been modelled using a distinct element method described initially by Cundall (1971, 1974). This work is similar to that described by Rice and Tse (1986) where the analysis considers the non-linear description of motion and includes the effects of inertia by defining two time scales: an inertial time scale and a state relaxation time scale. In such a scheme, numerical efficiency is achieved by solving the full equations for inertia and state relaxation only in a transit region where both time scales are significant. The present work adopts a different approach which results in great computational efficiency whilst always considering the full non-linear problem with inertia. Some results are shown in Figure 2 for the problem parameters given in Table 1. Figure 2 shows a sequence of shear stress response curves resulting from a slight velocity perturbation. Figure 2a shows a system for which the spring constant is slightly above critical whilst Figures 2b, c, d, e all have spring constants less than critical and progressively decreasing in value. Figure 2e shows true stick-slip behavior with the spring constant, k, defined as shown, as indicated by Rice and Tse (1986). This work is being extended to examine the development of chaotic motion in systems with two state variable constitutive laws. The work forms the basis for modelling fault systems embedded in a jointed medium.

References:

P.A. Cundall. A computer model for simulating progressive large scale movements in blocky rock systems. Proceedings of the Symposium of the International Society of Rock Mechanics, (Nancy, France, 1971), Vol. 1, Paper No. II-8, 1971.

P.A. Cundall. Rational design of tunnel supports: A computer model for rock mass behavior using interactive graphics for the input and output of geometrical data, Tech. Report MRD-2074, Missouri River Division, U.S. Army Corps of Engineers, 1974; NTIS Report No. AD/A-001 602, 1974.

J.H. Dieterich. Modelling of rock friction, 1, Experimental results and constitutive equations, J. Geophys. Res., 84, 2161-2168, (1979).

J.H. Dieterich. Constitutive properties of faults with simulated gouge. In Mechanical Behavior of Crustal Rock, Vol. 24, pp. 103-120. Geophysical Union Monograph, 1981.

R.R. Rice and S.T. Tse. Dynamic motion of a single degree of freedom system following a rate and state dependent friction law. J. Geophys. Res., 91, 521-530, 1986.

A.L. Ruina. Friction laws and instabilities: A quasi-static analysis of some dry frictional behavior. Ph.D. Thesis, Division of Engineering, Brown University, 1980.

A.L. Ruina. Slip instability and state variable friction laws, J. Geophys. Res., 88, 10359-10270, 1983.

Table 1

Problem parameters used in verification study of single-state variable friction law (see Ruina, 1983; Rice and Tse, 1985)

σ_n = 73.36 MPa

τ = 0.6 σ_n

A = 0.69 MPa

B = 1.38 MPa

L = 1.35 μm

V_* = 1.91 μms^{-1}

V_o = 1.62 to 2.03 μms^{-1}

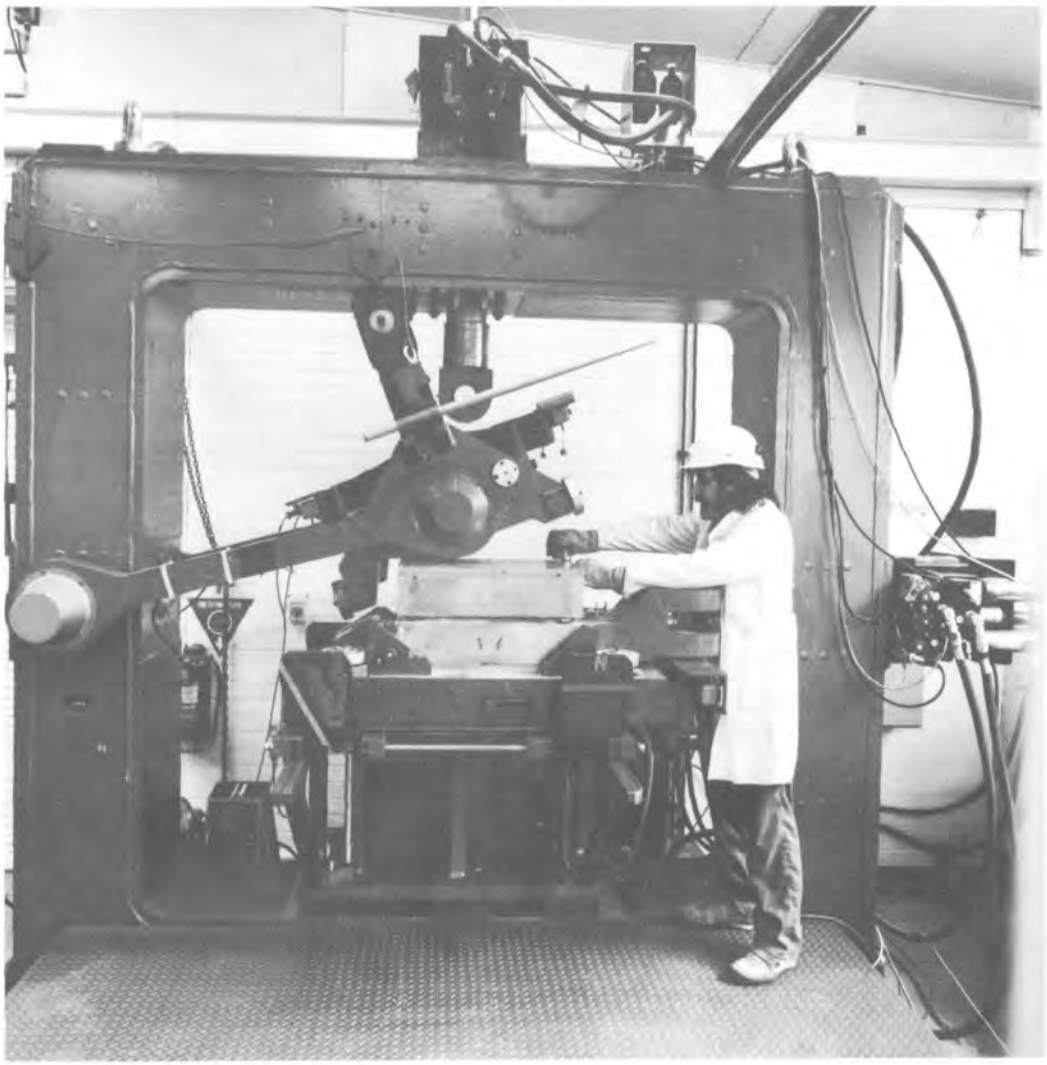

Figure 1: Large capacity shear frame. The 880 KN servo-controlled actuators can be seen at the top and far right of the frame. The arm which supplies the horizontal reaction is shown in raised position to expose the two steel boxes which house the rock specimens encased in plaster.

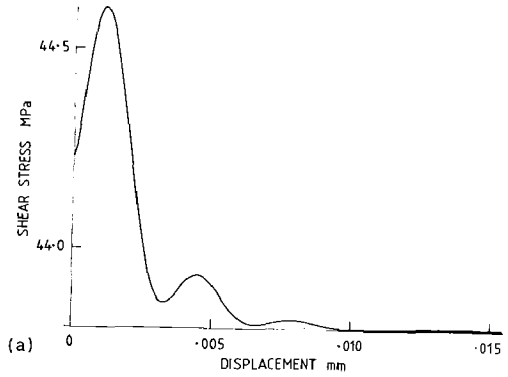

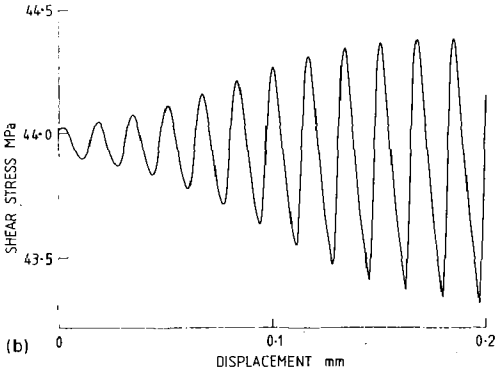

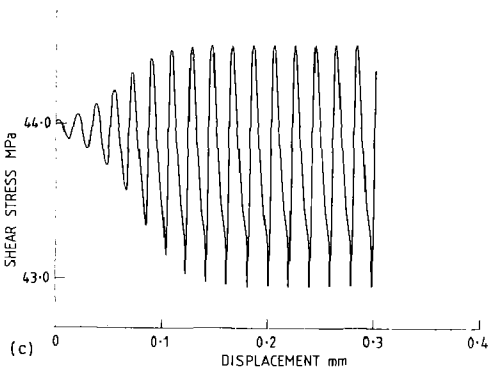

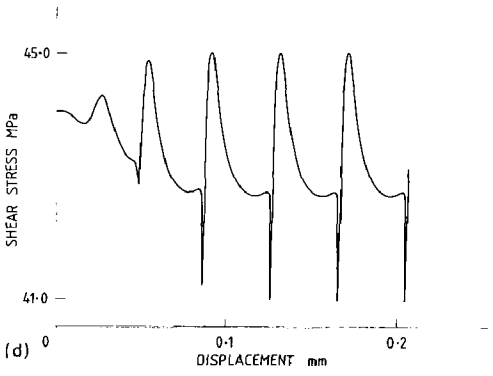

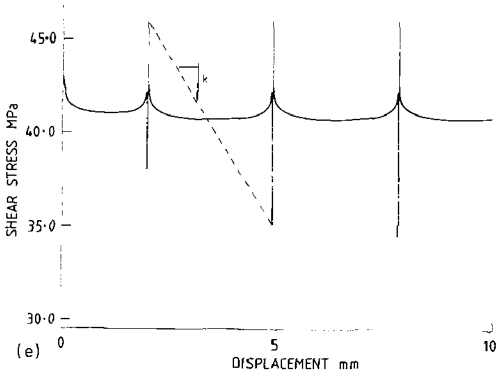

Figure 2: Some representative stress-displacement curves following load point velocity jump perturbations. (a) is for spring stiffness k > critical spring stiffness k_{cr}. (b), (c), (d), (e) are for k < k_{cr} and for k progressively decreasing in magnitude.

Earthquakes and the Statistics of Crustal Heterogeneity

9930-03008

Bruce R. Julian

Branch of Seismology
U.S. Geological Survey
345 Middlefield Road - MS77
Menlo Park, California 94025
(415) 323-8111 ext. 2931

Investigations

Both the initiation and the stopping of earthquake ruptures are controlled by spatial heterogeneity of the mechanical properties and stress within the earth. Ruptures begin at points where the stress exceeds the strength of the rocks, and propagate until an extended region ("asperity") where the strength exceeds the pre-stress is able to stop rupture growth. The rupture termination process has the greater potential for earthquake prediction, because it controls earthquake size and because it involves a larger, and thus more easily studied, volume within the earth. Knowledge of the distribution of mechanical properties and the stress orientation and magnitude may enable one to anticipate conditions favoring extended rupture propagation. For instance, changes in the slope of the earthquake frequency-magnitude curve ("b-slope"), which have been suggested to be earthquake precursors and which often occur at the time of large earthquakes, are probably caused by an interaction between the stress field and the distribution of heterogeneities within the earth.

The purpose of this project is to develop techniques for determining the small-scale distributions of stress and mechanical properties in the earth. The distributions of elastic moduli and density are the easiest things to determine, using scattered seismic waves. Earthquake mechanisms can be used to infer stress orientation, but with a larger degree of non-uniqueness. Some important questions to be answered are:

** How strong are the heterogeneities as functions of length scale?

** How do the length scales vary with direction?

** What statistical correlations exist between heterogeneities of different parameters?

** How do the heterogeneities vary with depth and from region to region?

Scattered seismic waves provide the best data bearing on these questions. They can be used to determine the three-dimensional spatial power spectra and cross-spectra of heterogeneities in elastic moduli and density in regions from which scattering can be observed. The observations must, however, be made with seismometer arrays to enable propagation direction to be determined. Three-component observations would also be helpful for identifying and separating different wave types and modes of propagation.

The stress within the crust is more difficult to study. Direct observations require deep boreholes and are much too expensive to be practical for mapping small-scale variations. Earthquake mechanisms, on the other hand, are easily studied and reflect the stress orientation and, less directly, its magnitude, but are often not uniquely determined by available data.

This investigation uses earthquake mechanisms and the scattering of seismic waves as tools for studying crustal heterogeneity.

Results

Stress field and tensile crack instability near a magma chamber

In the last semiannual report, we reported work in progress to combine published mathematical results to model the stress field around a cylindrical magma chamber. This work is now complete, and includes the effects of: (1) gravity acting on the density contrast between the magma and the country rocks; (2) excess pressure in the magma; and (3) tectonic stress. We are planning to use this result to refine previous results on unstable propagation of tensile cracks, which had been based on the much simpler (but less realistic) stress field due to pressure and remotely applied stress in an infinite, non-gravitating medium. These previous results show that catastrophic propagation of tensile cracks, causing earthquakes, is possible in the upper crust, but the predicted rupture dimensions are too small to explain the largest recent earthquakes at Long Valley caldera. Using the more realistic stress field will probably have the effect of increasing the predicted size of earthquakes.

Determination of earthquake source mechanisms

It has been suggested that the non-double-couple mechanisms of some of the large earthquakes near Long Valley caldera can be explained by catastrophic tensile failure caused by high fluid pressure. An unresolved problem is whether any of the smaller earthquakes have similar unusual mechanisms. It has proven impossible to answer this question using only P-wave first motions recorded by the current seismograph network in the area; these data allow (but do not require) most earthquake mechanisms to have significant non-double-couple components. To obtain more powerful constraints on this question, we have extended the computer program that determines seismic focal mechanisms by linear-programming methods so that it can handle amplitude data, in addition to first motions. The program now can analyze inequality constraints involving seismic-wave amplitudes, so that, for example, upper and lower bounds on the amplitudes may be treated. In addition, we have written a suite of related programs for focal-sphere plotting of first motions and focal mechanisms, computing the moment tensor of a general specified mechanism, and decomposing derived mechanisms into volumetric, double-couple and CLVD components. We plan to use the inversion program to analyze a suite of well recorded earthquakes, and, if necessary, to extend the program further to treat amplitudes of known magnitude but unknown sign, and amplitude ratios.

Mechanism of volcanic tremor

We have continued investigations on modeling volcanic tremor as a flow-induced vibration of the walls of cracks transporting magma. In particular, we have obtained a system of algebraic equations that can be used to predict the approximate amplitude and frequency of tremor as functions of magma viscosity, crack dimensions, and driving pressure. These equations must be solved numerically, but this is far

easier than integrating the differential equations of motion numerically. We are presently analyzing data to test whether the amplitude-frequency behavior of tremor agrees with the predictions of the theory.

Long Valley caldera dilatometer

In order to gather data on the earthquake mechanisms at Long Valley caldera, the USGS installed a Sacks-Evertson dilatometer in the autumn of 1983 near the Devil's Postpile, about 3 km southwest of the caldera. Since September, 1984, both low- and high- frequency data have been telemetered to Menlo Park. About 21 months of low-frequency data have now been collected. The average secular strain rate during this interval has been high, about 9 parts per million per year, although comparable rates attributed to processes in or near the borehole have been observed at other dilatometers in California. The signal thus may contain a large component of geophysical origin. If so, the cause must be within a few kilometers of the instrument, and probably at depths of less than about 3 kilometers. The observed strain rate was very high (about 20 to 40 microstrain per year) during the spring season of 1985, and then dropped to nearly zero during the summer. A similar high rate has been observed during the spring of 1986. If the rate decreases again during the summer it will suggest that these unusual changes are an annual phenomenon, possibly related to hydrological processes.

Reports

Chouet, Bernard, and Julian, Bruce R., 1985, Dynamics of an expanding fluid-filled crack: J. Geophys. Res., v. 90, no. B13, pp. 11,187-11,198.

Julian, Bruce R., 1986, Analysing seismic-source mechanisms by linear-programming methods: Geophys. J. R. Astron. Soc., v. 84, pp. 431-443.

Julian, Bruce R., and Sammis, Charles G., 1985, Instabilities in the propagation of tensile cracks (abs): EOS Trans. AGU, V. 66, no. 46, p. 1065.

Julian, Bruce R., and Sipkin, Stuart A., 1985, Earthquake processes in the Long Valley caldera area, California: J. Geophys. Res., v. 90, no. B13, p. 11,155-11,169.

Experimental Rock Mechanics

9960-01180

Stephen H. Kirby
Branch of Tectonophysics
U.S. Geological Survey, MS/977
345 Middlefield Road
Menlo Park, California 94025
(415) 323-8111, Ext. 2872

Investigations

1. Effects of polymorphic phase transformations on mechanical instabilities and strain localization in shear zones.

2. Physical mechanisms of deep earthquakes.

3. Deep aseismic fault zones, as revealed by the study of xenoliths brought up by basalts along major intraplate fault zones.

Results

1. John Pinkston has confirmed the large effect of trace concentrations (~0.2%) of hydrous minerals on reducing the frictional strength of Harbison-Walker dunite at 400°C and confining pressures up to 700 MPa. Prior heat treatment at 600°C greatly strengthens this rock. Laura Stern has studied the prograde metamorphic reactions by heating experiments on a low density mineral separate and doing subsequent powder X-ray mineral identification. The initial alteration assemblage is serpentine (lizardite), talc, tremolite and chlorite. Heat treatment to 600°C removes all serpentine and chlorite. By 900°C, virtually all traces of hydrous phases disappear. The strengthening by prior heat treatment at 600°C appears to correlate with the loss of serpentine and possibly chlorite along grain boundaries. To our knowledge, this is the first study that shows a significant weakening effect of hydrous alteration (retrograde) metamorphic reactions and this has implications for the rheologies of shear zones in the upper 20-30 km of the lithosphere.

2. Kirby and Art McGarr organized the first AGU special session on Deep Earthquakes, Polymorphic Phase Changes and the Mechanics of Deep Subduction held in December 1985 at the Fall Annual Meeting. The important connection between phase transitions and deep earthquakes was emphasized and Kirby reported the discovery of a new form of high-pressure

faulting found in experiments on materials that are deformed in the stability field of high pressure phases. It was emphasized that localized phase changes under metastable conditions may apply to the instabilities leading to deep earthquakes.

3. The mylonitic peridotite xenoliths of NE China are being studied by Kirby, B. C. Hearn (USGS, Reston) and He Yongnian and Lin Chuanyong (State Seismological Bureau, Beijing, China). Our preliminary investigation confirms the high-stress, high-strain and strain-rate origin of these rocks and points to their being samples of the aseismic shear zone that is the deep counterpart of the seismically active Tancheng Lujiang rift zone. Quantitative estimates of in-situ pressure, temperature and tectonic stress are being pursued based on mineral chemistry and rock textures.

Reports

Kirby, S. H., 1985b, Localized polymorphic phase transformations as mechanisms for deep earthquakes: Trans. Am. Geophys. Union, v. 66, p. 1086.

Kirby, S. H., Hearn, B. C., He, Y., and Lin, C., 1985, Geophysical implications of mantle xenoliths: evidence for fault zones in the deep lithosphere: Trans. Am. Geophys. Union, v. 66, p. 1066.

Kirby, S. H., Hearn, B. C., Jr., He, Yongnian, and Lin, Chuanong, 1986, Geophysical evidence of mantle xenoliths: evidence for fault zones in the deep lithosphere of eastern China: U.S. Geological Survey Circular, Kirby, S. H., Nielson, Jane, and Noller, J., eds. (in press).

Kirby, S. H., Nielson, J., and Noller, J., eds., 1986, Geophysics and petrology of the deep crust and upper mantle: U.S. Geological Survey Circular (in press).

Kronenberg, A. K., and Kirby, S. H., 1985, The hydrolytic weakening defect in quartz: equilibrium or metastable: Trans. Am. Geophys. Union, v. 66, p. 1140.

Kronenberg, A. K., Kirby, S. H., Aines, R. D., and Rossman, G. R., 1985, Solubility and diffusional uptake of hydrogen in quartz at high pressures: implications for hydrolytic weakening: Journal of Geophysical Research (accepted, in press).

Kronenberg, A. K., Kirby, S. H., and Pinkston, J. C., 1985, Compression of biotite single crystals perpendicular to cleavage: Trans. Am. Geophys. Union, v. 66, p. 1085.

3-D Fault Behavior with Rate Dependant Fault Constitutive Laws and Coupling to the Asthenosphere.

14-08-0001-22043

Victor C. Li (P.I.), N. Fares and H.S. Lim
Department of Civil Engineering
Massachusetts Institute of Technology
Cambridge, MA 02139
(617) 253-7142

Investigations

During the last funding period, two lines of investigations were followed. First, surface deformations at a strike-slip fault is studied with two different fault models in an attempt to verify the accuracy of lithosphere/asthenosphere coupling in the modified Elsasser model. Second, efforts towards developing a 3-D Green's function was initiated.

Results

I. Study of Surface Deformation Fields at a Strike-slip Plate Boundary

We consider the deformation of an elastic plate of thickness H with an edge crack of length $a(\equiv H - \ell)$, and is loaded at the base of the plate by imposed displacement rate $\dot{u} = \pm V_{pl}/2$ for $y \gtrless 0$, as shown in figure 1. This loading configuration represents an extreme case of lithosphere/asthenosphere coupling where the elastic lithosphere is driven by a rigid asthenospheric foundation moving at uniform velocity consistent with the far field plate motion.

For this extreme case, 2-D elasticity theory leads to a governing equation for the only non-vanishing displacement rate component $\dot{u}(y,z)$:

$$\nabla^2 \dot{u} = 0$$

subject to the boundary conditions indicated in figure 1.

Solution to this boundary value problem has been obtained by means of analytic conformal mapping technique and the details are reported in Li et al. 1986. Here we summarize the resulting expressions relevant to the present discussion:

(1) Displacement rate in body:

$$\dot{u}(y,z) = \frac{V_{pl}}{2} Re \int_0^p \frac{dt}{F\sqrt{(1-t^2)(1-k^2t^2)}}$$

where $k = \sin\beta$

$$F = \int_0^{\pi/2} \frac{d\theta}{\sqrt{1 - k^2\sin^2\theta}} \qquad \text{(complete elliptic integral of the first kind)}$$

$$p = Re\sqrt{1 + \tanh^2\alpha \,/\, \tan^2\beta}$$

$$\alpha \equiv \pi(y + iz)/2H \quad ; \quad \beta \equiv \pi a/2H \quad ; \quad \gamma \equiv \pi y/2H$$

(2) Surface displacement rate (at z = H)

$$\dot{u}_s(y) = \frac{V_{pl}}{2}\left[1 - \frac{1}{F}\int_{1/k}^{\lambda} \frac{dt}{\sqrt{(t^2-1)(k^2t^2-1)}} \right]$$

where $\lambda \equiv \sqrt{1 + \coth^2\gamma/\tan^2\beta}$

(3) Stress rate in body:

$$\dot{\tau}_{yx} - i\dot{\tau}_{zx} = \frac{iG(V_{pl}/2F)(\pi/2H)\operatorname{sech}\alpha}{\cos\beta\sqrt{\tan^2\beta + \tanh^2\alpha}}$$

(4) Surface strain rate (at z = H):

$$\dot{\gamma}(y) = \frac{(V_{pl}/2F)(\pi/2H)}{\cos\beta\,\sinh\gamma\sqrt{\tan^2\beta + \coth^2\gamma}}$$

A characteristic of the modified Elsasser model is the incorporation of the coupling tractions as body forces in the lithospheric plate. For the edge-cracked plate boundary geometry, these body forces become part of the loads σ in figure 2. This problem has been dealt with in Spence and Turcotte, 1974, among others. We compare the strain rates $\dot{\gamma}$ at the fault trace based on figure 1 and figure 2. Their ratio as a function of aseismic shear zone extent a (≡ plate thickness - locked ligament) is shown in figure 3, based on equivalent loading of equal net force transmitted across the locked ligament. It is seen that for typical

locked ligament size of say, 8-15 km. in a 45 km. thickness ($a = 0.67 - 0.82H$), the error in surface strain rate estimation due to the Elsasser approximation is less than 5%.

We are now extending this study of the surface strain rate to any distance from the fault trace, and not just at the fault trace, based on the work of Li and Rice (1986).

II. Development of 3-D Green's Function

The complete elastostatic response (i.e. displacements and stresses at all locations and for all time) of a (3-D) dislocation dipole in a solid medium consisting of an elastic layer over a viscoelastic foundation is sought. The available solutions in the literature only calculated the surface deformations associated with such sources with either an elastic or a viscoelastic half-space.

The complete response is needed in order to set up the integral equations which model the quasi-static rupture evolution of a fault having specified stress-slip constitutive relations until instability.

The exact solution for a source in an elastic layer over an elastic half-space (3-D) can be found through a transform technique and can be written in terms of improper integrals of the form:

$$\sigma_{ij},\ u_i \simeq \int_0^{\infty} \frac{\sum_{i=0}^{m} \alpha_i k^i \exp(\beta_i kz)}{\sum_{i=0}^{n} \gamma_i k^i \exp(\delta_i kz)} J_p(kr)\, dk$$

In the above integrals, α_i's and γ_i's may depend on both the elastic properties of the half space and the layer.

In order to extend this solution from an elastic half-space to a viscoelatic half-space via the correspondence principle (analytically), the solution has to be rewritten in a form which separates the material parameters from the geometric dependencies (r,θ,z) in the form of a sum of products of pairs of functions in which the first function of each pair depends solely on the material parameters and the second function of each pair depends solely on the geometric dependencies.

Before applying this approach to the 3-D case, the antiplane problem was investigated also using a transform technique. The improper integrals were shown to lead to a solution in the form of an infinite number of dislocation dipole "image" sources for the

complete solution. For the 2-D case (still being investigated) the approach suggests a solution in terms of an infinite number of "images" made of dislocation dipoles as well as higher order sources.

Finally, another starting point for the same problem which is being investigated is suggested by Rice 1985, in which the solution to a source in two dissimilar elastic half-spaces (Rongved 1953) in terms of Papkovich-Neuber potentials is exploited in an "extended" image technique for elastostatic problems of one layer between two half-spaces.

Reports and Publications

1. Li V.C., Lim H.S. and Cohen S.C., "Near Fault Surface Deformation Based on the Modified Elsasser Model.", Trans. Amer. Geophys. U., 1986 in press.

2. Li V.C. and Rice J.R.,"Crustal Deformation in Great California Earthquake Cycles.", in preparation, 1986.

3. Li V.C., "Mechanics of Shear Rupture Applied to Earthquake Zones.", to be published as a chapter of "Rock Fracture Mechanics", (B. Atkinson, ed.), Academic Press 1986.

4. Li V.C. and Fares N., "Rupture Processes in the Presence of Creep Zones.", in "Earthquake Source Mechanics", AGU 1986, in press.

5. Fares N. and Li V.C., "An Indirect Boundary Element Method for 2-D Finite/Infinite Regions with Multiple Displacement Discontinuities.", J. Eng. Frac. Mech., 1986 in press.

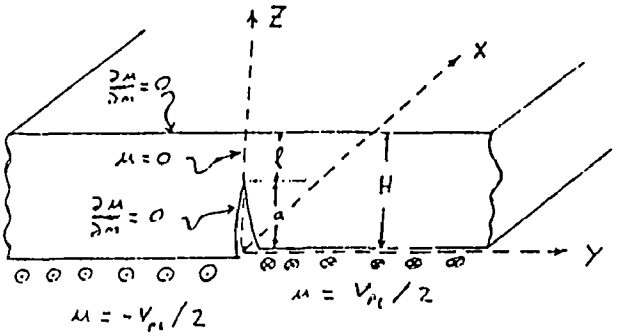

Figure 1

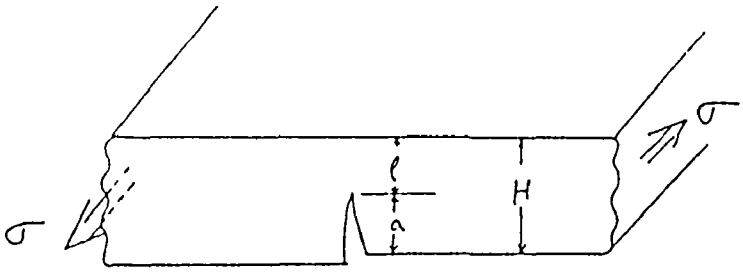

Figure 2

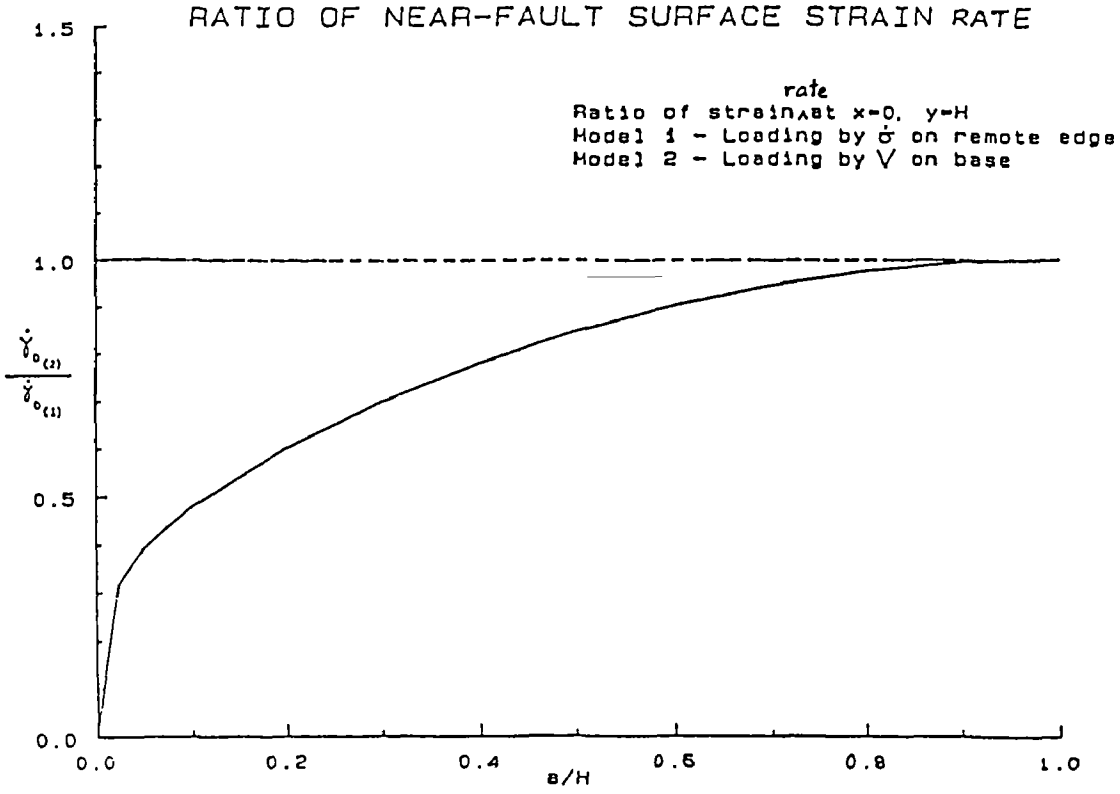

Figure 3

Rock Deformation

9950-00409

Eugene C. Robertson
Branch of Engineering Geology and Tectonics
U.S. Geological Survey
922 National Center
Reston, VA 22092
(703) 648-6792

Investigations

Characteristics of faults, such as, rupture length, displacement, and surface area have been correlated with earthquake magnitude (Bonilla et al, 1984; Scholz, 1982), and it would be useful to correlate fault zone thickness with magnitude as well. Correlation of thickness of gouge and breccia has been made with total displacement (Robertson, 1983, 1984) and recently with total fault length. A tentative effort to correlate fault gouge and breccia thickness with earthquake magnitude has been attempted.

Results

The careful review of 58 historical earthquakes and associated faults of Bonilla, Mark, and Lienkaemper (1984) provides data on rupture length, surface displacement, and surface-wave magnitude M_S of these shallow-focus events. Although outcrops of a number of earthquake faults have been excavated to study seismicity and displacement, relatively few studies provide data on thickness of the crushed zones mostly on strike-slip faults (Hill and Beeby, 1977; Sieb, K. E., 1978a, 1978b; Tanna Fault Research Group, 1983; Tsuya, 1944; and Wallace, 1977.) Therefore, it seemed useful to make a tentative correlation of fault zone gouge and breccia thickness with earthquake magnitude by doing a cross-correlation with fault length based on data in the studies of Bonilla et al (1984) and Robertson (1983).

A rather speculative result is shown in Figure 1; the nearly dip-slip normal and reverse faults, types A and B of Bonilla et al (1984, Table 3) are used on the right side of Figure 1, (crosses), and fault length-thickness data (Robertson, 1983) are used on the left side (circles). Uncertainties in determining fault length are described by Bonilla et et al (1984); their rupture lengths are for particular earthquakes, whereas total fault lengths are used in the thickness correlation. The single event fault length is estimated to differ from the total length by a factor of 2 or 3, but no correction was attempted. Superimposing the fault lengths on the obscissa, the thickness of gouge and breccia can be correlated with presumably near-maximum earthquake magnitude by juxtaposing linear trend lines through the two plots. This speculative correlation obviously needs

corroboration by a field investigation; in measuring thickness, care will be needed to consider only gouge and breccia and should not include jointed rock.

References

Bonilla, M. G., Mark, R. K., and Lienkaemper, J. J., 1984, Statistical relations among earthquake magnitude, surface rupture length, and surface fault displacement U.S. Geological Survey Open-File Report 84-256, 37 p.

Hill, R. L. and D. J. Beeby (1977). Surface faulting associated with the 5.2 magnitude Galway Lake earthquake of May 31, 1975, Mojave Desert, San Bernardino County, California, Geol. Soc. Am. Bull. 88, 1378-1384.

Robertson, E. C., 1983, Relationship of fault displacement to gouge and breccia thickness, Amer. Inst. Min. Met. Petrol. Engr., Mining Engineering, v. 35, no. 10, p. 1426-1432.

Robertson, E. C., 1984, Rock deformation report, Summaries of Technical Reports, vol. 19, National Earthquake Hazards Reduction Program, U.S. Geological Survey Open-File Report 85-22, p. 459-460.

Scholz, C. H., 1982, Scaling laws for large earthquakes: Consequences for physical models, Seis. Soc. Am. Bull., v. 12, p. 1-32.

Sieh, K. E. (1978a), Pre-historic large earthquakes produced by slip on the San Andreas fault at Pallet Creek, California. J. Geophys. Res. 83, 3907-3939.

Sieh, K. E., (1978b), Slip along the San Andreas fault associated with the great 1857 earthquake. Bull. Seismol. Soc. Am. 68, 1421-1448.

Tanna Fault Trenching Research Group (1983). Trenching study for Tanna fault, Izu, at Myoga. Shizuoka Prefecture. Japan. Bull. Earthquake Res. Inst., Univ. Tokyo 58, 797-830 [in Japanese].

Tsuya, H. (1944). Geological observations of earthquake faults of 1943 in Tottori Prefecture, Tokyo Imp. Univ. Earthquake Res. Inst. Null. 22, 1, 1-32.

Wallace, R. E. (1977). Profiles and ages of young fault scarps, north-central Nevada. Geol. Soc. Am. Bull. 88, 1267-1281.

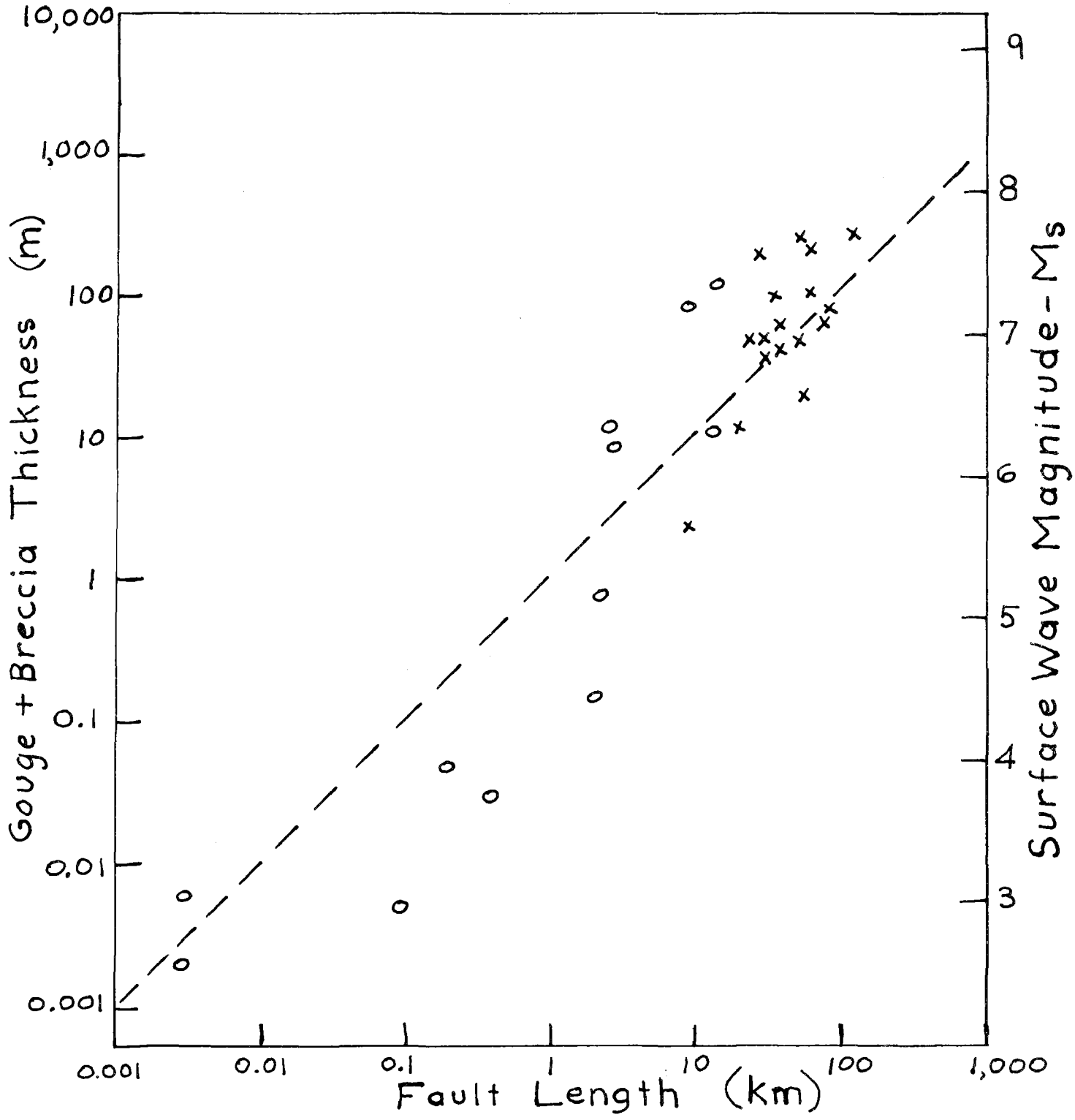

Figure 1. Correlation of thickness of fault gouge and breccia with near-maximum surface wave earthquake magnitude by using common scale of fault length and assuming linearity of trends of points. Circles are for length-thickness data (Robertson, 1983) and crosses are for length-magnitude data (Bonilla et al, 1984).

Heat Flow and Tectonic Studies

9960-01177

John H. Sass
Branch of Tectonophysics
U.S. Geological Survey
2255 North Gemini Drive
Flagstaff, AZ 86001
(602) 527-7726
FTS: 765-7226

Arthur H. Lachenbruch
Branch of Tectonophysics
U.S. Geological Survey
345 Middlefield Road
Menlo Park, CA 94025
(415) 323-8111, ext. 2272
FTS: 467-2272

Investigations:

1. Heat flow and tectonics of the Western United States: Thermal conductivities were measured and further interpretation was carried out on temperature data from the Ventura and Santa Maria Basins.

The active phase of the Salton Sea Scientific Drilling Project (SSSDP) was successfully completed on March 31-April 1, 1986.

Detailed analysis of data near Cajon Pass was carried out resulting in estimates of heat flow to 1.7 km.

A critical comment on previously published steady-state models for extension in the Great Basin prompted a re-examination of these models and some additional calculations on transient effects.

Results:

Heat flow and tectonics of the Ventura Basin. The onshore Ventura Basin, California, is An east-west trending structure with a sedimentation history extending from the Cretaceous through Holocene, and containing perhaps the thickest Quaternary section in the world (up to 5 km) and the thickest Pliocene section in the world (up to 4200 m). Quaternary subsidence/uplift rates have exceeded 1 cm/yr for 100,000 yr or more. Temperature profiles from 12 oil wells were used in this study. Thermal conductivity measurements were taken on cores obtain from other wells in the Oxnard and Ventura Avenue fields, and on surface samples obtained from outcrops. Preliminary data indicate that vertical heat flow may vary with depth. Heat flow in the interval between the zone disturbed by rapid Quaternary deposition and the mid-Miocene Conejo Volcanics averages 44±3 mW/m^2, a relatively low value for the region. Fragmentary data from the Oligocene through mid-Miocene interval suggest a heat flow of about 60 mW/m^2, a value more in keeping with regional averages. Thermal conductivity is poorly constrained in the thickest Pleistocene through Holocene sequence at Fillmore, but data suggest that near-surface heat flow there may be as low as 35 mW/m^2. These preliminary data suggest two major transients in the thermal data: (1) an earlier transient associated with the deposition of late Miocene to Pliocene sediments following initial sequestration of the central Ventura basin; and (2) a later transient associated with rapid Quaternary sedimentation. Pre-Quaternary heat flow on the Oxnard Shelf averages

48±8 mW/m^2 versus 45±3 mW/m^2 in the Santa Clara Trough; however, no logged holes in the trough penetrate the Miocene. When Miocene gradients are excluded, the shelf heat flow averages 44±2 mW/m^2, indicating no systematic differences between the trough and the shelf.

Salton Sea Scientific Drilling Project: State 2-14, the Salton Sea Scientific Drilling Project (SSSDP), was spudded on October 24, 1985, and reached a total depth of 10,564 ft (3.2 km) on March 17, 1986. There followed a period of logging, a flow test, and downhole scientific measurements. The scientific goals were integrated smoothly with the engineering and economic objectives of the program and the ideal of "science driving the drill" in continental scientific drilling projects was achieved in large measure. The principal scientific goals of the project were to study the physical and chemical processes involved in an active, magmatically driven hydrothermal system. To facilitate these studies and data collection, namely: (1) core and cuttings, (2) formation fluids, (3) geophysical logging, and (4) downhole physical measurements, particularly temperatures and pressures. In all four areas, the results obtained were sufficient to meet the stated scientific goals.

Thermal Studies at the Cajon Pass Borehole: An obstacle to understanding earthquakes and the tectonic forces that drive them is our ignorance of the magnitude of the stresses on earthquake faults. Attempts to estimate these stresses from calculated effects of their frictional heating on the San Andreas fault suggest an upper limit of about 200 b; greater average stresses should produce a local heat-flow anomaly and none has been observed. By contrast, stress measurements made to a maximum depth of about 1 km near the San Andreas fault, when extrapolated through the seismogenic zone, suggest average shear stresses ∿1 Kb, a result consistent with laboratory measurements of rock friction. The resolution of these contradictory estimates, the "stress-heat flow paradox," is a principal scientific objective of the Cajon Pass Drilling Project. The most popular models are: 1) the average stress is high (∿1 Kb) and the anomalous heat is not detected because it is carried off by circulating ground water, 2) the average stress is low (∿0.1 Kb) because fluid pressure is anomalously high or friction coefficients are anomalously low at depth. Ideally, measurements of either heat flow, stress or fluid pressure as a function of depth could independently resolve the paradox but there are other unknowns and redundancy will be needed. Measurements in the existing Cajon Pass well reveal a complex thermal regime that we do not fully understand. The thermal gradient is high (∿35°C/km) and it is the same in the sandstone and underlying granite despite their contrasting conductivities. High heat flow in the granite may be due to the rapid local erosion implied by Ray Weldon's mapping or to high fault stress; the uniformity of gradient may be due to structural complexities or hydrologic effects near the granite contact. Careful thermal, hydrologic and stress measurements to 5 km could resolve many of these questions.

Debate over the use of steady-state results for models of an extending lithosphere. In a comment to JGR, Jean-Claude Mareschal criticized our use of steady-state heat-flow results in "Models of an extending lithosphere and heat flow in the Basin and Range Province," A. H. Lachenbruch and J. H. Sass, GSA Memoir 152, 1978. His point was that such processes would take hundreds of million of years to approach a steady-state, and are not applicable to extension confined to the Cenozoic Era (tens of millions of years). However, we believe that Mareschal's time estimates are inappropriate

because he used the wrong boundary condition and an unrealistic lithosphere thickness, and he neglected relevant effects of the physics of intrusion. We presented a time-dependent analytical solution for simultaneous intrusion and extension of the lithosphere to show that Mareschal's time estimates are probably too large by an order of magnitude.

Reports:

DeRito, R. F., 1986, The effects of weak crust upon the strength of the continental lithosphere (abstract): U.S. Geological Survey Circular, in press.

DeRito, R. F., Cozzarelli, F. A., and Hodge, D. S., 1986, A forward approach to the problem of temperature and the long-term thickness of the mechanical lithosphere: Journal of Geophysical Research, in press.

Lachenbruch, A. H., Sass, J. H., Moses, T. H., Jr., and Galanis, S. P., Jr., 1986, Thermal Studies at the Cajon Pass Borehole (abstract): EOS, v. 67, p. 379-380.

Lachenbruch, A. H., 1986, Reply to Comment by J. C. Mareschal: Journal of Geophysical Research, in press.

Lachenbruch, A. H., Sass, J. H., Lawver, L. A., Brewer, M. C., Marshall B. V., Munroe, R. J., Kennelly, J. P., Jr., Galanis, S. P., Jr., and Moses, T. H., Jr., Temperature and depth of permafrost on the Alaskan Arctic Slope: Pacific Section - SEPM Special Publication and U.S. Geological Survey Professional Paper 1399 (Branch approval, March 1986).

Lachenbruch, A. H., and Marshall, B. V., Climatic warming: Geothermal evidence from permafrost in the Alaskan Arctic (Branch approval, March 1986).

Pollack, H. N., and Sass, J. H., 1986, Thermal regime of the lithosphere, in Haenel, R., Rybach, L., and Stegena, L., eds., Handbook of Terrestrial Heat-Flow Density Determination (Guidelines and Recommendations of the International Heat Flow Commission), in press.

Sass, J. H., and Elders, W. A., 1986, Salton Sea Scientific Drilling Project--Scientific Program: GRC Transactions, in press.

Sass, J. H., Hendricks, J. D., Priest, S. S., and Robison, L. C., 1986, The Salton Sea Scientific Drilling Program--A progress report: U.S. Geological Survey Circular 974, p. 60-61.

Fractal Heterogeneity of Faults

14-08-0001-G1161

C. H. Scholz
Lamont-Doherty Geological Observatory
and Dept. Geological Science, Columbia Univ.
Palisades, NY 10964
(914)359-2900

Investigations:

Studies have been made or are underway of the geometry of active faults, using fractal analysis. Two scale ranges have been studied, the micro and macro scale, 10^{-5}-1 M, which can be measured with profilometers, and the mega scale, 10^{3}-10^{6} M, by the analysis of maps.

Results:

1. Fractal Geometry of Faults and Faulting
   (Scholz, Aviles)

The Alquist-Priolo (1:24,000) fault hazard maps of the San Andreas fault system were digitized and analysed using the spectral technique. These results were compared with our earlier work, using profilometers, of the topography of joints and other natural rock surfaces. It was found that these surfaces were fractal, or nearly fractal, over the entire 10 decade spectral band studied, but that the fractal dimension is itself a function of scale.

These results have consequences in terms of the size distribution of asperities and earthquakes, and with regard to scaling of frictional constitutive relations that may apply to real faults.

2. Fractal Analysis of Characteristic Segments of the San Andreas fault
   (Aviles, Scholz, Boatwright)

A thorough study of variations in fractal dimension along the San Andreas fault was carried out. Because the segmentation of the fault into strands was found to create problems with the spectral technique, this study employed the ruler method. It was found that all sections of the San Andreas fault were fractal at the megascale, with considerable variation of fractal dimension along strike. No obvious correlation was found between the seismic behavior of different fault segments and the fractal dimension.

3. Profilometry Studies of Active Fault Surfaces
   (Scholz, Brown, Boitnott)

A joint investigation with Power and Tullis of Brown Univ. is underway of the topography of slickensided fault surfaces using profilometers. They made measurements in the field of a number of slickensided fault surfaces in Nevada and Utah, using our field profilometer, which was modified for remote field use. Measurements on a smaller scale were made from samples from the same outcrops using our lab profilometer.

Results so far show that these surfaces are fractal out to a length scale of 10M, but that they are strongly anisotropic. They tend to be much less jagged, when measured parallel to the slip direction, than other rock surfaces we have measured, and about as jagged when measured perpendicular to slip.

Reports

Scholz, C. H. and C. A. Aviles, Fractal geometry of faults and faulting, in 5th Ewing Symposium, Earthquake Mechanics (ed. S. Das, J. Boatwright, C. Scholz) Ewing V. 6, AGU, in press, 1986.

Aviles, C. A., C. H. Scholz, and J. Boatwright, Fractal Analysis of Characteristic segments of the San Andreas fault, J. Geophys. Res., in press, 1986.

Systems Analysis of Geologic Rate Processes

9980-02798

Herbert R. Shaw and Anne E. Gartner
Branch of Igneous and Geothermal Processes, U.S. Geological Survey
MS-910, 345 Middlefield Road, Menlo Park, CA 94025
(415) 323-8111, X4169, X4170

Objective: The work on this project has the objective of dynamic interpretation of paleoseismic data compiled by Shaw and others (1981). An aspect is the interpretation of self-similarity and fractal geometry of fault sets.

Results: The study of faulting in the conterminous U.S. by Shaw and others (1981) emphasized the discovery of a crude invariance over time and space of the distribution of fault lengths showing evidence of movement during the latest 15 m.y. (map data from Howard and others, 1978). On that basis it was inferred that faulting is, broadly speaking, a fractally self-similar branching process (see semi-annual report, v. XXI, p. 442-445) operating in the steady-state over times of the order of a million years in large crustal provinces (e.g., the faulting regions of Howard and others, 1978). However, it is known that at longer times there are variations in rates of deformation at the scale of plate tectonics, and at shorter times there are conspicuous local variations in faulting rates (e.g., along the San Andreas fault system).

The above scale-dependent observations are consistent with the idea that fractal dimensions of fault systems are variable, as previously discussed, but that they may also be roughly constant within certain domains of time and size. Expressed in terms of proportionalities between numbers and lengths of fault segments, as described in Shaw and others (1981), departures from the steady state can occur by various combinations of two kinds of tendency: 1) The total counts can be shifted to higher or lower levels at constant proportionalities of fault numbers and lengths (i.e., counts of fault movements at every length can transiently either increase or decrease together), or (2) The counts of shorter to longer faults can vary disproportionately (i.e., transiently there can be a higher than steady-state count of movements on short faults and a smaller than steady-state count on long faults, or vice versa).

From a paleoseismic point-of-view these possible types of deviations are of relatively long term compared to catalogs of historic seismicity. They may, however, be indicating some of the same types of effects that are now beginning to be revealed by the documentation of seismic cycles (e.g., Ellsworth and others, 1981; Mogi, 1985). This possibility is illustrated in Figures 1 and 2, using the data from Shaw and others (1981) for the U.S. as a whole compared with the more localized scale of faulting in southern California over the same approximate time intervals.

In Figure 1, it is seen that the proportions of small to long faults, as shown by the slopes of the regression lines, decrease in the younger age categories both for the U.S. data as a whole and for the restricted sets of data for southern California (data derived from the maps of Ziony and others, 1974). As discussed by Howard and others (1978), it is not possible to say unequivocally what is the youngest movement on a given

fault. The age classes refer only to the stratigraphic criteria that define the youngest recognizable offsets. Thus, except for the class of historic movements, no definite time interval can be assigned to either the steady state or to transient excursions from it. There is, however, evidence that a roughly constant limit is achieved over some time longer than the historic interval (slopes in Figure 1 approach an approximately constant value at the older ages).

Figure 2 explores the implication of assuming that the historic faulting data are representative of current activity simultaneously with the implication that at other times or over large enough domains the steady-state slope might be achieved during a time interval of comparable duration (200 years was arbitrarily chosen as the basis of comparative normalization). This hypothetical construction has consequences that seem to be categorically in accord with the idea of a systematic seismic cycle in California, as follows: (1) The steady-state assumption applied to all faulting in the U.S. produces a paleoseismic frequency-magnitude curve that agrees with Algermissen's (1969) curve of U.S. seismicity to within less than half a magnitude unit at a given frequency within the range of his regression curve. (2) The paleoseismic frequency-magnitude curves derived from the historic faulting record agree in slope with curves based on a 174-yr record of California earthquakes (1800-1974; data from Real and others, 1978, Toppozada and others, 1979). (3) Both the historic faulting and seismicity represent transient excursions that reflect relatively suppressed activity on smaller faults and enhanced activity on longer faults during the past 200 years or so relative to the curves assumed to reflect steady-state values at other times (this can be seen by projecting the historic fault-derived curves to large magnitudes and shifting them upward to agree with the 174-yr California record).

A general implication is that the overall energy of faulting deformation becomes transiently shifted from a broad distribution among many small faults to a more focused distribution along the larger faults over times within an approximate 200-yr window (within that time there are also sympathetic changes in number-length relations occurring more locally over times as short as decades). This interpretation agrees with the conclusions of Shaw and others (1981) that tectonic energy is effectively channeled by a fractally dendritic distribution of active faults. It appears that the area of "collection" of the tectonic energy that feeds California seismicity may be more widely distributed than has been acknowledged by emphases on localized histories. This possibility combined with the fact that the assessments of faulting underestimate activity, suggests not only that there is a wealth of unexploited geologic information relevant to present-day seismicity, but that the study of systems of small faults may represent a bellwether for premonitory analysis of large events on the longer faults. We are currently exploring these implications for the comparative seismicity of northern and southern California.

References Cited:

Algermissen, S. T., 1969, Seismic risk studies in the United States: World Conference on Earthquake Engineering, 4th, Chilean Association for Seismology and Earthquake Engineering, Santiago, Chile, v. 1, p. 1-10.

Ellsworth, W. L., Lindh, A. G., Prescott, W. H., and Herd, D. G., 1981, The

1906 San Francisco earthquake and the seismic cycle, in D. W. Simpson and P. G. Richards, eds., Earthquake prediction, Washington, D.C., American Geophysical Union, p. 126-140.

Howard, K. A., and others, 1978, Preliminary map of young faults in the United States as a guide to possible fault activity: U.S. Geoloical Survey, Miscellaneous Field Studies, Map MF-916.

Mogi, Kiyoo, 1985, Earthquake prediction: New York, Academic Press.

Real, C. R., Toppozada, T. R., and Parke, D. L., 1978, Earthquake epicenter map of California: California Division of Mines and Geology, Map Sheet 39.

Shaw, H. R., Gartner, A. E., and Lusso, F., 1981, Statistical data for movements of young faults of the conterminous United States; paleoseismic implications and regional earthquake forecasting: U.S. Geological Survey, Open File Report 81-946, 353 pp.

Toppozada, T. R., Real, C. R., Bezore, S. P., and Parke, D. L., 1979, Compilation of pre-1900 California earthquake history: California Division of Mines and Geology, Open File Report OFR 79-6 SAC.

Ziony, J. I., Wentworth, C. M., Buchanan-Banks, J. M., and Wagner, H. C., 1974, Preliminary map showing recency of faulting in coastal southern California: U.S. Geological Survey, Miscellaneous Field Studies, Map MF-585.

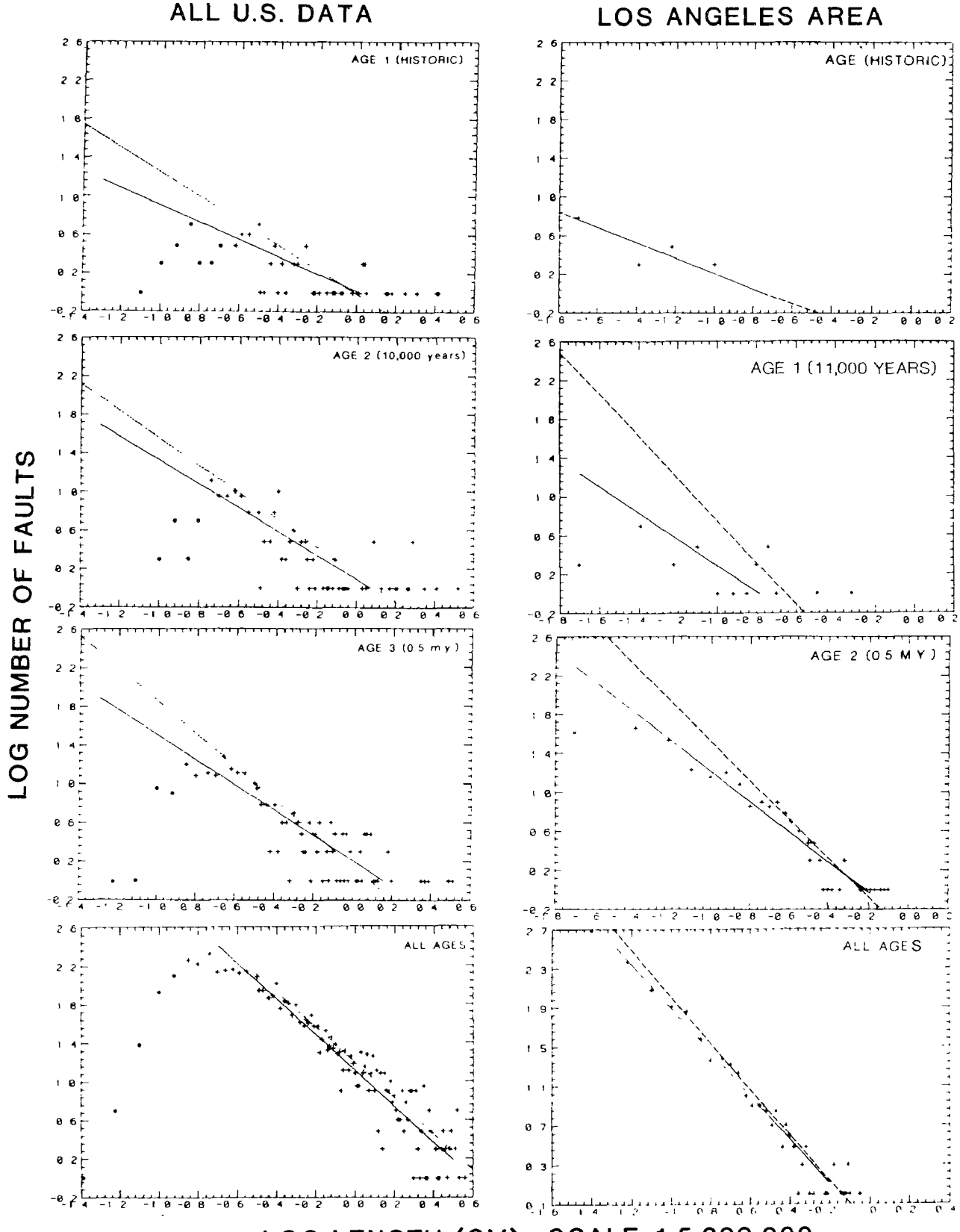

Figure 1. Statistics of faulting derived from maps of Howard and others (1978) and Ziony and others (1974), as compiled by Shaw and others (1981): 1 cm = 50 km. A. All US data; B. Los Angeles area.

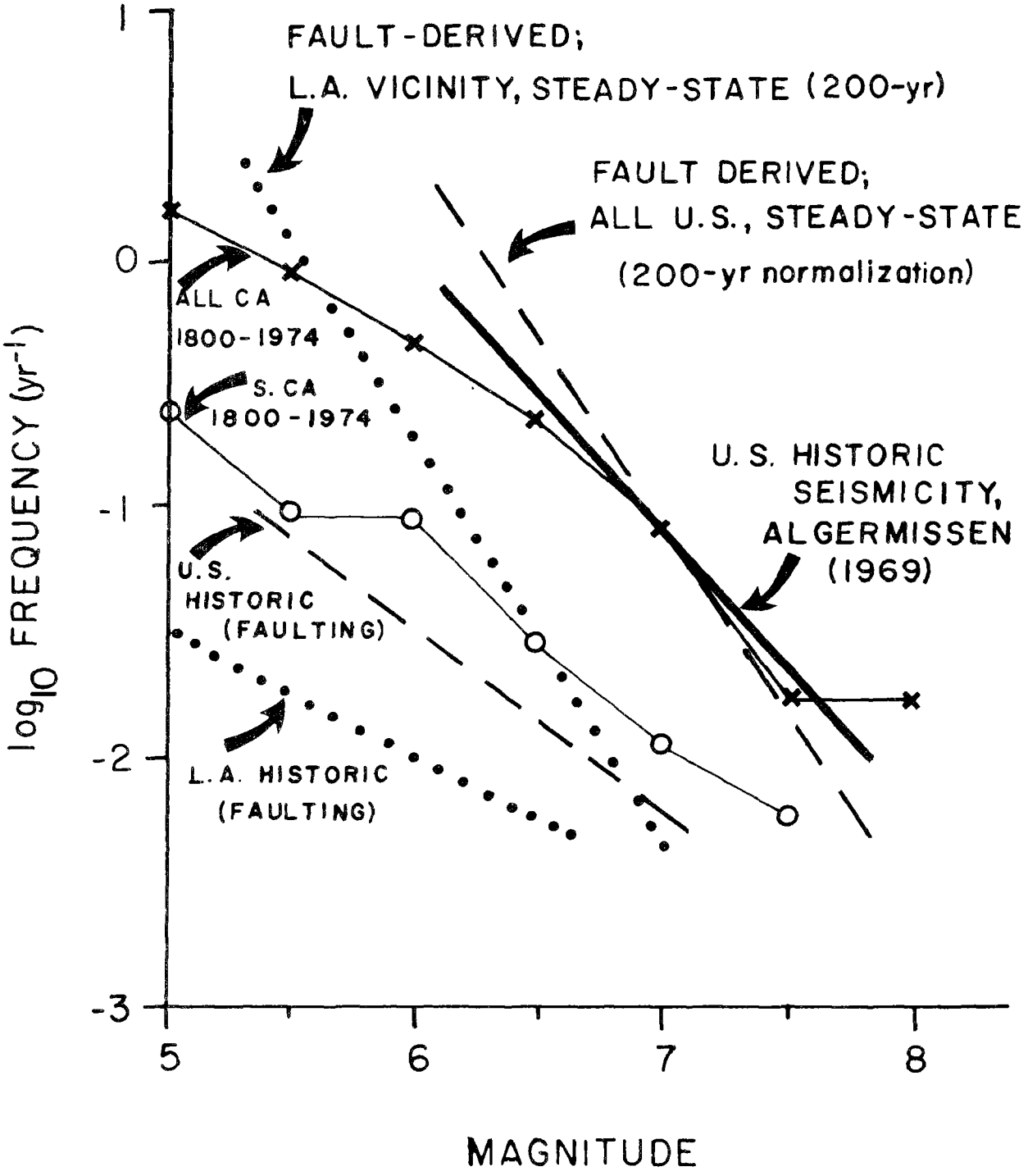

Figure 2. Comparison of U.S. and California seismicity with paleoseismicity calculated from fig. 1. U.S. seismicity from Algermissen (1969); California seismicity from Real and others (1978) and Toppozada and others (1979). Frequency-magnitude data calculated from fault length according to equation: M = 1.235 + 1.243 log L (L in meters); see Shaw and others (1981).

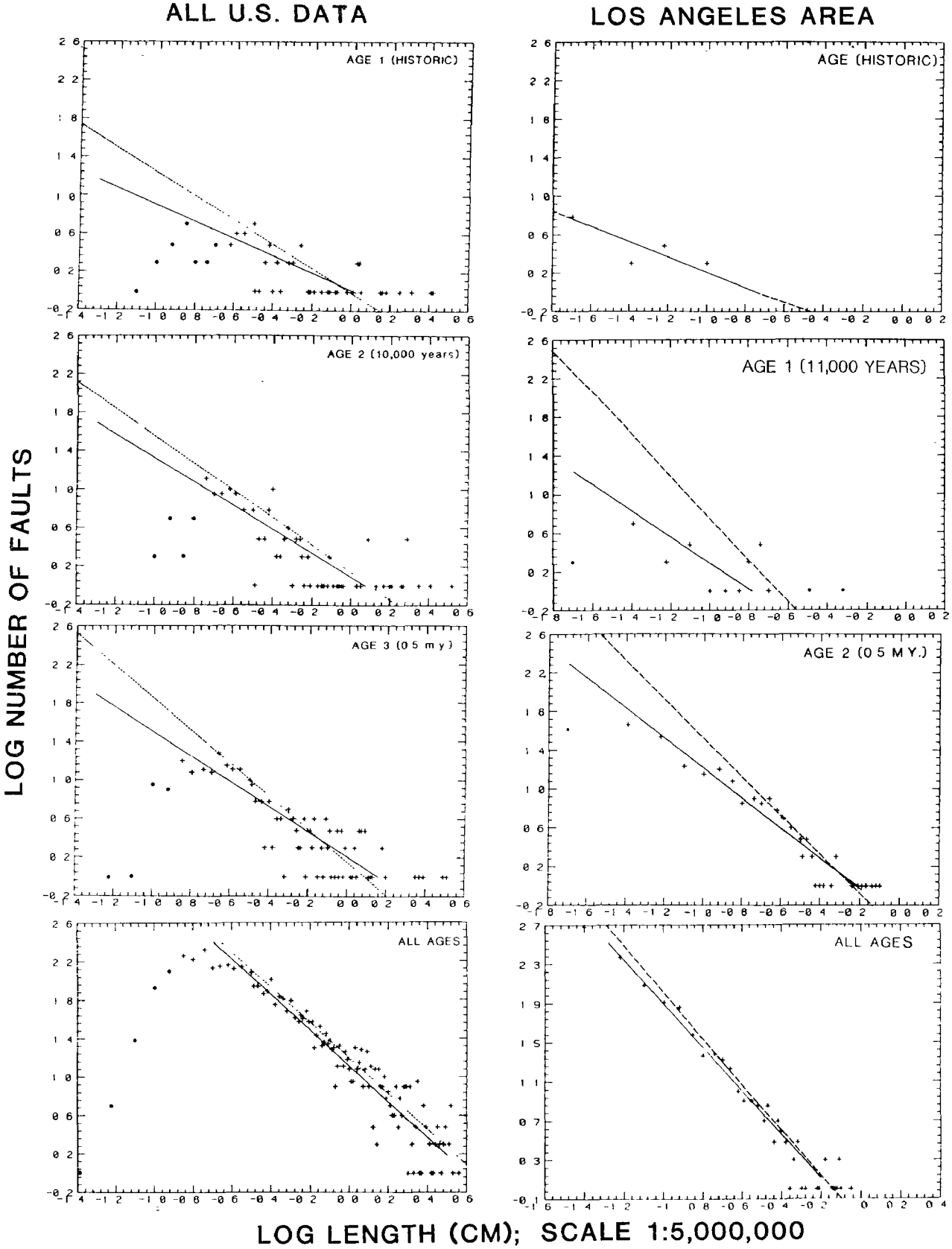

Figure 1. Statistics of faulting derived from maps of Howard and others (1978) and Ziony and others (1974), as compiled by Shaw and others (1981): 1 cm = 50 km. A. All US data; B. Los Angeles area.

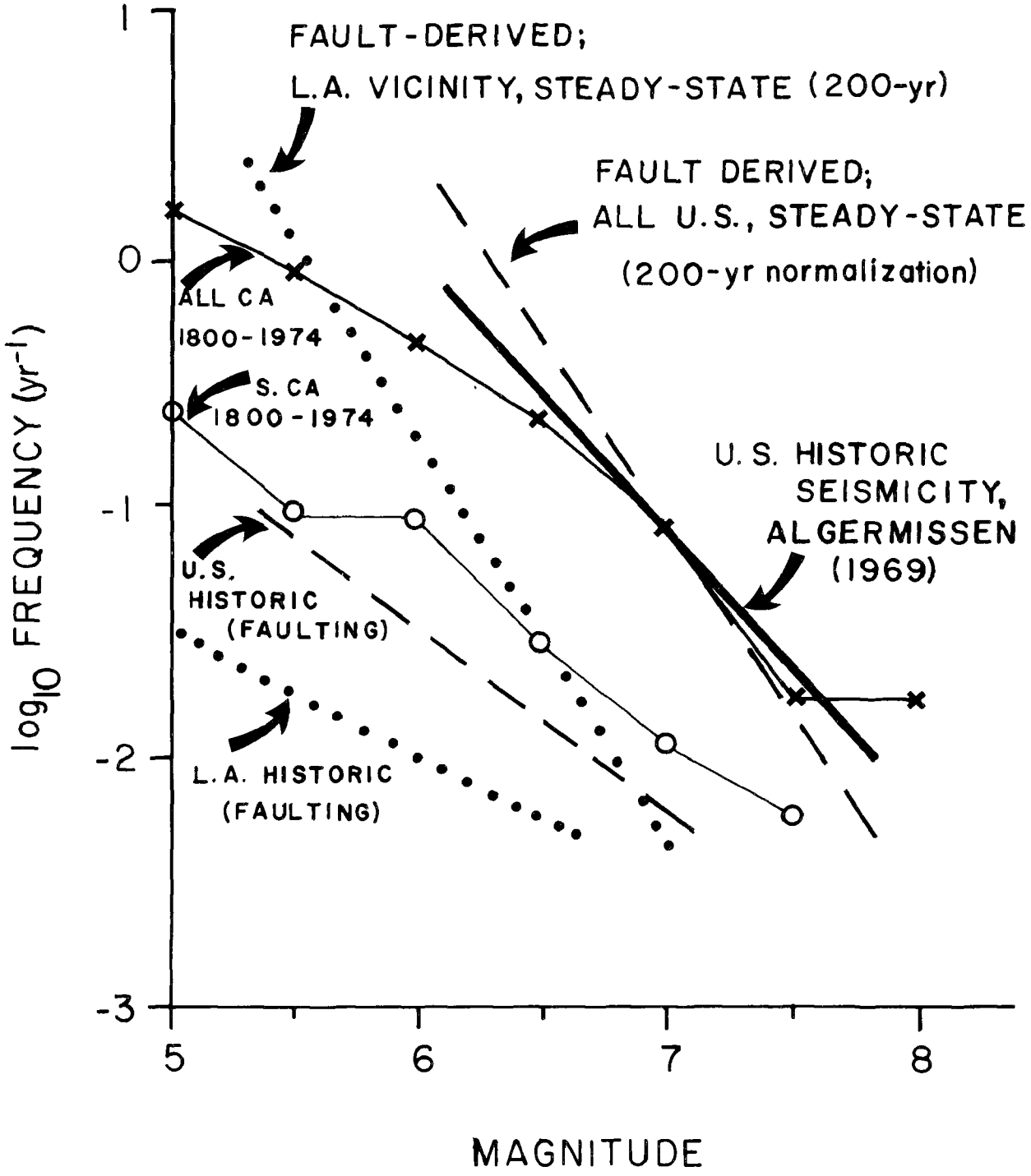

Figure 2. Comparison of U.S. and California seismicity with paleoseismicity calculated from fig. 1. U.S. seismicity from Algermissen (1969); California seismicity from Real and others (1978) and Toppozada and others (1979). Frequency-magnitude data calculated from fault length according to equation: M = 1.235 + 1.243 log L (L in meters); see Shaw and others (1981).

Modeling of Induced Seismicity and Implications for Earthquake Prediction

14-08-0001-G-1162

David W. Simpson
Lamont-Doherty Geological Observatory of Columbia University
Palisades, N.Y., 10964
(914) 359-2900

Objective - To model the effects of reservoir loading on the pore pressure in a medium with spatial variations in hydraulic and elastic parameters.

Results - We are working on a model in which temporal and spatial concentrations of high pore pressure can result from zones of material with high values of Skempton's pore pressure coefficient "B". In these zones, the initial elastic compaction due to surface loading of a reservoir leads to a transient pore pressure excess over the surrounding material, resulting in transient weakening. This pore pressure transient may be responsible for the induced seismicity at those sites where there is an immediate response in seismicity to changes in water level. At those sites where there is a considerable delay between the water level changes and seismicity, diffusion of pore pressure from the surface may be more important.

Critical to modeling induced seismicity is the ability to handle the generation of pore fluid pressures due to external loads and to let this excess pore pressure dissipate dynamically. Such a modeling ability can help analyze other related problems of interest such as response of aquifers to earth tides and barometric effects. As the first step in the modeling program, we have modified the computer program TRUST (Narasimhan and Witherspoon, 1978), a three-dimensional, saturated-unsaturated flow simulator of deformable media, to handle pore pressure generation and dissipation due to periodic or nonperiodic total stress changes. The new capability is currently being tested against problems related to response of a well piercing a confined aquifer to periodic barometric pressure changes. Our first application of this program to induced seismicity problems is in analysis of the response of a half space subjected to a finite load imposed by a surface water reservoir. The model is being extended to more general cases involving heterogeneities within the half space. After consideration of the effects on simple geometric models, we will attempt to mimic the response of specific reservoir sites (eg. Nurek, Aswan, Kariba) where detailed data are available on geology and seismicity.

The pore pressure generation in a water saturated system in response to asymmetrical, finite surface loads has to be evaluated based on general 3-dimensional stress-strain theory. In order to do this, we are using the computer program ADINA (Adina, 1981). Currently this program is being validated against analytical solutions for simple surface loads, to confirm that it will give the kinds of information needed for pore pressure generation relevant for reservoir induced seismicity. In addition, we also hope to use ADINA output to provide us with spatial variations in bulk compressibility of the rock matrix due to local variations in deformation constraints in a heterogeneous system. The pore pressure generation magnitudes and the compressibility variations obtained from ADINA form inputs for the fluid flow simulation in program TRUST.

Adina Engineering Inc., 1981; Automatic Dynamic Incremental Nonlinear Analysis, Report AE 81-1, Adina Inc.,Waterton Mass, 235 pp.

Narasimhan, T.N. and P.A Witherspoon, 1978; Numerical model for saturated-unsaturated flow in deformable porous media 2. The algorithm; Water Resources Res., 14, 255-261.

Induced Seismicity at Toktogul Reservoir, Soviet Central Asia

14-08-0001-G-1168

David W. Simpson and William Leith
Lamont-Doherty Geological Observatory
of Columbia University
Palisades, NY 10964
(914) 353-2900

As part of the US-Soviet scientific exchange program in earthquake prediction, we have been studying the induced seismicity at Toktogul reservoir in Soviet Central Asia since 1978. At Toktogul, one of the largest reservoirs in the world, significant bursts of seismicity followed reservoir filling in 1978 and 1979. Before reaching 75% of capacity, however, the reservoir water level dropped in 1982 and has remained low since then, partly due to the filling of Kurupsai reservoir, downstream. At Kurupsai, bursts of seismicity have accompanied two reservoir filling episodes. These earthquakes have occurred beneath the reservoir, somewhat upstream from the dam in an area where faults have been mapped at the surface.

Based on our previous studies at Nurek reservoir (USSR) and Aswan reservoir (Egypt), we expect intense microseismicity to resume in the future as the water level at Toktogul exceeds its previous maximum, and we suspect a long-term hazard at Toktogul for a large induced event on the Talas-Fergana fault. We are also studying the regional seismicity in detail, because there has been a dramatic increase in regional seismicity rate in the last three years. Seismicity rates now appear similar to a period about 40 years ago. The recent series has included three earthquakes of magnitude M > 6, and four occurrences of multiple, shallow, magnititude ~5 events in the last two years. We have also found important similarities between the Talas Fergana fault (which intersects Toktogul reservoir) and the southern San Andreas fault. These include off-fault seismicity, block fault rotations and Quaternary fault offsets, which make this study an important complement to current research on the tectonics and seismicity of the San Andreas fault.

References

Simpson, D. W., M. W. Hamburger, V. D. Pavlov, and I. L. Nersesov, Tectonics and seismicity of the Toktogul reservoir region, J. Geophys. Res. v. 86, p. 345-358, 1981.

Leith, W., M. Hamburger and A. Teremetsky, Preliminary result from trenching and geomorphologic studies of the Talas-Fergana fault, USSR, EOS Trans. AGU, v. 67, p 375-376, 1986.

Fault Patterns and Strain Budgets

9960-02178

Robert W. Simpson
U.S. Geological Survey
Branch of Tectonophysics
345 Middlefield Road, MS/977
Menlo Park, California 94025
415-323-8111, ext. 4256

Investigations

Program DIS3D, written by Scott Dunbar to calculate elastic fields in a half-space caused by slip on rectangular dislocations, has been patched up by Laurie Erickson of Stanford and myself and applied to several problems. Although the program has not yet been thoroughly tested, the ability to calculate elastic fields at depth and not just at the free surface will clearly be of great importance in many tectonophysics problems. I have also used Dunbar's subroutines to generalize Crouch's two-dimensional displacement-discontinuity approach for solving elastic boundary value problems to three dimensions. Two applications of these programs are described here.

Results

Coseismic slips recorded at six creepmeters on the San Andreas fault at the time of the January 26, 1986 magnitude 5.3 Tres Pinos earthquake, about 10 km southeast of Hollister, agree in their sense of motion with the sizes of the static shear stress changes predicted from a simple dislocation model of the earthquake. From south to north, the sense of motion observed on the creepmeters was RL, LL, RL, RL, RL, LL (S. Schulz, written commun., 1986). Figure 1 shows, in map view, horizontal shear stress resolved onto planes parallel to the San Andreas fault (which is parallel to the left edge of the figure), caused by 4 m of RL slip on a 1 km square dislocation centered at a depth of 7.5 km. The dislocation is vertical and strikes N5°W, which is close to the orientation of the inferred focal mechanism. The sense (RL or LL) of static shear stress change predicted by the dislocation model agrees with the observed sense of stepping on the creepmeters. This implies that the near-surface portion of the San Andreas fault in this vicinity is capable of responding to imposed stresses on the order of tenths of bars. It also suggests that nearby creepmeters need not have the same sense to their coseismic

steps if they sample different lobes in the static stress change field, and that oppositely directed creepmeter responses on nearby instruments do not necessarily imply noisy data.

A second application of the programs is the calculation of the static stress changes imposed on the San Andreas fault by the magnitude 6.7 Coalinga earthquake of May 2, 1983. The preferred dislocation model of Mavko and others (1985) was used to represent the Coalinga event. Figures 2a, b, and c show the horizontal shear stress, normal stress, and changes in the Coulomb failure criterion on the plane of the San Andreas fault in the vicinity of Parkfield. Mavko and others (1985) plotted these quantities at the Earth's surface. It is interesting to note that the largest static stress changes are predicted to occur at the Earth's surface and are on the order of 1 to 2 bar. The outline of the rectangular dislocation representing Coalinga has been projected onto the plane of the San Andreas fault and appears on the left side as a parallelogram. It should be noted that the Coulomb failure criterion is not linear because of the presence of an absolute value, so that Figure 2c truly represents the changes in the Coulomb criterion only if the pre-existing right-lateral shear stresses on the fault are everywhere greater than the imposed left-lateral stress. Because the creepmeter at MM1 slipped in a left-lateral sense for over a year after the Coalinga earthquake, it is unlikely that this assumption is correct--at least near the surface--and Figure 2c should be regarded with caution.

Figure 2d shows the slip adjustments and the redistribution of horizontal shear stress that would occur if the upper 4 km of the San Andreas fault were frictionless and moved so as to cancel the static shear stresses imposed by the Coalinga dislocation. Arrows pointing to the right represent left-lateral adjustments; the largest arrow corresponds to an adjustment of 0.02 m. Left-lateral creep was observed for over a year on the Middle Mountain creepmeter, indicated by MM in Figure 2. The calculated near-surface adjustments tend to increase and redistribute the stresses at seismogenic depths and might be responsible in part for changing patterns of seismicity near Middle Mountain in the months after the Coalinga shock (Poley and Lindh, 1985).

References Cited

Mavko, G. M., Schulz, S., Brown, B. D., 1985, Effects of the 1983 Coalinga, California earthquake on creep along the San Andreas fault, Bull. of the Seismological Society of America, v. 75, p. 475-489.

Poley, C. M., and Lindh, A. G., 1985, Recent seismicity at Parkfield, CA: EOS, Transactions of The American Geophysical Union, v. 66, p. 982.

Schulz, S. S. and Burford, R. O., 1985, Changes in fault creep rates near Parkfield, California, since the 1966 earthquake, EOS, Transactions of The American Geophysical Union, v. 66, p. 985.

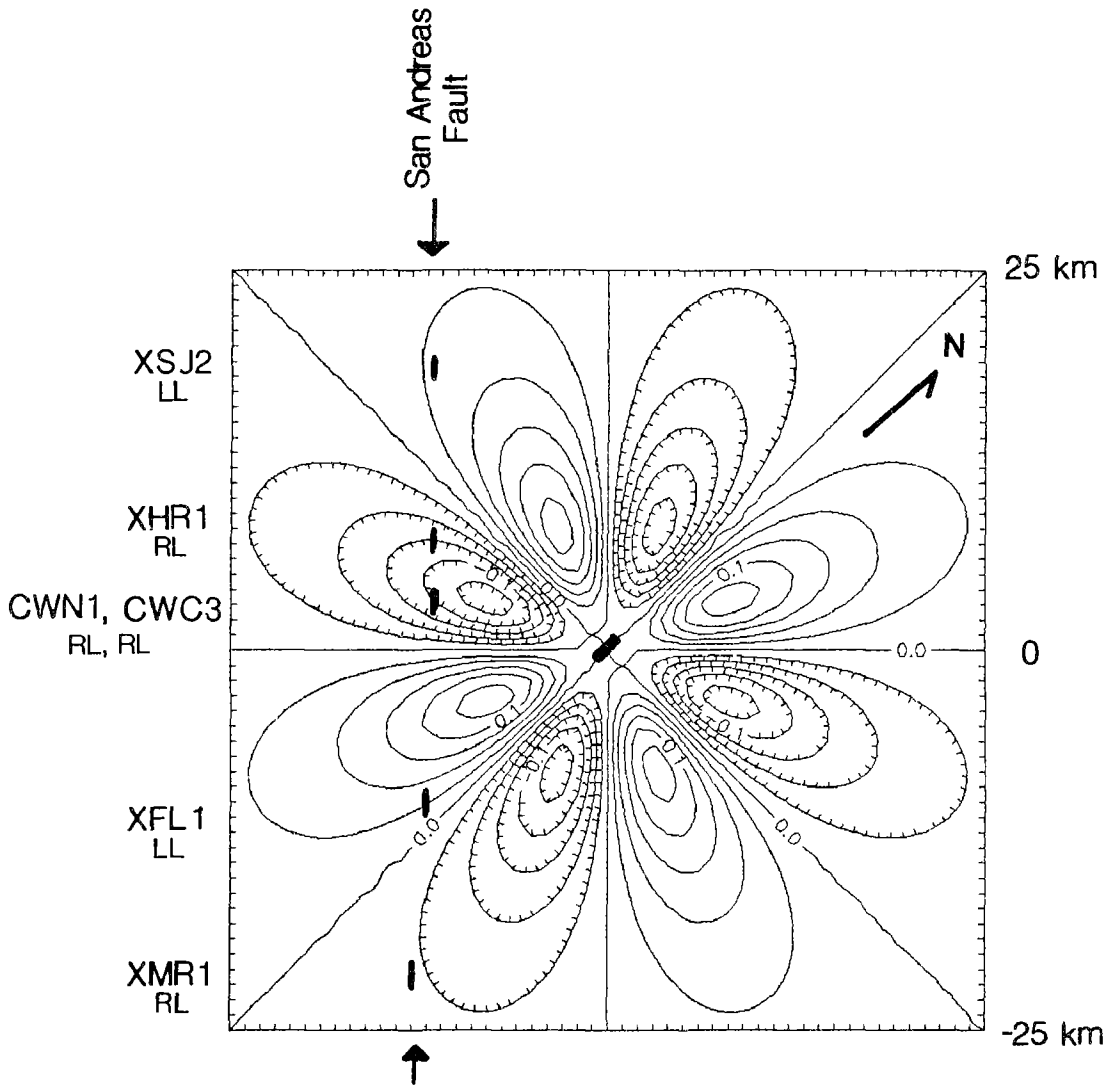

Figure 1. Static horizontal shear stress changes resolved onto planes parallel to the San Andreas fault, which is parallel to left edge of figure. Stresses were generated by a dislocation model for the Tres Pinos 26 January 1986 earthquake. Epicenter is located at the center of the figure; tics along edges of plot at 1 km interval; contour interval is 0.025 bar with hachures on negative contours. Negative shear is RL, positive is LL. Names of creepmeters and sense of observed coseismic slip are indicated along left margin. Locations of creepmeters are marked by short lines.

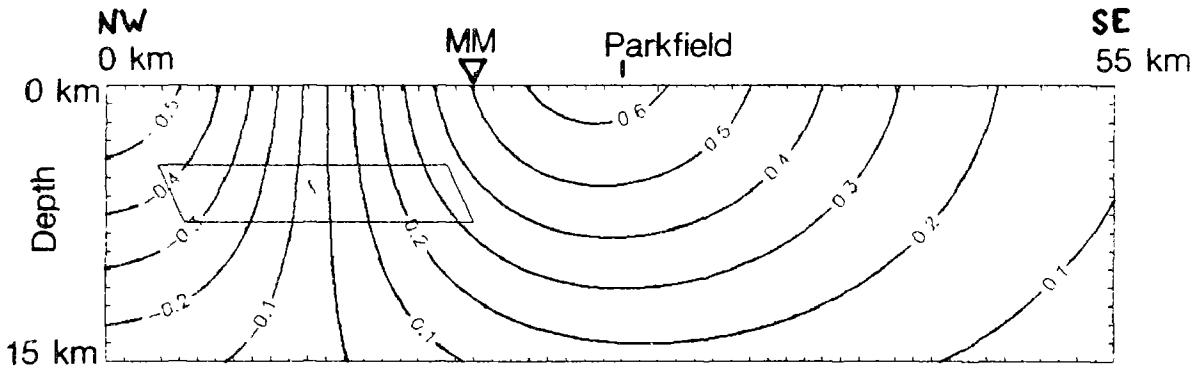

Figure 2a. Static horizontal shear stress change on plane of San Andreas fault from Coalinga earthquake. Contour interval 0.1 bar; positive is LL.

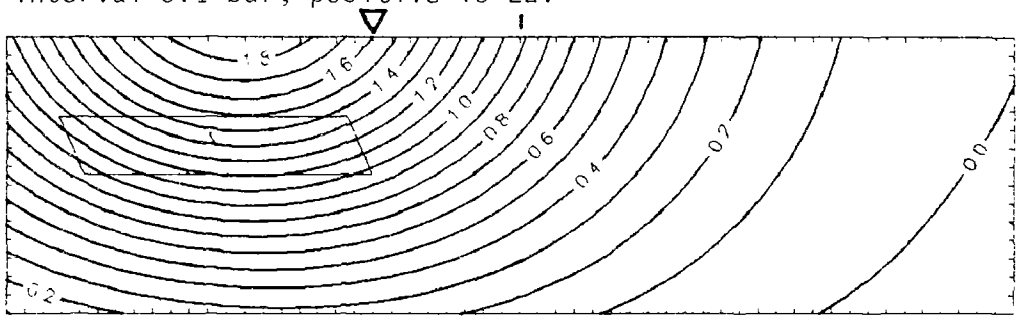

Figure 2b. Static normal stress change on plane of San Andreas fault from Coalinga earthquake. Contour interval 0.1 bar; positive is extensional.

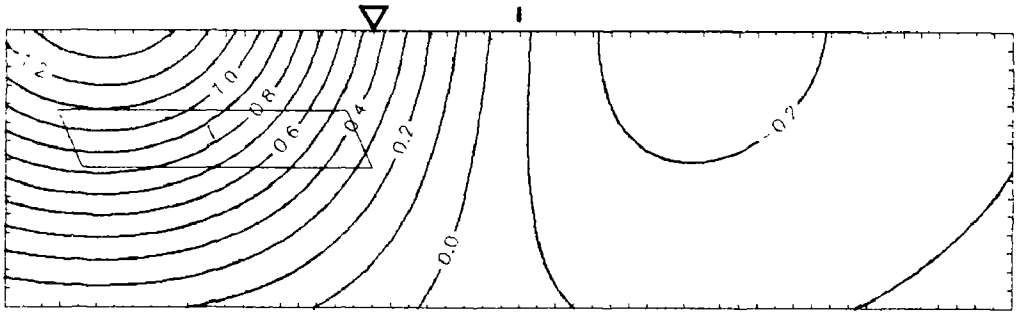

Figure 2c. Increment to Coulomb failure criterion from Coalinga earthquake. Friction 0.6; contour interval 0.1 bar; positive values closer to failure. See text for caution.

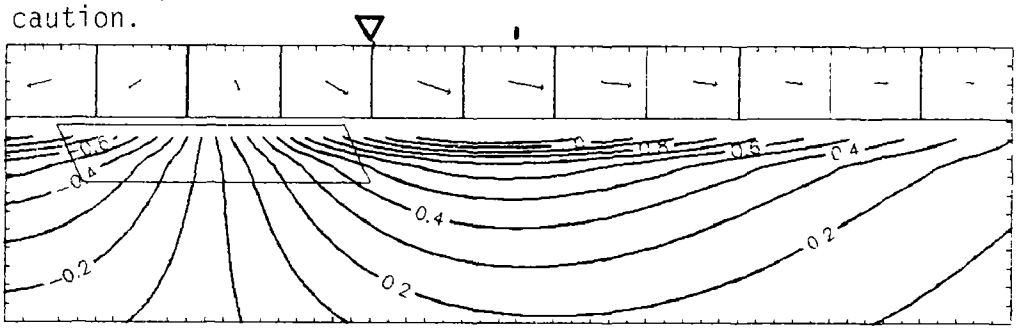

Figure 2d. Horizontal shear stress if upper 4 km is frictionless and readjusts to shear stresses imposed by Coalinga earthquake. Arrow in center block represents about 2 cm of LL adjustment.

Geophysical, Geological and Geochemical Characterization of Granitic Rock Associated with the San Andreas Fault System

14-08-0001-G-945

Donald J. Stierman*
Alan E. Williams
Institute of Geophysics and Planetary Physics
The University of California
Riverside, California 92521
(714) 787-4611

Objective: Understanding the constitutive nature and rheological properties of seismically active regions in the crust is fundamental to scientific earthquake prediction. Important factors controlling the strength of rocks, and, hence, the failure process, include the confining pressure, temperature, and pore fluid pressure as well as the frictional behavior of the minerals. Petrologic and geochemical methods are used to study cataclastic rocks to determine the physical setting of their genesis. Calibration of the relationships between rock properties and geophysical signatures of fault zone rocks permit us to extrapolate data obtained from boreholes downward into the seismic zone.

Investigations:

1. Petrographic, mineralogic and isotopic analysis of cataclastic quartz diorite from the 600 m deep Stone Canyon well.

2. Comprehensive analysis of engineering and geophysical information from the Stone Canyon well.

3. Gravity measurements across the San Andreas fault near Lake Hughes and Stone Canyon.

Data acquisition, analysis and results:

1. Petrographic examination of approximately 30 thin sections from throughout the Stone Canyon well identified three basic deformational textures, all attributable to shearing. Photomicrographs and petrographic descriptions have been made, as no previous reports of these features can be found in the literature. Alteration and incomplete cementation has left these rocks quite fragile; it is unlikely that structures found in these cores would long survive in outcrop. Although in some hand samples the deformational structures appear mylonitic, microscopic examination shows that deformation was associated with brittle failure. Breccia in these deformation zones is sometimes cemented by calcite or dolomite. While the plagioclase and quartz grains in these deformation zones ruptured in brittle failure, phyllosilicate segregations appear to form ductilely and coalesce into relatively planar bands of clay gouge along fracture surfaces. These rocks contain structures that appear to represent several stages in the development of fault gouge.

*Now at: Geology Department, The University of Toledo, Toledo, Ohio 43606 (419-537-2046)

2. A total of 60 mineralogic analyses were performed: about 10 of fresh rock samples, about 30 bulk analyses of deformed rock, and about 20 clay-rich concentrates, mostly from slicked fracture surfaces. This study documents the formation of montmorillonite as an alteration product in this quartz diorite. It appears that the montmorillonite forms as an alteration of biotite, perhaps in a manner similar to diagenesis in argillaceous sediments. The association of montmorillonite with the foliated and fractured deformation structures suggests that, despites its overall low bulk abundance, this low-friction clay may define planes of weakness when deformed and aligned, thus controlling the bulk strength of the rock. Further analysis of the mineralogy of the foliated rock and slickensided fractures are necessary to test this hypothesis.

3. Stable Isotope Analyses: a total of 41 analyses, including: 2 water samples (^{18}O only - Stone Canyon well water and local surface/spring water); carbonate samples (^{13}C and ^{18}O - 5 vein samples from upper section of well, 8 whole-rock samples from representative depths, and 9 samples from marble collected at the surface in the Gabilan Range); silicates (^{18}O only) - 9 whole-rock samples, 11 clay-rich concentrates, and 4 separates (2 each, quartz and plagioclase) from zones found to be depleted in ^{18}O. Large negative shifts in whole-rock silicate and plagioclase ^{18}O values imply interaction of some rocks with large quantities of fluids at relatively high temperatures, while moderate to large positive ^{18}O shifts in clay minerals indicate reactions at much lower temperatures. Moderate temperatures may be involved in the water-rock interaction of most of the analyzed samples. Carbonate isotope analyses generally suggest low temperatures of formation, and ^{13}C and ^{18}O values are typical of marine limestones, suggesting that dissolution of local marine carbonates and reprecipitation along the fault zone may be the ultimate source of carbonate in the Stone Canyon cores.

4. Fluid inclusion geothermometry was attempted on calcite samples from 6 different depths, but no workable inclusions could be found. Analysis of what appeared to be fluid inclusions in calcite cementing one breccia suggested minimum depositional temperature of 200°C, but this result could not be repeated and is thus not reliable.

5. Limited electron microprobe analysis was used to identify and compare the chemical composition of primary biotite and secondary montmorillonite.

6. Analysis of driller's notes, temperature gradient measurements, electrical logs and water levels in the Stone Canyon well show that fluid pressure at the bottom of the well is about 4 bars above hydrostatic and that several fracture systems intercepted during drilling contained fluids at pressures above hydrostatic. Other fracture systems encountered at shallower depths may have been permeable but show evidence of fluids escaping, rather than entering, the column of drilling mud. Fluid permeability of rocks at the bottom of the well was estimated at 10^{-7} cm/sec (about 0.2 millidarcy), but there is some uncertainty in this value due to the unknown condition of the intake at the base of the casing.

7. The Stone Canyon well is artesian, flowing at about 5 l/day. Water flowing from this well is a chloride brine similar to oil-field brines, not water pressurized from precipitation in nearby mountains. Because these brines do not originate in granitic rocks, it is likely that they are directly linked to frac-

tures extending into the seismogenic zone. We speculate that the rotation of least principal stress from horizontal to vertical about 300 m below the surface controls which fractures (vertical or horizontal) inflate in response to pressurized fluids rising from depth. This would mean that wells drilled to monitor fluid pressure or geochemical variations originated at seismogenic depths would have to be at least 300 m in depth. The influence of such a system of fractures (as they respond to changes in stress or fluid pressure) on nearby strain or tilt transducers should also be evaluated.

8. Gravity measurements were taken at 87 new stations on both sides and within the San Andreas fault zone near Lake Hughes, on the locked segment of the San Andreas fault, and at 48 new stations near Stone Canyon on the creeping section of the fault. These data have been interpreted in conjunction with undergound gravity measurements made previously in the Elizabeth Tunnel, where the Los Angeles Aqueduct crosses the San Andreas fault, and in the Stone Canyon well. Subsurface data reduce the ambiguity that limits our ability to distinguish between different structural models in this complex geological regime. Near Lake Hughes, analysis subsurface data shows that the densities of rocks on both sides of the fault are about 0.1 $g\text{-}cm^{-3}$ lower than estimates (published previously) based on hand samples. A minor (5 mgal) gravity low is associated with the fault itself. In the vicinity of Stone Canyon, the gravity decrease associated with the fault is steeper and narrower than reported for profiles to the north and south. This restricts the fault to a virtually vertical plane consistent with its mapped trace, which in turn confirms in situ densities (derived from a previously reported borehole gravity study) about 0.13 $g\text{-}cm^{-3}$ lower than those measured in those hand samples solid enough to prepare and measure. Gravity data are consistent with the hypothesis that rocks such as those collected at Stone Canyon do extend to seismogenic depths, but additional analysis is needed to further restrict and adequately constrain structural models.

Reports:

Kazi, Wallid M., A gravity survey in the vicinity of the San Andreas fault near Lake Hughes, California; M.S. thesis, Dept. of Earth Sciences, The University of California, Riverside, 1985.

Marryott, Robert A., A. E. Williams and D. J. Stierman (abstract), Petrologic and geochemical studies of granitic rocks of the San Andreas fault; EOS, 45, 1097.

Stierman, Donald J. (Abstract), The relevance of measurements in deep boreholes to earthquake prediction research, EOS, 45, 1097.

Stierman, Donald J. (abstract), Natural earthquakes triggered by pore pressure fluctuations, Earthquake Notes, 55, 19.

Stierman, Donald J. and A. E. Williams, Cover photo, EOS, July 24, 1984.

Stierman, Donald J. and A. E. Williams, Hydrologic and geochemical properties of the San Andreas fault at the Stone Canyon well, Pure & Applied Geophysics, 122, 403-424, 1985.

Stierman, Donald J. and J. H. Healy, A study of the depth of weathering and its relationship to the mechanical properties of near-surface rocks in the Mojave Desert, Pure & Applied Geophysics, 122, 425-439, 1985.

Reports in Preparation

Marryott, Robert A., Some petrologic and geochemical characteristics of cataclastic rocks from the Stone Canyon well, San Benito County, California; M.S. Thesis, Dept. of Earth Sciences, The University of California, Riverside, 1986.

EARTHQUAKE FORECAST MODELS

9960-03419

William D. Stuart
U.S. Geological Survey
Branch of Tectonophysics
Pasadena, California 91106
(818) 405-7816

Investigations

1. Analyzing an earthquake instability model for subduction zones. Model is plane strain, and fault dip may vary with position of fault. Fault constitutive law is slip and slip-rate dependent.

2. Analyzing related plane stress model for application to the San Andreas fault near Parkfield, California.

Results

Development and testing of solution methods are nearly completed. Preliminary simulations produce results consistent with some features of geodetic observations.

Reports

Stuart, W. D., Instability model for recurring large and great earthquakes in southern California, Pure Appl. Geophys., 122, 793-811, 1985.

Stuart, W. D., Forecast model for large and great earthquakes in southern California, submitted to J. Geophys. Res., 1986.

An Experimental and TEM Study of Cataclastic Flow in Quartzo-Feldspathic Rocks

Jan Tullis

Department of Geological Sciences
Brown University
Providence, RI 02912
(401) 863-1921
14-08-0001-G-1180

Investigations

In order to understand the factors governing whether fault slip is stable or unstable, it is important to determine the operative grain scale deformation mechanisms and relate these to the empirical constitutive laws. One of the important deformation mechanisms within the gouge along fault zones is cataclastic flow, which involves distributed, intragranular cracking and rotation and frictional sliding of the resulting fragments. We have undertaken an experimental study, over a wide range of T and P, of the conditions and mechanisms of cataclastic flow in feldspar and in quartz aggregates. Because the deformation products include extremely fine-grained material, transmission electron microscopy (TEM) is an important part of the study. We have been working on three different aspects of the problem to date:

1. Location and nature of the transition from brittle faulting to ductile cataclastic flow for anorthosites, over a range of T and P.

2. Location and nature of the transition from cataclastic flow to dislocation creep of albite aggregates, as a function of increasing T at moderately high P.

3. Location and nature of the transition from brittle faulting to cataclastic flow, and from cataclastic flow to dislocation creep, for quartz aggregates, as a function of T and P.

Results

1. Anorthosites (An_{77}) have been deformed at a strain rate of 10^{-5}/sec, at pressures of 500, 1000, and 1500 MPa and temperatures from 24 to 700°C. One of the major results to date is that confining pressure alone, at room temperature, is insufficient to stabilize cracking and produce cataclastic flow; at all three pressures investigated, the anorthosite samples failed suddenly and audibly, with the formation of a through-going fault, and subsequent deformation involves unstable sliding with quasi-periodic audible stress drops. These results on the effect of increasing pressure at room temperature are in agreement with those on other silicate rocks such as granite (which fails brittley to pressures of at least 2500 MPa). However, they are in contrast to the early results of Heard on Solnhofen limestone, which showed a transition to ductile behavior (presumably cataclastic flow, since the strength was pressure sensitive) at about 100 MPa.

Our results to date on anorthosite show that the transition to cataclastic flow is promoted by increasing temperature at moderate to high pressure. At 300-500°C at 500, 1000, and 1500 MPa, samples show some distributed grain-scale faulting and some ductile shear zones of more localized deformation; the localization seems to be governed in part by the occurrence of grains with their cleavage planes in appropriate orientations. At 700°C at 1000 and 1500 MPa, samples show uniformly distributed cataclastic flow; the original twins in all the grains serve as markers to show that the deformation has occurred almost entirely by grain-scale faulting on the cleavages. We are about to begin TEM investigations of some of these samples to determine whether the transition from brittle faulting to cataclastic flow with increasing temperature is associated with the onset of dislocation generation and limited mobility, and if so just what the interaction is with progressive strain.

2. Albite aggregates have been deformed to moderately high strains at 1500 MPa, at strain rates of 10^{-5} and 10^{-6}/sec and temperatures from 500 to 1000°C; detailed optical and TEM analyses have been done on the deformed samples in order to elucidate details of the transition from cataclastic flow to dislocation creep. There are several important conclusions to date. First, the optical microstructures in the two fields are the opposite of what is generally expected. In the cataclastic flow field the original grains undergo a very homogeneous flattening; this apparently occurs by grain-scale faulting which involves such close spacing and small individual offsets that it is often barely detectable optically. These microstructures are very similar to those expected for the lower temperature portions of the dislocation creep regime, based on previous results for quartz aggregates. On the other hand, in the dislocation creep field, the original grains remain as internally undeformed augen, while undergoing recrystallization along the margins, and the (weaker) recrystallized grains take up almost all of the sample strain. These microstructures are very similar to what one would have expected for "cataclasis" along original grain margins. These experimental results may be helpful in guiding more accurate interpretations of deformation mechanisms and conditions from observations of microstructures in naturally deformed feldspathic rocks.

TEM observations have helped to elucidate the processes occurring within the cataclastic flow regime as well as the nature of the transition to dislocation creep. Although low strain samples show the onset of limited dislocation mobility at about 500°C at 1500 MPa and 10^{-6}/sec, samples shortened 50% or more at these conditions show few visible dislocations; instead, there are regions a few um across with no deformation features, directly against regions or semi-planar zones of extremely finely crushed material (average grain size < 0.1 um). This crushing is not at all obvious as such on the optical scale; rather it produces apparently continuous although patchy undulatory extinction, and thin deformation bands along the grain-scale faults. Thus interpretations of optical microstructures from low-grade naturally deformed rocks must be made with caution.

The transition from cataclastic flow to dislocation creep is associated with changes in mechanical behavior. At conditions where dislocation mobility is extremely limited, cataclastic flow produces steady state flow. However, with increasing temperature, samples show marked strain weakening behavior; this appears to result because the extremely fine crushed material is able to undergo dynamic recrystallization. These results may have important implications

for the localization of ductile deformation along the sites of earlier brittle fractures.

3. Preliminary experiments have been done on quartzites and a novaculite. One significant conclusion from these experiments is the role of porosity in inducing cataclastic flow. Previous room temperature experiments by Hadizadeh and Rutter on a quartzite with 7% porosity showed a transition from brittle fracture to ductile cataclastic flow at a pressure of about 600 MPa (at a strain rate of 10^{-4}/sec). Our room temperature experiments on a quartzite with about 1% porosity show brittle fracture up to 1000 MPa (at a strain rate of 10^{-5}/sec). Therefore it appears that the crushing associated with pore collapse during pressurization of the porous quartzites must serve to stabilize cracking and prevent the formation of a single through-going fracture.

Reports

Tullis, J. and Yund, R.A., 1985, Cataclastic flow of feldspar: an experimental study: Geol. Soc. Amer. Abst. with Prog., 17, 737-738.

Hadizadeh, J. and Tullis, J.A., 1986, Transition from fracture to cataclastic flow in Anorthosite: both P and T are required: Amer. Geophys. Union Trans., 67, 372-373.

EXPERIMENTS OF ROCK FRICTION CONSTITUTIVE LAWS APPLIED TO EARTHQUAKE INSTABILITY ANALYSIS

USGS Contract 14-08-0001-G-1185

Terry E. Tullis
John D. Weeks
Department of Geological Sciences
Brown University
Providence, Rhode Island 02912
(401) 863-3829

Investigations

1. We have continued work on determining the detailed constitutive behavior for frictional sliding of calcite marble, kaolinate clay and artificial crushed granite gouge.

2. We have investigated the high velocity frictional behavior of granite by numerical modeling of experimental stick slip events, using a modification of the Ruina state variable constitutive law.

3. We have continued our theoretical investigation of the stability of a spring-and-slider block frictional system, using the theories developed by Gu, et al. (1984). Since our modeling of experimental data has shown that two state variables are needed to match our experimental results, we are examining how changes of the values of the constitutive parameters affects the stability of a frictional system characterized by two state variables.

Results

1. We have made an important step in understanding the micromechanical processes of frictional sliding by finding that we are able to relate the strength of intact samples of calcite aggregates to **a** in the friction constitutive law, supporting the notion that plastic deformation of calcite at the real area of contact on frictional surfaces is appropriate to explain the frictional resistance. We were able to do this for calcite because the strength, ductility, and deformation mechanisms of calcite are well known as a result of a large number of studies; we have used results of Heard and Raliegh (1972) for flow of calcite at 25^0 C. Since we do not know the real area of contact on the sliding surface we cannot directly compare the frictional results with the flow data. Instead, we compare the fractional change in frictional resistance per decade change in sliding velocity to the fractional change in intact sample strength per decade change in strain rate. Reasonable estimates of the strain rate in our experimental slip zone indicate that the flow data covers an appropriate range of strain rates for this comparison. From Heard and Raliegh's flow data, we conclude that the fractional change in resistance per decade change in strain rate is 0.0174, implying that the ratio of **a** to the coefficient of friction should be 0.0076. For our experiment at 15 MPa normal stress, μ was .78 so that the predicted value of **a** is .006. The actual value that we find for **a** as determined from the data in Figure 1 is between 0.008 and 0.009, good agreement considering the nature of the two data sets and the preliminary nature of the comparison. An interesting further implication of this agreement is that the real area of contact of our samples is about 24 percent of the apparent area, determined from the ratio of the frictional strength to the flow strength of intact samples. This is in good agreement with real area of contact on Indiana limestone as a function of normal stress found by Logan and Teufel (1986) using an entirely different method. However, this could be inaccurate if the strength of the bonding across the sliding surface is not the same as for an intact sample, as might happen if surface contaminants reduced the bond strength or if geometric irregularities added to the sliding resistance.

2. In our continuing effort to develop constitutive laws that accurately reflect frictional behavior, we have made simulations of stick slip events in granite using a constitutive law having a transition from velocity weakening at low velocity to velocity strengthening at high velocity. Our evidence for the existence of such a high velocity transition is shown in Figure 2, where we compare an experimental sequence of abrupt increases in load point velocity with a series of theoretical simulations. If the slope of the steady state line were constant as is the case for the constitutive equations presented by Ruina, each of the velocity steps in the sequence should be identical, and neglecting inertia, the stress would drop to zero. Simulations made with a constitutive law having a high velocity transition, the results of which are shown below the data in Figure 2, reproduce the small stress drops at higher velocity as well as the nearly constant minimum stress regardless of the maximum stress reached. To produce such a transition in our numerical simulations, the magnitude of **b** in the state variable friction law was changed over a range of velocity according to the equation $\mathbf{b} = \mathbf{b}_0 / (1 + (V/V_t)^E)$ where V_t is the velocity at which **b** has fallen to one half its low velocity value and E is a measure of the velocity range over which **b** falls from $\mathbf{b}_0$ to zero. We feel it is more reasonable that at higher velocity the frictional resistance be velocity strengthening rather than independent of velocity as has been assumed by others since the data for dolomite and calcite (our work) and halite (Shimamoto and Logan, 1986) show such behavior, and there is no reason to suppose that the strength of the deforming material at the sliding surface should lose its rate dependence at high velocity. In addition to the success in simulating features of the friction-displacement curves, the phase plane plot is of interest as well, as shown in Figure 3. The stability boundary derived from the Ruina law having no dependence on absolute velocity is still important. The minimum stress reached by trajectories starting below the boundary is strongly dependent on the starting point, whereas those above the boundary fall to a nearly constant minimum stress. Also, trajectories above the boundary are concave upward during the first acceleration, whereas those below are concave downward, a difference that might be useful as a short term precursor for earthquakes. A significant departure from the Ruina law caused by the high velocity transition to velocity strengthening is that even for trajectories that start above the stability boundary, sliding eventually stops accelerating and the trajectory drops below the boundary. Thus, the modified law provides a means of recovery from instability.

3. We have continued our numerical investigation of the stability and behavior of a frictional system in which two state variables describe the frictional response of the sliding surface. It has been found that the values of the constitutive parameters are widely variable and appear to be functions of rock type, fault roughness, gouge composition, the presence of pore fluids and temperature. For this reason, it is desirable to understand how different values of the parameters affect the stability and behavior of sliding. It is difficult to study the effects of the parameters **a**, $\mathbf{b}_1$, $\mathbf{b}_2$, L_1, and L_2 individually, because changing any single one changes the critical stiffness and consequently affects stability in much the same way as changing machine stiffness. It is possible, on the other hand, to change pairs of parameters in such a way that K/K_{cr} remains unchanged. For the following discussion, K/K_{cr} was held constant while $\mathbf{b}_1$ and $\mathbf{b}_2$ or L_1 and L_2 were changed. In Figures 4 and 5 stability surfaces are shown for which K/K_{cr} was held constant at 1.63, the same value as has been used in simulations of experimental granite data, using the stiffness of our experimental apparatus. Increasing $\mathbf{b}_2$ while decreasing $\mathbf{b}_1$ so as to maintain a constant value of K/K_{cr} has two effects: The sharp drop-off at high values of ψ_2 is moved towards the origin and the slope along the $\phi = 0$ plane is steepened. In fact, it was found that this slope is 0.9 times $\mathbf{b}_2$, regardless of the value of $\mathbf{b}_1$ and K/K_{cr} (this relationship depends on the values chosen for L_1, L_2, and **a**). The net effect is that in Figure 4a the region that will evolve stably is smaller than in Figure 4b which has a larger value of $\mathbf{b}_1$. Similar effects are found if L_1 and L_2 are changed, as in Figure 5, although in this case the slope of the surface is only slightly affected, the main difference between Figures 5a and b being that a longer L_2, as in Figure 4b, moves the drop-off away from the origin, resulting in a larger volume of stable points.

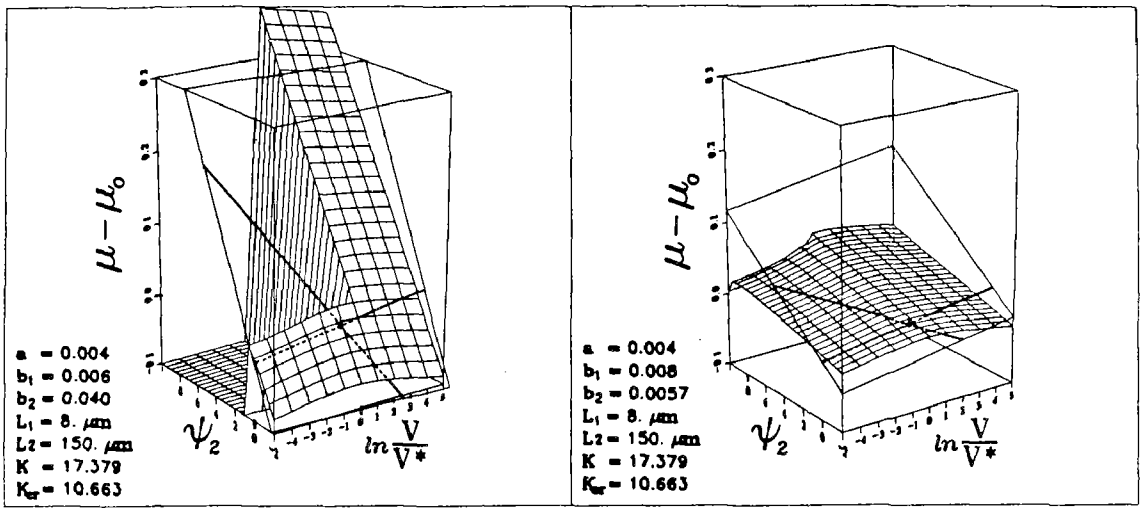

Figure 4. Stability surfaces for a frictional system described by a two state variable law, plotted on axes of $\phi = \ln(V/V_*)$, $\mu - \mu_o$, and ψ_2 (the more slowly evolving state variable). The steady state and constant state lines have been drawn in and dashed where they lie below the surface. The origin is indicated by a dot at the intersection of these lines. This pair of surfaces is drawn for two different values of b_1 and b_2, while keeping the value of K/K_{cr} constant at 1.63. Changing these values affects the position of the steady state line, the slope of the stability surface in the ψ_2 direction, the position of the surface drop-off, and the height of the surface above the origin. The plane upon which $\psi_1 = \psi_2$ has been indicated; the steady state and constant state lines lie in this plane.
A. $b_1 = 0.006$, $b_2 = 0.040$.
B. $b_1 = 0.008$, $b_2 = 0.0057$.

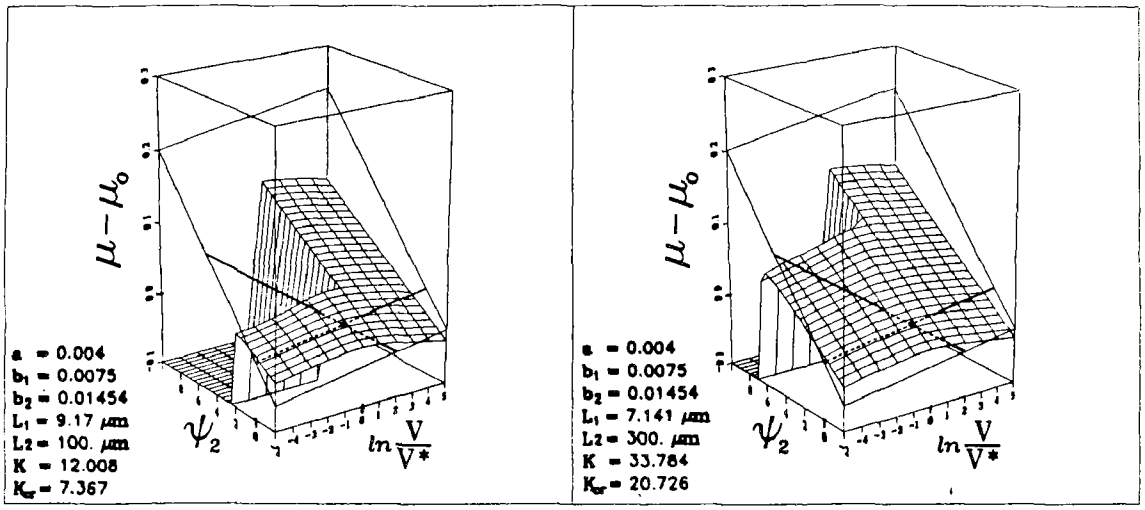

Figure 5. Stability surfaces for differing values of L_1 and L_2, while keeping K/K_{cr} constant at 1.63. The principal effect of changing these values is to alter the position of the surface drop-off. The positions of the the steady state and constant state lines do not depend on L_1 and L_2, so they are unchanged in these two figures.
A. $L_1 = 9.17\ \mu m$, $L_2 = 100\ \mu m$.
B. $L_1 = 7.141\ \mu m$, $L_2 = 300\ \mu m$.

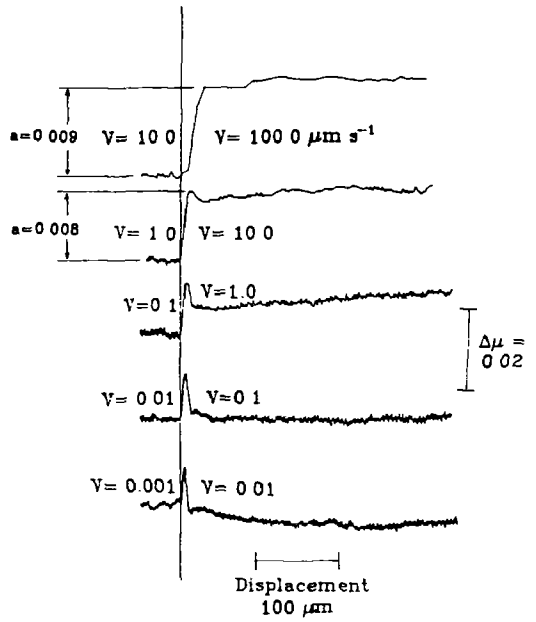

Figure 1. Traces from an experiment on calcite marble at 15 MPa normal stress showing the effect of ten-fold increases in load point velocity over a wide range of starting velocities. As the velocity increases, the magnitude of the short term stress relaxation due to an evolving state variable decreases until between 10 and 100 μm s^{-1} the transient effect has entirely disappeared, leaving only the instantaneous direct effect. There also appears to be a longer term evolution that changes sign with velocity so that at 0.01 μm s^{-1} there is a long term decrease and by 1.0 μm s^{-1} there is a long term increase.

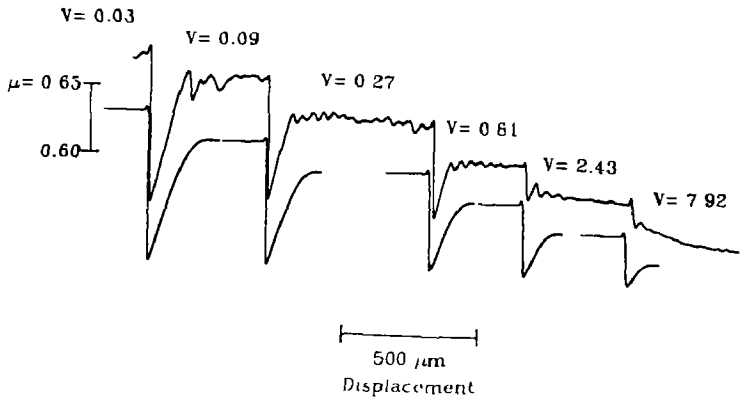

Figure 2. Unstable events following each of a series of three-fold increases in load point velocity; upper continuous traces are data from an experiment on Westerly granite, lower traces are simulations calculated using the modified constitutive law. The parameters used to calculate the simulations are **a**= 0.004, b_o = 0.024, L = 40 μm, V_T = 100 μm s^{-1}, and E = 1.4. For the first three velocity changes, the simulations match the changing stress drops very closely. At V= 2.43 the simulation fails to match the abrupt change to stable sliding. It also does not incorporate a second state variable capable of reproducing the long term relaxation seen especially strongly at V= 7.29 μm s^{-1}. Two-fold jumps earlier in the same experiment were stable, in agreement with simulations.

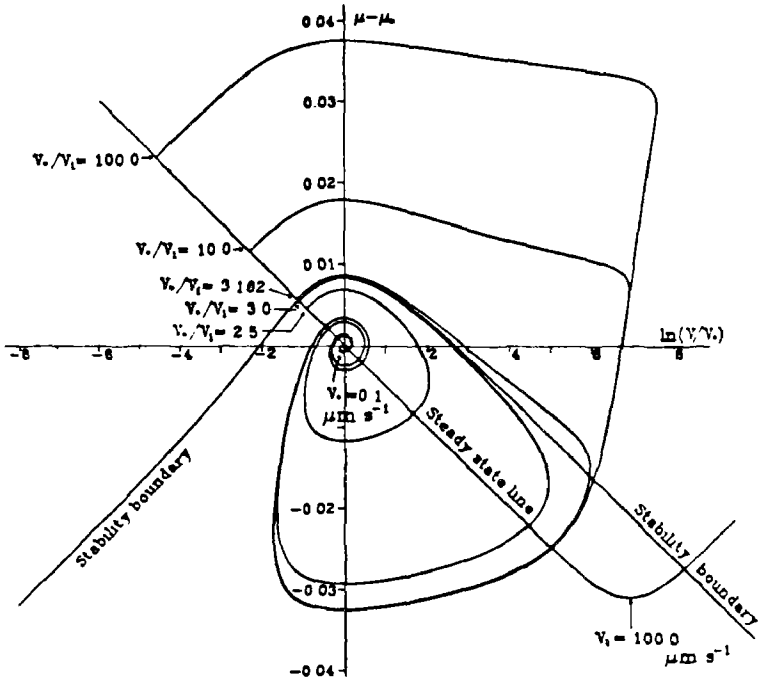

Figure 3. Calculated trajectories on the phase plane for several load point velocity jumps of different sizes, for a constitutive law having a transition from velocity weakening at low velocity to velocity strengthening at high velocity. All the trajectories are evolving to steady state at V_* = 0.1 μm s^{-1}. The stability boundary is shown for a constitutive law having a linear relation to log velocity, as in Gu et al. (1984). At low velocity, the modified steady state line coincides with the linear law while at high velocity there is a transition to a slope of **a**. For trajectories above the boundary, the high velocity accelerating portion is concave up and the minimum stress is the same for any starting velocity V_1 while below the boundary the curves are concave down and the peak velocity and minimum stress depend strongly on starting velocity. This can be compared with Figure 1, in which trajectories are shown that were calculated using the linear steady state line, and the unstable trajectories go to infinite velocity, always above the stability boundary.

Stress and Pore Pressure Changes Due to Annual Water Level Cycles in Seismic Reservoirs

Contract 14-08-0001-22022

Evelyn A. Roeloffs, Taechin F. Cho and Bezalel C. Haimson
University of Wisconsin-Madison
1509 University Avenue
Madison, WI 53706
608-262-2563

Investigations

Two-dimensional finite element modeling of strength changes caused by a time-dependent reservoir load on the surface of a porous elastic half-space have been carried out. Three types of models are considered: a uniform half space, layered half spaces, and a full space into which thin dipping layers of high diffusivity have been introduced in order to model the hydraulic behavior of faults and joints. Strength changes have been calculated for normal, reverse, and strike-slip faulting environments for a reservoir load that increases over a period of about three years to either a steady or an annually varying level. Current investigations are addressing the effects of rapid changes in water level.

Results

Using a two-dimensional finite element program that solves the coupled equations of elasticity and fluid flow, we have calculated time dependent strength changes produced by reservoir impoundment for several layered porous elastic half spaces. The models under study have near-surface layers with relatively high diffusivity and Skempton's constant; these layers quickly equilibrate to pore pressures comparable to those at the bottom of the reservoir and are the sites of broad zones of weakening for many fault orientations. The presence of such near-surface layers can also decrease the time required for deeper, less permeable layers to experience elevated pore pressure. For the layered models considered so far, the largest strength changes are comparable in size to those in a uniform half space, but may be more or less extensive and may occur at different times. The differences between strength change distributions in layered as opposed to uniform media is due primarily to modification of the fluid pressure distribution by non-uniform diffusivity. The stress fields in the two types of media are similar.

In a second type of non-uniform model, the hydraulic properties of joints and faults are simulated by introducing elements of high aspect ratio. The diffusivity of these elements is 1000 times greater than that of the surrounding medium, but the same elastic properties are used for all elements. In the model studied, these elements dip 60 degrees. Water level is assumed to rise exponentially to a steady level with a time constant of one year. For this type of model, fluid diffusion is facilitated along

the highly diffusive layers. The resulting effective stress decrease diminishes strengthening and intensifies weakening near these layers. However, the strength changes for the model with highly diffusive layers are of the same order of magnitude as those for the uniform half space.

Reports

Roeloffs, E. A., 1985, Stress and Pore Pressure Changes Due to Annual Water Level Cycles in Seismic Reservoir, (abstract), EOS, Trans. Am. Geophys. Union, Vol. 66, No. 18.

Deep Hole Desalinization of the Dolores River

9920-03464

William Spence
National Earthquake Information Center
U.S. Geological Survey
Denver Federal Center
Box 25046, Mail Stop 967
Denver, Colorado 80225
(303) 236-1506

Investigations

This project relates to monitoring the seismicity of the region of the intersection of the Delores River and Paradox Valley, southwest Colorado. The project is a component of the Paradox Valley Unit of the Colorado River Basin Salinity Control Project and is being performed for the U.S. Bureau of Reclamation with support from the Induced Seismicity Program of the USGS. In this desalinization project, it is proposed to pump approximately 30,000 barrels/day from brine-saturated rocks beneath the Dolores River through a borehole to the Madison-Leadville limestone formation of Mississippian age, some 15,000 feet below the surface. There is a possibility of seismicity being induced by this desalinization procedure, especially in the long term. The project objectives are to establish a pre-pumping seismicity baseline and, during the pumping phase, to closely monitor the discharge zone for possible induced seismicity. If induced seismicity does occur, it should be possible to relate it to formation characteristics and to the pumping pressure and discharge rates.

Results

A 10-station seismograph network is centered at the location of the proposed injection well. This high-gain network has a diameter of about 80 kilometers, and has been in operation since September 1983. Seismic data are brought to Golden, Colorado, via microwave and phone line transmission. These data are fed through an A/D converter and then through an event detection algorithm. The network has operated at high quality, except for two periods when it was decommissioned by lighting strikes. Analysis procedures have been considerably complicated by a high rate of blasting activity in the region, but means have been developed to distinguish the occurrence of natural earthquakes to good reliability.

Notable regional earthquake activity are a swarm of shallow events (maximum magnitude 3.2) near Carbondale, Colorado, a magnitude 3.4 shallow earthquake near Blue Mesa Reservoir, Colorado, and a magnitude 2.8 earthquake that was preceded by three events and followed by four events all located about 25 km SE of Grand Junction, Colorado. In the vicinity of the network, the earthquake catalog is complete to about magnitude 2.0. Most of the seismicity in the area of the network is in the shallow crust. However about 10 earthquakes have focal depths greater than 20 km, with several events at the depth intervals 30-35 km and 50-55 km. These results indicate

that microearthquakes are distributed throughout the crust of the Colorado Plateau, with an occasional event in the upper mantle. The shallow and deeper earthquakes follow a diffuse north-south trend, parallel to the eastern boundary of the Colorado Plateau. These early results, combined with a lack of historical seismicity at the zone of the Paradox Valley seismic network, indicate that any seismicity induced by deep-well injection near Paradox Valley should be identifiable as such.

Report

Martin, Richard A., Jr., and Spence, William, 1986, Seismicity studies in the eastern Colorado Plateau of southwestern Colorado [abs.]: Rocky Mountain Section of GSA Annual Meeting, Flagstaff, Ariz.

Spence, W., and Chang, P-S., 1985, Seismic monitoring in the region of the Paradox Valley, Colorado (Annual report, July 1984 - June 1985, U.S. Bureau of Reclamation, Deep well injection site, Paradox Valley Unit, Colorado River Basin Salinity Control Project), 11 p.

Regional and National Seismic Hazard and Risk Assessment

9950-01207

S. T. Algermissen
Branch of Engineering Geology and Tectonics
U.S. Geological Survey
Denver Federal Center, MS 966
Denver, CO 80225
(303) 236-1611

Investigations

1. A field intensity survey was undertaken following the January 31, 1986, Chardon, Ohio earthquake (m_b=4.9, NEIS).

2. A portable, microcomputer-based system for rapid field collection and evaluation of post-earthquake damage data is under development.

3. Continuing investigations into statistical treatment of errors using historical earthquake data in seismic hazard analysis.

4. Continuing development of a program to produce hazard maps from historical earthquake locations by specifying probabilistic variability of future earthquake locations and magnitudes in lieu of defining seismic source zones.

Results

1. A preliminary isoseismal map of the 1986 northeastern Ohio earthquake (fig. 1) was prepared. The highest intensity found, Modified Mercalli intensity VI, occurred within approximately a 15-km (10-mi) radius from the instrumental epicenter. An extension of the area of intensity VI appears on the southeast. Damage within the intensity-VI isoseismal consisted primarily of wall cracks, cracked or fallen plaster, fallen ceiling tiles, and fallen loose chimney bricks. Fallen plaster generally occurred only in older buildings. Popping out of light-weight ceiling tiles, usually along the juncture between the ceiling and an outside wall, occurred where the intensity based on other indicators was V or VI.

The isoseismals in figure 1 are shown as dashed because additional data will soon be available from the results of the USGS intensity questionnaire survey. When all the data have been combined, the isoseismals will be finalized.

The "valley" of low intensities running from southwest to northeast across the isoseismals may also appear somewhat different with the inclusion of questionnaire data. There is no apparent correlation of this area of low intensity with regional bedrock geology. However, an area of kames and eskers corresponds to the southwestern section of the low in the intensity pattern.

2. The microcomputer-based damage survey system permits damage data to be rapidly entered from standardized forms using an optical scanner. A digitizing tablet and plotter permits the entering and replotting of maps to control the damage survey and insure complete coverage. Data can be subjected

to preliminary analysis in the field which will provide feedback while conducting the survey. Data can also be transmitted via modem to the mainframe VAX computer for further analysis. The hardware components of this system have been brought into operation and software for communication between devices and decoding of input has been implemented. Standardized damage survey forms have been completed for single family dwellings. Forms are under development for damage assessment of steel-framed and reinforced concrete structures.

3. Results of investigations on the effects of observational errors in fitting magnitude relationships, presented in FY-85 Semi-Annual Technical Reports are summarized in a journal paper that is currently under revision following internal technical review.

4. Using modest values of earthquake location variability the development of hazard maps based on historical earthquake locations can help reveal spatial patterns in historic data which may correlate with geologic structure. Larger values of location variability results in smooth regional hazard maps that provide useful comparisons with maps produced using standard hazard estimation techniques that require delineation of seismic source zones.

Reports

Algermissen, S. T., 1986, Some problems in ground motions assessment in the United States [abs.]: Earthquake Notes, v. 57, no. 1, p. 24.

Bender, Bernice, 1986, Modeling source zone boundary uncertainty in seismic hazard analysis: Seismological Society of America Bulletin, p. 329-341.

Campbell, K. W., 1986, An empirical estimate of near-source ground motion for a major, m_b=6.8, earthquake in the Eastern United States: Seismological Society of America Bulletin, v. 76, p. 1-17.

Hanson, S. L., and Perkins, D. M., 1985, Auxiliary programs for support of seismic hazard analysis: U.S. Geological Survey Open-file Report 85-615, 115 p.

Hopper, M. G., 1985, Estimation of earthquake effects associated with a great earthquake in the New Madrid seismic zone, in Hays, W. W., and Gori, P. L., eds., A workshop on "Continuing actions to reduce potential losses from future earthquakes in Arkansas and nearby states": U.S. Geological Survey Open-File Report 83-0846, p. 31-112.

Hopper, M. G., and Algermissen, S. T., 1985, Kinds of damage that could result from a great earthquake in the central United States: Earthquake Information Bulletin, v. 17, no. 3, p. 84-97.

Oaks, S. D., and Algermissen, S. T., 1986, Site response in the Salt Lake City area determined from intensity data from historic earthquakes: Earthquake Notes, v. 57, no. 1, p. 14.

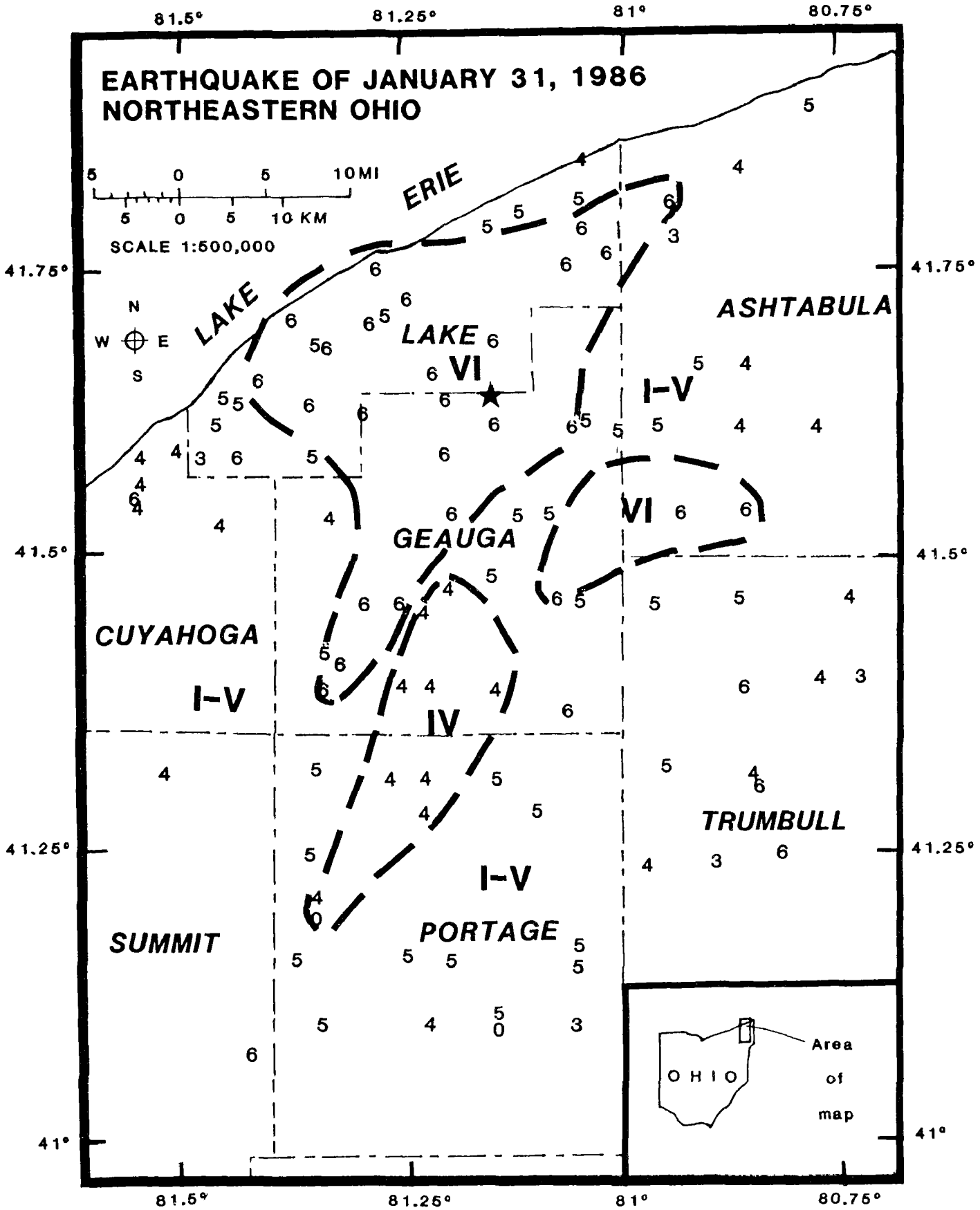

Figure 1.--Preliminary interior MM isoseismals for the earthquake of January 31, 1986, *northeastern Ohio*. Site intensities are shown by Arabic numerals. Isoseismal intensities are denoted by Roman numerals. Star shows the location of the main shock epicenter. The isoseismal lines are shown as dashed because all the data are not yet in. When the data set is complete the lines will be finalized.

Regional and Local Hazards Mapping in the Eastern Great Basin

9950-01738

R. Ernest Anderson
Branch of Engineering Geology and Tectonics
U.S. Geological Survey
Box 25046, MS 966, Denver Federal Center
Denver, CO 80225
(303) 236-1684

Investigations

1. Continued field mapping and analysis of data pertaining to earthquake hazards along the Wasatch fault zone. (Machette, Nelson, Personius, Scott)

2. Continued analysis of surface-rupture data and other effects of the 1983 Borah Peak, Idaho, earthquake. (Crone, Machette, and Bucknam)

3. Continued analysis and interpretation of exploratory trenching across the Lost River fault, Idaho. (Schwartz and Crone)

4. Continued analysis of data bases that might reflect segmentation of the Wasatch fault zone. (Wheeler)

5. Completed report describing neotectonic framework and its relationship to seismicity, central Sevier Valley, Utah. (Anderson and Barnhard)

6. Continued development of statistical and other procedures to identify significant or reproducible concentrations and alignments of epicenters. (Wheeler)

Results

1. Compilation of a set of 1:50,000-scale maps of Quaternary deposits and fault traces along the Wasatch fault zone is proceeding according to schedule with "final" decisions as to stratigraphic framework and publication format agreed upon. These maps show six types of genetic units (alluvial terrace and fan, lacustrine, colluvium, glacial, and eolian) divided into as many as six age categories (late Holocene, mid to early Holocene, Provo, Bonneville, young pre-Bonneville, and old pre-Bonneville). Fault data, such as amount of offset, scarp height, and scarp morphology, are shown at selected points along the fault zone. Also included are detailed geologic maps at 1:10,000 scale at key localities along individual segments of the fault zone.

   Mapping of the Weber segment of the Wasatch fault zone (Kaysville segment of previous report, southern two-thirds of Ogden segment of Schwartz and Coppersmith, 1984) is proceeding on schedule. Detailed mapping of scarps at the northern end of the segment indicates that (1) the mountains that make up the Pleasant View salient just north of North Ogden mark a nonconservative barrier to rupture propagation on this

segment, and (2) there have been at least two and probably three late Holocene surface-faulting events on this part of the segment.

A radiocarbon age of 2,110+100 yrs BP on a buried A horizon has been obtained from the exposure of the fault at Garner Canyon in Ogden described in the previous report. Two scarp-derived colluvial wedges overlying the dated horizon indicate that there have been two surface-faulting events of 1-1.5 m on the fault at this site in the last 2,000 yrs or less. Two other ages are pending. The ages of these events are similar to those obtained by trenching the central part of this segment near Kaysville (Swan and others, 1980).

Over 120 scarp profiles have been measured across the Weber segment of the fault using the computer-assisted PG-2 photogrammetric plotter in Central Regional Geology Branch (with the help of Chuck Pilmore). Comparison with field-measured profiles shows that scarp height and displacement values obtained from plotter-measured profiles are about the same as field values for scarps greater than 5 m high. In some areas, older photography has been used to measure profiles across scarps that were destroyed over 30 yrs ago.

2. and 3.
Analysis of the 1983 Borah Peak earthquake and paleoseismic data from the area has led to an improved understanding of the segmented characteristics of the Lost River fault zone and has strengthened the conclusion that the fault zone represents an extremely valuable analog for comparison with the Wasatch fault zone.

4. For most or all of the history of the Wasatch fault, four large footwall salients between Nephi and Brigham City have acted as persistent segment boundaries. Other segment boundaries, mostly near the north and south ends of the fault, might have been active sporadically during Quaternary time.

These conclusions arise from examining transverse anomalies (TA's) in six data types: Bouguer gravity, aeromagnetic intensity, instrumental seismicity, shape of the fault trace (salients), smoothed topography of the Wasatch Range and San Pitch Mountains, and pre-Cenozoic structures. The resulting 26 TA's satisfy seven geological and statistical criteria. These criteria insure that the TA's reliably reflect the operation of major segment boundaries that persisted through most or all of the Cenozoic evolution of the Wasatch fault.

Median width of the 26 TA's is 11 km, or 3 percent of the fault's length in Utah. A few TA's in various data types likely would coincide along the fault just by chance, but at four places TA's in 4-6 data types coincide: the Pleasant View, Salt Lake City, Traverse Mountains, and Payson salients. Accordingly, at these four places probably the Wasatch fault has been persistently segmented. The most likely way for these salients to cause segmentation is as nonconservative barriers to rupture propagation, across which slip vectors change orientation (King and Nabelek, 1985, Science, v. 228, p. 984-987).

The six data types are associated pairwise to various degrees, depending on how many of their TA's coincide along the fault. Aeromagnetic intensity and pre-Cenozoic structures are perfectly associated, followed by Bouguer gravity and aeromagnetic intensity. No data type is strongly associated with instrumental seismicity, but salients come closest (Jaccard coefficient = 0.60). The data types whose TA's are most characteristic and most diagnostic of the persistent segment boundaries are aeromagnetic intensity, instrumental seismicity, and salients. No data type has TA's that are strongly diagnostic or strongly characteristic of the segments between or beyond the persistent segment boundaries.

Other workers have sought evidence of the operation of segment boundaries in more recent parts of the geologic record along the Wasatch fault (Mayer and Maclean, 1986, Geological Society of America Abstracts with Programs, v. 18, no. 2, p. 155; Machette, Personius, and Nelson, as summarized in volume XXI of this series, U.S. Geological Survey Open-File Report 86-31, p. 474; Schwartz and Coppersmith, 1984, Journal of Geophysical Research, v. 89, p. 5681-5698). These more recent records show segment boundaries at the four salients, but also show boundaries variously in the northern and southern parts of the fault, beyond the salients. Thus, the central, most populous part of the Wasatch fault is characterized by persistent segment boundaries, whereas the less populous end parts of the fault might contain nonpersistent segment boundaries that have been active sporadically during Quaternary time.

5. Two areas of concentrated seismicity in central Sevier Valley coincide with anomalous concentrations of late Quaternary deformation suggesting a genetic relationship. Both areas contain late Quaternary fault scarps suggestive of normal faulting and microseismicity suggestive of strike-slip faulting, and each is broadly consistent with east-west extension. Both areas are located at complex structural junctures where the geometry and vergence directions of major structures show dramatic on-strike contrast. Transverse zones of structural accommodation in which stress is likely concentrated are required in both areas and probably explain the concentration of seismicity and late Quaternary deformation.

6. In the Midcontinent and East some epicentral alignments are accepted by most workers but others are less obvious and of disputed validity. Although perceived alignments are subjective, if they can be shown to be reproducible they can be taken to be reliable, and might identify seismogenic fault zones. To develop and test procedures for identifying reproducible epicentral alignments, a convenient data set is one with no uncertainties in map locations. Mapped locations of outcrops of uraniferous breccia pipes near the Grand Canyon constitute such a data set. On a map of 92 pipe locations, nine independent interpreters each drew perceived alignments and assigned each alignment to a certainty class (certain, probable, or possible). Of several criteria for distinguishing reproducible from nonreproducible alignments, the most effective selects those alignments that were assigned to the same certainty class by a majority of interpreters. Of 126 alignments, six satisfy this criterion. Thus, if enough interpreters are used, it should be feasible to demonstrate the reproducibility and reliability of subjectively perceived alignments of epicenters.

Reports

Anderson, R. E., and Barnhard, T. P., 1986, Genetic relationship between faults and folds and determination of Laramide and neotectonic paleostress, western Colorado Plateau-transition zone, central Utah: Tectonics, v. 5, no. 2, p. 335-357.

Forman, S. L., and Machette, M. N., A review of thermoluminescence dating, in Morrison, R. B, ed., Quaternary non-glacial geology of the conterminous United States, Chapter 17--Dating methods applicable to the Quaternary: Geological Society of America, Decade of North American Geology, 15 ms p., 2 figures (Branch Approval).

Machette, M. N., 1986, History of Quaternary offset and paleoseismicity along the La Jencia fault, central Rio Grande rift, New Mexico: Bulletin of the Seismological Society of America, v. 76, no. 1, p. 259-272.

Machette, M. N, in press, Quaternary movement along the La Jencia fault, New Mexico: U.S. Geological Survey Professional Paper 1440, 150 ms. p., 17 figures, and 23 tables (Directors Approval).

Machette, M. N., Rosholt, J. N., and Bush, C. A, 1986, Uranium-trend ages of Quaternary deposits along the Colorado River, Grand Canyon National Park, Arizona [abs.]: Geological Society of America Abstracts with Programs, v. 18, no. 5, p. 393.

Nelson, A. R., and VanArsdale, R. B., 1986, Recurrent late Quaternary movement on the Strawberry normal fault, Basin and Range-Colorado Plateau transition zone, Utah: Neotectonics, v. 1, no. 1, p. 1-30.

Nelson, A. R., 1986, Use of lithofacies codes in paleoseismological studies of normal faults in unconsolidated sediments [abs.]: Geological Society of America, Abstracts with Programs, v. 18, no. 2, p. 163.

Nelson, A. R., and Sullivan, J. T., Late Quaternary history of the James Peak fault, southernmost Cache Valley, north-central Utah, in, Hays, W. W., and Gori, Paula, eds., Assessment of regional earthquake hazards and risk along the Wasatch Front, Utah: U.S. Geological Survey Professional Paper (Branch Approval).

Personius, S. F., 1986, The Brigham City segment--a new segment of the Wasatch fault zone, northern Utah [abs.]: Geological Society of America Abstracts with Programs, v. 18, no. 5, p. 402.

Wheeler, R. L., 1986, Selecting reliable alignments of mapped points: Structural control of breccia pipes on the Marble Plateau, northern Arizona [abs.]: Geological Society of America Abstracts with Programs, v. 18, no. 5, p. 422.

Implementation of Research Results and Information Systems for Regional and Urban Earthquake Hazards Evaluation, Southern California

9950-03836

William M. Brown III
Branch of Engineering Geology and Tectonics
345 Middlefield Road, MS-998
Menlo Park, California 94025
(415) 856-7112/7119

Investigations:

This project is part of a long-range regional earthquake hazards evaluation for Southern California, directed by the U.S. Geological Survey. This phase of the project is oriented towards (1) Summarizing results of recent earth-science research on evaluating earthquake hazards; (2) Presenting examples of ongoing earthquake-hazard reduction efforts; and (3) Determining what additional scientific and technical information is needed and which hazard-reduction techniques are most effective. This phase draws upon research results published in U.S. Geological Survey Professional Paper 1360 (1985), and is intended to direct future research efforts based upon evaluation of those results.

The evaluation began during April-September 1985 with distribution of materials from Professional Paper 1360 and selective invitations for written statements on earthquake hazards evaluation. The distribution was directed to a multidisciplinary group of about 80 people from a variety of professions involved with the earthquake hazard for Southern California. These people were requested to prepare formal responses to those materials, and to present their analyses and recommendations at a major multidisciplinary workshop convened during November 12-13, 1985, at the University of Southern California, Los Angeles, California.

The workshop, "Future Directions in Evaluating Earthquake Hazards of Southern California" focused on (1) Evaluating earthquake and surface-faulting potential; (2) Predicting seismic intensities for response planning and loss estimation; (3) Predicting ground motion for earthquake-resistant design; (4) Predicting major earthquakes for preparedness planning; (5) Evaluating earthquake groundfailure potential for development decisions; and (6) Evaluating the shaking hazard for redevelopment decisions. Each of these elements was introduced from a scientific perspective, and was then evaluated by those who apply the scientific information.

Results:

The workshop consisted of a formal program of 80 presenters, moderators, panelists, and commentators during an intensive two-day session involving a plenary session and three working groups each day. Total participation, including speakers and audience, was 350. Those on the program represented a significant aggregation of the most prominent workers in earthquake hazards evaluation, reduction, and response for Southern California. The audience included scientists, engineers, attorneys, insurance actuaries, emergency

response officials, government officials, educators, geotechnical consultants, and representatives of many other professions. The workshop program and a roster of attendees are available from the address at the head of this article.

All presenters, moderators, panelists and commentators submitted written papers and statements for the workshop proceedings. All proceedings were recorded on audiotapes, and transcribed, condensed, and edited for publication. The bulk of work during October 1985 - March 1986 was directed toward compiling and editing the workshop proceedings for publication in the NEHRP "Redbook" Open-File Report Series. As of March 31, 1986, all materials had been assembled, and about two-thirds had been edited.

Reports:

Ziony, J. I., editor, 1985, Evaluating earthquake hazards in the Los Angeles Region -- An earth-science perspective: U.S. Geological Survey Professional Paper 1360, 505p.

Seismic Hazards of the Hilo 7 1/2' Quadrangle, Hawaii

9950-02430

Jane M. Buchanan-Banks
Branch of Engineering Geology & Tectonics
U.S. Geological Survey
David A. Johnston Cascades Volcano Observatory
5400 MacArthur Boulevard
Vancouver, Washington 98661
(206) 696-7996

Investigations

1. Part-time work continued on preparing a geologic map of the Hilo 7 1/2' quadrangle for publication.

2. Revised manuscript from Branch of Western Technical Reports on structural damage and ground failures from November 1983 Kao'iki earthquake.

Results

A geologic map of the Hilo 7 1/2' quadrangle has been drafted onto a stable base and a general description of the map area, together with an explanation of the lithologic units, has been prepared in draft form. Finalization awaits study of thin sections. A paper on radiocarbon dates obtained from within the Hilo and adjacent quadrangles is in progress.

One month was spent reviewing and revising manuscript of the Kao'iki earthquake damage as a result of a Branch of Western Technical Reports edit.

Seismic Hazard Studies, Anchorage, Alaska

9950-03643

A. F. Espinosa
Branch of Engineering Geology and Tectonics
U.S. Geological Survey, MS 966
Denver Federal Center, Box 25046
Denver, CO 80225
(303) 236-1597

Investigations

1. A successful field seismological experiment was conducted in Anchorage, Alaska, and vicinity from September 14 through November 1, 1985. The field instrumentation deployment and data collection were completed using 11 portable digital system. Twenty-eight local and regional events were recorded. The data are being played back for editing analysis purposes. The topic of "Ground Amplification Studies in Areas Damaged by the Alaskan Earthquake of March 28, 1964: Anchorage, AK" will contribute further knowledge on site response (engineering zonation) obtained in different geologic environments.

2. A suite of isoseismal maps for Alaska has been compiled and drawn. A map composed of all the intensity distributions (MMI) is being released shortly. Intensity attenuation studies are being made from the above data base.

3. A "completeness" of the seismicity catalogue is being investigated in order to use lower magnitude thresholds in (a) spatial and magnitude-temporal distribution of shallow ($h \leq 33$ km) and intermediate ($33 < h \leq 100$ km) seismicity ($M_S \geq 5.5$) occurring within a specified area in the period of time which uses (a) historical and (b) instrumentally recorded earthquakes. This effort is part of the seismicity study being carried out in this project for the Anchorage and vicinity region in Alaska.

4. A damage evaluation for the City of Anchorage, sustained from the 1964 Alaskan earthquake, is in the editing stage. The damage data to dwellings along 15 street and DeBarr Blvd. in Anchorage, Alaska, will be catalogued and used in seismic-risk studies of the area. This information and local surficial geological data is planned to be used in order to evaluate transfer-function amplification curves in Anchorage and to ascertain any existing correlation between damage and soil conditions in the area.

5. A suite of seismicity maps and depth cross sections for the Anchorage and vicinity region in Alaska are being prepared. A technique has been developed to map the subducting plate on a three-dimensional finite-difference display for Anchorage and vicinity. ISC, USGS, and Menlo Park's local seismicity data files are used to perform the geometrical

mapping of the lithosphere in this region. A paper is being presented at the spring AGU meeting which discusses the technique and application of 3-D mapping of convergence zone-Alaska and the Aleutian Islands region.

6. The intensity catalogue covering the period 1900 through 1981 for the State of Alaska has been undergoing a very careful editing process during the last 2 years.

7. A model which incorporates the concept of seismotechnistratigraphic cells as a method for delineation of subsurface geology beneath Anchorage, Alaska, and its application to seismic hazards studies is under study and a paper is being presented on this subject

8. The geologic map of the northwestern quarter of the Tyonek A-4 quadrangle at 1:31,680 scale has been revised and completed and being edited. Also, the geologic map of the Tyonek B-4 quadrangle has been reviewed. These two maps are in the process of being edited and will be released shortly.

9. A report describing the geology and geophysics of the Tikishla Park hole, drilled in Anchorage in 1984, has been completed.

10. An open-file report describing cuttings from shot holes drilled for the Trans-Alaska Crustal Transect Project in the Copper River basin in 1985 has been completed.

11. The first draft of a USGS Bulletin interpreting results from geotechnical testing of cores from four drill holes in the Tyonek Formation has been completed.

12. Contributions consisting of surficial geology input to the geologic map of the Gulkana B-1 quadrangle, covering about half of the map (which is being prepared as an adjunct to the Trans-Alaska Crustal Transect Project), is nearly completed.

13. The northeastern sheet of the three-sheet geologic materials map of the Municipality of Anchorage has been checked and further editing is being done.

Reports

Bartsch-Winkler, Susan, and Schmoll, H. R., 1986, Origins of convoluted and hummocky bedded sequences, lower Knik Arm, upper Cook Inlet, Alaska, U.S.A. [abs.]: International Sedimentology Congress Proceedings, Canberra, Australia, v. 1, p. 105.

Espinosa, A. F., Brockman, S. R., and Michael, J. A., 1986, Modified Mercalli intensity distribution for the most significant earthquakes in Alaska, 1899-1981: U.S. Geological Survey Map 86-203.

Espinosa, A. F., and Rukstales, 1986, Seismological mapping of the Benioff zone in Alaska and the Aleutian Islands in central western South America [abs.]: EOS [Transactions of the American Geophysical Union], v. 67, p. 303.

Odum, J. K., Compilation of field and laboratory geotechnical test data for

U.S. Geological Survey drill holes 1C-79, 2C-80, CW81-2, and CE82-1, Beluga resource area, upper Cook Inlet region Alaska: U.S. Geological Survey Open-File Report. (in press)

Odum, J. K., Yehle, Y. A., Schmoll, H. R., and Gilbert, Chuck, 1986, Genralized interpretation of geologic materials from shot holes drilled for the Trans-Alaska Crustal Transect project, Copper River basin, Alaska, Mey 1985: U.S. Geological Survey Open-File Report. (in press)

Schmoll, H. R., Espinosa, A. F., and Odum, J. K., 1986, Subsurface mapping at Anchorage, Alaska: a tool for delineation of seismotechnistratigraphic (STS) cells: International Association of Engineering Geologists, 5th International Congress, Buenos Aires, 1986, 15 p.

Schmoll, H. R., and Yehle, L. A., 1986, Pleistocene glaciation of upper Cook Inlet basin, Alaska, in Hamiston, T. D., Reed, K. M., and Thorson, R. M., eds., Glaciation in Alaska; the geologic record: Anchorage, Alaska Geological Society, p. 193-218.

_____, Surficial geologic map of the northwest quarter of the Tyonek A-4 quadrangle, Alaska: U.S. Geological Survey Miscellaneous Field Studies Map, scale 1:31,680. (in press)

Yehle, L. A., Odum, J. K., Schmoll, H. R., and Dearborn, L. L., Overview of the geology and geophysics of the Tikishla Park drill hole, USGS A-84-1, Anchorage, Alaska: U.S. Geological Survey Open-File Report. (in press)

Yehle, L. A., and Schmoll, H. R., 1985, Surficial geologic map of the Tyonek B-4 quadrangle, Alasks: U.S. Geological Survey Geologic Quadrangle Map, scale 1:63,360 (in press)

Soil Development as a Time-Stratigraphic Tool

9540-03852

Jennifer W. Harden
Branch of Western Regional Geology
U.S. Geological Survey
345 Middlefield Road, MS 975
Menlo Park, California 94025
(415) 323-8111 ext. 2039

Investigations

1. Slip-rate study near Yucaipa, California along the San Andreas Fault: Jennifer Harden, Jonathan Matti.

2. Slip-rate study along the Calaveras Fault near Tres Pinos: Jennifer Harden, Kathy Harms, Malcolm Clark.

3. Geochronology-soil chronology-remote sensing study of outwash fans near Independence, California.

Results

1. Slip rates on the "southern branch" of the San Andreas fault near Yucaipa were constructed using fluvial terraces and soil development. Three surficial units, about 14, 30 and 100 ka old, were displaced about 0.5 to 1.0 km along the fault. Averaged to the present, Holocene rates are about 12 to 25 mm/yr; rates averaged to 30 and 100 ka decrease to about 8 to 16 mm/yr. This strand of the fault appears to have been less active in the Late Pleistocene, suggesting that other faults or fault strands may have been more active (publication no.).

2. Dated soils near Merced, California were compared to four dated soils in the San Francisco Bay Area. Rates of soil development appear to be quite similar, probably due to the similarity in climates and parent materials of the study areas. Based on the Merced and Bay Area dated localities, ages of fluvial terraces near Tres Pinos, California were estimated from degree of soil development. At least two terraces, approximately 20 and 40 ka old, were offset by the Calaveras Fault. Slip rates for these age-spans (averaged to present) will be provided using soils to match up similar-aged surfaces across the fault (publication no.).

3. Eight outwash fans along the eastern front of the Sierra Nevada were identified by A. Gillespie using multi-spectral imaging. At least 5 of those fans can be dated by their stratigraphic relationship to basalt flows dated by Ar 39-40 and K-Ar methods. Backhoe pits were excavated on each of the 8 fans, and 2-3 replicate soils were described and sampled. Soil data will provide calibration for deposits 10 to 1800 ka in age. Soils will then be used to correlate and date deposits in the region where basalts are absent.

Reports

Harms, K.K., Harden, J.W., Hoose, S.N., and Clark, M.M., 1984, Estimating slip rates along the Calaveras Fault, California, Using soils chronology and geometry of stream terraces: Earthquake Notes, v. 55, no. 1, p. 9.

Harden, J.W., Harms, K.K., Mark, R.K., and Clark, M.M., 1986, Soil development as a tool for studying seismogenic faults, Soil Science Society of America Abstracts, Annual Meeting, Chicago, Illinois, December 4-9, 1986.

Harden, J.W., Matti, J.C., and Terhune, C.L., 1986, Quaternary slip rates along the San Andreas fault near Yucaipa, California, derived from soil development on fluival terraces: Geological Society of America Abstracts with Program, v. 18, no. 2, p. 113. Cordilleran Meeting, Los Angeles, California, Programs with Abstracts.

Harden, J.W., Sarna-Wojcicki, A.M., and Dembroff, G., 1986, Soils developed on coastal and fluvial terraces near Ventura, California, in Harden, J.W., (ed): A series of soil chronosequences in the western United States, U.S. Geological Survey Bulletin 1590-B (in press). Director's approval, November 1985.

Terhune, C.L., Harden, J.W., and Matti, J.C., 1986, Application of a quantified field index of soil development to distinguish relative ages of geomorphic surfaces for regional geologic mapping: Geological Society of America Cordilleran Meeting, Los Angeles, California, Programs with Abstracts.

Seismic Slope Stability
9950-03391

Edwin L. Harp
Branch of Engineering Geology and Tectonics
345 Middlefield Road
Menlo Park, CA 94025
(415) 856-7124

Investigations

1. Continued development of an engineering criteria to evaluate seismic stability of rock slopes.

2. Conducted comparison of landslide distribution data from the 1980 Mammoth Lakes, California earthquakes with susceptibilities to seismic-induced failure as predicited by the above-mentioned criteria. This was to evaluate the applicability of the criteria to regions of future possible seismic-induced rock-fall hazards such as the Wasatch Front near Salt Lake City, Utah.

Results

1. Evaluation of rock-mass-quality index, Q, as described by Barton (1974), although adequate for tunnel design, has several shortcomings when used to predict the susceptibility of a rock slope to seismic failure. The quantitative index underrates the effect of the orientation of major, throughgoing joints or fractures. It also underrates the effect of the openness of joints and fractures on the susceptibility of rock slopes. Experimantation with assigning various numerical values to each of these factors in the rating classification indicates that satisfactory results may be obtained by increasing the standard numerical weights twofold in each descriptive category.

2. Comparison of landslide distribution data from the 1980 Mammoth Lakes earthquakes with modified rock-mass-quality indices obtained by field measurements at 92 rock-fall source areas shows a strong correlation despite uncertainties in the spatial variation in the seismic shaking that may have been due to the seismic source or to the extremely rugged topography within the area. The modified version of the rock-mass-quality index will be used to rate the susceptibility to seismic-induced failure of rock slopes along the Wasatch Front near Salt Lake City, Utah where measurements of joints and fracture characteristics have been and will continue to be gathered through summer 1986.

Reports

Harp, E.L., Wilson, R.C., Keefer, D.K., and Wieczorek, G.F., 1986, Seismically induced landslides: current research of the U.S. Geological Survey: Proceedings of conference of International Association of Engineering Geologists, Engineering Problems in Seismic Areas, p. [illegible].

References

Barton, N., Lien, R., and Lunde, J., 1974, Engineering classification of rock masses for the design of tunnel support: Norwegian Geotechnical Institute no. 106, 48p.

Urban Hazards Seismic Field Investigations and the Study of the Effects of Site Geology on Ground Shaking

9950-01919

Kenneth W. King
Branch of Engineering Geology and Tectonics
U.S. Geological Survey
Denver Federal Center, MS 966
Denver, CO 80225
(303) 236-1591

Investigations

The general objective of this project is to improve the understanding of how the shallow underlying geology affects ground shaking. The specific objectives of this 6-month period are to compare the site response numbers derived by Hays and King (1982) (who ratioed pseudo-relative-velocity algorithms (psrv)), against ratios derived from smoothed Fourier amplitudes; to develop a more detailed ground response of the Salt Lake City area in the low- to medium-response areas of the Hays and King report; and, to examine the feasibility of correlating the derived site response with the geotechnical data derived from high-resolution shallow seismic reflection profiles.

Ground motions induced by a NTS nuclear test were recorded at eight sites in Salt Lake City and five sites in the Provo area. Detailed high-resolution shallow-reflection profiles were made at five of the sites. The data has been analyzed and is now in process of being written for the USGS Wasatch paper.

A seismic field investigation at the Laguna Indian Reservation is near completion. The program investigated the cause of the damage to structures in the village of Paguate. The project called for a damage investigation of 240 structures, design of a damage scale for adobe type structures, study of attenuation and ground response by using down-hole blasts outside the village as the energy source, and establishing the periods and dampings of approximately 50 of the structures. The project was 90-percent completed within this reporting period.

Several test profiles were made to improve the methods of using shallow high-resolution reflections to identify changes in the upper 200 feet. The methods are improving rapidly. We are integrating an IBM-XT into the field system to allow pertinent decisions to be made on line without returning to the laboratory.

Results

1. The new site response data and analysis methods on the Salt Lake-Provo data agree very closely with the Hays and King (1982) report. The PSRV ratios are very similar to the smoothed Fourier ratios. The study confirmed the repeatability of the process and made a more detailed site response map of the Salt Lake area.

2. The on-going evolution of shallow high-resolution reflection methods continue to show improvements. We were able to identify correctly a tunnel in

coal at approximate 45-foot depth. The experiment was repeated at another site with similar success. The data from the Wasatch area looks good with correlations now in process. In another experiment we were also able to identify the bottom of a landslide. These results and/or experiments may be combined into one open-file report.

3. The Wasatch strong-motion network continued in stand-by ready mode. The equipment was inspected by Menlo personnel. The underlaying unconsolidated sediments will be profiled using the reflection methods.

4. Several reports are now in progress and hope to be in review or published in the next 6-month period.

Determining Landslide Ages and Recurrence Intervals

9950-03789

Richard F. Madole
Branch of Engineering Geology and Tectonics
U.S. Geological Survey
P. O. Box 25046, MS 966
Denver, Colorado 80225
(303) 236-1617

Investigations

Study to date has determined that slope-movement recurrence intervals can be documented by stratigraphic relations and ^{14}C ages from three kinds of deposits found in three different locations on slope failures. The stratigraphic relations and locations are those of lateral ridges (features resembling lateral moraines), translocated pond deposits, and landslide-dammed lake deposits. Stratigraphic and chronologic data from these kinds of deposits associated with the Manti slide, Sanpete County, Utah, provide a measure of the activity of this feature for late Holocene time.

Results

Six ^{14}C ages from deposits associated with the Manti slide indicate that at least 5-6 episodes of major slope movement have occurred here in the past 3000-3500 years (Table 1). Slope movement occurred sometime during 3400-3200 B.P., at about 2930 B.P., 2750 B.P., 2000 B.P., at least once during 300-20 B.P., and in the latter part of the 1970's.

On the basis of a ^{14}C age of 3110+60/-50 yr B.P. (DIC-3212), it is estimated that Manti Canyon was dammed by a landslide in the vicinity of the present toe of the Manti slide at sometime between 3400 and 3200 B.P. It is not clear whether damming was caused by the Manti slide or North slide, which extends into Manti Canyon from the north, opposite the Manti slide. Approximately 11.5 m of lake deposits are exposed above the level of Manti Creek upstream from the landslide dam. Most of the 11.5 m section consists of laminated clayey silt and silty clay. The section becomes progressively more coarse in the upper 3-4 m and is capped by 2 m of clast-supported gravel. The upper half of the gravel is predominantly medium to large cobbles, whereas the lower half is chiefly pebbles. The coarsening-upward sequence represents the in-filling of the lake and re-establishment of a coarse-bedload stream, similar to the present creek, across the area.

The 3110+50/-60 yr B.P. age is of charcoal collected from a sandy interval between the laminated lake beds and the capping layer of gravel. This ^{14}C age is a minimum for the time of landslide damming because more than 9 m of lake deposits (bottom of section not exposed) had accumulated prior to deposition of the charcoal-bearing sediment. Given the high sediment load of Manti Creek, the 9 m or so of lake deposits could have accumulated within 100-200 years. The spillway for the landslide-dammed lake was in the topographic low, part of which is preserved, south of the present course of Manti Creek. For some unknown reason, Manti Creek later cut a channel across, rather than around, the toe of North slide.

The largest slope failure in the late Holocene history of the Manti slide occurred about 2930±60 yr B.P. (DIC-3211). On the basis of the size and continuity of the lateral ridge formed at that time, the magnitude of movement is considered to have been much larger than any movement that has occurred since. The ^{14}C age of 2930±60 yr B.P. (DIC-3211) is of relatively clean charcoal collected from the upper part of a buried soil exposed in a trench excavated across a lateral ridge.

Charcoal from the basal layer of translocated pond deposits found on the hilltop west of Cottonwood Reservoir provided a ^{14}C age of 2740+100/-90 yr B.P. (DIC-3239). The larger analytical error associated with this age is due to the small amount of charcoal used in the assay. The possibility exists that the 2740+100/-90 age and the 2930±60 age (DIC-3211) described above may relate to a single event that occurred about 2850 B.P. Without more information, however, I favor the interpretation that the two ages represent separate episodes of slope failure.

Major movement occurred again on the Manti slide about 2000 B.P. This movement formed a low, lateral ridge locally along the north side of the Manti slide. At one locality, site MC-5 of Table 1, pond deposits were squeezed or thrust laterally and came to rest at the crest of the newly formed lateral ridge. The soil that formed in the pond sediment provides a measure of the degree of soil development that can be expected in 2000 years on the crests of lateral ridges. This soil consists of a weakly developed A/AC/C profile only 11 cm thick. An A horizon, typically 5 cm thick, overlies a 5-cm-thick AC horizon that is defined mainly by color. The AC horizon is distinctly lighter in color than the A horizon but darker than the C horizon. Color contrasts are distinct because the parent material is derived chiefly from Flagstaff Limestone (Paleocene) and is light gray to white, whereas A horizons in this area are dark gray to black.

Movement comparable to that of the 1970's occurred at least one other time on the Manti slide in the past 20-250 years. Translocated pond deposits, now on the slope below where the jeep road crosses the upper part of the slide, contained a stump of a relatively large tree. The outermost wood of the stump provided a ^{14}C age of "modern", which is to say that it is too young to be assayed accurately by the ^{14}C method.

Relationships between the times of slope movements and possible causes of these movements have not been established. The ^{14}C ages obtained thus far, however, do permit conclusions to be drawn about the use of soil studies to date the formation of lateral ridges. Contrary to statements made in previous semiannual reports, differences in soil development on segments of lateral ridges cannot be relied on solely to differentiate and correlate ridge segments and, thereby, to identify the number of ridge-forming slope movements.

Soils are not destroyed by the movement that forms lateral ridges. The soil buried by the lateral ridge at site MC-7 (Table 1) about 2930±60 yr B.P. (DIC-3211) is similar to the surface soil on the crest of the lateral ridge. The surface soil profile consists of A/Cox/Cn horizons. The A horizon is typically 27-29 cm thick, has a strong, medium, subangular blocky structure, and is leached to depths of 17-20 cm. The Cox horizon extends from a depth of 29 cm to 129 cm and is composed of slightly oxidized, highly calcareous diamicton derived chiefly from Flagstaff Limestone.

The surface soil at site MC-7 represents considerably more development than would be expected in 3000 years. This conclusion is based primarily on comparison with the amount of soil that has formed in 2000 years at site MC-5, which is just a few hundred meters from site MC-7. The conclusion is also supported, however, by comparisons with late Holocene soils developed in a variety of other areas and environments, most of which are more favorable to soil formation than is site MC-7.

TABLE 1.--^{14}C ages from Manti slide, Sanpete County, Utah

^{14}C Age	Lab. No.	Site No.	Material	Deposit
3110+60/-50	DIC-3212	MC-11	Charcoal	Landslide-dammed lake
2930±60	DIC-3211	MC-7	Charcoal	Lateral ridge, buried soil
2740+100/-90	DIC-3239	MT-1	Charcoal	Translocated pond deposit
2070±60	DIC-3229	MC-5A	Humus	Lateral ridge, displaced pond sediment
1980+50/-60	DIC-3230	MC-5B	Charcoal	Lateral ridge, buried soil
Modern	DIC-3231	MU-1	Wood	Translocated pond deposit

Analysis of Earthquake Ground Shaking Hazard For the Logan - Brigham City Region, Utah

14-08-0001-G1189

M.S. Power, R.R. Youngs, and F.H. Swan III
Geomatrix Consultants
One Market Plaza, Spear Street Tower,
San Francisco, CA 94105 (415) 957-9557

Objectives: We are conducting an assessment of the ground motion hazard for the Logan-Brigham City region using the same probabilistic approach that was used to analyze the hazard for the Salt Lake City - Ogden - Provo urban corridor. The seismic hazard is expressed as levels of peak ground acceleration having certain probabilities of being exceeded during a specified time period. The results of this study will be shown on regional maps as contours of peak ground acceleration for selected probabilities of exceedance. Acceleration response spectra corresponding to selected probabilities of exceedance will be presented for representative locations in the study region for use in further establishing the damage potential of ground motions to buildings.

The basic approach for probabilistic seismic hazard analyses incorporates the inherent uncertainties in the location, time of occurrence and size of future earthquakes and the uncertainties in the resulting ground motions at a site to evaluate the probability of exceeding a specified ground motion level in a specified time period. Specifically, these factors are incorporated in three probability functions:

1. A probability distribution for the distance from a site to the earthquake rupture surface is developed from the geometry of the identified seismic sources and a relationship between earthquake magnitude and rupture size.

2. A probability distribution for the rate of occurrence of earthquakes of various sizes (magnitudes) is developed from a recurrence relationship for each seismic source.

3. A probability distribution for the resulting ground motion levels at a site a specified distance from a specified size earthquake is developed from appropriate attenuation relationships.

In a basic seismic exposure analysis, it is assumed that the source characterization parameters required to develop the above probability distributions (fault length, dip and width, maximum earthquake magnitude, and earthquake recurrence rate) are known with certainty. In fact, there usually is uncertainty in these parameters arising from less than complete knowledge of the seismogenic processes at work. These uncertainties can significantly affect the estimated seismic hazard levels. In the present study, the uncertainties in characterizing the potential sources of future seismicity are explicitly incorporated in the analysis in order to express the uncertainty in the estimated seismic hazard levels in the study region.

Results: Two types of seismic sources have been characterized for use in the seismic hazard analyses: known faults and distributed areal sources of seismicity. Geologic studies by numerous investigators have identified a number of active or potentially active faults in the region. The locations of faults significant to the study are shown in Figure 1. These faults are believed to be capable of generating moderate to large magnitude earthquakes, and the Wasatch fault and East Cache fault have evidence of Holocene surface rupture. The maximum earthquake magnitudes and recurrence rates for large magnitude events on these faults have been characterized based on geologic and paleoseismic data.

Evaluations of the historical and instrumental seismicity catalog for Utah have been used to characterize the recurrence rates for smaller magnitude earthquakes. These evaluations, together with the results of other published studies indicate that much of the smaller magnitude seismicity cannot be directly associated with mapped faults. Consequently, distributed area sources of small to moderate magnitude earthquakes are being included in the model of the regional seismicity.

At the present time, there is uncertainty as to the appropriate attenuation characteristics for the study region. The approach taken in this study is to use several attenuation relationships and test the sensitivity of the computed hazard levels to these relationships.

Reports: Power, M.S., Schwartz, D.P., Youngs, R.R., and Swan, F.H. III, Analysis of earthquake ground-shaking hazard for the Salt Lake-Ogden-Provo region: Paper presented at the Workshop on Evaluation of Regional and Urban Earthquake Hazards and Risk in Utah, Salt Lake City, August 14-16, 1984.

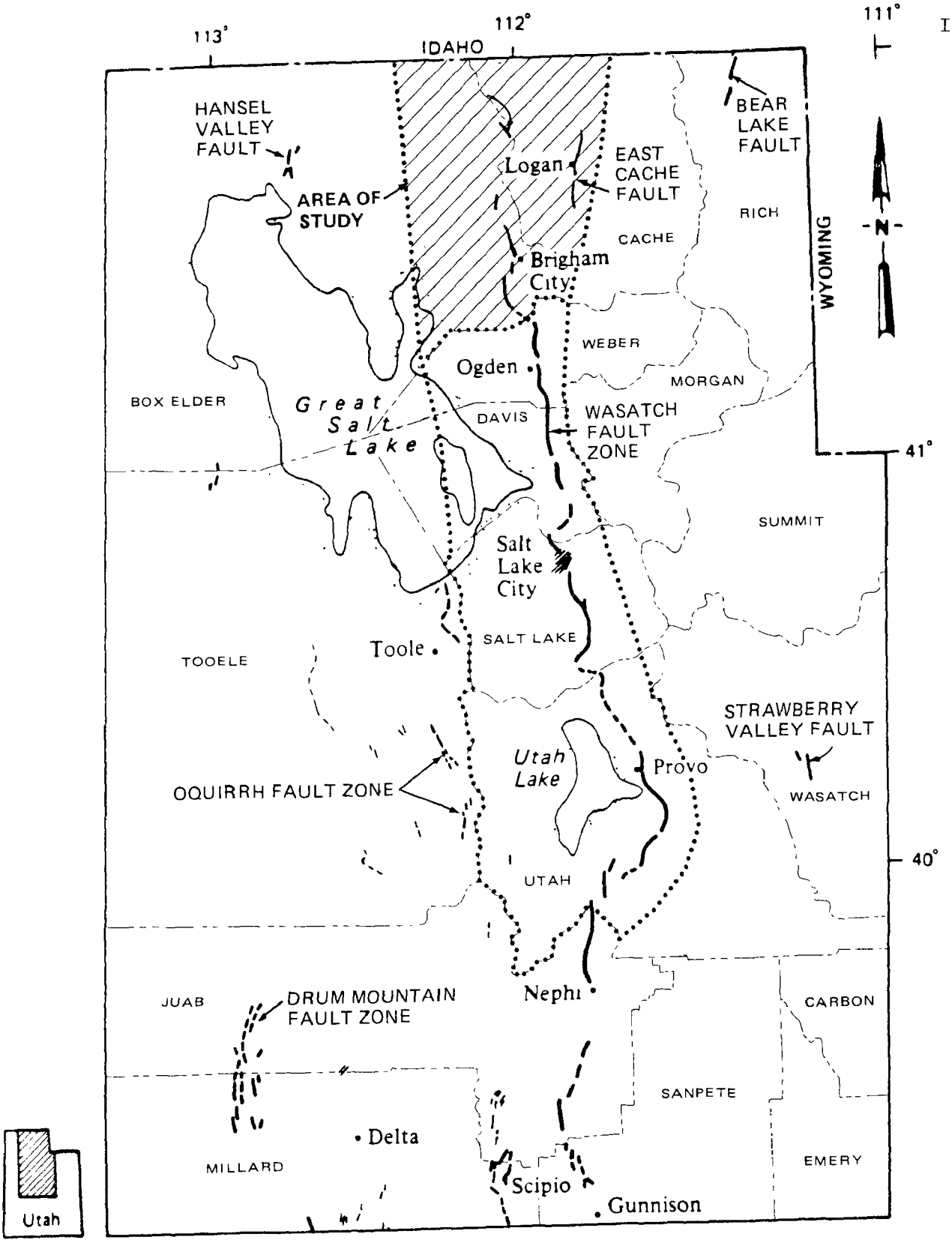

(Summarized from Anderson and Miller, 1979, Buchnam and Anderson, 1979a; Cluff and others, 1970, 1973, 1974, Everitt and Kaliser, 1979, Nelson, 1982; Woodward-Clyde Consultants, 1982)

Figure 1. REGIONAL LOCATION MAP

Source Properties of Great Basin Earthquakes

9950-03835

Arthur C. Tarr
Branch of Engineering Geology and Tectonics
U.S. Geological Survey
Box 25046, MS 966, Denver Federal Center
Denver, CO 80225
(303) 236-1605; (FTS) 776-1605

Investigations

Four investigations were pursued during this reporting period:

1. Analysis of digital data recorded at the Nevada Test Site.
2. Development of field computer system for urban hazards seismic studies.
3. Site Characterization Plan chapter for the proposed Yucca Mountain high-level nuclear waste repository.
4. Information systems element of the Wasatch Front regional and Urban Hazards Evaluation.

The objective of the first investigation was to analyze digital seismic data that had been recorded in 1981 by DR-100 portable seismic systems and in subsequent years by the permanent Southern Great Basin Seismic Network (SGBSN). One goal in this investigation was to implement software for the rapid spectral analysis of large quantitites of digital waveform data. Another goal was to compare source parameters, such as stress drop, from earthquakes in different seismic regimes at the Nevada Test Site. This investigation is in support of the Southern Great Basin Seismic Studies project (9950-02151).

The objective of the second investigation was to design a microcomputer system that could be used in the field to support the activities of the Urban Hazards Seismic Field Investigations project (9950-01919). Some of these activities include multi-channel refraction and reflection profiles of the upper 100 m to determine basement depth and seismic parameters of Quaternary deposits. Analysis of seismic data in the field is expected to improve the productivity of seismic field experiments by reducing guesswork in laying out spreads and in selective filtering of data channels.

The objective of the third investigation was to prepare the seismology section of the geology chapter of a Site Characterization Plan (SCP) the USGS is preparing for Department of Energy. The SCP is for the proposed Yucca Mountain repository near the Nevada Test Site. The goal for each section of the SCP is to synthesize existing information about the proposed site and summarize the state of knowledge of the geology in the surrounding southern Great Basin.

The objective of the fourth investigation was to contribute to the information systems element of the Wasatch Front Regional and Urban Hazards Evaluation study.

The information delivery system has been described in previous reports and is scheduled to be completed in FY 1986.

Results

Extensive software revision was performed during the reporting period to streamline the increasing data processing load resulting from voluminous digital data sets acquired during the last year. This software and assistance were provided for the digital seismic data analyses of four projects: South Carolina Seismic Network (9950-01195); Regional and National Seismic Hazard and Risk Assessment (9950-01207); Urban Hazards Seismic Field Investigations (9950-01919); and Chaco Seismology Study (9950-03816). In addition, computer programs used for computing seismic moment, stress drop, and other source parameters were improved during the reporting period. The effect of the improvements was to reduce the scatter of the moment and stress drop estimates and consequently, to provide more accurate values of moment magnitude M_L.

Research continued into small magnitude earthquakes recorded at Jackass Flats during 1981. As reported previously, stress drops determined for a set of ten well-recorded earthquakes were significantly smaller than typical stress drops for earthquakes of similar seismic moment in California. Similarly, determinations of peak ground motion parameter $R\mathbf{v}$ (where R is distance and $\mathbf{v}$ is the peak velocity) are up to 10 to 20 times smaller than McGarr's (1984) empirical formula relating $R\mathbf{v}$ to seismic moment. We conclude that seismic waves from southern NTS earthquakes suffer from significant anelastic attenuation, possibly in the near-surface crust under the recording sites, yielding reduced amplitude and frequency of the peak ground motion and shifting the apparent corner frequency of the source spectrum to lower values, thereby producing unexpectedly low stress drops.

Hardware for the field computer was purchased during the reporting period. A standard IBM PC/XT was modified with an accelerator board (9.54 MHz numerical coprocessor and 8086 CPU) to permit high-speed computations, such as FFTs and matrix inversions. The system was equipped with a high-resolution monitor for quality graphics, a dot-matrix printer for graphical output, and a mouse for phase picks and other waveform processing operations.

Preparation of the seismology section of SCP Chapter 1 (Geology of the southern Great Basin and Yucca Mountain) required full-time participation for approximately three months. The synthesis drew upon published results of research and new results scheduled to be published by the end of calendar year 1986. Many of the new results come from analysis of seismic data acquired by the Southern Great Basin Seismic Network (SGBSN) and refinements of seismic hazards assessment due to more realistic modeling of source zones.

The seismicity and seismic hazard of the southern Great Basin and the site of the Yucca Mountain repository are characterized as follows:

- The pattern of regional seismicity, as defined by historical epicenters within 400 km of Yucca Mountain, consists of the north-south-trending Nevada-California seismic belt, the southern end of the Intermountain seismic belt in southwestern Utah, and the diffuse East-West seismic belt encompassing the Nevada test Site (NTS). Six major earthquakes, magnitude $M \geq 6.5$, have occurred in the Nevada-California seismic belt and two (1857, 1952) on or near the San Andreas fault. The nearest major earthquake (1872 Owens Valley) was about 150 km west of Yucca Mountain. Yucca Mountain is located in a large, historically quiescent area that includes the southwest quadrant of NTS and the eastern Mojave Desert.

- The pattern of local seismicity, as defined by hypocenters within 150 km of Yucca Mountain and determined by the 53-station SGBSN, is a widespread but diffuse background corresponding principally to the East-West seismic belt, punctuated by clusters of intense activity and by larger, nearly aseismic (or quiescent) areas. Yucca Mountain is in a locally-quiescent area characterized by few hypocenters and low seismic energy density.

- Most seismically active areas of the southern Great Basin occur in regions of major Tertiary northeast-trending left-lateral shear; notable among these are the Rock Valley, Pahranagat, and Gold Mountain shear zones. Seismicity is also located in some north-trending fault zones; examples are found at Indian Springs Valley and Sarcobatus Flat, and along the Thirsty Canyon, Yucca, and Pahute Mesa fault zones.

- Focal depths of hypocenters range from 1 km above sea level to 17 km. The depth distribution has two broad peaks at 0-2 km and 5-8 km and a distinct minimum at 3.5 km. Depth profiles in active areas frequently show earthquake patterns extending from the surface to 10 km or more.

- Epicenter and depth patterns, combined with nodal planes determined from first-motion studies, can sometimes be associated with mapped faults or structural grain having north to northeast trends. In other cases, associations among hypocenter patterns, nodal planes, and mapped faults cannot be drawn unequivocally.

- The direction of minimum principal stress, determined from focal mechanisms, is approximately N60°W; intermediate and maximum principal stresses are approximately equal in magnitude. This stress configuration favors right-lateral strike-slip and north-striking faults, normal slip on northeast-striking faults, and left-lateral strike-slip on ENE-striking faults.

- The largest mean peak horizontal acceleraton at Yucca Mountain calculated under deterministic assumptions is 0.4 g; the calculation assumes full-length rupture of 17 km ($M = 6.8$) on the Bare Mountain fault at a distance of 14 km. Using probabilistic methods and conservative assumptions, the acceleration has less than 4 percent probability of being exceeded during the 30-year emplacement period and 14 percent probability during the 90-year (maximum) preclosure period.

Activity in the fourth investigation consisted principally of reviewing a copy of a draft UGMS bibliography of geologic hazards in Utah.

REFERENCE CITED

McGarr, A., 1984, Scaling of ground motion parameters, state of stress, and focal depth: Journal of Geophysical Research, v. 89, 6969-6979.

Quaternary Framework for Earthquake Studies
Los Angeles, California

9540-01611

John C. Tinsley
Branch of Western Regional Geology
U.S. Geological Survey
345 Middlefield Road, MS 975
Menlo Park, California 94025
(415) 323-8111, x 2037

Investigations

1. Completed a collection and compilation of geologic and geotechnical data enabling us to characterize probable levels of relative ground motion using geologic parameters along the Wasatch Front from Logan, Utah, to Provo, Utah. (J.C. Tinsley, K.W. King, D. Carver, D. Trumm and K. Parish).

2. Completed drilling and subsurface sampling studies, emphasizing the Salt Lake City area. The objective is to use the site specific data, including down-hole measurements of P-wave and S-wave velocities to improve predictions of site-dependent earthquake generated ground motion in the Wasatch region (J. Tinsley, A.M. Rogers, K.W. King and D. Carver).

3. Continued field study of late Quaternary alluvial fans, related terrace deposits and soils along the San Gorgonio Pass fault zone, to determine the neotectonic history of the Pass and the remarkable zone of reverse faults that mark the zone of convergence. (J.C. Tinsley, J.C. Matti, L.M. Wells).

Results

1. Geologic data include about 1000 water well logs, foundation investigations and soils reported compiled from public agencies and private consultants, for about 70 USGS relative ground-motion instrument stations in the Logan, Ogden, Salt Lake City and Provo areas. This effort was greatly facilitated by Loren D. Anderson, Professor of Geotechnical Engineering, Utah State University, Logan, UT, who has maintained files of geotechnical data compiled during studies to evaluate liquefaction in the Wasatch region. The objective of our study is to predict relative ground response for the Wasatch region in terms of sets of geologic properties of materials beneath the instrument sites. Measurements of P-wave and S-wave velocities were completed in the Provo area using down-hole techniques (K. W. King). These and other geologic and geotechnical data are to be correlated with ground-motion amplification data, to comprise a regional evaluation of the ground shaking hazard in the Wasatch region. The data base will include in-situ data at as many of our ground-motion instrument sites as possible (40 to 60 sites from Logan, Utah to Provo, Utah. A manuscript for inclusion in a U.S.G.S. Professional Paper dedicated to evaluation earthquake hazards in the Wasatch region, Utah, is in preparation.

2. In July or August, 1986, U.S. Geological Survey personnel will commence exploratory drilling and sampling at 20 to 30 sites in the Salt Lake City area. These localities are sites at which recordings of ground motion were made from 1973 until as recently as January, 1986, and include sites at which K.W. King and D. Carver have recorded high-resolution seismic profiles using .50 caliber and .30 caliber rifles and 12 ga. shotgun slugs. The drilled and sampled holes will be cased and velocity logging will commence as soon as practicable. This study extends to the Wasatch region the methodology of a study by Rogers, Tinsley and Borcherdt (1985) for the Los Angeles region.

3. Soils were described and sampled, and samples were submitted to the soil laboratory at the University of New Mexico for analysis by Dr. L.D. McFadden. Initial results pertaining to the slip-rate studies of the San Gorgonio Pass fault zone are anticipated by mid-Autumn. Additional soil samples will be obtained throughout the late Spring and early Summer. Trenching on Millard Canyon fan will start in June, 1986.

Publications

Fumal, T.E., and Tinsley, J.C., 1985, Delineating seismically-distinct units, in Ziony, J.I. (ed.), Evaluating earthquake hazards in the Los Angeles region, an earth-science perspective: U.S. Geological Survey Professional Paper 1360, p. 127-149.

McFadden, L.D., and Tinsley, J.C., 1985, The rate and depth of pedogenic carbonate accumulation in soils--Formulation and testing of a compartment model, in D.L. Weide (ed.), Soils and Quaternary geology of the southwestern United States: Geological Society of America Special Paper 203, p. 23-41.

Rogers, A.M., Tinsley, J.C., and Borcherdt, R.D., 1985, Predicting relative shaking response, in Ziony, J.I. (ed.), Evaluating earthquake hazards in the Los Angeles region, an earth-science perspective: U.S. Geological Survey Professional Paper 1360, p. 221-247.

Tinsley, J.C., and Fumal, T.E., 1985, Mapping Quaternary sedimentary deposits for estimating the severity of shaking, in Ziony, J.I. (ed.), Evaluating earthquake hazards in the Los Angeles region, an earth-science perspective: U.S. Geological Survey Professional Paper 1360, p. 101-125.

Tinsley, J.C., Youd, T.L., Perkins, D.M., and Chen, A.T.F., 1985, Evaluating liquefaction potential, in Ziony, J.I. (ed.), Evaluating earthquake hazards in the Los Angeles region, an earth-science perspective: U.S. Geological Survey Professional Paper 1360, p. 236-315.

Tinsley, J.C., and Rogers, A.M., in press, Suggested directions in earthquake ground-shaking microzonation research, in Proceedings of workshop XXXII, Future directions in evaluating earthquake hazards of southern California, Nov. 12-13, 1985 Los Angeles: U.S. Geological Survey Open-File Report _____.

Ziony, J.I., Evernden, J.F., Fumal, T.E., Harp, E.L., Harztell, S.H., Joyner, W.B., Keefer, D.K., Spudich, P.A., Tinsley, J.C., Yerkes, R.F., and Youd, T.L., 1985, Predicted geologic effects of a postulated magnitude 6.5 earthquake along the northern Newport-Inglewood zone, in Ziony, J.I. (ed.), Evaluating earthquake hazards in the Los Angeles region, an earth-science perspective: U.S. Geological Survey Professional Paper 1360, p. 415-441.

Tinsley, J.C., Youd, T.L., Perkins, D.M., and Chen, A.T.F., (in press), Improving predictions of liquefaction potential in Brown, William M. (ed.) Proceedings of Conference XXXII -- Workshop on future directions in evaluating earthquake hazards of southern California: U.S. Geolgoical Survey Open-File Report _____.

Liquefaction Risk Map for Boston

14-08-0001-G1188

Robert V. Whitman
Herbert H. Einstein
Daniele Veneziano

Department of Civil Engineering
Massachusetts Institute of Technology
Cambridge, MA 02139
(617)253-7127

This study was formally established 1 December 1985, with work commencing 1 February 1986. The study has three major components: 1) the determination of liquefaction susceptibility of different soils; 2) estimation of earthquake intensities, recurrence intervals and based thereupon the shaking hazard at different locations; 3) combining of 1 and 2.

Geologic Characterization

Ground conditions are used in two basic ways to establish liquefaction susceptibilities:

1. Natural sediments and artificial fill which have been loosely deposited and remained in this condition are potentially liquefiable. Ground conditions can thus be subjectively categorized based on geological and man-influenced history.

2. Geotechnical properties, notably SPT values, are established from boring records. Correlations among SPT, other geotechnical properties and natural geologic characterization are used to interpolate among widely-spaced groups of borings.

Geologic characterization can thus be used directly to establish liquefaction potential and indirectly to correlate with geotechnical properties indicating liquefaction potential. Geologic characterization as used in this context involves both natural ground and artificial fill. This is particularly important in Boston where the greater part of the city is located on fill.

Ample, although to some extent controversial, information is available concerning the natural geology. Literature searches have been conducted in the files of the USGS, Boston office, and in the geology libraries of M.I.T. and Harvard. The results obtained so far were discussed with Dr. B. Stone, USGS. The basic stratigraphy underlying the Boston Peninsula and surrounding areas in Cambridge and Brookline, was determined. Controversies are mainly related to the age and association of different deposits with particular periods (4 major ice advances versus 2 with a limited readvance). The information is, however, sufficient to start correlating it with the boring log information.

Originally, it was thought that fills would not be very problematic in the context of earthquake liquefaction in the Boston area. However, in addition to revealing a very complex history geographically, temporally and technically, initial review of available information also showed that many fill deposition procedures potentially produced loose soils in this area. This part of the work was therefore intensified. So far the work has consisted of archival studies in the Boston Public Library, Boston Athenaeum and the M.I.T. libraries. At the present time the search is being expanded to the archives of a number of public atuhorities. The quality and quantity of the information is uneven. It is usually relatively detailed regarding the time and the particular area filled, while material properties and filling procedures are not always mentioned. Nevertheless, interesting differences could be established. In Back Bay, for instance, in addition to the well-known dumping of Needham sand-gravel from railroad cars, dredging and deposition with a suction dredge of material from the Charles River bottom, and also dumping from scows of material dredged from the river, were used. The latter two procedures can lead to loose deposits.

At the present time more information is collected concerning the South Bay and Dorchester areas, as well as concerning some of the very old fills. Further work will involve Cambridge.

Ground Motion Models for the Eastern United States

During this reporting period, we have addressed the problem of earthquake attenuation in the Eastern United States (EUS), under joint sponsorship of USGS and EPRI. In the past, attenuation models in the EUS have been obtained mainly by an indirect method which combines MM intensity attenuation relationships appropriate to the EUS with "intensity-to-ground-motion" conversions from the Western United States (WUS). Recently, instrumental data from a few moderate-size earthquakes has become available in the EUS, from which direct estimation of ground motion is possible. We have obtained direct estimates of attenuation from this data, using a regression model with random coefficients that recognizes variations of attenuation from earthquake to earthquake.

The main focus of our work has been however the development of a new statistical technique to compare and combine direct and indirect estimates of ground motion. The proposed method utilizes information on macroseismic and instrumental measures of ground motion from several geographical regions. Differences in attenuation among the regions are permitted and means are given to describe these differences either deterministically or probabilistically. Diagnostic quantities are calculated to verify the compatibility of assumptions about the similarity of attenuation in different regions with available data. The method has been used to estimate how peak ground acceleration (PGA) and spectral velocities at 1 and 10 herz for 5% damping ($S_V(1)$ and $S_V(10)$) attenuate in the EUS. These estimates are based on instrumental and MM intensity information from that region and instrumental data from the WUS. The proposed regressions for horizontal motion on rock are

$$\ell nPGA = 2.53 + 1.10\, m_{Lg} - 1.17 \ell nR - 0.003\, R$$

$$\ell nS_V(10) = -1.54 + 1.11\, m_{Lg} - 1.04\, \ell nR - 0.003\, R$$

$$\ell nS_V(1) = -6.96 + 2.10\, m_{Lg} - 1.10\, \ell nR - 0.003\, R$$

where PGA is in cm/sec^2, S_V is in cm/sec, and R is hypocentral distance in km. These relationships are consistent with results from the method of attenuated spectra and random vibration analysis. A by-product of the analysis is the finding that taking the attenuation of MM intensity into account has almost no influence on the attenuation of PGA and $S_V(10)$ and only a small influence on the attenuation of $S_V(1)$. Another finding is that, for the above parameters, scaling of attentuation with magnitude is much higher in the EUS than in the WUS. Attenuation with distance displays statistically non-significant differences between the two regions, up to a few hundred kilometers from the source.

A paper based on the above work has been submitted for publication in the Bulletin of the Seismological Society of America.

Worldwide Standardized Seismograph Network (WWSSN)

9920-01201

Russ Wilson
WWSSN Project Chief
Branch of Global Seismology and Geomagnetism
U.S. Geological Survey
Albuquerque Seismological Laboratory
Building 10002, Kirtland AFB-East
Albuquerque, New Mexico 87115-5000
(505) 844-4637

Investigations

1. Technical and operational support were provided to each station in the Worldwide Standardized Seismograph Network (WWSSN) as needed and required.

2. Eighty-six (86) modules and components were repaired, and six hundred thirty-two (632) separate items were shipped to support the network during this period.

3. A continuous flow of high-quality seismic data from the cooperating stations within the network is provided to the users in the seismological community.

Hot Pen Conversion:

1. All WWSSN stations were informed that as of October 1, 1985, they were to record on only four channels, three LP channels and one Z-SP channel. However, a few stations are recording on three SP channels and one Z-LP channel. The following stations have not responded: ARE, GSC, KOD, NDI, NNA, NUR, and POO.

2. The following stations were notified that as of October 1, 1985, USGS will discontinue supplying photographic paper and chemicals: AAM, ATL, EPT, GEO, LPS, MAN, MSO, NIL, PAL, RCD, RIV, SOM, and NME.

3. The following stations were discontinued with no action taken: CAI, KBL, MHI, SHI, TAB, and TPM.

4. There are now eighty-eight (88) WWSSN stations in operation.

5. During the month of November 1985, six (6) hot pen conversion kits were built at the Albuquerque Seismological Laboratory (ASL) and installed at the WWSSN station ALQ: three (3) LP operating at mag. 3000; one (1) low gain LPZ operating at mag. 30; one (1) SPZ operating at mag. 200K; and one (1) low gain SPZ operating at mag. 2K.

6. At 9:00 a.m. on March 13, 1986, a pre-proposal bidders conference was held at the Albuquerque Seismological Laboratory. This conference was held for the demonstration of a working model of a heated pen conversion kit and to answer all questions asked by the bidders. The following companies attended this conference:

    1. Kinemetrics, Inc.
       San Gabrial, California

    2. Teledyne Geotech
       Garland, Texas

    3. R&D Associates
       Albuquerque, New Mexico
       (R&D Associates have advised us that they will not be a bidder.)

7. Springnether Instrument Company
   Saint Louis, Missouri
   (This company did not attend the conference but will submit a bid.)

National Map of Liquefaction Hazard

14-08-0001G1187

T. Leslie Youd
Dept. of Civil Engineering
Brigham Young University
Provo, Utah 84602
(801) 378-6327

Objective: One of the key tools for evaluating earthquake hazards is a map showing liquefaction hazard. The purpose of this project is to prepare a national liquefaction hazard map for the 48 contiguous U.S. states. This map will show contours of a parameter termed liquefaction severity index (LSI) which is indexed to the anticipated severity of damage as a consequence of liquefaction of susceptible sediments. LSI will be contoured to provide an estimate of severity of expected liquefaction effects with a high degree of probability of not being exceeded in a given period of time. This LSI value, however, applies only to areas underlain by liquefiable sediment. The actual locations of liquefiable sediments will not and indeed cannot be effectively mapped at a national scale.

Data Acquisitions and Analysis: The first six months of work on this project have involved modifications and verification of a computer program and revision of attenuation relationships required for the analysis.

1. A copy of a usable computer program and seismic input files was obtained from Dave Perkins and his colleagues at USGS in Golden Colorado. This program was modified as necessary to run on Brigham Young University computers and to perform the required analyses and to accept our LSI input data files.

2. An LSI attenuation correlation developed for the western U.S. was adapted to the eastern U.S. by adjusting the correlation on the basis of intensity attenuation with distance from large earthquakes and then verifying the adjusted correlations with the few LSI datum points available for the eastern U.S.

Geophysical and Tectonic Investiagations of the Intermountain Seismic Belt

9930-02669

Mary Lou Zoback
U.S. Geological Survey
Branch of Seismology
345 Middlefield Road, Mail Stop 977
Menlo Park, California 94025
(415) 323-8111, Ext 2367

Investigations

1. Analysis of the state of stress and modern deformation of the northern Basin and Range province.

2. Investigations of tectonic stress on the Atlantic continental shelf.

Results

1. The current stress regime of the actively extending northern Basin and Range province has been constrained using a variety of observations. The data include deformation data (focal mechanisms and fault slip studies), in-situ stress (hydraulic fracturing) measurements, borehole elongation ("breakouts") analyses and alignment of young volcanic vents. Integrated, the data indicate significant regional and temporal variations both in principal stress orientations and magnitudes, as well as relative magnitude variations with depth. Approximately E-W extension appears to characterize both the eastern and western margins of the province, whereas a NW to N 60°W least principal stress orientation characterizes the active parts of the interior of the province. Abundant strike-slip focal mechanisms from many areas in the province suggest a stress regime in which the maximum horizontal stress and the vertical stress have similar mangitudes. Detailed observations of faulting in the region of combined normal and strike-slip faulting in the Sierra Nevada - Northern Basin and Range boundary zone suggest temporal variations, possibly quite large, in both stress orientation and relative magnitudes. Limits on variations in stress field are simply illustrated with field observations from a single site, the Owens Valley area of westernmost California.

   Owens Valley was the site of M 8+ earthquake in 1872. Although a prominent NNW-trending east-facing vertical scarp (typically 1 m to up to 3 m high) was formed during the earthquake, a recent careful field investigation of the fault zone indicates that for most of the fault trace the dominant sense of offset was right-lateral strike-slip (S. Beanland, 1986, oral comm.). Beanland estimates that the ratio of lateral to vertical offset during the 1872 event may range from 4:1 to as great as 10:1. Morphology of the fault trace and the fact that the uplifted block is sometimes on the eastern side not western side of the fault, indicate a very steep dip for the fault (we have estimated ~ 85°E). For much of its length the fault runs through Owens Valley, and is located 5 to 20 km east of the subparallel Independecne Fault, which is a part of the Sierran frontal fault zone. Late Pleistocene slip on the Independence fault has been dominantly dip-slip, no evidence of lateral slip has been detected (Gillespie, Ph.D thesis, Caltech, 1982).

Figure 1 gives a lower hemisphere plot of these two faults and ranges in possible slip direction for specified stress orientations. Using an estimated S_3 orientation of N 80°W, the observed contrasting sense of offset can be explained only with very large fluctuations in the relative magnitude of S_{Hmax}. For the nearly pure normal dip-slip on the Independence fault S_{Hmax} must be close in magnitude to S_{hmin} whereas the Owens Valley fault appears to have slipped under a regime where S_{Hmax} and S_v were approximately equal. Thus the approximately N-S horizontal principal stress has had large fluctuations in relative magnitude, possibly accompanied by horizontal rotations.

2. Horizontal principal stress orientations were inferred from wellbore elongations ("breakouts") obtained from standard industry dipmeter logs run in petroleum exploration wells on the Atlantic outer continental shelf. Twenty-seven of 43 dipmeter logs analyzed yielded clear and consistently-oriented wellbore elongations. Results of the analysis by area (from north to south) are as follows: Georges Bank (9 wells, total depths between 4.30 and 6.66 km)-maximum horizontal compressive stress (S_{Hmax}) orientation approximately E-W; Baltimore Canyon (16 wells, total depths between 3.74 and 5.58 km)-S_{Hmax} orientation between N 50°E and N 70°E; and the Southeast Georgia Embayment (2 wells, total depths between 1.83 and 2.13 km)-S_{Hmax} orientation between N 8°E and N 23°E. All wells lie within 70 km of the continental slope and the inferred least horizontal principal stress orientations are aligned perpendicular to the local trend of the continental slope suggesting that the stress field may be dominated by flexural effects related to sedimentary loading or by instability related to the topographic free face of the slope itself. However, focal mechanisms of earthquakes directly adjacent onshore indicate compressional deformation (thrust and strike-slip faulting) resulting from NE to ENE maximum horizontal compressive orientation. The absence of seismicity and lack of high resolution seismic reflection data in the offshore fields preclude characterization of the style of deformation (compressional or extensional) that might currently be occurring in those areas. It appears that the state of stress on the continental margin is broadly consistent with the NE to ENE maximum horizontal compression characterizing most of mid-plate North America, however continental slope affects are locally large enough to rotate the horizontal principal stresses by as much as 40°.

Reports

1. Dart, R. W. and Zoback, M. L., 1986, Principal stress directions on the Atlantic Continental Shelf from the orientations of borehole elongations: U.S. Geological Survey Open-File Rept. 86-?.

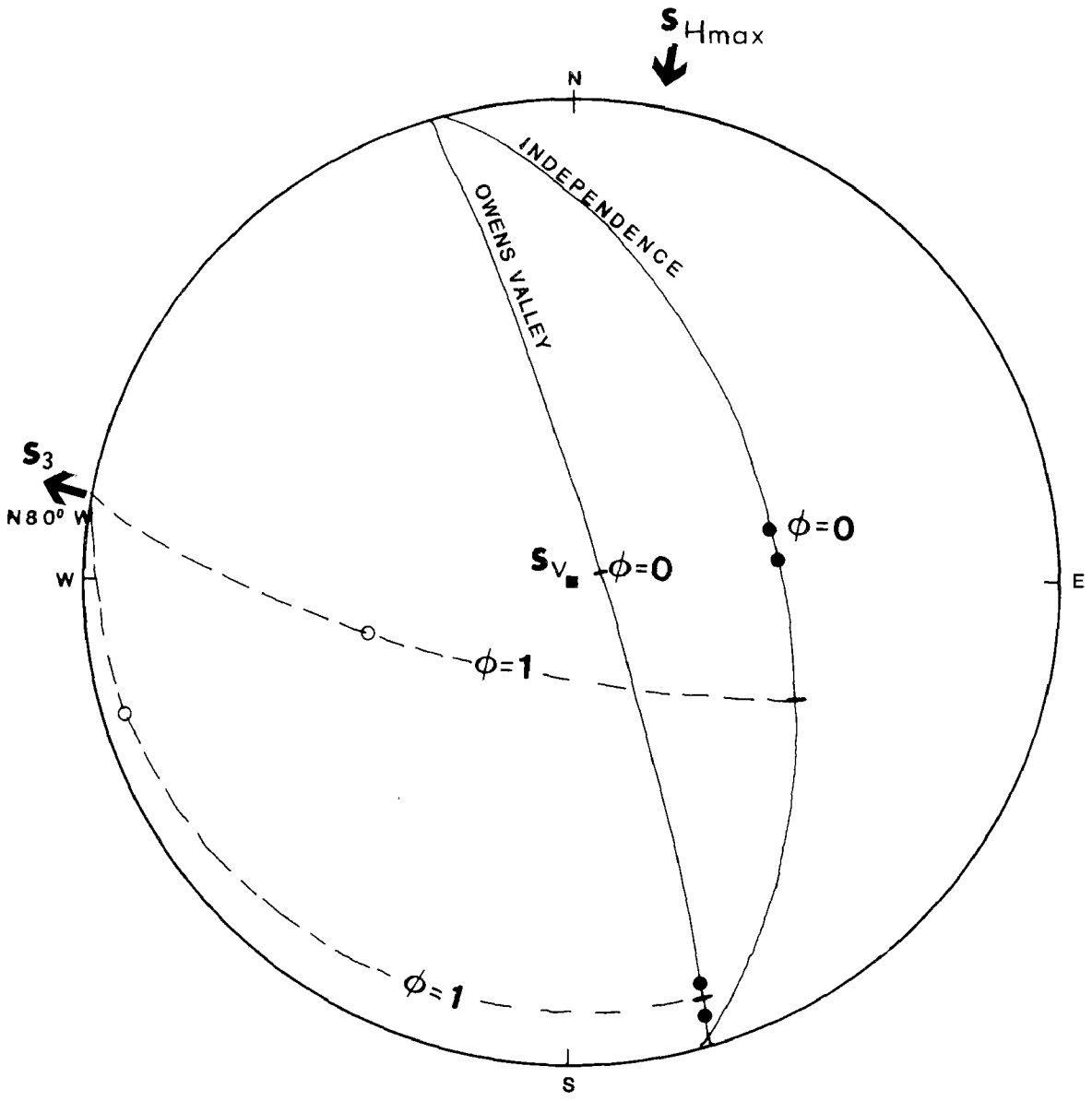

Figure 1: Lower hemisphere stereographic projection of the Independence and Owens Valley faults. Fault normals indicated by open circles. Range of observed slip vectors given by solid circles (see text). Possible slip vectors for stress field shown (and assuming $S_1 = S_V$) are indicated by bars on the fault plane. End members of range of slip vector defined by $\emptyset = 0$ ($S_2 = S_3$, down-dip slip) where $\emptyset = \frac{S_2 - S_3}{S_1 - S_3}$ and by

$\emptyset = 1$ ($S_1 = S_2$, transitional to strike-slip faulting stress regime), see description of technique in Angelier (1979, Tectonophysics, v. 56, p. 17-26).

Wasatch Front County Hazards Geologists Program

14-08-001-G991

Gary E. Christenson
Utah Geological and Mineral Survey
606 Black Hawk Way
Salt Lake City, Utah 84108
(801) 581-6831

Investigations: The principal objective of this program is to facilitate geologic hazards reduction in urban planning along the Wasatch Front. This is being accomplished by providing funding to county governments to hire staff geologists for a 3-year period to collect information, compile maps and reports, and work with planners on a day-to-day basis. The geologists are employees of the counties but receive technical supervision, schedules, and work plans from the UGMS. Three geologists have been placed in the planning departments of five Wasatch Front counties (Mike Lowe - Weber and Davis Counties; Craig Nelson - Salt Lake County; Robert Robison - Utah and Juab Counties) and are undertaking data collection and compilation in the first year of this three-year program. Basic geologic, hydrologic, and soils information has been collected, indexed, and placed in a library at each county office. Site-specific engineering geologic and geologic hazards information is being collected and indexed on 1:24,000 USGS topographic quadrangles. In addition, county geologists are aiding both city and county planners by providing information needed for immediate decision-making, reviewing geotechnical reports, answering public inquiries, investigating hazard events, and performing site investigations for public facilities. Work by the county geologists is reviewed by UGMS to maintain technical quality and bimonthly meetings are held to provide a forum for discussion of issues and monitoring of progress.

During the year beginning June 1986, basic-data maps depicting soils, geology, depth to ground water, and slope will be compiled and used along with information collected during the first year to derive interpretive maps depicting slope stability, seismic hazards, and soil-foundation conditions. These interpretive maps will be user-oriented and directed toward use by planners in developing and implementing hazards ordinances. Other assistance to cities and counties performed during the first year will continue as time allows.

Results: Much new and important hazards information has been identified and brought to the attention of environmental planners, including:

1) Recent mapping of liquefaction hazards completed in Davis and Salt Lake Counties and in progress in Utah and Weber Counties by Utah State University and Dames and Moore.

2) Surficial mapping of the Wasatch fault completed for Salt Lake County and underway in all other counties by the USGS.

3) Unpublished fault trenching data from seismic hazards site investigation reports by local consultants.

4) Quantitative slope stability analyses for slopes and existing landslides under static and dynamic (earthquake) loading.

5) Various research and mapping projects being funded under the USGS NEHRP addressing relative ground shaking, seismic slope stability, flooding due to tectonic subsidence, and rockfall hazards along the Wasatch Front.

This information is being used to identify hazards at proposed developments, review geotechnical reports, perform site investigations, and compile hazards maps. The county geologists have also provided input in the review of proposed hazards ordinances, attended planning commission meetings to discuss proposed developments and other concerns, suggested topics to be addressed in site investigation reports in hazard areas, and provided geologic input into decisions regarding zoning changes and exemptions from ordinances. Interim reports at the end of each year and a final report at the end of the program will be presented to the County Commissions, Planning Commissions, and Councils of Governments (city mayors) of each participating county.

Development of Seismic Hazard Maps for Puget Sound

USGS Contract No. 14-08-0001-21306

Steven M. Ihnen and David M. Hadley
Sierra Geophysics, Inc.
P.O. Box 3886
Seattle, WA 98124
(206) 881-8833 until 1 June 1986
(206) 822-5200 thereafter

Investigations: A set of maps have been constructed which estimate the risk of seismic ground shaking in the Puget Sound, Washington area as measured by peak horizontal ground acceleration (PGA). A hybrid technique for risk assessment has been developed which incorporates the effects of soil type and subsurface focusing into the risk estimate.

Results: A "base risk" map has been prepared using the program SEISMIC.EXPOSURE (NOAA, 1982). The "base risk" map is computed by assigning earthquake frequency-magnitude curves to user-specified seismic zones. The result is an estimate of the PGA for which there is an X percent chance of exceedance in T years. Figure 1 shows the base risk map for Puget Sound. The quantity contoured is the PGA for which there is a 5% chance of exceedance in 50 years. This is equivalent to the PGA for which once exceedance can be expected every 1000 years, on average.

Figure 1 shows a general pattern of high PGAs to the northwest, where the subducted slab is shallow, ranging to lower PGAs in the southeast, where the slab is deep.

Soil effects have been incorporated into this map by digitizing the surface geology of Puget Sound and applying a correction adapted from the theoretical modeling studies of Apsel, et al. (1983). A very conservative approach was used which should result in fairly low predicted PGAs. The result is shown in Figure 2. The general pattern of highs to the NW and lows to the SE seen in the previous figure is apparent here also, but it is now modified by the presence of soils. High PGAs occur in regions of soft soil, especially along lakeshores and in streambeds. The high PGAs present in the northwest corner have been moderated by the presence of bedrock at the surface there.

Ihnen and Hadley (1984, 1986a) pointed out that subsurface focusing can cause large increases in PGA at some sites. Incorporation of focusing into the risk map cannot be done in a rigorous way, since focusing is both hypocenter- and focal-mechanism-dependent. An approximate technique was developed which allows estimation of the increase or decrease in PGA associated with focusing. The risk map in Figure 3 includes this focusing estimate. Approximately 30% of the study area experiences focusing of some degree. Highest PGAs for which there is a 5% chance of exceedance in 50 years are about 60% of g, but only in one or two isolated areas. The average PGA in this area is around 30% of g.

Details of the risk mapping procedure may be found in Ihnen and Hadley (1986b).

References and Reports:

Apsel, R.J., D.M. Hadley and R.S. Hart, 1983, Effects of earthquake rupture shallowness and local soil conditions on simulated ground motions, U.S. Nuclear Regulatory Commission/CR-3102/UCRL-15495.

Ihnen, S.M. and D.M. Hadley, 1984, Prediction of strong ground motion in the Puget Sound region: the 1965 Seattle earthquake, Sierra Geophysics Report SGI-R-84-113.

Ihnen, S.M. and D.M. Hadley, 1986a, Prediction of strong ground motion in the Puget Sound region: the 1965 Seattle earthquake, to appear in Bull. Seism. Soc. Amer., August 1986.

Ihnen, S.M. and D.M. Hadley, 1986b, Seismic Risk maps for Puget Sound, Washington, Sierra Geophysics Report SGI-R-86-127.

National Oceanic and Atmospheric Administration, 1982, Development and initial application of software for seismic exposure evaluation, Volume 1, software description.

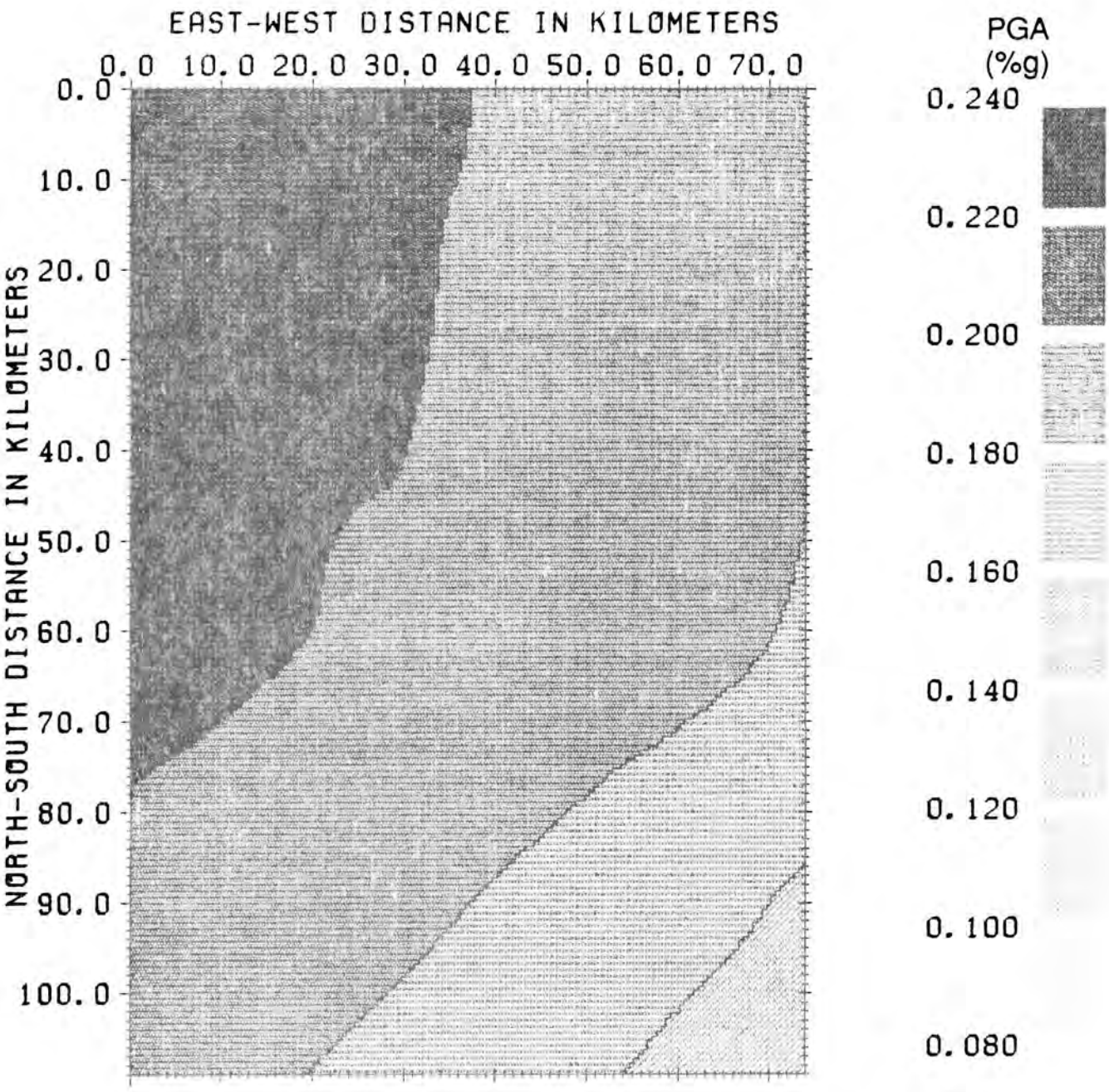

FIGURE 1 - "Base risk" map for Puget Sound earthquakes. Contours are of PGA for which there is a 5% chance of exceedance in 50 years. Origin of coordinates at NW corner of map is at 48N, 123W, and the area covered is one degree by one degree.

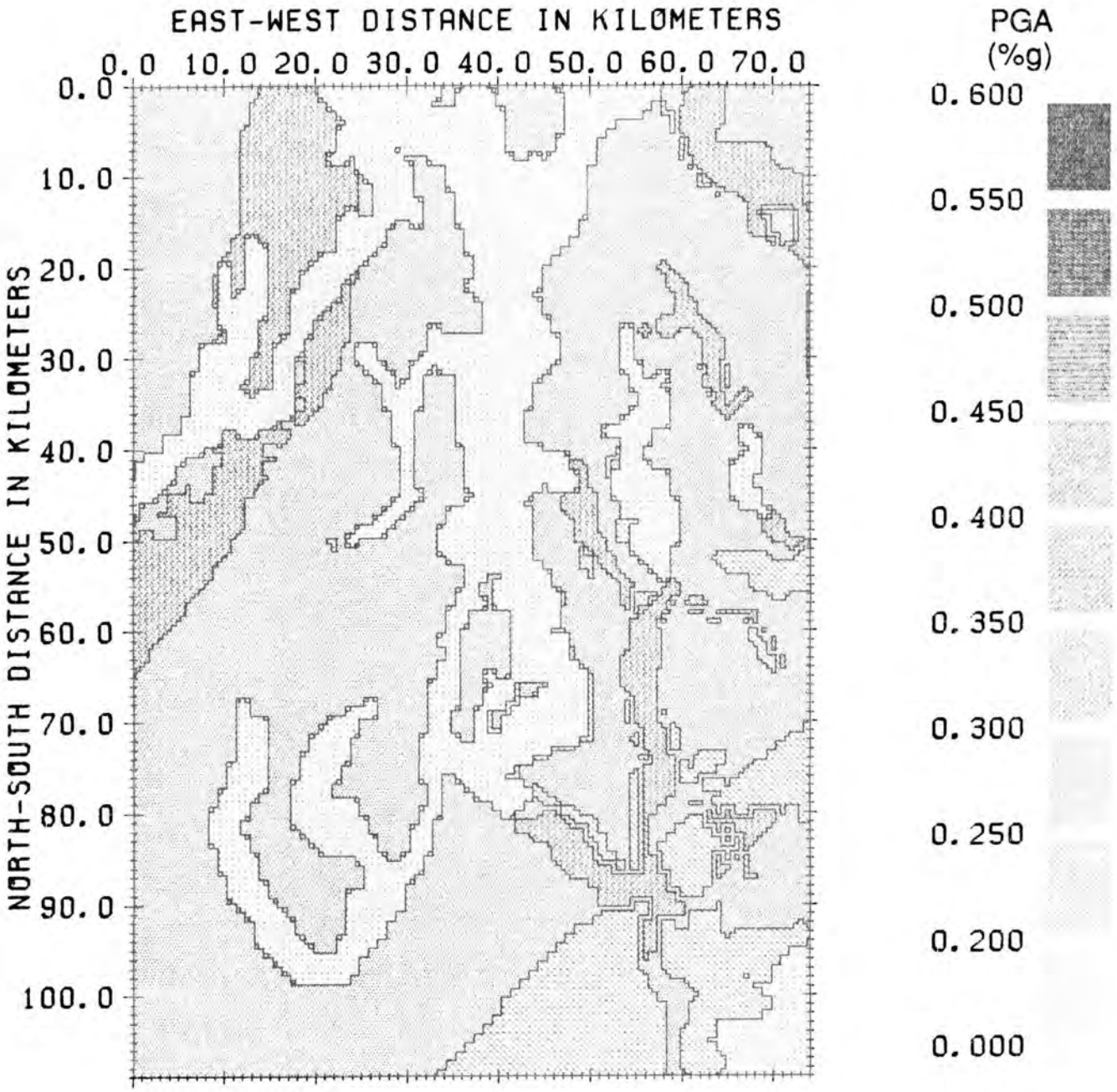

FIGURE 2 - Risk map including effect of soils. Contours, area, and scale same as Figure 1.

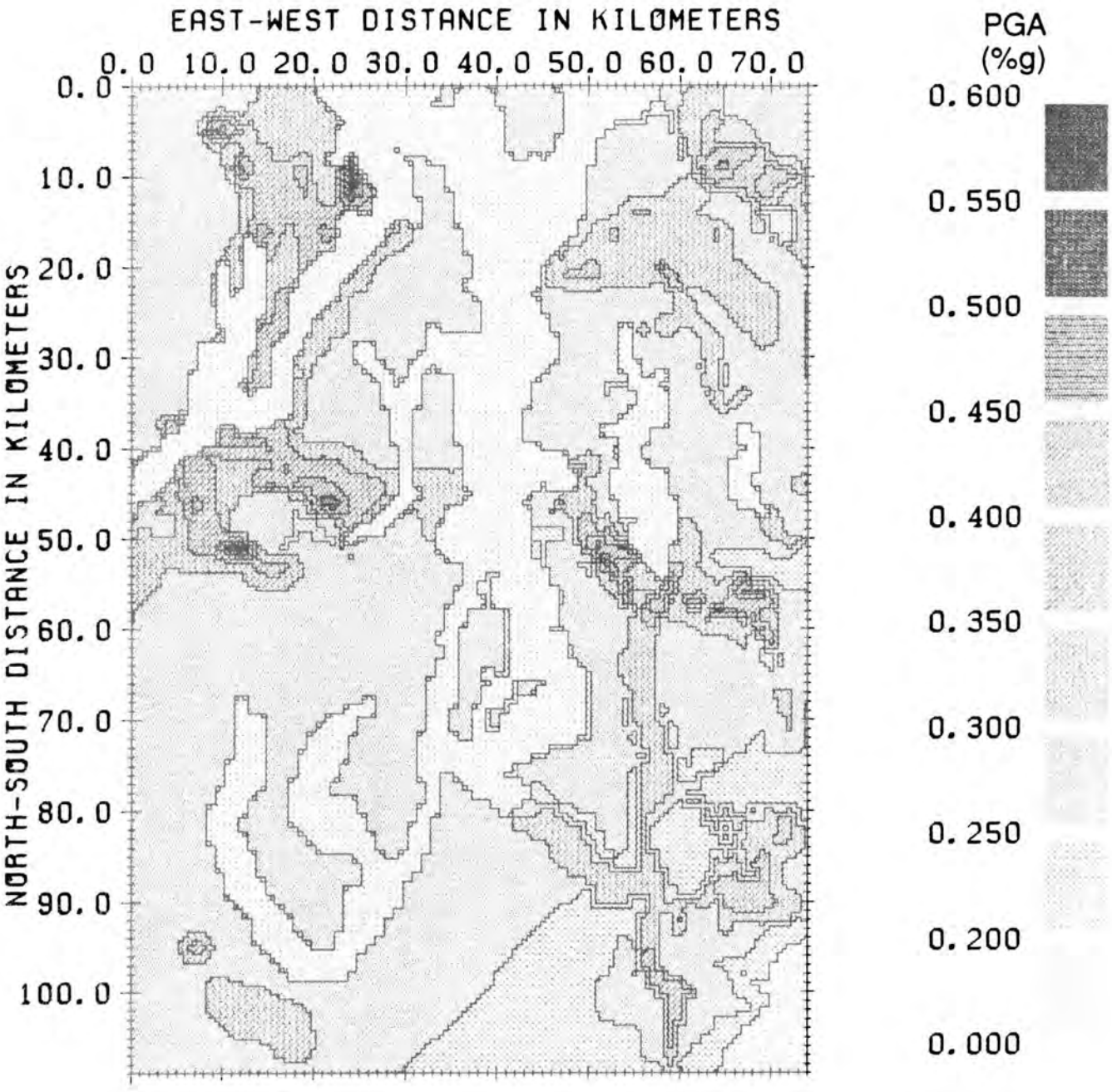

FIGURE 3 - Risk map including soils and an estimate of focusing. Contours, area, and scale same as Figure 1.

Effect of Lateral Heterogenieties on Strong Ground Motion

14-08-0001-21257

C.A. Langston
440 Deike Building
Department of Geosciences
The Pennsylvania State University
University Park, PA 16802
(814) 865-0083

Investigations

1. Simulation of high frequency strong ground motions over plausible three-dimensional geologic structure.

2. Study of anomalous site effects in the Pasadena, California area for the San Fernando earthquake.

3. Teleseismic waveform modeling of the April 13, 1949 Puget Sound Earthquake.

4. Study of strong ground motions from the April 13, 1949 Puget Sound earthquake.

Results

1. A ray theory algorithm was succesfully developed which allows the computation of body wave responses at the free surface of a velocity model consisting of homogeneous layers separated by curved three-dimensional surfaces. Dislocation point sources can be placed anywhere within the model.

2. A study was made of the effect of alluvium geometry on the propagation of short-period body waves using standard propagator matrix methods and the ray tracing technique for 3-D structure. A working assumption was made that differing wave incidence angles and azimuths between the waves excited by the San Fernando earthquake and events studied by Gutenberg caused the descrepancy in expected site amplifications observed during the San Fernando earthquake in the Pasadena area. Amplification does not occur for plane layer responses of grazing S wave incidence. Synthetic seismograms constructed for S wave point sources at various depths and locations outside of a 3-D model of Pasadena alluvium structure indicate that particle motion can be quite complex from off-azimuth conversions and reverberations within the structure. The effective amplification can also be variable due to local shadow zones for the direct waves, particularly for shallow incidence angles. However, these effects tend to be homogenized if a finite source is assumed and that the

principal effect of low velocity alluvium is to amplify wave amplitudes by factors of two or more. These results generally agree with Gutenberg's observations since he analyzed waves of lower incidence angle compared to the San Fernando event and found high amplifications with considerable amplitude scatter. 3-D structures can be constructed to reconcile the San Fernando data with this result, but are clearly non-unique.

3. Eight long period three component teleseismic records from the magnitude 7.1 1949 Olympia, Washington earthquake were collected. P, SH, and SV first motions and SH to SV amplitude ratios from those records, in combination with data from three stations at regional distances were utilized in a grid testing routine which constrained the focal mechanism. Both forward and inverse body wave modeling techniques were utilized to gain further insight into source parameters. Identification of the pP phase in each teleseismic record places the event at 54 km depth. Distinct pulses, assumed to be source effects, are observed in the far field waveforms. Analysis of these pulses for directivity effects made possible discrimination between the fault and auxiliary planes. The plane taken to represent the fault surface strikes east-west ±15°, dips N45E ±15°, and has nearly pure left lateral slip. The source model preferred has an eastward propagation of forty km. Surface reflections of successive source pulses indicate an upward component of propagation of five km. The focal mechanism is significantly different from those obtained in previous studies based on just P wave first motions. Evidence of polarity reversals in data sets used in the earlier studies indicates that errors in polarity may have led to errors in the previously determined focal mechanisms. The event is assumed to have occurred in the subducted Juan de Fuca Plate. The T axis, gently dipping to the southeast, supports other evidence that the Juan de Fuca plate dips to the southeast in a zone between segments of the plate north and south of the event's location. The fault plane's slip is taken to indicate that subduction is still active beneath Washington, and that motion of the two segments is probably independant.

4. Bounds on the earthquake location and rupture of the magnitude 7.1 Puget Sound event of April 13, 1949 were determined using depth and source mechanism constraints from a previous teleseismic study of the event and characteristics of local strong ground motion recordings. The 9 second S - instrument trigger time seen in the Seattle acceleration recordings places the event at least 60 km from Seattle. Strong motion velocity at the Olympia Highway Test Laboratory(OHT) is characterized by an impulsive and rectilinear S wave. The low amplitude of the vertical component of initial S motion suggests that either the source is within 5 km of OHT for a pure

incident SV wave or located along an azimuth of N158° if the wave is SH. The combined constraint of minimum distance from Seattle and the S polarization angle implied by the teleseismic data focal mechanism place the initiation of rupture 5 to 10 km N to NNE of OHT at 47.13°N 122.95°W. This is approximately 20 km west of previously determined epicenters. The duration of rupture inferred from the S wave duration at OHT is consistent with the teleseismic rupture model where left-lateral slip occurs on the northward dipping east-west fault plane.

Reports

Baker, G.E. (1985). Source parameters of the magnitude 7.1, 1949, south Puget Sound, Washington earthquake determined from long-period body waves, M.S. Thesis, University of Washington.

Baker, G.E. and C.A. Langston (1986). Source parameters of the magnitude 7.1, 1949, south Puget Sound, Washington earthquake determined from long-period body waves, preprint.

Langston, C.A. and G.E. Baker (1986). Source parameter constraints from strong ground motions of the April 13, 1949, Puget Sound earthquake, preprint.

San Andreas Segmentation: Cajon Pass to Wallace Creek

9910-03983

David P. Schwartz, Robert V. Sharp, and Ray J. Weldon
Branch of Engineering Seismology and Geology
U.S. Geological Survey
345 Middlefield Road, MS 977
Menlo Park, California 94025
(415) 323-8111, ext. 2689

Investigations

This is a new project. The goal is to refine existing and/or develop new segmentation and fault behavior models for the San Andreas fault between Wallace Creek and Cajon Pass.

1. Develop new slip rate data from Wallace Creek to south of Cajon Creek. Emphasis will be placed on obtaining longer term rates (one to several thousand years), which help in evaluating segmentation and fault behavior models. Especially important will be defining rates at locations where changes in structural complexity of the fault system occur, such as the Tejon Pass region and the San Andreas-San Jacinto confluence. Quaternary mapping and preliminary trenching will be conducted at appropriate sites.

2. Critically review published and unpublished data and, where possible, existing field relationships to define and quantify uncertainties in: a) timing, displacement, and lateral extent of individual past earthquakes; and b) location-specific slip rate estimates. This includes new measurements of offset streams and other geomorphic features at sites where slip rate and slip per event have previousy been measured. The 1857 slip distribution is included in this review.

3. Map and characterize the style of secondary faulting along the San Andreas, particularly near the junction with the San Jacinto fault on the south and near Liebre Mountain on the north. The former locality is where a slip rate step occurs and the 1857 rupture appears to have ended. The latter is a change (decrease) in the amount of offset associated with the 1857 rupture and where a previous (1720?) rupture decreased or stopped at its northern end. The recognition of distinctive structural settings that may correspond with the end of rupture segments is a major component of segmentation modeling, and can also provide important insight into processes of rupture initiation and termination.

Results

1. Five potential sites for slip rate and recurrence studies were located during reconnaissance of the fault between Tejon Pass and Pitman Canyon. Two sites, named 96 St. and Wrightwood, have been selected for study during FY 1986.

   a. The 96 St. site, located 6 km southeast of Littlerock Creek and 8-1/2 km northwest of Pallett Creek, exposes an offset sequence of fluvial, pond, and colluvial deposits. Charcoal from a carbon-rich burn layer exposed in a natural cut into the upthrown block of the fault has yielded a radiocarbon date of 1070, +50, -60 ^{14}C yr B.P. Exploratory trenches and gully exposures show the fault is a well-defined zone

containing two traces that are consistently 5 to 8 m apart at the surface. The west trace is vertical and was the main slip surface (3 m? to 4-1/2 m?) in 1857. The east trace varies in dip from 20 to 60 degrees SW and likely joins the west trace at a shallow depth. Microgeomorphic relationships suggest 50 to 75 cm of slip on the east trace in 1857. The trenches show that charcoal, either as burn layers or as disseminated detrital charcoal, occurs throughout the stratigraphic sequence. This site appears to have good potential for yielding a 1100 year, and possibly longer term, slip rate. Additional trenches will be excavated in June.

b. The Wrightwood site is located near the mouth of Government Canyon, approximately 4 km northwest of Wrightwood. A natural stream cut exposes a sequence of layered peats displaced by minor faults immediately west of the main fault trace. A radiocarbon age of 3520, +60, -50 ^{14}C yr B.P. was obtained from the highest peat in the section (1.5 m below ground surface), and an age of 4990±90 ^{14}C yr B.P. was obtained on a peat 0.5 m lower in the section. A trench is planned for July/August to better expose site stratigraphy. The site appears to have the potential to yield long term slip rates, and may provide information on the fault history prior to the Pallett Creek sequence.

c. Control points have been surveyed at the 96 St. and Wrightwood sites, and large scale topographic maps of each site are being made in conjunction with Sherman Wu, USGS Flagstaff.

2. Reconnaissance has been made along the fault between Gorman and Cajon Pass for the specific purpose of reviewing estimates of the slip distribution of the 1857 event. Our initial observations in Leona Valley and at the 96 St. site suggest that slip on parallel traces may be more common than recognized and that at some localities previous estimates of 1857 slip may be minima.

3. a. A map of active secondary faults along the San Andreas fault between Palmdale and Indio is being prepared with John Matti to better characterize the neotectonic setting of the fault. Preliminary results show domains on the order of fifteen to thirty km wide where either normal or reverse secondary faults dominate. These domains suggest that different parts of the fault zone are experiencing slight extension or compression that may be an important control in rupture propagation. The 1857 rupture terminated at the boundary between a compressional and extensional domain. The domains appear to relate to geometric complexities in the fault system.

b. On-going paleomagnetic studies in Plio-Pleistocene sediments along the San Andreas fault are providing long term slip rates with which to compare Holocene estimates. Detailed structural mapping along the Punchbowl and Lieber Mountain faults has begun to characterize the tectonic setting of the San Jacinto-San Andreas junction and the big bend in the San Andreas, respectively.

Reports

None.

Historical Normal Fault Scarps: Wasatch Front and Vicinity

9910-NEW

David P. Schwartz
Branch of Engineering Seismology and Geology
U. S. Geological Survey
345 Middlefield Road, MS 977
Menlo Park, California 94025
(415) 323-8111, ext. 2689

Investigations

This is a new project. The goal is to study historical normal fault scarps in the Great Basin to calibrate geological techniques used to identify individual past earthquakes and the amount of displacement during each, quantify earthquake recurrence intervals, and evaluate earthquake recurrence models and fault segmentation models. For FY 1986 the project will concentrate on the 1983 Borah Peak, Idaho surface rupture and associated scarps of the Lost River Range.

The Borah Peak surface rupture, in conjunction with other scarps along the Lost River Range, provides a unique opportunity to study major aspects of fault scarp morphology, earthquake recurrence, and fault segmentation. Trenching of the 1983 surface faulting at Doublespring Pass Road (Schwartz and Crone, 1985; Schwartz and Crone, in preparation) has shown that only one other event, with similar displacement to that of 1983, occurred along this reach of the fault during the past 15,000 years. Additional trenching along the northern part of the 1983 rupture, where Scott and others (1985) have proposed a distinct "Warm Springs" segment, and along the adjacent "Mackay" segment to the south that did not rupture in 1983, has the potential to constrain the timing of past events and to clearly demonstrate normal fault segmentation for the first time. This study has major implications and applications for segmentation modeling and seismic hazard analysis of other normal faults, especially long fault zones. The Lost River Range bears many structural similarities to the Wasatch Range and may serve as a dynamic model for interpreting observations made along the Wasatch fault zone.

1. Exploratory trenching at three sites. Site 1 will be near Gooseberry Creek along the northern end of the 1983 surface rupture. The purpose of trenching at this locality is to evaluate whether the pre-1983 scarp, which is larger than the 1983 slip at this location, represents the same event as the pre-1983 event observed in the Doublespring Pass Trench. Test pits will also be excavated along the 1983 rupture to search for datable material that can be used to place tighter constraints on the timing of the pre-1983 earthquake. Sites 2 and 3 will be at Lower Cedar Creek and Pete Creek, respectively, on the proposed Mackay segment. A trench excavated at site 2 by T. Haitt in 1976 is reported to contain Mazama ash and a datable organic horizon. However, the documentation of trench stratigraphy, the number of past events, and the relationship between faulting and datable deposits is poor and inconsistent. This site has the potential to date the most recent event south of the 1983 rupture. Site 3 is near the north end of the proposed Mackay segment. This site

is critical for characterizing the behavior of the segment (one trench is insufficient) and for showing differences in timing of events across a proposed segment boundary.

2. Map variability in morphology of the 1983 scarp. The type and extent of scarp morphology associated with the 1983 surface rupture (vertical free face, colluvium covered scarp, scarp with rotated blocks, folding instead of brittle failure, *etc.*) will be documented and cataloged. Information on variability in morphology and complexity of a scarp along its length can be used to better interpret trench exposures across other normal faults.

Results

Forthcoming.

Reports

None.

Investigations of the Applicability of Fuzzy Calculus to Seismic Risk Determination for the Eastern United States

84-21993

Charles C. Thiel Jr.
Auguste C. Boissonnade
Haresh C. Shah
John A. Blume Earthquake Engineering Center
Stanford University
Stanford, California
(415) 723-1502

Objective:

The development of seismic risk assessments for use in the eastern United States, or for most other areas where there is limited instrumental data and earthquake activity, depends on clearly being able to interpret subjective data on historic activity. This entails several distinct problems:

1. interpretation of historic information that is usually subjective and not easily quantified;

2. assignment of uncertainty to instrumental and qualitative data where the recording instruments performance and/or original data are not available for calibration; and

3. processing these data in a rational method that does not assume that the data has qualities inappropriate to their value.

The premise of this project is that the methods of fuzzy set theory offer the opportunity to assess such data in ways that better represent the value of the data and modeling techniques that present conclusions consistent with these data. The research effort has lead in several directions; firstly, to explore the dependencies of building performance and how data collected from such observations can vary with the quality of the structure; secondly, on the formulation of expert systems (loosely described as a branch of artificial intelligence) that allow the logical interrelationship of risk factors and statements of cause-effect; thirdly, processing approaches for fuzzy data, particularly system identification problems; and, fourthly, applications to seismic catalog data.

Discussion of Results:

The first model developed was the one which explored the interpretation of observed structural damage data. This issue is central to the assignment of intensities and epicentral magnitudes and the development of attenuation relationships. Current techniques are less than satisfactory since they rely

on a subjective evaluation of historic data that is often second hand (or further removed) and interpreted in terms of undefined standard structures. The influence on building earthquake performance of the quality of architectural design, engineering design, construction and age and alteration is examined, [1,2]. Expert opinions on estimating vulnerability is implemented through the formulation of a linear model developed using Fuzzy Set Theory. It shows that variations in quality can change substantially a building's expected vulnerability; so much so, that observed damage variability may be more easily attributed to quality variations than to the level of ground motion observed. The model suggests that the influence of the condition of the structure and the foundation system have an overwhelming effect on the damage that is observed. This effect can be so large as to effectively remove the inferential ability of a single observation from a structure of unknown quality. The key parameters in this analysis are specifications of the damage level, and the building's quality attributes.

A persistent problem in the formulation of overall rules that relate an observation to a conclusion in fuzzy set theory, expert systems or other artificial intelligence systems, is how a series expert derived rules, in the form "If A then B with confidence C", can be reduced to one overall or summary rule. The methods commonly used, based on Mandami's papers in the middle 1970's, have the property that they do not reproduce the data on which they are bases in any "optimal" sense. This formulation has the disadvantage that it tends to give results of very low maximum possibility when the expert rules on which they are based are at odds. While this is satisfactory for many applications, it yields results which are not very useful in our case. This lead to developed of a least square measure to find the summary rule that minimizes the difference between the summary rule and the individual data from which the rule is derived, [3], which is much more satisfactory for seismic risk determinations.

The methods discussed above were applied to interpretation of seismic intensity data, [4]. The concept of seismic intensity involves many complex factors. It attempts to provide in a single measure of the many consequences of an earthquake. Two fuzzy classification methods were used to interpret data: the fuzzy classification system discussed above and fuzzy equivalent relation. The technique shows great promise. The examples given in the paper demonstrate that both methods yield reasonable results when the data are well behaved. An essential choice must be made when assessing which method is used; that is, do you want your ignorance (differences or contradictions) in the data to rule interpretation and therefore imply little or nothing is determined, or whether you want the "best" fit to the data.

The thoughts on how to develop models for seismic risk determination are summarized in the paper "System Identification and Information Processing in Seismic Vulnerability Analysis of Structures" Seismic vulnerability analysis generally involves processing many judgments which are based on experience and much data that is ill-defined or conjectural. A cascade model was developed and presented in this paper for combining site hazard, design, architectural and building characteristics data that incorporates both specific and vague information and data. The cascade model is Bayesian in approach in that new information is used to update prior estimates of vulnerability. The development of the seismic vulnerability evaluation model

depends on rules which encode as a set of relations between linguistic variables.

Papers published to date:

The following papers resulting from the research effort have been published or submitted for publication:

1. Thiel, C.C. and A.C. Boissonnade, "Predicting the Influences on Seismic Building Performance", Presented at the US-Italy Workshop on Existing Buildings, Verena, Italy and Published in Proceedings of the US-Italy Workshop on Existing Buildings, edited by G. Grandori, Politecnico di Milano, Italy, 1985.

2. Thiel, C.C. and A.C. Boissonnade, "Predicting the Influences on Seismic Building Performance", a revised and extended version of the above paper submitted for publication in the Journal Earthquake Spectra.

3. Boissonnade, A.C., W.-M. Dong, H.C. Shah and F.S. Wong, "Identification of Fuzzy Systems in Civil Engineering", in Fuzzy Mathematics in Earthquake Researches, F. Deyi and L. Xihui editors, Seismological Press, Beijing, pp 48-71, 1985.

4. Dong, W.-M., A.C. Boissonnade, H.C. Shah and F.S. Wong, "Fuzzy Classification of Seismic Intensity", in Fuzzy Mathematics in Earthquake Researches, F. Deyi and L. Xihui editors, Seismological Press, Beijing, pp 129-146, 1985.

5. Thiel, C.C. and A.C. Boissonnade, "System Identification and Information Processing in Seismic Vulnerability Analysis of Structures", Proceedings, First International Conference on Applications of Artificial Intelligence to Engineering Problems, London, England, Computational Mathematics Institute, Southampton, England, pp. 277-286, 1986.

6. Lamarre, Michelle, W.-M. Dong, "Evaluation of Seismic Hazard with Fuzzy Algorithm" submitted to special issue on approximate reasoning in information systems, Journal of Information Sciences, to be published in the Fall of 1986.

Earthquake Hazards Studies, Metropolitan Los Angeles-Western Transverse Ranges Region

9540-02907

R. F. Yerkes
Branch of Western Regional Geology
345 Middlefield Road MS 975
Menlo Park, California 94025
(415) 323-8111 x2350

Investigations and results

1. Historic earthquake data (Paia Levine and W.H.K. Lee). HYP071 now revised to be interactive relative to station weighing; graphics revised to run on any 8 1/2 x 11 format printer. A series of interactive, interlocking programs were written to permit selection of catalogued events on basis of geographic location, magnitude, number and quality of first-motion arrivals, etc. Programs have been written to automate the revised HYPO program; the programs reformat, standardize, and collate station lists, phase data, and specific instructions for each group of events considered. Using these programs, all 1979 events recorded by CIT/USGS network in southern California region and having good first motions have been set up and are ready for further processing.

2. Earthquake hazard studies (Yerkes). The western Transverse Ranges in the region of the Ventura basin are the locus of extreme north-south convergence (up to 23 mm/yr by some estimates), as indicated by dated marine terraces rising at rates of 6-8 mm/yr, several seismically active reverse faults tens of kilometers in length (including San Fernando and 1971 San Francisco earthquake; Anacapa and 1973 Pt. Mugu earthquake), as well as isolated clusters of seismicity having thrust/reverse fault-plane solutions. The specific loci of the convergence and uplift have not been isolated or identified. As one approach, a series of detailed structure sections, using subsurface well data to depths of 5+ km, have been constructed across the 20 km-long Rincon-San Miguelito-Ventura oil field anticlinal structures. From these sections a detailed structure contour map of a common datum has been made. The sections and map show the 5 km-thick Pliocene-Pleistocene marine section to be tightly folded, with steep overthrust limbs offset up to 1 km on reverse faults such as the Javon Canyon on the south. Uplifted 45,000 yr BP marine terrace deposits are preserved on both the hanging-wall and foot-wall blocks of this fault; their elevations indicate a relative rate of vertical movement of slightly more than 1 mm/yr on the fault. In addition, a N-S structure section, using deep exploratory wells, has been constructed across eastern Santa Barbara Channel. This section indicates that compressive structure is restricted to the north part of the channel, north of the Mid-Channel fault zone. Combining the apparent shortening in the channel with that across the Rincon-San Miguelito structure onshore (south of the Red Mountain fault) indicates a convergence rate of about 12.5 mm/yr.

3. Quaternary stratigraphy, chronology, and tectonics, Ventura area (Sarna-Wojcicki). This investigation is presently concentrating on: improvement of age control for Quaternary marine deposits in onshore sections such as

those of the Ventura basin, developing more detailed oxygen-isotope records, and correlation of marine and continental sequences. We completed a trial set of oxygen-isotope analyses of benthic forams from the Quaternary upper Pico Formation in Balcom Canyon near Ventura (assisted by K.A. McDougall, Branch of Paleontology and Stratigraphy, Menlo Park; Jim Gardner, Branch of Marine Geology, Menlo Park; and K.V. Matthews, Brown University, Rhode Island). These data represent variations in oxygen-isotope composition for about 75,000 yrs, from about 1.21 to 1.135 Ma, indicating variations in ocean volume for this period. Age control is provided by previously-dated tephra in the same sequence and inferred sedimentation rates. The Balcom Canyon record shows greater detail than is available from deep-sea cores owing to faster sedimentation rates and consequently much smaller effects of bioturbation. Because of the ability to control the sampling interval and the greater sedimentation rates, the present Balcom Canyon sampling interval represents about 3,000 yrs. versus 6,000 yrs. for deep-sea sampling intervals. Analysis and testing continue.

Reports

Levi, Shaul, Schults, D.L., Yeats, R.S., Stitt, L.T., and Sarna-Wojcicki, A.M., 1986, Magnetostratigraphy and paleomagnetism of the Saugus Formation near Castaic, Los Angeles County, California, in Ehlig, Perry, ed., Neotectonics and faulting in southern California, Guidebook and Volume, Geological Society of America Annual Meeting, Cordilleran Section, March 25-27, p. 103-108.

Sarna-Wojcicki, A.M., Morrison, S.D., Meyer, C.E., and Hillhouse, J.W., Correlation of upper Cenozoic ash beds in sediments of the western United States and northeastern Pacific Ocean, and comparison with biostratigraphic and magnetostratigraphic data. Submitted to G.S.A. Bulletin, 57 ms p. Director approved.

Experimental Investigation of Liquefaction Potential

9910-01629

Thomas L. Holzer

Branch of Engineering Seismology and Geology
U.S. Geological Survey
345 Middlefield Road, MS 977
Meno Park, CA 94025
(415) 323-8111 ext 2760

Investigations

1. Design and installation of an instrumented site in Parkfield, California, to measure pore pressures in sands and strong ground motion during the predicted Parkfield earthquake.

2. Magnitudes of ground settlement during liquefaction and the effect of the densification on the liquefaction resistance to future earthquakes are being evaluated.

Results

1. Subsurface exploration in Cholame Valley, California, has found a saturated medium- to coarse-grained sand which has the potential to generate excess pore pressures during the predicted Parkfield earthquake. Detailed analysis of standard penetration and cone penetration test data indicates the upper part of the deposit is susceptible to liquefaction at the magnitude of strong ground motion anticipated during the predicted earthquake. A system with six pore pressure transducers and four borehole accelerometers is being designed to be installed in the summer of 1986.

2. Settlements caused by liquefaction equal up to five per cent of the thickness of the liquefying sand. Despite the densification, field investigations suggest that liquefaction of many deposits recurs.

Reports

Bennett, M.J., 1985, Subsurface investigation of ground failure at the San Fernando Valley Juvenile Hall, Sylmar, California (abstract): Association of Engineering Geologists, 28th Annual meeting, Winston-Salem, N.C., Abstracts with Programs, p. 57.

Chen, A.T.F., 1986, PETAL2 - Penetration testing and liquefaction, An interactive computer program: U.S. Geological Survey, Open-File Report 86-178, 31 p.

Tinsley, J.C., and Youd, T.L., 1985, Liquefaction-related ground failure in U.S. geological Survey Professional Paper 1360, p. 434-436.

Near Lithologic and Seismic Properties

9910-01168

W.B. Joyner
J.F. Gibbs

Branch of Engineering Seismology and Geology
U.S. Geological Survey
345 Middlefield Road, MS 977
Menlo Park, California 94025
(415) 323-8111, ext. 2754, 2910

Investigations

Measurement of seismic velocity and attenuation to determine the effect of local geology on strong ground motion and to aid in the interpretation of seismic source parameters.

Results

We cooperated with J. Boatwright in the determination of shear-wave attenuation to a depth of 150 meters in a borehole near Coalinga.

We also obtained additional downhole shear-velocity data at recording sites for the Coalinga earthquake sequence.

Reports

Boatwright, J., Porcella, R.L., Fumal, T.E., and Liu, H.-P., 1986, Direct estimates of shear wave amplification and attenuation from a borehole near Coalinga, Cailfornia: *Earthquake Notes*, v. 57, p. 8-9.

Boore, D.M., and Joyner, W.B., 1986, Prediction of earthquake ground motion at periods of interest for base-isolated strutures: *Proceedings of ATC Seminar on Base Isolation and Passive Energy Dissipation*, San Francisco, California, March 1986, Applied Technology Council, in press.

Joyner, W.B., 1986, Predictive mapping of earthquake ground motion *in* Workshop on Future Directions in Evaluating Earthquake Hazards of Southern California: *U.S. Geological Survey Open-File Report*, in preparation.

Techniques for Applying Earthquake Hazard Map Data--San Francisco Bay Area, California

14-08-0001-G1166

Jeanne B. Perkins
Association of Bay Area Governments
Metrocenter
Eighth and Oak Streets
Oakland, CA 94607
[P.O. Box 2050--Oakland, CA 94604]
(415) 464-7934

For the past several years, ABAG has been developing computer-based maps and map files of the San Francisco Bay Area depicting earthquake hazards. The information currently is underutilized. ABAG will be helping selected local governments make more effective use of the information with the objective of helping them develop more strategies for reducing potential earthquake-related losses. First, ABAG staff will be conducting a survey of several local government staff in the Bay Area to identify past applications and potential needs of the user community. Next, staff will select potential applications and develop techniques to aid in the use of ABAG's regional database. Finally, ABAG will be preparing materials to document the new techniques, inform other local governments in the region of potential ways that actual communities have used the data, and aid others in developing similar regional capabilities. ABAG's Earthquake Preparedness Program will provide for continuing user support and interaction.

Due to other demands on the time of key project staff, minimal work has occurred on this project at this time.

Regional Syntheses of Earthquake Hazards in Southern California

9910-03012

Joseph I. Ziony
Branch of Engineering Seismology and Geology
U.S. Geological Survey
345 Middlefield Road, MS 977
Menlo Park, California 94025
(415) 323-8111, ext. 2944

Investigations

During this reporting period, our efforts were directed toward:

1. Organizing and holding a multidisciplinary workshop on southern California earthquake hazards to review recent scientific results and to identify priorities for future research.
2. Compilation of a 1:250,000-scale map showing late Quaternary faults and recent seismicity for the onshore and offshore Los Angeles region.
3. Initiating detailed geologic field studies along the Elsinore fault zone between Corona and Lake Elsinore in order to document late Quaternary offsets, estimate fault slip rates, and evaluate segmentation of the zone.

Results

1. We convened a workshop, "Future Directions in Evaluating Earthquake Hazards of Southern California", in Los Angeles at the University of Southern California on November 12 and 13, 1985. The USGS, FEMA, NSF, California Office of Emergency Services, California Division of Mines and Geology, California Seismic Safety Commission, Southern California Earthquake Preparedness Project, and Southern California Association of Governments jointly sponsored the workshop. About 330 people participated, including geologists, seismologists, engineers, planners, and emergency management experts. Numerous private firms, universities, and governmental units were represented.

   The workshop summarized key results of recent earth-science research on evaluating earthquake hazards; examined current activities where hazard information is being used in southern California to reduce potential earthquake losses; and discussed what additional scientific information is needed and which hazard-reduction techniques are most effective. Separate working group sessions explored the following topics in depth:

   - Evaluating earthquake and surface-faulting potential for hazard reduction actions.
   - Predicting seismic intensities for response planning and loss estimation.
   - Predicting ground motion for earthquake-resistant design.
   - Predicting major earthquakes for preparedness planning.
   - Evaluating earthquake ground-failure potential for development decisions.
   - Evaluating the shaking hazard for redevelopment decisions.

Workshop proceedings, including papers of the speakers and panelists and summaries of individual working group discussions, currently are being edited for release as a USGS "redbook" open-file report. These published proceedings will aid in transferring southern California's successful hazard-reduction efforts to other earthquake-prone regions.

2. A 1:250,000-scale map showing epicenters of $M_L \geq 2$ earthquakes (A, B, C, and P quality) during 1978-1984 was compiled by Lucy Jones for the Los Angeles region between longitudes 120°00'W and 116°45'W and latitudes 33°15'N and 34°45'N. These data will be combined with surface traces of late Quaternary faults being evaluated and compiled from the most recent available geologic maps for the same region.

Reports

Ziony, J.I., Earthquake and Surface-faulting potential in southern California--Current knowledge and major unresolved questions, for *Proceedings, Southern California Earthquake Hazards Workshop*, 10 p. (approved by Director).

Depth to bedrock map in the greater Tacoma area, Washington

9950-04073

Jane M. Buchanan-Banks
Branch of Engineering Geology and Tectonics
U.S. Geological Survey
David A. Johnston Cascades Volcano Observatory
5400 MacArthur Boulevard
Vancouver, Washington 98661
(206) 696-7996

Investigations

The Puget Lowland is a densely populated urban area with a high potential for damaging earthquakes. In 1949, a 7.1 magnitude earthquake with an epicenter between Tacoma and Olympia, and in 1965, a 6.5 magnitude earthquake with an epicenter between Seattle and Tacoma caused eight deaths and millions of dollars in damage. Most structural damage was associated with areas of thick, loosely consolidated sediments.

The purpose of this new project is the reduction of earthquake-related geologic hazards in the dense population centers in and near Tacoma and Olympia, Washington, through identification and delineation of areas with thick sediment cover that could produce strong seismic-related ground shaking and slope failures.

Results

1. Compilation of a bibliography of the geology of the Puget Sound region was begun, and copies of some appropriate publications were obtained.

2. Water-well records of Pierce County were obtained from USGS Water Resources Division, Tacoma, and locations of all wells deeper than 200 ft were plotted on a 30 X 60 ft map of the Tacoma area.

A Systems Approach to Wasatch Front Seismic Risk Problems

14-08-001-22013

Craig Taylor and John Wiggins
NTS Engineering
1650 South Pacific Coast Highway
Redondo Beach, CA 90277
(213) 316-2257

Investigations

1. Develop a data base structure, including selection of a basic geographic reference and microzonation scheme, and construct building data and lifeline network component data formats for earthquake risk studies.

2. For Salt Lake and Davis Counties, Utah, gather and input data on State-owned buildings, natural gas supply facilities, culinary water supply facilities, and local geoseismic hazards.

3. Using seismic energy sources mapped at depth, develop seismic risk procedures and programs that will produce figures of merit for State insurance analysis and that will estimate expected pipeline breaks in natural gas and culinary water systems.

4. Produce figures of merit for State building earthquake insurance analysis and evaluate expected pipeline breaks in natural gas and culinary water systems inventoried.

Results

Although "moderate" in terms of excepted earthquake occurrences, the Wasatch Front region has local factors that tend to increase earthquake risks significantly. Our analysis has shown that these include:

(1) Limited seismic resistance of many older buildings.

(2) High spectral dynamic amplification factors potentially affecting many exposures in Salt Lake and Davis Counties.

(3) High-to-moderate liquefaction susceptibilities potentially affecting one-fifth of all buried conduits in these counties.

(4) Limited seismic resistance of many utility facilities currently in-place.

(5) Proximity of facilities to the Wasatch normal fault zone modeled at depth.

and (6) Location of some critical facilities within the Wasatch fault zone.

Fifty-two earthquake events with magnitudes ranging from 5.5 to 7.3 were modeled in order to provide both risk-based and single-event loss estimates. Smaller events were randomized on north-south trending lines. The larger ($Ms \geq 6.4$) twelve events were associated with a three-dimensional model of the Wasatch normal fault, which dips and plunges under facilities. For the Salt Lake segment of the Wasatch fault, the model used was based on preliminary findings by Bruhn and others. For the Ogden segment, this model was constructed on the assumption of constant plunge and trend angles. The two largest events ($7.0 < Ms < 7.5$) were defined as having fault rupture lengths equal to fault segment lengths.

PML estimates for State-owned buildings were derived from these two largest events. These were based on shaking intensities only. Basement rock shaking intensities were derived from K. Campbell's near source horizontal peak ground velocity attenuation functions. Distances from the Wasatch fault zone modeled in three dimensions were derived for all microzones (township sections) containing potential exposures. Virtually no exposure in the two counties was more than ten miles from the fault. Dynamic amplification factors for each microzone were adapted from studies by Rogers, Hays, and others of relative ground motion response in the study area. For State-owned buildings, construction data were derived from Utah State Division of Facilities Construction and Management and valuation data were obtained from the Utah State Office of Risk Management. Structural Facilities, Inc. used raw data along with extensive familiarity in the local buildings, code changes, and construction practices in order to categorize buildings for their seismic vulnerabilities. For the bulk of structures, those at the University of Utah, initial categorizations--based on frame and construction data, were revised based on inspection and visual rating techniques. Revisions suggested that initial categorizations tend to be pessimistic.

These PML events produced extremely high loss estimates. At the mean level, over 32 percent of buildings and contents replacement values, respectively, were expected to be lost. Downtime estimates often approached two-thirds of a year for many buildings. Estimates of deaths,

severe injuries, and moderate injuries were three percent, four percent, and ten percent, respectively, of occupants. Since these estimates may have been biased by high dynamic amplification factors, basement rock intensities were then used. But estimates of deaths, severe injuries, and moderate injuries fell only to two percent, three percent, and eight percent, respectively. Key parameters in these high loss estimates were therefore (1) the limited seismic resistance of many buildings (and the assumption that casualty ratios are directly associated with degree of building damage), (2) the proximity of buildings to the Wasatch normal fault zone, and (3) the magnitude of the events ($7.0 < Ms \leq 7.5$) postulated.

Along with shaking hazards, liquefaction and fault rupture hazards were considered in analyzing culinary water and natural gas system earthquake response. Major results are that:

(1) Those microzones having the highest risk-based rates of damage to buried conduits have high liquefaction susceptibilities;

(2) In larger ($Ms \geq 6.4$) magnitude events, expected damage from shaking alone is extremely extensive in culinary water systems;

(3) Over seventy percent of all long-term expected direct water supply pipeline damage is due to smaller magnitude events;

(4) Even local ($M_L \cong 5.5$) smaller magnitude events close to a given water system can yield over 100 expected breaks per million feet of culinary water piping; larger magnitude events can produce up to 400 expected breaks per million lineal feet of culinary water piping; these breaks in larger events are more evenly spread throughout the utility networks as a result of the extremely high shaking estimates for those events;

(5) In larger magnitude events originating from the Ogden segment of the Wasatch fault, aqueducts conveying potentially ample water supplies are likely to be damaged by fault ruptures; these damages, along with high overall expected breaks and damage outside the fault zone imply that Davis County water systems cannot be relied on for immediate assistance to Weber County systems after these events;

(6) Break rates were much lower to natural gas piping, which was modeled as being virtually impervious to shaking damage. Nonetheless, these rates can exceed 50 breaks per million lineal feet of piping in the largest magnitude events postulated; and

(7) Moderate earthquake events outside the study area can cause damage to buried conduits within the study area.

These and other preliminary results suggest numerous further possible investigations including

(i) more detailed investigations of liquefaction susceptibilities and soil effects in microzones with high exposures, liquefaction susceptibilities, and dynamic amplification factors

(ii) more detailed investigations of non-piping performance and also network reliabilities in moderate magnitude events, which are more likely to occur than larger magnitude events,

(iii) inspection and rating of selected State-owned buildings for life-safety hazards

(iv) more detailed investigations of the subsurface configuration of the Ogden segment of the Wasatch fault, including discussions of discontinuities/continuities with the Salt Lake segment

(v) more detailed analyses of source-to-site transmission path wave propagation effects potentially affecting shaking intensity estimates

and (vi) superior procedures both for defining liquefaction severities and for defining response of various types of piping to those severities.

Global Digital Network Operations

9920-02398

Howell M. Butler
Branch of Global Seismology and Geomagnetism
U.S. Geological Survey
Albuquerque Seismological Laboratory
Building 10002, Kirtland AFB-East
Albuquerque, New Mexico 87115-5000
(505) 844-4637

Investigations

The Global Digital Network Operations presently consists of 16 SRO/ASRO and 14 DWWSSN stations. The primary objective of the project is to provide technical and operational support to keep these stations operating at the highest percentage of recording time possible to provide high-quality digital seismic data to the seismic research community. This support includes operational supplies, replacement parts, repair service, modification of existing equipment, training installation of systems, and on-site maintenance and calibration. A service contract provides technicians to perform on-site maintenance and installations, as well as to perform repair-and-test of seismometers and all replaceable units that comprise the various network systems. Contract technicians are also provided for special projects such as on-site noise surveys, special telemetered system installations, system renovations, and evaluation and testing of seismological and related instrumentation.

The following station maintenance activity was accomplished:

ANMO - Albuquerque, New Mexico - SRO - Five maintenance visits.
BCAO - Bangui, Central African Republic - SRO - One maintenance visit.
BDF - Brasilia, Brazil - DWWSSN - One maintenance visit.
BOCO - Bogota, Columbia - SRO - One maintenance visit.
CHIO - Chiang Mai, Thailand - SRO - Three maintenance visits.
COL - College, Alaska - DWWSSN - One maintenance visit.
KONO - Kongsberg, Norway - ASRO - One maintenance visit.
LEM - Lembang, Indonesia - DWWSSN - One maintenance visit.
LON - Longmire, Washington - DWWSSN - One maintenance visit.
SHIO - Shillong, India - SRO - Two maintenance visits.
ZOBO - Zongo Valley, Bolivia - ASRO - Two maintenance visits.

System Installations:

A new SRO system was installed at Bar Giyyora, Israel (BGIO) during March.

A DWWSSN system was assembled, tested, and installed at ASL as a control system for China digital system test.

Special Activity:

Seismic site surveys were made in the countries of Ivory Coast, Central African Republic, Botswana, and South Africa.

Tests were conducted on the Teledyne-Geotech modified 36000, 44000, and 55000 borehole seismometers.

A new IBM PC/XT was installed and programmed for shop maintenance history and inventory control system.

Results

The Global Digital Network continues with a combined total of 30 SRO/ASRO/DWWSSN stations. The main effort of this project is to furnish the types of support at a level needed to keep the GSN at the highest percentage of operational time in order to provide the highest quality digital data for the worldwide digital data base.

U.S. Seismic Network

9920-01899

Marvin A. Carlson
Branch of Global Seismology and Geomagnetism
U.S. Geological Survey
Denver Federal Center
Box 25046, Mail Stop 967
Denver, Colorado 80225
(303) 236-1506

Investigations

U.S. Seismicity. Data from the U.S. Seismic Network are used to obtain preliminary locations and magnitudes of significant earthquakes throughout the United States and the world.

Results

As an operational program, the U.S. Seismic Network operated normally throughout the report period. Data were recorded continuously in real time at the NEIS main office in Golden, Colorado. At the present time, 100 channels of SPZ data are being recorded at Golden on develocorder film. This includes data telemetered to Golden via satellite from both the Alaska Tsunami Warning Center, Palmer, Alaska, and the Pacific Tsunami Warning Center, Ewa Beach, Hawaii. A representative number of SPZ channels are also recorded on Helicorders to give NEIS real-time monitoring capability of the more active seismic areas of the United States. In addition, 15 channels of LPZ data are recorded in real time on multiple pen Helicorders.

Data from the U.S. Seismic Network are interpreted by record analysts and the seismic readings are entered into the NEIS data base. The data are also used by NEIS standby personnel to monitor seismic activity in the United States and worldwide on a real time basis. Additionally, the data are used to support the Alaska Tsunami Warning Center and the Pacific Tsunami Warning Service. At the present time, all earthquakes large enough to be recorded on several stations are worked up using the "Quick Quake" program to obtain a provisional solution as rapidly as possible. Finally, the data are used in such NEIS publications as the "Preliminary Determination of Epicenters" and the "Earthquake Data Report."

Development is continuing on an Event Detect and Earthquake Location System to process data generated by the U.S. Seismic Network. We expect the new system to be ready for routine operational use by summer of 1986. At that time, the use of develocorders for data storage will be discontinued. Ray Buland and David Ketchum have been doing most of the developmental programming for the new system. A Micro Vax II will be used as the primary computer of the Event Detect and Earthquake Location System. It will replace the VAX 750 which has been used for system development.

In April, the Albuquerque to Golden long line telemetry system was upgraded by installing a digital telemetry system which uses modems to transmit the seismic data. It was the last long line on which an analog frequency modulation telemtry system was still being used. The digital systems are less susceptible to electronic noise and make it possible to transmit data from up to 36 short-period vertical seismometers on one long line.

Earth Structure and its Effects upon Seismic Wave Propagation

9920-01736

George L. Choy
Branch of Global Seismology and Geomagnetism
U.S. Geological Survey
Denver Federal Center
Box 25046, Mail Stop 967
Denver, Colorado 80225
(303) 236-1506

Investigations

1. Use of body wave pulse shapes in infer Earth structure. Develop methods of generating synthetic waveforms that correctly incorporate the frequency dependent effects that arise from source directivity and from propagation through the Earth. Apply these methods to obtain: (a) constraints on frequency-dependent Q_α and Q_β of the Earth over a continuous frequency band from several Hz to tens of seconds; and (b) constraints on the fine structure of velocity and attenuation at the base of the outer core and the top of the inner core.

2. Source parameters from GDSN data. Develop methods to extract source parameters from digitally recorded data by applying propagation corrections to waveforms. Incorporate these corrections in semi-automatic on-line computation of source parameters of large earthquakes.

Results

1a. We have obtained broadband records of displacement and velocity from deep earthquakes recorded by stations of the GDSN, RSTN and GRF array. The rupture processes of these earthquakes were derived using the P waveforms. The derived rupture processes then enabled us to derive the t^*_β operators for SH-type body waves. Differences between S and ScS body waves provided strong constraints on differential attenuation in the Earth. The mid-mantle between depths of 400 and 1600 km contributes primarily to the attenuation of low frequencies (0.01 to 0.1 Hz). Below the mantle depth of 2000 km, the P and SH waveforms suggest little or no attenuation exists in the band of 0.01 to 5.0 Hz for the propagation paths investigated.

1b. We are extending methods developed by Choy and Cormier (1983) that will make it possible to separate and identify individual branches of the PKP(DF) interference head wave to within 4° of the cusps of the PKP travel-time curve. In anticipating the completion of these techniques, we have compiled a library of broadband PKP waveforms from simple deep-focus earthquakes that occurred from approximately 1978 to the present.

2. We are incorporating into an algorithm for computing radiated energy a feature for correcting velocity spectra for the effects of frequency-dependent attenuation. We have applied the algorithm for computing the energy flux of two recent earthquakes (the Coalinga earthquake of May 2, 1983, and the Borah Peak earthquake of October 28, 1983). We are extending the method to examine the log-averaged P-wave acceleration spectra of large earthquakes using teleseismically recorded digital data.

Reports

Boatwright, J., and Choy, G. L., 1986, Teleseismic estimates of the energy radiated by shallow earthquakes: Journal of Geophysical Research, v. 91, p. 2095-2112.

Choy, G. L., and Cormier, V. F. 1986, Direct measurement of the mantle attenuation operator from broadband P and S waveforms: Journal of Geophysical Research (in press).

Cormier, V. F., and Choy, G. L., 1986, Seismic velocities and attenuation at the Inner Core Boundary [abs.]: EOS (American Geophysical Union, Transactions) (in press).

Systems Engineering

9920-01262

Harold E. Clark, Jr.
Branch of Global Seismology and Geomagnetism
U.S. Geological Survey
Albuquerque Seismological Laboratory
Building 10002, Kirtland AFB-East
Albuquerque, New Mexico 87115-5000
(505) 844-4637

Investigations

1. Design, develop, and test microprocessor-based seismic instrumentation.

2. Design, develop, procure, and test special electronic systems required by seismic facilities.

3. Design, develop, and test microprocessor/computer software programs for seismic instrumentation and seismic recording systems.

Results

1. Ten China Digital Seismic Network (CDSN) power systems have been shipped to the People's Republic of China. Nine CDSN power systems have been installed at the nine CDSN seismic stations. The tenth CDSN power system is being installed at the Beijing Depot Repair Facility.

2. Eight CDSN Field Digital Recording Systems are being installed in the People's Republic of China. The first two systems were installed in February 1986, at the Beijing Seismograph Station and at the Beijing Depot Repair Facility. The last two CDSN Field Digital Recording Systems will be air shipped in early May 1986. The nine station CDSN network will be installed and completed in the June/July 1986 time period.

3. The Albuquerque Seismological Laboratory (ASL) CDSN Field Digital Recording System was installed in the ASL vault. This system will remain at ASL for operational tests and future program development.

4. The CDSN Depot Repair parts are being ordered. The majority of the CDSN test equipment has been installed at the CDSN Depot Facility. The CDSN Depot Facility was used during the installation of the first two CDSN Systems to repair minor shipment damage and parts that had vibrated loose in shipment.

Reanalysis of Instrumentally-Recorded U.S. Earthquakes

9920-01901

J. W. Dewey
Branch of Global Seismology and Geomagnetism
U.S. Geological Survey
Denver Federal Center
Box 25046, Mail Stop 967
Denver, Colorado 80225
(303) 236-1506

Investigations

1. Relocate instrumentally recorded U.S. earthquakes using the method of joint hypocenter determination (JHD) or the master event method, using subsidiary phases (Pg, S, Lg) in addition to first arriving P-waves, using regional travel-time tables, and expressing the uncertainty of the computed hypocenter in terms of confidence ellipsoids on the hypocentral coordinates.

2. Evaluate the implications of the revised hypocenters on regional tectonics and seismic risk.

Results

Jim Dewey has been working with Dave Hill, Bob Engdahl, and Bill Ellsworth on a review of the seismicity of the 48 continguous states, to be published in a GSA Memoir on the Geophysical Framework of the Contiguous United States, edited by L. C. Pakiser and W. D. Mooney. The review summarizes evidence, from well-studied seismic sources, that most large earthquakes in the western United States occur on preexisting faults. There is indirect evidence that at least some strong central and eastern United States earthquakes also occur on preexisting faults. Well-observed faults are segmented geometrically and in their seismological properties. Fault segments that produce large earthquakes typically are quiescent for long periods between the large earthquakes. In many intraplate sources, the causative fault planes do not outcrop at the surface with the same orientation that they have at depth; either they do not outcrop at all, or their corresponding surface fault scarps have orientations that differ by tens of degrees from the orientations at depth. For a few well-studied sources, available data from geology or exploration geophysics provide no basis for postulating that the earthquakes occur on preexisting faults. Application of global plate tectonic models to the understanding of specific earthquake source regions has been particularly effective for regions in and near the Pacific-North American plate boundary in California. The hypothesis that a great thrust-fault earthquake might someday occur in the Pacific Northwest is based on analogy with subduction zones elsewhere in the world that appear similar from a plate-tectonic standpoint, and plate-tectonic models have been put forth to explain some characteristics of midplate seismicity in the central and eastern United States.

Reports

None in preceding six months. Reports completed earlier in this project are referenced in other Technical Reports volumes.

Global Seismology

9920-03684

E. R. Engdahl
and
J. W. Dewey

Branch of Global Seismology and Geomagnetism
U.S. Geological Survey
Denver Federal Center
Box 25046, Mail Stop 967
Denver, Colorado 80225
(303) 236-1506

Investigations

1. Depth Phases. Develop procedure for the global analyses of earthquake depth phases and source characteristics using broadband seismograms of body waves.

2. Earthquake Location in Island Arcs. Develop practical methods to accurately locate earthquakes in island arcs.

3. Subduction Zone Structure. Develop techniques to invert seismic travel times simultaneously for earthquake locations and subduction zone structure.

4. Global Synthesis. Synthesize recent observational results on the seismicity of the earth and analyze this seismicity in light of current models of global tectonic processes.

Results

1. Depth Phases. Because most large earthquakes are complex events, depth phases recorded on conventional seismograms commonly are incorrectly read and reported. It is now possible for reporting agencies, such as the National Earthquake Information Center, to use broadband digital waveforms routinely to obtain better estimates of focal depth, to identify subevents in complex earthquakes and to improve focal mechanism determinations. Displacement and velocity records of body waves in the frequency range from 0.01 to 5 Hz can now be routinely obtained for most earthquakes with $m_b > 5.5$. These records are obtained either directly or by multichannel deconvolution of waveforms from digitally recording seismograph stations such as those of the Global Digital Seismograph Network, the Regional Seismic Test Network, and the Gräefenberg Array. Once the distortion of the seismograph filter is removed, many seismograms show the source-time functions of the direct and surface-reflected phases, even for shallow events in which depth phases may overlap the direct wave. A systematic procedure has been developed for analyzing broadband seismograms that identifies depth phases and subevents (for complex earthquakes). An inherent advantage of this procedure over conventional methods is that focal mechanisms generally can be more clearly resolved from the polarities of depth phases. In particular, the phase sP,

which is better defined on broadband records, provides additional valuable constraints on focal mechanism determinations.

2. Earthquake Location in Island Arcs. Joint Hypocenter Determination is used to compute locations of teleseismically well-recorded earthquakes (magnitude 4.5 or larger) that occurred from 1964 through March 1985, in and near the aftershock zone of the Chilean earthquake of March 3, 1985. The 1985 mainshock nucleated in a region that had experienced a swarm of teleseismically recorded earthquakes that began 10 days before the main shock. The most precisely located foreshock epicenters fall in an equidimensional area of about 20 km that is free of, but surrounded by, the most precisely located 1985 aftershock epicenters. This distribution of seismicity is consistent with foreshock activity occurring as preliminary failure of an asperity that ruptured completely in the course of the mainshock. The seismically active thrust interface appears to consist of a shallow thrust zone and the deep thrust zone separated by 20 km in the plane of the interface. The low seismicity region between the two thrust zones is centered at a depth of approximately 35 km. A similar pairing of deep and shallow thrust zones has been documented for northern Honshu, Japan, by Kawakatsu and Seno (JGR, v. 88, p. 4215). Both the deep and shallow Chilean thrust zones may be activated in large earthquakes. 1985 aftershocks of magnitude less than 6.0 were heavily concentrated in the shallow thrust zone, and the 1985 mainshock nucleated near the downdip extremity of the shallow thrust zone. The deep thrust zone produced at least one, and probably two, aftershocks of magnitude 6.0 or greater the first day after the 1985 mainshock, but few shocks of magnitude between 4.5 and 5.9. The large thrust-fault earthquake of July 1971, nucleated in the deep thrust zone at the north end of the 1985 aftershock zone; virtually all of its aftershocks were in the shallow thrust zone.

3. Subduction Zone Structure. Two independent location and velocity inversion techniques have been applied to travel-time data from well-recorded central Aleutian earthquakes. In both studies, slabs extending at least 100 km beneath the deepest seismicity (~275 km) seem to be indicated. Spencer and Engdahl (Geophys. J., v. 72, p. 399-415, 1983) used a cylindrically symmetric slab model with fixed position and thickness to estimate slab length and maximum fractional slowness contrast (amplitude) between the slab and surrounding mantle. Their data included P and S arrivals at local stations, and P arrivals recorded teleseismically. They found the slab length not well resolved, there being a tradeoff between a short, high velocity slab and a longer, lower velocity one. The model which gave the smallest variance at the 95-percent confidence level had an amplitude of 7 percent and a length of 386 km. Engdahl and Gubbins (EOS, v. 66, p. 1086, 1985) used a structure parameterized with cubic splines that provides a specification of velocity at each point of a gridded arc cross section. They used as data P and S arrivals at stations of a local network and P, pP, and sP arrivals recorded at teleseismic stations. The velocity anomalies produced by their inversion describe a thin slab (60-80 km thick) of high velocity, dipping at an angle of about 60° to the north, with a velocity anomaly of 10 percent at the bottom of the model (400 km depth).

4. Global Synthesis. The sythesis study is currently in outline form. Approximately half the synthesis is outlined in full sentences or paragraphs that are intended to be included directly into the final publication. The other half is outlined with a skeleton listing of topics that will be covered. Related work continues on a project to produce a map of the seismicity of North America for the Geological Society of America's Decade of North American Geology series. A subset of these data was used to produce a United States seismicity map for the "Geophysical Framework of the Continental United States" Memoir.

Reports

Dewey, J. W., Choy, G. L., and Nishenko, S. P., 1985, Asperities and paired thrust zones in the focal region of the Chilean earthquake of March 3, 1985 [abs.]: EOS (American Geophysical Union, Transactions), v. 66, p. 950.

Engdahl, E. R., and Gubbins, D., 1985, Simultaneous travel-time inversion for earthquake location and subduction zone structure [abs.]: EOS (American Geophysical Union, Transactions), v. 66, p. 1086.

Engdahl, E. R., and Billington, S., 1986, Focal depth determination of central Aleutian earthquakes: Bulletin of the Seismological Society of America, v. 76, p. 77-93.

Engdahl, E. R., and Choy, G., 1986, Global analyses of earthquake depth phases and source characteristics using broadband seismograms of body waves [abs.]: EOS (Transactions, American Geophysical Union), v. 67 (in press).

Engdahl, E. R., and Gubbins, D., 1986, Aseismic extension of the central Aleutian slab [abs.]: EOS (Transactions, American Geophysical Union), v. 67 (in press).

Engdahl, E. R., and Kind, R., 1986, Interpretation of broadband seismograms from central Aleutian earthquakes: Ann. Geophysicae (in press).

Seismic Observatories

9920-01193

Leonard Kerry
Branch of Global Seismology and Geomagnetism
U.S. Geological Survey
Denver Federal Center
Box 25046, Mail Stop 967
Denver, Colorado 80225
(303) 236-1500

Investigations

Recorded and provisionally interpreted seismological and geomagnetic data at observatories operated at Newport, Washington; Cayey, Puerto Rico; and Agana, Guam. Continued operation of the Puerto Rican Seismic Telemetry Network from the main base located in Cayey, Puerto Rico. Operated advanced equipment for gathering research data for universities and other agencies at Cayey, Puerto Rico, and Agna, Guam. At Agana, Guam, a 24-hour standby duty was maintained to provide input to the Tsunami Warning Service operated at Honolulu Observatory by NOAA and to support the Early Earthquake Reporting function of the National Earthquake Information Service. Continued to telemeter long- and short-period seismic data on a real-time basis from Newport Observatory, Newport, Washington, to NEIC, Golden, Colorado; Pacific Tsunami Warning Center, Honolulu, Hawaii, and Alaska Tsunami Warning Center, Palmer, Alaska, to give support in the operation of their disciplines.

Results

Provided data on an immediate basis to the National Earthquake Information Service and the Tsunami Warning Service. Continued to send seismograms obtained from the WWSSN Systems operated at Agana, Guam, and Cayoy, Puerto Rico, to NEIS for use in the ongoing U.S. Geological Survey programs. Analog seismic records and digital seismic tape records were obtained from the Agana, Guam SRO system and forwarded to ASL for use in ongoing U.S. Geological Survey and other users' programs. Data from advanced research equipment was forwarded to universities or other agencies working in conjunction with U.S. Geological Survey. Seismic data from the Puerto Rican net was provided on a continuing basis to the University of Puerto Rico for their use in studying and research of the seismicity of the Puerto Rican area.

Responded to requests from the public, interested scientists, universities, state, and Federal agencies regarding geophysical data and phenomena.

Global Seismograph Network Evaluation and Development

9920-02384

Jon Peterson
Branch of Global Seismology and Geomagnetism
U.S. Geological Survey
Albuquerque Seismological Laboratory
Building 10002, Kirtland AFB-East
Albuquerque, New Mexico 87115-5000
(505) 844-4637

Investigations

Work continued on the development and deployment of the China Digital Seismograph Network.

Cooperation with IRIS has continued with plans developed for upgrading components of the Global Digital Seismograph Network.

Results

Assembly and testing of data systems and the data management system for the China Digital Seismograph Network (CDSN) were completed, and the equipment was shipped to China. During March the demonstration system was installed at the Baijatuan station outside Beijing. Both systems were brought on line without difficulty. Data from the Baijatuan station included an unexceptably high level of system noise. Follow-up tests at Albuquerque isolated the source, and modifications to the systems are being made to eliminate the noise. A schedule for installing the remaining eight stations beginning in May has been approved by the Chinese.

The immediate goals of an IRIS/USGS program to improve the global networks are to upgrade some GDSN stations and to modernize and expand the capabilities of the ASL data collection facility. Five DWWSSN stations have been designed to receive Streckeisen VBB seismometers. The broadband seismometers will replace the WWSSN short-period and long-period seismometer currently in use. A prototype system is being assembled at ASL. Funds are also being provided from the IRIS program to purchase the hardware needed to begin development of a new data collection facility that will include the capability to acquire real-time data via satellite telemetry.

Digital Data Analysis

9920-01788

Stuart A. Sipkin
Branch of Global Seismology and Geomagnetism
U.S. Geological Survey
Denver Federal Center
Box 25046, Mail Stop 967
Denver, Colorado 80225
(303) 236-1506

Investigations

1. Moment Tensor Inversion. Apply methods for inverting body phase waveforms for the best point source description to research problems.

2. Computation of Free Oscillations. Study the effects of anelasticity on free oscillation eigenfrequencies and eigenfunctions.

3. Earthquake Location Technology. Study techniques for improving the robustness, honesty, and portability of earthquake location algorithms.

4. Real Time Earthquake Location. Experiment with real-time signal detection, arrival-time estimation, and event location for regional earthquakes.

5. Broadband Body-wave Studies. Use broadband body phases to study lateral heterogeneity, attenuation, and scattering in the mantle.

6. Data Collection Center. Develop a state-of-the-art data collection center to handle digital waveform data collection for the next decade.

7. NEIS Monthly Listing. Contribute both fault plane solutions (using first-motion direction) and moment tensors (using long-period body-phase waveforms) for all events of magnitude 5.8 or greater when sufficient data exist. Contribute waveform/focal sphere figures of selected events.

Results

1. Moment Tensor Inversion. A catalog of moment tensors for all sufficiently large events during 1981-1983 has been completed and submitted for publication. A special study has been done for the 51 IASPEI events. A new, objective method for comparing source mechanisms has been developed. This method has been used to compare the moment tensor solutions to the USGS first-motion fault-plane solutions and to the Harvard CMT solutions.

2. Computation of Free Oscillations. A journal article describing comparisons of exact calculations and first order perturbation theory is being prepared. A new result has been obtained which seems to imply that a layer of extremely low Q can mechanically decouple wave propagation above and below the layer.

3. Earthquake Location Technology. A location program based on the R-estimator was tested against the program used by the NEIS to produce the monthly listing. In this test, all published events for March 1985 were relocated neglecting analyst instructions for P waves. Overall, the R-estimator preformed very well. The few descrepancies discovered remain to be analyzed.

4. Real-time Earthquake Location. The real-time system developed in cooperation with the Instituto Nazionale di Geofisica (Italian Government) is being implemented in Golden, Colorado, for the United States' seismic network. The system is being generalized to handle both digital and analog telemetry, different sample rates, and asynchronous channel timing. Dedicated microcomputer hardware has been procured for the near-real-time back-end system. Software for regional and teleseismic on-line event location is being tested. The current prototype is processing 128 analogue channels. A color graphics workstation is being procured for doing the analysis.

5. Broadband body-wave Studies. Two high-quality digitally recorded broadband data sets have been collected, one from the Gräfenberg Array (GRF) in West Germany, and the other from the Regional Seismic Test Network (RSTN) in North America. The suitability of the multiple ScS waveforms from the GRF array for studies of lateral heterogeneity and attenuation (including frequency dependence) are being investigated. Software for waveform processing is being developed and tested.

6. Data Collection Center. A new data collection system for the Albuquerque Seismological Laboratory is being implemented. By basing the hardware on 32-bit microcomputer and local area network technologies, it appears to be possible to achieve low cost, high reliability, and the flexibility to economically expand the capacity of the system from today's modest requirements to the full output of the proposed IRIS network a decade hence. The system requirements have been specified, and equipment has been ordered. The planning for implementation is now being done.

7. NEIS Monthly Listing. Since May 1981, fault plane solutions for large events have been contributed to the Monthly Listing. Beginning in November 1982, moment tensors and waveform/focal sphere plots are also being contributed. In the last six months, the fault plane solutions and moment tensors of approximately 80 events were published.

Reports

Presgrave, B. W., Needham, R. E., and Minsch, J. H., 1985, Seismograph station codes and coordinates, 1985 edition: U.S. Geological Survey Open-File Report 85-714.

Sipkin, S. A., 1986, Moment tensor solutions estimated using optimal filter theory for 51 selected earthquakes, 1980-1984: Physics of the Earth and Planetary Interiors (submitted).

Sipkin, S. A., 1986, Estimation of earthquake source parameters by the inversion of waveform data: Global seismicity, 1981-1983: Bulletin of the Seismological Society of America (submitted).

Seismicity and Tectonics

9920-01206

William Spence
Branch of Global Seismology and Geomagnetism
U.S. Geological Survey
Denver Federal Center
Box 25046, Mail Stop 967
Denver, Colorado 80225
(303) 236-1506

Investigations

Studies carried out under this project focus on detailed investigations of large earthquakes, aftershock series, tectonic problems, and earth structure. Studies in progress have the following objectives:

1. Generalize the role of the slab pull force in determining the primary tectonic features at subduction zones and in contributing to stresses that cause subduction zone earthquakes (W. Spence).

2. Provide tectonic setting for and analysis of the 1974 Peru gap-filling earthquake (W. Spence and C. J. Langer).

3. Examine the source properties (focal mechanism and depth) of aftershocks following large thrust earthquakes in subduction regions by using digital surface-wave data (C. Mendoza).

4. Determine the maximum depth and degree of velocity anomaly beneath the Rio Grande Rift and Jemez Lineament by use of a 3-D, seismic ray-tracing methodology (W. Spence and R. S. Gross).

Results

1. In spite of the recognized strong influence of the slab pull force in moving tectonic plates, the influence of this force in causing tectonic phenomena occurring on the order of days to several years generally has been neglected. In addition to reviewing evidence that the slab pull force is responsible for most steady-state features associated with mature subduction zones, this study considers a time-dependent model that describes the slab pull force and the weaker ridge push force through a cycle of great subduction zone earthquakes. The steady-state and short-term behaviors of a predominant slab pull force are demonstrated to be consistent with most seismic and tectonic data that exist for mature subduction zones. Slab pull forces can explain double seismic zones associated with old, rapidly subducting plates, the transition from extensional faulting in the upper mantle to compressional faulting below depths of about 300 km, the sudden increase in curvature of subducted plate at depths of 20-40 km, and possibly can provide some of the excitation function for the Chandler wobble.

2. The great 1974 Peru thrust earthquake (M_S 7.8, M_W 8.1) occurred in a documented seismic gap, between two earthquakes each with magnitude of about 8, occurring in 1940 and 1942. Additional major earthquakes occurred in this region in 1966 and in 1970; all but the 1970 shock represent thrust faulting. The stress release of the October 3, 1974, main shock and aftershocks occurred in a spatially and temporally irregular pattern. The multiple-rupture main shock produced a tsunami with wave heights of 0.6 ft at Hawaii and which was observed, for example, at Truk Island and at Crescent City. The aftershock series essentially was ended with the occurrence of a M_S 7.1 aftershock on November 9, 1974. The several years of preseismicity data to this earthquake include an unusually clear example of the "Mogi donut" pattern.

3. Love and Rayleigh-wave signals recorded by the Global Digital Seismograph Network provide source-parameter information for moderate-magnitude aftershocks that followed the large (M_S 7.7) Colombia earthquake of 12 December 1979. Love/Rayleigh amplitude ratios observed in a 30-80 second passband are compared against theoretical values calculated for a suite of source models fixed at independently determined depths. In addition, a reference earthquake with known focal mechanism and depth is used to calibrate the procedure and to minimize the path and size effects. Source mechanisms compatible with the amplitude data and observed P-wave first motions are obtained. These mechanisms serve to identify subsidiary faulting not associated with the main shock rupture.

Similar surface-wave techniques are being implemented in the analysis of the aftershock sequence that followed the large (M_S 7.8) Chile earthquake of 3 March 1985. The earthquake ruptured about 1/3 of the rupture length inferred for the great (M_S 8.2-8.4) Valparaiso earthquake of 1906. By comparing the spectra observed in a 20-50 second period range, focal depths can be estimated and source mechanisms can be computed for the aftershocks. The aftershock properties should provide additional constraints on the faulting geometry produced by the main shock of 3 March 1985.

4. To a depth of about 160 km, the upper mantle P-wave velocity beneath the Rio Grande rift and Jemez lineament is 4-6 percent lower than beneath the High Plains Province. A 3-D, P-wave velocity inversion shows scant evidence for pronounced low P-wave velocity beneath the 240-km-long section of the Rio Grande rift covered by our array. However, the inversion shows a primary trend of 1-2 percent lower P-wave velocity underlying the northeast-trending Jemez lineament, down to a depth of about 160 km. The Jemez lineament is defined by extensive Pliocene-Pleistocene volcanics and late Quaternary faults. The upper mantle low-velocity segment beneath the Jemez lineament is at most 100 km wide and at least 150-200 km long, extending in our inversion from Mt. Taylor through the Jemez volcanic center and through the Rio Grande rift. A Backus-Gilbert resolution calculation indicates that these results are well-resolved.

Reports

Mendoza, C., 1985, Aftershock source properties from digital surface-wave data: The 1979 Colombia sequence [abs.]: EOS (American Geophysical Union, Transactions), v. 66, p. 963.

Spence, W., 1985, Can slab pull cause shallow, decouping earthquakes? [abs.]: EOS (American Geophysical Union, Transactions), v. 66, p. 1077.

Spence, W., 1986, The 1977 Sumba earthquake series: evidence for slab pull force acting at a subduction zone: Journal of Geophysical Research (in press).

Spence, W., 1986, Slab pull and the earthquake cycle: Journal of Geophysical Research (submitted).

United States Earthquakes

9920-01222

Carl W. Stover
Branch of Global Seismology and Geomagnetism
U.S. Geological Survey
Denver Federal Center
Box 25046, Mail Stop 967
Denver, Colorado 80225
(303) 236-1500

Investigations

1. Ninety-two earthquakes in 21 states and Puerto Rico were canvassed by a mail questionnaire for felt and damage data. Twenty-three of these occurred in California, and 20 in Alaska. The most significant events were the California earthquake of January 26, 1986, magnitude 5.3 m_b, and the Ohio earthquake of January 31, 1986, magnitude 4.9 m_b.

2. Hypocenters and magnitudes for earthquakes in the United States for the period October 1, 1985, through March 31, 1986, have been computed and published in the Preliminary Determination of Epicenters (PDE) Weekly Listing.

Results

Both the January 1986, California and Ohio earthquakes were assigned a maximum intensity of VI; however, the Ohio event was felt over an estimated area of 225,000 km^2 compared to 35,000 km^2 for the one in California. The California quake was located near Tres Pinor and caused only minor damage in the form of cracked plaster, masonry, and chimneys; the Ohio quake was located between Chardon and Painesville and caused similar damage.

Seismicity maps for the conterminous United States, Alaska, and the world showing earthquakes located during the month of the publication were included in each Monthly Listing of the PDE.

Reports

Reagor, B. G., Stover, C. W., and Algermissen, S. T., 1985, Seismicity map of the state of Montana: U.S. Geological Survey Miscellaneous Field Studies Map MF-1819.

Stover, C. W., 1985, United States earthquakes, 1982: U.S. Geological Survey Bulletin 1655, 141 p.

Stover, C. W., Reagor, B. G., and Algermissen, S. T., 1986, Seismicity map of the sate of Arizona: U.S. Geological Survey Miscellaneous Field Studies Map MF-1852.

Stover, C. W., Reagor, B. G., and Algermissen, S. T., 1986, Seismicity map of the state of Idaho: U.S. Geological Survey Miscellaneous Field Studies Map MF-1857.

Stover, C. W., Reagor, B. G., and Algermissen, S. T., 1986, Seismicity Map of the state of Utah: U.S. Geological Survey Miscellaneous Field Studies Map MF-1856.

Data Processing Section

9920-02217

John Hoffman
Branch of Global Seismology and Geomagnetism
U.S. Geological Survey
Albuquerque Seismological Laboratory
Building 10002, Kirtland AFB-East
Albuquerque, New Mexico 87115-5000
(505) 844-4637

Investigations

1. Data Management Center for the China Digital Seismograph Network. The data processing system for the China Digital Seismograph Network has been installed in Beijing, People's Republic of China, and is presently operational. Additional software is presently being written in Albuquerque and will be installed later this year.

2. Data Processing for the Global Digital Seismograph Network. All of the data received from the Global Network and other contributing stations are reviewed and checked for quality.

3. Network-Day Tape Program. Data from the Global Network stations are assembled into network-day tapes which are distributed to regional data centers and other government agencies.

Results

1. Data Management Center for the China Digital Seismograph Network. The PDP 11/44 computer system was disassembled, packaged in large wooden crates, and shipped to Beijing, People's Republic of China, in December 1985. Approximately 50 percent of the software had been completed and thoroughly checked prior to shipment of the computer system. In February 1986, we departed Albuquerque for Beijing to install the computer system and train the Chinese in both operation and maintenance of the computer. The equipment was installed without incident during the first week, and an additional two weeks were spent training the Chinese. A large amount of software had to be written for this problem. New device drivers were needed, the event detection program required considerable modification, and new code had to written for the very long-period data. This very long-period code also had to be enclosed in the network-day tape program at the ASL. The remaining software is presently under development at the Albuquerque Seismological Laboratory and will be completed in May 1986. We are scheduled to install this software in June and provide final training for the Chinese at that time.

2. Data Processing for the Global Digital Seismograph Network. During the past six months, 793 digital tapes (281 SRO/ASRO, 348 DWWSSN, and 164 RSTN) from the Global Network and other contributing stations were edited, checked for quality, corrected when feasible, and archived at the Albuquerue Seismological Laboratory (ASL). The Global Network is presently comprised of 12 SRO stations, 4 ASRO stations, and 14 DWWSSN stations. In addition,

there are six contributing stations which include Glen Almond, Canada, plus the five RSTN stations which are supported by Sandia National Laboratories. During the next six months, nine stations will be installed in the People's Republic of China, and after processing their data at the Data Management Center described in item one above, it will be forwarded to the Albuquerque Seismological Laboratory for additional processing and ultimate inclusion in the network-day tape program.

3. Network-Day Tape Program. The network-day tape program is a continuing program which assembles all of the data recorded by the Global Digital Seismograph Network plus the contributing stations for a specific calendar day onto one magnetic tape. This tape includes all the necessary station parameters, calibration data, frequency response, and time correction information for each station in the network. An edition of the National Earthquake Information Center Newsletter containing information on the various digitally recording seismograph stations and the network-day tape program was distributed in December 1985. These newsletters are published twice a year and copies are forwarded to all digital data users.

Reports

Hoffman, J.P., Buland, R., and Zirbes, M., December 1985, National Earthquake Information Center Newsletter, v. 4, no. 2, 12 p.: Available from Albuquerque Seismological Laboratory, Albuquerque, New Mexico.

Seismic Review and Data Services

9920-01204

R. P. McCarthy
Branch of Global Seismology and Geomagnetism
U.S. Geological Survey
Denver Federal Center
Box 25046, Mail Stop 969
Denver, Colorado 80225
(303) 236-1513

Investigations and Results

Technical review and quality control were carried out on 482 station months of seismograms from the Worldwide Standardized Seismograph Network (WWSSN). Seventy-two station months of Seismic Research Observatory (SRO and ASRO) seismograms were provided to the National Earthquake Information Service (NEIS) for their PDE programs on a current basis. An average of 30 WWSSN current station months were supplied monthly for the NEIS fault-plane solution program.

No annual WWSSN Station Performance Reports were sent during this period. Preparations are in progress. Overall standards still remain high operationally. The timing systems remain remarkably stable with the average daily timing error less than 50 milliseconds at most stations.

Monthly reports covering the analog and digital records received from the WWSSN, DWWSSN, SRO, and ASRO networks were distributed to officials and researchers in the U.S. Geological Survey and DOD. Advice and consultations are still being provided to users, government officials, university and government researchers, and to the public sector.

Over 12,000 microfiche WWSSN seismogram copies were supplied to 47 researchers on special orders. Six hundred and thirty-one (631) station months of WWSSN microfiche copies were sent to eight standing-order customers, totaling about 606,000 copies. The total for special and standing orders was 618,000 copies. The microfilming quality control on the master films indicates excellent workmanship by the contractor. Spot checks on copies furnished to users also indicated high quality. Over 400 station months of original WWSSN seismograms were returned to the stations, and 120 station months of U.S. Geological Survey WWSSN, SRO, and other network seismograms were archived at the National Archives Records Center in Denver.

Data Processing, Golden

9950-02088

Robert B. Park
Branch of Engineering Geology and Tectonics
U.S. Geological Survey
Box 25046, MS 966, Denver Federal Center
Denver, CO 80225
(303) 236-1638

Investigations

The purpose of this project is to provide the day-to-day management and systems maintenance and development for the Golden Data Processing Center. The center supports Golden-based Office of Earthquakes, Volcanoes, and Engineering investigators with a variety of computer services. The systems include a PDP 11/70, several PDP 11/03's and PDP 11/23's, a VAX/750, a VAX/780 and two PDP 11/34's. Total memory is 14 mbytes and disk space will be approximately 6 G bytes. Peripherals include five plotters, ten mag-type units, an analog tape unit, five line printers, 5 CRT terminals with graphics and a Summagraphic digitizing table. On order is a laser disk to be used for archiving data. Dial-up is available on all the major systems and hardwire lines are available for user terminals on the upper floors of the building. Users may access any of the systems through a Gandalf terminal switch. Operating systems used are RSX11 (11/34's), Unix (11/70), RT11 (LSI's) and VMS (VAX's).

The three major systems are shared by the Branch of Global Seismicity and Geomagnetism and the Branch of Engineering Geology and Tectonics.

Results

Computation performed is primarily related to the Global Seismology and Hazards programs; however, work is also done for the Induced Seismicity and Prediction programs as well as for DARPA, ACDA, MMS, U.S. Bureau of Reclamation and AFTAC, among others.

In Global Seismology and Geomagnetism, the data center is central to nearly every project. The monitoring and reporting of seismic events by the National Earthquake Information Service is 100 percent supported by the center. Their products are, of course, a primary data source for international seismic research and have implications for hazard assessment and prediction research as well as nuclear test ban treaties. Digital time series analysis of Global Digital Seismograph Network data is also 100 percent supported by the data center. These data are used to augment NEIS activities as well as for research into routine estimation of earthquake source parameters. The data center is also intimately related to the automatic detection of events recorded by telemetered U.S. stations and the cataloging of U.S. seismicity, both under development.

In Engineering Geology and Tectonics, the data center supports research in assessing seismic risk and the construction of national risk maps. It also provides capability for digitizing analog chart recordings and maps as well as analog tape. Also, most, if not all, of the research computing related to the hazards program are supported by the data center.

The data center also supports equipment for online digital monitoring of Nevada seismicity. Also, it provides capability for processing seismic data recorded on field analog and digital cassette tape in various formats. Under development is a portable microprocessor-based system to be used by the field investigations group to do preliminary analysis and editing of temporary local networks and the GOES Satellite Event Detect System. Recent acquisitions include the VAX/750, laser plotter, three additional tape drives, two HP plotters, DECNET/ETHERNET, and 400 MB of disk storage. A VAX-based accounting system has been developed for an up-to-date reporting capability on branch projects.

National Earthquake Information Center

9920-01194

Waverly J. Person
Branch of Global Seismology and Geomagnetism
U.S. Geological Survey
Denver Federal Center
Box 25046, Mail Stop 967
Denver, Colorado 80225
(303) 236-1500

Investigations and Results

The Quick Epicenter Determinations (QED) continues to be available to individuals and groups having access to a 300-baud terminal with dial-up capabilities to a toll-free watts number or a commercial telephone number in Golden, Colorado. The time period of data available in the QED is approximately three weeks (from about two days behind real time to the current PDE in production). The QED program is available on a 24-hour basis, 7 days a week. From October 1, 1985 through March 31, 1986, we have had approximately 850 log-ins.

The weekly publication, Preliminary Determination of Epicenters (PDE) continues to be published, averaging about 90 earthquakes per issue. The QED, PDE Monthly Listing and Earthquake Data Report (EDR) continue to be prepared on the VAX/1180 with very little down time encountered.

Telegraphic data are not being received from the USSR on magnitude 6.5 or greater earthquakes at this time. We are attempting to find out what the problems may be.

Data from the People's Republic of China via the American Embassy are being received in a very timely manner and in time for the PDE publication. We continue to receive four stations on a weekly basis from the State Seismological Bureau of the People's Republic of China and about 22 by mail, which are in time for the Monthly. We have rapid data exchange (alarm quakes) with Centre Seismologique European-Mediterranean (CSEM), Strasbourg, France, and Instituto Nazionale de Geofisica, Rome, Italy, and data by telephone from Mundaring Geophysical Observatory, Mundaring, Western Australia.

The Monthly Listing of Earthquakes is up to date. As of March 31, 1986, the Monthly Listing and Earthquake Data Report (EDR) were completed through November 1985. A total of 6,562 events were published for the 6-month period. Solutions continue to be determined when possible and published in the Monthly Listing and EDR for any earthquake having an m_b magnitude $\geq$ 5.8. Centroid moment tensor solutions from Harvard University continue to be published in the Monthly Listing and EDR. Moment tensor solutions are being computed by the U.S. Geological Survey and are also published in the above publications. Waveform plots are being published for selected events

having m_b magnitudes $\geq$ 5.8. Beginning with the month of October 1985, depths for selected events were obtained from broadband displacement seismograms and waveform plots published in the Monthly.

The Earthquake Early Alerting Service (EEAS) continues to provide information on recent earthquakes on a 24-hour basis to the Office of Earthquakes, Volcanoes, and Engineering scientists, news media, other government agencies, foreign countries, and the general public. Thirty-seven releases were made from November 1, 1985 through March 31, 1986. The most significant earthquake released during the period was the magnitude 5.0 earthquake in Ohio on January 31, 1986.

Reports

Earthquake Information Bulletin, "Earthquakes," v. 17, no. 1, July-August 1984; "Earthquakes," v. 17, no. 2, September-October 1984; "Earthquakes," v. 17, no. 3, November-December 1984.

Monthly Listing of Earthquakes and Earthquake Data Reports (EDR); six publications from June 1985 through November 1985. Compilers: W. Jacobs, L. Kerry, J. Minsch, R. Needham, W. Person, B. Presgrave, W. Schmieder.

Person, Waverly J., Seismological Notes: Bulletin of the Seismological Society of America, v. 75, no. 5, November-December, 1985; v. 75, no. 6, January-February 1986; v. 76, no. 1, March-April 1986.

Preliminary Determination of Epicenters (PDE); 26 weekly publications from October 4, 1985 to March 27, 1986, numbers 37-85 through 10-86. Compilers: W. Jacobs, L. Kerry, J. Minsch, W. Person, B. Presgrave, W. Schmieder.

Presgrave, Bruce, Needham, R., and Minsch, J., Seismograph station codes and coordinates 1985: U.S. Geological Survey Open-File Report 85-714.

Quick Epicenter Determination (QED) (daily): Distributed only by electronic media.

National Earthquake Catalog

9920-02648

J. N. Taggart
Branch of Global Seismology and Geomagnetism
U.S. Geological Survey
Denver Federal Center
Box 25046, Mail Stop 967
Denver, Colorado 80225
(303) 236-1506

Investigations

1. Assumed responsibility for copying historical seismograms and distribution of copies on October 1, 1985.

2. Began development of a database and accession software to show the status of each of six million filmed archival (master) copies of Worldwide Standardized Seismograph Network (WWSSN) and Canadian Seismograph Network (CSN) seismograms.

Results

1. Since 1977, the International Association of Seismology and Physics of the Earth's Interior/United Nations Educational, Scientific, and Cultural Organization have sponsored a program to film as many as possible of the world's historical (pre-1963) seismograms of earthquakes before they are lost or undergo further deterioration. The intent of this effort is to provide filmed copies of the historical seismograms to the research community at nominal cost. With funds supplied by the Survey and administered by the National Oceanic and Atmospheric Administration (NOAA), four large 16-mm flow-through cameras were purchased and have been loaned to stations in the United States, South America, Egypt, and the Soviet Union. Through 1985, over 500,000 seismograms have been filmed from 18 stations in the United States and 10 stations in other countries. A NOAA inventory report was published in June 1985, listing the dates and film reel numbers of the historical seismograms that are archived for each station.

Responsibility for the filming and distribution of copies of the historical seismograms was transferred from NOAA to this project on October 1, 1985. The archival films were moved shortly thereafter from Boulder to Denver, Colorado. In response to the widely distributed inventory report, numerous inquiries concerning the availability and cost of the films for specific earthquakes have been received by NOAA and passed on to us. Currently we cannot duplicate films of individual seismograms, but have a contract for the somewhat costly duplication of entire reels of film. To avoid needless cost, we check the seismograms before recommending that the requestor purchase the reel. This examination reveals that (1) the quality of many of the films is poor, especially where the original seismogram was recorded on smoked paper; (2) time marks are difficult to identify; (3) components commonly are unlabeled; (4) system gains may be so low that only great earthquakes are recorded at teleseismic distances; and (5) system response characteristics are seldom available on the reels. As a result of these

problems, we plan to develop a database of quality control parameters to show the degree of usefulness of the individual reels, and the available dates and components. Furthermore, it is apparent that much tighter quality controls should be imposed on future filming of historical seismograms.

2. Responsibility for photographing and distributing filmed 70-mm and microfiche copies of WWSSN seismograms and 35-mm copies of CSN seismograms was transferred on July 1, 1985, from NOAA to the Branch of Global Seismology and Geomagnetism, National Earthquake Information Center (NEIC). The NEIC sends archival films of requested seismograms to a contractor for duplication. Numerous large orders have been received, some of which contain overlapping requests for the same seismograms. Development is underway on a database that will show the status of each master copy of WWSSN and CSN seismograms in the archival files. The database contains the name, code, reference number, operational starting date, closing date (if any), and typical instrumentation constants of every WWSSN and CSN station site. The main part of the database consists of a 300-character record of archival status for each day beginning with 01 September 1961. Pairs of coded characters show the existence and location of master copies of the long- and short-period seismograms for each station. About 40 symbols are required to take care of the possibilities. Interactive software transparently codes or decodes the symbols, but creates a simplified output display or printout that is easy for the user to understand.

National Strong-Motion Network: Data Processing

9910-02757

A.G. Brady
Branch of Engineering Seismology and Geology
U.S. Geological Survey
345 Middlefield Road, MS 977
Menlo Park, California 94025
(415) 323-8111, ext. 2881

Investigations

1. *Routing Processing.* The selection of the long-period limit for noise removal continues to be a prime concern in the preparation of corrected acceleration data. Important data sets from the Coalinga (1983) aftershocks, the Imperial Valley (1979) aftershocks, and the Hawaii (1983) earthquake are currently under investigation.

2. *Database.* The goals for the INGRES database on the DEC VAX have been revised downwards due to budget and manpower restrictions. We plan on complete in-house retrieval capability and complete table preparation for currently-used tables.

3. *Time-Dependent Structural Response.* Using the horizontal components from some significant historical earthquakes, 1940 and on, the displacement response for simple elasto-plastic oscillators has been investigated. The period range of these oscillators has been that of tall buildings, from 1 to 6 seconds. When we confine our attention to peak responses in the plastic regime, that would be in the same direction, and therefore more damaging, than the immediately preceeding peak, then the distribution of these peak amplitudes is similar to that for a completely elastic system. This result holds regardless of the ductility factor, that is, the ratio of the maximum peak amplitude to the amplitude when the elastic limit is reached.

Results

1. *Routing Processing Results.* Digitizing (D), computer processing (P), and report preparation (R) of strong-motion accelerograms continues: 15 records (D), Hawaii, 16 November 1983; 5 records (D), New Hebrides, May-September 1984; 7 records (P), Imperial Valley aftershock, 15 October 1979, 2318:40; 5 records (R), Solomon Islands, December 1981-March 1983; 5 records (P,R), Hollister Differential Array, January 26, 1986.

Reports

Perez, V., Brady, A.G., and Safak, E., 1986, Reversing cyclic elasto-plastic demands on structures during strong-motion earthquake excitation: *Third U.S. National Conference on Earthquake Engineering*, Charleston, South Carolina, August 1986.

Silverstein, B.L., and Brady, A.G., 1985, Processed strong-motion records from the Coalinga, California aftershock of July 22, 1983, 0239 GMT: *U.S. Geological Survey Open-File Report 85-250*, 229 p.

Brady, A.G., and others, Preliminary report on records from the USGS-maintained strong-motion network in the Hollister area, January 26, 1986: *U.S. Geological Survey Open-File Report 86-156*.

Silverstein, B.L., Brady, A.G., and Mork, P.N., 1986, Processed strong-motion records from the southern Alaska earthquake of January 1, 1975, 0355 GMT: *U.S. Geological Survey Open-File Report 86-191*.

National Strong-Motion Network: Engineering Data Analysis

9910-02760

A.G. Brady and G.N. Bycroft

Branch of Engineering Seismology and Geology
U.S. Geological Survey
345 Middlefield Road, MS 977
Menlo Park, California 94025
(415) 323-8111, ext. 2881

Investigations

1. *Differential ground motion.* Further investigation into soil-structure interaction. Development of integration and filtering procedures to determine differential ground displacements from the differential array at El Centro and Hollister. Development of a new form of spectra which includes both inertial and differential displacements. Calculation of these differential spectra for the El Centro 1979 and Morgan Hill 1984 earthquakes. Figure 1 shows the ratio of the maximum strain occurring in a simple bridge span when the differential inputs are those from the Hollister differential array, to the maximum strains occurring when the inputs are equal, for various span frequencies. It is seen that for stiff structures (*i.e.*, omega 1 large) the differential ground motion loading is more important than the inertial loading.

2. *Analysis of Structural Records.* A modal analysis has been completed using the actual recorded accelerograms from the Morgan Hill earthquake excitation of a three-span freeway bridge. Peak accelerations reached 0.1 g at ground level and 0.16 g in the box girder. The integrated displacements at frequencies higher than 3 Hz permit the identification of the fundamental modes and frequencies. The horizontal modes, along and transverse to the deck, have frequencies of 3.8 and 3.9 Hz, and include ground level motions up to 90% of peak deck motion. The soil-structure system clearly contributes to these modes.

Reports

Brady, A.G., and Celebi, M., 1986, Fundamental modal behavior of an earthquake-excited bridge: *Third U.S. National Conference on Earthquake Engineering*, Charleston, South Carolina, August 1986.

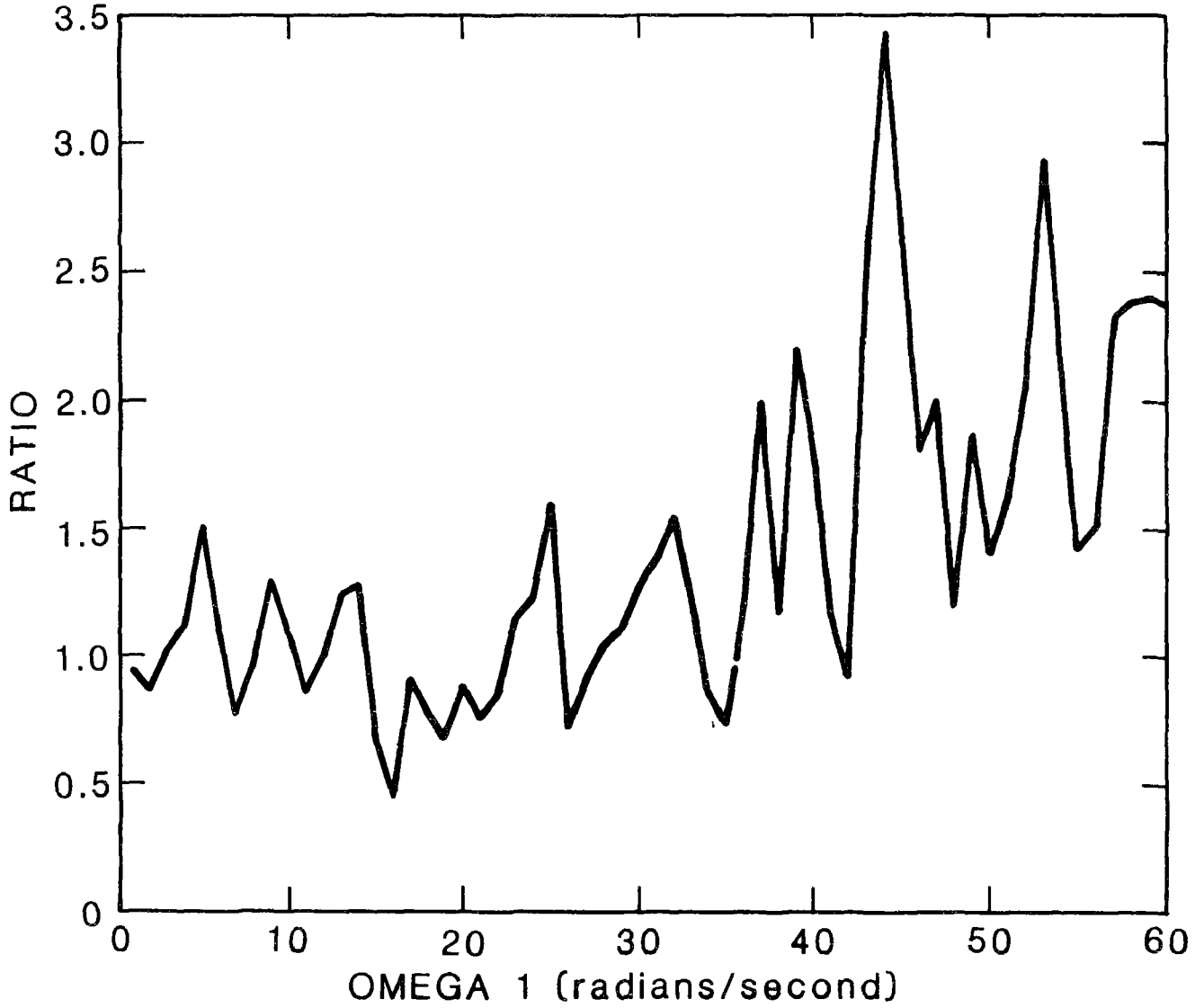

Figure 1. Ratio of maximum strain in the deck of a simple bridge span when subjected to the differential inputs provided by stations 1 and 3 of the Hollister array, 24 April 1984, to the maximum strain occurring when the inputs are equal. The two lowest fundamental transverse modes have equal frequencies, increasing on the x-axis. The structure has zero damping.

National Strong Motion Data Center

9910-02085

Howard Bundock
Branch of Engineering Seismology and Geology
U. S. Geological Survey
345 Middlefield Road, MS 977
Menlo Park, California 94025
(415) 323-8111, ext. 2982

INVESTIGATIONS

The objectives of the National Strong Motion Data Center are to:

Maintain a strong capability for the processing, analysis and dissemination of all strong motion data collected on the National Strong Motion Network and data collected on portable arrays;

Support research projects in the Branch of Engineering Seismology and Geology by providing programming and computer support including digitizing, graphics, processing and plotting capabilities as an aid to earthquake investigations;

Manage and maintain computer hardware and software so that it is ready to process data rapidly in the event of an earthquake.

The Center's facilities include a VAX 11/750 computer operating under VMS Version 4.2, a PDP 11/70 and two PDP 11/73 computers running RSX-11M+. The Center's computers are part of a local area network with other branch, OEVE, Geologic Division, and ISD computers, and we have access to computers Survey-wide over Geonet. Project personnel join other office branches and ISD in the support of the OEVE VAX 11/780-5.

Investigations during the first six months of FY86 included research into the implementation of a precise plan to insure the security of our computer project on a normal basis and also in case of a major disaster or emergency such as a fire or earthquake. Project personnel studied better methods of data access from our VAX 11/750, such as having data reside on disks shared by both our PDP 11/70 and the Branch VAX. The project researched ways of connecting individual microcomputers to our local area network. As an ongoing policy, the project has kept its hardware up to current revision levels, and operating system, network, and other software at the most recent versions. Programs have been written to digitize and display surface contours and fault systems and work is proceeding to include the plotting of earthquake hypocenters on these figures for definition of fault planes.

RESULTS

As a result of these and previous investigations, the project has:

Written and implemented a Continuity of Operations Plan to insure the security of our Branch computers, and participated in the writing and implementation of the same plan for the OEVE VAX 11/780-5;

Purchased, installed, and trained branch personnel in the use of a terminal server and related software, which allows eight terminals to access any computer on our local area network directly. Users can run up to four sessions at once with any computers on the net;

Ordered hardware and software to connect scientists' microcomputers to our network so that they can access data on any of the other micros or minicomputers on the network;

Ordered a 456MB Winchester type disk to be dual-ported with the ES+G PDP 11/70 and VAX 11/750 for easy interchange and access of data from either of the systems;

Obtained information concerning the procedure involved in accessing the CRAY at the San Diego Supercomputer Center through Information Systems Division in Reston, with whom project personnel worked previously to obtain this access. The link to this center will be used by scientists needing high speed processing for modelling, and to keep U.S.G.S. scientists current with new processing methods;

Shared in planning which resulted in the upgrade of the OEVE VAX to a higher speed 11/780-5.

Managed and maintained system hardware and software.

REPORTS

none.

Structural Response in Support of National Strong Motion Program

9910-02759

Mehmet Celebi, A. Gerald Brady, Erdal Safak, and Richard Maley
Branch of Engineering Seismology and Geology
U.S. Geological Survey
345 Middlefield Road, MS 977
Menlo Park, California 94025
(415) 323-8111, ext. 2394

Investigations

1. Selection of structures to be recommended for strong-motion instrumentation. This process is enhanced through advisory committees in seismically active regions of the United States.

2. Study of the performance of a roof diaphragm during the 24 April 1984 Morgan Hill Earthquake.

3. Implementation of structural instrumentation and design of instrumentation schemes.

4. Site response studies and structural damage correlation during the 3 March 1985 Chile earthquake.

5. Structural characteristic evaluation during the 19 September 1985 Mexico earthquake.

Results

1. The advisory committee(s) in San Bernardino, California reached its recommendations and a list of prioritized structures have been identified. An open-file report has been issued. Other committee(s) in Charleston (South Carolina), Boston, St. Louis (New Madrid area), Hawaii, Alaska, and Los Angeles and Orange Counties (California), are currently active, and of these, some are in the process of finalizing reports.

2. Records obtained from West Valley College (Saratoga, California), a gymnasium with a large roof diaphragm, during the 24 April 1984 Morgan Hill Earthquake (M=6.1) were studied to evaluate its performance. The studies showed that in plane deformation patterns of the roof diaphragm do not reproduce well with the current design/analyses procedures. A technical paper resulted.

3. As part of structural response study efforts through strong-motion instrumentation, and in accordance with recommendations of committees, two new structures are being instrumented. These are the 1100 Wilshire Building (33 stories) in Los Angeles and the Charleston Place Building (8 stories) in Charleston, South Carolina.

4. After the 3 March 1985 Chile earthquake (M_S=7.8), and as a result of observation of damages on ridges, as well as alluvial and sandy sites, site response studies were conducted. The results showed that there were topographical and geological amplification and these two factors contributed to the patterns of responses observed during post-earthquake surveys.

5. Approximately 15 structures in Mexico City were tested in January 1986. Some of these structures were tested in 1962 also. Studies are being finalized on the changes of dynamic characteristics of these structures.

Reports

Celebi, M.K. (Chairman), *et al.*, 1985, Report on recommended list of structures for seismic instrumentation in San Bernardino County, California: *U.S. Geological Survey Open-File Report 85-583.*

_____, 1986, Implications of Mexico and Chile earthquakes of 1985 as related to base isolated structures (*Summary of invited talk for ASCE/County of San Bernardino/California Seismic Safety Commission Seminar on Implementation of Base Isolation*), February 1986.

Celebi, M., (editor), 1986, Seismic site-response experiments following the March 3, 1985 central Chile earthquake: *U.S. Geological Survey Open-File Report 86-90.*

Celebi, M.K., Brady, G.A., Safak, E., and Converse, A.M., 1986, Performance of an earthquake excited roof diaphragm: *Third ASCE Engineering Mechanics Specialty Conference on Dynamic Response of Structures*, March 31-April 2, 1986, University of California at Los Angeles, Los Angeles, California.

STRONG-MOTION INSTRUMENTATION NETWORK DESIGN, DEVELOPMENT, AND OPERATIONS

9910-02763, 02764, 02765

Richard P. Maley
Edwin C. Etheredge

Branch of Enginering Seismology and Geology
345 Middlefield Road, MS 977
Menlo Park, CA 94025
(415) 323-8111, ext. 2881

Investigations

The Strong-Motion laboratory, in cooperation with several federal, state, and local agencies and advisory engineering committees, designs, develops, and operates an instrumentation program in 41 states and Puerto Rico. Program goals include: (1) recording of potentially damaging ground motion in regional networks, and in closely spaced sensor arrays; and (2) monitoring the structural response of buildings, bridges and dams with sensors placed in critical locations. The present coordinated network consists of more than 1,000 recording units installed at approximately 600 ground sites, 32 buildings, 4 bridges, 54 dams, and 2 pumping plants.

New Instrumentation

Eleven ground motion stations were installed in the western United States: 2 in southern California, 2 in the San Francisco Bay area, 4 in northern Nevada (extended Reno area), 1 in Seattle and 2 on the Island of Hawaii. A three-instrument structural array was established for the Corps of Engineers at Willow Creek dam in eastern Oregon. Planning continues for new ground motion stations in northern and southern California and for several structural instrumentation projects underway including a 33-story building in Los Angeles, a 7-story building in San Diego, a water pipe bridge equipped with a base isolation system near Riverside, a 6-story building in Seattle and an 8-story building in Charleston, South Carolina.

Recent Earthquake Records

More than 90 earthquake records were obtained during the past 6 months from instrumentation located in California and Hawaii. The following summarizes some of the more important results.

Earthquake Date	Magnitude	Location	Records	Peak Acceleration
2 October 1985	5.0	Redlands, CA	14	Ground .09 g Structure .06 g (Loma Linda VA Hospital)
28 November 1985	4.5	Bear Valley, CA	6	Ground .09 g
14 January 1986	4.6	Bear Valley, CA	7	Ground .22 g
26 January 1986	5.5	Hollister, CA	17	Ground .29 g
9 March 1986	3.5	Claremont, CA	4	Ground .10 g Structure .14 g (Live Oak Dam)
31 March 1986	5.3	Mt. Lewis, CA (12 mi SE of Fremont)	11	Ground .15 g Structure .39 g (Livermore VA Hospital)

Figure 1 shows the station locations and peak accelerations for the magnitude 5.5 January 26 earthquake.

Records of the 31 March earthquake from the Livermore VA hospital, located about 16 km from the epicenter, are shown in figure 2. The VA hospital is a 6-story reinforced concrete building completed in 1949 and is instrumented by SMA-1 accelerographs located at the basement and roof levels with interconnections for starting and timing signals.

Reports

Maley, R. P., and Porcella, R. L., 1985, The National strong-motion instrumentation network in the central and eastern regions of the United States, Eastern Section Seismological Society of America, Knoxville, October 16, 1985.

Maley, R., Celebi, M., Etheredge, E., and Johnson, J., 1986, The strong ground motion and structural instrumentation program in the southeastern United States, Technology Transfer & Development Council, The Citadel, Charleston, S.C., Jan 1986, 13 p.

Brady, A. G., Etheredge, E. C., Maley, R. P., Mork, P. N., Silverstein, B. A., Johnson, D. J., and Acosta, A. V., 1986, Preliminary report on records from the USGS-maintained strong-motion network in the Hollister Area, January 26, 1986, USGS Open File Report 86-156, 43 p.

Maley, R. P., Melebi, M., Etheredge, E., Johnson, D., and Porcella, R., 1986, The strong ground motion and structural instrumentation program in the southeastern United States, Annual Meeting of the Seismological Society of America, Charleston, S.C., April 1986.

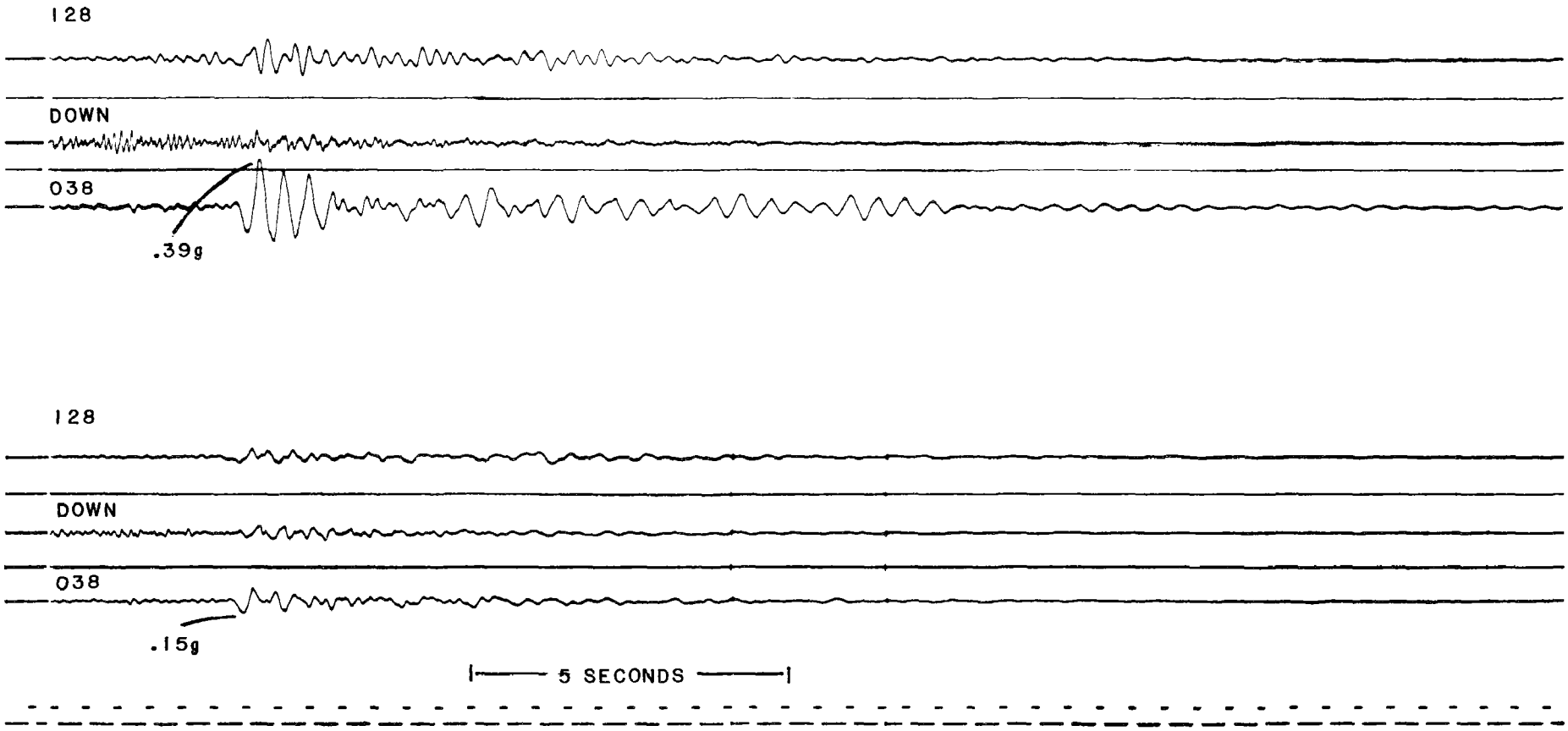

FIGURE 2. ACCELERATION RECORDS FROM THE LIVERMORE VA HOSPITAL, EARTHQUAKE OF 31 MARCH 1986.

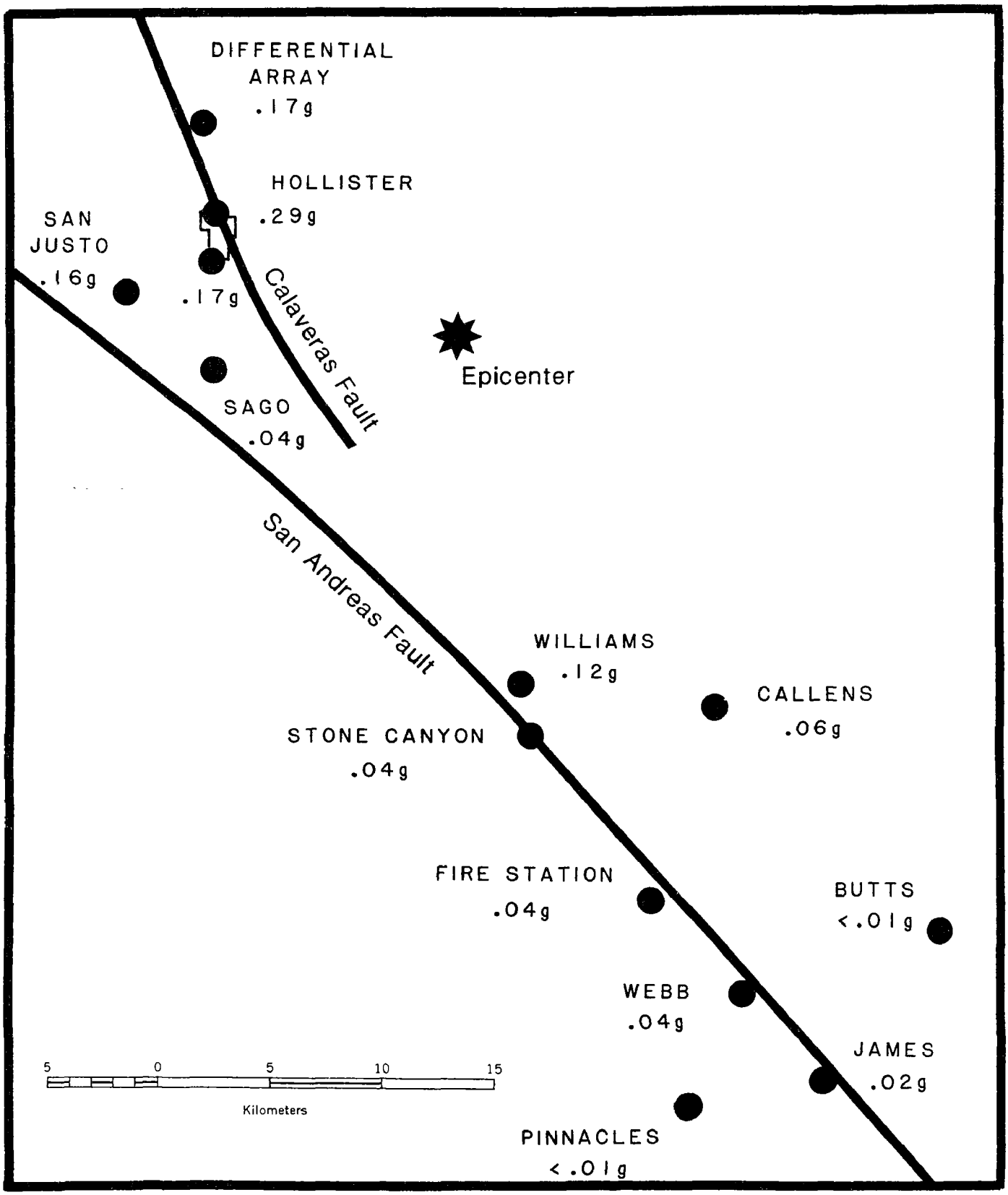

FIGURE 1. STRONG-MOTION STATIONS AND PEAK ACCELERATIONS FROM THE EARTHQUAKE OF 26 JANUARY 1986.

General Earthquake Observation System (GEOS)
GEOS Analysis and Playback Systems (GAPS)

9910-03009

Gary L. Maxwell and Roger D. Borcherdt
Branch of Engineering Seismology and Geology
U.S. Geological Survey
345 Middlefield Road, MS 977
Menlo Park, California 94025
(415) 323-8111 ext. 2318 and 2910

Investigations

1. Development and construction of a portable, broad band, high-resolution digital data acquisition capability for seismology and engineering (GEOS).

2. Development of mini- and micro-computer systems (hardware and software) for retrieval, processing, and archival of large volumes of digital data (GAPS).

3. Development of hardware and software components to improve functionality, versatility, and reliability of digital data acquisition and retrieval systems.

Results

Design features and modifications incorporated in the General Earthquake Observation System (GEOS) during this report period with assistance from J. Sena, C. Dietel, M. Kennedy, G. Jensen, and J. VanSchaack include:

1. Host software improvements to improve system reliability and to improve sensitivity of trigger algorithm to a wider spectrum of seismic activity (near-source impulsive, full coda encapsulation).

2. Improvements in hardware electronics for the reduction of noise and improvement of system performance; *e.g.*, refinement of WWVB radio antenna electronics for better reception.

3. Refinements in maintenance and deployment procedures to enhance quality control and assure successful deployment.

4. Completion of evaluation of new circuit modules for overall improvements to system capabilities: 28 K word EPROM/RAM program memory module, and 16-by-16 bit arithmetic multiplication module. Efforts to produce production-level versions of these boards are underway at this time.

Longer term development efforts that are nearing completion during this report period include:

1. Receipt of new, modern, high-density, low-power tape cartridge recorders for incorporation into new systems has been completed. All recorders have been successfully evaluated for read/write characteristics and for power consumption.

2. Evaluation of small, versatile AC/DC inverters for use in trickle-charging individual units has been completed. These small chargers are desirable in that they monitor the condition of the GEOS internal battery packs for evidence of load loss, and keep the batteries in a continuous charged state, while exhibiting a satisfactory resilience to generating electronic noise. Procurement of enough chargers to satisfy an array of 100 instruments is planned.

3. Modifications to the engineering drawings and artwork in anticipation of building additional systems is nearly underway. Most of the modules in the GEOS system require a few minor changes; performing such changes at this time will save hours of labor required to modify the modules at a later time.

4. Final construction of 270 channel high resolution (16 bit, 96 dB), broad band (DC-500#2) data acquisition capability should be completed within next report period.

Enhancements intiated or completed on the GEOS analysis and playback systems (GAPS) include:

1. Initiation of procurements to improve the floating point processing power of the PDP-11/73 playback system by 10-20%. Improvements should be complete within next report period.

2. Evaluation of new, state-of-the-art, portable, ruggedized minicomputers is underway. It is now possible to package a system with the computational speed and online storage of the existing systems which will fit under the seat of a passenger airline and be powered by a portable generator. Evaluation of other existing products is underway, with the possibility of an RFP being placed on the market for such a system in the next report period.

Reports

Algermissen, S.T. (ed.), 1985, Preliminary report of investigations of the central Chile earthquake of March 3, 1985: *U.S. Geological Survey Open-File Report 85-542*.

Borcherdt, R.D. (ed.), 1986, Preliminary report on aftershock sequence for earthquake of January 31, 1986 near Painsville, Ohio: *U.S. Geological Survey Open-File Report 86-181*.

Cranswick, E., Wetmiller, R., and Boatwright, J., 1985, High-frequency observations and source parameters of microearthquakes recorded at hard-rock sites: *Bulletin, Seismological Society of America*, p. 1535-67.

Boatwright, J., 1985, Characteristics of the aftershock sequence of the Borah Peak, Idaho, earthquake determined from digital recordings of the events: *Bulletin, Seismological Society of America*, p. 1265-84.

Ground Motion Prediction for Critical Structures

9910-01913
David M. Boore
William B. Joyner

Branch of Engineering Seismology and Geology
U.S. Geological Survey
345 Middlefield Road, MS 977
Menlo Park, California 94025
(415) 323-8111, Ext. 2698, 2154

Investigations

1. Study the investigation of amplitudes from Wood-Anderson instruments in southern California.

2. Investigate the specification of design motions for base-isolated structures.

3. Predict ground motions and response spectra in eastern North America.

Results

1. Studies of almost 10,000 amplitude readings taken from Wood-Anderson instruments from over 900 earthquakes demonstrates that Richter's distance correction used in the computation of local magnitudes (M_L) leads to values that are too high for large earthquakes and too small for small earthquakes. The bias is generally less than 0.25 units, however. New station corrections have been determined. There is no indication that the attenuation correction is a function of magnitude.

2. Direct prediction of response spectra from theory or observations at periods and dampings of interest for the design of base-isolated structures indicates that the resulting motions can be sensitive functions of the earthquake magnitude. The motions may be considerably larger than expectations conditioned by working with short-period motions.

3. A stochastic model with constant stress parameter of 100 bars produces a reasonable fit to the sparse strong motion data from earthquakes in eastern North America; predictions based on the scaling law proposed by Nuttli are much lower than the observations. With this validation of the basic model, theoretical attenuation models as a function of magnitude have been derived for response spectra.

Reports

Boore, D. M., The effect of finite bandwidth on seismic scaling relationships, Proc. Fifth Ewing Symposium on Earthquake Source Mechanics, American Geophysical Union, in press, 1986.

Boore, D., The prediction of strong ground motion, NATO Advanced Studies Institute on Strong Ground Motion, Ankara, Turkey (in press).

Boore, D. and G. Atkinson, Prediction of ground motion and spectral response parameters in eastern North America, (submitted to Bulletin of the Seismological Society of America).

Boore, D. and W. Joyner, Prediction of earthquake ground motion at periods of interest for base-isolated structures, Applied Technology Council ATC-17 (in press).

Haar, L. C., Mueller, C. S., Fletcher, J. B., and Boore, D. M., Comments on "Some recent Lg phase displacement spectral densities and their implications with respect to prediction of ground motions in eastern North America" by R. Street, Bull. Seismol. Soc. of America 76, 291-295, 1986.

Joyner, W. B. and Boore, D. M., On simulating large earthquakes by Green's function addition of smaller earthquakes, Proc. Fifth Ewing Symposium on Earthquake Source Mechanics, American Geophysical Union, in press, 1986.

Safak, E. and D. Boore, On nonstationary stochastic models for earthquakes, (paper for presentation at Earthquake Engineering meeting in Charleston, S.C., August, 1986).

Safak, E. and D. Boore, On low-frequency errors of commonly-used stochastic ground motion models, (submitted to ASCE J. of Engineering Mechanics).

NORTHWEST U.S. SUBDUCTION ZONE RISK ASSESSMENT 9930-03790

Thomas H. Heaton
Branch of Seismology
U.S. Geological Survey
525 S. Wilson Avenue
Pasadena, CA 91106
(818) 405-7814

The purpose of this project is to assess the potential seismic hazards due to large shallow thrust earthquakes along the Cascadia subduction zone of the northwestern United States. Although there is good evidence for a convergence rate of 3 to 4 cm/yr, there have been no large historic shallow thrusting earthquakes along this plate boundary. One interpretation of this low seismicity suggests that the plate motion is accomodate through aseismic slip. However, we have shown that the Cascadia subduction zone shares many features with subduction zones in southern Chile, southwestern Japan, and Colombia. Each of these subduction zones has experienced very large historic subduction earthquakes and they appear to be strongly coupled with relatively little aseismic slip. If the Cascadia subduction zone is also strongly coupled, then considerable elastic strain energy may have accumulated along its greater than 1000 km length during the last several centuries. If earthquakes similar to those in southern Chile, Colombia, and southwestern Japan are possible along the coast of the northwestern United States, then earthquake sequences having earthquakes as large as M_w 8 1/4 to 9 1/2 can be postulated. Estimating the nature of strong ground motions that might result from such earthquakes has been our primary objective for the first half of 1986.

Since the work on estimating ground motions in the northwestern United States is drawing to a close, this project is currently in a state of transition. The project is currently being reorganized and future work will center on seismic studies that utilize the southern California short-period telemetered array.

INVESTIGATIONS

1. Fifty-six recordings of strong ground motion from twenty-five shallow subduction earthquakes of $M_w > 7.0$ were used to characterize the nature of strong ground motions that might result from shallow subduction earthquakes as large as M_w 8 1/4 .

2. In order to estimate the ground motions for events larger than those for which strong motion data are available (M_w 8 1/4), we simulate ground motions of very large earthquakes by summing the motions from smaller ones. This procedure is often referred to as the empirical Green's function technique. We apply this technique

in such a way that it is compatible with teleseismic P-wave data from very large subduction earthquakes of the type that we have postulated for the Cascadia subduction zone.

3. We estimate the accuracy of earthquake locations produced by the application of several location procedures and assuming the present configuration of the southern California short-period network. Forward models utilizing ray tracing and assuming realistic horizontal variations in seismic velocity structure are used to synthesize mislocation vectors.

RESULTS

1. There are many examples of relatively strong shaking at surprisingly large distances from large subduction earthquakes. Peak accelerations in excess of 0.05 g at distances in excess of 150 km are relatively common from large subduction earthquakes. In contrast, we know of no recordings that have exceeded 0.05 g at comparable distances from earthquakes in the western United States. For a given magnitude and distance of the observer from an earthquake, there is typically an order of magnitude difference between the amplitudes of the largest and smallest observed ground motion. Although much of this scatter appears to be due to site effects, there are still relatively large variations in the ground motions for several different earthquakes observed at the same site. The way in which this scatter is treated affects design ground motions at least as much as the determination of the magnitude and distance of the design earthquake.

2. An earthquake similar to the 22 May 1960 Chilean earthquake (M_w 9.5) is the largest event that is considered to be plausible for the Cascadia subduction zone. This event has a moment which is two orders of magnitude larger than the largest earthquake for which we have strong motion records. The empirical Green's function technique is used to synthesize strong ground motions for such giant earthquakes. Observed teleseismic P-waveforms from giant earthquakes are also modeled using the empirical Green's function technique in order to constrain model parameters. The teleseismic modeling in the period range of 1.0 to 50 sec strongly suggests that fewer Green's functions should be summed than is required to match the long-period moments of giant earthquakes. It appears that a large portion of the moment associated with giant earthquakes occurs at very long periods that are outside of the frequency band of interest for strong ground motions. In Figure 1, we summarize our results by showing response spectra (5% damping) for an average site located abut 50 km inland and assuming that subduction earthquakes of differing sizes occur along the adjacent subduction zone. In Figure 2, we show synthetic ground motion time histories resulting from a model of the Chilean earthquake (M_w 9 1/2) and assuming a site abut 50 km from the coast. This particular model produced some of the largest motions that we feel are appropriate for these conditions and we believe that average motions will be somewhat smaller.

3. We have devised a technique to test the ability of various earthquake location methods to produce accurate hypocentral solutions in structurally complex areas. In this technique a basin is idealized as the intersection of a cylinder, in which there is a layered velocity model, with a layered half-space. Synthetic travel-times are produced by three-dimensional ray tracing through this model from a lattice of hypocenters to stations of the southern California array. Solutions produced by any location method using our synthetic phase times can then be compared directly to the "true", initial location.

The current study considers a horizontal basin that strikes N40W, is 5 km deep at its axis and 50 km wide. This configuration was chosen to simulate the Imperial Valley of southern California. Location methods that are being evaluated include the standard CIT catalog location method, the master event technique, the use of median delays, the use of calibration blast delays, and JHD. One aim of this project is to better understand the strengths and weaknesses of these location methods so that they may be correctly applied in a variety of seismic studies.

Figure 3 shows cross-sectional plots of hypocenter mislocation vectors for a grid of synthetic earthquakes located using different methods. The calculated solution is represented by a star and is connected to the true location by a solid line. Only "A" quality solutions are plotted. Figure 3a illustrates the effect of using an inappropriate velocity model (this is the same model used for routine CIT catalog locations). Figure 3b shows the improvement gained by use of a "nearly correct" model. These locations are slightly improved by using the median residuals of the whole data set as delays (figure 3c). Significant accuracy is gained in figure 3d by the use of a master event (black dot).

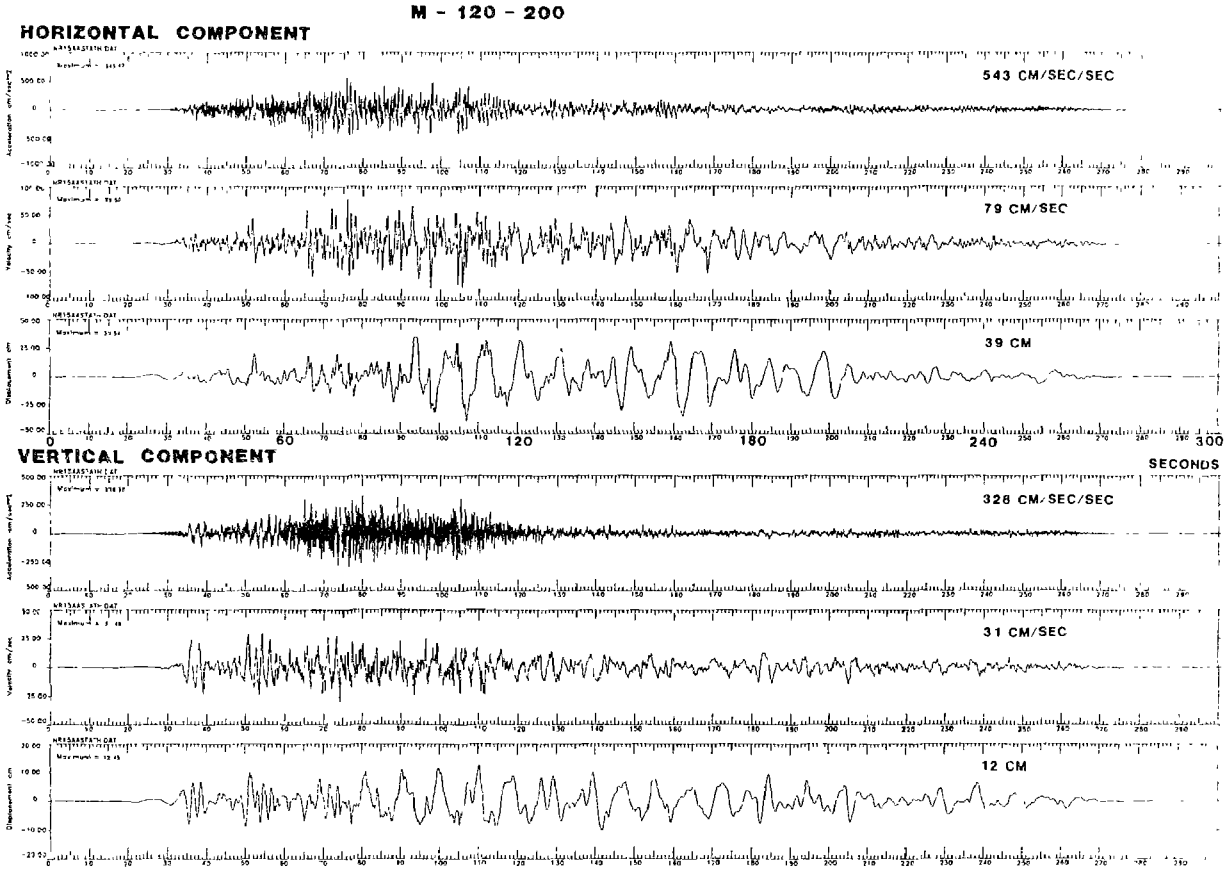

Figure 1

Figure 2

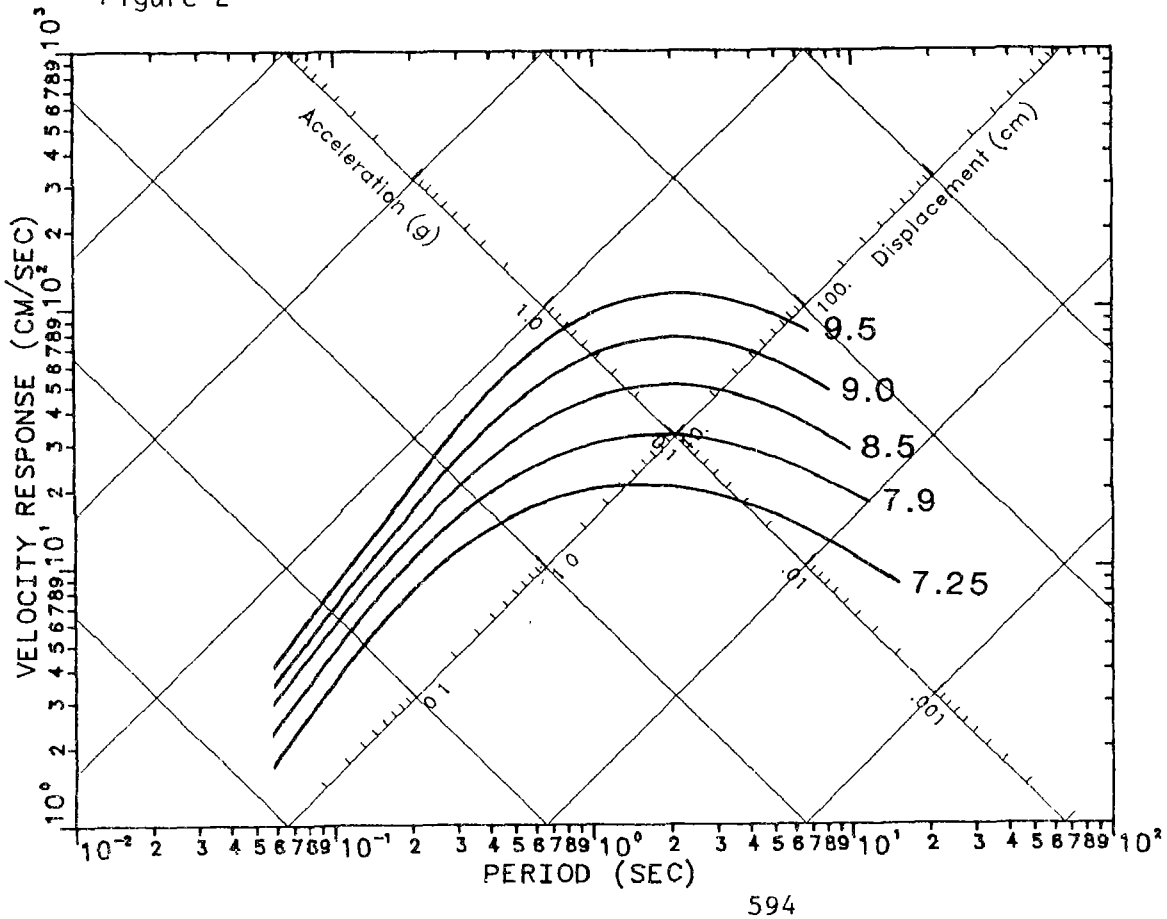

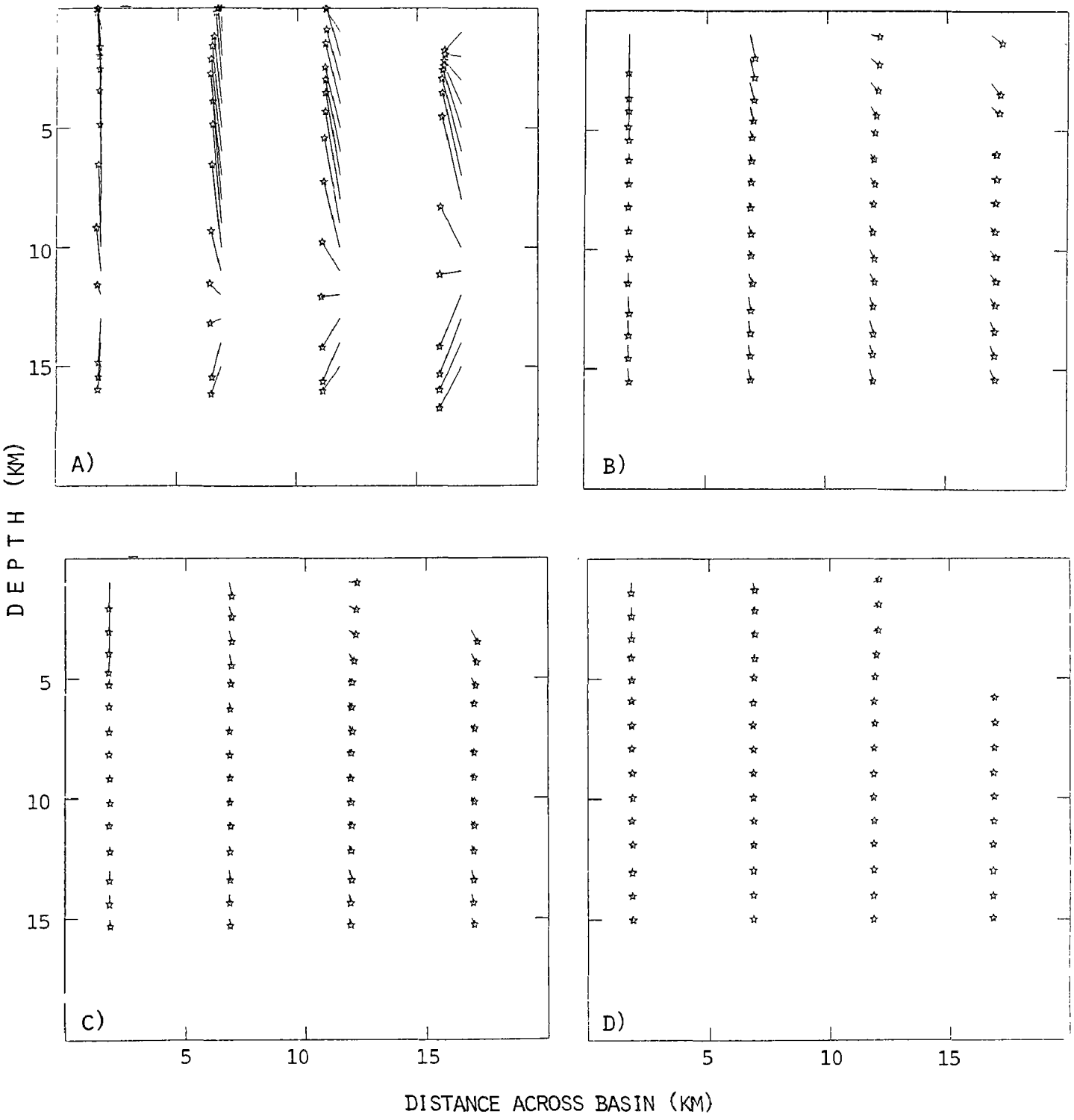

Figure 3

Precise Velocity and Attenuation Measurements in Engineering Seismology

9910-02413

Hsi-Ping Liu
Branch of Engineering Seismology and Geology
U.S. Geological Survey
345 Middlefield Road, MS 977
Menlo Park, California 94025
(415) 323-8111, ext. 2731

Investigations

1. Construction and testing of a borehole geophone leveling device which levels two orthogonally-oriented horizontal geophones to 0.1° from an initial maximum tilt of 10.5°.

2. Measurement of seismic shear-wave amplification and attenuation from a borehole near Coalinga, California (in collaboration with 9910-02676, Strong Motion Data Analysis and Source Mechanism Studies).

3. Design and construction of a borehole geophone locking device using a DC-powered linear actuator. The objective is to develop a 3-component borehole geophone package which can be locked rapidly at selected depths for seismic velocity and attenuation measurements.

Results

1. Horizontal electromagnetic geophones of natural period greater than 0.5 s need to be leveled to better than 1.5°. This requirement demands a leveling device for using such geophones in a borehhole when the axis of the geophone package deviates from the vertical by more than 1.5° after emplacement. Using Bendix flexural pivots as rotational axes, a gimbal leveling device has been constructed which levels two orthogonally-oriented horizontal geophones to 0.1° from an intial maximum tilt of 10.5°. This leveling device is designed to fit into a borehole-geophone package 12.7 cm (5 in) in outside diameter.

2. A 150 m deep borehole in Pleasant Valley, California has been logged using the pneumatically powered shear-wave generator developed under this project (Liu et al., 1985). The site is underlain by 38 m of clay, overlying interbedded sand and gravel. First arrival times and first zero crossing times were picked to obtain the shear-wave velocity structure, which increases gradually from 200 m/s at the surface to 540 m/s at 55 m depth. There is a narrow zone from 105 - 120 m with a velocity of 900 m/s, below which the velocity decreases to about 600 m/s. The shear-wave attenuation has been evaluated using the spectral-ratio technique. The resulting estimates of Q range between 5 and 20, with no significant increase with depth.

3. Using a DC-powered linear actuator, a low-cost borehole-geophone locking device has been designed. The locking force which pushes the geophone package sideways to the borehole wall can be adjusted up to 890 N (220 lbf). The entire package, designed to operate in a 10.2 cm-(4 in)diameter hole, is now under construction at the U. S. Geological Survey.

Reference Cited

Liu, H.-P., R. E. Warrick, and R. E. Westerlund, 1985, A pneumatic shear-wave generator with repeatable signal, EOS, Transactions of the American Geophysical Union, v. 56, p. 962.

Reports

Liu, H.-P., J. J. Fedock, and Fletcher, J. B., 1986, Mode identification of an arch dam by a dynamic air-gun test: 3rd U. S. National Conference on Earthquake Engineering, Proceeding Papers, Charleston, South Carolina, director approval.

Boatwright, J., R. Porcella, T. Fumal, and H.-P. Liu, 1986, Direct estimates of shear-wave amplification and attenuation from a borehole near Coalinga, California, Earthquake Notes, v. 57, p. 8.

Strong Ground Motion Prediction in Realistic Earth Structures

9910-03010

P. Spudich
Branch of Engineering Seismology and Geology
U.S. Geological Survey
345 Middlefield Road, MS 977
Menlo Park, California 94025
(415) 323-8111, ext. 2395

Investigations

1. Development of an automated iterative procedure for determining earthquake rupture behavior based on near-source ground motion records.

2. Studies of the S wave coda of aftershocks of the 1984 Morgan Hill earthquake.

Results

1. In collaboration with G. Beroza of MIT, we have developed an iterative procedure for modeling strong motion records and finding rupture mechanisms. Ground motions are linearly related to the amount of slip on the fault but are nonlinearly related to rupture time. Consequently, to invert for rupture time, an iterative procedure is employed. Using the isochrone formalism, it is computationally rapid to calculate the partial derivatives of seismograms with respect to rupture time and slip amplitude on the fault. The inverse of this partial derivative matrix is multiplied by 'residual' seismograms to obtain a perturbation to the current slip and rupture time model. We usually obtain convergence in 5-10 iterations. Preliminary results for the 1984 Morgan Hill earthquake indicate that there was significant deceleration of the rupture under Anderson Dam.

2. Using an array analysis technique reported on previously, T. Bostwick and I have examined the composition of waves comprising the S wave coda in aftershocks of the 1984 Morgan Hill earthquakes. At some stations a significant proportion of the coda energy appears to consist of waves that reverberate in a shallow region beneath the station, whereas this reverberation is largely absent at others. We are checking to see whether this phenomenon affects coda-Q measurements.

Reports

None.

Evaluation of the Effects of Large Earthquakes:

Development of an Earthquake Planning Scenario for the Hayward Fault

14-08-0001-21828

James F. Davis and Karl V. Steinbrugge
California Department of Conservation
Division of Mines and Geology
1416 Ninth Street
Sacramento, California 95814
(916) 445-1923

Objective: A large earthquake on the Hayward fault in the highly urbanized San Francisco Bay area poses one of the greatest hazards to lives and property in the nation. Knowledge of the plausible regional effects of such an earthquake on major lifelines and critical structures is basic to contingency planning at all levels of government responsibility and within the private sector. The regional evaluation of lifelines and critical structures that comprise an earthquake planning scenario for a specific earthquake is developed in three phases: (a) an isoseismal map is produced that characterizes the regional distribution of seismic intensity and potential for ground failure, i.e., surface rupture, liquefaction, landsliding, (b) inventories of lifelines and critical structures within the area impacted by the scenario earthquake are compiled and (c) the planning scenario is developed based on postulated damage to various lifeline components, given the regional pattern of projected shaking and ground failure developed in (a).

Results: The final report has been prepared, reviews completed, and printing (by Division of Mines and Geology) scheduled. Highlights of this planning scenario include:

The Scenario Earthquake: This planning scenario is based on the maximum credible earthquake that could occur on the Hayward fault. The assumed characteristics of the scenario earthquake are: a Richter magnitude of 7.5 (M7.5) that results from rupture of the entire 100-kilometer (62-mile) length of the fault from San Pablo Bay to east of San Jose; surface faulting that produces horizontal offsets of up to 10 feet; potentially damaging shaking that contiues for 30-40 seconds within 25 km (16 miles) of the fault; frequent aftershocks that continue for many weeks, including events of M6 or larger.

Deaths and Injuries: Deaths resulting from this scenario earthquake are estimated to range from 1,000-4,000 depending upon the time and day of occurrence. Hospitalized casualties are estimated to be 3 times the number of deaths; significant non-hospitalized casualties are estimated at 30 times the number of deaths.

Hospitals near the Fault: Eight of the 26 general acute care hospitals (99 beds or more) in Alameda and Contra Costa Counties are located within one mile of the Hayward fault. This represents a bed capactiy of 2,300 of a total of 6,200 available in these major facilities (about 35 percent).

Public Schools: Earthquake resistant public school buildings are generally well distributed throughout populated areas and provide a major resource for mass shelter and feeding. Some substantial damage to several schools can be anticipated, however, because of close proximity to the fault. Also, schools located in the hills east of the fault will be functionally impaired due to disrupted utility services. The Hayward fault traverses the University of California campus where about 20 percent of the floor space is in buildings classified as seismically poor or very poor, some of which can be expected to partially or totally collapse.

Trans-Bay Bridges: The trans-Bay bridges will be temporarily closed due to ground and structural failures at the bridge approaches. Roadway clearance, emergency repairs, detours, and bridge inspections will preclude or severely restrict use of these structures during the initial post-earthquake hours.

Major Freeway Routes: All of the major freeway routes to the East Bay from the east and south either cross the fault or are otherwise vulnerable to damage by strong shaking and ground failures. Major routes subject to surface fault offset (up to 10 feet) include Interstate 80 at San Pablo, Interstate 580 in East Oakland, Interstate 680 at Fremont and south to Milpitas, Route 24 west of the Caldecott Tunnel and most of Route 13 (Warren Freeway). Ground failures due to liquefaction and strong ground shaking cause major damage along Route 17 from Richmond to San Jose.

Airports: Performance of runways at the major Bay area airports when subjected to prolonged shaking is questionable, and liquefaction and differential settlement may render all or portions of many runways unusable by larger aircraft. For planning purposes, San Jose Municipal Airport is assumed to be available for larger transport aircraft. San Francisco and Oakland International, Hayward Municipal, and other secondary Bay area airports should be available for limited use by small aircraft and helicopters. Alameda Naval Air Station will be closed.

BART: BART will be shut down due to the lack of electrical power and need to assess and repair damage. Principal damage will be to the Berkeley Hills tunnels which will be closed indefinitely as a result of fault rupture. Damage to a few elevated spans is postulated in the East Bay. The trans-Bay tube and the subway systems survive with no major damage.

Railroads: Rail service to the Bay area from the east and south will be curtailed due to fault rupture, ground failures at various locations around the Bay perimeter, and structural damage to numerous bridges. Rail service via the coast route from southern California to San Francisco will be restored rapidly but all other lines to and from the Bay area will be blocked for at least the initial 72-hour post-earthquake period.

Electrical Power: Electrical power facilities in the East Bay are particularly vulnerable to damage from the scenario earthquake, and the time required to restore full power will be prolonged. While the resources may be available to rapidly deal with repairs to the system, the general confusion and damage to other lifelines such as communications and highways will complicate restoration efforts. Realistically, power is unlikely to be restored to many areas for several days or longer.

Water Supply: Water supply systems in the East Bay will be severely crippled in this scenario earthquake. Displacement along the Hayward fault will heavily damage all major tunnels, aqueducts and the many distribution systems that cross the fault. The flow of water crossing the fault will be reduced to 10% for the first 24 hours. Restoration of water service to all areas east of the fault in the East Bay hills will be greatly delayed. In the Alquist-Priolo zone, temporary pipe similar to that provided to many residences after the 1971 San Fernando earthquake may be used. Restoration of full service could take months.

Natural Gas: Horizontal displacement of up to 10 feet across the fault zone will cause hundreds of breaks in mains, valves, and service connections. Secondary ground failures resulting from high intensity shaking will result in many additional breaks in the system in the proximity of the fault zone. Some fires will occur in streets due to broken gas mains; structural fires will occur as a result of broken service connections. Fault rupture will also cause damage to the larger diameter transmission pipelines where they cross the fault at San Pablo and Fremont. As a result of damage to these transmission facilities, natural gas will be unavailable to all of the East Bay from San Pablo on the north to Milpitas on the south.

Petroleum Refineries and Products: The six major refineries in the San Francisco Bay area are in Contra Costa County, all are subject to damage by shaking, and all have facilities located near the Bay margin that are subject to damage by ground failure. Refineries may also suffer damage by fire and operations will curtailed by loss of utility services. All major pipelines transporting petroleum fuels to the Bay area (including the south Bay) cross the Hayward fault either at San Pablo or Fremont and all are vulnerable to damage by surface fault rupture.

Reports: (In press) Steinbrugge, K.V., Davis, J.F., Lagorio, H.J., Bennett, J.H., Borchardt, Glenn, and Toppozada, T.R., 1986; Earthquake Planning Scenario for a M7.5 Earthquake on the Hayward Fault in the San Francisco Bay Area: California Division of Mines and Geology Special Publication 78, 220 pp.

EVALUATION OF SEISMICITY ALONG THE COAST RANGES-SIERRAN BLOCK BOUNDARY ZONE, CALIFORNIA

U.S.G.S. Contract 14-08-0001-22019

Ivan G. Wong
Woodward-Clyde Consultants
1390 Market Street, Suite 250
San Francisco, California 94102
(415) 553-2000

INVESTIGATIONS

The faults within the boundary region between the Coast Ranges tectonic province and the Sierran crustal block of California have probably been the source of several earthquakes of M_L greater than 6 during historical times. However this zone (?) has generally not been recognized as a source of significant earthquakes and has received very little scientific attention because of (1) the lower level of seismicity and hence apparent seismic hazard relative to the adjacent San Andreas fault system, and (2) until recently, the lack of association with any significant earthquakes.

The somewhat surprising occurrence of the damaging 2 May 1983 Coalinga earthquake (M_L 6.7) has now focused greater attention on the seismicity along the western margin of the Great Valley and the resulting seismic hazard. We suggest that the Coalinga earthquake and several other significant earthquakes including the 19 and 21 April 1892 Winters earthquakes (two of the largest earthquakes felt in the San Francisco Bay Area in historical times with estimated M_L 6.75 - 7 and M_L 6.25 - 6.75, respectively) may be associated with the Coast Ranges-Sierran Block boundary zone (Wong, 1984).

In this study, we propose to analyze and interpret available seismographic data from the U.S. Geological Survey, the California Division of Water Resources, U.S. Bureau of Reclamation and Woodward-Clyde Consultants for selected events during the period 1969 to the present. The objectives will be to spatially and temporally characterize the contemporary seismicity, and to define the style and orientation of faulting and tectonic stresses along the boundary from the town of Red Bluff southeast to San Luis Dam. This will be accomplished principally by refining earthquake locations and crustal velocity structure, the determination of fault plane solutions and the integration of current geologic data. Based on earlier results, reverse faulting for at least the largest earthquakes and a northeast-southwest-trending tectonic compression seem to characterize the Coast Ranges-Sierran Block boundary zone (Wong and Ely, 1983). Detailed studies have been and are currently being conducted by the USGS and U.S. Bureau of Reclamation for the southern portion of the zone.

RESULTS

Literature research was conducted to refine the location of Coast Ranges-Sierran Block boundary which presently is not well defined because of the lack of surficial expression. This information was used to define a study area which includes the area within 20 km on either side of the boundary extending from Los Banos north to Red Bluff (Figure 1). The east-west extent of the study area was selected to insure inclusion of significant geologic features that may influence the seismicity in the region given the uncertainties in the location of the boundary and its role in contemporary seismotectonics.

A set of 153 earthquakes of $M_L \geq 2.0$ for the study area was selected from the USGS hypocentral data files (Figure 2). From this set, 20 earthquakes of $M_L \geq 3.0$ were selected to be relocated utilizing all available data including readings collected from networks operated by the University of California at Berkeley, California Department of Water Resources and Woodward-Clyde Consultants. Single event solutions are currently being refined utilizing velocity models for the Coast Ranges and the Great Valley based on recent refraction results obtained from Bob Colburn, U.S.G.S. Systematic residual errors will be searched for to evaluate the suitability of the velocity models especially with regards to early arrivals as usually observed at stations along the Sierran foothills. The latter are crucial in providing adequate azimuthal station coverage. If necessary station corrections will be calculated and applied. The velocity models will also be systematically varied to test for sensitivity of the hypocenters to the models. Upon finalization, the subset of 20 events will be used in some form of group location technique to relocate the rest of the data set. These studies are being performed in close cooperation with Dr. Jerry Eaton, U.S.G.S.

REFERENCES

Wong, I. G. 1984. "Re-evaluation of the 1892 Winters, California Earthquakes Based Upon a Comparison with the 1983 Coalinga Earthquake," EOS Transactions, American Geophysical Union, Vol. 65, pp. 996-997.

Wong, I. G. and R. Ely, 1983. "Historical Seismicity and Tectonics of the Coast Ranges-Sierran Block Boundary: Implications to the 1983 Coalinga, California Earthquakes," The 1983 Coalinga Earthquakes, California Division of Mines and Geology Special Publication 66, pp. 89-104.

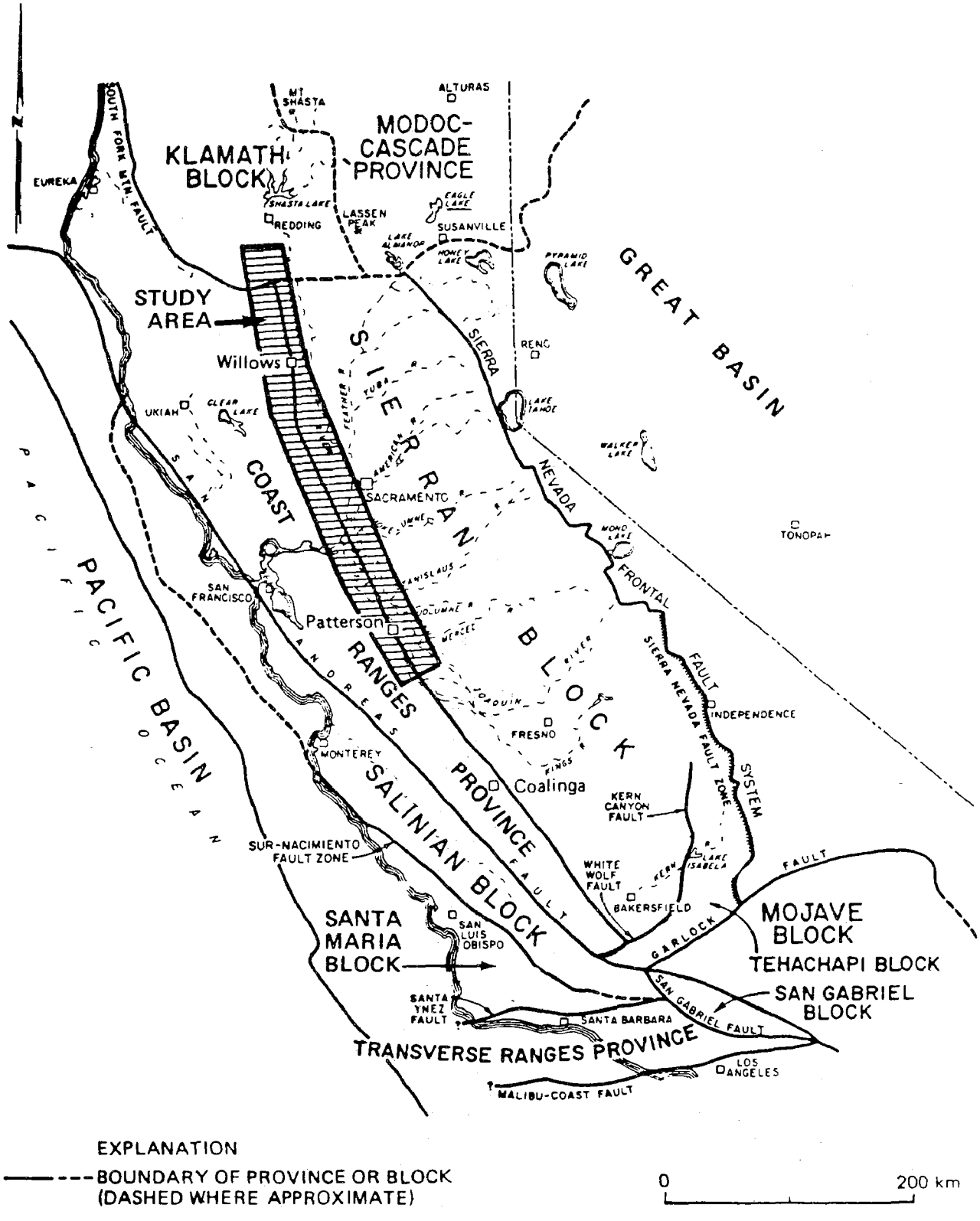

Figure 1. Tectonic provinces and crustal blocks of California

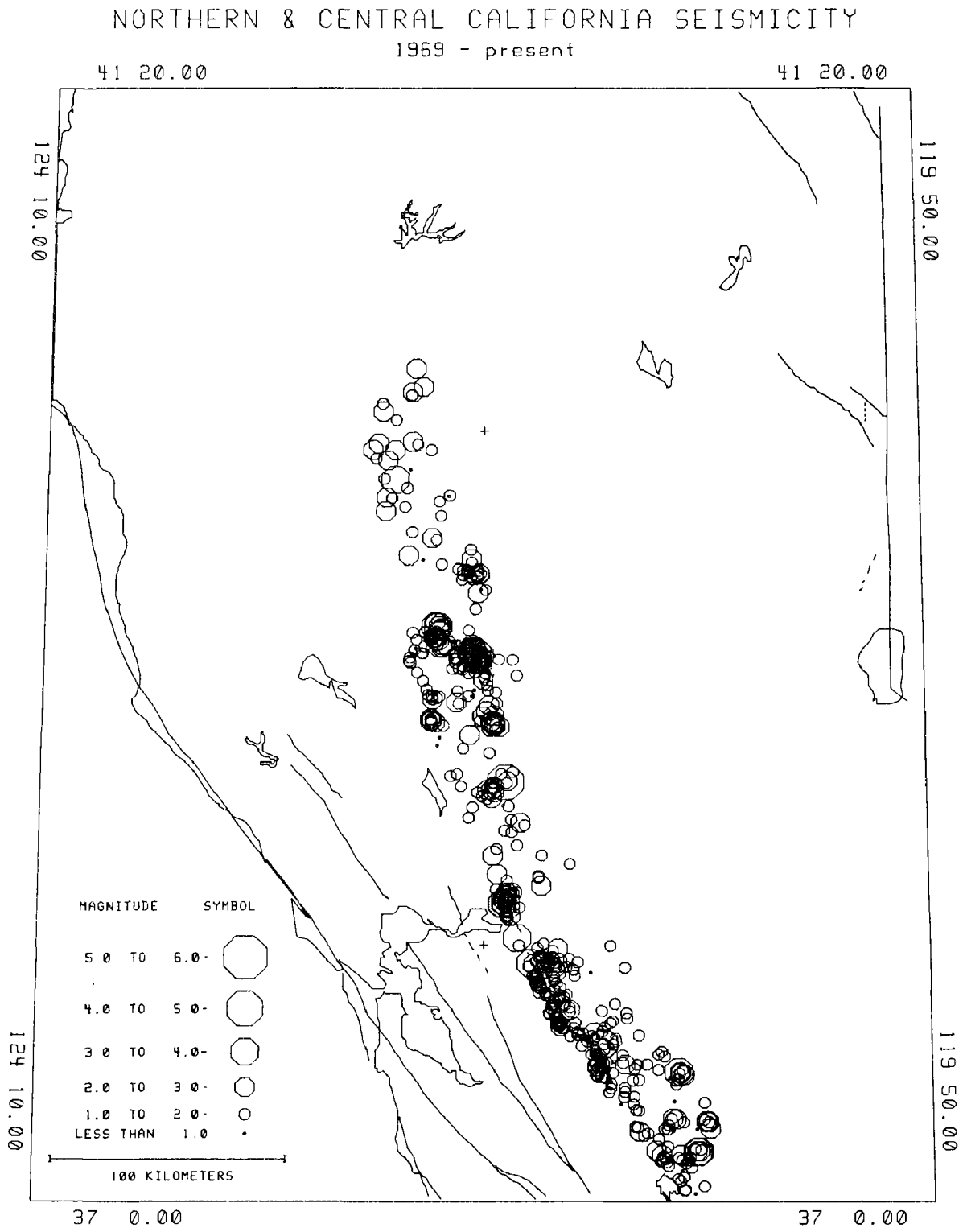
NORTHERN & CENTRAL CALIFORNIA SEISMICITY
1969 - present
41 20.00
41 20.00
124 10.00
119 50.00
124 10.00
119 50.00
37 0.00
37 0.00
MAGNITUDE SYMBOL
5.0 TO 6.0-
4.0 TO 5.0-
3.0 TO 4.0-
2.0 TO 3.0-
1.0 TO 2.0-
LESS THAN 1.0
100 KILOMETERS

Figure 2

INDEX 1

INDEX ALPHABETIZED BY PRINCIPAL INVESTIGATOR

INDEX 2

INDEX ALPHABETIZED BY INSTITUTION

San Diego State University	Rockwell, T. K.	192
San Francisco State University	Galehouse, J. S.	324
Sierra Geophysics, Inc.	Ihsan, S. M.	520
Southern California, University of	Aki, K.	202
Southern California, University of	Hauksson, E.	61
Southern California, University of	Henyey, T. L.	334
Southern California, University of	Teng, T.	41
Stanford University	Thiel, C. C., Jr.	532
U.S. Geological Survey	Algermissen, S. T.	477
U.S. Geological Survey	Allen, R. V.	309
U.S. Geological Survey	Anderson, R. E.	480
U.S. Geological Survey	Andrews, D. J.	129
U.S. Geological Survey	Atwater, B. F.	130
U.S. Geological Survey	Bakun, W. H.	310
U.S. Geological Survey	Bekins, B.	7
U.S. Geological Survey	Bonilla, M. G.	133
U.S. Geological Survey	Boore, D. M.	589
U.S. Geological Survey	Brady, A. G.	576
U.S. Geological Survey	Brady, A. G.	577
U.S. Geological Survey	Brown, R. D.	134
U.S. Geological Survey	Brown, W. M., III	484
U.S. Geological Survey	Buchanan-Banks, J. M.	486
U S. Geological Survey	Buchanan-Banks, J. M.	542
U.S. Geological Survey	Bucknan, R. C.	48
U.S. Geological Survey	Bundock, H.	579
U.S. Geological Survey	Burford, R.	316
U.S. Geological Survey	Butler, H. M.	547
U.S. Geological Survey	Byerlee, J. D.	413
U.S. Geological Survey	Byerlee, J. D.	415
U.S. Geological Survey	Carlson, M. A.	549
U.S. Geological Survey	Celebi, M.	581
U.S. Geological Survey	Choy, G. L.	51
U.S. Geological Survey	Choy, G. L.	207
U.S. Geological Survey	Choy, G. L.	551
U.S. Geological Survey	Clark, H. E., Jr.	553
U.S. Geological Survey	Clark, M. M.	135
U.S. Geological Survey	Cockerham, R. S.	209
U.S. Geological Survey	Dewey, J. W.	554
U.S. Geological Survey	Dieterich, J. H.	417
U.S. Geological Survey	Diment, W. H.	55
U.S. Geological Survey	Engdahl, E. R.	556
U.S. Geological Survey	Espinosa, A. F.	487
U.S. Geological Survey	Fletcher, J. B.	218

U.S. Geological Survey	Sato, M.	272
U.S. Geological Survey	Schulz, S. S.	276
U.S. Geological Survey	Schwartz, D. P.	528
U.S. Geological Survey	Schwartz, D. P.	530
U.S. Geological Survey	Segall, P.	390
U.S. Geological Survey	Shaw, H. R.	447
U.S. Geological Survey	Silverman, S.	396
U.S. Geological Survey	Simpson, R. W.	456
U.S. Geological Survey	Sims, J. D.	108
U.S. Geological Survey	Sipkin, S. A.	561
U.S. Geological Survey	Spence, W.	475
U.S. Geological Survey	Spence, W.	563
U.S. Geological Survey	Spudich, P.	403
U.S. Geological Survey	Spudich, P.	598
U.S. Geological Survey	Stein, R. S.	405
U.S. Geological Survey	Stewart, S. W.	37
U.S. Geological Survey	Stover, C. W.	566
U.S. Geological Survey	Stuart, W. D.	465
U.S. Geological Survey	Taggart, J. N.	574
U.S. Geological Survey	Tarr, A. C.	502
U.S. Geological Survey	Tinsley, J. C.	506
U.S. Geological Survey	Van Schaack, J.	45
U.S. Geological Survey	Van Schaack, J.	47
U.S. Geological Survey	Wallace, R. E.	124
U.S. Geological Survey	Ward, P. L.	286
U.S. Geological Survey	Weaver, C. S.	126
U.S. Geological Survey	Wentworth, C. M.	172
U.S. Geological Survey	Wesson, R. L.	411
U.S. Geological Survey	White, R. A.	292
U.S. Geological Survey	Wilson, R.	512
U.S. Geological Survey	Yerkes, R. F.	535
U.S. Geological Survey	Ziony, J. I.	540
U.S. Geological Survey	Zoback, M. L.	515
U.S. National Bureau of Standards	Levine, J.	253
Utah Geological And Mineral Survey	Christenson, G. E.	518
Utah, University of	Arabasz, W. J.	3
Utah, University of	Smith, R. B.	115
Washington, University of	Crosson, R. S.	17
Washington, University of	Crosson, R. S.	53
J. H. Wiggins Company/NTS	Taylor, C.	543
Woodward-Clyde Consultants	Wong, I. G.	602
Wisconsin, University of, Madison	Roeloffs, E.	473

687-925/58335